UNIVERSITY OF SOUTHAMPTON

FACULTY OF ENGINEERING, SCIENCE AND MATHEMATICS

School of Chemistry

BINDING ANIONS USING SIMPLE NEUTRAL MOLECULES

By

Jennifer Ruth Hiscock

Thesis for the degree of Doctor of Philosophy

September 2010

Dedicated to my grandfather, William Edward Chambers who received his PhD in 1946 and was an inspiration to me until his death in 2010.

UNIVERISTY OF SOUTHAMPTON

ABSTRACT

FACULTY OF ENGINEERING, SCIENCE AND MATHEMATICS

SCHOOL OF CHEMISTRY

Doctor of Philosophy

BINDING ANIONS USING SIMPLE NEUTRAL MOLECULES

By Jennifer Ruth Hiscock

This thesis reports a number of novel neutral, hydrogen bond donating anion receptors and describes their anion coordination properties in both the solution and solid states.

A set of ten urea/thiourea linked indole/carbazole groups were found to have high affinities for a variety of oxo-anions in highly competitive DMSO solutions. Of these receptors, the diindolylurea motif was found to be excellent for the binding of dihydrogen phosphate. This group of receptors were found to form 1:1 complexes in solution with various anions but more complex 2:1 and 3:1 receptor:anion complexes were observed in the solid state. Deprotonation of the bound protonated oxo-anion was observed with these 2:1 and 3:1 complexes.

The basic diindolylurea motif was then extended by the incorporation of further NH bond donor groups from amide, indole and carbazole functionalities. This group of receptors were found to form 1:1 complexes in both the solution and solid states, with the binding mode dependent of the geometry of the anion. These compounds also showed spontaneous crystallisation with sulfate in as little as 20 minutes. These receptors showed high affinities for the oxo-anions and gave the first examples of solution state deprotonation of bound protonated oxo-anions.

A set of three dimensional indole-based receptors was also synthesised, utilising the TREN and pin-wheel scaffolds. These receptors contain between six and fifteen NH bond donor groups that give a range of anion binding modes, some too complex to be defined, that generally show a preference for the oxo-anions. Again, an example of deprotonation of the bound protonated oxo-anion was observed.

Original work published by Gale and co-workers[1,2] and Jurczak and co-workers[3] was also extended by synthesising seven indolylyamide based anion receptors. In the solution state, the majority of receptor:anion combinations form a 1:1 complex but the solid state showed only 2:1 anion:receptor complex formation, giving similar selectivity for both oxo-anions and fluoride as the parent receptor.

Contents

DECLARATION OF AUTHORSHIP

I, **Jennifer Ruth Hiscock**, declare that the thesis entitled

Binding anions using simple neutral molecules

and the work presented in the thesis are both my own, and have been generated by me as the result of my own original research. I confirm that:

- this work was done wholly or mainly while in candidature for a research degree at this university;
- where any part of this thesis has previously been submitted for a degree or any other qualification at this university or any other institution, this has been clearly stated;
- where I have consulted the published work of others, this is always clearly attributed;
- where I have quoted from the work of others, the source is always given. With the exception of such quotations, this thesis is entirely my own work;
- I have acknowledged all main sources of help;
- where the thesis is based on work done by myself jointly with others, I have made clear exactly what was done by others and what I have contributed myself;
- parts of this work have been published as:

"1,3-Diindolylureas: high affinity dihydrogen phosphate receptors" C. Caltagirone, P.A. Gale, J.R. Hiscock, S.J. Brooks, M.B. Hursthouse and M.E. Light, *Chem. Commun.* 2008, 3007-3009

.

"1,3-Diindolylureas and 1,3-diindolylthioureas: anion complexation studies in solution and the solid state" C. Caltagirone, J.R. Hiscock, M.B. Hursthouse, M.E. Light and P.A. Gale, *Chem. Eur. J.*, 2008, **14**, 10236-10243.

"Fluorescent carbazolylurea anion receptors" J.R. Hiscock, C. Caltagirone, M.E. Light, M.B. Hursthouse and P.A. Gale, *Org. Biomol. Chem.* 2009, **7**, 1781-1783.

"2-Aminoindole based anion receptors" C. Caltagirone, P.A. Gale, J.R. Hiscock, M.B. Hursthouse, M.E. Light and G.J. Tizzard, *Supramolecular Chem.*, 2009, **21**, 125-130.

"Anion-anion proton transfer in hydrogen-bonded complexes" P.A. Gale, J.R. Hiscock, S.J. Moore, C. Caltagirone, M.B. Hursthouse and M.E. Light, *Chem. Asian J.*, 2010, **5**, 555-561

"Fluorescent carbazolylurea and carbazolylthiourea based anion receptors and sensors" J.R. Hiscock, C. Caltagirone, M.E. Light, M.B. Hursthouse, and P.A. Gale, *Supramol. Chem.*, 2010, DOI: 10.1080/10610271003637087

"Acyclic indole and carbazole-based sulfate receptors" P.A. Gale, J.R. Hiscock, C.Z. Jie, M.B. Hursthouse and M.E. Light, *Chem. Sci.*, 2010, **1**, 215-220

Signed: ……..

Date:…….

Acknowledgements

Firstly and foremost, I would like to thank my supervisor, Prof. Philip A. Gale, for all his help, support and guidance over the last three years. I would also like to thank my second supervisor, Prof. Mike B. Hursthouse, for giving me the opportunity to study for the PhD. I would like to thank all the members of the Gale group past (Gareth, Matthew, Peter, Jo, Sergio, Roberto, Christine), present (Cally, Steve, Sam, Sarah, Natalie, Marco) and the temporary visitors (Agnieszka, Masafumi).

An especially large thank you goes to Dr. Claudia Caltagirone, who taught me most of the practical skills I needed to undertake my PhD, would not let me quit, worked with me on many joint projects with endless patience and has become a lifelong friend.

I would also like to thank the University of Southampton and the ESPRC for the funding I have recieved and the NMR, MS and stores staff for all their advice and assistance.

Special thanks go to Dr. Mark E. Light for his endless patience, time and early morning starts involved in teaching me how to run and solve my own crystal structures.

Finally I would like to thank my family for the encouragement, support and help that they have given to me to enable me to reach this point in my academic career, especially my mother (Susan Hiscock) for proof reading my entire thesis in record time.

Abbreviations

Å	Ångström
Ac_2O	Acetic anhydride
AcO^-	Acetate
AcOH	Acetic acid
Act.	Actual
Anal.	Analysis
Ar	Aryl (general text) /aromatic (NMR)
a.u.	Atomic units
BOC	Butoxycarbonyl
Br	Broad resonance (NMR)
Bu	Butyl
BzO^-	Benzoate
^oC	Degrees Centigrade
Calcd.	Calculated
CDI	1,1'-Carbonyldiimidazole
$CHCl_3$	Chloroform
d	Doublet (NMR)
DCM	Dichloromethane
Decomp.	Decomposed
DMAP	4 – (Dimethylaminopyridine)
DMF	Dimethylformamide

DMSO	Dimethylsulfoxide
DNA	Deoxyribonucleic acid
E	Error
Et	Ethyl
EtOH	Ethanol
Equ.	Equivalents
FTIR	Fourier transform infra-red spectroscopy
Fmoc	Fluorenylmethyloxycarbonyl
g	Grams
HOBt	1-Hydroxybenzotriazole
hr	Hour(s)
HRMS	High Resolution Mass Spectrometry
Hz	Hertz
ITC	Isothermal titration calorimetry
IR	Infra-red spectroscopy
J	Coupling constant (NMR)
K	Kelvin
K_a	Association constant
LRMS	Low Resolution Mass Spectrometry
m	Meta
m	Multiplet (NMR)
M	Molarity

Me	Methyl
MeCN	Acetonitrile
MeOH	Methanol
mins	Minutes
mol	Mole(s)
mmol	millimole(s)
m.p.	Melting point
MS	Electrospray (Mass spectrometry)
m/z	Mass to charge ratio (Mass Spectroscopy)
NEt_3	Triethylamine
NMR	Nuclear magnetic resonance spectroscopy
o	Ortho
p	Para
Ph	Phenyl
Pd/C	Palladium/carbon catalyst
ppm	Parts per million
Pr	Propenyl
i-Pr	*iso*-propenyl
PyBOP	(Benzotriazol-1-yloxy)tripyrrolidinophosphonium hexafluorophosphate
q	Quartet (NMR)
Sat.	Saturated
t	Triplet (NMR)

TBA	Tetrabutylammonium
TEA	Tetraethylammonium
TMA	Tetramethylammonium
TREN	Tris(2-aminoethyl)amine
Tert	Tertiary
UV-vis	Ultraviolet – visible spectroscopy
^{o}	Degree
Φ	Fluorescence quantum yield
$\{^{1}H\}$	Proton decoupled (carbon NMR)

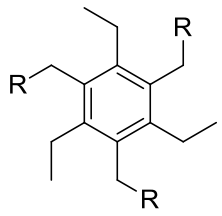

Pin-wheel scaffold

Chapter 1 – Introduction

1.1 Supramolecular Chemistry

In 1987, Jean-Marie Lehn, who was responsible for the invention of the term "supramolecular", won, along with Charles Pederson and Donald Cram, the Nobel Prize for research into this branch of chemistry. He described supramolecular chemistry as "chemistry beyond the molecule" with the aim of "developing highly complex chemical systems from components interacting by non-covalent intermolecular forces".[4] Supramolecular chemistry is study of the non-covalent interactions between molecules. This is often referred to as a host-guest scenario in which reversible; intermolecular interactions are used to hold together two or more chemical species, thus forming a supermolecule with the larger molecule being referred to as the host and the smaller as the guest. There are many examples in nature of this type of interaction. The first time this idea was described was when Fisher looked at enzyme-substrate interactions and described the "lock and key" principle. The enzyme-substrate complexes exhibit host-guest interactions, with the enzyme acting as the host and the substrate the guest. These two chemically distinct species are complementary to each other and join together like a lock and a key. See Figure 1.1.1 for illustrated detail.[5]

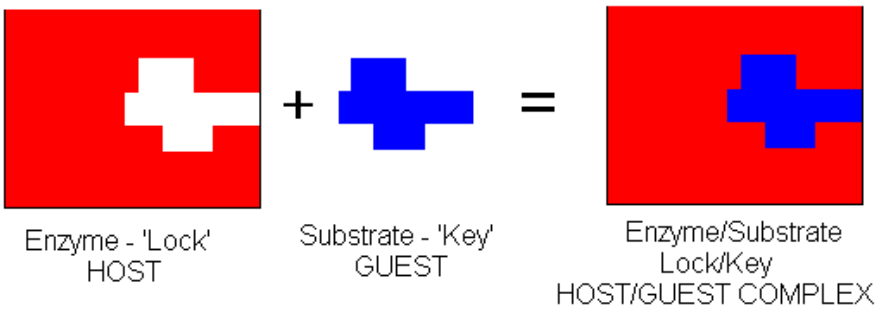

Figure 1.1.1 Illustration of the host/guest principle with the "lock and key principle". The two different components display a complementary shape allowing the two parts to join together to form the final complex.

Another important example of the supramolecular chemistry at work in nature is the formation of the DNA double helix from two independent strands. The DNA double

helix resembles a twisted ladder and it is the rungs of this ladder which are created when the two separate strands come together, held by non-covalent interactions.

Both of these examples show how non-covalent interactions can be used to join two or more molecules reversibly to form a supramolecule. It is this reversibility of binding that allows enzymes to perform catalysis and DNA to store and transfer biological information. These show selectivity; the host only interacts with a specific guest. A particular enzyme will only interact or bind a particular substrate and a guanine nucleotide will only pair with a cystine nucleotide, when forming the DNA double helix. [5]

There are a number of different intermolecular non-covalent interactions that contribute to the stability of the host-guest complex.

1. Hydrogen bonds are created between hydrogen bond donor groups (X) and hydrogen bond acceptor groups (A). The strength of this bond increases with the increase in electronegativity of both X and A. The hydrogen acts like a bridge between X and A, with optimal interaction being achieved at 180°. Weak, mainly electrostatic hydrogen bonds have bond energies of 4 $kJmol^{-1}$ whereas the stronger, mainly covalent bonds have energies of 120 $kJmol^{-1}$. [5-8]
2. Van der Walls forces are some of the weakest interactions, with bond energies <5 kJ mol^{-1}. These forces are based on electrostatic interactions formed by the proximity of an adjacent nucleus causing the polarisation of the electron clouds. Although the individual bond energies are small, the sum of multiple interactions can be great. [5,6]
3. Electrostatic interactions can be split into three main types, illustrated in Figure 1.1.2. The first, ion-ion interactions, are similar in strength to a covalent bond and have bond energies between 100 and 350 kJ mol^{-1}. The second, ion-dipole interactions, involve an ion and a polar molecule with a complementary, partial charge. These interactions have bond energies between 50 and 200 kJ mol^{-1}. The third, and weakest, are dipole-dipole interactions, which have bond energies of 5-10 kJ mol^{-1}. These are formed when atoms carrying partial charges are aligned. [5,6]

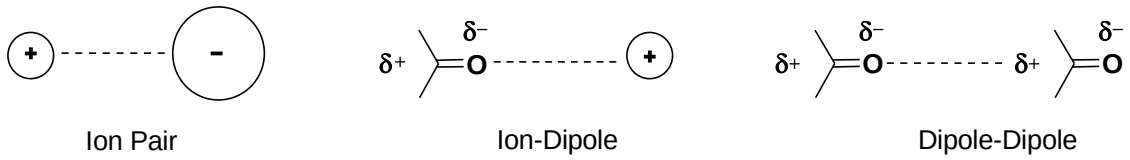

Figure 1.1.2 Three types of non-covalent electrostatic interactions.

4. π-π stacking interactions can be split into two main types (Figure 1.1.3). Although many variations have been seen, face-to-face and edge-to-face interactions occur between the electron-rich π-cloud and electron-deficient hydrogen atoms of aromatic rings. The edge-to-face is the more favoured interaction. [5,6]

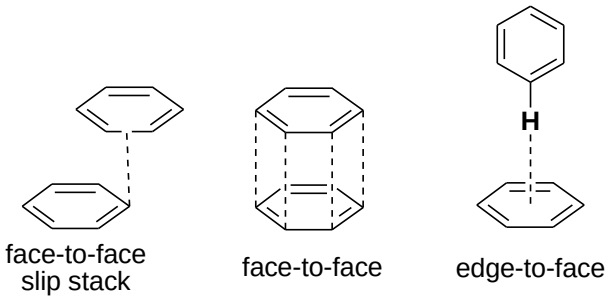

Figure 1.1.3 Two variations of π-π stacking interactions; face-to-face and edge-to-face. The face-to-face stacking is also illustrated in the two main observed forms.

1.2 Anion recognition

Anions are found everywhere in the natural world. Nitrates and phosphates are present in the earth and ground water systems. Integral to plant growth and health, they are also present in pesticides and fertilizers that can cause environmental damage. This can occur through organism poisoning and uncontrolled plant growth in contaminated ground water and surface runoff. [9] Chloride anions are responsible for maintaining an electrochemical gradient across cell membranes and are essential for the control of the water content of our mucous membranes. The absence of this anion in the mucus produced by our body systems is an effect of the genetic disease, cystic fibrosis. Anions are also an essential part of most enzyme substrate/co-factor complexes and form the polyphosphate backbone of DNA. Phosphate anions also act as the energy currency in our body systems in the form of ADP and ATP. Anions are critical to life and their importance often overlooked.[9]

The idea of an anion receptor is based on host-guest chemistry but the design is challenging for some of the reasons stated below.

- The radius of an anion is much larger than that of the equivalent isoelectric cations e.g. Cs^+ has a radius of 1.81 Å while I^- has a radius of 2.06 Å, meaning that it has a lower charge-to-radius ratio. [10]

- Anions can also become protonated in lower pH conditions, which can become a problem when designing protonated anion receptors. [5]
- Anions also have a wide range of geometries, meaning that each receptor needs to be specifically designed to optimise complementary anion:receptor binding. The different anion geometries are listed below with examples. [10]

1. Spherical – F^-, Cl^-
2. Linear – SCN^-, CN^-
3. Trigonal planar – HCO_3^-, NO_3^-
4. Tetrahedral – $H_2PO_4^-$, SO_4^{2-}
5. Octahedral – $Fe(CN)_6^{4-}$, $Co(CN)_6^{3-}$
6. Complex shapes – DNA, RNA[10]

- Solvent effects are also crucial. Polar solvents form strong interactions with both the free receptor and the anion and these electrostatic interactions often dominate over the recognition forces between the receptor and anion.[10]

In order to design an effective and selective anion receptor, these problems must be overcome. Although ion pairing is a strong interaction, it is not directional. This means that this interaction may be out-competed by the use of the highly directional hydrogen bond, the position of which can be tailored to meet the optimal 180° angle to interact with the geometry and size of a specific anion. Another important design consideration is the reduction of self-association. This reduces the effectiveness of anion/receptor affinity. Size specific, pre-organised receptors with specifically placed anion binding groups designed with a particular anion in mind, are the key for successful selective anion binding. It is these synthetic and design challenges, combined with the importance of anions, that makes anion binding a growing and ever more exciting area of supramolecular chemistry.

The first example of anion binding by a synthetic anion receptor was reported in 1968 by Simmons and Park (**1**) and was based around a tripodal ammonium bridged design. This charged receptor showed evidence of binding chloride anions, with a binding constant of 4 M^{-1} in a 50 % TFA solution. The position of the ammonium's hydrogen atoms pointing into the interior of the capsule when binding chloride was confirmed in 1975 by Marsh and

co-workers, using X-ray crystallography, although the full structure was not completely elucidated.[11]

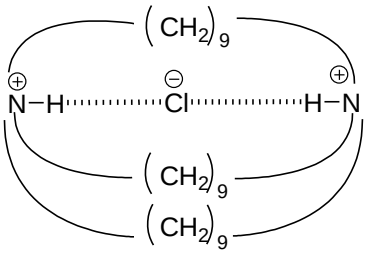

1

There are two main classes of synthetic anion receptors; those which utilise metals and those which do not. The non-metallic systems can be further divided into two subsections; neutral and charged. It is these non-metallic neutral systems that will be the focus of this thesis.

1.3 Neutral synthetic anion receptors

1.3.1 Amide based receptors

The first neutral hydrogen bonding anion receptor (**2**) was reported in 1986 by Pascal and co-workers. This design utilises the tripodal capsule design, binding the anion through three hydrogen bonds from amide NHs. This receptor was found to bind fluoride in a DMSO-d_6 solution. Anion binding was determined by ^{1}H and ^{19}F NMR spectroscopic studies.[12]

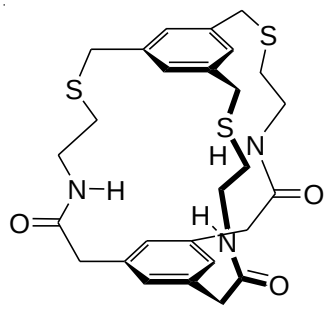

2

This original tripodal-based design was followed by anion receptors from Reinhoudt and co-workers. In this case, the receptors were based on a smaller TREN scaffold, with a design loosely based on naturally-occurring phosphate binding proteins.

The four analogues (**3-6**) were obtained from the relevant acid chloride by reaction with TREN, giving the presence of NEt_3 in yields of 70-90%. These receptors were found to be selective for dihydrogen phosphate, with binding constants of 4700 M^{-1}, which is x 10^2 higher than those obtained for sulfate or chloride. The binding constants were obtained by proton NMR titrations with the appropriate TBA salt. [13]

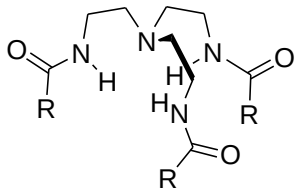

3 R = CH_2Cl
4 R = $(CH_2)_4CH_3$
5 R = C_6H_5
6 R = 4-$MeOC_6H_4$

More recent work by Smith and Davis and co-workers has shown that simple amido-functionalised TREN receptors are able to bind and transport anions. Smith and co-workers observed chloride transport through a polar phase, a non-polar phase and a second polar phase (U tube experiment). Davis and co-workers observed chloride transport through a vesicle biphospholipid membrane *via* OH-Cl^- bonding. Examples of the receptors used for anion transport from Smith and co-workers (**7**) and Davis and co-workers (**8**) are shown below.[14] [15]

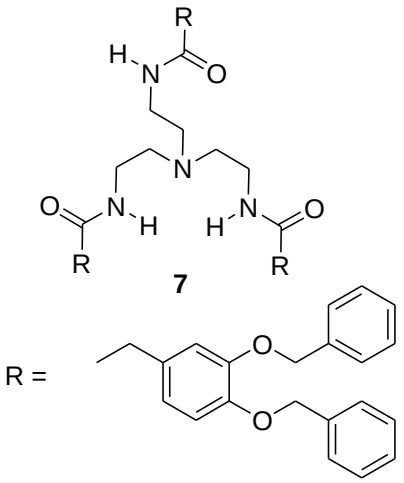

7

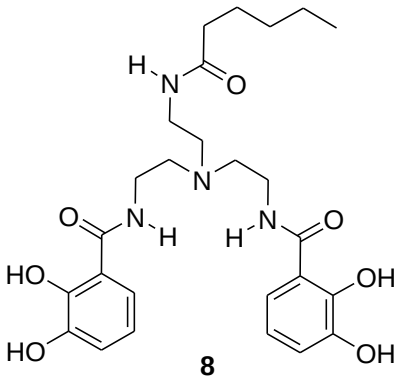

8

In 1997, Crabtree and co-workers synthesised a set of simple planar cleft receptors. Receptors **9** and **10** contain two amide groups, each of which form a single hydrogen bond to an anion. These 1:1 binding conformations were confirmed by Job plot in the solution state and illustrated with x-ray crystal structure of receptor **9** with bromine, (Figure 1.3.1.1)

(N···Br 3.44 and 3.64 Å). The bromide anion sits slightly above the plane of the central aryl ring (N-H···Br angles of 166° and 172°).[16]

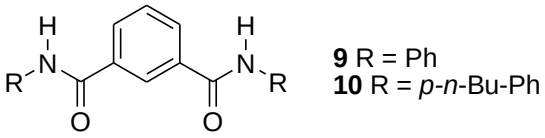

9 R = Ph
10 R = *p*-*n*-Bu-Ph

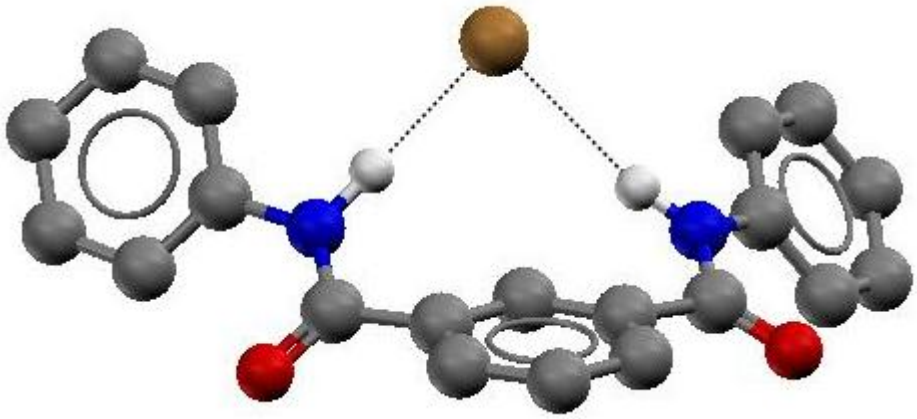

Figure 1.3.1.1 Crabtree and co-workers' simple amide isophthalamide-based anion receptor **9,** complexed with bromide.

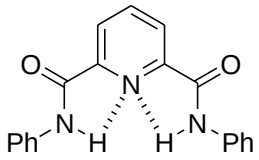

11

In 1999, Crabtree and co-workers synthesised an analogue of **9** and **10**. Receptor **11** was more soluble than its predecessor, enabling ^{1}H-NMR studies to be carried out. This receptor exhibits pre-organisation of the amide NH's into the binding cleft due to the favourable intramolecular interactions between the pyridinyl N and the amide NH. Binding constants and stoichometries were determined by ^{1}H NMR experiments in CD_2Cl_2 with the TBA or tetraphenylphosphate salt of the anion. Both receptors **10** and **11** show selectivity for chloride over the other anions tested in the following series:

Receptor **10**: Cl^- 61000 M^{-1} > F^- 30000 M^{-1} > OAc^- 19800 M^{-1} > Br^- 7100 M^{-1} > I^- 460 M^{-1}.

Receptor **11**: Cl^- 24000 M^{-1} > F^- 1500 M^{-1} > OAc^- 525 M^{-1} > Br^- 57 M^{-1} > I^- < 20 M^{-1}.

Although the binding constants for compound **11** are lower than those found with compound **10**, the pyridine based receptor exhibits far greater selectivity for chloride because of the pre-organised design. [17]

Other receptors synthesised, utilising the same pyridine diamide base unit as reported by Crabtree and co-workers [16,17] and others[18-21], also exhibit increased selectivity when the amide groups are pre-organised by these intramolecular bonds.

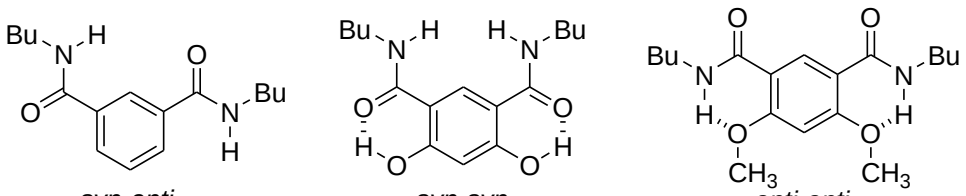

syn-anti **12** *syn-syn* **13** *anti-anti* **14**

The increase in selectivity for binding anions due to pre-organisation was shown by Gale and co-workers with the synthesis of receptors based on the isophthalamide unit. A set of analogous receptors (**12-14)** was synthesised, each with the different predicted predominant conformation as shown. Receptors **12**, **13** and **14** exhibit *syn-anti*, *syn-syn* and *anti-anti* conformations respectively. The conformation is controlled by the presence of different groups at the 4 and 6 position in the central aromatic ring. The crystal structure of **13** (Figure 1.3.1.2a) shows a predominant syn-syn conformation (O···O 2.55-2.75 Å) while the crystal structure of **14** (Figure 1.3.1.2b) exhibits anti-anti only (N···O 2.67-2.68 Å). ^{1}H NMR titration experiments were conducted with **12** and **13** in MeCN-d_3 and both were shown to have a preference for chloride over iodide and bromide. The pre-organisation of **13** into the syn-syn conformation, due to the substitutions on the aromatic ring, increases the binding constant with chloride from 195 M^{-1} (**12**) to 5230 M^{-1}. [22] This large increase in binding constant is due to the NH pre-organisation into the centre of the cleft. Unlike the examples of pre-organisation shown by Crabtree etc.[16-22], the NH bond donor groups are not involved in pre-organisation and so are free to bind the anion. The pre-organisation of **14** into the anti-anti conformation caused a negative effect. There was no evidence of anion binding as the NHs are facing out of the cleft, the hydrogen binding to the methoxy groups. [22]

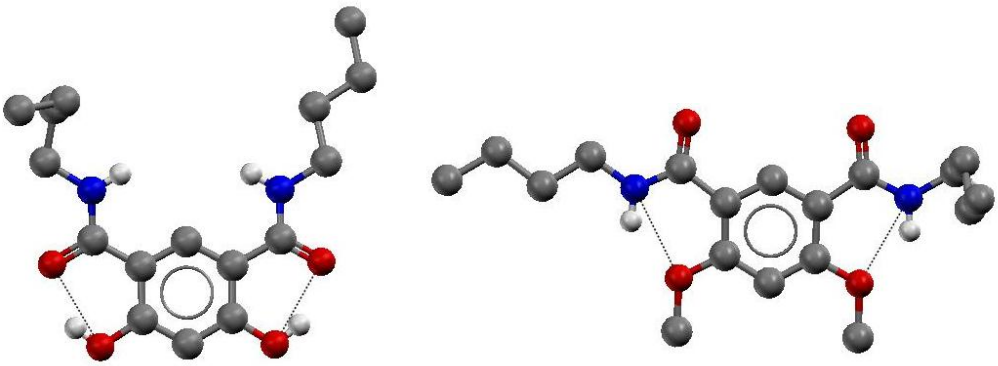

Left Figure 1.3.1.2a Gale and co-workers isophthalamide based receptor **13** pre-organised into the *syn-syn* conformation. **Right Figure 1.3.1.2b** Gale and co-workers isophthalamide based receptor **14** pre-organised into the *anti-anti* conformation.

A similar bis-amide isophthalamide-based receptor to those synthesised by Crabtree and co-workers [16,17] and Gale and co-workers [22] was synthesised by Hughes and Smith. Receptor **15** was pre-organised with the addition of the Lewis-acidic boronate groups, interacting with the carbonyl oxygen atoms. This leaves the amide NH free to interact with the anions.[23]

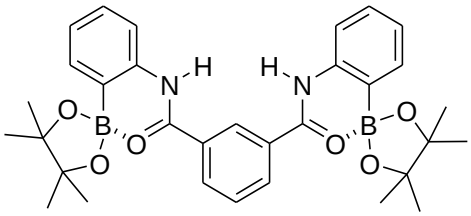

15

Research into isophthalamide- and pyridine-2,6-carboxamide-based symmetrical anion receptors is still current today, with further examples synthesised by Ghosh and co-workers[24] and Yatsimirsky and co-workers[25].

Thordarson and co-workers synthesised receptor **16** which, in non-polar solvents such as hexane, aggregates to form one-dimensional hydrogen bonding networks with additional molecular bonds that are strong enough to result in gel formation. ^{1}H MNR studies were carried out in acetone-d_6. However, due to aggregation effects with the receptor, analysis was difficult. The data was fitted to both 1:1 and 1:2 anion:receptor binding models and bromide, iodide, nitrate and acetate were found to fit the 1:2 model better. Chloride was the only exception, appearing to prefer the 1:1 binding conformation.

This pyromellitamide-based receptor has a similar selectivity for small anions as the other isophthalamide receptors previously discussed ($Cl^- > OAc^- > Br^- > NO^{3-} = I^-$). Receptor **16** uses the same NHs to bind the anions as it does to aggregate and form gels. Anion binding events are therefore able to stimulate the dissociation of the gel in a cyclohexane solution. The time taken for the gel to dissociate with different anions correlates qualitatively with the strength of anion binding ($Cl^- > OAc^- > Br^- > NO^{3-} > I^-$).[26]

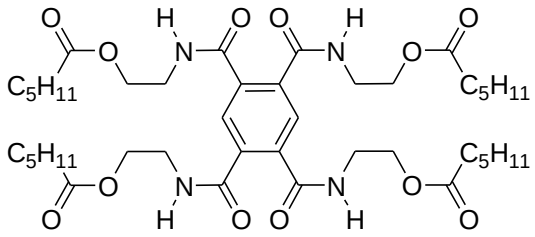

16

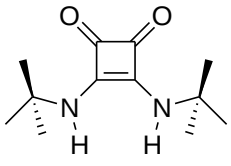

17

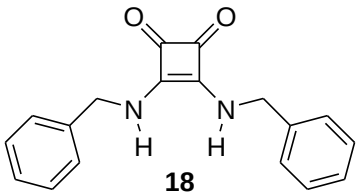

18

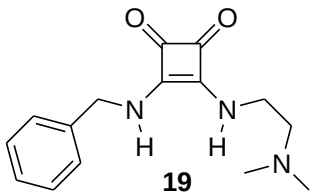

19

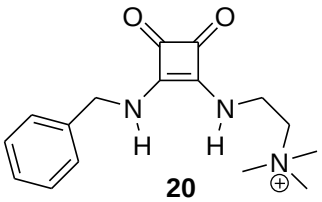

20

Prohen and co-workers synthesised a group of simple squaramido-based compounds. Each receptor contains two amide-like groups (compounds **17**-**20**). Proton NMR titration studies were preformed in a DMSO-d_6 solution with TMA acetate and fitted to a 1:1 binding model. Binding constants of 217 M^{-1}, 1980 M^{-1}, 1120 M^{-1} and 14200 M^{-1} were calculated for receptors **17**-**20** respectively. The advantage of the squaramido base unit is that the NH groups are less convergent than those in the isophthalamide-based receptors. This means that these receptors can form hydrogen bonds more efficiently with oxo-anions such as acetate and benzoate because the hydrogen bond formed between the anion and receptor is closer to the optimal 180° bond angle. The introduction of a positive charge (**20**) gives extra electrostatic interactions that cause a power of ten increase in binding constant over the neutral receptors tested. [27]

Incorporating a rigid scaffold into anion receptor design, functionalised with anion binding groups, increases the pre-organisation of the receptor, resulting in greater anion affinity by reducing flexibility. The selectivity of the receptor can be tailored towards a particular anion, depending on the size and geometry of that anion.

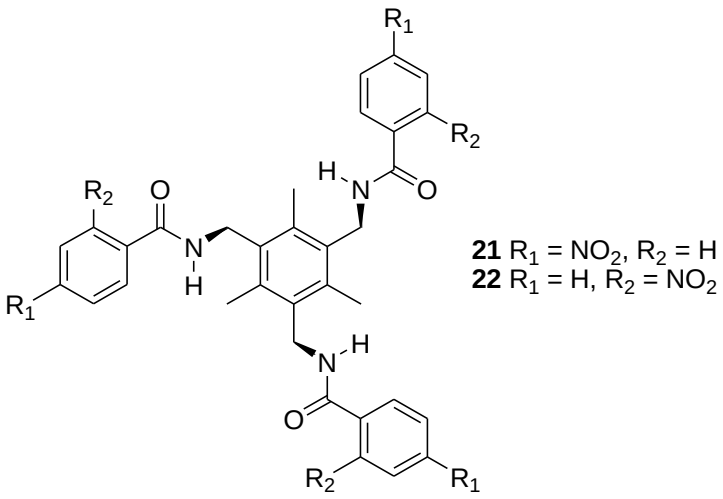

21 $R_1 = NO_2$, $R_2 = H$
22 $R_1 = H$, $R_2 = NO_2$

Ghosh and co-workers have utilised a 1,3,5-trimethyl-2,4,6-triaminobenzene scaffold, functionalised with three amide NH bond donor groups, to give receptors **21** and **22**. Solid state analysis was carried out with both the receptors and the TBA salts of acetate, chloride, fluoride and nitrate. Receptor **21** has been shown to effectively encapsulate, in a staggered dimeric capsule, hydrated acetate $[(AcO)_2(H_2O)_4]^{2-}$, hydrated fluoride $[F_2(H_2O)_6]^{2-}$, hydrated chloride $[Cl_2(H_2O)_4]^{2-}$, and two nitrate anions in the solid state. Receptor **22** only formed a dimeric capsule with hydrated fluoride $[F_2(H_2O)_6]^{2-}$. Monomeric units were formed with other anions. Although a 1:1 complex between anion and receptor was observed in the solid state, ^{1}H NMR Job plot experiments in DMSO-d_6 with TBA acetate indicated a 3:1 anion:receptor binding conformation in the solution state.[28,29]

In further extension of this work, Ghosh and co-workers went on to synthesise a bistripodal and amide-based receptor (**23**). In the solid state, when crystallised with TBA nitrate, receptor **23** shows a 4:1 anion:receptor complex (Figure 1.3.1.3). In the solution state, Job plot experiments show 3:1 binding conformation with nitrate. 4:1 stoichometries were seen with other anions such as dihydrogen phosphate and acetate in a DMSO-d_6 solution.[30]

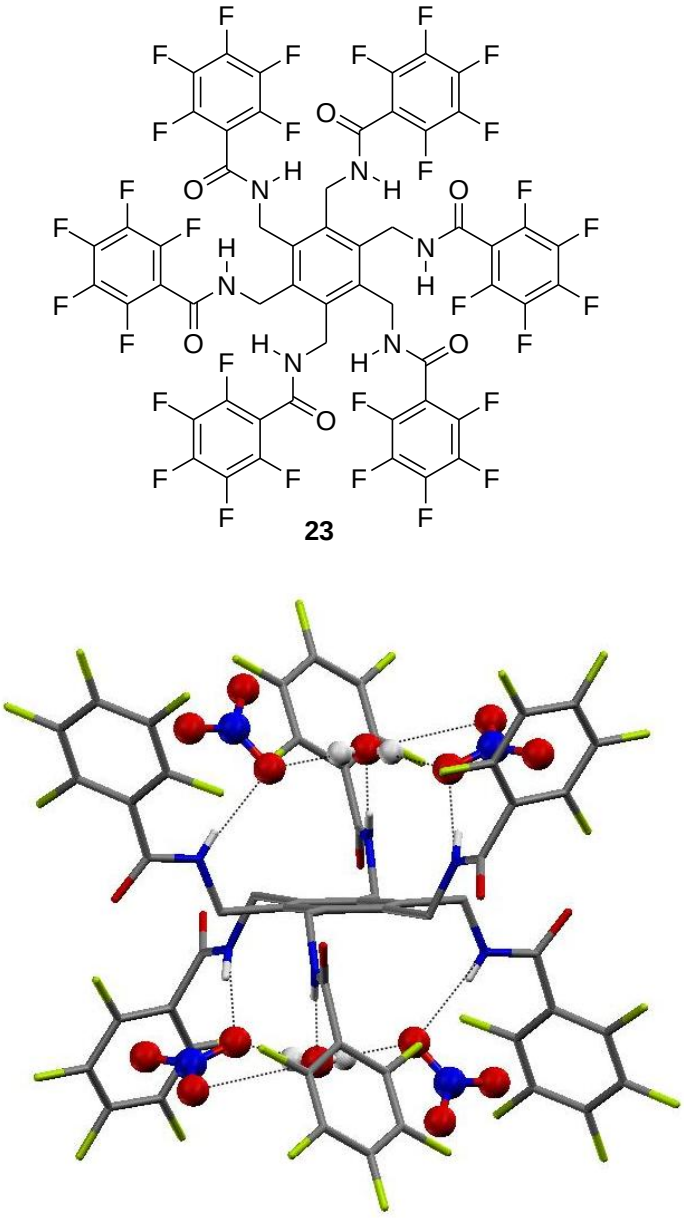

Figure 1.3.1.3 Ghosh and co-worker's bistripodal receptor **23**, complexed with four nitrate anions and two H_2O molecules.

Gong and co-workers used cyclohexane as a receptor scaffold. The use of the axial sites for the amide substituents allows convergence of the hydrogen bonding array, pre-organising the NH bond donor groups to coordinate with the anion. The original receptor (**24**) replaced the pyridinium ion with an anthracene substitution. This receptor (**25**) acts as a fluorescent chemosensor for dihydrogen phosphate over all the other TBA salts tested in 9:1 MeCN:MeOH, giving a 505 nm excimer emission when the sample was irradiated at 368 nm.[31]

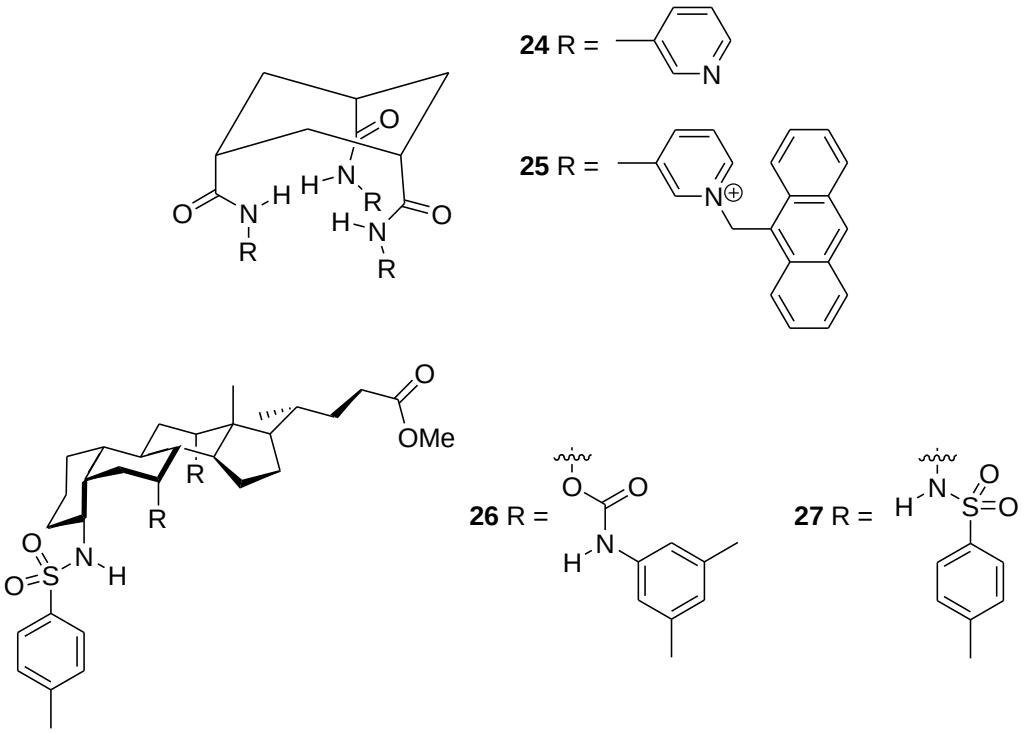

Groups of more complex anion receptors can be based on natural products such as steroids. Pandey and co-workers have produced macrocyclic anion receptors, based on deoxycholic acid.[32] Early examples by Davis and co-workers in 1997 used of cholic acid as an anion receptor scaffold and produced a group of receptors termed 'cholapods'. These acyclic receptors contain analogues of the amide functionality (sulfonamide in the case of receptor **26**, and sulfonamide biscarbonate in the case of receptor **27**) appended to the cholic acid scaffold. The sulfonamide functionalities are forced into a pre-organised convergent array by adopting the axial positions on the rigid cholic acid ring system. The binding constants for **26** and **27** were analysed using ^{1}H NMR titration studies in CD_3Cl. The relatively small, rigid binding site predisposed these receptors towards the smaller halide anions, showing selectivity for fluoride over the other halide and tosylate anions tested. Receptor **27** showed stronger anion binding than receptor **26** due to the increase in pre-organisation of the anion binding groups. The binding constant for fluoride and receptor **26** was 15400 M^{-1} while the binding constant for receptor **27** and fluoride was too large to be calculate by the methods used.[33]

The pinnacle of anion design today is the synthesis of macrocyclic receptors. These receptors are generally more efficient than acyclic receptors at binding anions as they form

more stable complexes with bound anions. This increase in thermodynamic stability is known as the macrocyclic effect. These more rigid structures can also cause an increase in the selectivity of anion binding as the cavity in the centre of the receptor can exclude anions that are too big or too small. The position of the hydrogen bond donating and accepting groups can favour the binding of different geometries of anion or shapes of molecule.

In 2001, Hamilton and Choi demonstrated the use of this macrocyclic effect with receptors **28-30**. The binding constants of these receptors to various anions were tested using ^{1}H NMR studies, with the majority of the results collected using a 2% DMSO-d_6/$CDCl_3$ solution and the TBA salts of the various anions. Compounds **28** and **29** were designed to bind tetrahedral oxo-anions. Job plot analysis found that these macrocycles had a 1:1 binding conformation with the tosylate anion through both the amide and the aryl protons. The central aryl protons contribute to the anion binding events, together with the amide protons, but the peripheral aryl protons outside of the central cavity did not contribute to the binding event. More complex and unusual binding conformations were observed with halide anions, nitrate, hydrogen sulfate and dihydrogen phosphate anions. At 0.0-0.5 equivalents of anion, a 1:2 anion:receptor sandwich complex was observed and this complex was stabilised by π- π stacking interactions. With increased equivalents of anion beyond this point, the usual 1:1 complex was observed. The authors suspect the receptors **28** and **29** have similar binding constants to a variety of anions and therefore different substitutions on the outside of the macrocycle have little effect on the overall binding of the anion to receptor. The strongest affinity between the anion and receptors was observed with the tetrahedral anions, nitrate and tosylate. Binding studies with dihydrogen phosphate and hydrogen sulfate exhibited slow exchange or the binding constants could not be determined due to complex binding events. The acyclic receptor **30** showed binding constants three orders of magnitude below that observed with the macrocyclic analogues (**28** and **29**)for various receptor anion combinations, confirming that the increase in anion affinity is due to the macrocyclic effect. [34,35]

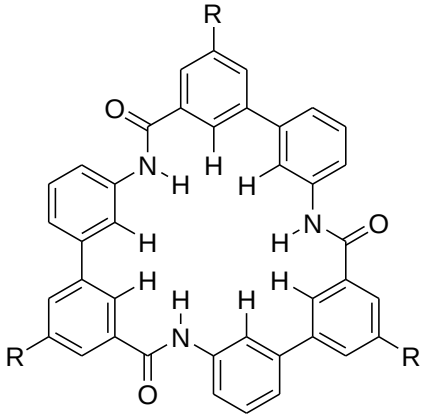

28 R = CO_2Et
29 R = NHBoc

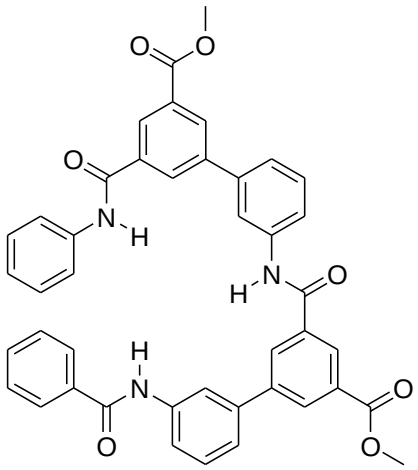

30

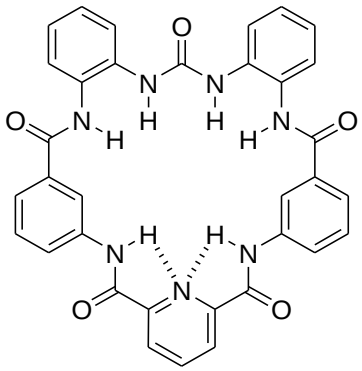

31

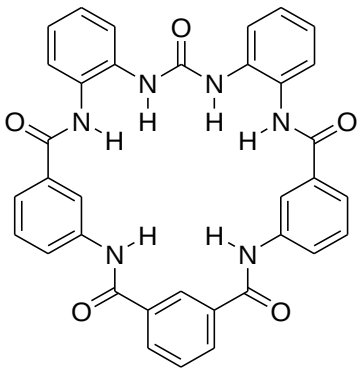

32

Gale and co-workers followed this work with macrocyclic receptors **31** and **32** that coordinate to anions though four amide NHs and two urea NHs. Binding constants were calculated by ^{1}H NMR titration studies using the TBA salt of the anion in 0.5% H_2O/ DMSO-d_6. Receptor **31** was shown to be selective for acetate over dihydrogen phosphate by two orders of magnitude. Receptor **32** was shown to have a lower affinity and selectivity for the oxo-anions and also exhibited low stability in H_2O/ DMSO-d_6 solutions. The increased stability of **31** is due to the intramolecular bonding between two of the amide groups and the nitrogen of the pyridine ring. This not only pre-organises the central cleft but also stops the macrocycle adopting a twisted conformation, as happens in the case of the isophthalamide group in receptor **32**. This helps to prevent amide hydrolysis in the H_2O/ DMSO-d_6 solution, allowing the receptor to remain stable. A range of acyclic analogues of **31** and **32** were synthesised but showed lower binding constants with anions

tested than receptor **31** and also a lack in selectivity between the different oxo-anions due to the loss of macrocyclic rigidity.[18]

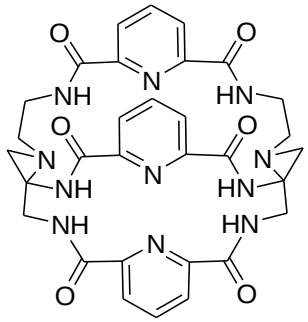

33

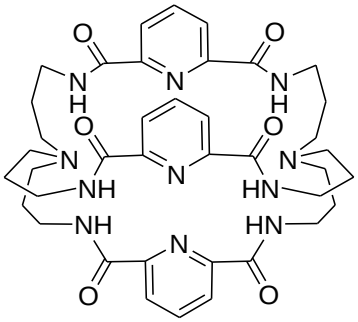

34

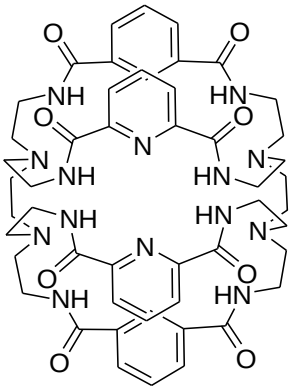

35

Bowman-James and co-workers took the macrocyclic receptor one step further, producing a set of three-dimensional, amido-cryptand receptors (**33-35**). These receptors are able to encapsulate an anion with three to four hydrogen bonding arrays. Binding constants were determined by ^{1}H NMR titration studies, using the TBA salt of the anion in a DMSO-d_6 solution. Receptors **33** and **34** are selective for fluoride, with binding constants > 10^5 M^{-1}. The cavity expansion from **33** and **34** causes a change in order of selectivity for the remaining anions tested. Receptor **33** binds chloride strongly, with a binding constant of 3000 M^{-1} when compared to receptor **34** (180 M^{-1}). However **34** binds hydrogen sulfate more strongly than **33**, with binding constants of 2700 M^{-1} and 68 M^{-1} respectively. Selectivity becomes based on size exclusion. Crystal structures of **34** with chloride (Figure 1.3.1.4a) and sulfate (Figure 1.3.1.4b) show two different binding stoichiometries, although both anions are bound within the amino-cryptand cleft and, in both cases, the tertiary amine sites on either end of the molecule become protonated because of the small amounts of HCl in the CH_3Cl used for crystallisation. Chloride is shown to bind in a 2:1 anion:receptor ratio, each anion being bound to the receptor by three NH bond donor groups and the OH group of a single bridging H_2O molecule. Sulfate is found to bind in a 1:1 binding stoichiometry through four NH bond donor groups and three OH groups of three bridging H_2O molecules. This complex exists as a dimer in the solid state due to π stacking interactions between the two receptors.[36]

By increasing the complexity of these cryptand receptors, a second generation amido-tricyclic cryptand receptor was synthesised. The binding constants were obtained under the same conditions as the studies carried out with **33** and **34** and the receptor **35** was found to be selective for bifluoride, with a binding constant of 5500 M^{-1}.[37]

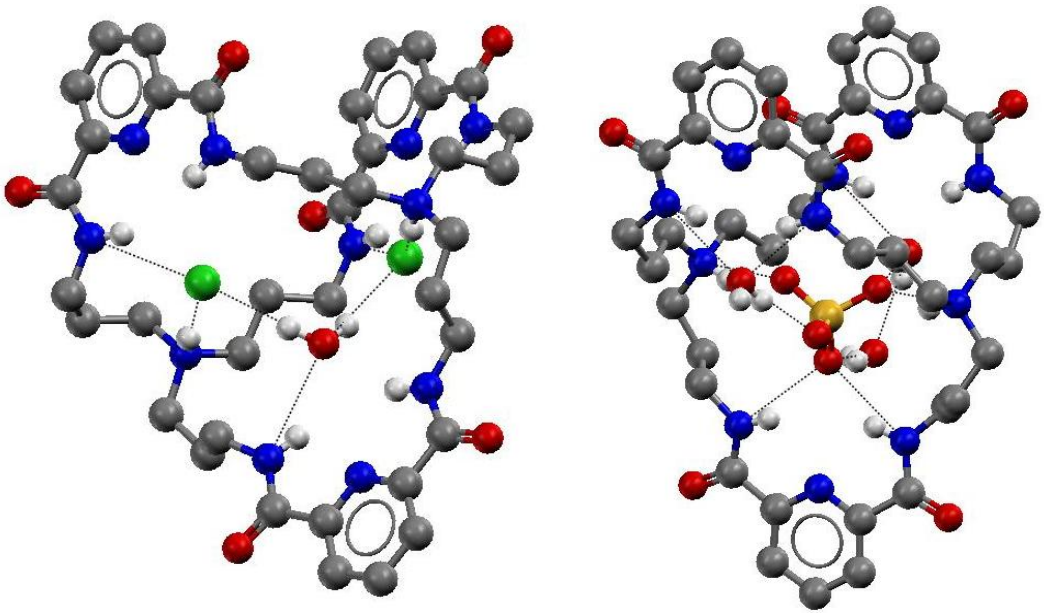

Left Figure 1.3.1.4a Bowman-James and co-worker's amido-cryptand based receptor **34**, complexed with two fluoride anions and a H_2O molecule. **Right Figure 1.3.1.4b** Bowman-James and co-worker's amido-cryptand based receptor **34**, complexed with a single hydrogen sulfate anion and three H_2O molecules.

Kubik and co-workers synthesised a hexapeptide macrocycle (**36**) that was able to bind anions in an aqueous environment. In a 80% D_2O/CD_3OD solution, a 1:1 complex was found with the sodium salt of benzosulfonic acid but 1:2 anion:receptor complexes were found with the sulfate and halide anions.[38] This led to the design of the molecular oyster **37**, which binds sulfate and halide anions in a 1:1 stoichiometry by sandwiching the anion between the two halves of the receptor. Binding studies carried out using both ITC and ^1H NMR studies in a 50 % D_2O/CD_3OD solution with the sodium salt of the anion at 298 K showed selectivity for sulfate. Binding constants for sulfate in this highly competitive environment were found to be (log K_a) 5.54 from the ^1H NMR and 4.55 from the ITC titration experiments.[39]

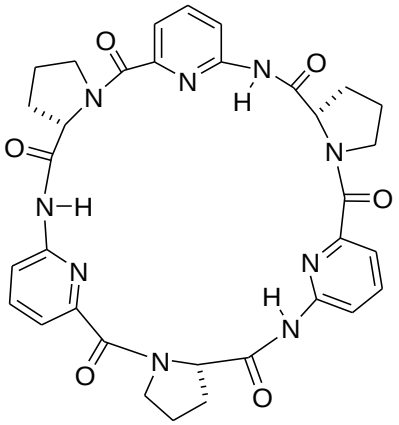

36

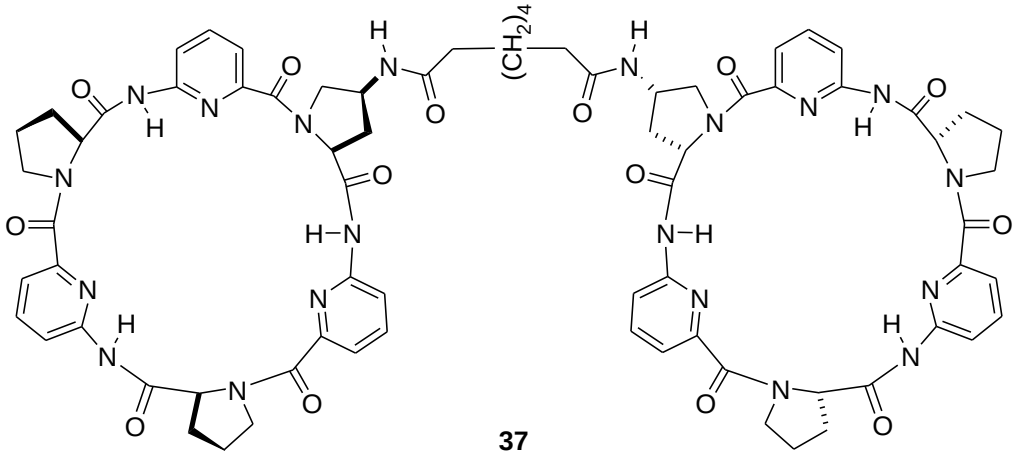

37

Similar to the rigid cholic acid scaffold utilised by Davis and co-workers [33], calix[4]arenes have been used to synthesise rigid anion receptors with high binding constants for a specific anion. The rigidity and ease of fictionalisation at four points around the macrocycle makes it a useful scaffold to suspend convergent hydrogen bonding arrays. The examples given by Ungaro and co-workers[40] and Beer and co-workers[41] utilise a strap from one side of the macrocyclic ring to the other that contains the hydrogen bonding array for binding anions. The strap also gives extra rigidity to the hydrogen binding array and helps pre-organise the binding cleft, thus increasing the affinity of the receptor for the anion.

Ungaro and co-workers synthesised receptors **38** and **39**. Binding constants were obtained by ^{1}H NMR titration in acetone-d_6 with the anions added as the TBA salts. These receptors are selective for carboxylate-based anions, with the highest binding constants observed for benzoate, followed by acetate, showing deviation from a TREN-based

receptor with a trend in binding according to basicity. Receptor **38** shows binding constants of 40100 M^{-1} and 10500 M^{-1} and receptor **39** shows binding constants of 44000 M^{-1} and 7100 M^{-1} for benzoate and acetate respectively. [40]

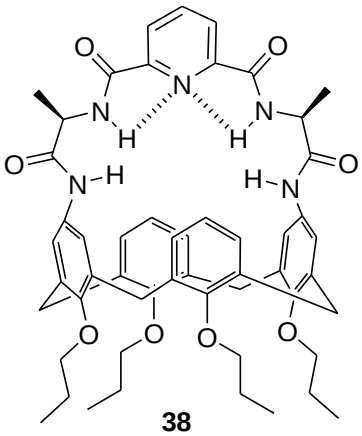

38

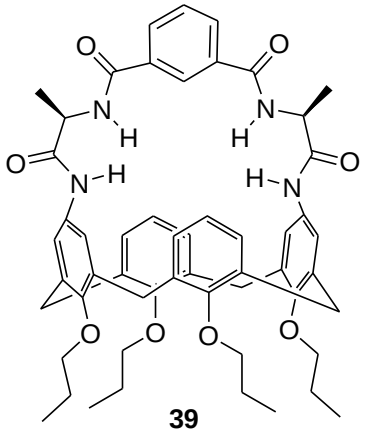

39

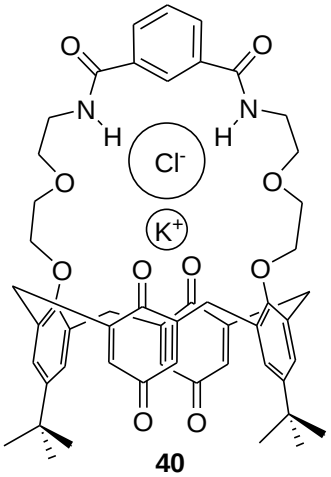

40

Beer and co-workers synthesised the first example of a neutral contact ion-pair receptor (**40**). The receptor binds the appropriate Group One metal (e.g. potassium) and the anion (e.g. chloride) from the ammonium salt as a contact ion pair. This ion pair binding is far stronger than is observed without the presence of the co-bound cationic guest. This receptor is able to act as an AND logic gate and is one of the first examples of the potential use of supramolecular chemistry in investigating operating systems in molecular computing.[41]

1.3.2 Urea and thiourea based receptors

Urea and thiourea functionalities contain two NH donor groups joined by single C=O/S group. Both these functionalities favour binding carboxylates (e.g. acetate or benzoate) but they can also be introduced to a larger, convergent hydrogen bonding array, tailored to bind larger oxo-anions such as dihydrogen phosphate. The predisposition for binding Y-shaped anions is because of the formation of hydrogen bonds with the optimum angle of 180°, as seen in Figure 1.3.2.1.

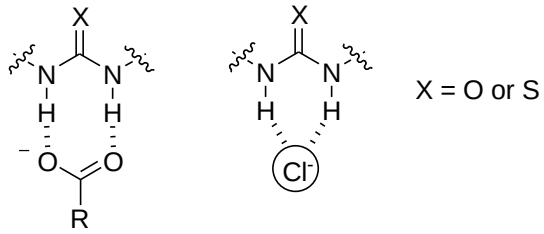

Figure 1.3.2.1 Formation of the optimum 180° hydrogen bond angle with the Y-shaped oxo-anions.

The main difference between the urea and the thiourea groups is the increased acidity of the thiourea NH groups. The larger sulfur atom accepts the partial negative charge created during the hydrogen bonding process more favourably than the oxygen atom due to the decreased charge density of the sulfur atom. Although the thiourea group is more acidic (and therefore should form hydrogen bonds more easily with anions then urea based receptors), other factors often perturb this so the efficiency of binding is not realised. Deprotonation of the hydrogen bonding array can occur with a sufficiently basic anion such as fluoride which forms the stable HF_2^- anion.[42] This anion can then be bound by the deprotonated receptor.[42-46]

The simple bis(4-nitrophenyl)urea receptor **41** was synthesised and studied for affinity various anions by Fabbrizzi and co-workers. Binding constants were determined by UV-Vis titrations in MeCN, using the TBA salt of the anion at 25 °C. This receptor shows a preference for oxo-anions, with the formation of a 1:1 complex. The strength of binding relies on the basicity of the oxo-anion. The more basic the anion, the more stable the hydrogen bonding complex and the higher the binding constant ($AcO^- > BzO^- > H_2PO_4^- > NO^{2-} > HSO_4^- > NO_3^-$). With fluoride in solution, there is formation of the HF_2^- anion. The first equivalent of fluoride binds to the receptor with a higher binding constant than that observed for acetate (log M^{-1} 6.61 and 7.38 for acetate and fluoride respectively). The second addition of fluoride induces the deprotonation of the urea group and formation of

the HF_2^- anion. Carbon dioxide introduced to the solution from the air then combines with H_2O and excess TBA cations to reprotonate the receptor and give $TBAHCO_3$, which binds to the reprotonated receptor to form a 1:1 receptor:bicarbonate complex. This was shown in the solid sate by the crystal structure, (Figure 1.3.2.2) produced by slow diffusion of TBAF and receptor **41** from MeCN and then THF in air.[47]

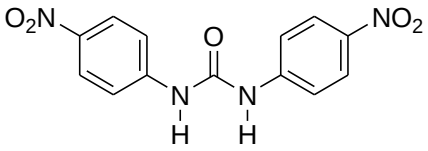

41

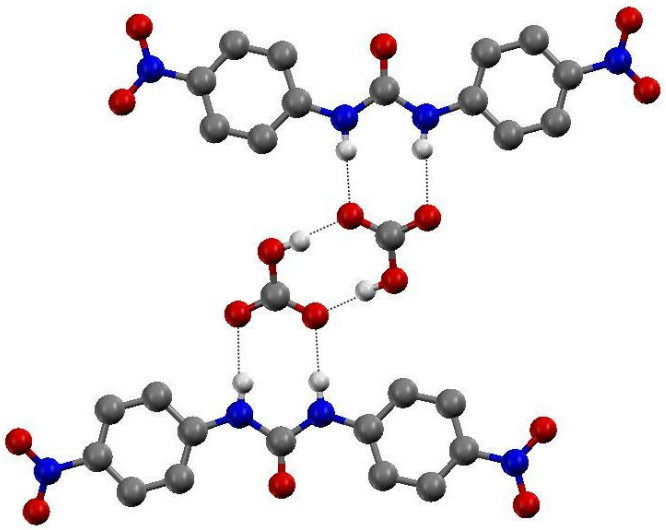

Figure 1.3.2.2 Complex with receptor **41** and bicarbonate crystallised by Fabbrizzi and co-workers from a solution containing TBA fluoride and receptor 41 open to the air.

Several acyclic, two-dimensional, fluorescent anion receptors have been synthesised using the urea/thiourea functionality to bind the anion. The hydrogen bonding arrays are attached to the fluorescent scaffold, which is commonly naphthalimide- or anthracene-based.

Receptors **42-45**, synthesised by Gunnlaugsson and co-workers, act as fluorescent photo-induced electron transfer (PET) chemosensors. The thiourea group binds the anion whilst the anthracene fluorophore causes these receptors to act as chemosensors. Information collected from ^{1}H NMR studies in DMSO-d_6 shows that both thiourea NH groups are involved in binding anions, forming a 1:1 complex. Florescence emission was

quenched upon the addition of fluoride, acetate and dihydrogen phosphate anions but chloride and bromide anions had no effect. The variations in the R groups were used to tune the acidity of the thiourea NH groups to alter the sensitivity of anion recognition. [48,49]

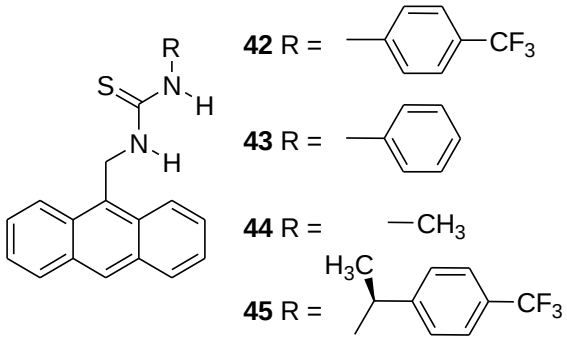

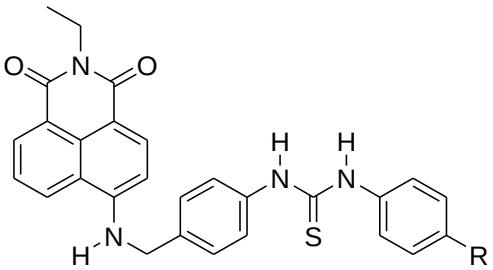

46 R = H
47 R = CF_3

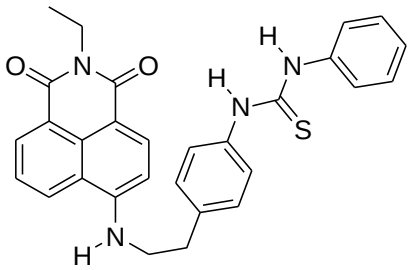

48

Gunnlaugsson and Pfeffer went on to synthesise further PET chemosensors, based on the thiourea unit but replacing the anthracene with a naphthalimide fluorophore. As before, these receptors were found to form 1:1 complexes with anions under the same conditions previously mentioned. Receptors **46** and **47** show similar properties to the receptors containing the anthracene moiety, sensing fluoride and acetate anions. However, in the case of receptor **48**, the addition of the naphthalimide NH coordinates to the phosphate anion along with the thiourea NHs. This increases the affinity of this receptor for the anion over receptors **46** and **47**. [50-52]

Naphthalimide scaffold receptors by Kondo and co-workers include a symmetrical cleft receptor (**49**), containing two thiourea groups. This receptor is more effective at binding anions than the single thiourea-containing, linear receptor **50**, both in affinity and selectivity. Binding constants were obtained by UV-Vis spectroscopy in MeCN with the order of selectivity as follows: $F^- > AcO^- > H_2PO_4^- > Cl^-$, showing a trend based on

basicity of the anion. Binding constants of 2.1 x 10^6 M^{-1} and 7.7 x 10^3 M^{-1} were obtained for fluoride and 1.1 x 10^5 M^{-1} and 3.7 x 10^3 M^{-1} for acetate for compounds **49** and **50** respectively. [53]

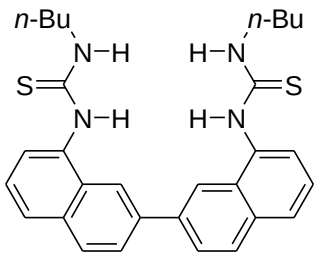

49

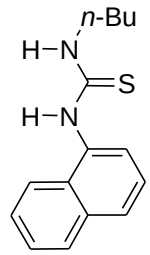

50

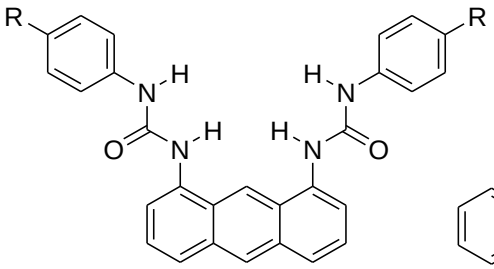

51 R = NO_2
52 R = H

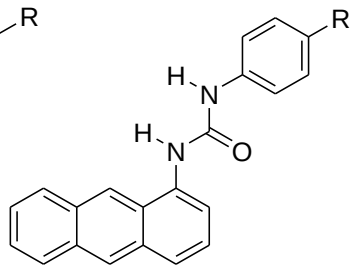

53 R = NO_2
54 R = H

Yoon and co-workers exchanged the thiourea group for a urea group and, as Kondo and co-workers [53], synthesised symmetrical binding clefts (**51-52**) with two urea groups, as well as linear receptors **53-54** with just a single urea group. ^{1}H NMR studies showed that strong hydrogen bonds were formed with both pyrophosphate and fluoride anions in the cases of receptors **51-52** in a DMSO-d_6 solution. The rigid scaffold provided by the anthracene moiety with the symmetrical cleft receptors introduces selectivity in binding. Receptor **51** was shown to act as a colorimetric sensor and receptor **52** to act as a fluorescent chemosensor for the detection of fluoride in DMSO.[54,55]

Urea-containing receptor **55**, synthesised by Pischel and co-workers, can not only sense anions but also to sense pH due to the fluorescent naphthalimide-based group (red). The tertiary amino group (green), when unprotonated, allows fluorescence quenching by PET. When this site is protonated, the fluorescence is not quenched as PET is inactive. The second site on the receptor (blue) is a urea group and, upon binding to anions such as acetate, PET is active as the site becomes electron-rich and therefore fluorescence is quenched. This quenching occurs even if the tertiary amino group is protonated. The

anions can now hydrogen-bond to the urea NHs and to the protonated amino site by a combination of electrostatic interactions. Reducing the effect of the positive charge activates PET. The combination of responses to these binding events makes this a molecular INH logic gate (a two input inhibit gate).[56]

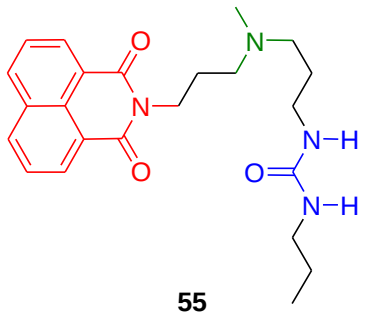

55

Pfeffer and co-workers have made the structures of their thiourea-containing receptors **56** and **57** more rigid with a [3]polynorborane framework to increase the efficiency and selectivity of anion binding. The receptor's cleft is far larger than those previously described by Kondo[53] and Yoon[54,55]. This predisposes these receptors to bind larger anions that can coordinate to both sides of the receptor's cleft. Binding constants and stoichometries were determined by ^{1}H NMR studies in DMSO-d_6 with the TBA salt of the anion. Acetate was found to form a 2:1 anion:receptor complex, each anion being bound by two hydrogen bonds. Dihydrogen phosphate formed a 1:1 complex, each anion being bound by four hydrogen bonds. The larger dihydrogen pyrophosphate anion formed a 1:2 anion:receptor self-assembled sandwich complex, each anion being bound by eight hydrogen bonds. Titrations with fluoride and receptor **57** produced a colorimetric change from yellow through to red with five equivalents of the anion due to the hydrogen bonding interactions and subsequent deprotonation of the receptor to form the HF_2^- anion.[57]

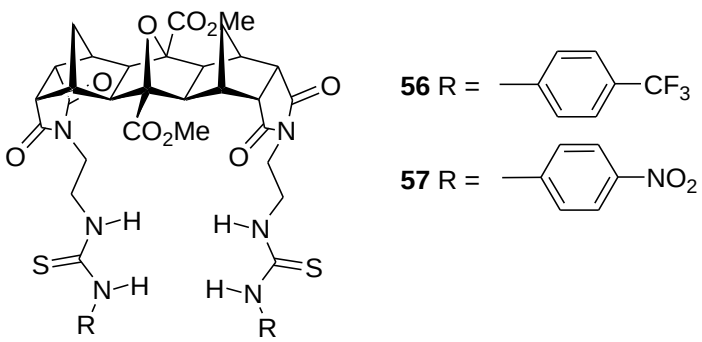

56 R = CF_3

57 R = NO_2

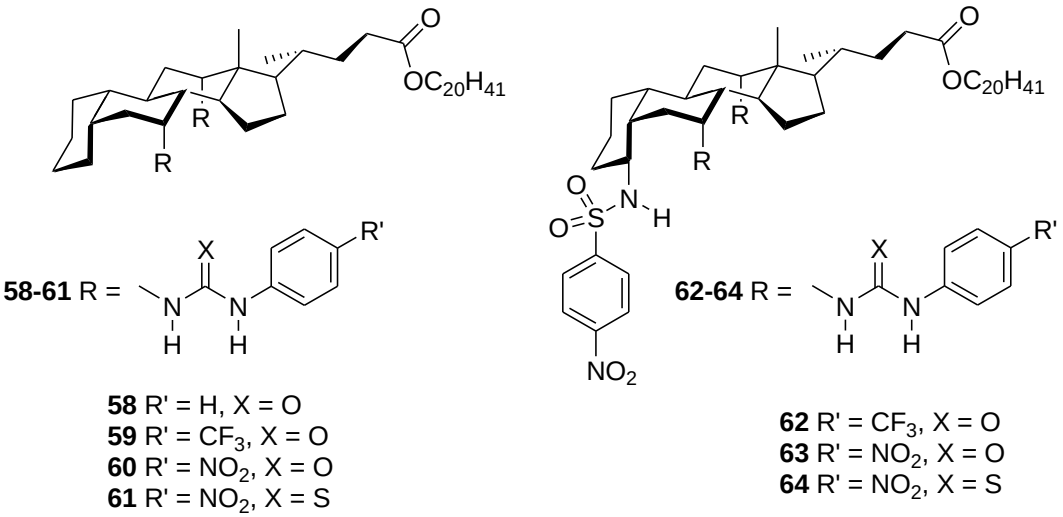

58 R' = H, X = O
59 R' = CF_3, X = O
60 R' = NO_2, X = O
61 R' = NO_2, X = S

62 R' = CF_3, X = O
63 R' = NO_2, X = O
64 R' = NO_2, X = S

Following on from previous work using the 'cholapod' scaffold to synthesise anion receptors based around the amide functionality, Davis and co-workers have synthesised a library of urea/thiourea based receptors (**58-64**). Binding stoichiometry was determined by ^{1}H NMR studies in $CDCl_3$ and was found to be predominantly 1:1, using the TEA salts of chloride and bromide. As the binding constants were found to be very high in this medium, they were determined by Cram's extraction method in H_2O-saturated $CHCl_3$ at 30 °C. The receptors were found to have greater affinity for chloride than bromide. The general increase in binding constant values from receptors **58-61** to receptors **62-64** can be attributed the additional nitrosulfonamide group. The more subtle increases in binding constant values observed within each general structure for receptors **58** to **60** and **62** to **63** is due to the increase in electron-withdrawing effects which occur when a different group is situated in the molecule, causing an increase in the acidity of the NH groups. The receptor with the least electron-withdrawing substituent has the lowest binding constants. The effect of the electron-withdrawing groups on the acidity of the NH bond donor groups are as follows; R = H<CF_3<NO_2. The interchange of the urea group for the more acidic thiourea group (receptors **62** and **64**) also increases the acidity of the NH bond donor groups, thus increasing the affinity of the receptor for the anion. The general trend observed here is the more acidic the NH group, the higher the binding affinity.[58]

This basic library was then expanded to incorporate more cholapod-based receptors that contain an increased number of NH bond donor groups. The effects of binding affinity with various anions for each receptor with varying, greater numbers of hydrogen bond

donor groups could then be further tested. A total of seven anions, including oxo and halide, were tested with receptors **58-65**. Receptor **65** was found to have the highest affinity with all the anions tested apart from acetate, where receptors **63** and **64** exhibited higher binding constants. Receptor **65** contains the highest number of NH bond groups in the form of three nitrophenyl-appended thiourea groups and produces the most acidic NH groups out of all those receptors tested.[59]

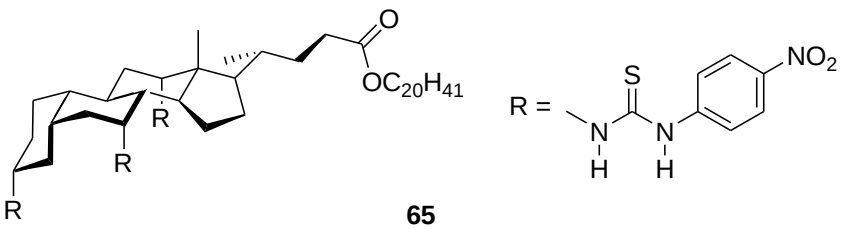

65

These cholapods have also been studied for potential anion transport across a lipid bilayer. They have been shown to transport chloride across vesicle and cell membranes. The steroidal-based scaffold, together with the alkyl chain, aids the receptor's movement across the membrane. These molecules therefore have potential in the medical field as a starting point to develop potential treatments for diseases such as cystic fibrosis by enabling anion transport across cell membranes.[60]

Gale and co-workers used the simple ortho-phenylenediamine unit as a symmetrical base unit from which to suspend NH bond donor groups, giving receptors **66-68**. The variations in hydrogen-bond donor groups change the receptor's affinity, efficiency and selectivity in anion binding. Binding constants were obtained by ^{1}H NMR titration in a DMSO-d_6/H_2O 0.5 % solution using the TBA salt of the anion. A range of oxo and halide anions were tested and all formed 1:1 complexes with the receptors. Receptors **66** and **67** showed similar binding activity and preference towards the different anions. A slight preference for binding dihydrogen phosphate over acetate was observed, with binding constants of 149 M^{-1}, 295 M^{-1} and 98 M^{-1}, 251 M^{-1} for receptors **66** and **67** respectively. This trend was reversed with receptor **68**, when binding constants of 3210 M^{-1} and 732 M^{-1} were observed for acetate and dihydrogen phosphate respectively. These binding constants are far higher than those observed for receptors **66** and **67**, showing how effectively the urea functionality binds carbonate-based anions compared with amide-based cleft receptors.[61,62]

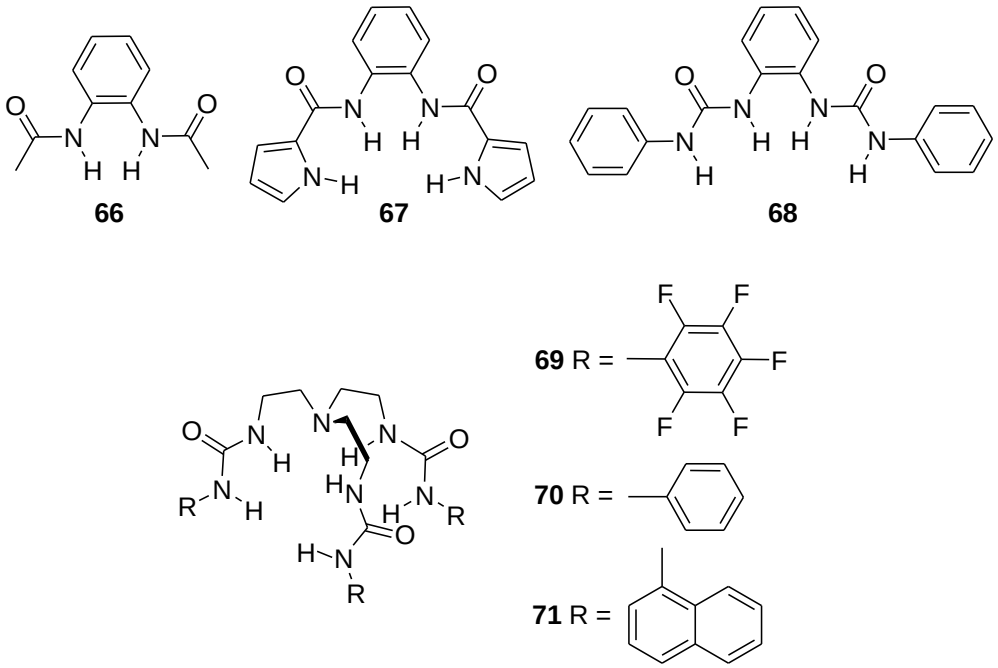

Ghosh and co-workers took urea-incorporated receptor design into the third dimension by using the TREN-based scaffold to suspend the urea functionalities. Binding studies were carried out *via* ^{1}H NMR titrations and DMSO-d_6 with receptors **69** and **70** and by fluorescence methods with receptor **71** because of the anthracene moiety. TBA salts of dihydrogen phosphate, acetate, nitrate and perchlorate anions were titrated with **69-71**. Selectivity was shown for dihydrogen phosphate with all three receptors. Binding constants of (log K) 5.52 M^{-1}, 4.04 M^{-1} and 4.60 M^{-1} were obtained for receptors **69**, **70** and **71** respectively with dihydrogen phosphate. The higher binding constant observed with **69** can be explained by the increased acidity of the NH bond donor groups due to the electron-withdrawing effects of the $–C_6F_5$ moieties. Receptor **69** is also able to dimerise to form a pseudo-dimeric cage in the solid state, encapsulating a dihydrogen phosphate dimer, as shown in Figure 1.3.2.3. The cage is held together by π-π stacking interactions and the dihydrogen phosphate is bound in the centre of the cage by hydrogen bonds between the receptor and the anions themselves.[63]

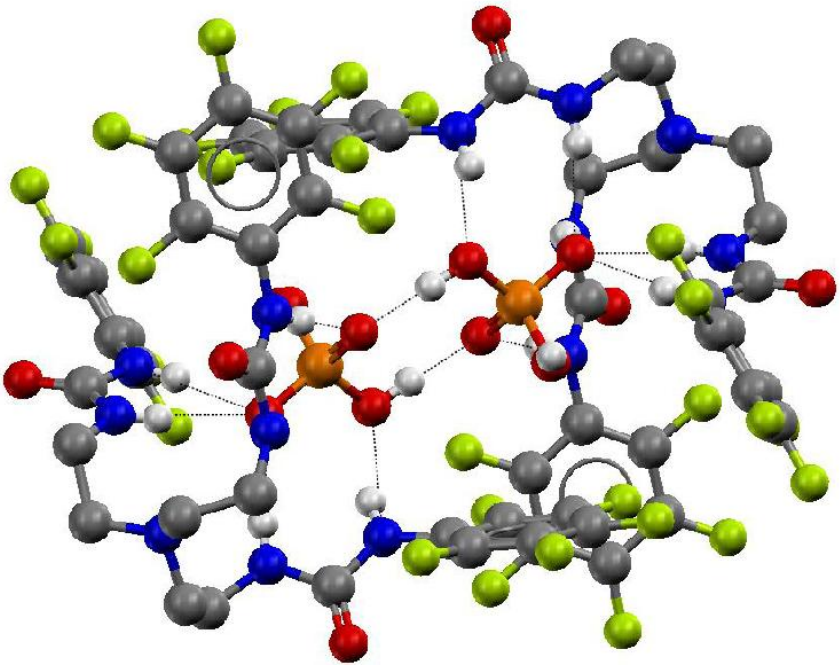

Figure 1.3.2.3 2:2 Anion:receptor complex with **69** and dihydrogen phosphate crystallised by Ghosh and co-workers from a solution containing TBA dihydrogen phosphate and receptor **69**.

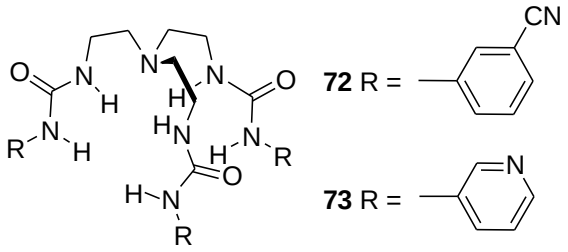

A second group of urea-functionalised TREN receptors (**72** and **73**) were synthesised by Moyer and co-workers. Unlike previous examples, these molecules were incorporated into a metal-organic framework. Crystal structures obtained from acetone/H_2O solutions show that receptor **72** forms a 2:1 receptor:anion complex with the silver sulfate salt. The crystal structure of this complex is shown in Figure 1.3.2.4. The sulfate anion is shown as a space filling model, illustrating how well this anion fits into the cavity created by the two receptors. Each anion is bound through twelve hydrogen bonds supplied by the six urea functionalities (N···O 2.85-3.11 Å) with bond angles between N-H···O of 124°-170°. Each complex is held together in a one-dimensional coordination polymer by interactions with two silver cations. Crystallisations were attempted with other silver salts but only crystals of the free ligand could be obtained. ^{1}H NMR studies in

acetone-d_6 with the silver salt of the anions indicated that sulfate gave by far the strongest interaction with receptor **72**. This may explain why the anion/receptor complexes were difficult to obtain. Attempted crystallisation with TMA sulfate was unproductive, which proved that the presence of the silver cation was crucial to complex formation.[64]

The introduction of the pyridine group in receptor **73** allows the formation of more rigid crystalline structures that are less soluble and more stable in aqueous solutions. This shows increased selectivity and efficacy for sulfate binding in more aqueous solutions because of the increased strength of bond between the metal centres and the pyridine groups. Crystals structures produced with cobalt, zinc, cadmium and magnesium sulfate salts from a 1:1 MeOH/H_2O solution all gave similar metal-organic frameworks from 2:1 receptor:anion complexs. Attempts to crystallise this receptor with other anion/cation combinations under the same conditions did not yield any crystals. Selective crystallisation of sulfate from a competitive mixture of anions was achieved.[65]

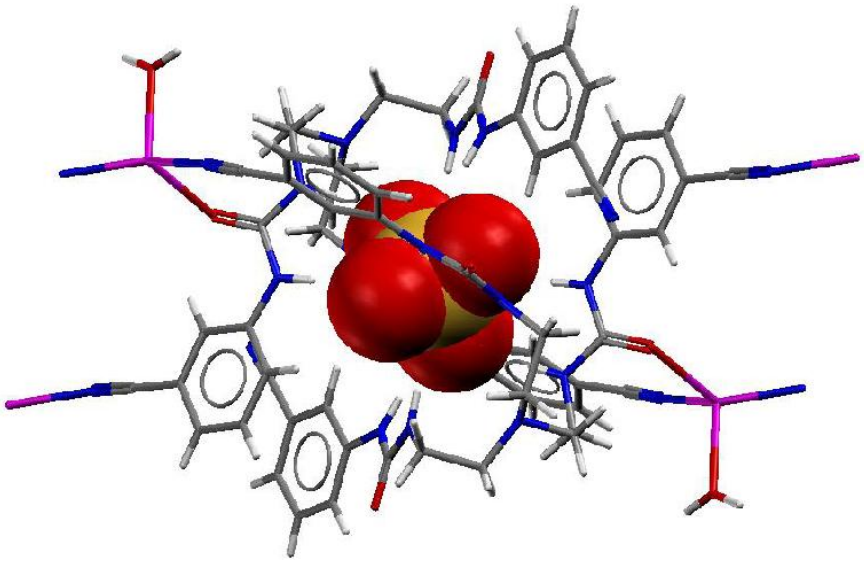

Figure 1.3.2.4 2:1 Receptor:anion complex with **72** and sulfate crystallised by Ghosh and co-workers from a solution containing silver sulfate and receptor **72**.

McDevitt, Anslyn and co-workers used the less flexible pin-wheel core as a tripodal scaffold from which to suspend different binding groups. Receptor **74** shows the general structure of the receptor with R_1, R_2 and R_3 representing the different side chains of the random amino acid moieties. The different combinations of R groups produces a combinatorial library of receptors. Thirty beads from this combinatorial library were chosen at random and incorporated into a micro-machined, chip-based array. An ionic

chromophore such as fluorescein was then introduced into the receptors. Some of the receptors bound the chromophore with a high affinity, while others do not bind the chromophore at all. When introduced to an aqueous solution of various nucleotide phosphates, the chromophore was displaced and/or the nucleotide phosphates was bound to the receptor. This happened at different rates depending on the receptor analogues. The different phosphates were bound by different degrees, depending upon the affinity of the receptor for the phosphate group. This process was monitored by a charge-coupled device recording the red(R), green(G) and blue(B) intensity of each bead over a period of time. This created diagnostic patterns for ATP (adenosine triphosphate) and GTP (guanosine triphosphate) through the combinatorial library of sensors and indicator-displacement assays in an aqueous solution.[66]

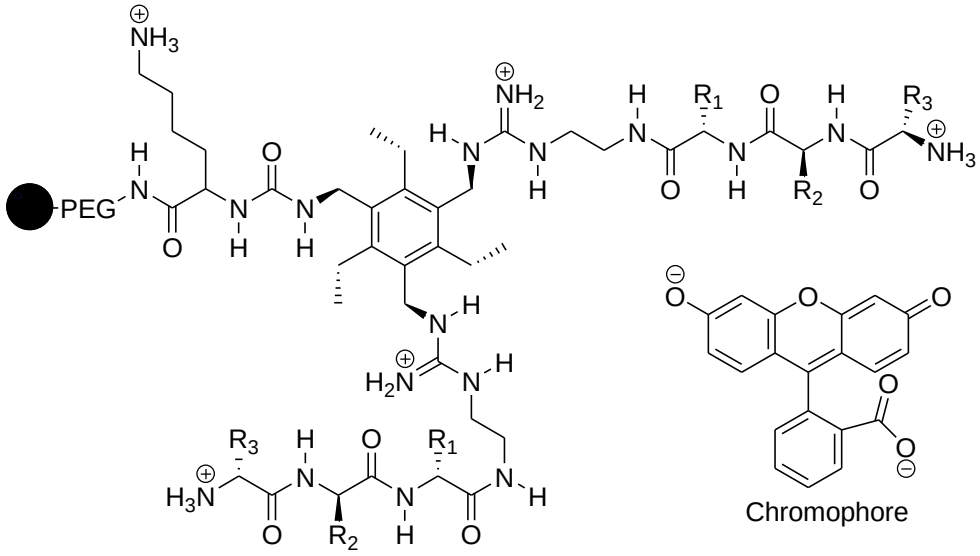

74

The calixarene-based receptor, **75**, synthesised by Fukazawa and co-workers, exhibits shape-selective dicarboxylate recognition. This receptor's hydrogen-bonding array contains four NH bond donor groups from two urea moieties. Binding constants were obtained from ^{1}H NMR studies in DMSO-d_6 using the TBA salt of the anion. Job plot experiments showed the 1:1 binding stoichiometry in this environment. All the dicarboxylate salts studied showed higher binding constants than the benzoate anion. This shows selective recognition for the dicarboxylate anions. In general, the *m*-phenyl biscarboxylates were bound with higher affinity, followed by *o*-phenyl biscarboxylates, with the lowest binding constants observed with the *p*-phenyl biscarboxylate anions. This

selectivity for the *m*-anions occurs because these anions form the optimal hydrogen-bonding angle and thus the strongest hydrogen bonds.[67]

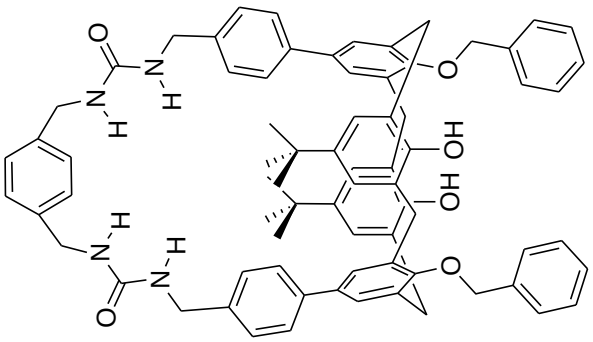

75

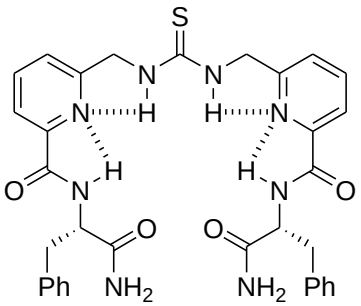

76

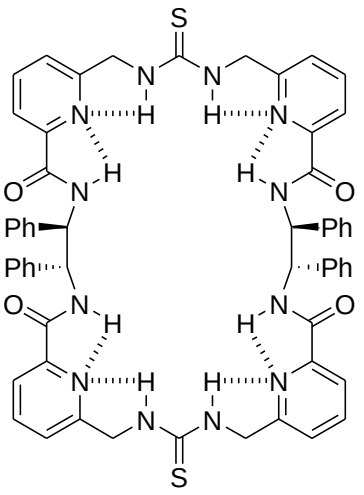

77

Refining work on shape-selective binding, Kilburn and co-workers synthesised acyclic (**76**) and macrocyclic (**77**) chiral receptors, capable of the enantioselective binding of amino acids. As seen in previously discussed examples, the pyridine-based scaffold is able to rigidify and pre-organise the structure of the receptor by intramolecular hydrogen bond formation. The intramolecular bond formation holds the NH bond donor groups directionally towards the centre of the hydrogen bonding cavity. ^{1}H NMR titration and studies were carried out in $CDCl_3$ with both enantiomers of Boc-protected amino acids, isolated as their TBA salts. Both receptors were found to form 1:1 complexes with the amino acid enantiomers. Due to the macrocyclic effects, receptor **77** was found to be far more enantiomerically selective than **76**, which only exhibited moderate selectivity. Binding events were also found to be dependent on the solvent in which the binding

studies were carried out. In a less polar $CDCl_3$ solution, the intramolecular hydrogen bonds were too strong to allow binding of N-boc-glutamate. However, in more polar solvents such as MeCN or DMSO, the intramolecular forces were weakened. Both ^{1}H NMR and calorimetry experiments showed selective binding of the N-boc-L-glutamate enantiomer over other amino acid enantiomers tested.[68,69]

Lee and Hong synthesised macrocyclic receptors **78** and **79**, with three thiourea groups. With this design, the receptor **79** was using the steric effects of the ethyl-R groups on the phenyl rings to increase the rigidity of the structure. Binding studies were carried out using ^{1}H NMR techniques and TBA salts of the anions in a DMSO-d_6 solution. Job plots were used to establish a 1:1 binding stoichiometry. Receptor **79** demonstrated higher binding constants in general and showed selectivity for acetate over other anions tested, with binding constants of 5300 M^{-1} and 1600 M^{-1} for acetate and dihydrogen phosphate respectively. The more flexible receptor **78**, although exhibiting lower binding constants overall, did show a change in selectivity to dihydrogen phosphate as the binding constants for dihydrogen phosphate and acetate were 800 M^{-1} and 320 M^{-1} respectively. This illustrates an alteration in the selectivity following increasing basicity of the anion.[70]

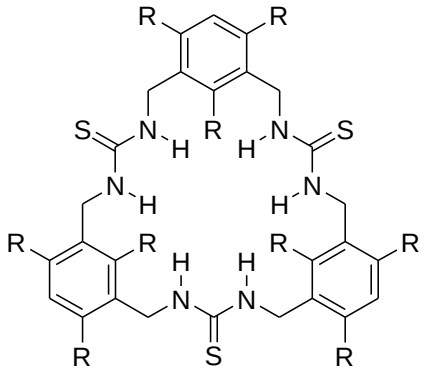

78 R = H
79 R = Et

A new approach to receptor design was taken by Meshcheryakov and co-workers. Instead of the traditional route of synthesis followed by investigation into the binding properties of the new receptor, receptor **80** was designed with the aid of molecular modelling techniques to optimise selectivity for the nitrate anion. Receptor **80** was designed with some similarities to **78** and **79**[70], containing three urea moieties linked by aromatic spacer groups.[71]

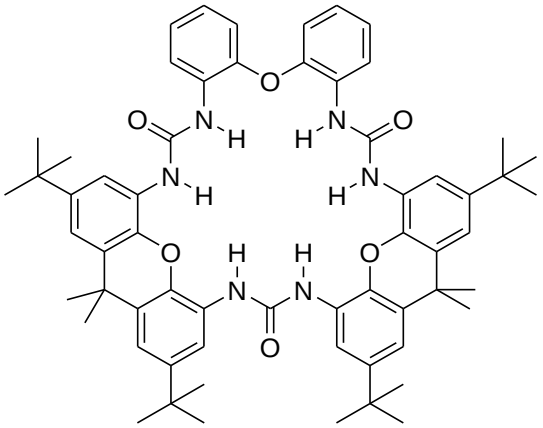

80

Reinhoudt and co-workers synthesised a variety of cleft (**81-84**) and macrocyclic receptors (**85-86**) containing a total of four urea/thiourea groups, giving eight NH hydrogen-donating bonds. Binding constants were obtained by ^{1}H NMR titrations in a DMSO-d_6 solution with the TBA salt of the anion. Binding stoichiometry was determined by Job plot analysis. The macrocyclic receptors **85-86** showed a 1:1 binding stoichiometry with all anions tested. Selectivity was shown with dihydrogen phosphate (binding constants approximately 10^3 M^{-1}) compared with other anions and chloride (binding constants of around 10 M^{-1}). The acyclic receptors **81-84** showed more complex binding stoichiometries. Dihydrogen phosphate was found to bind in a 2:1 anion:receptor complex with binding constants in the region of 10^7 M^{-2}, whereas chloride exhibited a 1:1 binding conformation with binding constants in the region of 10^3 M^{-1}.[72]

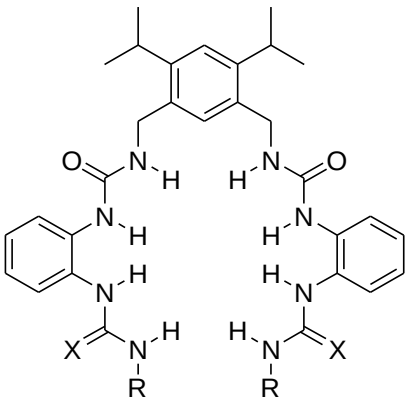

81 R = C_3H_7, X = O
82 R = Ph, X = O
83 O, R = SO_2Ph, X = O
84 R = Ph, X = S

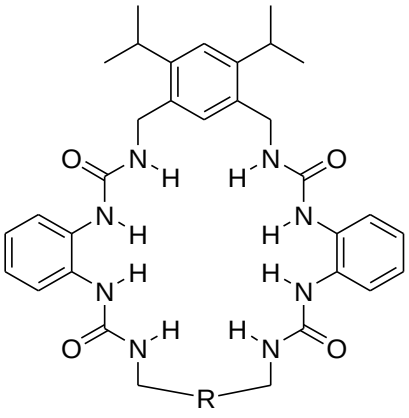

85 R = Ph
86 R = CH_2CH_2

A group of tripodal/cryptand based receptors, **87-91** were synthesised by Tobe and co-workers. These receptors incorporate three thiourea functionalities, giving six hydrogen-bond donor groups. Binding constants were determined by ^{1}H NMR studies in CD_2Cl_2 at 373 K but, because of problems experienced with peak broadening and slow exchange, binding stoichiometries were determined by Job plot. A 1:1 binding stoichiometry was observed with both receptors **87** and **88** but the steric hindrance of the various aromatic substituents and the entropic cost of cooperative binding impeded the binding event, producing smaller binding constants than were expected. Receptor **89** showed more complex binding events. A 1:1 binding complex was observed with the halide anions whereas a 2:1 anion:receptor complex was observed with acetate and dihydrogen phosphate. This change in binding stoichiometry is due to the increased binding ability of this receptor over receptors **87** and **88** as steric hindrance is overcome. The cryptand-based receptors **90** and **91** all show 1:1 binding stoichometries. The strong intramolecular hydrogen bonding between the thiourea groups in receptor **91** explains why the binding constants for this receptor and acetate, chloride and fluoride anions are so much smaller than those for receptor **87**. Binding constants of 116 M^{-1} and 3030 M^{-1} were obtained for acetate with receptors **91** and **87** respectively.[73]

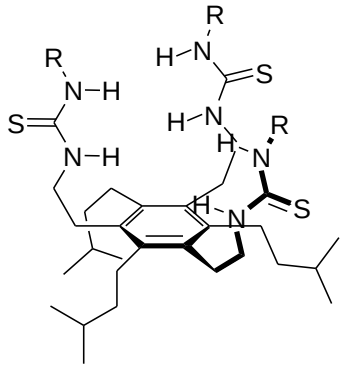

87 R = *n*Bu
88 R = Bn
89 R = Ph

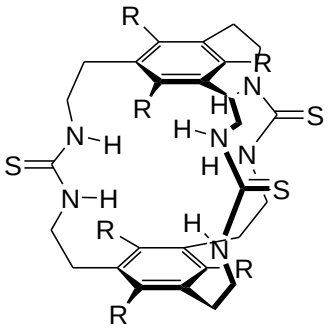

90 R = Me
91 R = $(CH_2)_2CH(CH_3)_2$

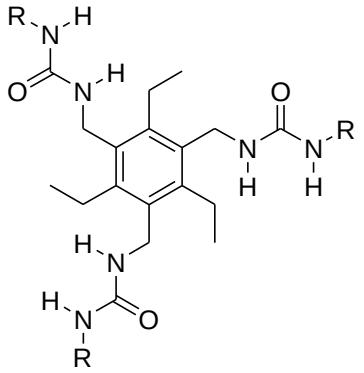

92 R = *tert* - octyl

Roelens and co-workers produced a set of simple 1,3,5-substituted 2,4,6-triethylbenzene (pin-wheel) based receptors with three simple urea groups. Receptor **92** shows binding affinity with monosaccharides. Binding constants (K_1) were obtained by ^1H NMR titration in $CDCl_3$ and calculated to be in the mid to high hundreds, with a slight preference shown for β-galactose. This receptor shows different affinities for the α and β enantiomers of the different monosaccharides. A three-constant equilibrium model was established to calculate appropriate binding constants for the interactions of this receptor with various monosaccharides, including 1:1, 2:1 receptor:anion interactions alongside receptor dimerisation.[74]

1.3.3 Aromatic NH based receptors

The introduction of aromatic NH bond donor groups into the design of anion receptors is a relatively recent idea. The amide, urea and thiourea groups can have poor solubility in organic solvents and also contain a hydrogen-acceptor group. This can lead to intra- or intermolecular bond formation that can impede anion binding, producing less effective anion receptors. Replacing these groups with pyrrole, indole or carbazole substituents prevents self-association and improves solubility in organic solvents. These groups also allow acidity of the NH bond donor group to be controlled, (Figure 1.3.4.1) and therefore allows control of some hydrogen bond formation properties between the receptor and prospective anion.[75,76]

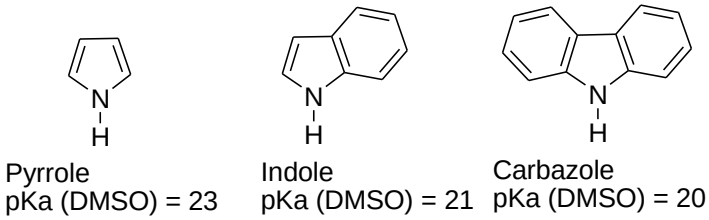

Figure 1.3.4.1 Illustration of the increasing acidity of different aromatic NH hydrogen bond donor groups in DMSO.

1.3.4.1 Pyrrole based receptors

Since the first introduction of the pyrrole group into the scaffold of anion binding receptors, many research groups have taken an interest in this functionality.[77,78]. The first example of a simple anion–pyrrole complex, reported in 2001, was crystallised from a solution pyrrole of TMA chloride by Gale and co-workers and can be seen in Figure 1.3.4.1.1.[79]

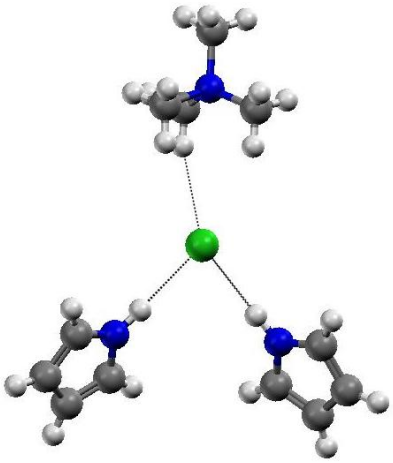

Figure 1.3.4.1.1 Crystal structure of pyrrole hydrogen bonded to chloride. This crystal structure was obtained from a solution of pyrrole and TMA chloride by Gale and co-workers.

Gale and co-workers went on to synthesise many acyclic cleft receptors, utilizing the pyrrole moiety. The first of these was based on 2,5-dicarboxamidpyrroles. This series of molecules consisted of eight different analogues, receptors **93-100**. The first four of these analogues to be synthesised compared the binding abilities of two and three hydrogen donating arrays of the symmetrical and asymmetric receptors. Binding studies were carried out by ^{1}H NMR titration using the TBA salt of the anion with compounds **93**, **95** and **96**. Unfortunately no information could be generated for **94** due to precipitation and

crystallisation issues. Receptors **93** and **95** were dissolved in CD_3CN, while titrations with compound **96** were carried out in a DMSO-d_6/H_2O 0.5 % solution due to solubility issues. Job plot analysis showed that all three receptors formed 1:1 complexes with the different anions. Only receptors **93** and **95** could be directly compared due to the solubility issues. These two receptors showed selectivity for benzoate, with binding constants of 202 M^{-1} and 2500 M^{-1} for **93** and **95** respectively. However, this was the only similarity in the binding trends. Receptor **95** showed selectivity of at least one order of magnitude over the other anions but **93** only showed selectivity by approximately 50 M^{-1}. Receptor **96** showed selectivity for dihydrogen phosphate (1450 M^{-1}), a selectivity of at least one order of magnitude over the other anions tested.[80,81]

The cleft design was then improved by incorporating electronegative chloro groups into the central pyrrole unit, increasing the acidity of the NH donor groups (receptors **97-100**). Proton NMR studies were carried out with receptors **97** and **98** in a variety of different deuterated solvents. These studies revealed the deprotonation of the central pyrrole group, producing the pyrrolate anion with several basic anions. This effect was most noticeable with the most basic anion (fluoride) in CD_2Cl_2. These pyrrolate anions self-assemble in solution and in the solid state to form dimers, held together by four hydrogen bonds between the amide and pyrrolate groups.[45] This process of spontaneous self-assembly was further explored with the synthesis of **99** and **100**, which, when deprotonated to give the dipyrrolate anions, formed chains of hydrogen-bonded molecules, each molecule bridging from one to the next.[82]

The last two receptors in this series (**101** and **102**) have nitro functionalities on the phenyl rings to increase the acidity of the hydrogen-bond donating group, increasing the affinity towards the anion. Proton NMR titration studies were carried out in CD_3CN and, in most cases, the binding affinities of these receptors were found to be enhanced when compared to others in the series. Deprotonation of receptor **102** was still observed with fluoride, causing a light yellow to blue colour change.[44]

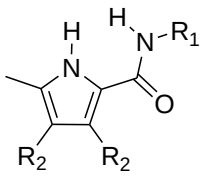

93 R_1 = n-Bu, R_2 = Ph
94 R_1 = R_2 = Ph

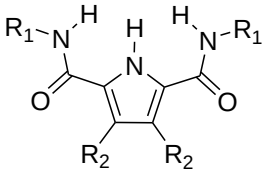

95 R_1 = n-Bu, R_2 = Ph
96 R_1 = R_2 = Ph
97 R_1 = Ph, R_2 = Cl
98 R_1 = n-Bu, R_2 = Cl

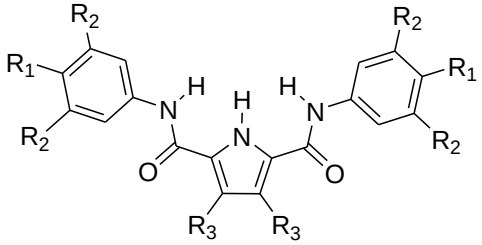

101 R_1 = NO_2, R_2 = H, R_3 = Ph
102 R_1 = H, R_2 = NO_2, R_3 = Ph

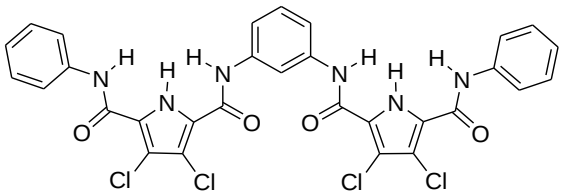

99

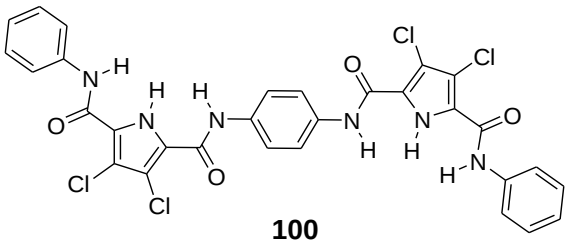

100

In collaboration with Sessler and co-workers, Gale and co-workers went on to synthesise receptor **103**. The binding constants were increased by the introduction of two extra pyrrole groups, which increased the number of hydrogen-bonding groups from three to five. Trends in selectivity changed when compared to receptor **96**'s binding constants. 5500 M^{-1} and 1450 M^{-1} were calculated for dihydrogen phosphate and 10300 M^{-1} and 560 M^{-1} calculated for benzoate for receptors **103** and **96** respectively in a DMSO-d_6 solution.

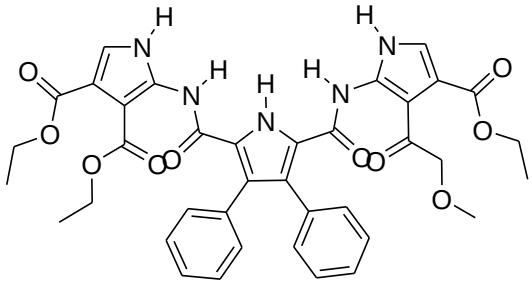

103

Gale and co-workers then went on to synthesise a group of bis-pyrrole receptors (**104**-**109**). Binding studies were carried out in DMSO-d_6/5% H_2O. Receptors **104** and **105** were found to be selective for dihydrogen phosphate, with binding constants > 10^4 M^{-1}. These receptors were unstable in solution over a period of time. The methyl groups were introduced at the R_5 position and increased the stability of receptors **106**-**109** dramatically.

The more stable receptor (**106**) shows selectivity of one order of magnitude for dihydrogen phosphate (1092 M^{-1}) but the binding constant was lower than that of **104** and **105**. Receptors **107** and **108** showed no real selectivity for one anion over another, with binding constants in the range of zero to the low hundreds. Receptor **109** showed a complete change in trend of selectivity, preferring the anions with increased basicity. Fluoride is bound selectively, with binding constants of 1450 M^{-1} and 83 M^{-1} for fluoride and dihydrogen phosphate respectively.[83,84]

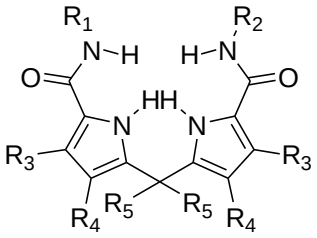

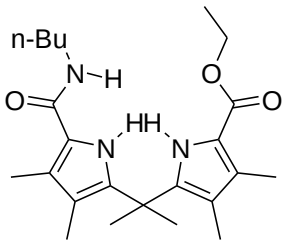

109

104 $R_1 = R_2$ = Ph, R_3 = Me, R_4 = Et, R_5 = H
105 $R_1 = R_2$ = n-Bu, $R_3 = R_4 = R_5$ = H
106 $R_1 = R_2$ = Ph, $R_3 = R_4 = R_5$ = Me
107 $R_1 = R_2$ = n-Bu, $R_3 = R_4 = R_5$ = Me
108 R_1 = Ph, R_2 = n-Bu, $R_3 = R_4 = R_5$ = Me

Sessler and co-workers explored the effect of pre-organisation and pyrrole position on anion affinity and selectivity by synthesising receptors **110** to **113**. Where binding conformations could be calculated *via* Job plot, a 1:1 stoichiometry was favoured. All binding constants were calculated by UV-Vis titration in dichloroethane, using the TBA salt of the anion. Receptor **110** favours the oxo-anions, showing selectivity for benzoate followed by acetate (binding constants of 43000 M^{-1} and 19000 M^{-1} respectively). Receptor **111** has bulky R group functionalities which interfere with anion binding causing the inhibition of anion binding with all anions apart from acetate (13900 M^{-1}). Replacing the pyridine unit with a phenyl group (**112**) almost completely inhibits all binding events with all anions, showing the importance of pre-organisation in receptor design. Receptor **113** investigates the change in position of the NH groups by reversing the connectivity of the amide groups. The only anion that shows appreciable affinity with this receptor is chloride (805 M^{-1}).[85]

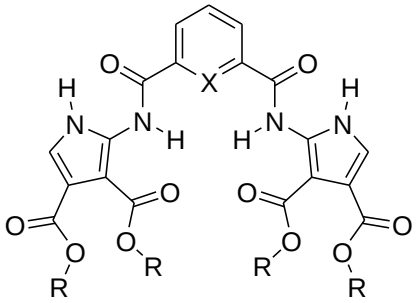

110 R = CH_2CH_3, X = N
111 R = $CH_2CH_2CH_3(CH_3)_3$, X = N
112 R = CH_2CH_3, X = CH

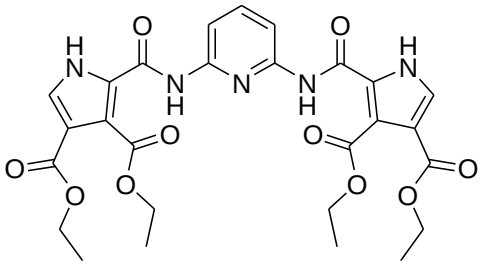

113

Sessler and co-workers also synthesised a terpyrrolic-based analogue of dipyrrolylquinoxalines (**114**),[86] already known for the sensing of anions. **116** acts as an improved colorimetric and fluorescent sensor for dihydrogen phosphate and halide anions in organic solutions. Fluorescence titrations were performed in CH_2Cl_2 with TBA salts of the anions to establish binding constants. Job plots were used to determine a 1:1 binding stoichiometry in solution. Binding constants were calculated for dihydrogen phosphate, (80 M^{-1} and 17500 M^{-1}) and for fluoride (18200 M^{-1} and 182000 M^{-1}) for receptors **114** and **115** respectively. This shows not only an increase in binding affinity for the new terpyrrolic analogue but also a dramatic increase in the selectivity for binding dihydrogen phosphate.[87]

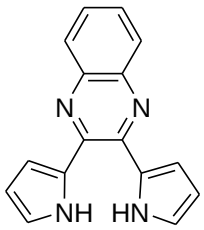

114

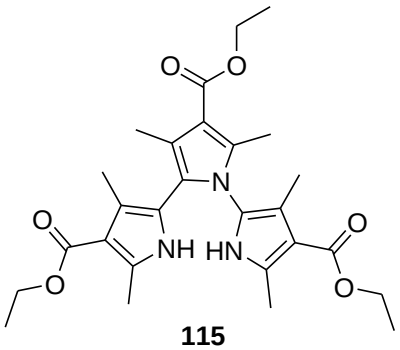

115

Schmuck and co-workers produced two zwitter ionic receptors (**116** and **117**), containing a positively charged guanidinium group and a negatively charged carboxylate group, which resulted in an overall neutral charge. Receptor **116** shows no interactions between the charge centres that could be detected by ^{1}H NMR in a DMSO-d_6, but

intramolecular interactions were observed with the larger receptor, **117**. It was found that this receptor is able to self-fold into a loop that is stabilised by six hydrogen bonds as well as the ionic charge attractions. This conformation was found to be stable even in the polar environment of the DMSO solution.[88]

A shorter guanidinium receptor (**118**) was then synthesised. It only contains one, instead of two, pyrrole groups and the carboxylate functionality of the zwitter ion is removed by ester protection. This molecule does not associate into a loop but dimerises in polar DMSO-d_6 solutions (confirmed by NMR titration and mass spectrum analysis). These dimers are suspected to be held together by a mixture of hydrogen bonding and π-π stacking. This dimerisation was found to be entropically driven and is dependent on the anion present in solution. Counter anions, such as chloride, that do not interfere with the π-π stacking, do not affect the dimerisation process. Counter anions, such as picrate, that do disrupt the π-π stacking and can form favourable ion pair interactions with the individual molecules, prevent the dimerisation of the subunits in solution.[89] This simple unit was then extended and produced receptor **119**. This was also found to dimerise in a DMSO-d_6 solution. Using ^{1}H NMR concentration experiments, **119** was found to have an dimerisation constant higher than expected (1080 M^{-1}). The picrate anion was again found to disrupt this dimerisation process. The binding constant for the receptor and picrate anion was calculated to be 2400 M^{-1}, (twice that of the dimerisation association complex), making this complex twice as stable and therefore more favourable. This process is found to happen even in the presence of chloride counter ions, giving a switchable, self-dimerising system.[90]

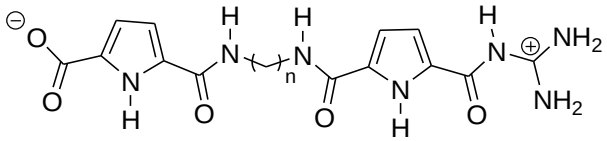

116 n = 2
117 n = 4

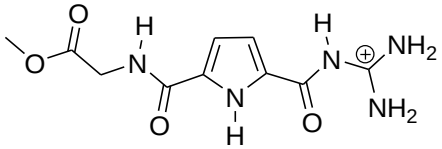

118

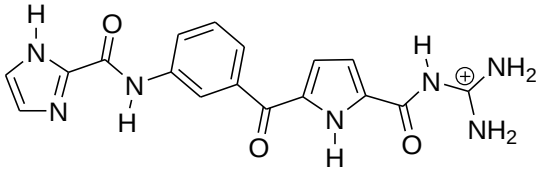

119

Four analogues (**120-123**) of the last set of receptors (**116-119**) were synthesised and incorporated into an amino acid sequence (H-alanine-receptor-valine-NH_2) *via* the Fmoc-protected amine and carboxylic acid functonalisation. This synthetic analogue for the amino acid, arginine, has an improved carboxylate binding site and could be used to probe the effects of carboxylate binding in naturally occurring peptide sequences that are rich in arginine.[91]

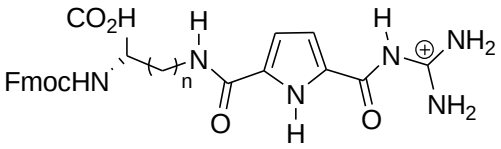

120-123 n = 1 - 4

As well as working with acyclic receptors, Sessler and co-workers have synthesised a number of macrocyclic, pyrrole-based molecules (**124-128**), analogues of sapphyrin. Receptors **125** and **126** were first studied in 1990. Crystals grown from a solution of **126** and HPF_6 showed that the receptor had been deprotonated and was binding fluoride through five hydrogen bonds. A crystal structure of **126** was also obtained that was doubly protonated, binding two hydrochloric acid molecules.[92] **124-126** were first synthesised in the 1980's by Woodward and co-workers.[93] Full solution studies of receptors **124-126** and **127** and **128** involving anions were not explored until 1996. X-ray crystal structures of compounds **124** and **125** showed that, in the solid state, the deprotonated receptors were able to bind diphenyl phosphate and monobasic phenyl phosphate respectively, forming 2:1 complexes of anion:receptor. The deprotonated form of receptor **125** was found to bind only one equivalent of either dihydrogen or monohydrogen phosphate. Binding constants were determined for **124-128** from ^{1}H and ^{31}P NMR titration studies in CD_3OD and aqueous bis-Tris buffer and UV-Vis studies in the same solution conditions. Both 1:1 and 2:1 anion:receptor complexation stoichiometry were observed in the solution state with receptor **125** and phenylphosphoric acid by analysing the shape of the titration curves. The complexes observed were found to be dependent on the pH of the titration solution, the more acidic solutions giving the 2:1 binding stoichiometry. Phosphate anions were added as free-acid and monobasic potassium, TBA or TEA salts. In every case, receptors **124-128** were shown to be effective phosphate receptors in their protonated forms. Receptors **125**

and **126** gave binding constantans of $>10^4$ M^{-1} in CD_3OD and 10^2 M^{-1} in 10 mM aqueous bis-Tris buffer at pH 6.1.[94]

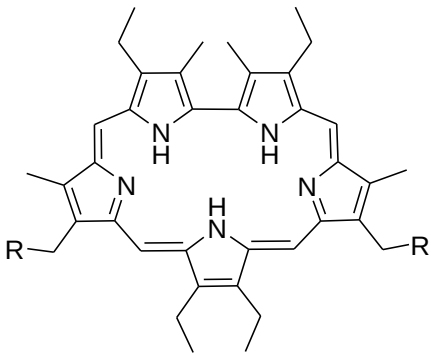

124 R = $CH_2CON(CH_2CH_2OH)_2$
125 R = CH_2CH_2OH
126 R = CH_3

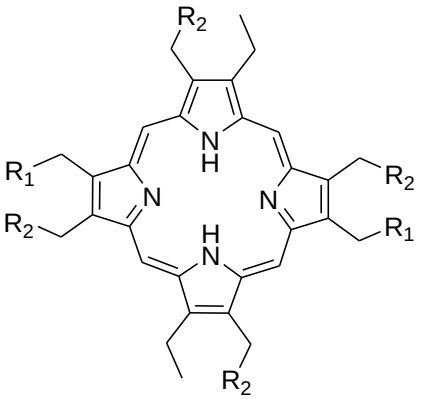

127 R_1 = $CH_2CON(CH_2CH_2OH)_2$, R_2 = H
128 R_1 = R_2 = CH_3

Sessler and co-workers went on to synthesise a macrocycle (**129**) based on 2,6-diamidopyridine scaffold. This new macrocycle contained four hydrogen bonds, two from pyrrole and two from amide functionalities. Binding constants and stoichometries were determined in the solution state by UV-Vis titrations in MeCN, using the TBA salt of the anion. Little interaction was noted with nitrate or bromide but 1:1 binding was found with chloride, cyanide, acetate and hydrogen sulfate. A slightly higher affinity was observed for hydrogen sulfate. All these anions had binding constants in the range of 12000 to 64000 M^{-1}, apart from chloride which only showed moderate binding affinity to the receptors. Dihydrogen phosphate was the only anion to show a 2:1 anion:receptor binding stoichiometry, with binding constants of 342000 M^{-1} and 26000 M^{-1} for the first and second binding events.[95]

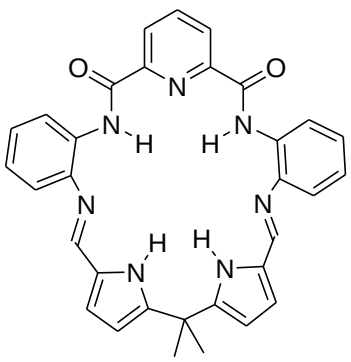

129

The success of receptor **129** led to the synthesis of receptor **130** and the reduction and oxidation of this receptor led to receptors **131** and **132**. This produced macrocycles with three, four and six hydrogen-bond donor groups. Binding constants were determined by the same methods as for **130** but there were no longer any 2:1 binding stoichometries. Receptor **130** showed increased selectivity for hydrogen sulfate and dihydrogen phosphate, with binding constants of 108000 M^{-1} and 29000 M^{-1} respectively. The reduced form of the receptor (**131**) showed selectivity for chloride (116000 M^{-1}), with binding constants for hydrogen sulfate and dihydrogen phosphate of 4700 M^{-1} and 15500 M^{-1} respectively. The oxidised form of the receptor, **132**, only showed affinity with bromide (2760 M^{-1}) out of all the anions tested. Receptor **129** has a large, flexible cavity whereas **130** has a rigidified cavity due to steric hindrance of the tolyl group. Both these receptors are selective for oxo-anions, hydrogen sulfate and dihydrogen phosphate but different binding stoichometries are observed with the two receptors. The increased number of hydrogen-bond donor groups and the increased flexibility in receptor **131** causes a change in anion binding selectivity towards the smaller spherical anions. Receptor **132** is the most rigid and planar of all the structures with the least number of hydrogen-bond donor groups and therefore shows little anion binding interaction. These examples show that it is possible for binding affinities to be fine-tuned by basic structural (redox) changes to the parent molecule.[96]

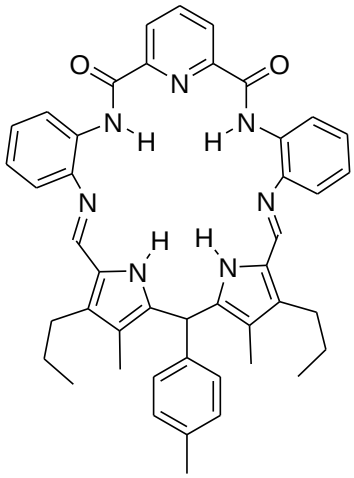

130

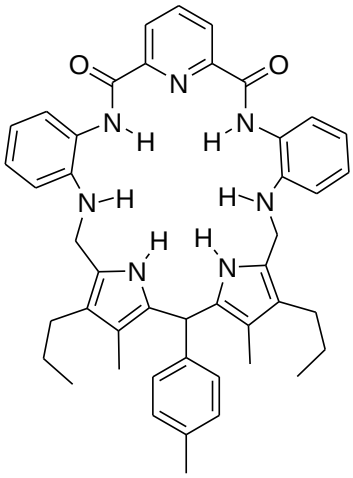

131

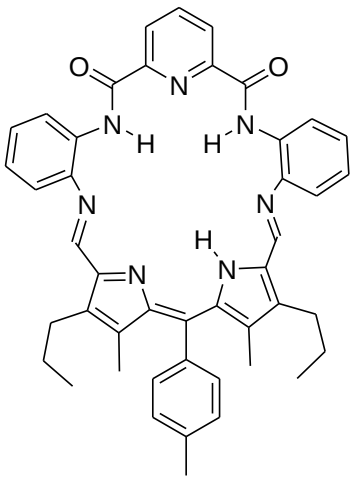

132

The macrocyclic anion receptors **133-136**, synthesised by Neri and co-workers, use calix[4]arene as a scaffold from which to suspend a total of eight hydrogen-bond donor

groups (four amide and four pyrrole). Receptors **135** and **136** have the flexibility of the macrocyclic ring reduced by the addition of crown ether groups. The acidity of the NH bond donor groups is also increased with the addition of nitro substitutions to the pyrrole rings as seen in receptors **134** and **136**. Binding constants were obtained by ^{1}H NMR titrations in DMSO-d_6/0.5% H_2O using the TBA salt of the anion. 1:1 binding stoichometries were determined by Job plot analysis. With receptor **133**, we see selectivity for dihydrogen phosphate (2500 M^{-1}) over acetate (65 M^{-1}) and the other range of anions tested. By increasing the acidity of the NH bond donor groups (**134**), a new trend in anion binding is observed, favouring the more basic anions. Acetate (1140 M^{-1}) is selectively bound over the other anions, including dihydrogen phosphate (315 M^{-1}). This trend is also seen with receptor **136**. The binding constants for the more basic anions are higher than those observed for **134** due to increased rigidity of the structure, which enhances anion binding. Receptor **135** does not exhibit increased binding constants for the anions when compared to receptor **133**. There is overall a loss in selectivity and anion binding affinity (dihydrogen phosphate 920 M^{-1}, acetate 460 M^{-1}) even though the structure is made more rigid because the NH bond donor groups no longer have the freedom to move into the optimal position for interaction with a tetrahedral anion such as dihydrogen phosphate.[97]

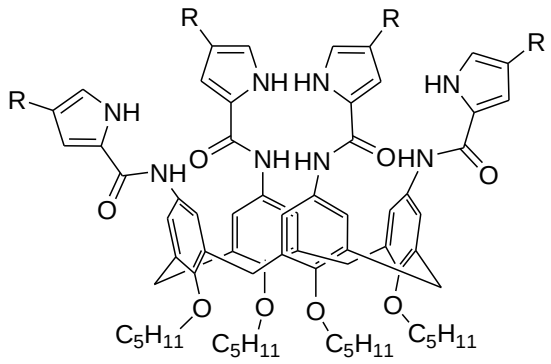

133 R = H
134 R = NO_2

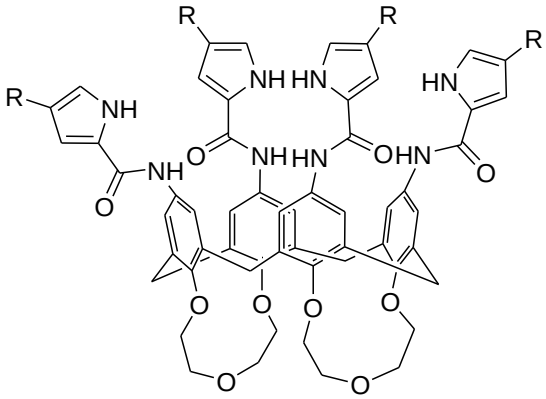

135 R = H
136 R = NO_2

The introduction of calix chemistry led to the synthesis of pyrrole-containing macrocycles, each pyrrole unit being separated by one carbon spacer unit. *meso*-Octamethylcalix-[4]-pyrrole (**137**) was first synthesised in 1886 by Baeyer[98] but the potential for these small molecules to act as anion receptors was not realised until 1996 by Gale, Sessler and co-workers. This simple molecule was the first pyrrole-based neutral

anion receptor. Crystal structures obtained with the free receptor show a 1, 3 alternate structure as shown in Figure 1.3.4.1.2. Upon anion binding to fluoride and chloride, a cone conformation is adopted[99] and each anion is bound by four hydrogen bonds. The small fluoride anion is able to fit snugly into the cone. The larger chloride anion appears to balance on top of the cone and the even larger bromide anion balances on top of the cone still further away from the receptor due to the larger size. This can be seen in Figures 1.3.4.1.3a-c the crystal structures of the caesium salts of fluoride, chloride and bromide and receptor **137**.[100]

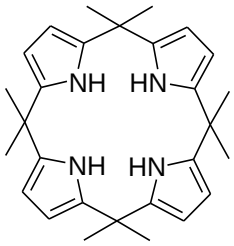

137

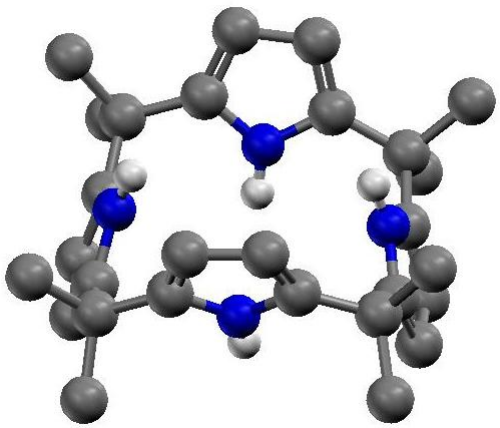

Figure 1.3.4.1.2 Crystal structure of **137** showing the free receptor 1,3 alternate conformation. Obtained by Gale and co-workers.

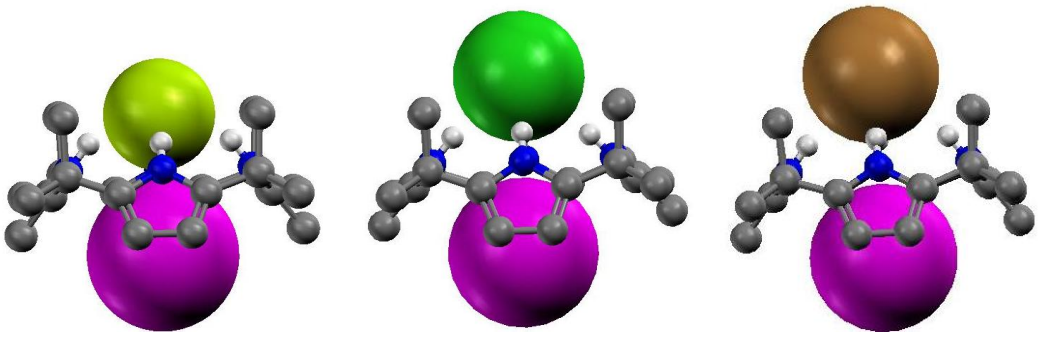

Left Figure 1.3.4.1.3a Crystal structure of **137** with CsF. The fluoride anion can be seen in the cone held by the four hydrogen bonds of receptor **137** and ionic interactions from the caesium**. Centre Figure 1.3.4.1.3b** Crystal structure of **137** with CsCl. The chloride anion can be seen balancing above the cone, held by the four hydrogen bonds of receptor **137** and ionic interactions from the caesium. **Right Figure 1.3.4.1.3c** Crystal structure of **137** with CsBr. The bromide anion can be seen furthest away from the cone, held by the four hydrogen bonds of receptor **137** and ionic interactions from the caesium. All complexes synthesised by Gale and co-workers.

An analogue of receptor **137**, tetraspirocyclohexylporphyrinogen (**138**), adds different groups to the outside of the macrocyclic ring. The position of the hydrogen-bond donor groups, the size and shape of the cleft and the substitutions on the outside of this macrocyclic ring (altering size, shape and conformation of the binding site) appear to be crucial to the anion binding. Both receptors **137** and **138** show selectivity in binding fluoride over other oxo- and halide anions, with **137** shown to be the most effective at selectively binding the anion. Binding constants for fluoride of 17170 M^{-1} and 3600 M^{-1} were obtained for receptor **137** and **138** respectively, although the remaining anion binding constants calculated for both anion receptor complexes are similar. Binding constants were calculated to a 1:1 binding stoichiometry, obtained by Job plot analysis through ^{1}H NMR titration in CD_2Cl_2 using the TBA salt of the anion. [99]

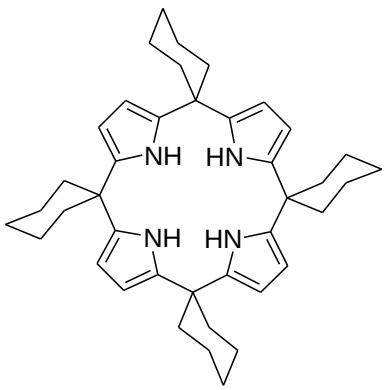

138

The selectivity of *meso*-octamethylcalix-[4]-pyrrole, (**137**) for different anions is also solvent dependent. Comparisons and studies by Schidtchen,[101] and Sessler and Gale [102] have shown a decrease in selectivity with the increase in polarity of the solution. With TBA chloride, binding constants ranging from 10^2 to 10^5 M^{-1} were calculated with both ITC and ^{1}H NMR techniques in a range of different solvents. Binding constants were also found to be dependent on the counter ion, with changes of 10^2 to 10^4 M^{-1} observed in CH_2Cl_2/CD_2Cl_2 with the chloride anion. This is due to the degree of cation inclusion into the cavity of the cup, which will affect the degree of ion pairing and, in turn, will contribute to the strength of anion binding interactions.

Receptor **137** was shown to act as a diatopic, anion-pair receptor with the caesium salts of the halide compounds. Inclusions of N-ethylpyridinium and TEA cations have also been shown with the halide counter ions. As the anion binds to the receptor, it causes a conformational change into the cone conformation. See caesium crystal structures, Figures 1.3.4.1.3a-c. The cation is able to slide into the vacant space.[100,102,103] **137** and **138** have also been shown to transport the caesium chloride ion pair across phospholipid bilayers. The effects of **138** are small compared to **137**, which is an effective chloride transporter.[104]

Sessler and co-workers synthesised five fluorinated analogues of **137**, receptors **139-143**. Binding constants were obtained by a combination of ^{1}H NMR and ITC techniques, which were found to give similar values. For most of the binding experiments, the raw data was fitted to a 1:1 binding model. The binding constants were obtained from dry DMSO and MeCN solutions, using the TBA salt of the anion. Fluorinated compounds **139-141** were compared to **137**. Trends in anion selectivity were found to be generally the same for the different anion/receptor combinations. Carboxylate anions were bound selectively over the halide anions tested with all four receptors in MeCN. Receptor **139** was shown to be the most effective at binding every anion apart from hypophosphite, which was more effectively bound by **140** and **141**. As cavity size increases, so do the binding constants of the larger anions. Bromide was more effectively bound by **141** because of the larger cavity size. This larger, more diffuse anion is more easily accommodated, making binding a more favourable process. Higher binding constants are observed with the fluorinated analogues of original calix pyrrole due to the electron-withdrawing effects of the fluoro groups. As previously explained, this increases the acidity of the pyrrole NH-bond donor groups.[105] This receptor has also been shown to be an effective chloride transporter across biphospholipid membranes of vesicals.[106]

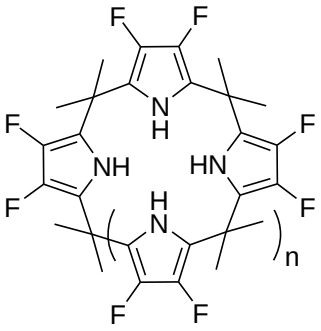

139 n = 1
140 n = 1
141 n = 1
142 n = 1
143 n = 1

Gale and co-workers improved the binding affinity of receptor **137** by adding a *meso*-appended 3,4,5-trisbromopyrrole functionality. The addition of this extra pyrrole group in receptor **144** greatly increases the binding affinity and selectivity for the carboxylate anions, benzoate and acetate, increasing the number of hydrogen-bond donor groups coordinating with the anion. Binding constants were determined by ^{1}H NMR titration in CD_2Cl_2 with the TBA salt of the anion. Binding constants were increased from 668 M^{-1} to $>10^4$ M^{-1} with acetate and 196 M^{-1} to $>10^4$ M^{-1} with benzoate by the addition of this *meso* functionality (**144**) to the basic calixpyrrole structure (**137**).[107]

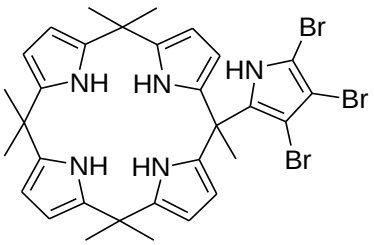

144

After the original interest in calix[4]pyrrole, modifications were made to improve anion binding affinity and selectivity. *meso*-Substitutions have been made on up to four points on the macrocycle. These early modifications have a limited effect on binding affinity and selectivity. Single arm modifications were then employed but were shown to be less effective than the addition of a 'strap' from one side of the receptor to another. This strap allows increased pre-organisation through rigidification of the structure, improving binding affinity and selectivity. 'Capped' calix[4]pyrroles have also been synthesised that take the idea of a 'strap' one step further by joining four arms together over the top of the macrocycle. However, these structures can be too rigid, reducing anion affinity and selectivity. It is because of this over rigidification that the 'strapped' macrocycles have

become the focus of modified calix[4]pyrrole research rather than the 'capped' molecules.[108]

Lee and co-workers published the first example of a 'strapped' calixpyrrole in 2002.[109] The strap of this receptor was based on an ester linkage, with no hydrogen-bond donating groups to aid the anion binding process. The anion binding trend was found to be based on size exclusion from the receptor molecule. Two years later, a set of receptors (**145-147**) with straps containing amide groups were synthesised. There were no size exclusion properties observed with receptors **145-147** and this is believed to be because of the flexibility and hydrogen bonding interactions of the strap. As the anions get larger, the strap tilts to one side, allowing the anion to interact with all six of the NH donor functionalities. This theory is supported by the binding stoichiometry evidence collected by ^{1}H NMR analysis with receptor **146**. When this receptor binds fluoride, a 1:1 anion:receptor complex is observed. The anion is small and can fit into the space inside the receptor without distorting it. Chloride anions are found to form a mixture of 1:1 and 1:2 anion:receptor complexes. This anion is slightly larger and begins to tilt the strap sideways so that it comes to sit slightly outside the binding array. This in turn allows interactions with a second receptor. The larger bromide anion also tilts the strap sideways and sits even further outside of the binding cleft, forming a purely 1:2 anion:receptor complex.[110]

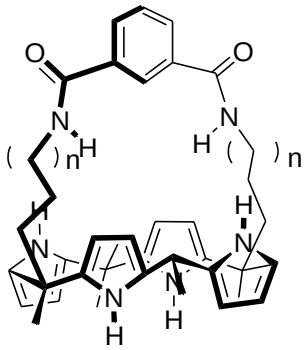

145 n = 1
146 n = 2
147 n = 3

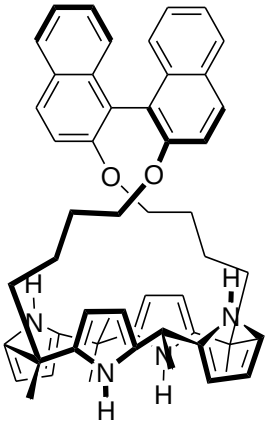

148

This group went on to synthesise a chiral-strapped calix[4]pyrrole (**148**). Chirality is introduced through the binol functionality. Binding constants were determined in dry MeCN by ITC and fitted to a 1:1 binding model, using the TBA salt of the anion. The anion binding properties of the (*S*) enantiomer of receptor **148** were analysed with the chiral enatiomeric anions; (*S*)-2-phenylbutyate and (*R*)-2-phenylbutyate. The *S*-enantiomer of the receptor selectively binds the *S* enantiomer of the anion with a binding constant of $1.0 \times 10^5\ M^{-1}$ over the *R* enantiomer of the anion ($9.8 \times 10^3\ M^{-1}$). This selectivity is due to unfavourable steric interactions of the *R* and *S* enantiomeric complex, showing enantiomeric anion recognition. The racemic mixture of anion and receptor forms favourable π-π interactions between the binol rings of the receptor and phenyl rings of the anion.[111]

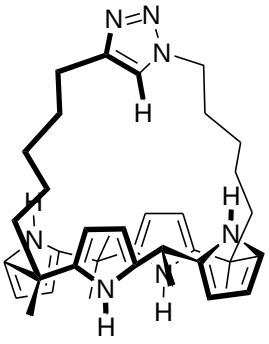

149

In 2009, Gale and co-workers synthesised a 1,2,3-triazole-strapped calix pyrrole (**149**). This receptor adopted an unexpected 1,2-alternate conformation in the solid state when crystallised with MeOH. Binding constants were obtained with TEA chloride by ITC

in both MeCN and CH_2Cl_2, fitting to a 1:1 binding model. Comparison was made with **137** and the strap was found to improve the affinity of chloride to calix[4]pyrrole in both solutions. This is due to the increased pre-organisation of the strap and the added CH interaction from the triazole functionality. This receptor has also been shown to transport chloride across a phospholipid bilayer. Unlike receptor **137**, which only transports chloride as a caesium chloride co-transporter, receptor **149** has been shown to transport chloride with a combination of ion-pair co-transport and chloride-nitrate antiport mechanisms. In a sodium nitrate solution, buffered to pH 7.2, chloride transport was shown to occur with every alkali metal chloride salt tested. The efficiency of anion transport was found to be dependent on the size of the counter cation. The larger, charge-diffuse cations were found to produce the most activity. With a change in extra-vesicular solution from sodium nitrate to a sodium sulfate solution, buffered to pH 7.2, an overall decrease in the activity of chloride transport was observed with each of the alkali metal chloride salts. Although the decrease in anion transport activity was minimal for caesium chloride, a more pronounced effect was observed as the size of the counter cation decreased. This shows that the larger alkali metal counter cations rely mainly on an ion-pair transport mechanism but the smaller alkali metal counter cations mainly rely on a chloride-nitrate antiport transport mechanism.[112]

1.3.4.2 Carbazole, indole, indolocarbazole and biindole based receptors

Despite the natural progression from pyrrole to indole-based anion receptors and the early synthesis of a synthetic indole-based receptor in 1996 by Black and co-workers[113], it was not until 2004 that Jurczak and co-workers[114] started to look at the carbazole functionality as a potential hydrogen-bond donating group in anion receptor design. In 2005, indole/indolocarbazole systems started to be examined for anion binding potential by Beer and co-workers [115] and Jeong and co-workers [116]. Since the early incorporation of these groups into the anion receptor, these functionalities have become a popular addition in the world of anion binding.[117,118]

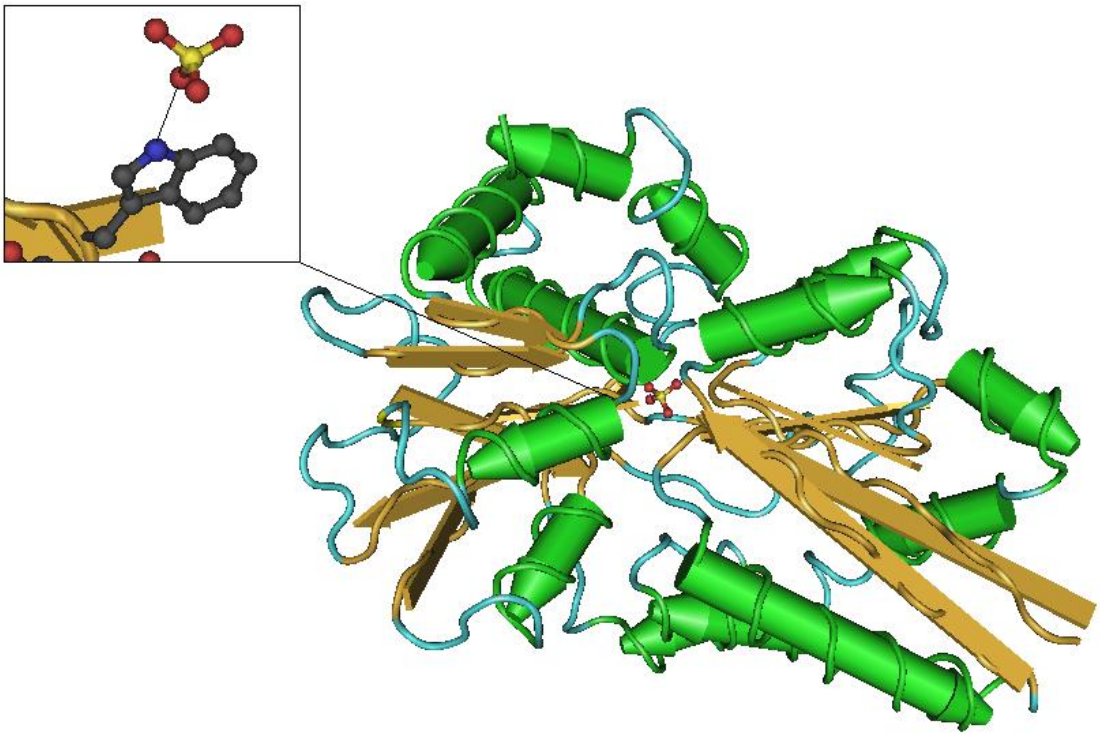

Figure 1.3.4.2 Protein X-ray crystal structure of the sulfate binding protein found in *Salmonella typhimurium*. The area of the protein crystal structure which contains the tryptophan 192 residue hydrogen bonding to the sulfate anion has been expanded and the tryptophan side chain shown. The hydrogen atoms and water molecules have been omitted for clarity.[119]

The indole group is naturally occurring in the amino acid, tryptophan, and is found to have some activity as a catalytic residue in enzymes. [120] Tryptophan is also crucial in the hydrogen binding of sulfate to the sulfate binding protein found in *Salmonella typhimurium* (Trp 192). This was confirmed by X-ray crystallography and is illustrated in Figure 1.3.4.2. [121-123] Two indole groups (Trp125 and 175) bind chloride in the enzyme, haloalkane

dehalogenase which is found in *Xanthobacter autotrophicus*.[124] Not only has this indole functionality been found to be both crucial to enzymatic activity but bisindolylmaleieides and indolocarbazoles have also been shown to prevent enzyme activity inhibiting protein kinase C activity.[125]

1.3.4.2.1 Carbazole based receptors

The first indole/carbazole-based building block used in anion receptor design was 1,8-diamino-3,6-dichlorocarbazole. Carbazole contains the most acidic NH –bond donor group out of the pyrrole, indole, and carbazole family. The chloro groups are electron-withdrawing, increasing the acidity of the hydrogen-bond donor groups of the carbazole still further. The anions were bound by three NH bonds. Binding constants were determined for chloride, benzoate and dihydrogen phosphate by ^{1}H NMR titration in a DMSO-d_6/H_2O 0.5 % solution, using the TBA salt of anion. Receptor **150** was shown to have similar selectivity for benzoate (1230 M^{-1}) and dihydrogen phosphate (1910 M^{-1}) over other anions tested. Receptor **151** shows increased binding constants for dihydrogen phosphate (19800 M^{-1}), becoming selective for this anion over benzoate (8340 M^{-1}). The rigidity given to the structure by the carbazole skeleton and the highly acidic hydrogen bond donor groups gives rise to the selectivity and high binding constants in competitive solutions.[114] The increase in binding constants and selectivity for receptor **150** over receptor **151** is due to the steric hindrance effects of the phenyl substituent of receptor **150**.

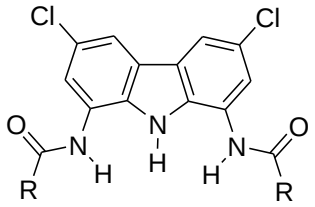

150 R = Ph
151 R = Pr

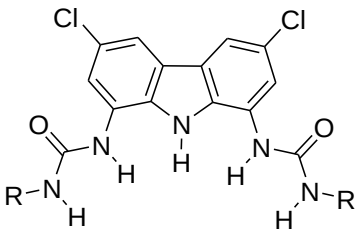

152 R =

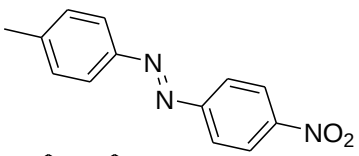

153 R =

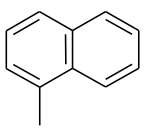

Figure 1.3.4.2.1 Full spectrum of colour observed by Kim and co-workers upon the addition of various anions to a solution of receptor **152.**

The same carbazole building block was utilised by Kim and co-workers three years later, attaching functionalities by a urea linkage. This produces two receptors, **152** and **153**, with five hydrogen bond donor groups used in the binding of the anion. The addition of chromogenic/fluorogenic functionalities visualises the binding events. The chemogenic anion sensing capabilities of receptor **152** (CH_3CN:DMSO 9:1) were analysed with one hundred equivalents of each anion. A visual inspection revealed six groups of colour changes for different anions as listed below. The full spectrum of colour change is shown in Figure 1.3.4.2.1:

1. No significant colour change from yellow (λmax = 419 nm): SCN^-, NO_3^-, ClO_4^-, I^-, Br^-
2. Yellow/orange colour change (λmax = 426 - 431 nm): Cl^-, HSO_4^-
3. Orange colour change (λmax = ~ 443 nm): OBz^-, OAc^-, glutarate
4. Red/orange colour change (λmax = ~ 450 nm): adipate, $H_2PO_4^-$, oxalate
5. Red colour change (λmax = ~ 460 nm): CN^-, $HP_2O_7^{3-}$
6. Dark blue to green colour change (λmax > 617 nm): OH^-, F^-, succinate, malonate (indicating deprotonation of the receptor)

Job plot experiments with **153** in DMSO-d_6 showed 1:1 binding conformation with acetate and pyrophosphate but 2:1 anion:receptor complex with fluoride. Different binding modes are observed with different anions/receptor combinations.[126]

Lin and Co-workers used a functionalised phenanthroline bridge to join two carbazole moieties at the three positions, resulting in receptor **154**. Binding constants were calculated using UV-Vis in DMF, with the anion added as the TBA salt. This receptor was shown to be selective for iodide over fluoride, chloride, bromide and acetate anions, with a binding constant of 5×10^4 M^{-1}. Job plot analysis confirmed a 1:1 binding stoichiometry with the iodide anion. Binding constants for other anions could not be calculated as the change in the UV-Vis spectra was too small. The selectivity of this receptor for the large spherical anion such as iodide can be explained by the rigid size, shape and position of the hydrogen bond donating groups in the binding cavity.[127]

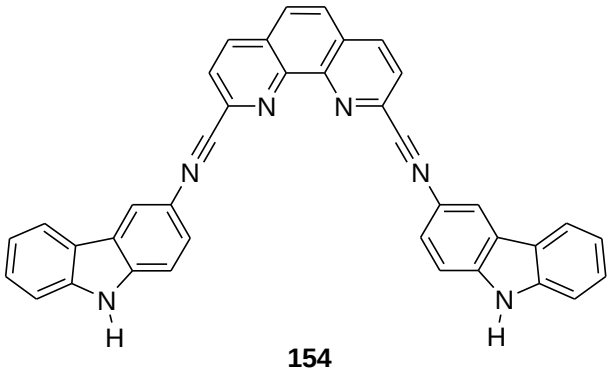

154

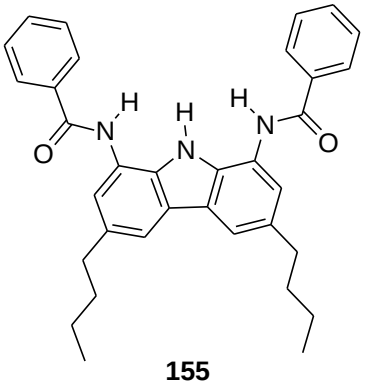

155

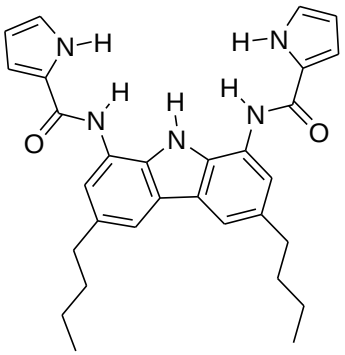

156

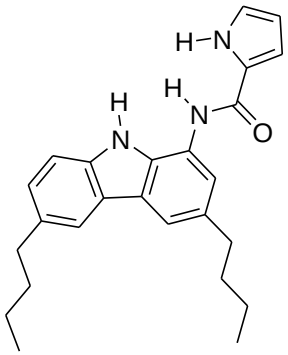

157

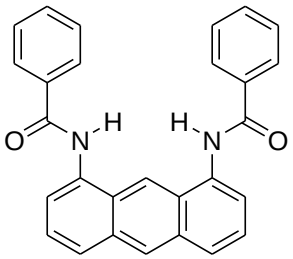

158

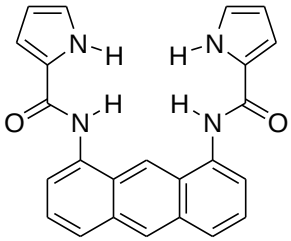

159

A set of five cleft receptors (**155-159**), synthesised by Gross and co-workers, is one of the most recent examples of carbazole-containing anion receptors. This group of receptors contains both carbazole and anthracene scaffolds and a range of different numbers and types of NH bond donor groups. In the solid state, only the amide and carbazole NH donor groups of receptor **156** are involved in the anion binding event with TBA salt of acetate or chloride. In the solution state (DMSO-d_6), ^{1}H NMR titrations were fitted to a 1:1 binding model. All binding events show the participation of every NH bond donor group in all receptors. Receptors **155**, **156** and **159** all show the binding trend $H_2PO_4^-$ > BzO^- > Cl^-, with binding constants for dihydrogen phosphate of 1400M^{-1}, 2000

$M^{-1}$and 2600 M^{-1} for receptors **155**, **156** and **159** respectively. Receptors **157** and **158** also show selectivity for dihydrogen phosphate, with binding constants of 880 M^{-1} and 160 M^{-1} respectively. They also show a higher affinity for chloride than for benzoate. The lower selectivity shown by **157** and **158** for dihydrogen phosphate and the alteration in anion binding trend is due to the change in hydrogen bonding array and the decreased numbers of NH bond donor groups available to interact with the anion.[128]

Sessler and co-workers utilised the calix-pyrrole chemistry to synthesise a calix-pyrrole/carbazole hybrid macrocycle (**160**). Binding constants were calculated using the static fluorescence quenching techniques in CH_2Cl_2 with the TBA salt of the anion. This macrocyclic receptor was found to be selective for acetate over other anions tested. Binding constants of 229000 M^{-1}, 220000 M^{-1} and 77000 M^{-1} were calculated for 1:1 acetate:receptor complexes in receptor concentrations of 0.5 µM, 1.0 µM and 10 µM thus showing a steady decrease. This decrease in binding constant between the 1.0 µM and 10 µM concentrations of receptor is due to the residual aggregation effects in solution at higher concentrations, decreasing the availability of the receptor for anion complex formation. This macrocyclic receptor was found to bind a variety of anions reasonably well, binding dihydrogen phosphate, chloride and the larger oxalate anions with moderate affinity. Crystal structures were obtained with benzoate, showing the anion receptor bending around the anion so the four pyrrole NH bond donor groups were involved in the binding process in a 1:1 complex. This is shown in Figure 1.3.4.2.2.[129]

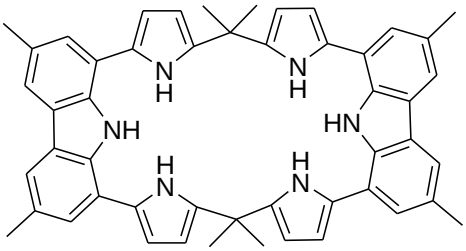

160

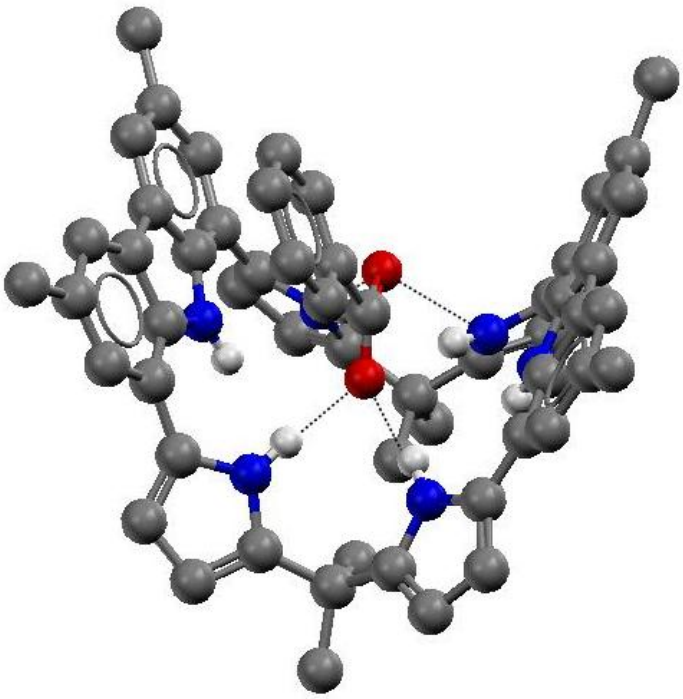

Figure 1.3.4.2.2 1:1 Complex of receptor **160** with benzoate. The crystal structure was obtained by Sessler and co-workers.

1.3.4.2.2 Indole based receptors

Continuing from work previously discussed by Sessler and co-workers in1999, which utilized quinoxalines as a scaffold to suspend pyrrole groups[86], Sessler and co-workers used the same scaffold again in 2006 to suspend indole moieties (**161-162**) [130]. Analogues of this receptor were synthesised by Yan and co-workers two years later (**163-164**)[131]. Binding constants for **161-162** were obtained by UV-Vis titration, carried out in CD_2Cl_2 using TBA salts of the anions. The results from titration and Job plot experiments indicated a 1:1 binding stoichiometry. During titration with dihydrogen phosphate and receptor **162**, a bathochromic shift was observed, resulting in a colour change from yellow to orange. Both **161** and **162** show selectivity for dihydrogen phosphate (**162 -** 20000 M^{-1}, **161 -** 6800 M^{-1}), with higher binding constants and a greater degree of selectivity observed for **162** due to the electron-withdrawing effect of the nitro group, which increases the acidity of the hydrogen bond donor groups. A change in the trend of selectivity was observed when the pyrrole groups of Sessler's original receptor was substituted by an indole group; dihydrogen phosphate anion was selectivity bound over the fluoride anion.

Binding constants for the completely rigidified analogues **163** and **164** were determined by a combination of UV-Vis and fluorescence titration in DMSO using the TBA salt of the anion. Receptor **163** was found to be selective for acetate (20602 M^{-1}) over fluoride (15531 M^{-1}) and other oxo- and halide anions tested. Receptor **164** showed a large increase in binding affinity for fluoride (152535 M^{-1}) but only a slight increase in affinity for acetate (24452 M^{-1}). The alteration in selectivity trend is due to the addition of the nitro group, increasing the acidity of the NH bond donor groups. The results from Yan and co-workers and Sessler and co-workers cannot be directly compared due to differing solvent conditions.

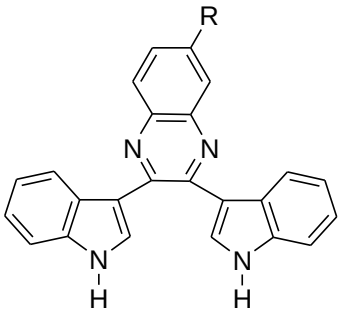

161 R = H
162 R = NO_2

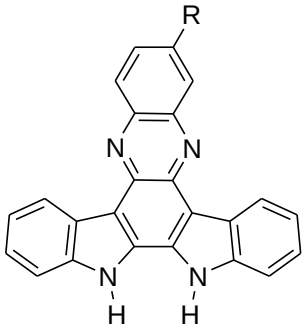

163 R = H
164 R = NO_2

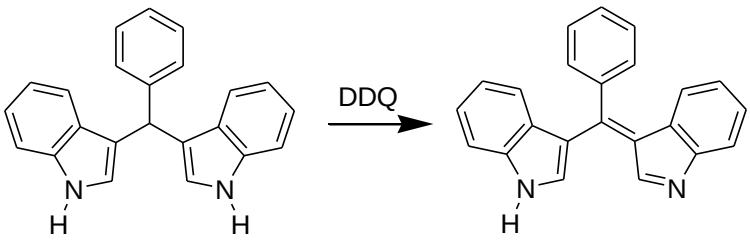

165 **166**

This bis(indolyl)methane-based receptor synthesised by Shao and co-workers (**165**) was oxidised by 2,3-dichloro-5,6-dicyanobenzoquinone (DDQ), to produce receptor **166**. This conjugated system, with a more acidic NH bond donor group, can act as a selective colorimetric anion sensor but this is dependent on the solvent system in use. The colour change events were explored using UV-Vis spectroscopy and the TBA salt of the anion. In an aprotic solvent, such as MeCN, a solution containing the receptor changed colour from yellow to red with fluoride and yellow to orange with acetate. This colour change is due to

deprotonation of the NH bond donor group. The more extreme colour change noted with fluoride is because of the basic nature of this anion and the favourable formation of the stable HF^- which encourages receptor:anion binding. With addition of H_2O to the solution of receptor **166** and fluoride (H_2O:MeCN 1:4), a colour change from yellow to red/pink was observed with hydrogen sulfate. The receptor has now become protonated because hydrogen sulfate can act as a weak acid in an aqueous solution with a pKa of 1.99. Hence the colour change.[132]

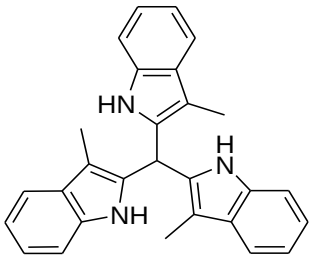

167

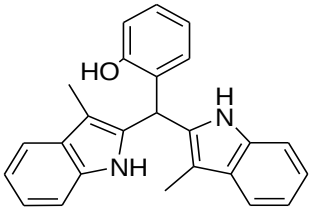

168

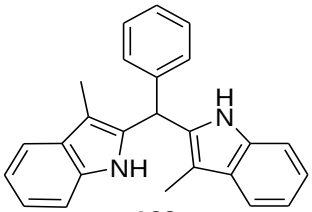

169

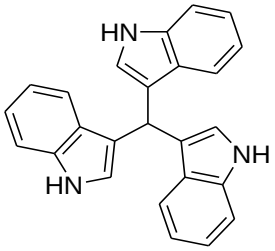

170

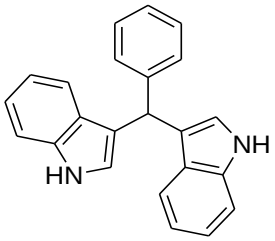

171

The indolylmethane-based structures, **167-171**, were further explored by Nishiki and co-workers. Anion binding chemistry was explored using ^{1}H NMR titration studies in $CDCl_3$ with the TBA salt of the anion. The Job plot method implied a 1:1 binding stoichiometry except in the case of **170**, which showed indications of more complex binding events. All of the hydrogen bond donor groups were seen to play a part in the anion binding process, including the OH of **168**. All receptors tested (**167**, **168** , **169**, **171**) showed a preference for binding chloride anions over the other anions tested. The strength of binding and the degree of selectivity for the anions decreased from receptor **167** (Cl^- = 1200 M^{-1}) > **168** (Cl^- = 150 M^{-1}) > **169** (Cl^- = 75 M^{-1}) > **171** (Cl^- = 26 M^{-1}). The difference between the binding constants for the different analogues of the receptor is due to the number of hydrogen-bond donor groups, the size fit of the chloride anion into the

receptor's cleft and the position of the hydrogen bond donor groups in the anion binding array.[133]

A further development in the use of indolylmethane-based anion receptors was made by Browning and co-workers, who synthesised a phosphate-containing analogue of Nishiki and co-workers' receptor (**167**) in create receptor **172**. Binding constants obtained by ^{1}H NMR titration in CD_2Cl_2, using the TBA salt of the anion, were fitted to a 1:1 binding model. Strong binding interactions and selectivity were observed with chloride (3920 M^{-1}) and acetate (2730 M^{-1}) and a strong interaction was also noted with fluoride but a binding constant could not be calculated for fluoride as the titration data did not fit cleanly to a 1:1 binding profile.[134]

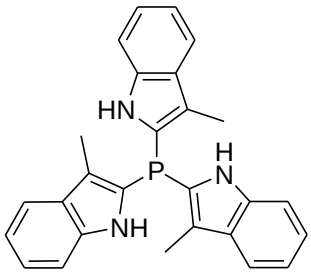

172

In 2007, Pfeffer and co-workers[135] and Gale and co-workers[2] synthesised two sets of asymmetrical, acyclic receptors, containing between three and four NH bond donor groups. Each receptor contains a single indole group, combined with amide/urea/thiourea groups. Both sets of binding constants were calculated by ^{1}H NMR titration using a 1:1 binding model and the TBA salt of the anion. Pfeffer and co-workers ran the experiments in DMSO-d_6 but Gale and co-workers used a slightly more polar 0.5 % H_2O solution with receptors **176-181**.

Pfeffer and co-workers found that receptors **173** and **174** bound dihydrogen phosphate (with binding constants of (log K) 3.5 and 3.5 respectively) over acetate (with binding constants (log K) of 3.1 and 2.8 respectively). Receptor **175** bound acetate over dihydrogen phosphate with binding constants (log K) of 3.9 and 3.4 respectively. The longer spacer unit of **175** alters binding geometry, compared to receptors **173** and **174** and therefore alters the trend and strength of anion binding. There is clear interaction of all four hydrogen bond donor groups when receptor **175** is bound to dihydrogen phosphate but the

contribution of the urea/thiourea groups is less evident with the binding of the first equivalent of the Y-shaped oxo-anion anions.[135]

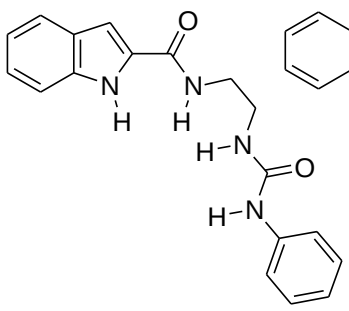

173

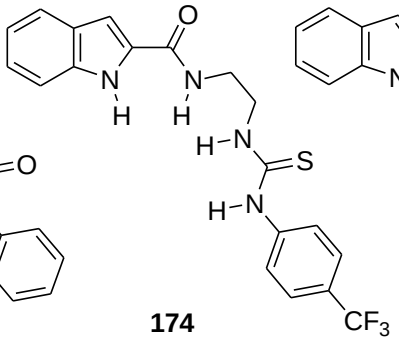

174

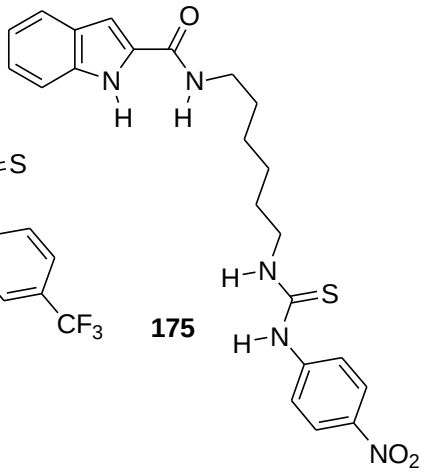

175

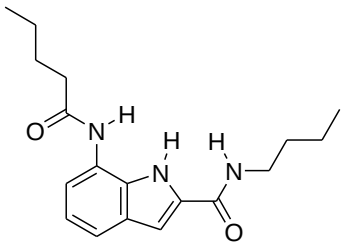

176

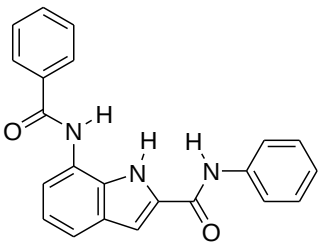

177

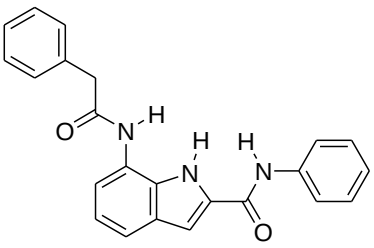

178

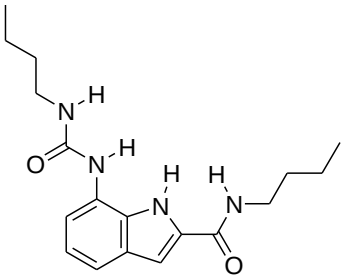

179

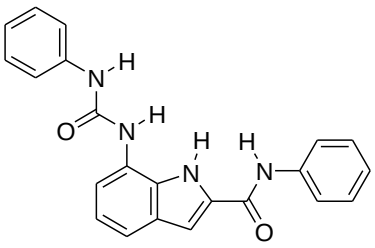

180

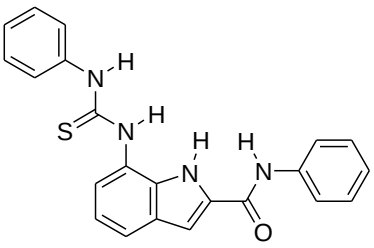

181

The receptors produced by Gale and co-workers can be split into two groups: the three NH bond donor group receptors **176-178** (containing one indole and two amide moieties) and the four NH bond donor group receptors **179-181** (containing one indole, one amide and one urea/thiourea moiety). Receptors **176-178** were found to bind acetate over other oxo- and halide anions tested, with binding constants of 425 M^{-1}, 650 M^{-1} and 900 M^{-1} for receptors **176-178** respectively. In the second group, **179-181**, the receptors were seen to bind to the anions through all three NH bond donor groups. The replacement of the amide for urea functionality in the seven position on the indole ring increased the affinity of the receptor towards all of the anions as well as increasing the degree of selectivity

towards acetate (2060 M^{-1} and 10000 M^{-1} for receptors **179** and **180** respectively). In these cases, it was only the urea and indole NH groups that could be seen to hydrogen-bond to the first equivalent of anion. The amide functionality appears to be involved in binding further equivalents of the anion. Binding constants with acetate for the more acidic thiourea-containing receptor **181** could not be calculated due to coalescence and peak broadening.[2] The utilisation of a specific part of the hydrogen bonding array to bind carboxylate anions is clear in both sets of receptors synthesised by Gale and co-workers and Pfeffer and co-workers.

Gale and co-workers[1] continued their work on acyclic indole receptors by the synthesis of two symmetrical cleft receptors, **182** and **183**, containing two indole groups and two amide groups. Shortly after the publication of these receptors, Jurczak and co-workers[3] produced a set of analogous compounds, **184-186**. Receptor **184** contains a centralised pyrrole group, adding a fifth hydrogen bond donating group. Binding constants were calculated by ^{1}H NMR titration in a DMSO-d_6/0.5 % H_2O solution. However Gale and co-workers also used a slightly more polar 5 % H_2O solution. The anion species were added using the appropriate TBA salt. Titration results were fitted to a 1:1 model (unless otherwise appropriate) and the binding event was observed through all available NH bond donor groups.

Gale and co-workers show the selective binding of fluoride over all other oxo/halide anions tested with receptor **182** in DMSO-d_6/0.5 % H_2O and DMSO-d_6/ 5 % H_2O solutions. Receptor **183** shows more complex binding events. In DMSO-d_6/0.5 % H_2O solution, titration results could not be fitted to a 1:1 or a 2:1 anion:receptor binding model. However in a 5 % H_2O solution, the titration data was fitted to a 2:1 binding model. Crystal structures of compound **183** with fluoride and chloride shows a 1:1 binding stoichiometry. This 1:1 conformation is not seen in the solution state with the halide anions. The fluoride anion can be seen encapsulated by the receptor, helicating around (see Figure 1.3.4.2.3a). The chloride anion is larger and so less well encapsulated by the receptor as seen in Figure 1.3.4.2.3b. This is an indication as to why chloride is bound so weakly by this type of receptor.[1]

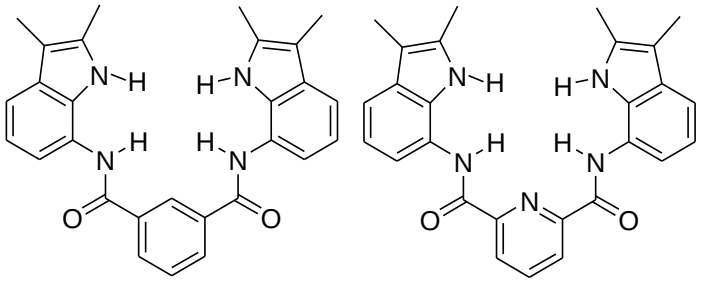

182 **183**

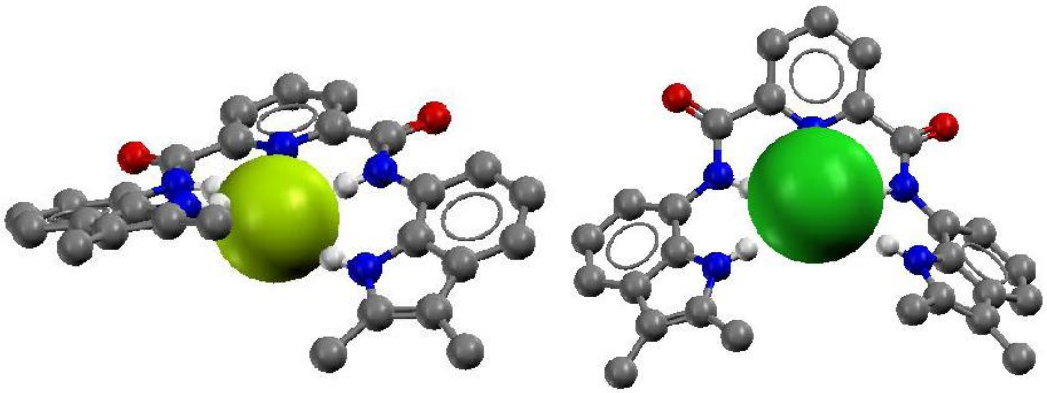

Left Figure 1.3.4.2.3a 1:1 Complex of receptor **183** with fluoride. The space-fitting anion clearly illustrates the size compatibility between the receptor's binding cleft and anion size. **Right Figure 1.3.4.2.3b** 1:1 Complex of receptor **183** with chloride. The space-fitting anion clearly illustrates the decreased size compatibility between the receptor's binding cleft and anion size. Both crystal structures were obtained by Gale and co-workers.

Although Jurczak and co-workers did not test their anion receptor with fluoride, we do see similar binding constants as observed by Gale and co-workers for acetate and dihydrogen phosphate, with selectivity for these anions over chloride. Receptor **184** shows no selectivity for acetate over dihydrogen phosphate. Receptors **185** and **186**, like receptor **183**, show a preference for dihydrogen phosphate over acetate. Receptor **182** sees this trend reversed.[1 3]

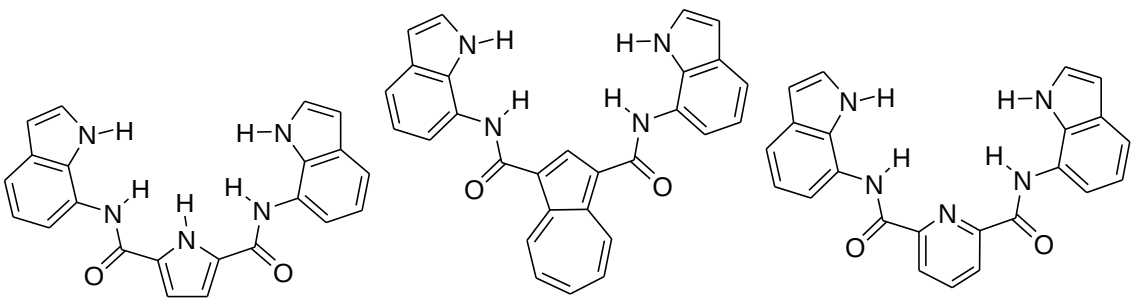

184 **185** **186**

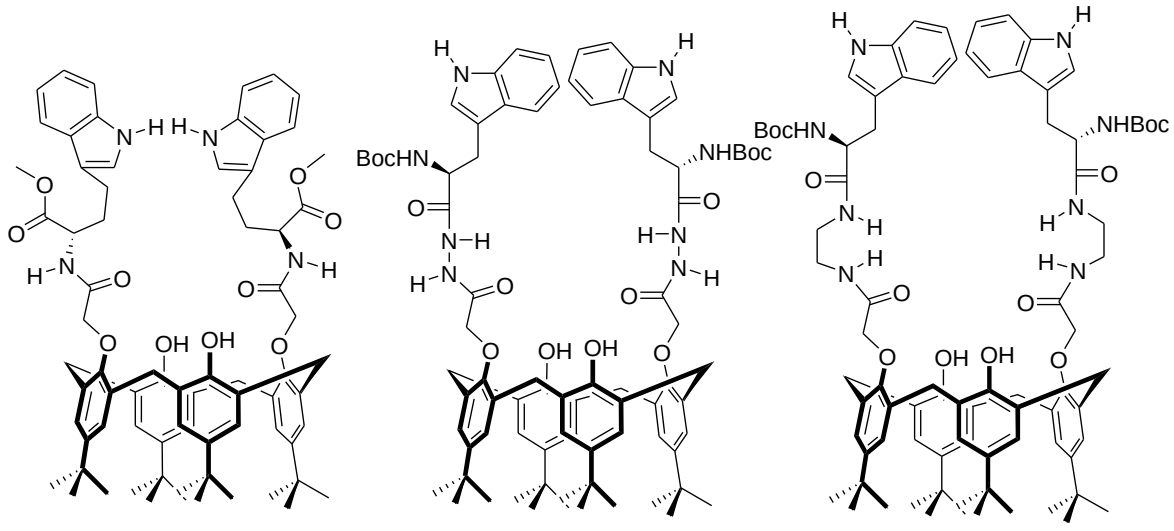

187 **188** **189**

He and co-workers were another group to utilise the calix[4]arene as a scaffold to suspend anion binding groups (*L*-tryptophan). In this case, these groups are chiral-producing receptors (**187-189**) and can be used to fluorescently sense different guest enantiomers. Where needed, the counter cation was TBA and the binding constants were determined by fluorescent titration in DMSO. Job plot ^{1}H NMR studies were carried out to find a 1:1 binding stoichiometry. These three analogues were tested with a range of larger molecules such as malate and tartrate and a range of amino acid derivatives. Receptor **187** showed selective quenching with *D*-alanine anion. A quenching of 48 % was observed with 155 equivalents of *D*-alanine anion, whereas the *L*-alanine anion only exhibited 10 % quenching after addition of 155 equivalents of anion. Receptor **188** shows selective quenching with *D*-malonate. An 88% quenching effect was observed with 165 equivalents of *D*-malonate, compared with an 11 % quenching effect as observed with 180 equivalents of *L*-malonate. The longer links in receptor **189** cause the two indole groups to interact (as the structure is less rigid), forming an excimer. When anions are added, this causes an excitement of fluorescence. Enantiomeric selectivity was shown in particular with *D*-phenylananinol over the *L* enantiomer.[136]

1.3.4.2.2 Indolocarbazole and biindole based receptors

2005 was the first time that indoles made an appearance in anion receptor chemistry in the form of indolocarbazoles. Beer and co-workers synthesised the first set of four indolocarbazoles, **190-193**, with different substituents in the 1, 3, 8 and 10 positions.

The indolocarbazole group is very rigid, forming a highly pre-organised, conjugated system. Binding constants were determined by UV-Vis spectroscopy in MeCN, using the TBA salt of the anion. Job plot and Specfit analysis showed a 1:1 binding stoichiometry in the solution state. A preference was found with all the receptors for benzoate over other halide/oxo-anions tested. This was most pronounced in **193**, which exhibits the largest binding constants because the electron-withdrawing bromide groups in the 3 and 8 positions increase the acidity of the NH bond donor groups. An increase in fluorescence emission was noted with fluoride, chloride and dihydrogen phosphate. Fluorescence quenching was noted with benzoate. No change was seen with hydrogen sulfate. This shows that the indolocarbazole group can be used as an anion sensor. In the solid state crystal structures showed a 1:1 complex of **191** with chloride, (shown in Figure 1.3.4.2.4a) and a 2:1 anion:receptor complex of **191** with fluoride, (shown in Figure 1.3.4.2.4b).[115]

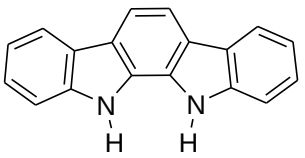

190

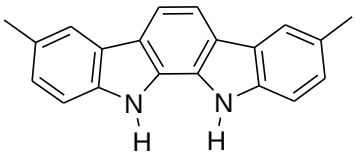

191

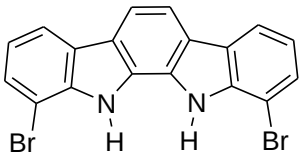

192

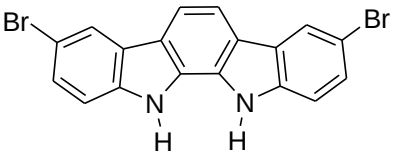

193

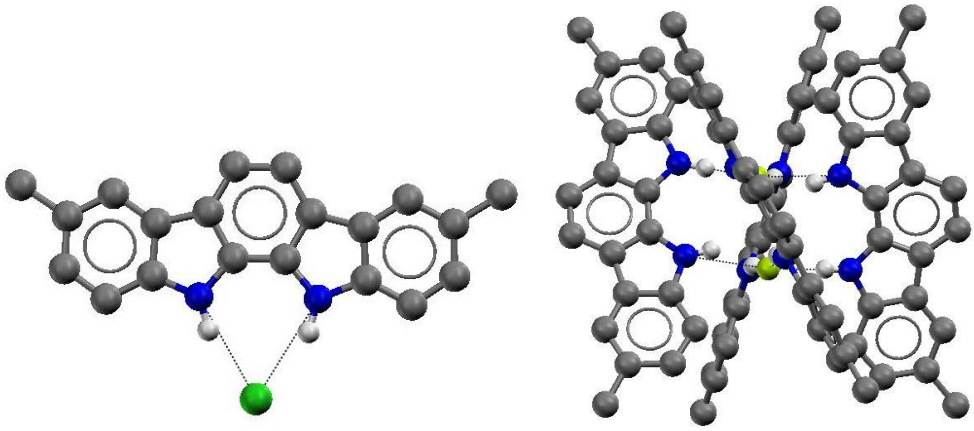

Left Figure 1.3.4.2.4a 1:1 Complex of receptor **191** with chloride. **Right Figure 1.3.4.2.4b** 1:2 Anion:receptor complex of receptor **191** with fluoride. Both crystal structures were obtained by Beer and co-workers.

Jeong and co-workers utilised a similar type of indolocarbazole scaffold. This biindole group of receptors, **194-196**, is more flexible than the indolocarbazole scaffold group and this set of symmetrical cleft receptors contains between two and six hydrogen bond donor groups, created by the addition of amide and urea groups to the biindole scaffold. Binding constants were calculated using UV-Vis titration in DMSO/0.1-0.2 % H_2O and the TBA salt of the anion. A 1:1 binding stoichiometry was confirmed by Job plot experiment. **194** was found to have a very weak affinity for the three anions tested (acetate, dihydrogen phosphate and hydrogen pyrophosphate), coordinating to the anion by two hydrogen bond donor groups of the biindole scaffold. **195**, with two extra amide groups, showed a high affinity for all three anions, with binding constants > 1 x 10^4 M^{-1}. A preference for hydrogen pyrophosphate over dihydrogen phosphate was found, with binding constants of 5.2 x 10^5 M^{-1} and 1.4 x 10^5 M^{-1} respectively. **196**, with six hydrogen bond donor groups exhibits high binding constants across the board, with a greater degree of selectivity shown for hydrogen pyrophosphate (> 6.0 x 10^6 M^{-1}) than dihydrogen phosphate (3.9 x 10^5 M^{-1}). This shows that the larger hydrogen bonding array is more effective in binding the larger anions, utilising all six NH groups. Only four of six NH groups were involved in binding the first equivalent of acetate and dihydrogen phosphate. This receptor was also tested for the ability to bind dicarboxylates such as malonate and adipate and showed binding constants greater than 1 x 10^5 M^{-1} but less than 9 x 10^5 M^{-1} in a DMSO/MeOH 9:1 solution. [137]

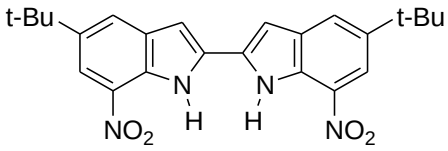

194

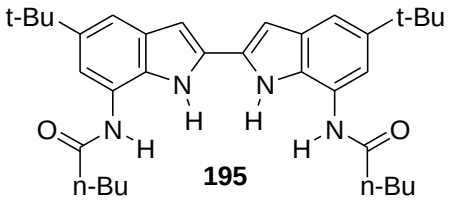

195

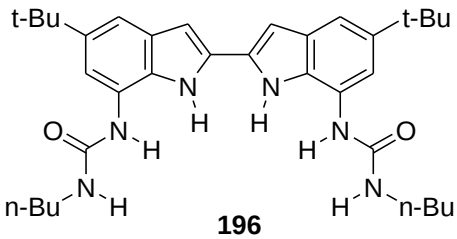

196

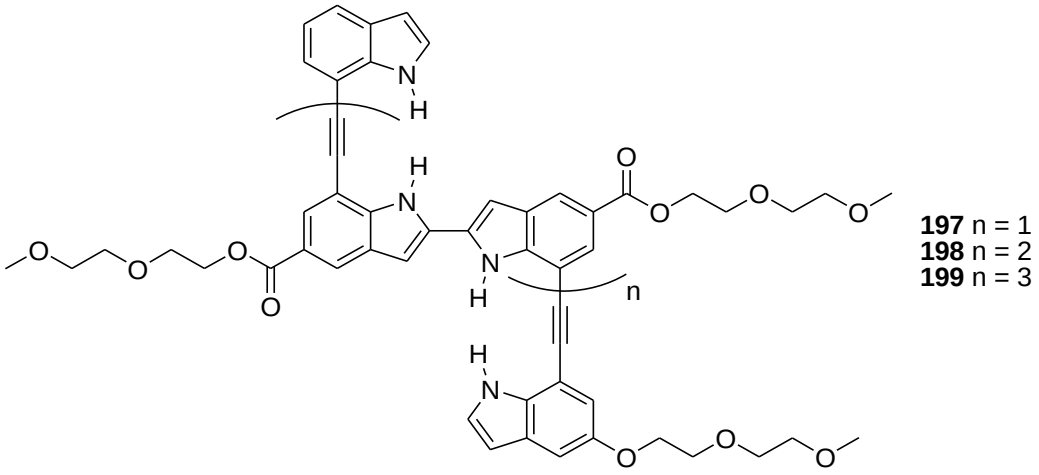

Jeong and co-workers went on to synthesise a range of symmetrical acyclic receptors, based on the diindole/indolocarbazole scaffold but with various appended groups that exhibit different anion binding properties.[138-140] These basic receptors led to the synthesis of more complex, larger receptors that act as foldmers. This means they can helically fold around the anion. The first foldmer receptors utilised the diindole scaffold and contain between one and three of these units. The binding constants for these three receptors, **197-199**, and TBA chloride were calculated by UV-Vis titration in MeCN and a 1:1 binding stoichiometry was confirmed by Job plot. In a 100% MeCN solution, binding constants of 1.3 x 10^5 M^{-1}, 1.2 x 10^6 M^{-1} and > 10^7 M^{-1} were calculated for receptors **197**, **198**, and **199** respectively. By adding 10% H_2O to increase the polarity of the solution, a more accurate binding constant was obtained for receptor **199** as an increase in polarity of solution lowers the binding constant because there is increased competition from the solvation effects. Binding constants could now be accurately calculated as 1.2 x 10^2 M^{-1} and 2.3 x 10^4 M^{-1} for **198** and **199** respectively, showing high binding constants even in this more competitive media. The increase in binding constants for receptors **198** and **199** is due to significant increase in NH bond donor groups and increased turns of the helix.[141,142]

A second type of helical folding receptor (**200**) follows on from previous examples by Jeong and co-workers, this time based on the more rigid indolocarbazole scaffold. Binding constants were determined by fluorescence titration, using the TBA salt of the anion in a MeCN/H_2O solution 9:1. A 1:1 binding stoichiometry was confirmed by Job plot experiments. This helical receptor was shown selectively bind sulfate (640000 M^{-1}) over the other range of anions tested (oxo/halide/cyanide/azide). Chloride is the next most

effectively bound anion, with a binding constant of 8800 M^{-1}. The sulfate anion is bound through all the NH and OH groups but the other anions do not bind through the hydroxyl groups. This difference in binding mode contributes to the difference in binding constants. The fewer hydrogen bonds formed in the anion: receptor complex, the lower the binding constant. This receptor is also able to fluorescently sense the sulfate anion with a fluorescent colour change from blue to green.[143]

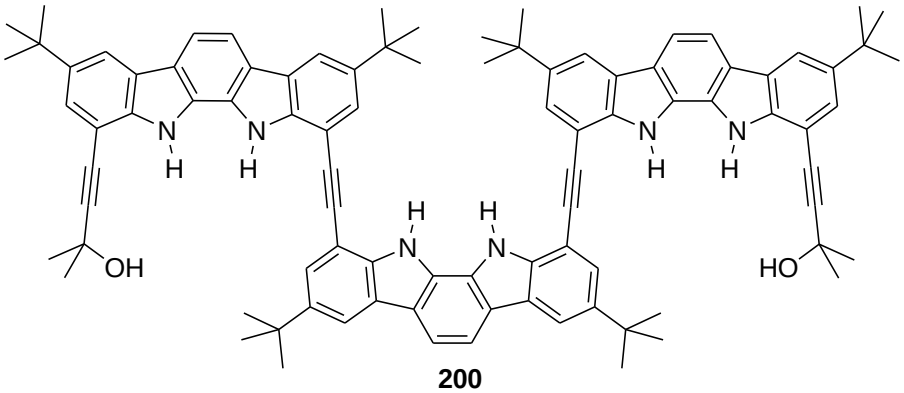

200

Jeong and co-workers have also explored the diindole and indolocarbazole groups in the synthesis of macrocycles **201-203**. These scaffolds make very rigid, square-type macrocycles, each containing four NH bond donor groups that are all involved in the binding process. Binding constants were calculated by UV-Vis titration in MeCN with the TBA salt of the anion. Binding stoichiometry was confirmed by Job plot experiment. Of the various anions tested (oxo/halide/cyanide/azide), fluoride was found to be the most effectively bound by approximately two orders of magnitude (2.0×10^8 M^{-1} and 5.6×10^8 M^{-1} for receptors **201** and **202** respectively). The calculated binding constants were similar for both receptors and the trend in anion binding seemed to be based on basicity and size of the anion because the smaller anions were also more effectively bound. These receptors were found to be able to act as chemosensors as the different anions produce different ^1H NMR chemical shifts; as all the binding processes observed are in slow exchange, qualitative and quantitative information about the species and the concentration of anion can be derived. Although most of the anions tested show a straight forward 1:1 binding complex, the larger spherical anions (bromide and iodide) are too large to fit into the cavity of the macrocycle and so are just able to perch on top of the macrocycle. This leads to a 1:2 anion:receptor binding event where the anion and receptor forms a sandwich complex.[116]

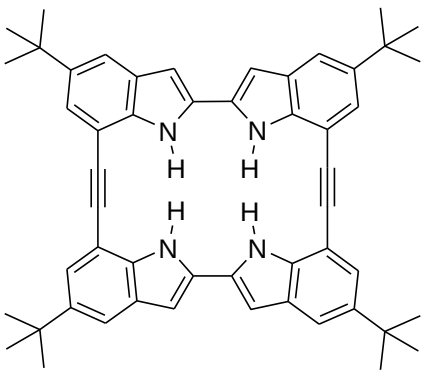

201

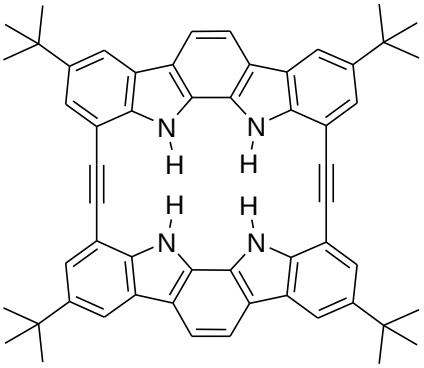

202

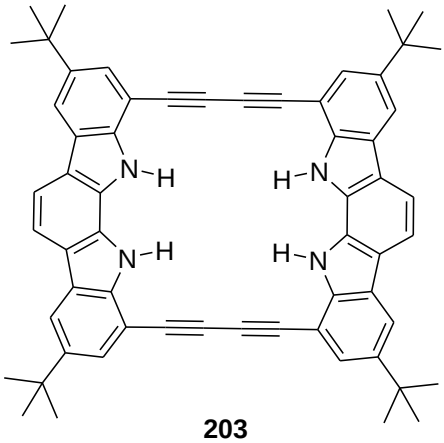

203

The slightly larger macrocycle **203** was synthesised by two years later. Binding constants and stoichometries were determined as before. However, in this case, the binding constants were calculated in a more polar acetone:MeOH 9:1 solution. Comparative studies were also undertaken with receptor **202**. The more competitive solvent conditions resulted in a decrease in binding constants for **202** and formation of more 2:1 anion:receptor complexes. A change in the trend of anion binding was also observed with receptors **202** to **203**. Higher binding constants were observed with iodide: receptor **203** complex (with binding constants 2400 M^{-1} and < 10 M^{-1} for **202** and **203** respectively) but chloride was bound less efficiently by the larger receptor, with binding constants of 1800 M^{-1} and 430 M^{-1} for receptors **202** and **203** respectively. Except for chloride, an increase in binding constant for all anions tested was observed with receptor **203**. The major reason for this is the increase in cleft size of the receptor, which allows the larger anion to better fit into the cleft, optimising the hydrogen bonding interactions. This is illustrated in the crystal structures shown in Figures 1.3.4.2.5a and b. Azide is able to bind side-on instead of end-

on in the larger cavity, optimising the hydrogen bonding interactions and therefore increasing the binding constant.[144]

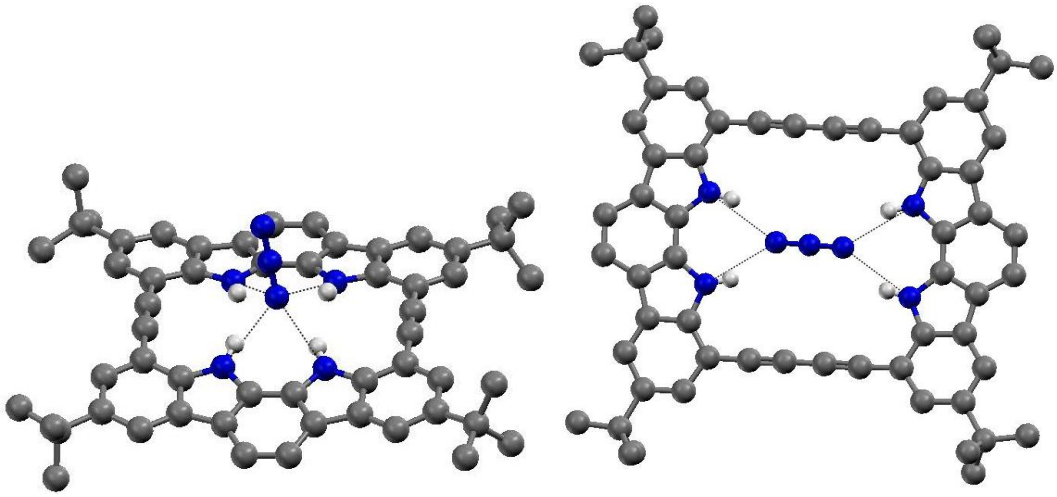

Left Figure 1.3.4.2.5a 1:1 Complex of receptor **202** with azide, showing end-on binding as the receptor's cavity is too small for side-on binding. **Right Figure 1.3.4.2.5b** 1:1 Complex of receptor **203** with azide, showing side-on binding as the receptor's cleft is now large enough to accommodate the anion. Both crystal structures were obtained by Jeong and co-workers.

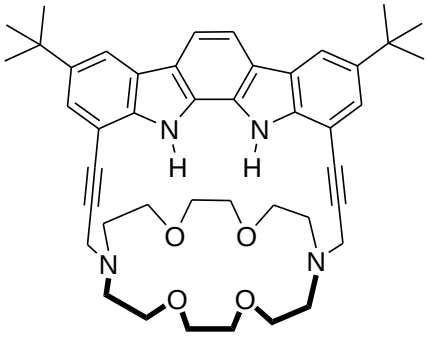

204

Jeong and co-workers have also utilised the indole carbazole group, attaching it as a strap to create to a diazocrown ether as an ion pair receptor (**204**). The crown ether is responsible for binding the cation and the indolocarbazole group is responsible for binding the anion. Binding constants were determined by ^{1}H NMR titration in CD_3CN/DMSO-d_6 9:1 with the TBA, Na, Li and K salts of chloride, bromide and iodide. Job plot experiment confirmed a 1:1 binding stoichiometry of anion:receptor. Anion binding was found to be dramatically enhanced with the addition of an alkali metal in the order of $Na^+ > K^+ > Li^+$, due to electrostatic interactions with the anion; the sodium alkali metal cation optimises

the inter-ionic distance and charge density interactions with the anion, leading to the larger increases in binding constant. The addition of a different cation does not alter the binding trend $Cl^- > Br^- > I^-$.[145]

Beer, Davis and co-workers have recently shown that, using sulfate templetation, indolocarbazole can be used to synthesise a pseudorotaxane, (**206**). ^1H NMR titrations with unsubstituted indolocarbazole, (**190**) in CD_3CN show the initial formation of a strong 1:2 anion:receptor complex formation. One of the indolocarbazole receptors was then replaced by a simple neutral isophthalamide based macrocycle, (**205**). This used the two NH bond donor groups in the macrocycle to coordinate to two oxygen atoms of the tetrahedral sulfate anion. The indolocarbazole was then threaded through the macrocyclic ring and held in place by hydrogen bonding to the remaining two oxygen atoms on the sulfate anion from the two NH bond donor groups. This process is shown in Scheme 1.3.4.2.1[146]

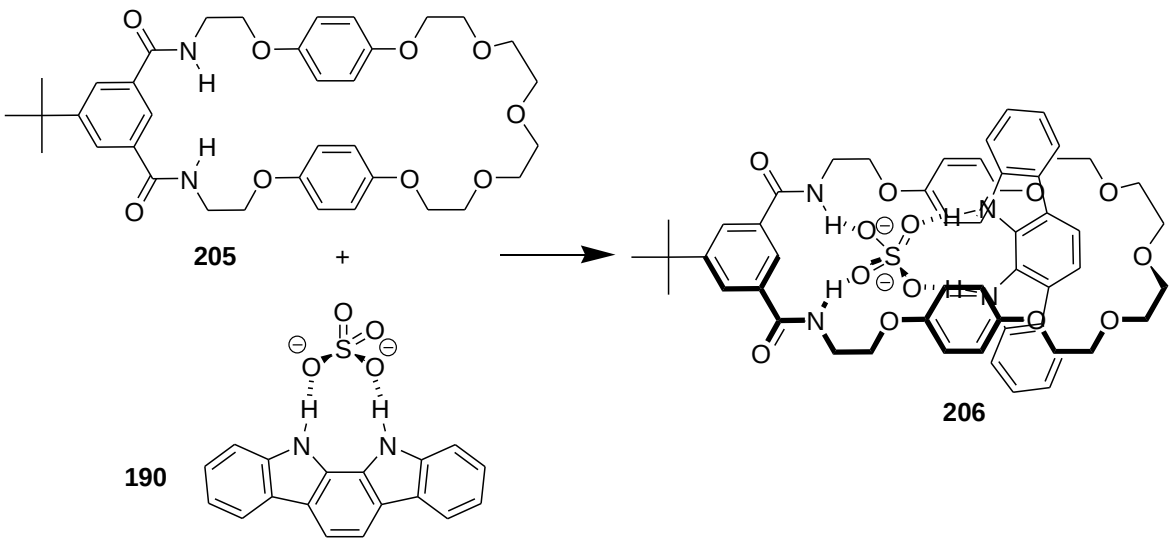

Scheme 1.3.4.2.1

Fang and Chou and co-workers used an extended diindole scaffold to synthesise a receptor (**207**) that is a selective chemosensor for fluoride. Binding with the fluoride ion produces both fluorescent and colorimetric changes that are visibly detected. This receptor was studied in DMSO with the TBA salt of the anion and a 1:1 binding conformation was determined from Job plot analysis. A green/yellow colour is observed with the receptor in DMSO. Addition of a wide range of different anions gave no change in colour except when the fluoride anion was used, when the colour changed from green/yellow to red. This

colour change was due to the deprotonation of the receptor by the fluoride anion. This process can be seen in Scheme 1.3.4.2.2.[147]

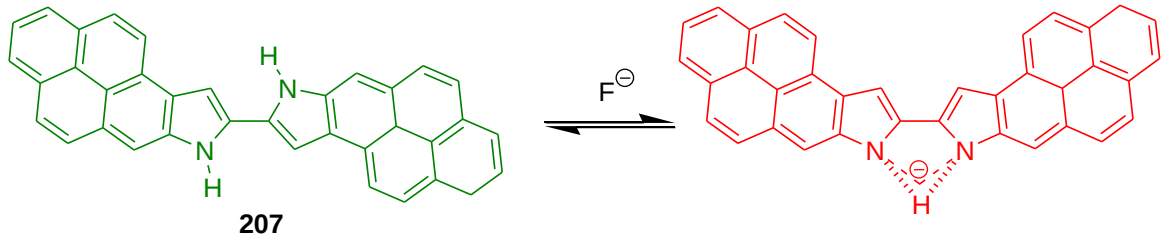

207

Scheme 1.3.4.2.2

1.4 Aims of this thesis

In this chapter, I have attempted to introduce and illustrate the importance of supramolecular chemistry, focusing upon the interactions between synthetic, neutral receptors and anions. From the broad range of examples synthesised and explored by many researchers from all over the world, I hope to have shown that hydrogen bond donating based anion receptors are one of the most important groups of synthetic molecules that can be used for the effective and selective binding and sensing of a broad range of anions.

I have demonstrated that there are a wide range of hydrogen bond donating groups that are used to construct anion receptors, with specific properties based on the hydrogen bond donating array. I have also shown that the presence of multiple hydrogen bond donating groups contained within a neutral receptor can effectively bind anions in a highly competitive environment.

In this thesis, I will discuss the synthesis, characterisation and anion binding properties of simple acyclic indole/carbazole based receptors, splitting them into the following groups for ease of comparison and increasing complexity of experimental results;

- Simple cleft receptors, containing three to four hydrogen bond donating groups, based on indole/carbazole moieties linked by urea/ thiourea functionalities.
- Extended symmetrical cleft receptors, containing between six and eight hydrogen bond donating groups, based on indole/carbazole moieties linked by amide and urea functionalities.

- Tripodal three dimensional receptors, containing between six and fifteen hydrogen bond donating groups, based on TREN and ‘Pin-wheel’ scaffolds.
- Simple symmetrical indole- and amide-based receptors, containing four to five hydrogen bond donor groups and comparing the effects of flexible and rigid spacers and electron-withdrawing groups.

Chapter 2 - Simple Urea And Thiourea Based Anion Receptors

2.1 Introduction

Urea and thiourea groups have been used extensively in anion binding scaffolds since the relatively early examples of synthetic anion receptor chemistry.[148,149] Sets of receptors have been synthesised that compare the roles of urea and thiourea functionalities directly in anion binding events[58 59 72]. As can be seen in Figure 1.3.4.2, interest has grown in the hydrogen bond donating group contained in the indole/carbazole aromatic skeleton over recent years. Initiated by the work of Jurczak and co-workers[114], these functionalities have been further explored by the groups of Gale[2], Jeong [116,118,137-139,141,143]and Beer[115], amongst others.

The set of receptors described in this chapter, which contain three to four NH bond donor groups, explore low molecular weight, anion binding clefts with hydrogen bond donating groups from indole/carbazole groups linked by urea/thiourea functionalities. These simple receptors explore the binding affinity, selectivity and fluorescence properties of a range of oxo-anions with these simple receptors, depending on the combination of urea, thiourea, indole or carbazole moieties.

2.2 Symmetrical diindolylurea hydrogen bond donating clefts

The work from this section of Chapter Two has been published previously[150,151]. Previous work from Gale and co-workers has shown that the incorporation of indole into the scaffolds of various groups of receptors leads to the selective binding of fluoride[1] and oxo-anions[2]. These oxo-anion receptors show limited use of the hydrogen bond donating groups as not all the NH bond donor groups are used fully in the coordination of some anions. This was seen both in the solution and solid phase experiments. The main functional parts of these receptors are the central urea-linked indole group. In collaboration with Claudia Caltagirone, a group of four symmetrical receptors was synthesised,

containing two indole groups joined by a urea functionality to improve selectivity for the oxo-anions and remove redundant parts of the parent receptor. The parent receptor was synthesised previously by Gale and co-workers (Scheme 2.2.1) but the new receptors were originally designed to selectively bind dihydrogen phosphate over other halide and oxo-anions in highly competitive solvent environments. It was hoped to improve on the previous receptors synthesised by Gale and co-workers [2] and the 1,3-diphenylurea (**208**) originally synthesised by Sitzmann and co-workers[152]. The binding constants for receptors **180**[2] and **208**[18]were calculated by Gale and co-workers using ^{1}H NMR titration studies in DMSO-d_6/0.5% H_2O with various TBA salts of halide and oxo-anions as shown in Table 2.2.1.

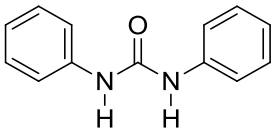

208

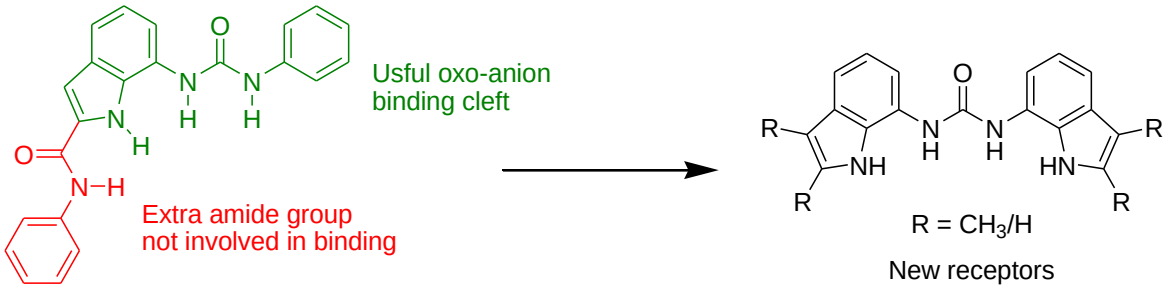

180

Scheme 2.2.1

Table 2.2.1 Anion binding constants (M^{-1}) for receptors **180** and **208**, measured in DMSO-d_6/0.5% H_2O at 298 K. Error not estimated to be more than ±15% for the simple **208**[18] and no more than ± 12% for receptor **180**[2]. Anionic guests were added as the TBA salt, with binding constants determined by ^1H NMR titration following the urea NH, fitting data to a 1:1 binding model using WINEQNMR[153].

Anion	208	180
$CH_3CO_2^-$	1260	10000
$H_2PO_4^-$	523	4950
$C_6H_5CO_2^-$	674	4460
Cl^-	31	38

2.2.1 Synthesis

The majority of the original synthesis of receptors **209** and **210** was designed by Claudia Caltagirone. Receptors **209** and **210** were synthesised by the two step process shown in Scheme 2.2.1.1, the first step being the reduction of the appropriate nitroindole to produce the relevant amine. Receptors **209** and **210** were then prepared by the reaction of this amine with triphosgene in a two-phase solution of saturated $NaHCO_3$ and DCM. The crude product was purified by a recrystallisation from methanol. Receptors **209** and **210** were isolated in 78% and 50% yields respectively.

The reduction of 1,3-dimethyl-7-nitroindole and 7-nitroindole was originally effected by the use of ninhydrin as the hydrogen source with a Pd/C 10% catalyst[2]. However after the original synthesis, reduction with hydrogen gas became the preferred method of hydrogenation because reaction completion was achieved in a much shorter period of time and the reaction workup was easier.

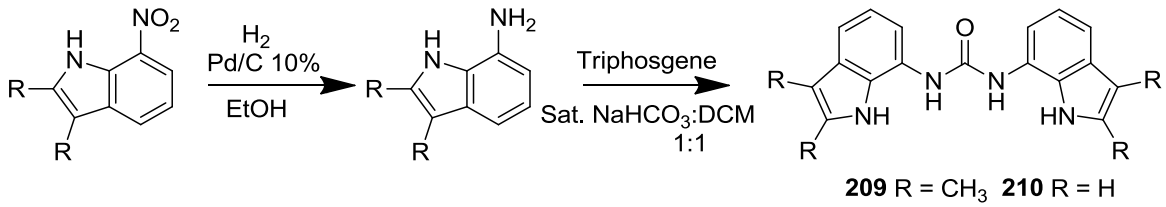

Scheme 2.2.1.1

2.2.2 Solution phase analysis

2.2.2.1 Proton NMR titration data

Anion binding constants for a wide range of anions were calculated for receptors **209** and **210**. The binding constants were determined by ^{1}H NMR titration with the TBA or TEA salt of the anion in various DMSO-d_6/H_2O solutions. Binding constants were determined by the computer program WINEQNMR[153] and fitted to a 1:1 binding model. Some Job plots[154] were produced to check the 1:1 binding mode that was strongly suggested by the titration data. The majority of the binding constants were generated by Claudia Caltagirone, with the majority of the binding stoichometries being determined by myself. Binding constants and Job plots were determined by following the downfield shift of the urea NH.

Table 2.2.2.1 Anion binding constants (M^{-1}) and percentage error for receptor **209**, measured in DMSO-d_6 and varying concentrations of water at 298 K. Anionic guests were added at the TBA salt of the anion with the exception of bicarbonate, which was added as the TEA salt of the anion. Binding constants were determined by ^{1}H NMR titration following the urea NH, fitting data to a 1:1 binding model using WINEQNMR.[153]

Anion	**DMSO-d_6/0.5% H_2O**	**E (%)**	**DMSO-d_6/10% H_2O**	**E (%)**	**DMSO-d_6/25% H_2O**	**E (%)**
$CH_3CO_2^-$	$>10^4$	-	567	6	a	-
$H_2PO_4^-$	$>10^4$	-	4790	4	a	-
HSO_4^-	50	10				
$C_6H_5CO_2^-$	$>10^4$	-	736	7	a	-
Cl^-	128	1	16	3		
[b]HCO_3^-	$>10^4$	-	545	4	a	-

a – No binding constant could be calculated due to the precipitation of the receptor/anion complex. [b] Added as the TEA salt of the anion.

The results of the anion binding studies with receptor **209** are shown in Table 2.2.2.1. In DMSO-d_6/0.5% H_2O, receptor **209** was found to bind the oxo-anions acetate, benzoate and dihydrogen phosphate strongly, with binding constants > 10^4 M^{-1}, and also showed an increase in affinity for the oxo-anions when compared to the receptors tested previously by Gale and co-workers[18] (Table 2.2.1). Exact numbers could not be calculated due to the limitations of the technique employed when working with binding constants >10^4 M^{-1}. Lower binding constants of 128 M^{-1} and 50 M^{-1} were calculated for chloride and hydrogen sulfate. It was found that all four of the NH groups were involved binding each of the anions. This can be seen by the downfield shift observed with all NH resonances involved in binding the anion.

As the binding constants observed with acetate, benzoate and dihydrogen phosphate were too high to measure in a DMSO-d_6/0.5% H_2O solution, exact binding constants were obtained in a more competitive DMSO-d_6/10% H_2O solution. All four NH bond donor groups were again observed to be binding the anions, forming a 1:1 complex. Increasing the polarity of the solution by increasing the percentage of water in solution created a more competitive environment, lowering the affinity of the anion to the receptor, thus giving smaller binding constants. This could be seen from the downfield shift of these resonances in the ^{1}H NMR titration data. High binding constants were observed with acetate (567 M^{-1}), benzoate (736 M^{-1}) and dihydrogen phosphate (4790 M^{-1}). Small binding constants were calculated for the halide anion, chloride (16 M^{-1}). Selectivity was observed for dihydrogen phosphate over the other carboxylate and halide anions, unlike the anion binding trends observed previously in the case of receptor **208** by Gale and co-workers[2], where acetate was selectively bound over dihydrogen phosphate (Table 2.2.1). An attempt was made to observe anion binding events in DMSO-d_6/25% H_2O. However, although receptor **209** was soluble in this solution, precipitation of the anion/receptor complex was observed upon addition of the TBA salt of anion to the receptor solution. This made monitoring any binding events in solution impossible.

Although the results from the bicarbonate anion cannot be directly compared because of the different counter ion (TEA), similar binding constants were observed as with the other carboxylate anions. A binding constant >10^4 M^{-1} was determined for TEA bicarbonate and receptor **209** in a DMSO-d_6/0.5% H_2O solution and 545 M^{-1} in a DMSO-

d_6/10% H_2O solution. Precipitation of the anion complex was seen in a DMSO-d_6/25% H_2O solution.

An analogous set of ^1H NMR titration experiments was then performed with receptor **210** and these results can be seen in Table 2.2.2.2. All four NH bond donor groups are involved in binding the anions in the various titration solutions. The participation of all four NH bond donor groups was shown by the downfield shift of the NH resonances in the ^1H NMR titration experiments. This receptor was again found to bind all anions in the variety of DMSO-d_6/H_2O solutions in a 1:1 binding stoichiometry. In DMSO-d_6/0.5% H_2O, the calculated binding constants are almost identical to those observed for receptor **209**, with binding constants $<10^4$ M^{-1} observed for oxo-anions acetate, benzoate and dihydrogen phosphate and much lower affinities observed with chloride (128 M^{-1}) and hydrogen sulfate (23 M^{-1}). Binding studies were repeated in a more competitive, polar DMSO-d_6/10% H_2O solution, allowing the calculation of precise binding constants for acetate, benzoate and dihydrogen phosphate. As with the previous receptor **209**, receptor **210** shows a low affinity for chloride (17 M^{-1}), moderate affinity for both acetate (774 M^{-1}) and benzoate (521 M^{-1}) and strong selective binding for dihydrogen phosphate (5170 M^{-1}). The loss of the four methyl groups of receptor **209** does cause some subtle alterations in binding strength and trend.

Receptor **210** has a higher affinity for dihydrogen phosphate over the other anions. Receptor **209** exhibits a trend in anion binding as follows:

$$H_2PO_4^- > OBz^- > OAc^- > Cl^-$$

Receptor **210** exhibits the following binding trend, exchanging the position of acetate and benzoate when compared to receptor **209**:

$$H_2PO_4^- > OAc^- > OBz^- > Cl^-$$

The loss of the four methyl groups in receptor **210** also made it possible to obtain binding constants in a DMSO-d_6/25% H_2O solution as there was no precipitation of the anion/receptor complex. Binding constants of 160 M^{-1} and 20 M^{-1} were calculated for dihydrogen phosphate and acetate respectively. The selective binding of dihydrogen phosphate over acetate is still observed, with a similar magnitude to that observed in the less polar DMSO-d_6/10% H_2O solution. Even in this highly competitive environment (DMSO-d_6/25% H_2O), we still see a moderate binding affinity with dihydrogen phosphate

and a 1:1 binding stoichiometry by this small neutral molecule. This is illustrated in the Job plot shown in Graph 2.2.2.1.

Table 2.2.2.2 Anion binding constants (M^{-1}) and percentage error for receptor **210**, measured in DMSO-d_6 and varying concentrations of water at 298 K. Anionic guests were added as the TBA salt of the anion with the exception of bicarbonate, which was added as the TEA salt of the anion. Binding constants were determined by ^{1}H NMR titration following the urea NH, fitting data to a 1:1 binding model using WINEQNMR[153].

Anion	**DMSO-d_6/0.5% H_2O**	**E (%)**	**DMSO-d_6/10% H_2O**	**E (%)**	**DMSO-d_6/25% H_2O**	**E (%)**
$CH_3CO_2^-$	$>10^4$	-	774	3	20	7
$H_2PO_4^-$	$>10^4$	-	5170	5	160	5
HSO_4^-	23	9				
$C_6H_5CO_2^-$	$>10^4$	-	521	6	a	-
Cl^-	128	3	17	3		
[b]HCO_3^-	9580	11	699	4	42	8

a – No binding constant could be calculated due to the precipitation of the receptor/anion complex. [b] Added as the TEA salt of the anion.

Although bicarbonate cannot be directly compared because of the different counter ion, similar binding constants were obtained as with the other carboxylate anions. A binding constant 9580 M^{-1} was determined for bicarbonate in a DMSO-d_6/0.5% H_2O solution, 699 M^{-1} in a DMSO-d_6/10% H_2O solution and 42 M^{-1} in a DMSO-d_6/25% H_2O solution. Although a higher binding constant was observed with bicarbonate and receptor **209** over receptor **210** in a DMSO-d_6/0.5% H_2O solution, it is receptor **210** that exhibits the slightly stronger binding affinity with this anion in the more competitive DMSO-d_6/10% H_2O solution.

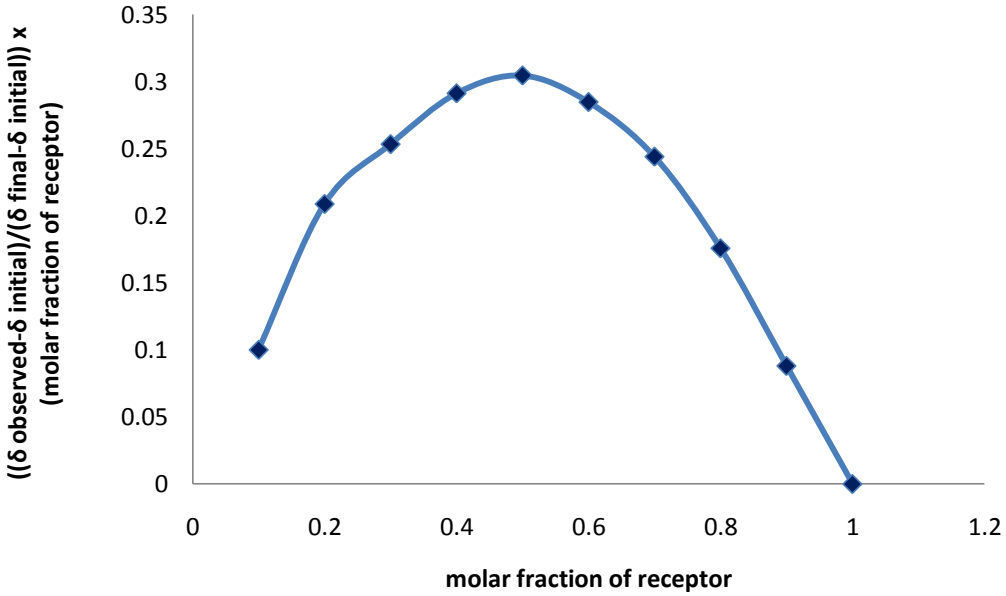

Graph 2.2.2.1 Job plot[154] of receptor **210** in a DMSO-d_6/25% H_2O solution at 298 K. Dihydrogen phosphate guest was added as the TBA salt with 1:1 binding stoichiometry determined by ^{1}H NMR following the urea NH.

2.2.3 Solid phase analysis

X-ray quality crystals of receptor **209** with TBA benzoate were produced by Claudia Caltagirone and were obtained by slow evaporation of a DMSO solution of receptor **209** with an excess of TBA benzoate.

The crystal structure obtained by single crystal X-ray diffraction is shown in Figure 2.2.3.1. The crystal structure shows a 1:1 binding stoichiometry as observed in the solution state, with the anion coordinated to the receptor by four hydrogen bonds, one from each of the NH bond donor groups. Each of the oxygen atoms of the benzoate anion is bound to the receptor by two hydrogen bonding interactions, one from the urea and one from the indole functionality. The hydrogen bonding interactions and hydrogen bonding angles for the benzoate complex, shown in Figure 2.2.3.1, are shown in Table 2.2.3.1. The hydrogen bonds from the nitrogen atoms of the receptor to the oxygen atoms of the anion range from N···O = 2.846(8)-2.907(8) Å and the bond angles range from N–H···O = 159.2°-175.7°.

Table 2.2.3.1 Hydrogen bonding table for crystal structure of receptor **209** and TBA benzoate that is shown in Figure 2.2.3.1, obtained by single crystal X-ray diffraction at 120K. *D* – hydrogen bond donor atom. *A* – hydrogen bond acceptor atom. *d* – distance in Å. ∠ - bond angle in °. H – hydrogen atom.

D–H···*A*	*d*(*D*–H) (Å)	*d*(H···*A*) (Å)	*d*(*D*···*A*) (Å)	∠(*DHA*) (°)
N1–H1···O3	0.88	2.00	2.846(8)	161.0
N2–H2···O3	0.88	2.04	2.907(8)	168.7
N3–H3···O2	0.88	1.99	2.866(8)	175.7
N4–H4···O2	0.88	2.06	2.902(8)	159.2

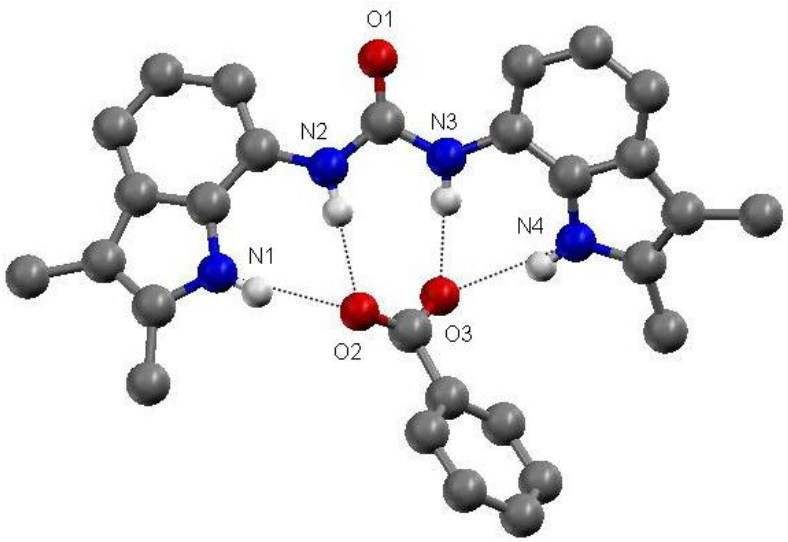

Figure 2.2.3.1 The benzoate complex of receptor **209**. Single X-ray crystal structure with TBA benzoate. The aromatic CH hydrogen atoms and the TBA counter ion have been omitted for clarity.

X-ray quality crystals of receptor **209** and TEA carbonate were produced by Claudia Caltagirone and were obtained by slow evaporation of an excess of the TEA bicarbonate and receptor from DMSO.

The structure of receptor **209**, produced by single crystal X-ray diffraction, is shown in Figure 2.2.3.2. This crystal structure shows a 1:2 anion:receptor binding stoichiometry, which differs from that observed in the solution state. A clear 1:1 binding conformation is observed in ^{1}H NMR studies with a DMSO-d_6/0.5% and 10% H_2O solution and TEA bicarbonate for both receptors **209** and **210**. Whereas, in the solid state, all eight NH bond donor groups of two receptors are involved in forming hydrogen bonds

to the single anion. The single anion is in the centre of the complex and is bound as the deprotonated carbonate anion. This deprotonation is the result of the crystallisation effects that cause the association of two receptors with a signal anion. The additional interactions from four further hydrogen bond donor groups cause the deprotonation of the bound anion. This is further discussed in Chapter Three. O3 and O5 are bound to the two receptors by three hydrogen bonds, two from the indole NH groups and one from the urea NH. O4 is bound to the receptors by two hydrogen bonds, both from a urea group. The hydrogen bonding interactions and hydrogen bonding angles for the complex shown in Figure 2.2.3.2 are shown in Table 2.2.3.2. The hydrogen bonds from the nitrogen atoms of the receptor to the oxygen atoms of the anion range from N···O = 2.739(2) - 2.9382(16) Å and the bond angles range from N–H···O = 151.3°-175.1°.

Table 2.2.3.2 Hydrogen bonding table for the complex shown in Figure 2.2.3.2 for crystal structure of receptor **209** and TEA carbonate, obtained by single crystal X-ray diffraction at 120K. *D* – hydrogen bond donor atom. *A* – hydrogen bond acceptor atom. *d* – distance in Å. ∠ - bond angle in °. H – hydrogen atom.

D–H···*A*	*d*(*D*–H) (Å)	*d*(H···*A*) (Å)	*d*(*D*···*A*) (Å)	∠(*DHA*) (°)
N6–H96···O4	0.995(18)	1.778(18)	2.739(2)	161.3(15)
N1–H91···O3	1.09(2)	1.726(19)	2.7865(19)	162.9(19)
N2–H92···O3	0.95(2)	1.84(2)	2.791(2)	175.1(14)
N3–H93···O5	0.805(18)	2.009(17)	2.805(2)	169.7(15)
N7–H97···O4	0.972(17)	1.881(18)	2.774(2)	151.3(16)
N8–H98···O3	0.79(2)	2.18(2)	2.915(2)	155(2)
N4–H94···O5	0.856(16)	2.099(16)	2.9382(16)	167(2)
N5–H95···O5	0.818(19)	2.109(19)	2.878(2)	156.6(17)

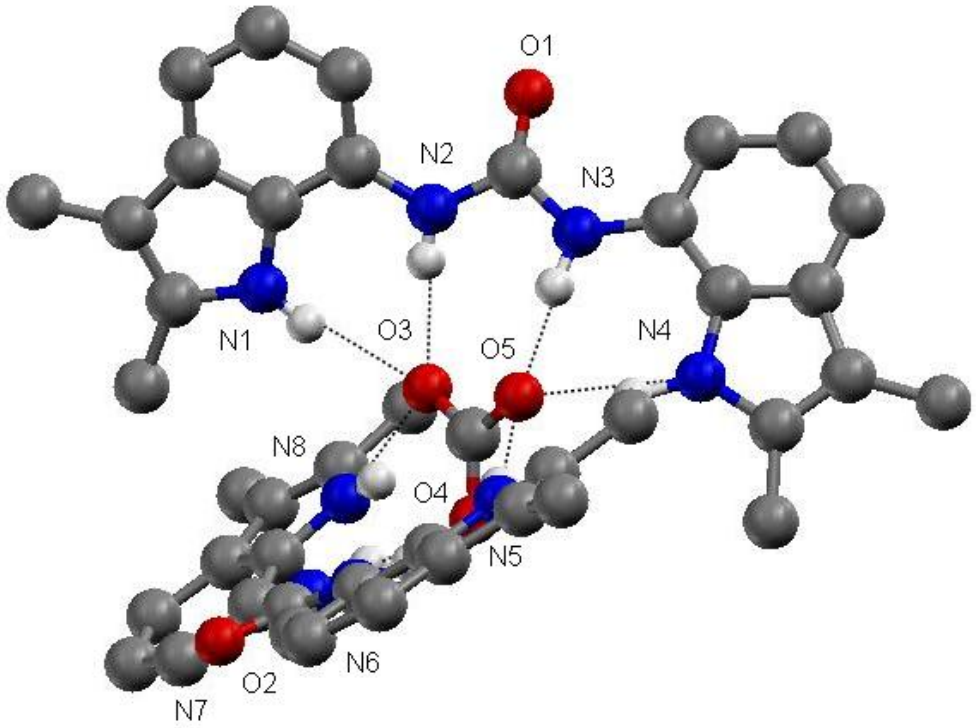

Figure 2.2.3.2 The carbonate complex of receptor **209**, produced by single crystal X-ray diffraction. The aromatic CH hydrogen atoms and the TEA counter ion have been omitted for clarity. Crystal was obtained from a DMSO solution containing receptor **209** and TEA bicarbonate.

X-ray quality crystals of receptor **210** and TBA phosphate were obtained by Claudia Caltgirone from a titration solution of receptor **210** with approximately six equivalents of TBA dihydrogen phosphate in DMSO-d_6/25% H_2O.

The structure of receptor **210** produced by single crystal X-ray diffraction is shown in Figure 2.2.3.3a and b. This complex shows a 1:3 anion:receptor stoichiometry, with all twelve NH bond donor groups coordinating to the four oxygen atoms of a single phosphate anion through the formation of twelve hydrogen bonds. From Job plot analysis (Graph 2.2.2.1), it is clear that, in a DMSO-d_6/25% H_2O solution, a 1:1 dihydrogen phosphate/receptor complex is formed. However, as with the carbonate complex (shown in Figure 2.2.3.2), single deprotonation of the bound anion is observed but in this case, there is a double deprotonation of the dihydrogen phosphate anion. As before, this phenomenon is a result of the crystallisation effects that cause three receptors to coordinate to a single anion and the twelve acidic hydrogen bonds formed from the receptor to the anion cause the deprotonation of the bound anion (see Chapter Three for further explanation). Each oxygen atom of the phosphate anion is bound to the receptor by three hydrogen bonds. O2

is bound by three indole NHs, one from each of the receptors. The remaining three oxygen atoms of the phosphate ion are bound by two urea NHs from one receptor and a third NH bond from the indole group of a second receptor. A helix is formed by the three receptors around the phosphate anion. The hydrogen bonding interactions and hydrogen bonding angles for Figure 2.2.3.3a and b are shown in Table 2.2.3.3. The hydrogen bonds from the nitrogen atoms of the receptor to the oxygen atoms of the anion range from N···O = 2.722(3) – 3.406(3) Å and the bond angles range from N–H···O = 140°-169°.

Table 2.2.3.3 Hydrogen bonding table for crystal structure, shown in Figure 2.2.3.3, of receptor **210** and TBA phosphate, obtained by single crystal X-ray diffraction at 120K. *D* – hydrogen bond donor atom. *A* – hydrogen bond acceptor atom. *d* – distance in Å. ∠ - bond angle in °. H – hydrogen atom. Symmetry transformations used to generate equivalent atoms: (i) –y+1,x–y,z (ii) –x+y+1,–x+1,z

D–H···*A*	*d*(*D*–H) (Å)	*d*(H···*A*) (Å)	*d*(*D*···*A*) (Å)	∠(*D*H*A*) (°)
N1–H91···O2	0.882(18)	1.905(19)	2.762(3)	163(3)
N2–H92···O3^{ii}	0.878(17)	1.95(3)	2.756(3)	152(4)
N3–H93···O3	0.885(17)	2.68(4)	3.406(3)	140(4)
N4–H94···O3	0.888(2)	1.884(2)	2.722(3)	169(3)
N3–H93···N4	0.885(17)	2.52(5)	2.924(3)	108(4)

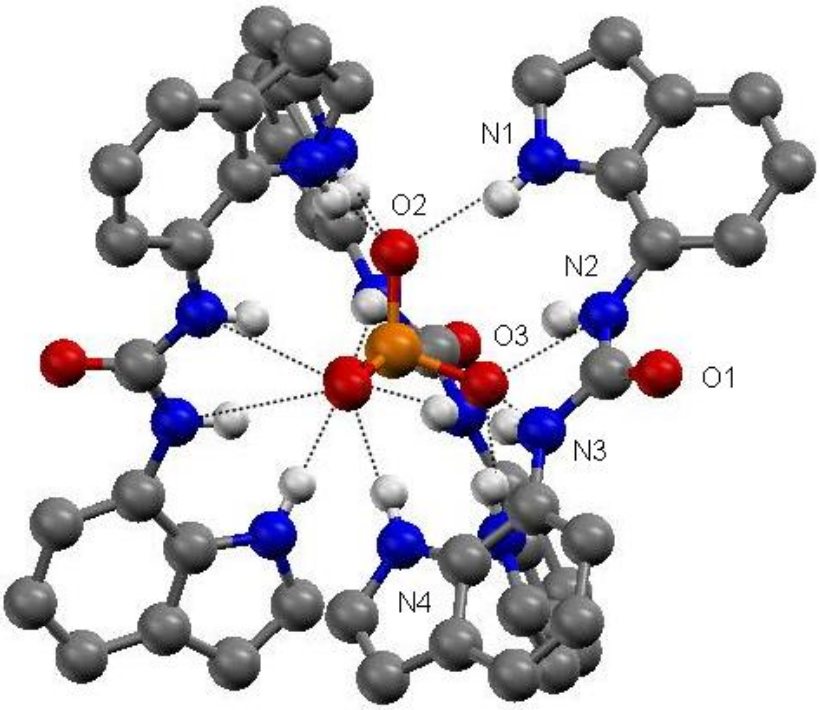

Figure 2.2.3.3a The phosphate complex of receptor **210**. Single X-ray crystal structure with TBA phosphate. The aromatic CH hydrogen atoms, solvent molecules and the TBA counter ion have been omitted for clarity.

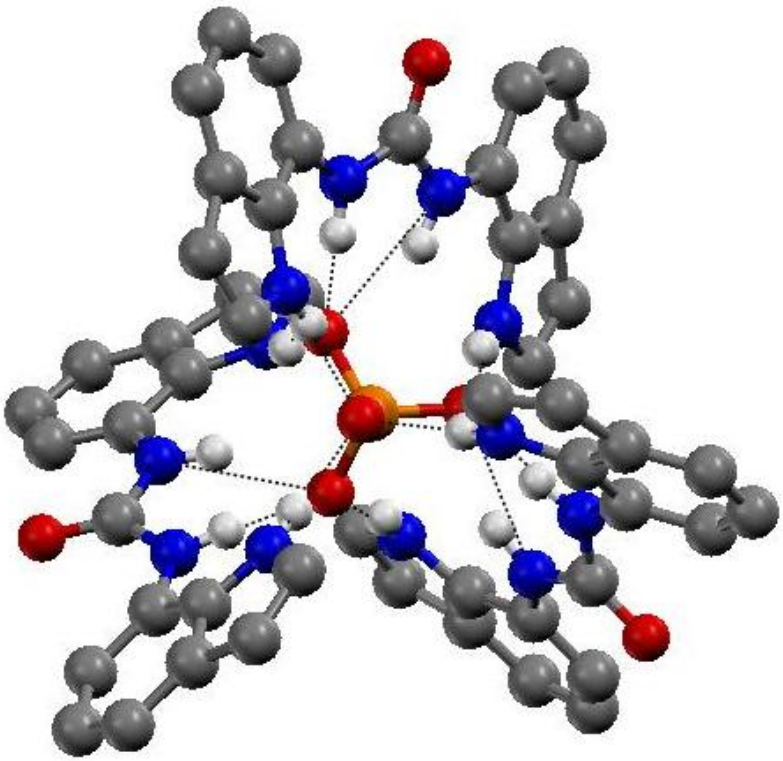

Figure 2.2.3.3b Top view. The phosphate complex of receptor **210**. Single X-ray crystal structure with TBA phosphate. The aromatic CH hydrogen atoms, solvent molecules and the TBA counter ion have been omitted for clarity

2.3 Symmetrical diindolylthiourea hydrogen bond donating clefts

The work from this section of Chapter Two has been published previously.[151] After the synthesis of the diindolylurea receptors **209** and **210** with strong oxo-anion binding properties in highly polar solutions, the thiourea analogues (**211** and **212**) of receptors **209** and **210** were synthesised. The substitution of the thiourea group for the urea group increases the acidity of the associated NH bond donor groups as the sulfur atom is more capable of stabilising the negative charge than the oxygen atom. The partial negative charge, produced during the anion binding process, is better diffused over the larger sulphur atom. The thiourea functionality can thus form more effective hydrogen bonds, increasing the potential strength with which the receptor can bind the anion.

2.3.1 Synthesis

This simple two step reaction process is shown in Scheme 2.3.1.1.The corresponding 7-nitroindole was reduced with a Pd/C 10% catalyst under a hydrogen atmosphere in ethanol. Receptors **211** and **212** were prepared by the reaction of the corresponding 7-aminoindole with thiophosgene in a two phase solution to yield the isothiocyanate of the amine. The isothiocyanate was then heated with a further addition of the relevant 7-aminoindole. Receptor **211** was purified by flash chromatography (DCM:MeOH 49:1) and receptor **212** was isolated by filtration of the reaction mixture. Receptors **211** and **212** were isolated in 29% and 83% yields respectively.

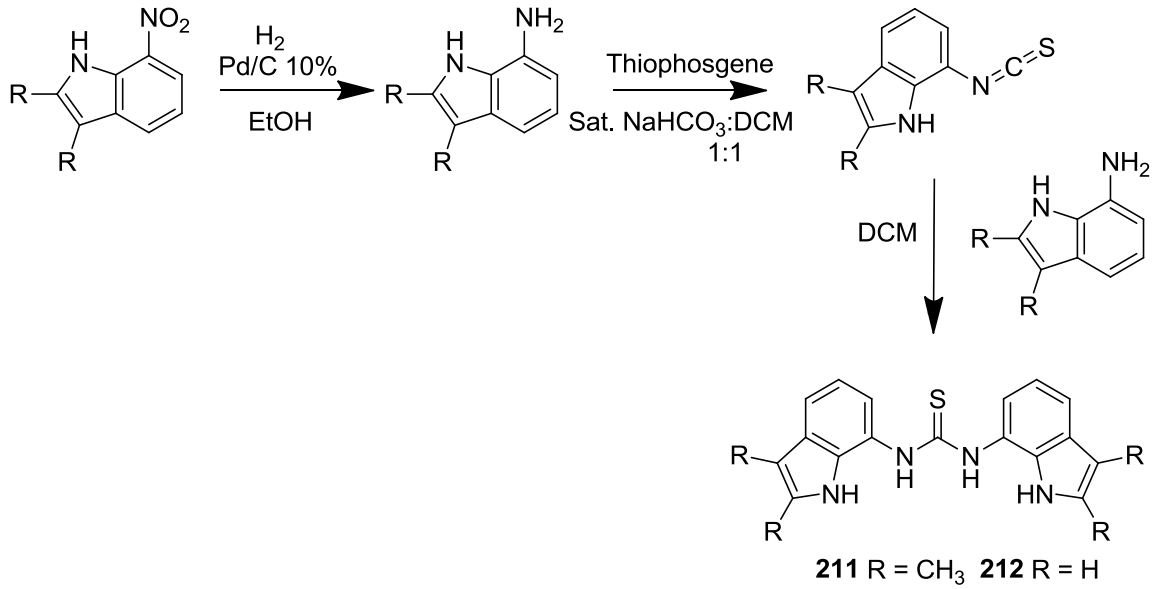

Scheme 2.3.1.1

2.3.2 Solution phase analysis

2.3.2.1 Proton NMR titration data

Anion binding constants were calculated for receptors **211** and **212** with a wide range anions. The binding constants were determined by ^{1}H NMR titration with the TBA or TEA salt of the anion in DMSO-d_6/0.5% H_2O solutions. The binding constants were determined by the computer program WINEQNMR[153] and fitted to a 1:1 binding model. Some Job plots[154] were produced to check the 1:1 binding mode that was suggested by the titration data and previous receptor analogues (**209** and **210**). The majority of the binding constants and Job plot were generated by myself with a some input from Claudia Caltagirone. Binding constants and Job plots were determined by following the downfield shift of an aromatic CH, as peak broadening was observed with the NH resonances upon addition of anion. However the downfield shift observed at the beginning of the ^{1}H NMR titrations of the indole and thiourea NH's does show that all four NH bond donor groups of both receptors are involved in binding the anion. The peak broadening and upfield shift of the NH signals, along with the upfield shift of the aromatic CH resonance used to calculate anion binding constants, can be seen in Figures 2.3.2.1 and 2.3.2.2.

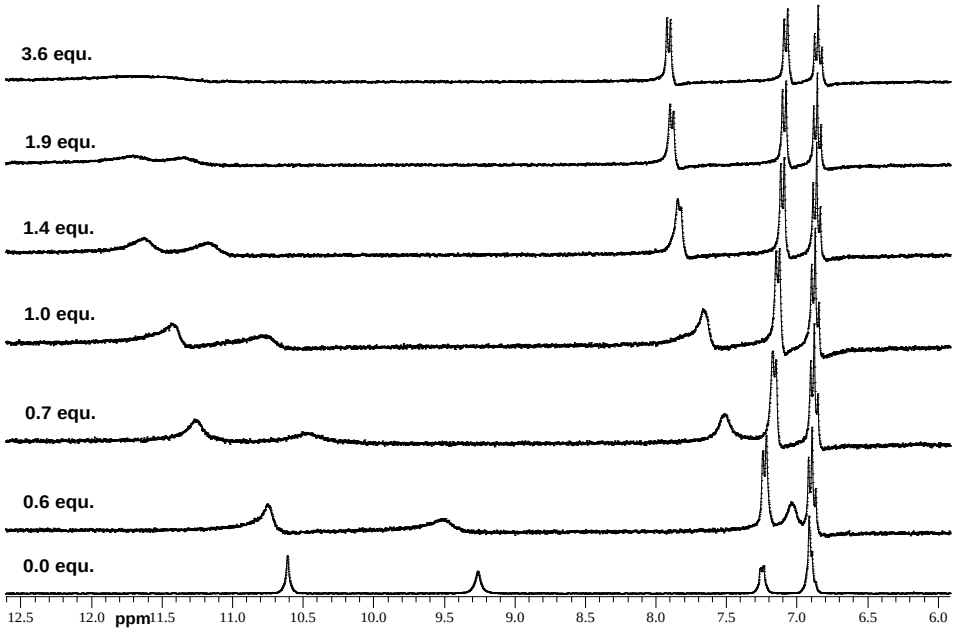

Figure 2.3.2.1 NMR Stack plot of receptor **211** *vs* TBA dihydrogen phosphate in DMSO-d_6/H_2O 0.5%, showing downfield shift and peak broadening of both the indole and urea NH bond donor groups and a downfield shift of the aromatic CH involved in binding the anion. This stack plot is taken from the pre-peer reviewed version of the supplementary information from the following article: Caltagirone, C.; Hiscock, J. R.; Hursthouse, M. B.; Light, M. E. and Gale, P. A., *Chem. Eur. J.*, **2008**, *14*, 10236-10243.

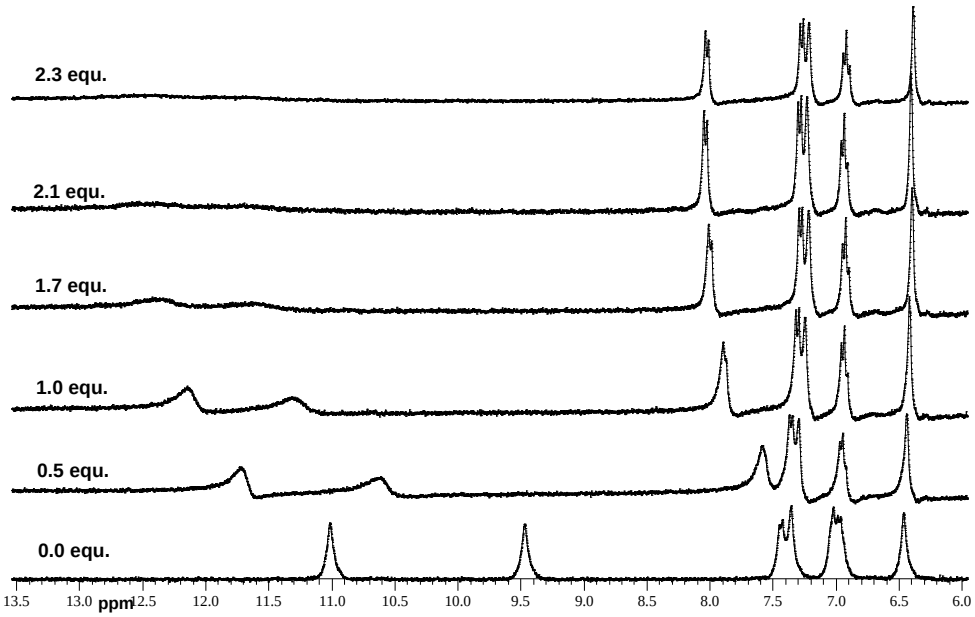

Figure 2.3.2.2 NMR Stack plot of receptor **212** *vs* TBA dihydrogen phosphate in DMSO-d_6/H_2O 0.5%, showing downfield shift and peak broadening of both the indole and urea NH bond donor groups and a downfield shift of the aromatic CH involved in binding the anion. This stack plot is taken from the pre-peer reviewed version of the supplementary information from the following article: Caltagirone, C.; Hiscock, J. R.; Hursthouse, M. B.; Light, M. E. and Gale, P. A, *Chem. Eur. J.*, **2008**, *14*, 10236-10243.

Table 2.3.2.1 Anion binding constants (M^{-1}) and percentage error for receptors **211** and **212**, measured in DMSO-d_6/0.5% H_2O at 298 K. Anionic guests were added as the TBA salt of the anion with the exception of bicarbonate, which was added as the TEA salt of the anion. Binding constants were determined by ^{1}H NMR titration following the urea NH, fitting data to a 1:1 binding model using WINEQNMR[153].

Anion	211	E (%)	212	E (%)
$CH_3CO_2^-$	2830	5	1620	12
$H_2PO_4^-$	3830	6	1630	7
F^-	a	-	205	9
$C_6H_5CO_2^-$	514	8	477	8
Cl^-	128	10	74	8
[b]HCO_3^-	477	14	a	-

a – No binding constant could be calculated due to the peak broadening of the receptor/anion complex.
[b] Added as the TEA salt of the anion

As shown in Table 2.3.2.1, there is a loss in affinity with all anions (when compared to the urea analogues **209** and **210**) apart from chloride, which still exhibits similar binding constants to those observed for **209** and **210** (128 M^{-1} and 74 M^{-1} for receptors **211** and **212** respectively). Although there is a substantial decrease in binding constants for the oxo-anions tested, there is also a general loss in selectivity for dihydrogen phosphate with both thiourea receptors. Receptor **211** shows a slight affinity for dihydrogen phosphate over acetate, with binding constants of 3830 M^{-1} and 2830 M^{-1} respectively. Any selectivity for dihydrogen phosphate over acetate is lost with receptor **212**. The two anions are now bound with almost identical affinities of 1620 M^{-1} and 1630 M^{-1}, for acetate and dihydrogen phosphate respectively.

Work by Soós and co-workers explore the energies of several different thiourea-containing molecules in solution with computer modelling. This work showed that the energy involved in the conformational interconversion that occurs in solution to bind anions with this type of compound makes this process unfavourable. This could be the reason for the lower binding constants observed with the thiourea, as opposed to the urea-containing compounds.[155]

A second potential reason for the loss in affinity of the anions for the receptor could be the size of the sulfur atom in the thiourea group compared to the smaller oxygen atom of the urea group. The larger size of the sulfur atom causes a distortion of the planar conformation of the receptors, therefore preventing the formation of optimum binding conformation and limiting binding affinity.

2.3.3 Solid phase analysis

X-ray quality crystals of receptor **212** and TEA bicarbonate were obtained in collaboration with Claudia Caltagirone and were produced by slow evaporation of an excess of the TEA bicarbonate and receptor **212** from DMSO.

The crystal structure of produced by single crystal X-ray diffraction is shown in Figure 2.3.3.1a. The crystal structure has a 1:1 binding stoichiometry as in the solution state. The anion is coordinated to the receptor by four hydrogen bonds, one from each of the NH bond donor groups but it is more true to say that the complex adopts a 2:2 binding conformation (as shown in Figure 2.3.3.1b). O1 and O3 are each bound by one hydrogen bond from the first receptor (N3 and N4). O2 of the bicarbonate anion is bound by two hydrogen bonds from a second receptor (N1 and N2). This pattern is then repeated to form layers of 2:2 complexes, with the bicarbonate anions bound in the centre of a receptor sandwich. The exact position of the bicarbonate anion could not be fixed because of the disorder in the crystal structure and therefore the position on the hydrogen atom of the bicarbonate anion could not be fixed and so is not shown. The hydrogen bonding interactions and hydrogen bonding angles of the complex, shown in Figures 2.3.3.1 a and b, are shown in Table 2.3.3.1. The hydrogen bond from the nitrogen atoms of the receptor to the oxygen atoms of the anion range from N···O = 2.797(4)-3.160(4) Å and the bonds angles range from N–H···O = 124°-169°.

The twisted nature of this receptor:anion complex further supports the idea that optimal binding cannot be achieved with the thiourea receptor due to the lack of planar conformation observed in the complexes involving receptors **209**, and **210**, shown in Figures 2.2.3.1, 2.2.3.2 and 2.2.3.3 a and b.

Table 2.3.3.1 Hydrogen bonding table for the crystal structure shown in Figures 2.3.3.1 a and b, of receptor **212** and TEA bicarbonate, obtained by single crystal X-ray diffraction at 120K. *D* – hydrogen bond donor atom. *A* – hydrogen bond acceptor atom. *d* – distance in Å. ∠ - bond angle in °. H – hydrogen atom. Symmetry transformations used to generate equivalent atoms: (i) –x,–y+1,–z (ii) x–1,y,z

D–H···*A*	*d*(*D*–H) (Å)	*d*(H···*A*) (Å)	*d*(*D*···*A*) (Å)	∠(*DHA*) (°)
N1–H91···O2^{i}	0.83(3)	2.13(3)	2.887(4)	152(3)
N1–H91···O3^{ii}	0.83(3)	2.62(3)	3.160(4)	124(3)
N2–H92···O2^{i}	0.73(3)	2.09(3)	2.797(4)	163(3)
N3–H93···O1	0.78(3)	2.06(3)	2.838(4)	169(3)
N4–H94···O3	0.78(3)	2.08(4)	2.835(4)	161(3)

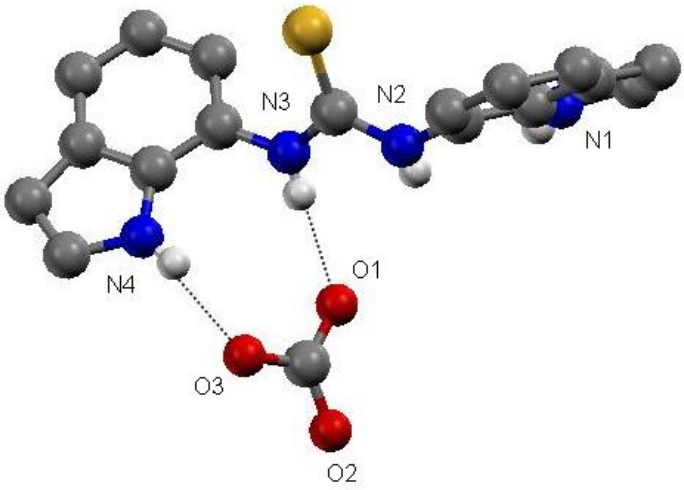

Figure 2.3.3.1a The bicarbonate complex of receptor **212**. Single X-ray crystal structure with TEA carbonate. The aromatic CH hydrogen atoms and the TEA counter ion have been omitted for clarity. The hydrogen of the bicarbonate anion could not be fixed so is not shown.

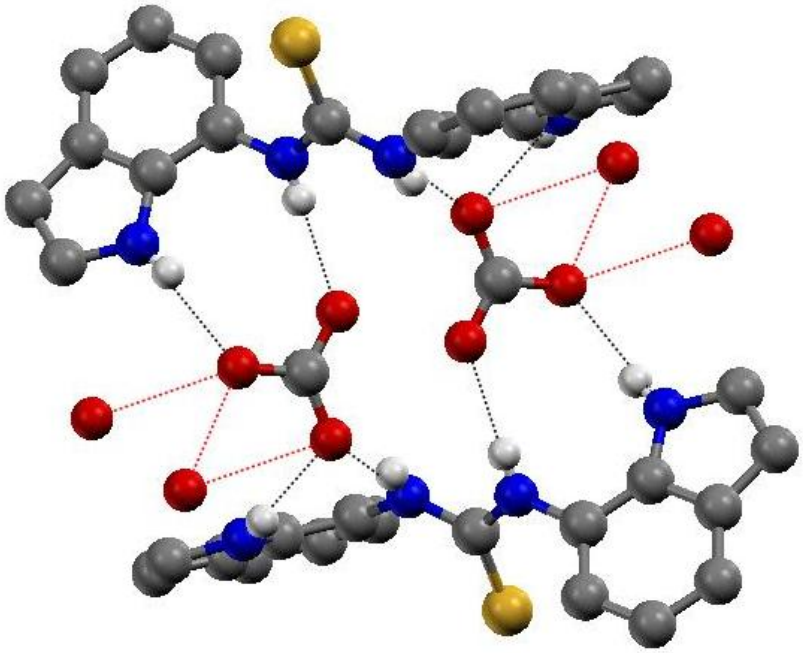

Figure 2.3.3.1b Extended structural veiw. The carbonate complex of receptor **212**. Single X-ray crystal structure with TEA bicarbonate. The aromatic CH hydrogen atoms and the TEA counter ion have been omitted for clarity. The hydrogen of the bicarbonate anion could not be fixed so is not shown. Red dashed bonds and unconnected oxygen atoms illustrate the next carbonate/receptor complexes in the chain.

X-ray quality crystals of receptor **212** with TBA chloride were obtained in collaboration with Claudia Caltagirone, and were produced by slow evaporation of a DMSO solution containing **212** and an excess of the TBA chloride.

The structure of produced by single crystal X-ray diffraction is shown in Figure 2.3.3.2. The crystal structure shows a 1:1 binding stoichiometry, as in the solution state. The anion is bound to the receptor by four hydrogen bonds, one from each of the NH bond donor groups but the receptor again adopts a twisted conformation that is not conducive to optimum hydrogen bond formation between anion and receptor. The hydrogen bonding interactions and hydrogen bonding angles for the crystal structure shown in Figure 2.3.3.2 are shown in Table 2.3.3.2. The hydrogen bonds from the nitrogen atoms of the receptor to the chloride anion range from N···Cl^- = 2.935(3)-3.307(2) Å and the bond angles range from N–H···Cl^- = 159°-171°.

Table 2.3.3.2 Hydrogen bonding table for crystal structure, shown in Figure 2.3.3.2, of receptor **212** and TBA chloride obtained by single crystal X-ray diffraction at 120K. *D* – hydrogen bond donor atom. *A* – hydrogen bond acceptor atom. *d* – distance in Å. ∠ - bond angle in °. H – hydrogen atom.

D–H···*A*	*d*(*D*–H) (Å)	*d*(H···*A*) (Å)	*d*(*D*···*A*) (Å)	∠(*DHA*) (°)
N1–H91···Cl1	0.85(3)	2.57(4)	3.377(3)	160(3)
N2–H92···Cl1	0.87(3)	2.33(3)	3.187(2)	165(3)
N3–H93···Cl1	0.80(3)	2.55(3)	3.307(2)	159(3)
N4–H94···Cl1	0.85(3)	2.42(3)	3.262(2)	171(3)

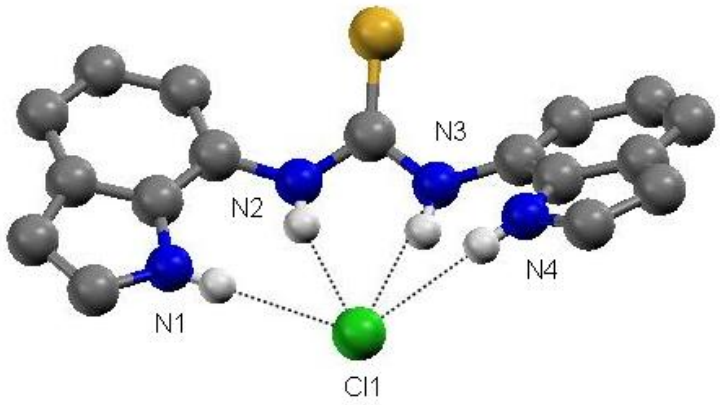

Figure 2.3.3.2 The chloride complex of receptor **212**. Single X-ray crystal structure with TBA chloride. The aromatic CH hydrogen atoms and the TBA counter ion have been omitted for clarity.

2.4 Symmetrical and asymmetrical carbazolylurea hydrogen bond donating clefts

The work from this section of Chapter Two has been published previously.[156,157] Due to the loss of selectivity and binding affinity observed when substituting the thiourea group for the urea group in the diindolylurea skeleton, the indole groups were interchanged for the carbazole group in an attempt to improve the design of receptors **209** and **210**. The carbazole moiety contains a NH bond donor group that is more acidic than that of the indole.[75,76] This should increase the affinity of the anion for the receptor with no alteration

of the planarity of the receptor, thus keeping the optimal anion binding conformation. A group of three carbazole urea analogues were synthesised and, because of the ease of synthesis of the carbazole isocyanate, asymmetrical as well as symmetrical receptors could be synthesised. Another property of the carbazole group it's fluorescent characteristic that lends the receptor to anion-sensing capabilities through the quenching of fluorescence.[115,126,136]

2.4.1 Synthesis

Synthesis of 1-nitrocarbazole was achieved from carbazole by a slight alteration to a literature procedure[158], using nitric and acetic acid. The crude product that was obtained, after precipitation from water, was purified by flash chromatography in CH_3Cl. 1-Nitrocabazole was then reduced to 1-aminocarbazole, using hydrogen gas and a Pd/C 10% catalyst in ethanol. Characterisation data agreed with previously published values, as shown in Scheme 2.4.1.1.[159]

Receptors **213** and **214** were then prepared as shown in Scheme 2.4.1.2, by the reaction 1-aminocarbazole in a two phase solution of saturated $NaHCO_3$ and DCM with triphosgene. This produced the carbazole isocyanate which, due to its reactivity, was used straight away by reacting with either 1-aminocarbazole and TEA in DCM/CH_3Cl to give receptor **213** in a 41% yield or with 7-aminoindole and TEA in CH_3Cl to give receptor **214** in a 26% yield.

215 was formed by a similar reaction with 1-aminocarbazole and phenylisocyanate in DCM, as shown in Scheme 2.4.1.3, giving a 69% yield.

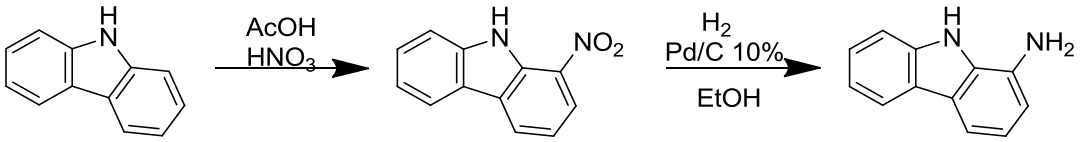

Scheme 2.4.1.1

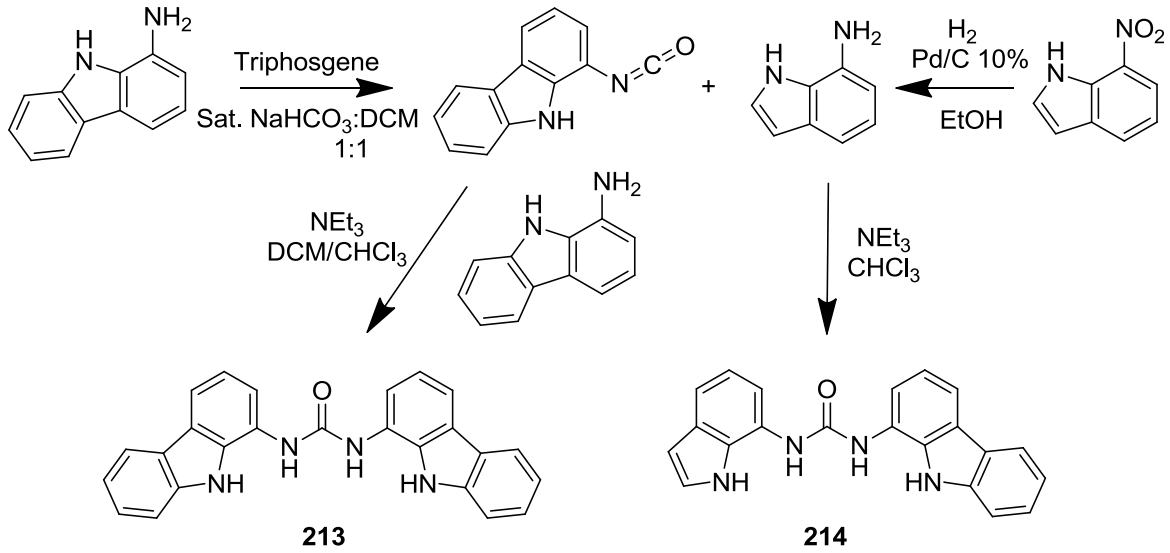

Scheme 2.4.1.2

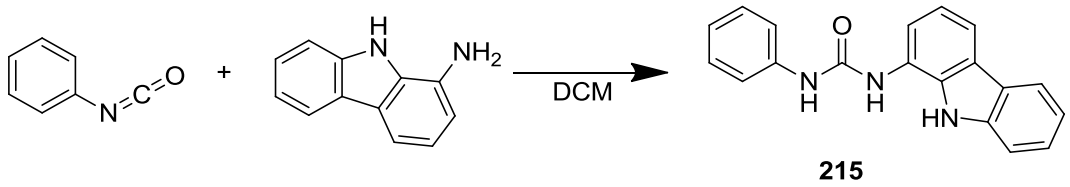

Scheme 2.4.1.3

2.4.2 Solution phase analysis

2.4.2.1 Proton NMR titration data

Anion binding constants were calculated for receptors **213**, **214** and **215** for a wide range anions. The binding constants were determined by ^{1}H NMR titration with the TBA or TEA salt of the anion in DMSO-d_6/0.5% H_2O. The binding constants were determined by the computer program WINEQNMR[153] and fitted to a 1:1 binding model, suggested by the titration data and previous receptor analogues (**209-212**). Binding constants were determined by following the downfield shift of a urea NH and are shown with error values in Table 2.4.2.1. High errors were calculated for receptors **214** and **215** with TBA fluoride due to peak broadening of the NH signals, which decreased the accuracy in ascertaining the exact signal positions. These numbers can therefore only be taken as a rough guide. The downfield shift observed during the ^{1}H NMR titrations show that all the NH bond donor groups of receptors **213-215** are involved in binding the anions.

Table 2.4.2.1 Anion binding constants (M^{-1}) and percentage error for receptors **213**, **214** and **215**, measured in DMSO-d_6/0.5% H_2O at 298 K. Anionic guests were added as the TBA salt of the anion with the exception of bicarbonate, which was added as the TEA salt of the anion. Binding constants were determined by ^1H NMR titration following the urea NH, fitting data to a 1:1 binding model using WINEQNMR[153].

Anion	213	E (%)	214	E (%)	215	E (%)
$CH_3CO_2^-$	$>10^4$	-	$>10^4$	-	$>10^4$	-
$H_2PO_4^-$	a	-	a	-	6140	10
$C_6H_5CO_2^-$	5670	10	5880	10	3420	10
F^-	b	-	154	46	36	19
Cl^-	102	5	139	6	85	1
$^cHCO_3^-$	$>10^4$	-	$>10^4$	-	$>10^4$	-

a – Does not fit a 1:1 or 2:1 anion:receptor binding model. b – Binding constant could not be calculated due to the peak broadening of the receptor/anion complex. [c] Added as the TEA salt of the anion.

There is a preference for the binding of acetate and bicarbonate over the other anions tested, with binding constants calculated to be $>10^4$ M^{-1} in a DMSO-d_6/0.5% H_2O solution. However, the numbers calculated for bicarbonate cannot be directly compared to the other results because of the TEA counter anion. Low affinities were observed with the halide anions, chloride and fluoride, and are comparable in magnitude to those observed with receptors **209-212**. The binding constants for chloride were calculated to be 102 M^{-1}, 139 M^{-1} and 85 $M^{-1}$for receptors **213**, **214** and **215** respectively, indicating that receptors **213** and **214** exhibit almost identical anion binding affinity and selectivity. Receptor **215**, which contains one less NH bond donor group than receptors **213** and **214**, showed a similar trend in anion selectively and only slightly lower binding affinity when compared to the receptors **213** and **214**.

Although the titration data for receptors **213** and **214** with dihydrogen phosphate could not be fitted to a 1:1 or 2:1 anion:receptor binding model, the titration data for dihydrogen phosphate with receptor **215** was fitted to a 1:1 binding model. Receptor **215** showed a preference for this anion over benzoate. The binding curves produced by the ^1H NMR titration data for receptor **213** and **214** with dihydrogen phosphate are shown in

Graphs 2.4.2.1 and 2.4.2.2. The data for receptor **213** is fitted to a 1:1 binding model and the data for receptor **214** is fitted to a 2:1 anion:receptor binding model. Neither model fits the trend in data points collected during the titration experiments, although this trend in data points can be seen with receptor **213**, it becomes more exaggerated with receptor **214**. Overall the binding events are similar.

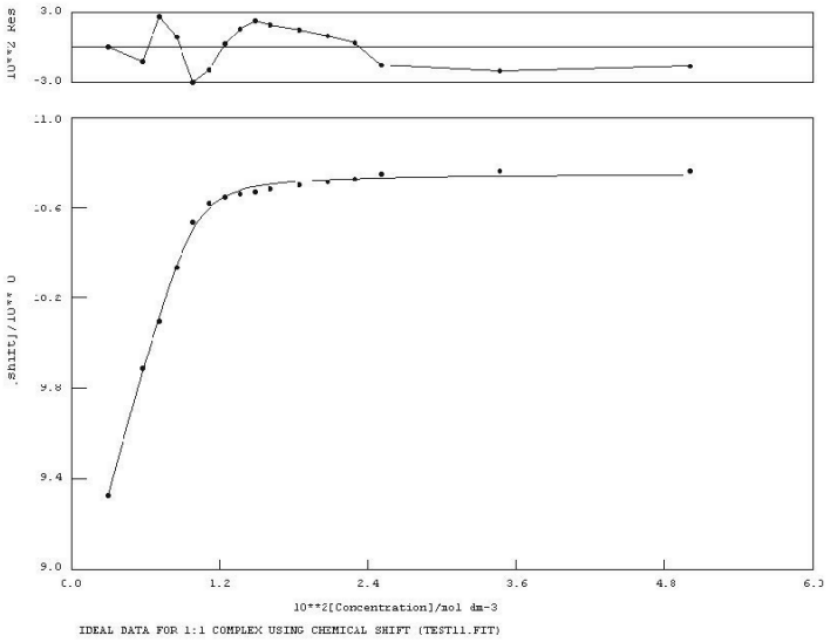

Graph 2.4.2.1 ^{1}H NMR titration curve of receptor **213** *vs*. TBA dihydrogen phosphate in DMSO-d_6/H_2O 0.5%. Fitted to a 1:1 binding model.[153]

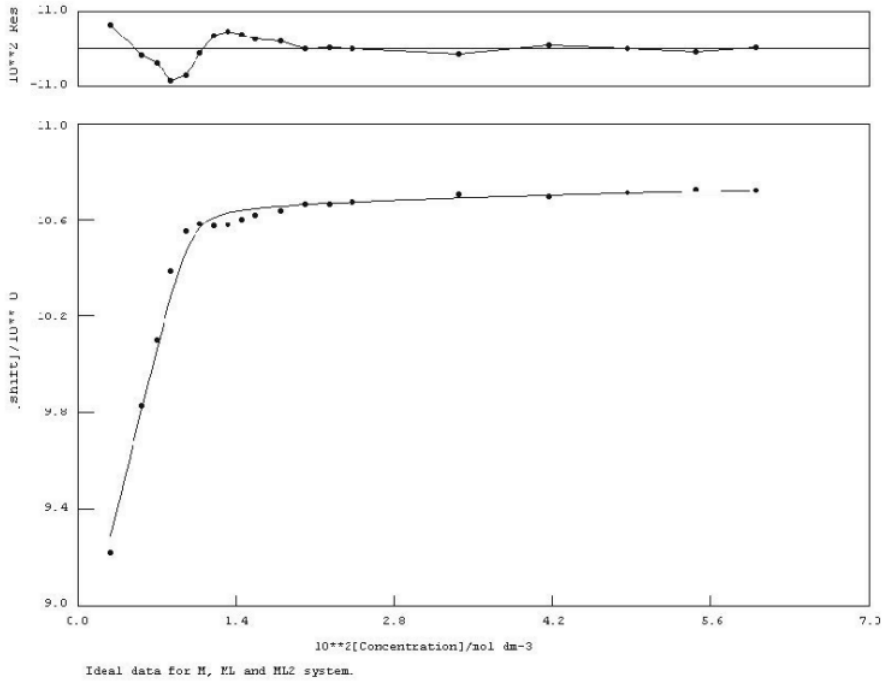

Graph 2.4.2.2 ^{1}H NMR titration curve of receptor **214** *vs.* TBA dihydrogen phosphate in DMSO-d_6/H_2O 0.5%. Fitted to a 2:1 anion:receptor binding model.[153]

2.4.2.2 Fluorescence studies

DMSO/0.5% H_2O solutions of the receptors **213-215** and different anions were tested for their fluorescence properties. Photographs of the different receptor/TBA salt combinations are shown in table 2.4.2.2. Fluorescence quenching was observed with all three receptors when binding benzoate. Fluorescence enhancements or slight change in colour seen with other anions can be attributed to the π-π stacking interactions observed in stronger concentrations of anion and receptor (1 M concentrations of receptor and 6 M concentrations of anion). These colour changes were not be identified in further solution studies of much weaker concentrations of receptor and anion as the π-π stacking effect was much decreased.

Table 2.4.2.2 Photographs of different combinations of receptor and anion in a DMSO/0.5% H_2O solution under a UV light. Approximate concentration: 0.1 M solution of receptor and 6 equivelents of anion.

Receptor	**Anion**					
	none	acetate	fluoride	dihydrogen phosphate	benzoate	chloride
213						
214						
215						

Further fluorescence studies were carried out by Claudia Caltagirone, using DMSO-0.5% H_2O with the TBA salts of the anions, except for the bicarbonate anion, which was added as the TEA salt. All three receptors showed a selective fluorscence quenching upon the addition of the benzoate anion. This quenching effect can be seen to the greatest extent with receptor **213**. Graph 2.4.2.3 shows fluorecence emission by receptor **213** when excited at 270 nm, with maxima at 363 and 376 nm. There is a decrease in the intencity of emissions at 363 and 376 nm as the concentrations of benzoate increase. There was a small increase in absorbance in the UV-Vis titration but no shift.

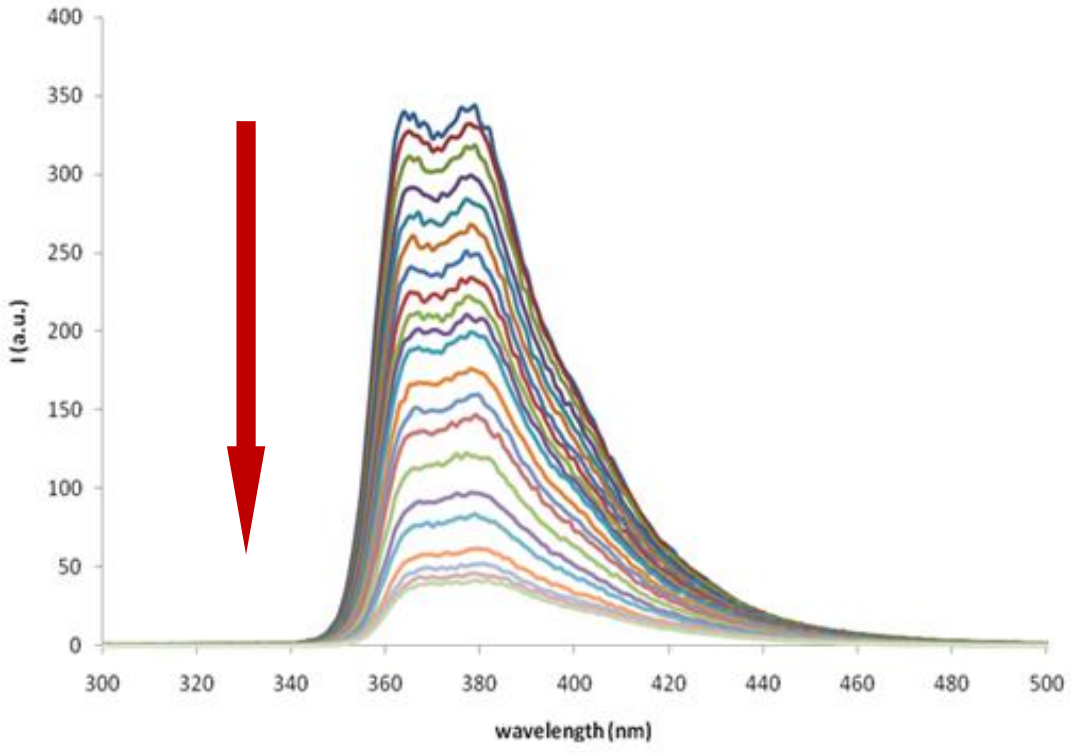

Graph 2.4.2.3 Fluorescence quenching of **213** in DMSO-0.5% H_2O upon the addition of TBA benzoate.

Graph 2.4.2.4 shows the effect on the fluorescence of receptor **213** when excited at 270 nm, following the addition of different amounts of anion to a DMSO-0.5% H_2O solution. Of all the anions tested (acetate, benzoate, chloride, fluoride, dihydrogen phophate, TEA bicarbonate), only chloride does not have any effect on the quenching of fluorescence. Benzonate exhibits almost full quenching of fluorescence but acetate only exhibits a partial quenching effect, (I_{res} = 50%). Dihydrogen phosphate and bicarbonate also exhibit a partial quenching effect in these cases (I_{res} = 70% approximately). Fluoride does exhibit a quenching of fluorescence but this only occurs after the addition of more than three equivelents of anion. This maybe an indication of the deprotonation of the receptor by the fluoride anion. This phenomenon has been seen in other examples of synthetic, neutral receptors that exhibit fluorescent sensing of anions.[147]

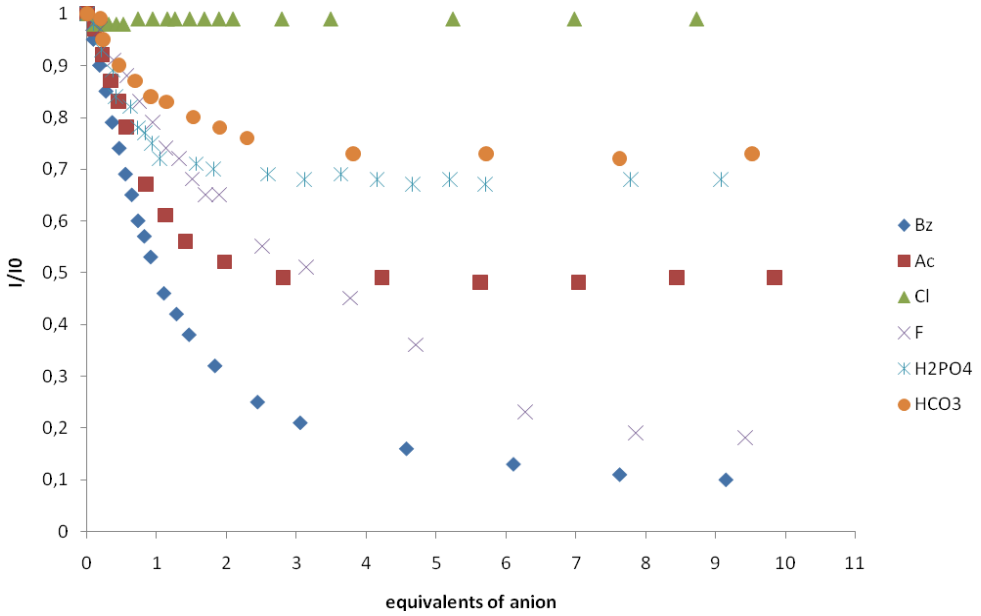

Graph 2.4.2.4 Effect of increasing anion concentration upon the relative fluorescence emission of receptor **213** in DMSO/0.5% water. This graph is taken from the following article: Hiscock, J. R.; Caltagirone, C.; Light, M. E.; Hursthouse, M. B. and Gale, P. A., *Org. Biomol. Chem.*, **2009**, *7*, 1781-1783.

Graph 2.4.2.5 shows the effect on the fluorescence of receptor **214** when excited at 270 nm, following the addition of different amounts of anion to a DMSO-0.5% H_2O solution. Of all the anions tested (acetate, benzoate, chloride, fluoride, dihydrogen phophate, TEA bicarbonate) benzoate again shows the largest fluorescence quenching effect (I_{res} = 36%). Acetate, bicarbonate, dhhydrogen phophate and fluoride anions show limited quenching effects with I_{res} = 70-80%, while chloride has little noticeable effect on flourescence emission.

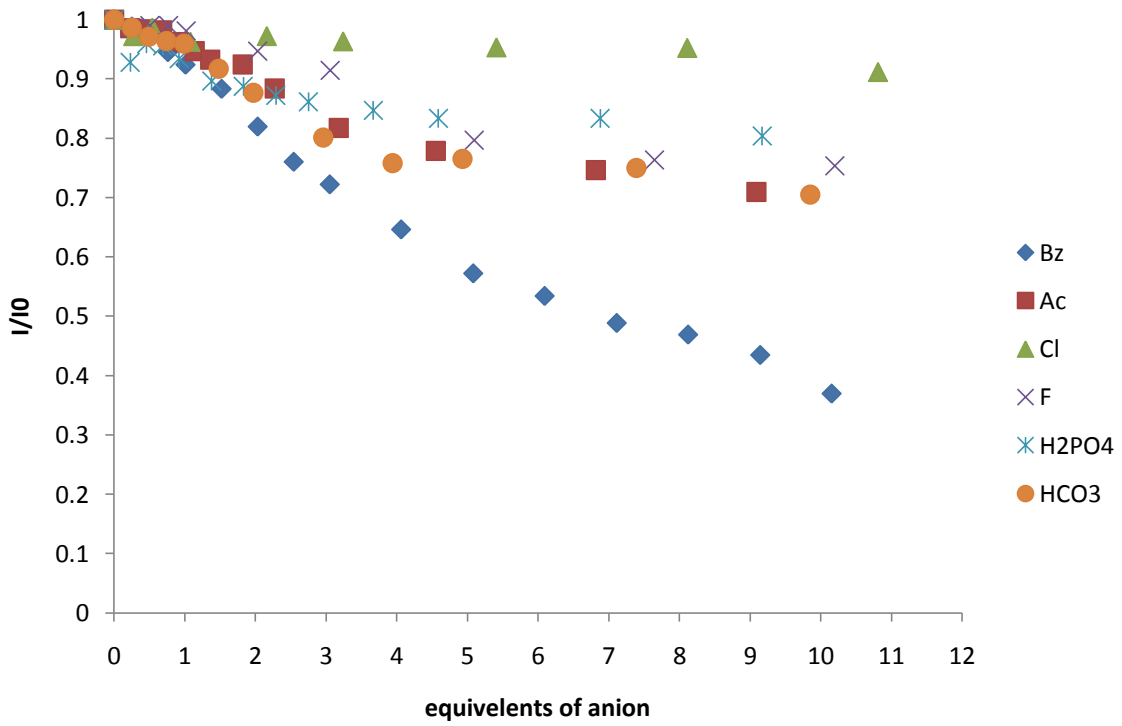

Graph 2.4.2.5 Effect of increasing anion concentration upon the relative fluorescence emission of receptor **214** in DMSO/0.5% water.This graph is taken from the supplementary information of the following article: Hiscock, J. R.; Caltagirone, C.; Light, M. E.; Hursthouse, M. B. and Gale, P. A., *Org. Biomol. Chem.*, **2009**, *7*, 1781-1783.

Graph 2.4.2.6 shows the effect on fluorescence of the receptor **215** when excited at 270 nm, following the addition of different amounts of anion to a DMSO-0.5% H_2O solution. Although this receptor still shows fluorescence quenching selectivity for benzoate, it is less obvious (I_{res} = 52%). The difference in I_{res} between benzoate and acetate, dihydrogen phosphate and fluoride is within 20%. Chloride still has a negligible quenching effect on the fluorescence of receptor **215**.

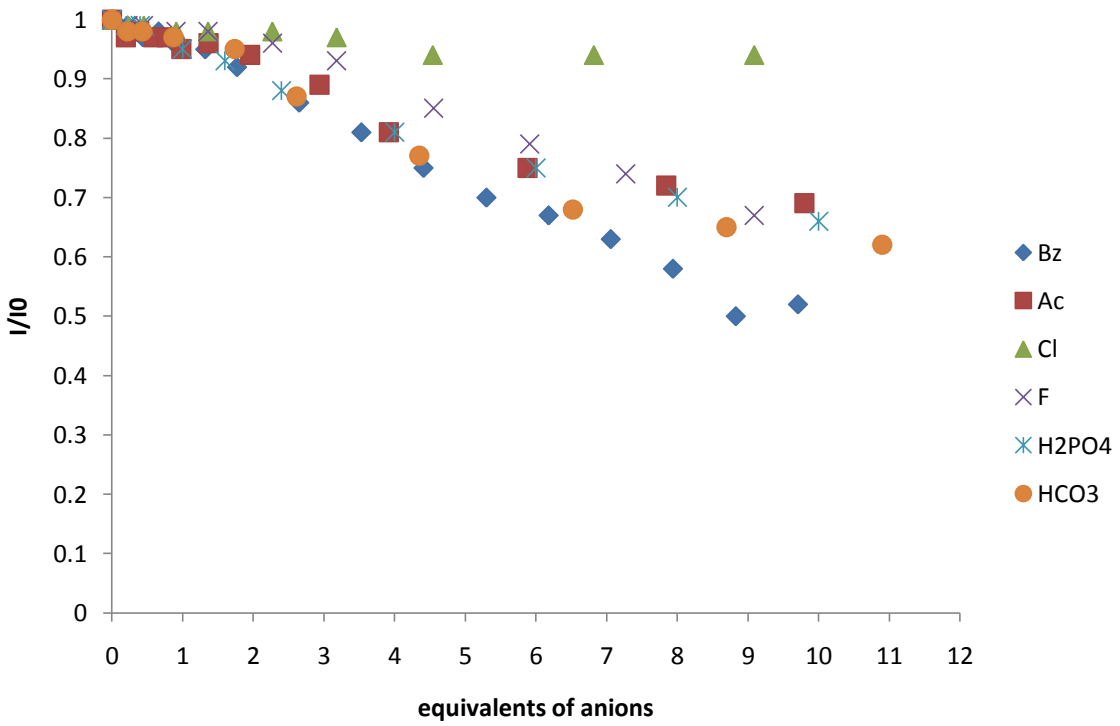

Graph 2.4.2.6 Effect of increasing anion concentration upon the relative fluorescence emission of receptor **215** in DMSO/0.5% water. This graph is taken from the supplementary information of the following article: Hiscock, J. R.; Caltagirone, C.; Light, M. E.; Hursthouse, M. B. and Gale, P. A., *Org. Biomol. Chem.*, **2009**, *7*, 1781-1783.

2.4.3 Solid phase analysis

X-ray quality crystals of receptor **213** were obtained by slow evaporation of the receptor from DMSO. The structure produced by single crystal X-ray diffraction is shown in Figure 2.4.3.1. The crystal structure shows receptor molecules in a twisted conformation, forming a tape which is held together firstly by two hydrogen bonds formed between the hydrogen bond donor and acceptor atoms of the urea group and secondly by the π- π stacking between the aromatic rings of the carbazole functionalities. The hydrogen bonding interactions and hydrogen bonding angles for the crystal structure shown in Figure 2.4.3.1 are shown in Table 2. 4.3.1. The hydrogen bonds from the nitrogen atoms of one receptor to the oxygen atoms of a second receptor N···O = 2.795(9) Å and the bond angle N–H···O = 146.0°.

Table 2.4.3.1 Hydrogen bonding table for crystal structure, shown in Figure 2.4.3.1, of receptor **213** obtained by single crystal X-ray diffraction at 120K. *D* – hydrogen bond donor atom. *A* – hydrogen bond acceptor atom. *d* – distance in Å. ∠ - bond angle in °. H – hydrogen atom. Symmetry transformations used to generate equivalent atoms: (i) –x+1,y,–z+3/2 (ii) x,y+1,z

D–H···*A*	*d*(*D*–H) (Å)	*d*(H···*A*) (Å)	*d*(*D*···*A*) (Å)	∠(*DHA*) (°)
N2–H2···O1^{ii}	0.88	2.02	2.795(9)	146.0

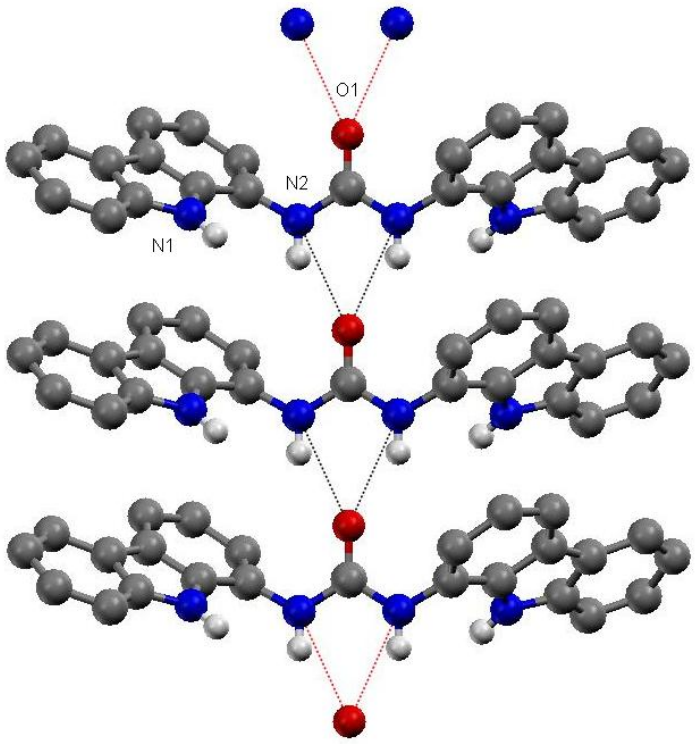

Figure 2.4.3.1 Receptor **213**. The aromatic CH hydrogen atoms and the TBA counter ion have been omitted for clarity.

X-ray quality crystals of receptor **213** and TBA benzoate were obtained by slow evaporation of an excess of the TBA salt and receptor from DMSO.

The crystal structure produced by single crystal X-ray diffraction is shown in Figure 2.4.3.2. There are two receptor anion complexes contained within the unit cell. However, as they are both practically identical, only one receptor anion complex is shown. The crystal structure shows a 1:1 binding stoichiometry as in the solution state, with the anion coordinated to the receptor by four hydrogen bonds. The four NH bond donor groups

bind to the two benzoate oxygen atoms, forming two hydrogen bonds to each of the two benzoate oxygen atoms. The receptor adopts a slightly twisted conformation but this is far less extreme than that observed in Figure 2.4.3.1. However this receptor still does not have the completely planar conformation observed in the diindolylurea-based receptors, **209** and **210**. The hydrogen bonding interactions and hydrogen bonding angles for the two similar benzoate complexes, as illustrated in Figure 2.4.3.2, are shown in Table 2.4.3.2. The hydrogen bonds from the nitrogen atoms of the receptor to the oxygen atoms of the anion range from N···O = 2.762(5)-2.996(5) Å and the bond angles range from N–H···O = 147.7°-178.6°.

Table 2.4.3.2 Hydrogen bonding table for the two analogues of the crystal structure of receptor **214** and TBA benzoate, as shown in Figure 2.4.3.2, obtained by single crystal X-ray diffraction at 120K. *D* – hydrogen bond donor atom. *A* – hydrogen bond acceptor atom. *d* – distance in Å. ∠ - bond angle in °. H – hydrogen atom.

D–H···*A*	*d*(*D*–H) (Å)	*d*(H···*A*) (Å)	*d*(*D*···*A*) (Å)	∠(*DHA*) (°)
N1–H901···O4	0.86	2.00	2.809(5)	157.3
N2–H902···O4	0.86	2.02	2.816(5)	152.9
N3–H903···O3	0.86	2.06	2.917(5)	178.6
N4–H904···O3	0.86	1.96	2.801(4)	165.4
N5–H905···O6	0.86	1.98	2.773(5)	153.0
N6–H906···O6	0.86	2.00	2.762(5)	147.7
N7–H907···O5	0.86	2.14	2.996(5)	174.9
N8–H908···O5	0.86	1.96	2.806(5)	167.0

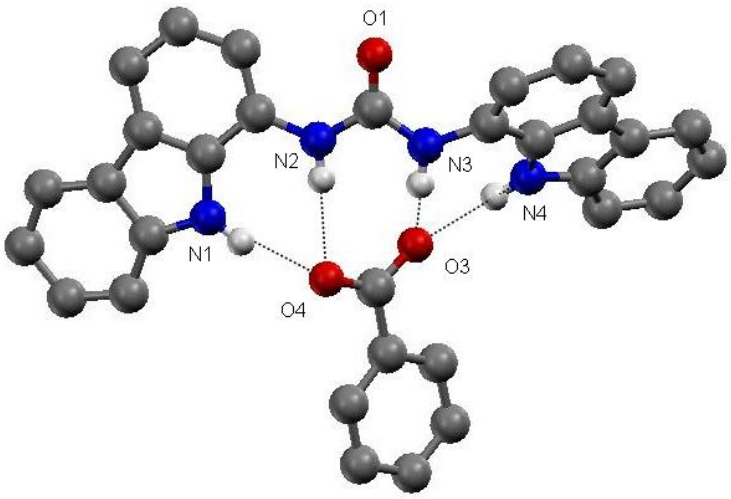

Figure 2.4.3.2 The benzoate complex of receptor **213**. Single X-ray crystal structure with TBA benzoate. The CH hydrogen atoms and the TBA counter ion have been omitted for clarity.

X-ray quality crystals of receptor **213** and TBA acetate were obtained by slow evaporation of an excess of the TBA salt and receptor from DMSO.

The crystal structure obtained by single crystal X-ray diffraction is shown in Figure 2.4.3.3. The crystal structure shows a 1:1 binding stoichiometry as in the solution state, with the anion coordinated to the receptor by four hydrogen bonds, one from each of the NH bond donor groups binding a single acetate anion with two hydrogen bonds to each of the acetate oxygen atoms. The receptor adopts a slightly twisted conformation as with the benzoate structure shown in Figure 2.4.3.2. The hydrogen bonding interactions and hydrogen bonding angles for the crystal structure shown in Figure 2.4.3.3 are shown in Table 2.4.3.3. The hydrogen bonds from the nitrogen atoms of the receptor to the oxygen atoms of the anion range from N···O = 2.781(2)-2.926(2) Å and the bond angles range from N–H···O = 127.6°-177.0°.

Table 2.4.3.3 Hydrogen bonding table for crystal structure of receptor **213** and TBA acetate, shown in Figure 2.4.3.3, obtained by single crystal X-ray diffraction at 120K. *D* – hydrogen bond donor atom. *A* – hydrogen bond acceptor atom. *d* – distance in Å. ∠ - bond angle in °. H – hydrogen atom. Symmetry transformations used to generate equivalent atoms: (i) x+1/2,–y+1/2,z–1/2

D–H···*A*	*d*(*D*–H) (Å)	*d*(H···*A*) (Å)	*d*(*D*···*A*) (Å)	∠(*DHA*) (°)
N1–H1···O2^{i}	0.86	1.96	2.781(2)	159.8
N2–H2···O2^{i}	0.86	1.95	2.809(2)	177.0
N3–H3···O3^{i}	0.86	2.10	2.926(2)	159.9
N4–H4···O3^{i}	0.86	2.21	2.820(2)	127.6

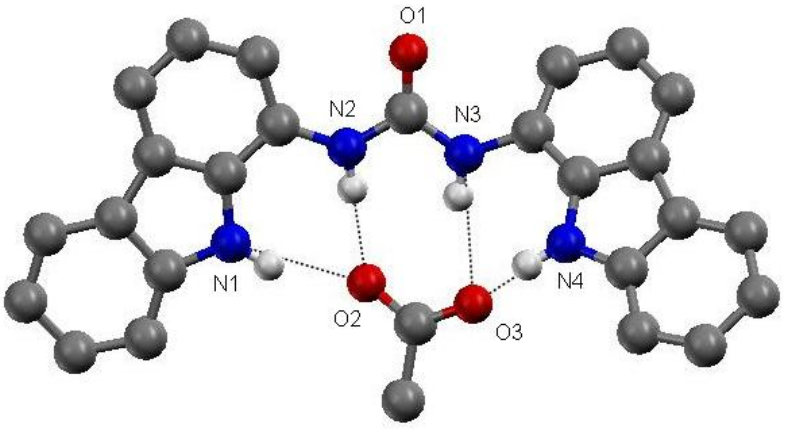

Figure 2.4.3.3 The acetate complex of receptor **213**. Single X-ray crystal structure with TBA acetate. The aromatic CH hydrogen atoms and the TBA counter ion have been omitted for clarity.

X-ray quality crystals of receptor **215** and TBA acetate were obtained by slow evaporation of an excess of the TBA salt and receptor from DMSO.

The crystal structure produced by single crystal X-ray diffraction is shown in Figure 2.4.3.4. A small amount of disorder involved the position of the acetate anion and was omitted for clarity. The crystal structure shows a 1:1 binding stoichiometry as in the solution state, with the anion coordinated to the receptor by three hydrogen bonds, one from each of the NH bond donor groups. Two hydrogen bonds are formed to one of the acetate oxygen atoms through the carbazole and a urea NH. The second urea NH hydrogen binds to the second of the two oxygen atoms of the acetate anion. The receptor adopts a

planar binding conformation, unlike that observed with receptor **213** (Figures 2.4.3.1-3) and more comparable to those of the diindolylurea complexes formed by receptors **209** and **210**. The hydrogen bonding interactions and hydrogen bonding angles for the simplified complex (Figure 2.4.3.4) are shown in Table 2.4.3.4. The hydrogen bonds from the nitrogen atoms of the receptor to the oxygen atoms of the anion range from N···O = 2.715(7)-2.993(7) Å and the bond angles range from N–H···O = 143.0°-164.0°.

Table 2.4.3.4 Hydrogen bonding table for crystal structure of receptor **215** and TBA acetate as shown in Figure 2.4.3.4, obtained by single crystal X-ray diffraction at 120K. *D* – hydrogen bond donor atom. *A* – hydrogen bond acceptor atom. *d* – distance in Å. ∠ - bond angle in °. H – hydrogen atom.

D–H···*A*	*d*(*D*–H) (Å)	*d*(H···*A*) (Å)	*d*(*D*···*A*) (Å)	∠(*DHA*) (°)
N1–H901···O2A	0.88	1.95	2.715(7)	144.8
N1–H901···O2B	0.88	1.98	2.732(5)	143.0
N2–H902···O3B	0.88	1.99	2.797(6)	151.5
N2–H902···O2A	0.88	2.15	2.993(7)	160.7
N3–H903···O3B	0.88	1.89	2.718(5)	156.9
N3–H903···O3A	0.88	1.95	2.811(7)	164.0

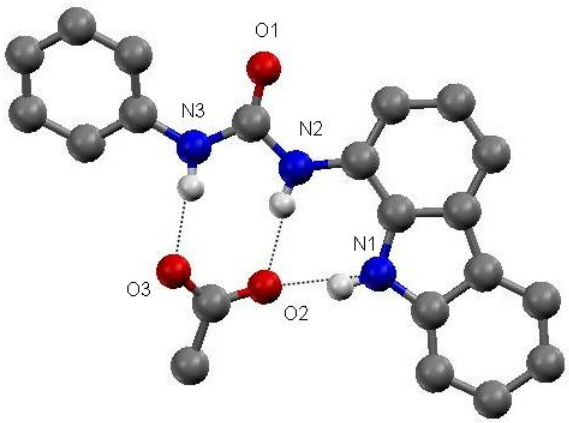

Figure 2.4.3.4 The acetate complex of receptor **215**. Single X-ray crystal structure with TBA acetate. The aromatic CH hydrogen atoms, disordered acetate anion and the TBA counter ion have been omitted for clarity.

2.5 Symmetrical and unsymmetrical carbazolylthiourea hydrogen bond donating clefts

The work from this section of Chapter Two has been published previously.[157] To complete the series of receptors, the thiourea versions (**216**-**218**) of the carbazolylurea receptors (**213-215**) were synthesised. These receptors contain the more acidic carbazole group instead of the indole moiety and also contain the more acidic thiourea instead of the urea functionality. Again, there is a loss of binding affinity as observed with the original set of diindole receptors (**209-212**). In this case, there is not the major loss in selectivity as was observed with the indolylurea receptors, **209** and **210**, compared to the indolylthiourea receptors, **211** and **212**, but there was a loss in anion selective fluorescence quenching with the thiourea analogues of receptors **213-215**.

2.5.1 Synthesis

1-Aminocarbazole was synthesised in the same way as previously described in 2.4.1.1. Receptors **216** and **217** were then prepared by reacting the 1-aminocarbazole in a two phase solution of saturated $NaHCO_3$ and DCM with thiophosgene (as shown in Scheme 2.5.1.1). This produced the carbazole isothiocyanate, which was reacted straight away with either 1-aminocarbazole and NEt_3 in $CHCl_3$ to give receptor **216** in a 36% yield or with 7-aminoindole in dry pyridine to give receptor **217** in a 48% yield. The crude product of receptor **216** was recrystallised from methanol/ether. Receptor **217** was recrystallised from hot methanol.

Receptor **218** was synthesised by a simple reaction with 1-aminocarbazole and phenylisothiocyanate in DCM, precipitating the final product with hexane, to give a 41% yield (as shown in Scheme 2.5.1.2).

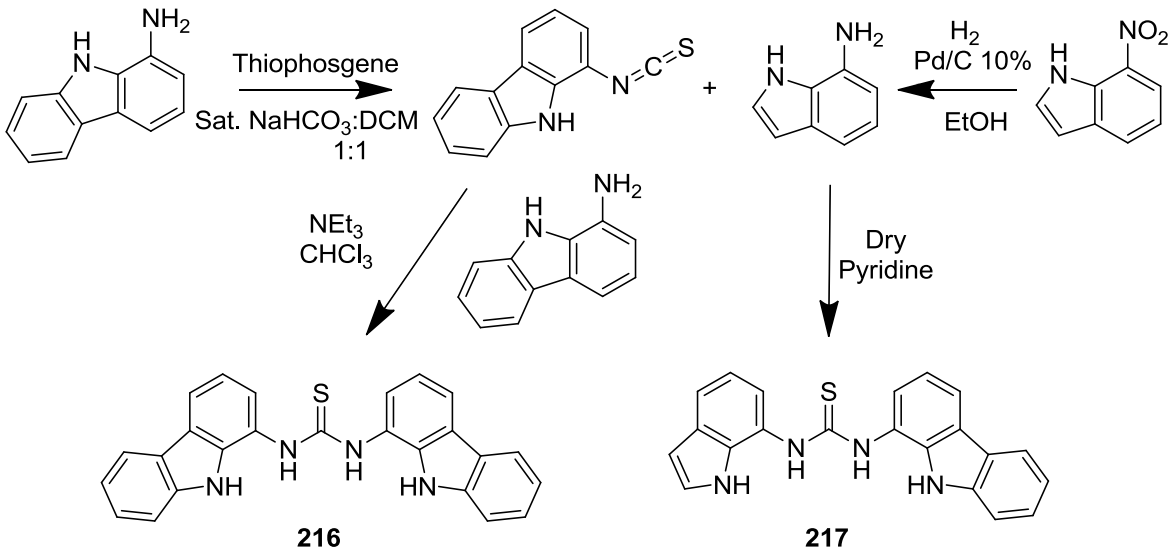

Scheme 2.5.1.1

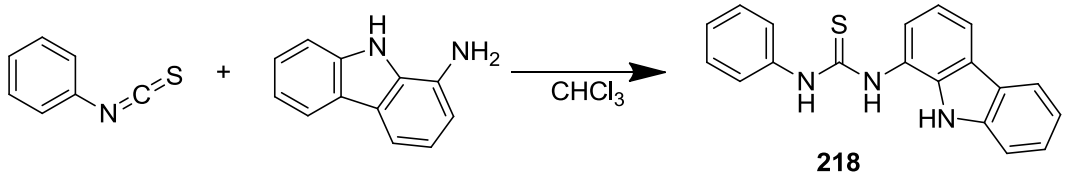

Scheme 2.5.1.2

2.5.2 Solution phase analysis

2.5.2.1 Proton NMR titration data

Anion binding constants were calculated for receptors **216**, **217** and **218** with wide range anions. The binding constants were determined by ^{1}H NMR titration with the TBA or TEA salt of the anion in DMSO-d_6/0.5% H_2O. The binding constants were determined by the computer program WINEQNMR[153] and fitted to a 1:1 binding model that was suggested by the titration data and previous receptor analogues (**209-215**). Binding constants were determined by following the downfield shift of a thiourea NH. No binding constants could be calculated for receptors **216-218** with TBA fluoride or TEA bicarbonate due to NH peak broadening. The downfield shifts observed during the ^{1}H NMR titrations show that all NH bond donor groups of the three analogues are involved in binding the anions. An overview

of the anion/receptor binding constants and the associated errors are shown in Table 2.5.2.1.

Table 2.5.2.1 Anion binding constants (M^{-1}) and percentage error for receptors **216**, **217** and **218**, measured in DMSO-d_6/0.5% H_2O at 298 K. Anionic guests were added as the TBA salt of the anion with the exception of bicarbonate, which was added as the TEA salt of the anion. Binding constants were determined by ^1H NMR titration following the thiourea NH, fitting data to a 1:1 binding model using WINEQNMR[153].

Anion	**216**	**E (%)**	**217**	**E (%)**	**218**	**E (%)**
$CH_3CO_2^-$	2230	9	1800	7	1780	16
$H_2PO_4^-$	687	8	1340	12	a	-
$C_6H_5CO_2^-$	658	3	675	7	870	5
F^-	a	-	a	-	a	-
Cl^-	15	10	17	10	23	6
[b]HCO_3^-	a	-	a	-	a	-

a – No binding constant could be calculated due to the peak broadening of the receptor/anion complex. [b] Added as the TEA salt of the anion.

As observed in the comparison between the diindolylthiourea receptors (**211-212**) and the diindolylurea receptors (**209-210**), the carbazolylthiourea receptors (**216-218**) show a general decrease in anion affinity when compared to the urea analogues (**213-215**). This can there be attributed to the same solution interconversion effects, or conformational effects, of the larger-sized sulfur atom of the thiourea group affecting the planar conformation of the receptor when binding the anion and causing a decrease in anion binding affinity. Graphs 2.5.2.1 and 2.5.2.2 show evidence for the argument that receptors **216-218** could not adopt a planar conformation, thus limiting the binding affinity of the receptors for the various anions. The strength of binding can be estimated by the overall change in chemical shift and the severity of the turning point shown on Graphs 2.5.2.1 and 2.5.2.2 to reach a plateau. The sharper the turn and the greater the overall change in chemical shift, the greater the affinity of that NH bond donor group with the anion. Both the carbazole and urea NHs show similar strong interactions between receptor **213** and the

benzoate anion. Although receptor **216** shows a similar strength interaction through the carbazole NH as observed with receptor **213**, a weaker interaction is observed through the thiourea NHs as would be expected if the receptor was twisted. This comparison could not be made with the diindolylurea/thiourea (**209**-**212**) due to the peak broadening observed with the NH signals of the thiourea-based receptors.

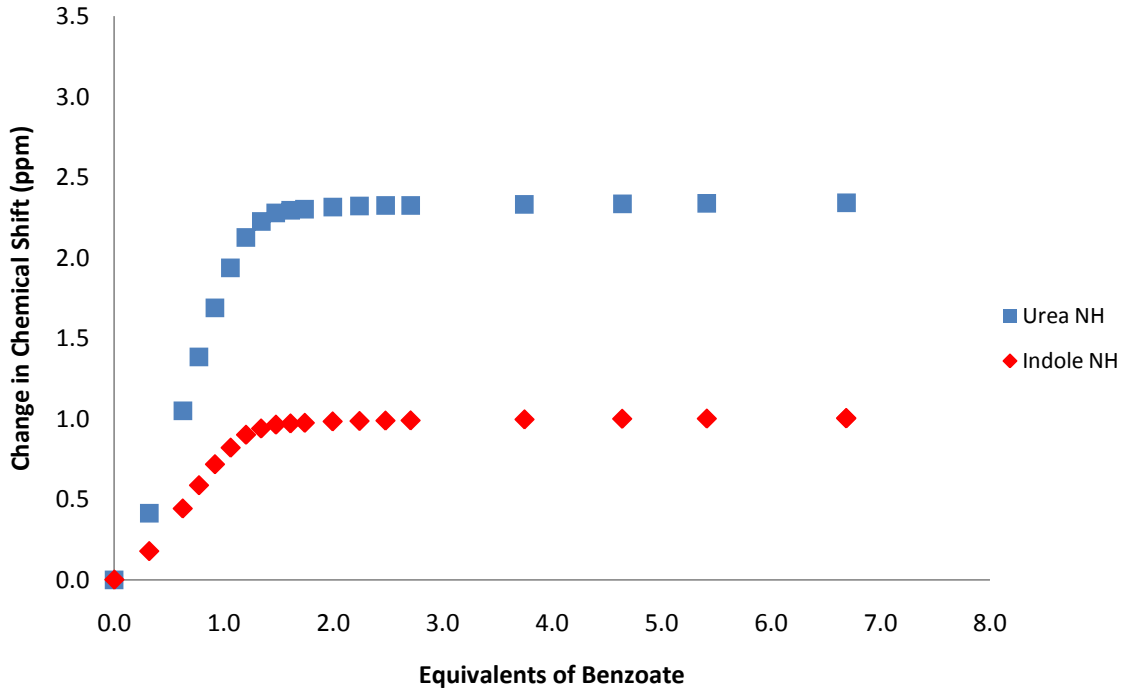

Graph 2.5.2.1 Effect of increasing benzoate concentration upon the change of chemical shift for receptor **213** in DMSO/0.5% water.

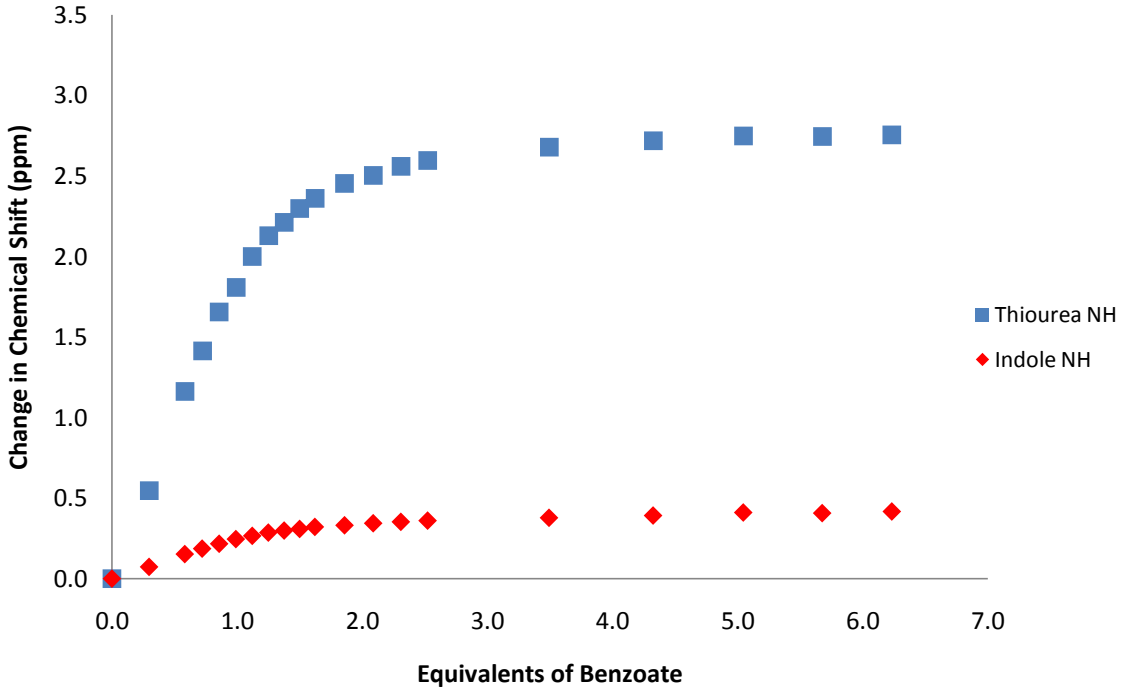

Graph 2.5.2.2 Effect of increasing benzoate concentration upon the change of chemical shift for receptor **216** in DMSO/0.5% water.

2.6 Conclusion

A set of urea/thiourea linked indole/carbazole receptors have been synthesised and their solution state anion binding properties have been explored using ^{1}H NMR titration and Job plot experiments. The fluorescence properties of these receptors have also been investigated by Claudia Caltagirone. The solid state anion binding properties were investigated by X-ray crystallography.

Receptors **209** and **210** have shown a high affinity and selectivity towards dihydrogen phosphate in highly polar DMSO-d_6/H_2O solutions. Replacing the urea group in these receptors with a thiourea group (**211** and **212**) has been shown to cause a loss in selectivity and affinity with anions, potentially due to either conformational interconversion effects[155] or the larger size of the sulfur atom twisting the receptor and preventing the adoption of a more favourable planar conformation.

Receptors **213-215** were shown to have a high affinity and selectivity towards acetate and bicarbonate anions. These receptors also show selective quenching effects upon

the addition of benzoate. The same loss in anion affinity, was observed with receptors **213-218** following the exchange of the urea for the thiourea functionality. The introduction of the thiourea group also meant that receptors **216-218** no longer were able to act as fluorescent sensors for the presence of particular anions.

X-ray analysis showed unusual 1:2 and 1:3 anion:receptor complexes with carbonate, phosphate and receptors **209** and **210** respectively. The formation of multiple hydrogen bonds to an anion from two or more receptors was found to cause the deprotonation of the bound anion (bicarbonate to carbonate and dihydrogen phosphate to phosphate). For further explanation, see Chapter Three.

Chapter 3 – Amide Appended Diindolylurea Anion Receptors

3.1 Introduction

The addition of extra hydrogen bond donor groups to allow a greater number of hydrogen bonds to form between the anion and the receptor is known to increase the affinity of an anion for a receptor. This chapter will discuss the effects of increasing the number of hydrogen bond donor groups upon anion binding events in the solution and solid states. Additional amide functionalities on the simple phosphate selective diindolylurea-based scaffold, as discussed in Chapter Two, will provide the extra hydrogen bond donor groups. Although there is little interaction of the amide functionality with the precursors of the diindolylurea receptors, synthesised from previous members of this group (receptors **179-181**)[2], we do see selective interaction of the amide functionality based on the anionic guest. The cleft receptors **219-222** have the ability to wrap around the anions with tetrahedral/trigonal planar geometries, utilising all NH bond donor groups. The geometric conformation changes depend upon the anion bound. This design takes inspiration from the indole-based foldmers synthesised by Jeong and co-workers.[116,138,139,141-143]

The most interesting effect that has resulted from the addition of two hydrogen bond donor groups (receptors **219** and **220**), and four hydrogen bond donor groups, (receptors **221** and **222**) onto the basic four hydrogen bond donor diindolylurea skeleton, (receptors **209** and **210**) was the discovery that bound oxo-anions, bicarbonate and dihydrogen phosphate, underwent deprotonation to give the 2- ion in both the solid and solution states. The interaction of this increased number of acidic hydrogen bond donor groups with the anion reduces the pK_a of the bound anion, resulting in deprotonation of the more acidic anion by excess free anion in solution. This deprotonation event can be seen in the solid state single X-ray crystal structure of the original diindolylurea receptors **209** and **210** when bound with bicarbonate and dihydrogen phosphate respectively. The anions are bound by multiple receptors that contribute between eight and twelve NH bond donor groups to a single anion (Figures 2.2.3.2, 2.2.3.3a and 2.2.3.3b). This effect, however, was

only seen in the solid state, not in the solution-based studies. Proton transfer events have been seen before in receptor/anion studies, but this has been from deprotonation of the receptor's acidic hydrogen bond donor groups by basic anions such as fluoride and dihydrogen phosphate.[44-46,50,82,160-168]

Receptors have shown sufate selectivity. Tripodal-urea functionalised acyclic and macrocyclic receptors have already been shown to selectively bind this anion, with attempts to remove the anion from the solution[64,65,169,170]. The binding of this anion is of great importance because of its roles in biological systems, in particular the role in disease[122,123,171,172]. The anion also has roles in environmental pollution[173] and hydrometallurgy[174-176]. The advantage with these receptors is the spontaneous crystallisation of the receptor/anion complex under certain conditions in as little as 20 minutes.

3.2 Symmetrical amide appended indolylurea hydrogen bond donating clefts containing six hydrogen bond donating groups

The work from this section of Chapter Three has been previously published.[177] This set of two symmetrical cleft receptors (receptors **219** and **220**) contain six hydrogen bond donor groups as opposed to the four hydrogen bond donor groups contained in the original diindolylurea receptors **209** and **210**. The extra two NH bond donor functionalities come from the additional amide functionality at the indole seven position. The aim of this functionality is to increase the anion binding affinity of these receptors by increasing the number of hydrogen bond donor groups.

3.2.1 Synthesis

Receptors **219** and **220** were synthesised in a four step process. The first step is an amide coupling reaction with 7-nitroindole-2-carboxylic acid to butylamine (receptor **219**) using PyBOP as the amide coupling agent. HOBt was used to catalyse the reaction in a dry DMF solution with a few drops of NEt_3. The crude product was precipitated from a concentrated chloroform/hexane solution to give a 25 % yield. The coupling was also performed using CDI in chloroform and the crude product was refined by flash chromatography methanol:DCM 1:49 to give a 74 % yield. This method became the preferred synthesis

method. The amide coupling with analine for receptor **220** was performed in accordance with previously published methods[2]. The coupling was also performed using PyBOP and a catalytic amount of HOBt in a dry DMF solution with NEt_3. The pure product was isolated by precipitation from the reduced DMF solution with chloroform and hexane to give a yield of 47 %. This method became the preferred synthesis method, although the CDI coupling was also found to be successful, giving a yield of 43 %. The type of amide coupling reaction chosen was based on the availability of reactants, size of reaction and the purity of the reagents, as some decompose over time.

The nitroamide compounds were then reduced with a solid Pd/C 10% catalyst in ethanol under a hydrogen atmosphere. A 100% yield was assumed. The amine was then reacted straight away with triphosgene in a two phase, 1:1, saturated $NaHCO_3$:DCM solution. Both receptors **219** and **220** were isolated from the reaction mixture with yields of 77 % and 88 % respectively. The synthetic route has been summarised in Scheme 3.2.1.1

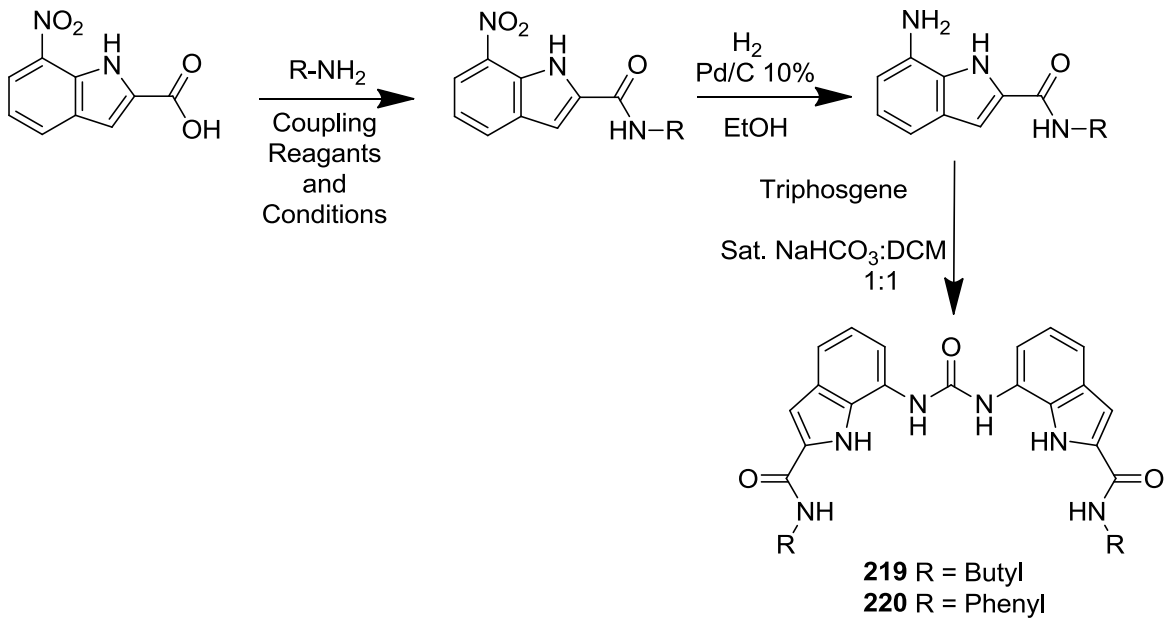

Scheme 3.2.1.1

3.2.2 Solution phase analysis

3.2.2.1 Proton NMR titration data

Anion binding constants were determined for receptors **219** and **220** with wide range anions. The binding constants were calculated from ^{1}H NMR titration with the TBA salt of the anion in various DMSO-d_6/H_2O solutions apart from bicarbonate, which was added as the TEA salt of the anion. The binding constants were obtained using the computer program WINEQNMR[153] with the titration data fitted to a 1:1 binding model. A Job plot[154] was produced to check the binding stoichiometry of dihydrogen phosphate and receptor **220** in a DMSO-d_6/10% H_2O solution. One to one binding modes of the remaining anion:receptor combinations in the various DMSO-d_6/H_2O solutions were strongly suggested by the titration data and previous generations of receptor (Chapter Two). Binding constants and Job plots were determined by following the downfield shift of the urea NH and aromatic CH resonances as there were conformational changes and peak broadening events that made it difficult to calculate binding constants from one ^{1}H NMR resonance. In general, there is a good correlation for the binding constants calculated using the urea NH and the aromatic CH resonances. Between four and six NH bond donor groups are involved in binding the anion to the receptors, depending on the geometry of the anion.

The binding constants and information derived from the ^{1}H NMR titration experiments for receptor **119** are shown in Table 3.2.2.1. This receptor shows a range of complex binding activity. In a DMSO-d_6/0.5% H_2O solution, high affinities are observed for the carboxylate anions, with binding constants $>10^4$ M^{-1}. There is little affinity shown for the chloride anion, with binding constants of 166 M^{-1} and 22 M^{-1} observed for the aromatic CH and urea NH respectively. Deprotonation of the bound anion is observed with dihydrogen phosphate. This is further discussed in 3.2.2.2. Increasing the polarity of the solution by increasing in the percentage of water in the solution to 10% prevents the deprotonation of the bound dihydrogen phosphate and the receptor becomes selective for the binding of this anion over the other carboxylate anions, with binding constants of $>10^4$ M^{-1} and 2314 M^{-1} observed for the aromatic CH and urea NH respectively. The lower binding constant observed for acetate (462 M^{-1}) could be due to a conformational change, indicated by the NH resonances of the ^{1}H NMR titration spectrums, which would prevent

optimal anion binding conditions. Data collected with fluoride could not be fitted to a 1:1 or 2:1 anion:receptor binding model. The data collected is illustrated in Graph 3.2.2.1.

Table 3.2.2.1 Anion binding constants (M^{-1}) and percentage error for receptor **219**, measured in DMSO-d_6 and varying concentrations of water at 298 K. Anionic guests were added as the TBA salt of the anion with the exception of bicarbonate, which was added as the TEA salt of the anion. Binding constants were determined by ^{1}H NMR titration following the urea NH, fitting data to a 1:1 binding model using WINEQNMR.[153]

	DMSO-d_6 0.5% H_2O				**DMSO-d_6 10% H_2O**			
Anion	**CH**	**E (%)**	**NH**	**E (%)**	**CH**	**E (%)**	**NH**	**E (%)**
$CH_3CO_2^-$	$>10^4$	-	$>10^4$	-	462	7	c	-
$H_2PO_4^-$	b	-	b	-	$>10^4$	-	2310	-
$C_6H_5CO_2^-$	$>10^4$	-	$>10^4$	-	1020	8	1100	4
Cl^-	166	1	22	9				
F^-	a	-	a	-				
[d]HCO_3^-	$>10^4$	-	2470	14	809	3	395	9

a – Data could not be fitted to a 1:1 or 2:1 anion:receptor binding model. b – Deprotonation of bound anion. c – Conformational change. [d] Added as the TEA salt of the anion.

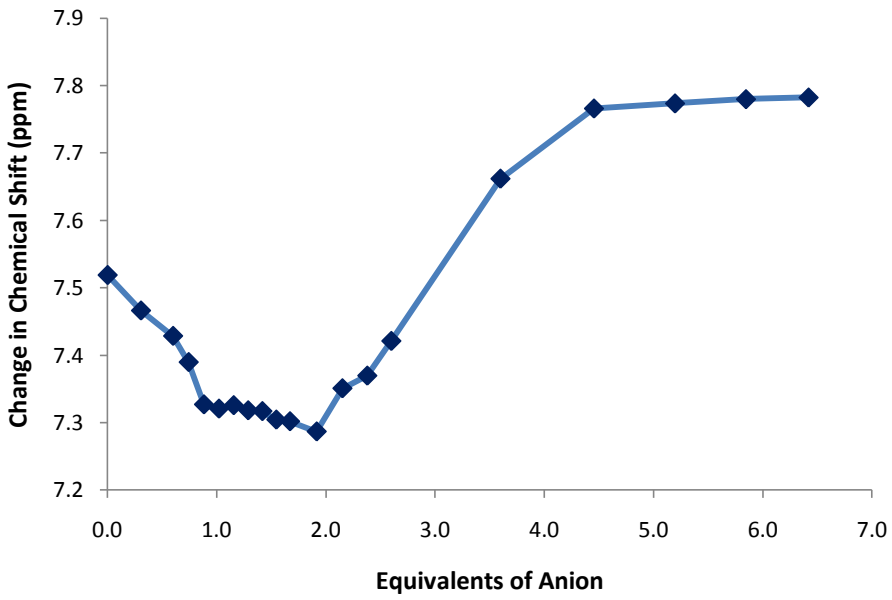

Graph 3.2.2.1 Change in chemical shift of the aromatic CH of receptor **219**, when binding TBA fluoride in a DMSO-d_6/0.5% H_2O solution.

The binding constants and information derived from the ^1H NMR titration constants for receptor **220** are shown in Table 3.2.2.2. The range of anions tested was extended for future comparison to receptors **221** and **222**. A small proportion of the ^1H NMR titration experiments were performed by Claudia Caltagirone. As with receptor **219**, receptor **220** shows complex binding activity with the different anions in a DMSO-d_6/0.5% H_2O solution. There is also low affinity shown towards chloride with binding constants calculated of 79 M^{-1} and $\leq$ 10 M^{-1} for the CH and NH groups respectively. A similarly low binding constant was also calculated for hydrogen sulfate. Carboxylate anions, acetate and benzoate, are also bound effectively, with binding constants calculated from the aromatic CH to be $>10^4$ M^{-1} but bicarbonate is not bound as effectively (2250 M^{-1}). Although there is no deprotonation of the bound anion observed with this receptor, a binding constant of 107 M^{-1} was calculated for the receptor/dihydrogen phosphate complex, which is much lower than that observed with receptor **219** in a far more competitive environment. Receptor **220** has lost the high affinity for dihydrogen phosphate due to the steric hindrance created in replacing the butyl chain for the phenyl ring. Data collected with fluoride could not be fitted to a 1:1 or 2:1 anion:receptor binding model. The data collected is illustrated in Graph 3.2.2.2.

Table 3.2.2.2 Anion binding constants (M^{-1}) and percentage error for receptor **220**, measured in DMSO-d_6 and varying concentrations of water at 298 K. Anionic guests were added as the TBA salt of the anion with the exception of bicarbonate, which was added as the TEA salt of the anion. Binding constants were determined by ^{1}H NMR titration following the urea NH, fitting data to a 1:1 binding model using WINEQNMR.[153]

	DMSO-d_6 0.5% H_2O				**DMSO-d_6 10% H_2O**			
Anion	**CH**	**E (%)**	**NH**	**E (%)**	**CH**	**E (%)**	**NH**	**E (%)**
$CH_3CO_2^-$	$>10^4$	-	8460	12	c	-	1420	6
$H_2PO_4^-$	107	8	b	-	d	-	d	-
HSO_4^-	18	14	≤10	-				
SO_4^{2-}	$>10^4$	-	$>10^4$	-	e	-	e	-
$C_6H_5CO_2^-$	$>10^4$	-	b	-	639	3	481	5
Cl^-	79	5	≤10	-				
F^-	a	-	a	-				
[f]HCO_3^-	2250	17	b	-	728	7	b	-

a – Deprotonation of receptor. b – Peak broadening prevented binding constant from being calculated. c – Conformational change. d – Data could not be fitted to a 1:1 or 2:1 anion:receptor binding model. e – Spontaneous crystallisation. [f] Added as the TEA salt of the anion.

This receptor was also found to have a high affinity for sulphate, with a binding constant of $>10^4$ M^{-1} calculated for urea NH. Increasing the percentage of water in the solution to 10 % was found to cause spontaneous crystallisation of the sulfate receptor complex (see 3.4 for further explanation). The more polar solution also caused an increase in the complexity of the dihydrogen phosphate binding model, which can no longer be fitted to a binding model. A trend in selectivity of the carboxylate anions can also be seen. Acetate is bound most favourably (1420 M^{-1} urea NH) and bicarbonate now bound more favourably than benzoate, with binding constants for the aromatic CH of 728 M^{-1} and 639 M^{-1} respectively, although these low values cannot be directly compared because of the difference in counter cation.

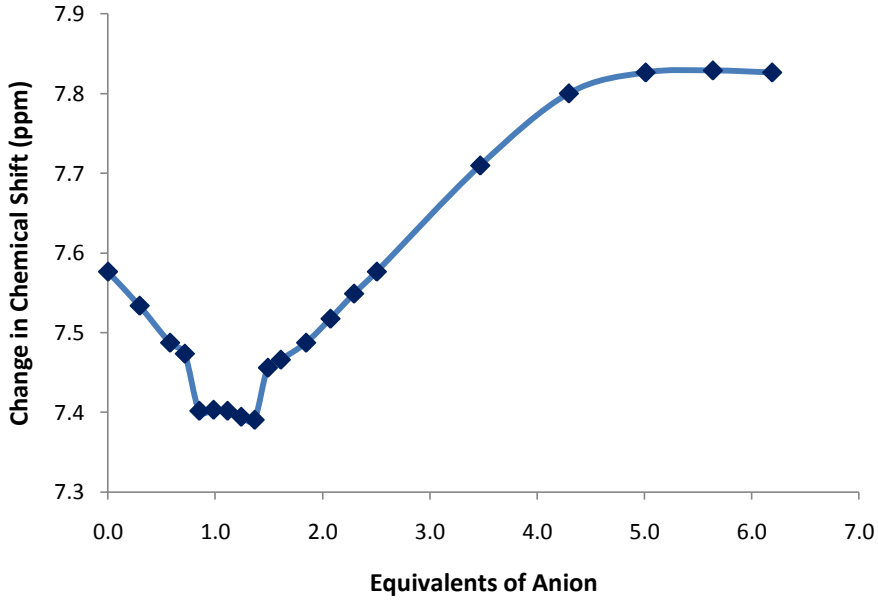

Graph 3.2.2.2 Change in chemical shift of the aromatic CH of receptor **220** when binding TBA fluoride in a DMSO-d_6/0.5% H_2O solution.

Evidence for changes in binding conformation of the different anion/receptor combinations is shown in Graphs 3.2.2.3 – 3.2.2.5, generated from the ^{1}H NMR titration data. There are two different binding modes observed with these two receptors. The first is the binding of the first equivalent of anion through four NH bond donor groups, two from the indole functionality and two from the urea functionality. The second is the binding of the first equivalent of the anion through all six urea, indole and amide NH bond donor groups. Similar binding modes are observed for each of the different anions with the two receptors. The downfield shift of the different hydrogen resonances following additions of anion indicates their involvement in the anion binding process.

Graph 3.2.2.3 shows the change in chemical shift of the different NH and CH resonances with the addition of equivalents of TBA benzoate to a DMSO-d_6/0.5% H_2O solution of receptor **219**. A downfield shift, producing similar shaped curves, is seen with the indole NH, urea NH and aromatic CH resonances but no change in chemical shift is seen for the amide NH. This shows that the anion is only coordinating to the receptor through the indole and urea NHs, but not through the amide NH bond donor groups.

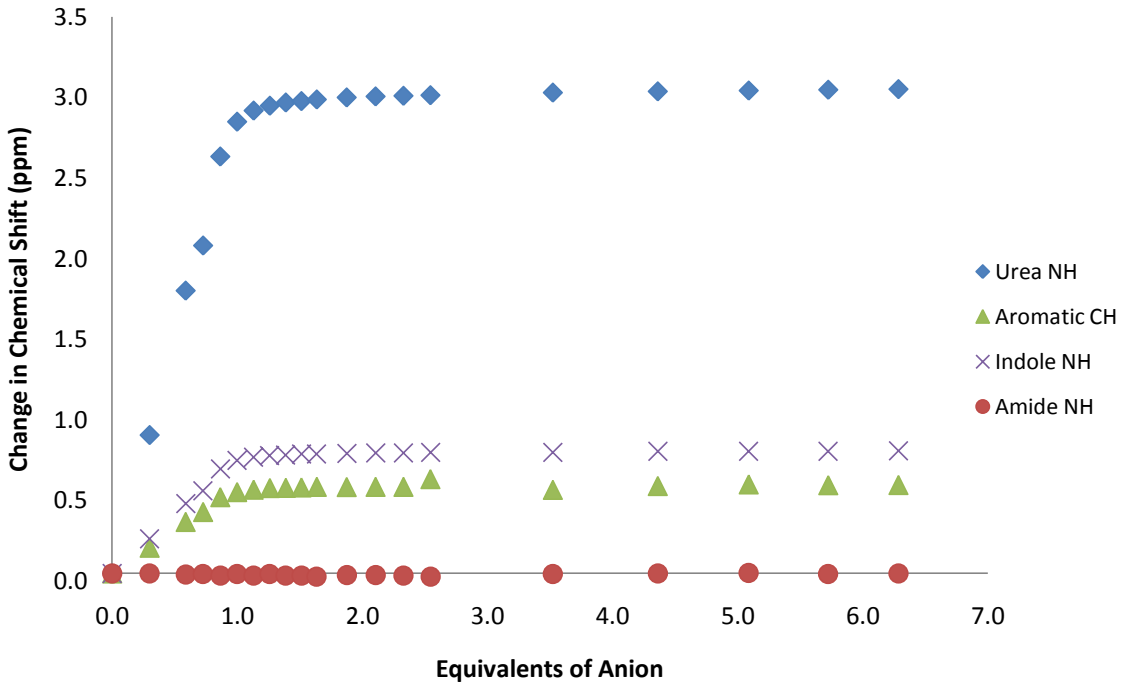

Graph 3.2.2.3 Change in chemical shift of the various resonances of receptor **219** with TBA benzoate, illustrating the interaction of the urea, indole, amide NH and aromatic CH functionalities with the anion in a DMSO-d_6/0.5% H_2O solution.

Graph 3.2.2.4 shows the change in chemical shift of the different NH and CH resonances with the addition of equivalents of TBA acetate to a DMSO-d_6/0.5% H_2O solution of receptor **220**. A downfield shift, producing similar shaped curves, is seen with the indole NH, urea NH and aromatic CH resonances. A change in chemical shift is only seen for the amide NH after the addition of more than one equivalent of anion. This means that the first equivalent of anion is only coordinating to the receptor through the indole NH, urea NH and aromatic CH. Further equivalents of anion are then binding through the two remaining amide NHs outside of the binding cleft.

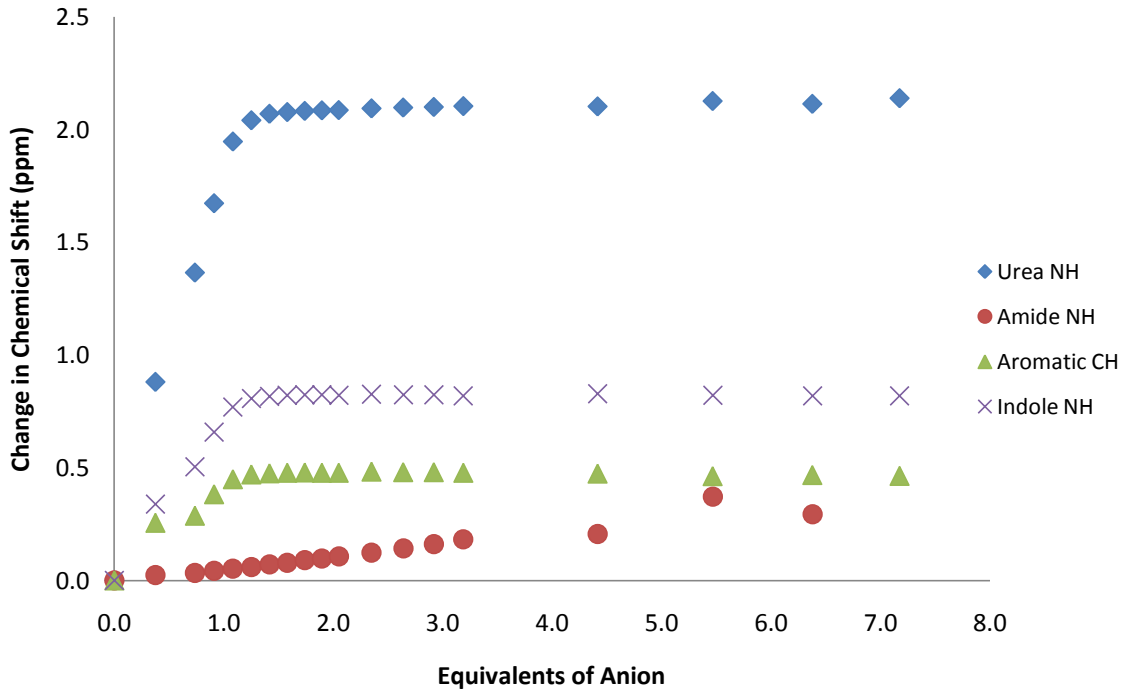

Graph 3.2.2.4 Change in chemical shift of various resonances of receptor **220** with TBA acetate, illustrating the interaction of the urea, indole, amide NH and aromatic CH functionalities with the anion in a DMSO-d_6/0.5% H_2O solution.

Graph 3.2.2.5 shows the change in chemical shift of the different NH and CH resonances with the addition of equivalents of TEA bicarbonate to a DMSO-d_6/0.5% H_2O solution of receptor **219**. A downfield shift, producing similar shaped curves, is seen with the indole NH, urea NH, aromatic CH and amide NH resonances. This is evidence for the second binding mode, with the first equivalent of anion bound by all six NH bond donor groups. This binding motif is also observed with dihydrogen phosphate, sulfate, hydrogen sulphate and is only found in the binding of tetrahedral and trigonal planar anions.

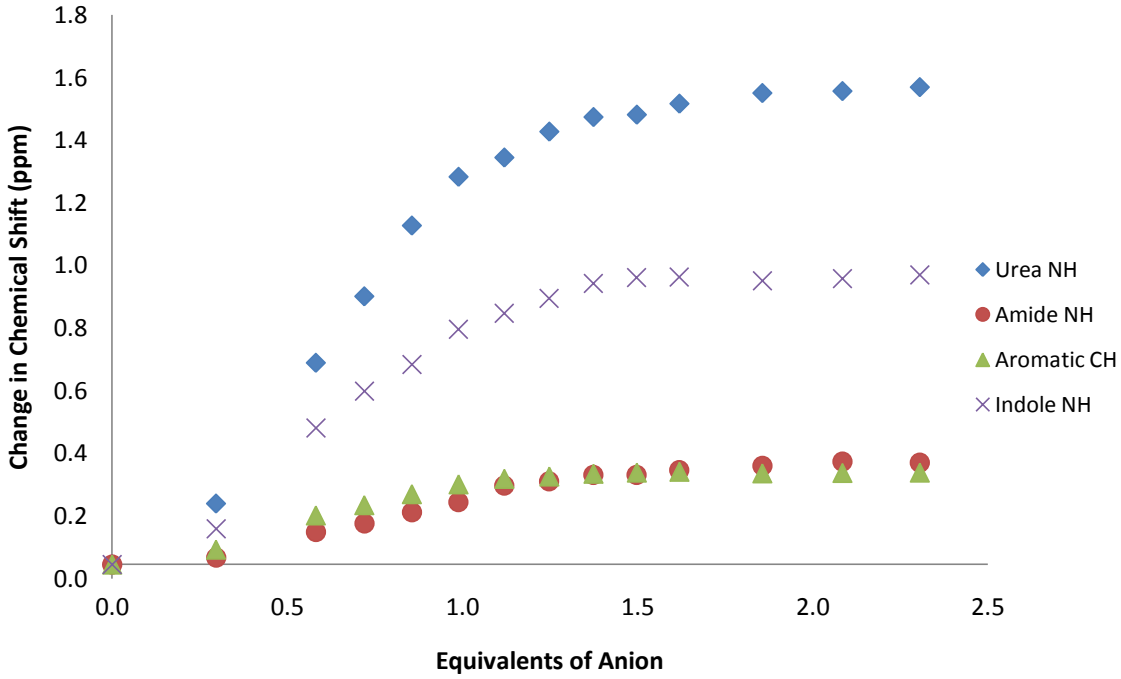

Graph 3.2.2.5 Change in chemical shift of various resonances of receptor **219** with TEA bicarbonate, illustrating the interaction of the urea, indole, amide NH and aromatic CH functionalities with the anion in a DMSO-d_6/0.5% H_2O solution.

3.2.2.2 Deprotonation of bound anions

The ^{1}H NMR titration of receptor **219** showed two processes occurring with the addition of TBA dihydrogen phosphate. The first, fast exchange event is observed between 0-1 equivalents of anion in a DMSO-d_6/0.5% H_2O solution of receptor. The second event is in slow exchange with anion concentrations greater than one equivalent. The first binding event, shown in Stack plot 3.2.2.1, shows a steady downfield shift of the all NH and aromatic CH bond donor groups involved in binding the anion. This steady downfield shift is typical of an anion binding to the receptor.

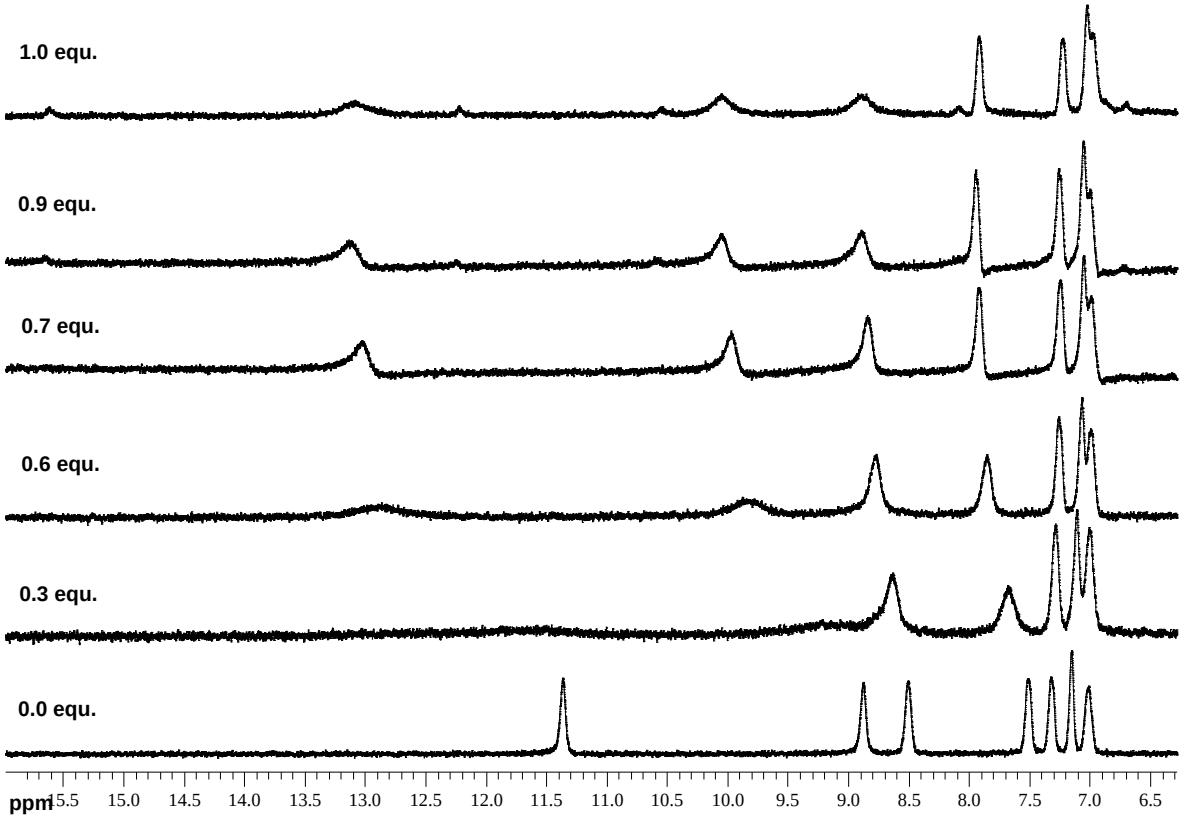

Stack plot 3.2.2.1 Receptor **219** with 0-1 equivalents of TBA dihydrogen phosphate, illustrating the fast exchange binding event of the anion to the receptor in a DMSO-d_6/0.5% H_2O solution.

The second, slow exchange process, which occurs with concentrations of anion greater than one equivalent, is shown in Stack plot 3.2.2.2. The resonances of the NH and CH bond donor groups that are involved in binding the first equivalent of anion jump downfield by as much as 2.5 ppm. This large downfield shift in indicative of a change in bound anion species that has a greater affinity for the receptor than the original anion species. This would be expected if the anion were to lose a proton, changing the formal charge on the anion from 1^- to 2^-. This increase in charge density would cause a change in chemical shift of the NH and CH resonances involved in the anion binding process and a further downfield shift is observed. This evidence supports the theory that the interaction from six acidic NH groups lowers the pK_a of the bound anion, allowing deprotonation by the more basic, free anions in solution.

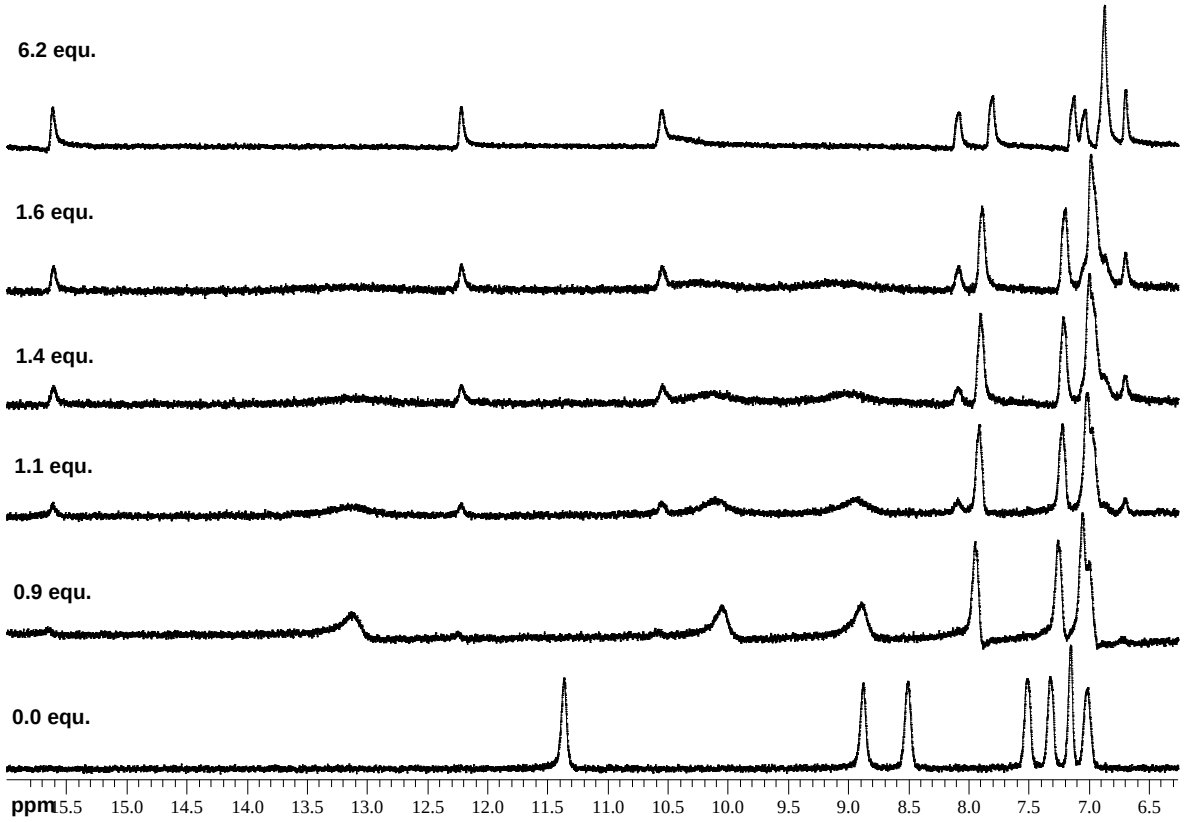

Stack plot 3.2.2.2 Receptor **219** with 0-6 equivalents TBA dihydrogen phosphate, illustrating the slow exchange deprotonation of bound dihydrogen phosphate and the binding of hydrogen phosphate in the receptor's cavity in a DMSO-d_6/0.5% H_2O solution.

To check this theory, 1.4 equivalents of dihydrogen phosphate were added to a DMSO-d_6/0.5% H_2O solution of receptor **219**, until new peaks of the hydrogen phosphate slow exchange binding event were just visible**.** Equivalents of TBA hydroxide were then added in order to force the deprotonation of the bound anion. The results from this experiment are shown in Stack plot 3.2.2.3, which shows an identical spectrum after addition of hydroxide as observed as was seen after the addition of excess dihydrogen phosphate in the original NMR experiment (Stack plot 3.2.2.2). As there is no change observed in the integration of the NH or CH resonances in either experiment, this cannot be deprotonation of the receptor but must instead be deprotonation of the bound anion.

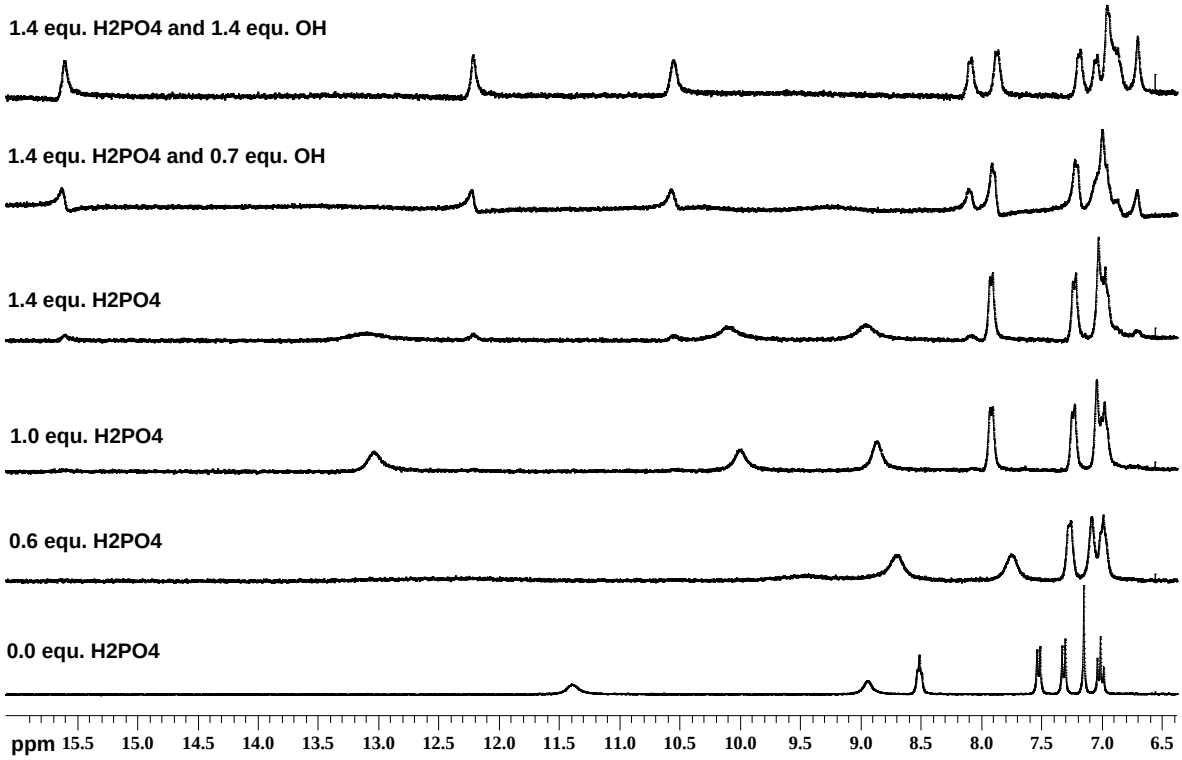

Stack plot 3.2.2.3 Receptor **219** with the addition of 0-1.4 equivalents TBA dihydrogen phosphate, followed by the introduction of TBA hydroxide to deprotonate the bound dihydrogen phosphate anion, illustrating both fast and slow exchange in a DMSO-d_6/0.5% H_2O solution. This stack plot is taken from the pre-peer reviewed version of the supplementary information from the following article: Gale, P. A.; Hiscock, J. R.; Moore, S. J.; Caltagirone, C.; Hursthouse, M. B. and Light, M. E. *Chem. Asian. J.*, **2010**, *5*, 555-561.

For completeness, Stack plot 3.2.2.4 shows that the addition of hydroxide to a DMSO-d_6/0.5% H_2O solution of the receptor **219** causes deprotonation of the receptor. The NMR results from this experiment were found to be in no way similar to those achieved with the addition of dihydrogen phosphate or a combination of dihydrogen phosphate and hydroxide.

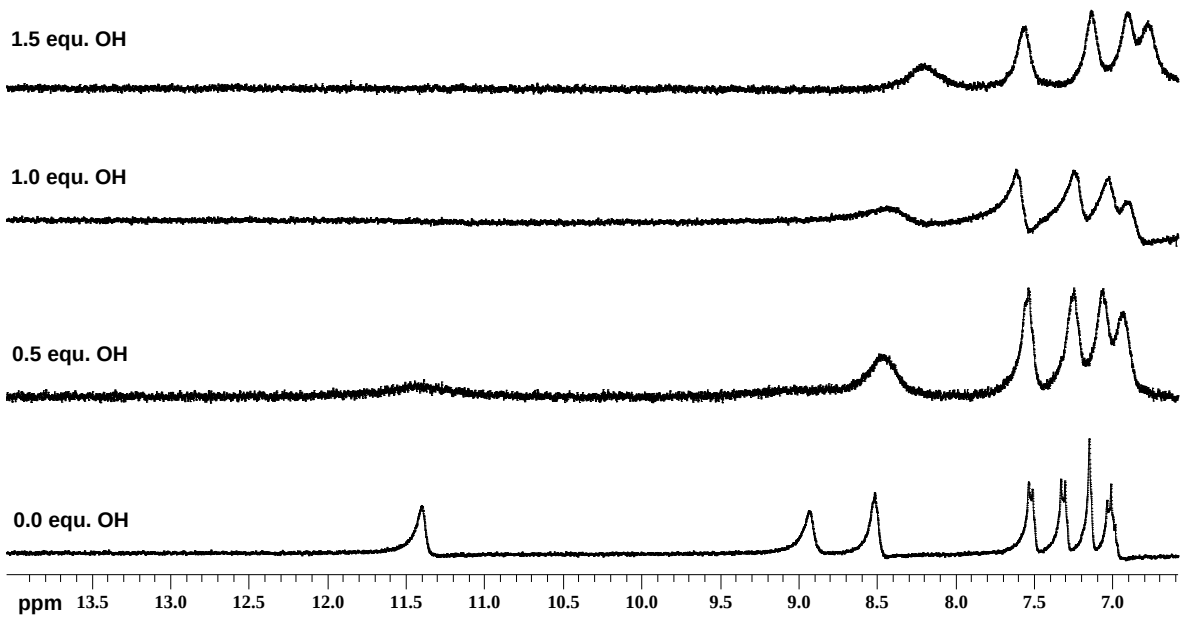

Stack plot 3.2.2.4 Receptor **219** with 0-1.5 equivalents TBA hydroxide, illustrating the deprotonation of the receptor in a DMSO-d_6/0.5% H_2O solution. This stack plot is taken from the pre-peer reviewed version of the supplementary information from the following article: Gale, P. A.; Hiscock, J. R.; Moore, S. J.; Caltagirone, C.; Hursthouse, M. B. and Light, M. E. *Chem. Ais. J.*, **2010**, *5*, 555-561.

3.2.3 Solid phase analysis

X-ray quality crystals were obtained of receptor **220** and TBA hydrogen phosphate from a DMSO solution of receptor **220** with exess TBA dihydrogen phosphate.

The crystal structure of receptor **220**, produced by single crystal X-ray diffraction, is shown in Figure 3.2.3.1. This complex shows a 1:1 anion:receptor binding stoichiometry, with all six NH bond donor groups coordinating to three of the four oxygen atoms of a single hydrogen phosphate anion. The binding stoichiometry and interaction through all six NH bond donor groups is the same as that observed in a DMSO-d_6/0.5% H_2O solution. Unlike receptor **219**, receptor **220** does not exhibit deprotonation of the bound anion in the solution state but the deprotonation event is observed in the solid state. The deprotonation of the bound anion in the solid state but not the solution state is also observed with the original diindolylurea receptors **209** and **210** (Figures 2.2.3.2, 2.2.3.3a and 2.2.3.3b). The crystallisation effects remove the solvent competition, causing stronger NHO bonds to form between the anion and receptor, therefore decreasing the pK_a of the bound anion

further than would normally be observed in the solution state and allowing the deprotonation of the bound anion.

Each of the three oxygen atoms of the anion that are not covalently bound to a hydrogen atom of the hydrogen phosphate anion are bound to the receptor by two hydrogen bonds. O7 is bound by the two urea NHs, while O5 and O6 are bound by one indole and one amide NH each. The hydrogen bonding interactions and hydrogen bonding angles for the complex (illustrated in Figure 3.2.3.1) are shown in Table 3.2.3.1. The hydrogen bonds from the nitrogen atoms of the receptor to the oxygen atoms of the anion range from N···O = 2.660(5) – 2.842(5) Å and the bond angles range from N–H···O = 152.1°-176.1°.

Table 3.2.3.1 Hydrogen bonding table for the crystal structure of receptor **220** and TBA hydrogen phosphate for the complex shown in Figure 3.2.3.1, obtained by single crystal X-ray diffraction at 120K. *D* – hydrogen bond donor atom. *A* – hydrogen bond acceptor atom. *d* – distance in Å. ∠ - bond angle in °. H – hydrogen atom. Symmetry transformations used to generate equivalent atoms: (i) –x+1,–y+2,–z+1 (ii) –x+1,–y+1,–z+1

D–H···*A*	*d*(*D*–H) (Å)	*d*(H···*A*) (Å)	*d*(*D*···*A*) (Å)	∠(*D*H*A*) (°)
N1–H801···O5	0.88	1.87	2.734(5)	166.0
N2–H802···O5	0.88	1.86	2.668(5)	152.1
N3–H803···O7	0.88	1.97	2.804(4)	156.5
N4–H804···O7	0.88	2.02	2.842(5)	155.4
N5–H805···O6	0.88	1.81	2.660(5)	160.6
N6–H806···O6	0.88	1.88	2.763(4)	176.1

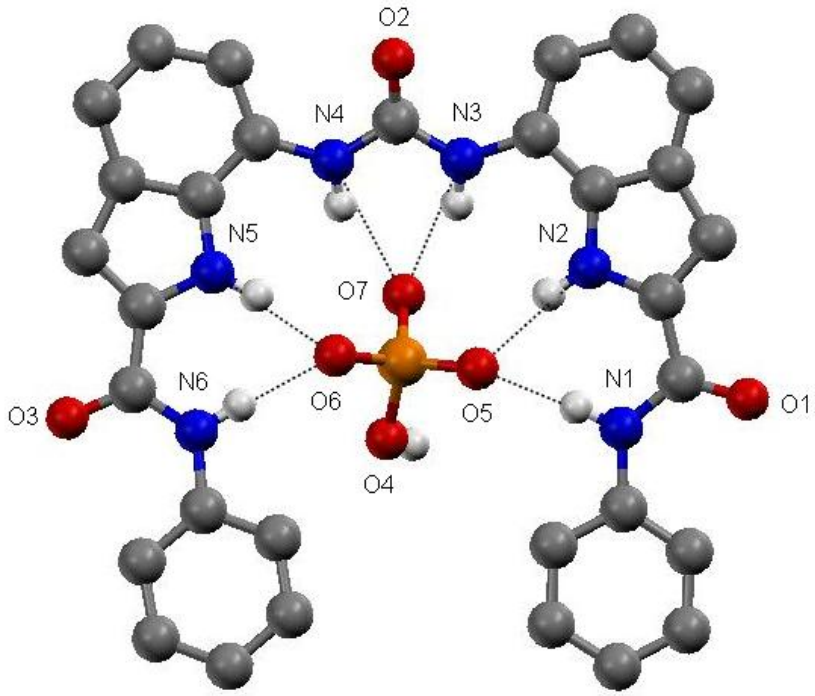

Figure 3.2.3.1 The phosphate complex of receptor **220**. Single X-ray crystal structure with TBA hydrogen phosphate. The CH hydrogen atoms, solvent molecules and the TBA counter ions have been omitted for clarity.

X-ray quality crystals were obtained of receptor **220** and TBA chloride from a DMSO solution of receptor **220** with excess TBA chloride, with help from Claudia Caltagirone.

The crystal structure of receptor **220** was produced by single crystal X-ray diffraction and is shown in Figure 3.2.3.2a. This complex shows a 2:1 anion:receptor binding stoichiometry. One chloride anion is bound in the central cleft by four hydrogen bonds, one bond from each of the urea and indole NHs. This is similar to the complex formed in the DMSO-d_6/0.5% H_2O solution, where the central indole and urea NHs are involved in binding the first equivalent of anion whilst the amide NHs are not utilised in the binding process. A second chloride ion is bound on the periphery of the receptor through two amide NHs, each contributing a single hydrogen bond to the chloride ion from adjacent receptors. This produces the chloride-interlinked structure shown in Figure 3.2.3.2b. The hydrogen bond interactions and hydrogen bonding angles for the complex shown in Figure 3.2.3.2a and b are shown in Table 3.2.3.2. The hydrogen bonds from the nitrogen atoms of

the receptor to the chloride atoms of the anion range from N···Cl = 3.156(3) – 3.405(3) Å and the bonds angles range from N–H···Cl = 155.0°-165.3°.

Table 3.2.3.2 Hydrogen bonding table for the crystal structure of receptor **220** and TBA chloride for the complex shown in Figure 3.2.3.3a and b, obtained by single crystal X-ray diffraction at 120K. *D* – hydrogen bond donor atom. *A* – hydrogen bond acceptor atom. *d* – distance in Å. ∠ - bond angle in °. H – hydrogen atom. Symmetry transformations used to generate equivalent atoms: (i) x,–y,z+1/2

D–H···*A*	*d*(*D*–H) (Å)	*d*(H···*A*) (Å)	*d*(*D*···*A*) (Å)	∠(*D*H*A*) (°)
N1–H901···Cl2^{i}	0.88	2.46	3.296(3)	159.7
N2–H902···Cl1	0.88	2.48	3.337(3)	163.2
N3–H903···Cl1	0.88	2.30	3.156(3)	163.2
N4–H904···Cl1	0.88	2.36	3.176(3)	155.0
N5–H905···Cl1	0.88	2.52	3.378(3)	164.0
N6–H906···Cl2	0.88	2.55	3.405(3)	165.3

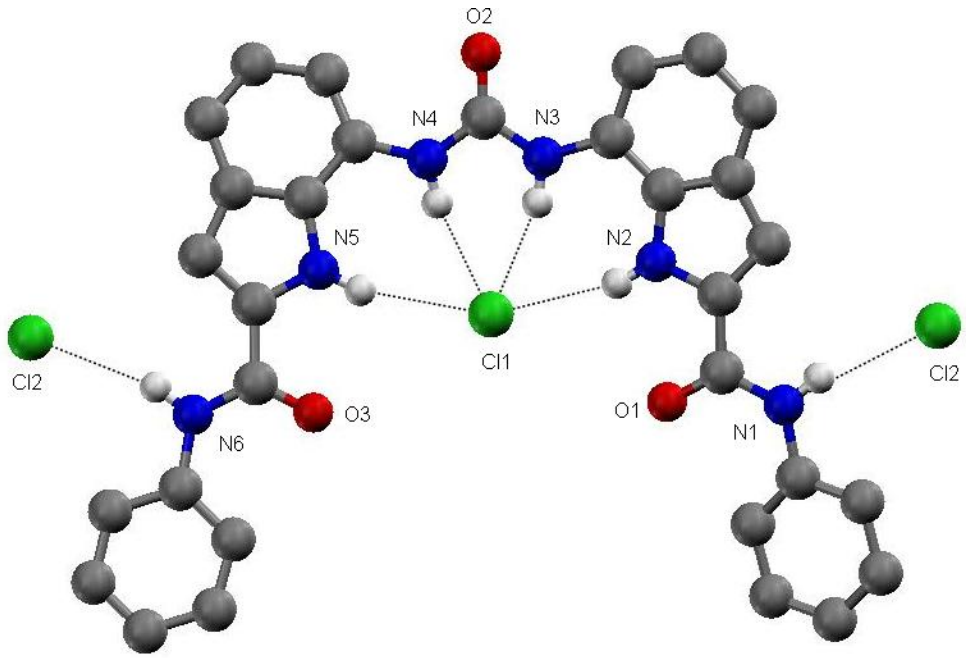

Figure 3.2.3.2a The chloride complex of receptor **220**. Single X-ray crystal structure with TBA chloride. The CH hydrogen atoms, solvent molecules and the TBA counter ions have been omitted for clarity.

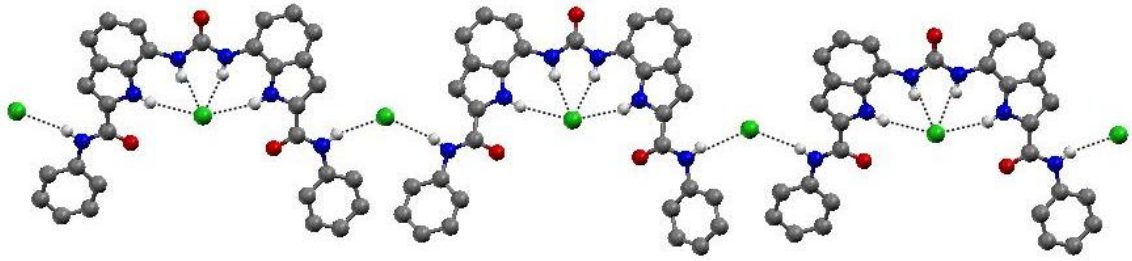

Figure 3.2.3.2b The chloride complex of receptor **220**. Single X-ray crystal structure with TBA chloride. The CH hydrogen atoms, solvent molecules and the TBA counter ions have been omitted for clarity.

3.3 Symmetrical amide appended diindolylurea hydrogen bond donating clefts containing eight hydrogen bond donating groups

The work from this section of Chapter Three has been previously published.[178] Receptors **221** and **222** are analogues of **209** and **210** and increase the number of hydrogen bond donating groups to eight overall. They are more complex receptors and resemble closely the foldmer receptors of Jeong and co-workers[116,138,139,141-143]. Binding of a single trigonal planar or tetrahedral anion occurs as the receptor wraps around the anion, using all eight hydrogen bond donor groups and binding it from 360 °, similar to a macrocycle. The first equivalent of Y-shaped and spherical anions are bound by a maximum of four hydrogen bond donor groups only. The interaction of all eight hydrogen bond donor groups to a single anion should greatly increase binding affinity towards these geometrically favoured anions, compared to previous analogues of the diindolylurea skeleton containing four (**209-210**) to six (**219-220**) NH bond donor groups. The properties of these receptors should be more exaggerated by these eight hydrogen bond donor receptors, **221** and **222**.

3.3.1 Synthesis

The synthesis of 1-nitrocarbazole and the reduction of both 7-nitroindole and 1-nitrocarbazole were achieved by methods previously described in Chapter Two, Schemes 2.2.1.1 and 2.4.1.1. However, the synthesis is also shown below as a part of reaction Schemes 3.3.1.1 and 3.3.1.2. The first step is an amide coupling reaction between 7-nitroindole-2-carboxylic acid and either 7-aminoindole (**221**) or 1-aminocarbazole (**222**),

using PyBOP as the amide coupling agent. HOBt was used to catalyse the reaction in a dry DMF solution with a few drops of NEt_3. The pure indoleamide and carbazoleamide compounds were obtained by dissolving the oil obtained from the reduced reaction mixtures in two phase solutions of DCM and washing with water. The diindole derivative was further purified by precipitation from methanol, giving yields of 89% and 70% respectively. The nitro compounds were then reduced in DMF with a solid Pd/C 10% catalyst under a hydrogen atmosphere. A 100% conversion was assumed and the amine, in a reduced amount of DMF, was finally reacted with triphosgene in a chloroform/saturated Na HCO_3 solution to give the product, which was purified by sonication in water, with yields of 71 and 79 % for compounds **221** and **222** respectively.

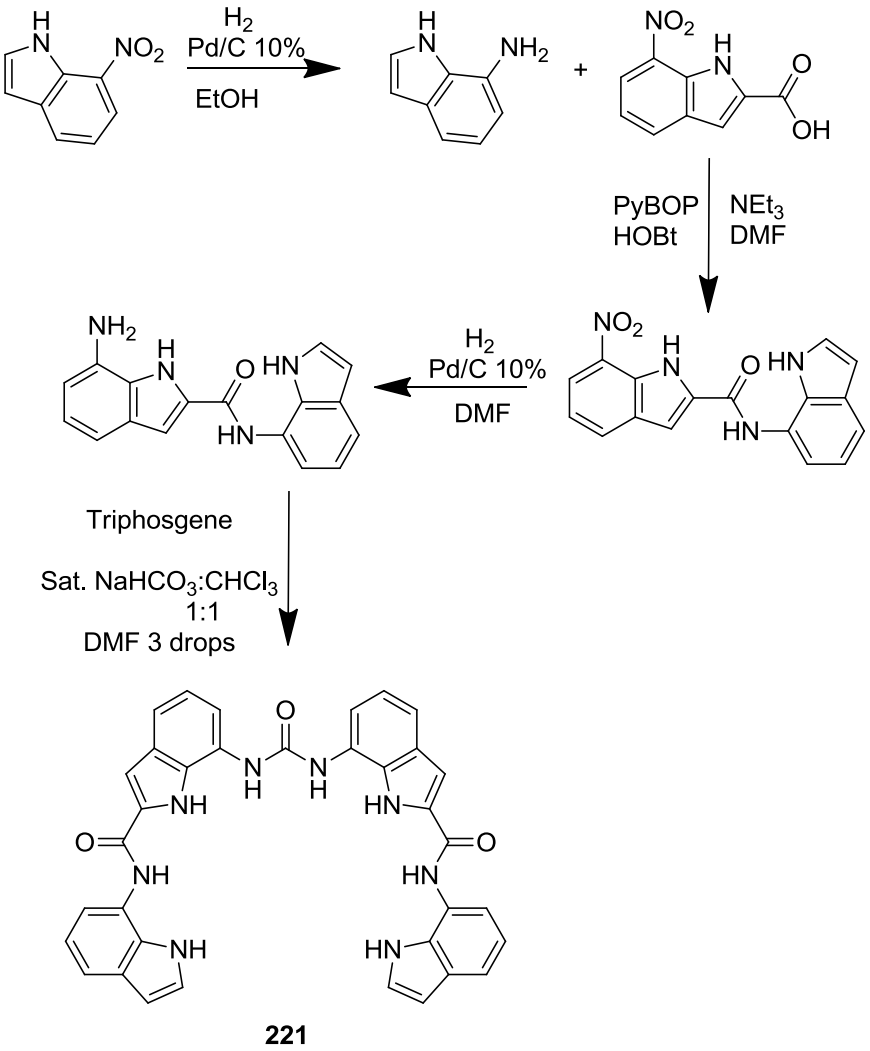

221

Scheme 3.3.1.1

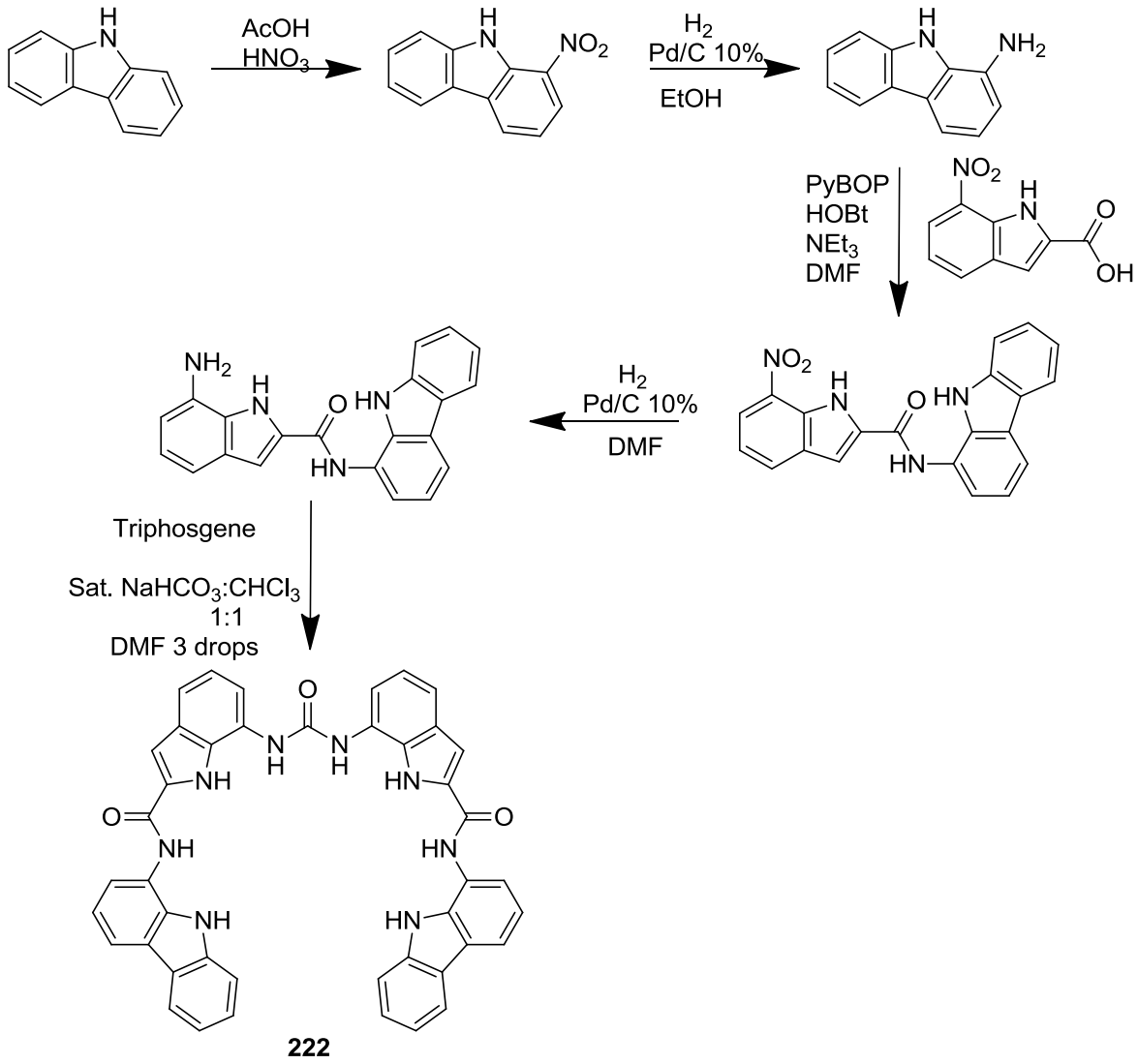

Scheme 3.3.1.2

3.3.2 Solution phase analysis

3.3.2.1 Proton NMR titration data

The ^{1}H NMR titration studies with receptors **221** and **222** were attempted with the TBA/TEA salts of the anions in various DMSO-d_6/H_2O solutions. Binding constants could not be obtained in most cases or could only be calculated approximately due to the complex nature of the binding processes. Some Job plots[154] were produced to try to identify the binding stoichometries involved in binding the anions but, for the most part, there were no clear results, again due to the complex equilibrium involved in the solution.

Limited information was gathered from the ^{1}H NMR data through observing the change of chemical shift of the different NH resonances with the addition of anion. This information is depicted in Graphs 3.3.2.1-3.3.2.9. The key for the interpretation of this data is shown in Figure 3.3.2.1. No data could be determined for the benzoate anion with receptors **221** or **222** because of the precipitation of the receptor: anion complex in both DMSO-d_6/H_2O 0.5% and 10% solutions. Deprotonation of bound dihydrogen phosphate and bicarbonate was observed for both receptors in DMSO-d_6/0.5% H_2O. Deprotonation of bound bicarbonate was also observed with both receptors in DMSO-d_6/10% H_2O.

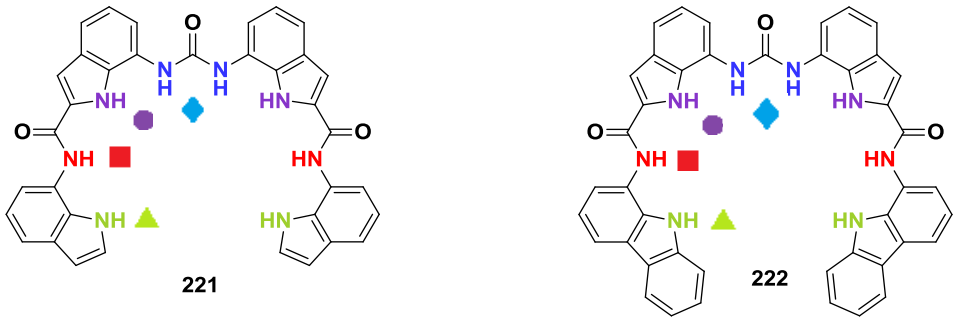

Figure 3.3.2.1 Key to structures of receptors **221** and **222**

Graph 3.3.2.1 shows the interaction of chloride with receptor **221** in a DMSO-d_6/0.5% H_2O solution. From the shape of the curve, the overall change in chemical shift and the change in chemical shift with each aliquot of anion added, there only appears to be a weak interaction with the anion. The binding stoichiometry is unclear from this Graph. Job plot analysis indicates a 1:1 anion:receptor binding mode for the urea NH but the binding stoichometries for the remaining three NH bond donor groups remains unclear, mainly due to the small change in chemical shift observed with the other NH resonances.

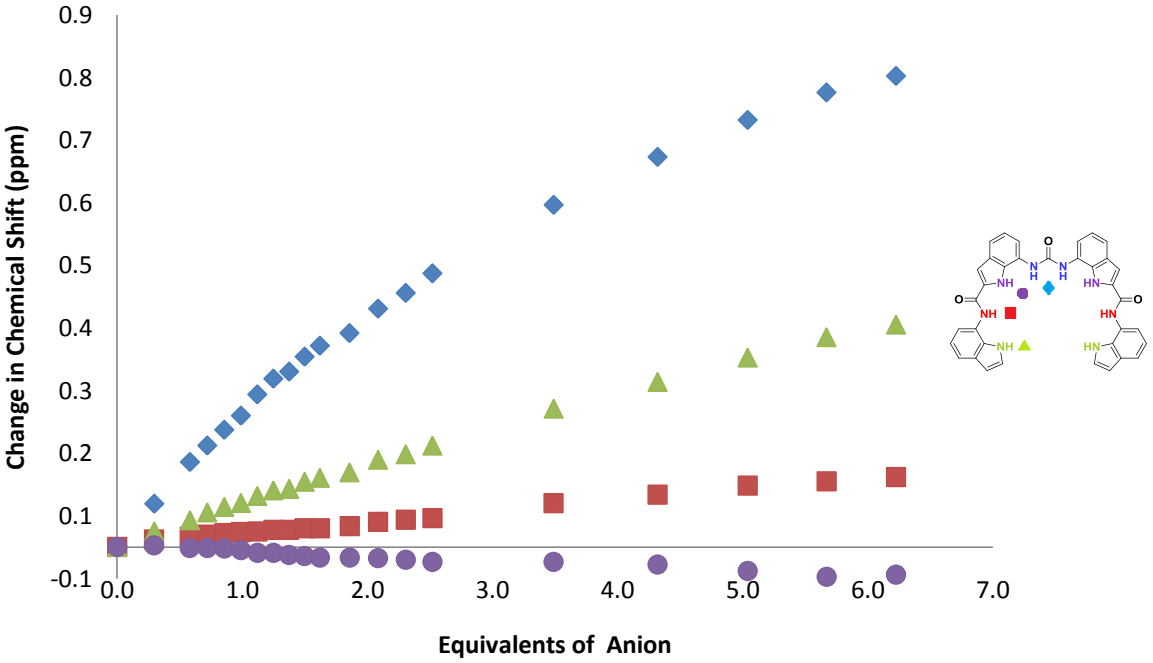

Graph 3.3.2.1 Change in chemical shift of the four different NH resonances of receptor **221** with TBA chloride, illustrating the interaction of the different NH functionalities with the anion in a DMSO-d_6/0.5% H_2O solution.

Graph 3.3.2.2 shows the interaction of acetate with receptor **221** in a DMSO-d_6/0.5% H_2O solution. From the shape of the curve, the overall change in chemical shift and the change in chemical shift with each aliquot of anion added, it is evident that there is a strong interaction with NH1 and NH4 (the diindolylurea part of the receptor) and the first equivalent of anion. Further changes in chemical shift after the addition of one equivalent of anion are indicative of the binding of further aliquots of anion. There is no real change in chemical shift observed with NH2 and 3(lower half of the receptor) until after the first aliquot of anion has been added. This indicates that these hydrogen bond donor groups are involved in binding further aliquots of anion as was seen with receptors **219** and **220** (Graph 3.2.2.4). Job plot analysis indicates a 1:1 anion:receptor binding mode for the urea NH1 and indole NH4 but more complex binding stoichometries are suggested for the remaining indole and amide NH groups.

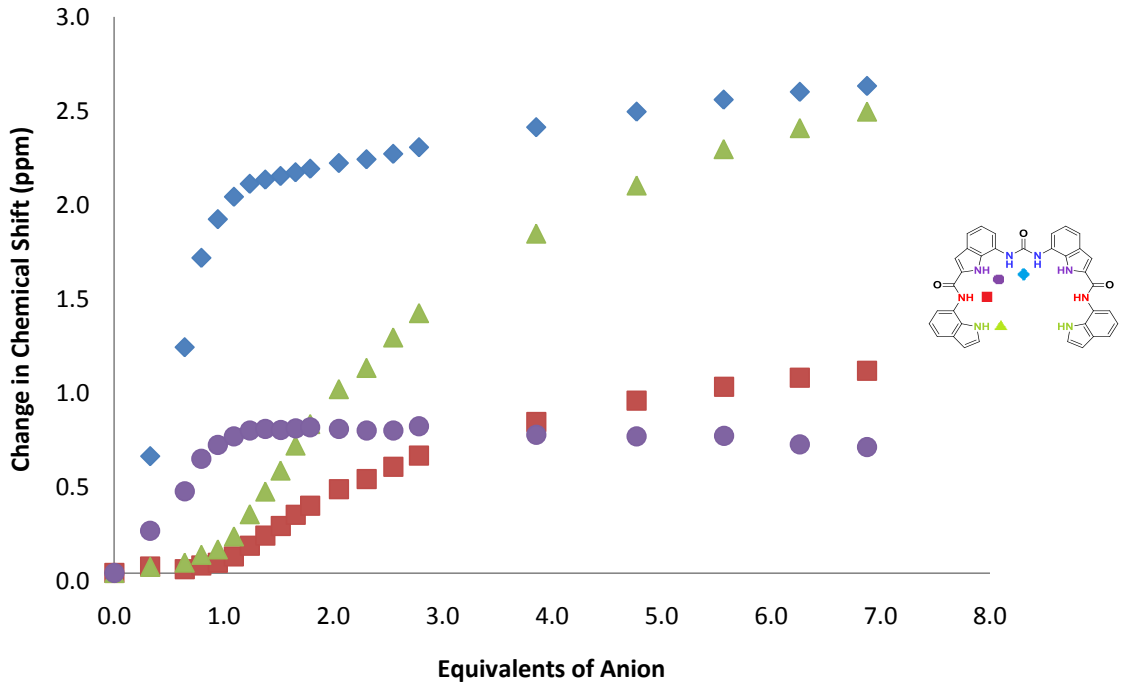

Graph 3.3.2.2 Change in chemical shift of the four different NH resonances of receptor **221** with TBA acetate, illustrating the interaction of the different NH functionalities with the anion in a DMSO-d_6/0.5% H_2O solution.

Graph 3.3.2.3 shows the interaction of sulfate with receptor **221** in a DMSO-d_6/0.5% H_2O solution. From the shape of the curve, the overall change in chemical shift and the change in chemical shift with each aliquot of anion added, it is evident that there is a strong interaction with all eight of the NH bond donor groups and the first equivalent of anion. There are further changes in chemical shift of all the NH groups after the addition of the first equivalents of the anion. This indicates a more complex binding stoichiometry than a straightforward 1:1 binding mode. Job plot analysis indicates complex binding, with all the NH resonances showing a combination of 1:1and 2:1 anion:receptor binding modes for all eight of the different NH bond donor groups.

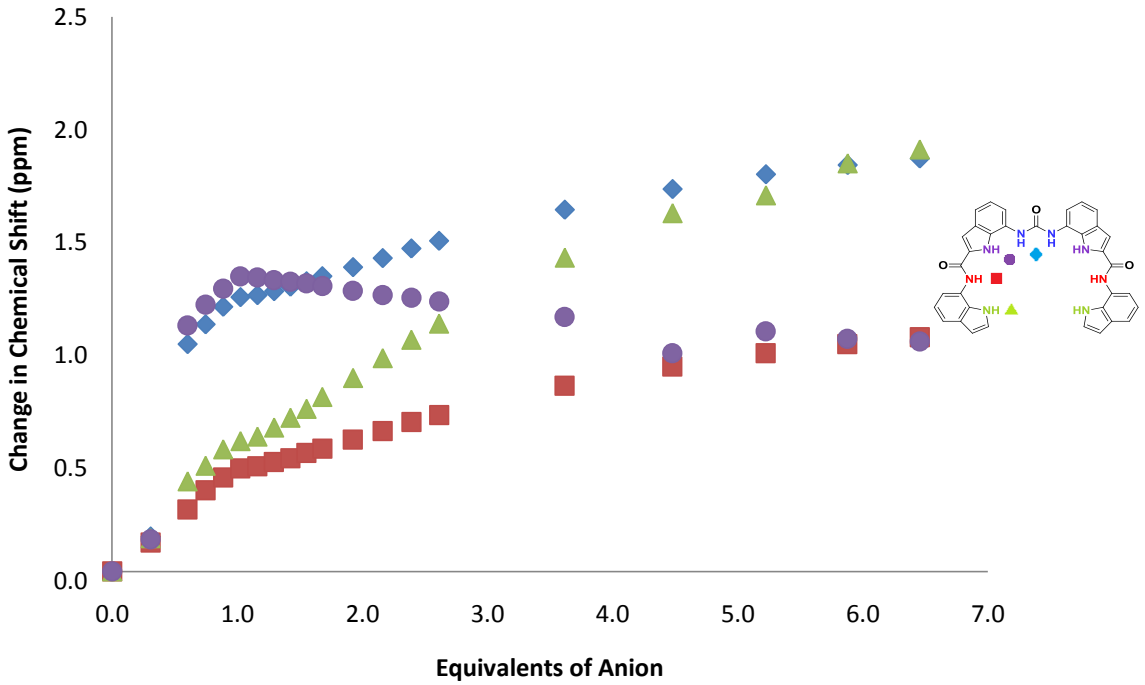

Graph 3.3.2.3 Change in chemical shift of the four different NH resonances of receptor **221** with TBA sulphate, illustrating the interaction of the different NH functionalities with the anion in a DMSO-d_6/0.5% H_2O solution.

Receptor **222** shows similar interactions with the different anions as receptor **221** but the binding stoichiometries are less clear cut and are more difficult to interpret. The change in chemical shift overall and the change with the addition of each aliquot of chloride, plus the shape of the curves, all indicate weak binding of the anion to the receptor and the binding stoichiometry is still ambiguous (Graph 3.3.2.4). No clear result can be guaged from the Job plot experiment and there is only a suspected 1:1 binding stoichiometry with the anion and urea NH as the peak of the graph cannot be clearly seen.

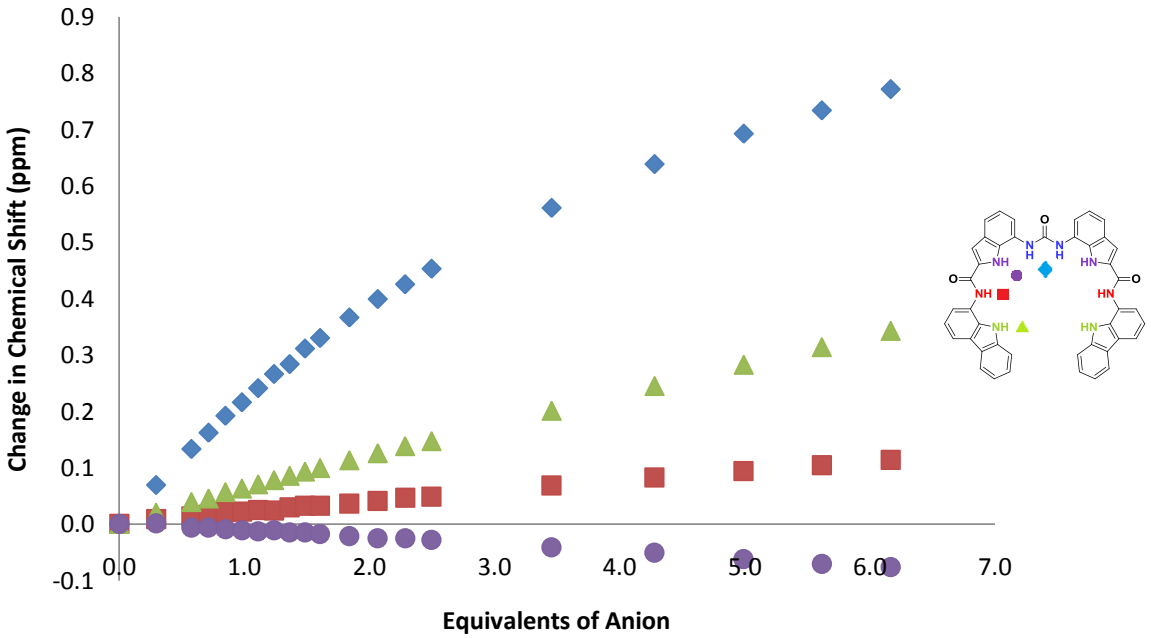

Graph 3.3.2.4 Change in chemical shift of the four different NH resonances of receptor **222** with TBA chloride, illustrating the interaction of the different NH functionalities with the anion in a DMSO-d_6/0.5% H_2O solution.

Graph 3.3.2.5 shows the interaction of acetate with receptor **222** in a DMSO-d_6/0.5% H_2O solution. As with receptor **221**, the shape of the curve, the overall change in chemical shift and the change in chemical shift with each aliquot of anion added indicate that there is a strong interaction between NH1 and NH4 (the diindolylurea part of the receptor) and the first equivalent of anion. Further changes in chemical shift after the addition of one equivalent of anion is indicative of the binding of further aliquots of anion. This is exceptionally clear with NH4 after the addition of three equivalents of anion. As with receptor **221**, NH2 and 3 are also involved in binding further aliquots of anion after the addition of one equivalent. Job plot analysis shows complex binding stoichometries with all four different NH moieties.

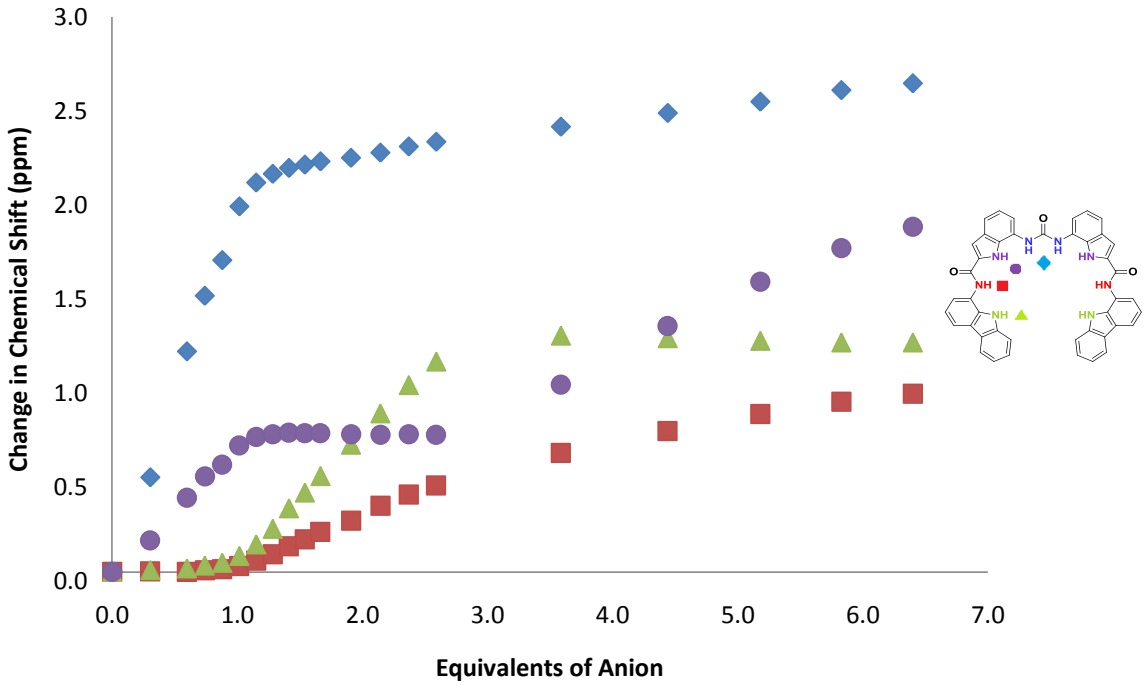

Graph 3.3.2.5 Change in chemical shift of the four different NH resonances of receptor **222** with TBA acetate, illustrating the interaction between the different NH functionalities and the anion in a DMSO-d_6/0.5% H_2O solution.

As with receptor **221**, receptor **222** binds the first equivalent of sulfate strongly through all eight NH bond donor groups in a DMSO-d_6/0.5% H_2O solution (Graph 3.3.2.6). Further equivalents of sulfate also appear to bind to the receptor, affecting the chemical shift of all eight different hydrogen bond donor groups. Job plot analysis shows complex binding stoichometries with all four different NH moieties.

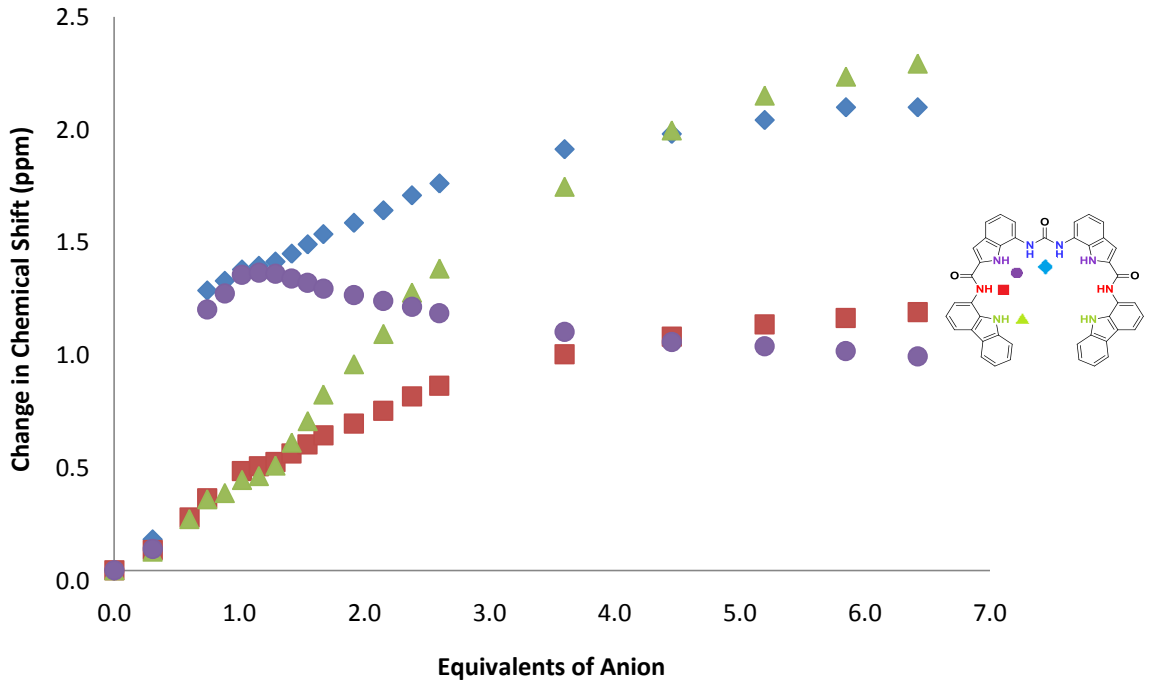

Graph 3.3.2.6 Change in chemical shift of the four different NH resonances of receptor **222** with TBA sulphate, illustrating the interaction between the different NH functionalities and the anion in a DMSO-d_6/0.5% H_2O solution.

In a DMSO-d_6/10% H_2O solution, the binding stoichometries of both receptors are greatly simplified. This is because the more competitive solvent environment decreases the affinity of the anions for the receptor. These solvent conditions produce binding curves for acetate (Graph 3.3.2.7 and 3.3.2.8), sulphate (Graph 3.3.2.9) and dihydrogen phosphate that resembled typical 1:1 binding curves. The binding constants were then estimated from the urea NH, which had shown evidence of 1:1 binding by Job plot analysis in DMSO-d_6/0.5% H_2O solutions with both receptors. These binding constants are shown in Table 3.3.2.1, but can only be used as estimations as more complicated binding stoichiometries were indicated by the titration data and Job plot analysis of the remaining NH bond donor groups.

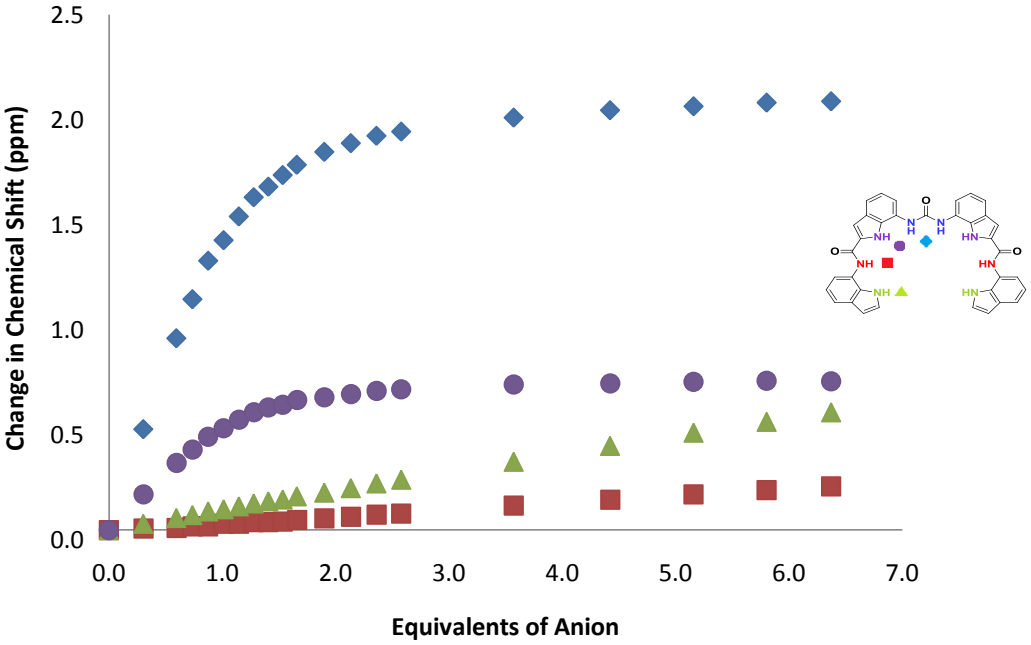

Graph 3.3.2.7 Change in chemical shift of the four different NH resonances of receptor **221** with TBA acetate, illustrating the interaction of the different NH functionalities with the anion in a DMSO-d_6/10% H_2O solution.

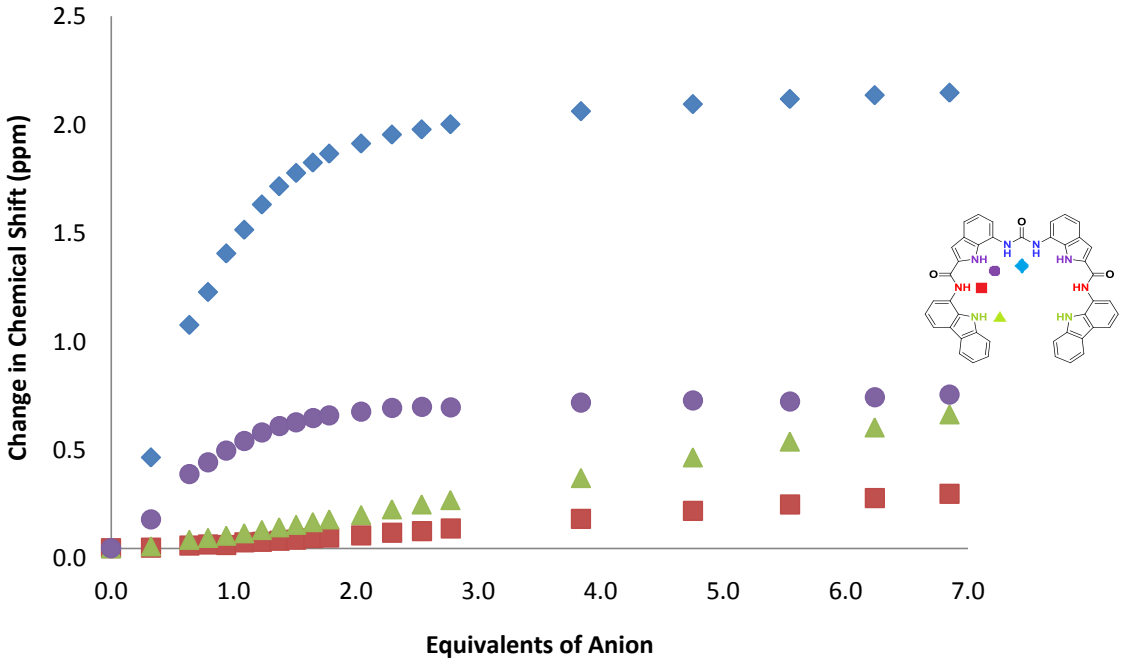

Graph 3.3.2.8 Change in chemical shift of the four different NH resonances of receptor **222** with TBA acetate, illustrating the interaction of the different NH functionalities with the anion in a DMSO-d_6/10% H_2O solution.

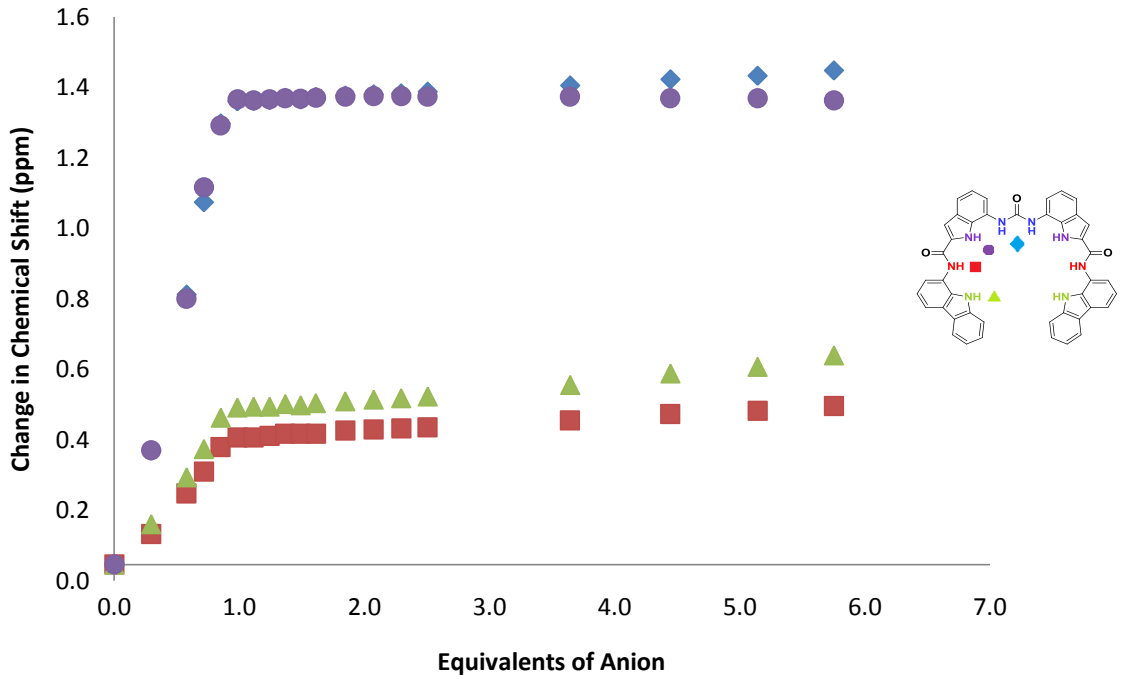

Graph 3.3.2.9 Change in chemical shift of the four different NH resonances of receptor **222** with TBA sulphate, illustrating the interaction of the different NH functionalities with the anion in a DMSO-d_6/10% H_2O solution.

Approximate anion binding constants were determined for receptors **221** and **222** with wide range anions. The binding constants were determined by ^{1}H NMR titration with the TBA salt of the anion apart from bicarbonate, which was added as the TEA salt in a DMSO-d_6/10% H_2O solution. The binding constants were determined by the computer program WINEQNMR[153] and fitted to a 1:1 binding model. This showed a preference for binding acetate (with estimated binding constants of 602 M^{-1} and 691 M^{-1} for receptors **221** and **222** respectively) over dihydrogen phosphate (binding constants of 122 M^{-1} and 315 M^{-1} respectively). Sulfate was bound with a binding constant of $>10^4$ M^{-1} by receptor **222**. A binding constant could not be generated with receptor **221** because of spontaneous crystallisation effects (see 3.4 for further details).

Table 3.3.2.1 Approximate anion binding constants (M^{-1}) and percentage error for receptors **221** and **222**, measured in DMSO-d_6/10% H_2O at 298 K. Anionic guests were added as the TBA salt of the anion with the exception of bicarbonate, which was added as the TEA salt of the anion. Binding constants were determined by ^1H NMR titration following the urea NH, fitting data to a 1:1 binding model using WINEQNMR.[153]

Anion	221	E (%)	222	E (%)
$CH_3CO_2^-$	602	2	691	5
$H_2PO_4^-$	122	11	315	11
SO_4^{2-}	a	-	$>10^4$/a	-
$^cHCO_3^-$	b	-	b	-

a – Spontaneous crystallisation. b – Deprotonation of the bound anion. ^{c} Added as the TEA salt of the anion.

3.3.2.2 Deprotonation of bound anions

As in the case of receptor **219** binding dihydrogen phosphate, similar deprotonation of bound anions was observed with receptors **221** and **222**. In these cases, deprotonation of both bicarbonate and dihydrogen phosphate was observed in DMSO-d_6 solutions containing up to 10% water.

The binding of receptor **221** with dihydrogen phosphate, followed by the deprotonation of the bound anion by excess anion in a DMSO-d_6/0.5% H_2O solution, is shown in Stack plots 3.3.2.1a and 3.3.2.1b. Both events were observed in fast exchange. Similar results were observed with dihydrogen phosphate and receptor **222**. The deprotonation of the bound dihydrogen phosphate was tested in the same way as previously discussed in 3.2.2.2; by the addition of hydroxide to a solution of the receptor and to a solution of the receptor/anion complex.

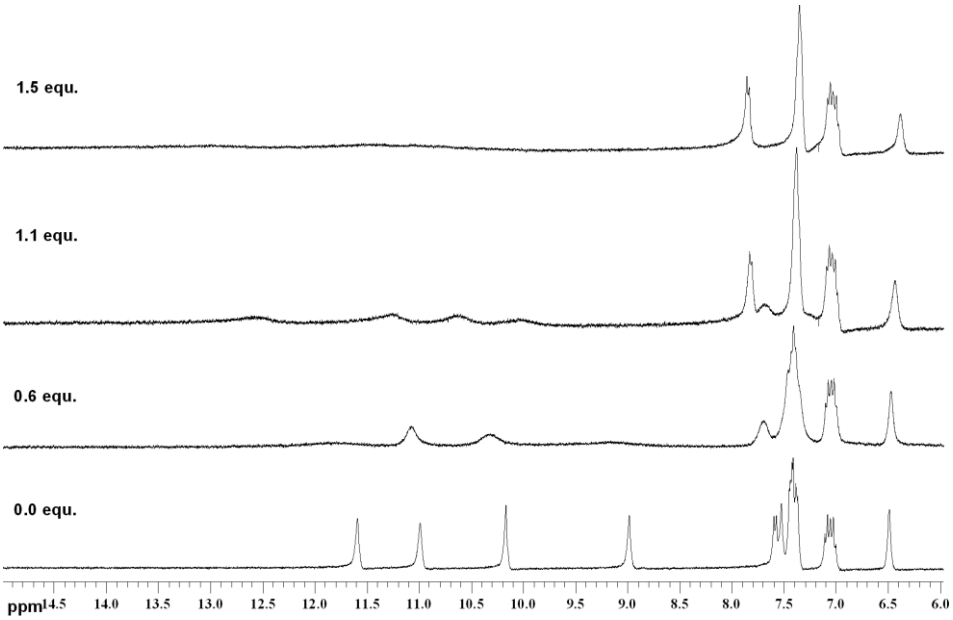

Stack plot 3.3.2.1a Receptor **221** with approximately 0-1.5 equivalents TBA dihydrogen phosphate, illustrating the fast exchange binding of dihydrogen phosphate in a DMSO-d_6/0.5% H_2O solution. This stack plot is taken from the supplementary information of the following article: Gale, P. A.; Hiscock, J. R.; Jie, C. Z.; Hursthouse, M. B. and Light, M. E., *Chem. Sci.*, **2010**, *1*, 215-220.

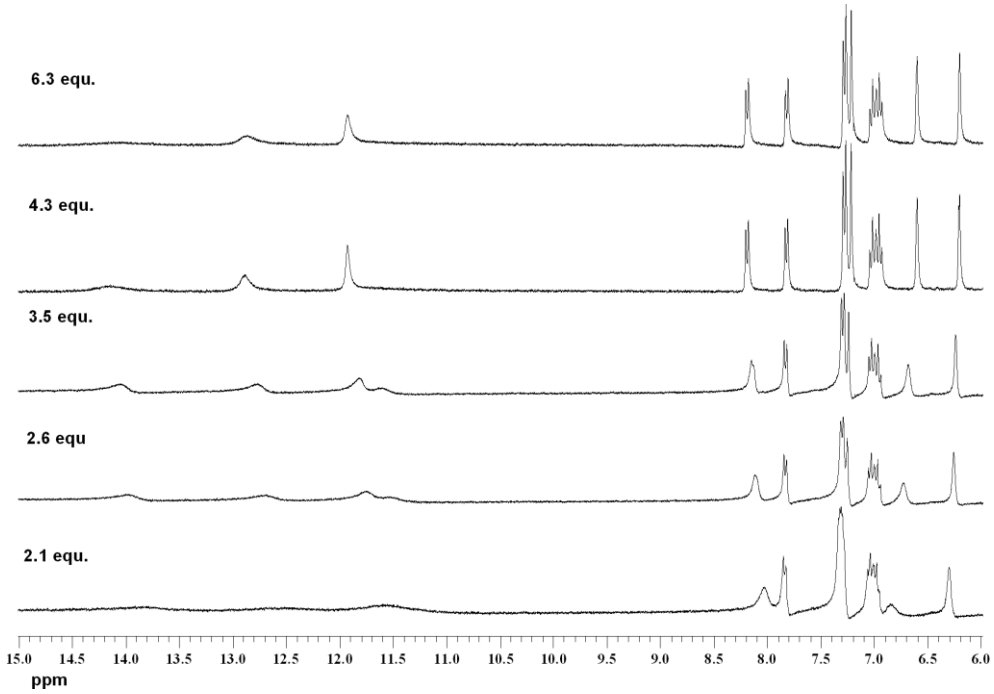

Stack plot 3.3.2.1b Receptor **221** with approximately 2-6 equivalents TBA dihydrogen phosphate, illustrating the fast exchange deprotonation of bound dihydrogen phosphate and the binding of hydrogen phosphate to the receptor in a DMSO-d_6/0.5% H_2O solution. This stack plot is taken from the supplementary information of the following article: Gale, P. A.; Hiscock, J. R.; Jie, C. Z.; Hursthouse, M. B. and Light, M. E., *Chem. Sci.*, **2010**, *1*, 215-220.

Stack plot 3.3.2.2 shows the deprotonation of receptor **221** and bound bicarbonate in a DMSO-d_6/0.5% H_2O solution. The deprotonation of the bicarbonate anion was also observed with receptor **222** in this solution and was still evident in the more polar DMSO-d_6/10% H_2O solutions with both receptors. Again, the deprotonation of the bound anion events were tested with the addition of hydroxide to a solution of the receptor and a solution of the receptor/anion complex.

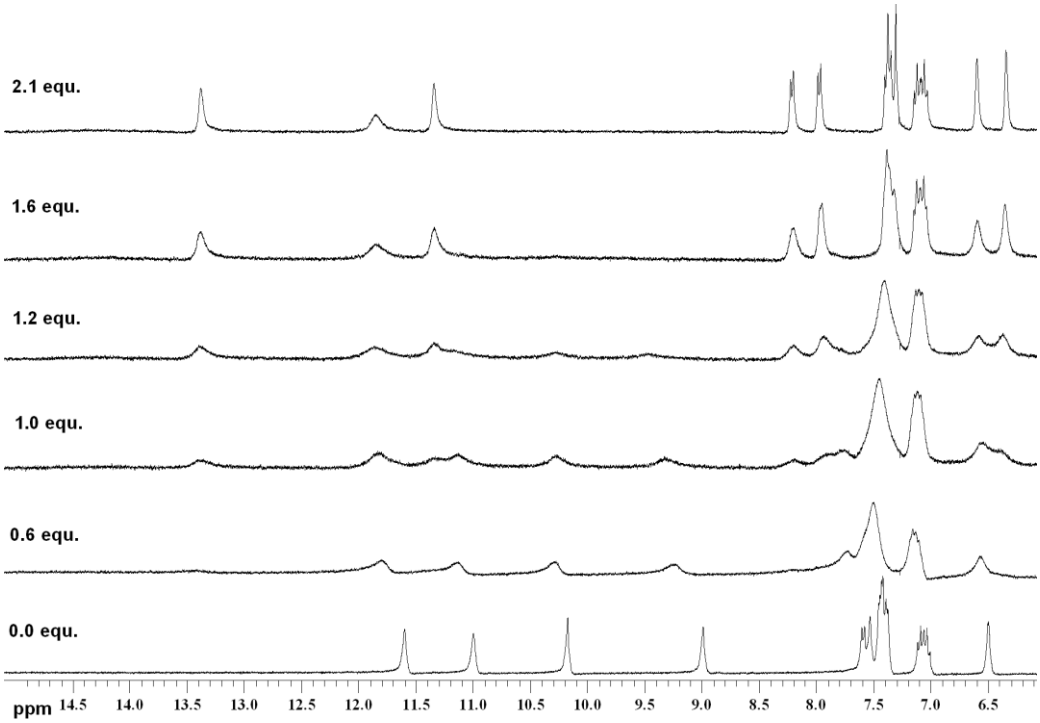

Stack plot 3.3.2.2 Receptor **221** with 0-2.1 equivalents TEA bicarbonate, illustrating the fast exchange process of bicarbonate binding the slow exchange deprotonation of the bound anion and the binding of carbonate to the receptor in a DMSO-d_6/0.5% H_2O solution. This stack plot is taken from the following article: Gale, P. A.; Hiscock, J. R.; Jie, C. Z.; Hursthouse, M. B. and Light, M. E., *Chem. Sci.*, **2010**, *1*, 215-220.

3.3.3 Solid phase analysis

X-ray quality crystals of receptor **221** and TBA benzoate were obtained from a DMSO solution of receptor **221** with excess of TBA benzoate.

The crystal structure of receptor **221** was produced by single crystal X-ray diffraction and is shown in Figure 3.3.3.3. This complex shows a 3:1 anion:receptor binding stoichiometry, with the four central urea and indole NHs involved in binding one anion through the formation of four hydrogen bonds. One indole and one urea NH forms a

hydrogen bond to each of the benzoate oxygen atoms. Two further benzoate anions are bound on the outside of the cleft by two hydrogen bonds each, one from the indole and one from an amide functionality. This similar to observations made in the solution state with both receptors and acetate in DMSO-d_6/0.5% and 10% H_2O.

The hydrogen bonding interactions and hydrogen bond angles for the complex shown in Figure 3.3.3.1 are shown in Table 3.3.3.1. The hydrogen bonds from the nitrogen atoms of the receptor to the oxygen atoms of the anion range from N···O = 2.717(4) – 2.840(4) Å and the bond angles range from N–H···O = 149.0°-167.6°.

Table 3.3.3.1 Hydrogen bonding table for the crystal structure of receptor **221** and TBA benzoate shown in Figure 3.3.3.1, obtained by single crystal X-ray diffraction at 120K. *D* – hydrogen bond donor atom. *A* – hydrogen bond acceptor atom. *d* – distance in Å. ∠ - bond angle in °. H – hydrogen atom.

D–H···*A*	*d*(*D*–H) (Å)	*d*(H···*A*) (Å)	*d*(*D*···*A*) (Å)	∠(*D*H*A*) (°)
N1–H901···O4	0.88	2.08	2.870(4)	149.0
N2–H902···O5	0.88	1.95	2.811(4)	167.5
N3–H3···O6	0.88	1.90	2.719(4)	153.4
N4–H904···O6	0.88	1.84	2.717(4)	173.1
N5–H905···O7	0.88	1.97	2.820(4)	161.1
N6–H906···O7	0.88	1.94	2.770(4)	155.8
N7–H7···O8	0.88	1.97	2.841(4)	167.6
N8–H8···O9	0.88	1.92	2.766(5)	159.8

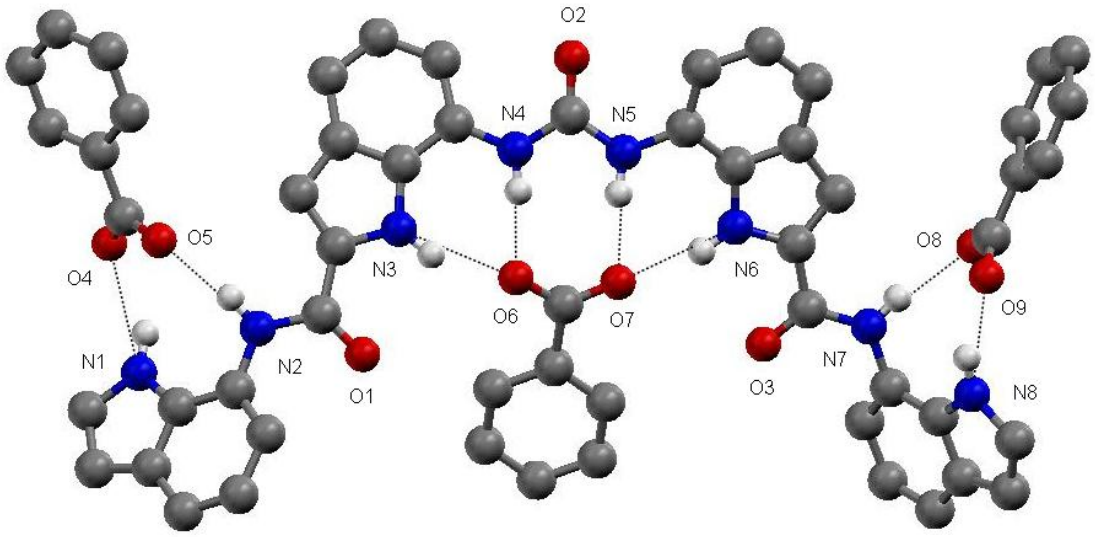

Figure 3.3.3.1 The benzoate complex of receptor **221**. Single X-ray crystal structure with TBA benzoate. The CH hydrogen atoms, slovent molecules and the TBA counter ions have been omitted for clarity.

X-ray quality crystals of receptor **221** and TBA sulfate were obtained from a DMSO solution of receptor **221** with excess TBA sulfate.

The crystal structure of receptor **221**, produced by single crystal X-ray diffraction, is shown in Figure 3.3.3.2. This complex shows a 1:1 anion:receptor binding stoichiometry, with all eight NH bond donor groups coordinating to the four oxygen atoms of a single sulfate anion. It is the acyclic nature of the receptor that allows this as the lower half of the receptor is free to twist round, adopting the optimum binding conformation for hydrogen bond formation to all four sulfate oxygen atoms. The binding stoichiometry and interaction through all eight NH bond donor groups is the same as that observed in a DMSO-d_6/10% H_2O solution. In a 0.5% water solution, more complex binding stoichometries were observed but all eight NH bond donor groups were still involved in binding the first equivalent of anion.

All eight hydrogen bond donor groups of the receptor contribute to the formation of a single hydrogen bond with an oxygen atom of the anion. In total, each oxygen atom is bound to the receptor by two hydrogen bonds. O5 forms two hydrogen bonds with both the urea NHs, O4 and O7 form two hydrogen bonds with an indole and amide NH and O6 is bound by the remaining two indole NH groups. The hydrogen bonding interactions and hydrogen bond angles for the complex shown in Figure 3.3.3.2 are shown in Table 3.3.3.2. The hydrogen bonds from the nitrogen atoms of the receptor to the oxygen atoms of the

anion range from N···O = 2.856(3) – 2.953(3) Å and the bonds angles range from N–H···O = 136.5°-177.2°.

Table 3.3.3.2 Hydrogen bonding table for the crystal structure of receptor **221** and TBA sulfate for the complex shown in Figure 3.3.3.2, obtained by single crystal X-ray diffraction at 120K. *D* – hydrogen bond donor atom. *A* – hydrogen bond acceptor atom. *d* – distance in Å. ∠ - bond angle in °. H – hydrogen atom.

D–H···*A*	*d*(*D*–H) (Å)	*d*(H···*A*) (Å)	*d*(*D*···*A*) (Å)	∠(*DHA*) (°)
N1–H901···O6	0.88	2.07	2.926(4)	164.7
N2–H2···O4	0.88	2.08	2.953(3)	170.3
N3–H3···O4	0.88	1.93	2.798(3)	168.8
N4–H4···O5	0.88	1.96	2.787(3)	157.2
N5–H5···O5	0.88	2.10	2.896(3)	150.9
N6–H6···O7	0.88	2.05	2.862(3)	154.1
N7–H7···O7	0.88	2.02	2.895(3)	177.2
N8–H8···O6	0.88	2.15	2.856(3)	136.5

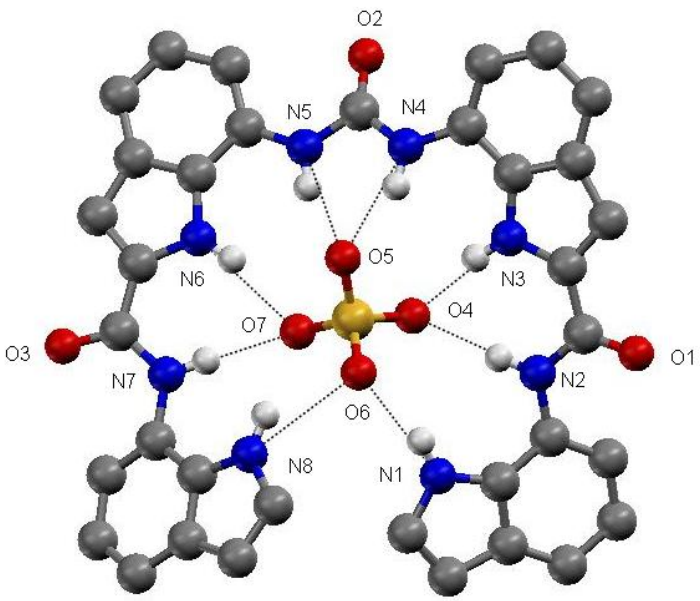

Figure 3.3.3.2 The sulfate complex of receptor **221**. Single X-ray crystal structure with TBA sulfate. The CH hydrogen atoms and the TBA counter ions have been omitted for clarity.

X-ray quality crystals of receptor **221** and TBA hydrogen phosphate were obtained from a DMSO solution of receptor **221** with excess TBA dihydrogen phosphate.

The crystal structure of receptor **221**, produced by single crystal X-ray diffraction, is shown in Figure 3.3.3.3a. This complex shows a 1:1 anion:receptor binding stoichiometry, with all eight NH bond donor groups coordinating to the four oxygen atoms of a single hydrogen phosphate anion. This complex is found to dimerise through hydrogen bonding interactions between the two hydrogen phosphate anions as shown in Figure 3.3.3.3b. The anions are shown as space-filling molecules to allow the anion and receptor molecules to be easily distinguished. As in the solution state (DMSO-d_6/0.5% H_2O), this receptor contributes enough acidic hydrogen bond donor groups to lower the pK_a of the bound anion, causing it to deprotonate.

All eight hydrogen bond donor groups of the two receptors contribute to the formation of a single hydrogen bond with one of the oxygen atoms of the anion. O5 forms hydrogen bonds with both of the urea NHs. O4 forms two hydrogen bonds, one from an indole NH and one from the amide NH. O6 is coordinated to the receptor by three hydrogen bonds, two from indole NHs and one from the remaining amide functionality. O7 is bound by a single indole NH. The hydrogen bonding interactions and hydrogen bond angles for the complex shown in Figure 3.3.3.3b are shown in Table 3.3.3.3. The hydrogen bonds from the nitrogen atoms of the receptor to the oxygen atoms of the anion range from N···O = 2.736(8) – 2.970(8) Å and the bond angles range from N–H···O = 135.0°-177.6°.

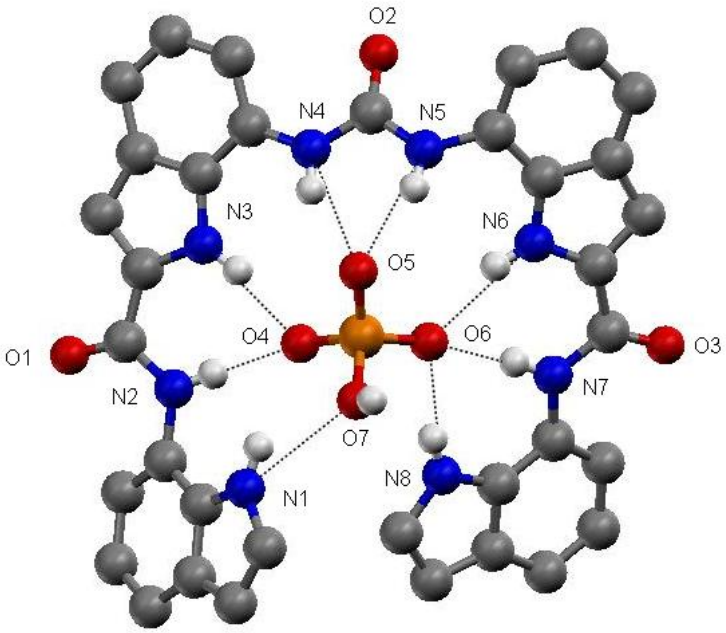

Figure 3.3.3.3a The hydrogen phosphate complex of receptor **221**. Single X-ray crystal structure with TBA hydrogen phosphate. The CH hydrogen atoms and the TBA counter ions have been omitted for clarity.

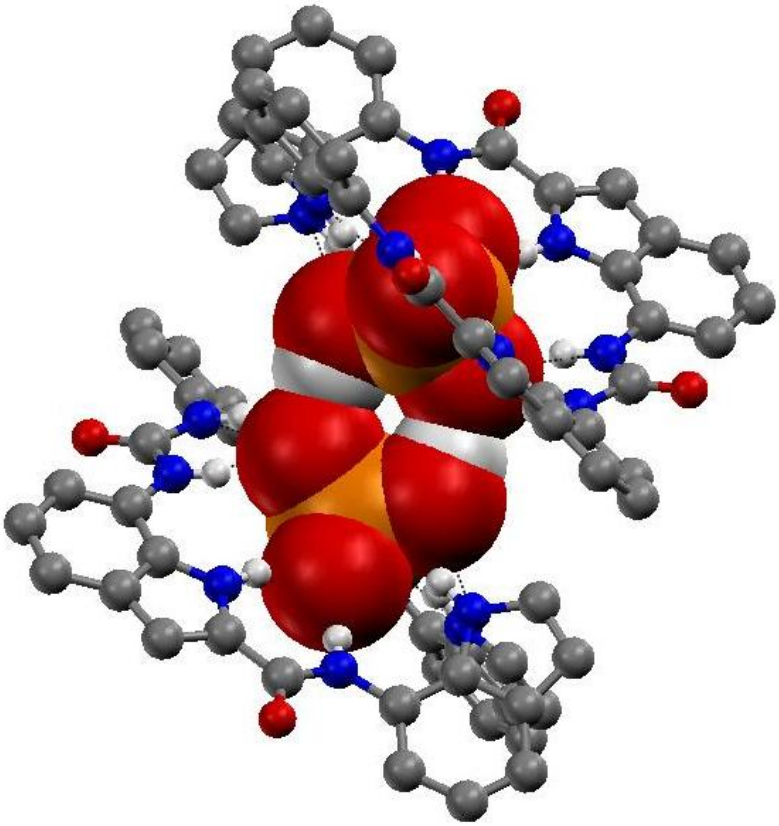

Figure 3.3.3.3b The dimer of the hydrogen phosphate complex of receptor **221**. Single X-ray crystal structure with TBA hydrogen phosphate. The CH hydrogen atoms and the TBA counter ions have been omitted for clarity.

Table 3.3.3.3 Hydrogen bonding table for the crystal structure of receptor **221** and TBA hydrogen phosphate shown in Figure 3.3.3.3b, obtained by single crystal X-ray diffraction at 120K. *D* – hydrogen bond donor atom. *A* – hydrogen bond acceptor atom. *d* – distance in Å. ∠ - bond angle in °. H – hydrogen atom. Symmetry transformations used to generate equivalent atoms: (i) –x+1,–y+1,–z

D–H···*A*	*d*(*D*–H) (Å)	*d*(H···*A*) (Å)	*d*(*D*···*A*) (Å)	∠(*D*H*A*) (°)
N1–H901···O7	0.88	2.28	2.970(8)	135.0
N2–H902···O4	0.88	1.91	2.790(8)	177.6
N3–H903···O4	0.88	1.89	2.736(8)	162.1
N4–H904···O5	0.88	2.01	2.818(8)	152.6
N5–H905···O5	0.88	1.96	2.764(7)	150.5
N6–H906···O6	0.88	1.96	2.815(7)	162.5
N7–H907···O6	0.88	1.96	2.838(8)	173.8
N8–H908···O6	0.88	1.94	2.782(7)	159.0
O7–H997···O5^{i}	0.86(6)	1.79(7)	2.645(7)	170(6)

X-ray quality crystals of receptor **222** and TBA hydrogen phosphate and dihydrogen phosphate were obtained from a DMSO solution of receptor **222** with excess TBA dihydrogen phosphate.

The crystal structure of receptor **222**, produced by single crystal X-ray diffraction, is shown in Figure 3.3.3.4a. This complex shows a 2:1 anion:receptor binding stoichiometry, with seven of the eight NH bond donor groups coordinating to the four oxygen atoms of a single hydrogen phosphate anion. The remaining NH is utilised in coordinating a dihydrogen phosphate anion. This complex is part of a chain of six phosphate-based anions, two hydrogen phosphate and four dihydrogen phosphate, capped at either end by a receptor molecule. The central two dihydrogen phosphate anions are highly disordered and the charge on these anions was decided on a charge balance basis. The full complex is shown in Figure 3.3.3.4b. As in the solution state (DMSO-d_6/0.5% H_2O), this receptor contributes enough acidic hydrogen bond donor groups to lower the pK_a of the bound anion, causing it to deprotonate to other anions in solution.

Seven of the eight hydrogen bond donor groups of the receptor contribute to the formation of a single hydrogen bond to an oxygen atom of the hydrogen phosphate anion apart from N8, which is involved in two hydrogen bonding events. O4 forms hydrogen bonds with both of the urea NHs. O6 is bound to the receptor by three hydrogen bonds, one from an indole NH, one from a carbazole NH and the third from the amide NH. O5 is coordinated to the receptor by two hydrogen bonds, one from an indole NH and one from the amide functionality. O7 is bound by a single carbazole NH. A dihydrogen phosphate anion is bound to the receptor by a single carbazole NH through O11. The anion chain is held together through several hydrogen bond interactions between the anions. The hydrogen bonding interactions and hydrogen bond angles for the complex shown in Figure 3.3.3.4b are shown in Table 3.3.3.4. The hydrogen bonds from the nitrogen atoms of the receptor to the oxygen atoms of the anion range from N···O = 2.662(4) – 3.047(3) Å and the bond angles range from N–H···O = 135.6°-175.1°.

Table 3.3.3.4 Hydrogen bonding table for the crystal structure of receptor **222** and TBA hydrogen phosphate and dihydrogen phosphate shown in Figure 3.3.3.4b, obtained by single crystal X-ray diffraction at 120K. *D* – hydrogen bond donor atom. *A* – hydrogen bond acceptor atom. *d* – distance in Å. ∠ - bond angle in °. H – hydrogen atom.

D–H···*A*	*d*(*D*–H) (Å)	*d*(H···*A*) (Å)	*d*(*D*···*A*) (Å)	∠(*D*H*A*) (°)
N1–H1···O11B	0.88	1.82	2.662(4)	159.1
N1–H1···O11A	0.88	1.99	2.741(3)	142.0
N2–H2···O5	0.88	2.01	2.869(3)	165.9
N3–H3···O5	0.88	1.89	2.738(3)	161.8
N4–H4···O4	0.88	2.01	2.819(3)	152.5
N5–H5···O4	0.88	1.96	2.792(3)	156.6
N6–H6···O6	0.88	1.90	2.754(3)	162.6
N7–H7···O6	0.88	1.89	2.768(3)	175.1
N8–H8···O7	0.88	2.31	3.037(3)	140.4
N8–H8···O6	0.88	2.36	3.047(3)	135.6
O7–H7A···O11A	0.84	1.99	2.603(3)	129.6
O7–H7A···O11B	0.84	2.16	2.696(4)	121.9
O7–H7A···O8B	0.84	2.57	3.319(4)	148.8
O8A–H8A1···O4	0.84	2.01	2.578(3)	124.3

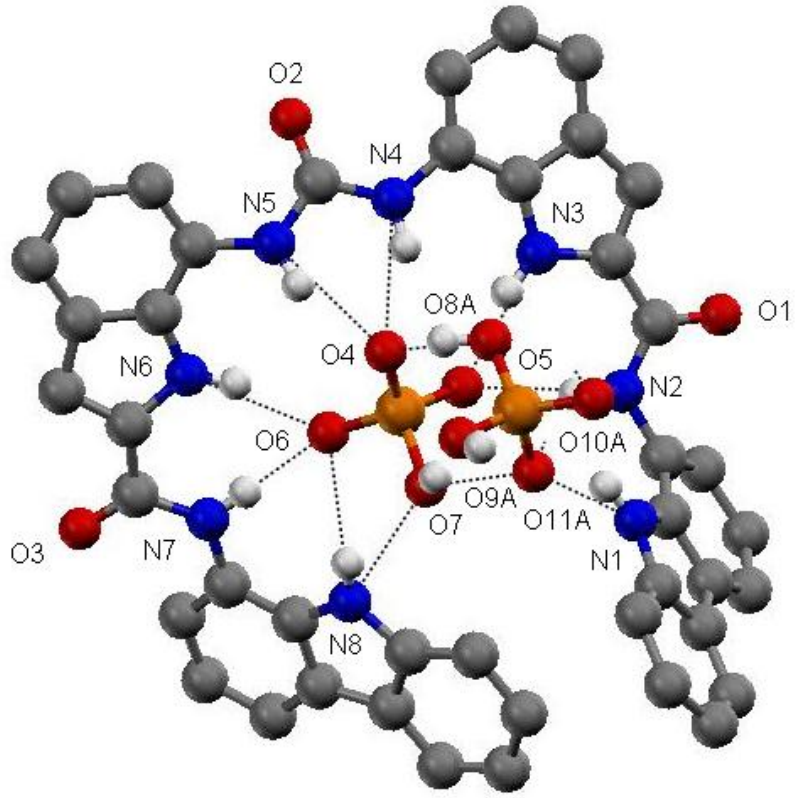

Figure 3.3.3.4a The hydrogen phosphate and dihydrogen phosphate complex of receptor **222**. Single X-ray crystal structure with TBA hydrogen phosphate. The CH hydrogen atoms and the TBA counter ion have been omitted for clarity.

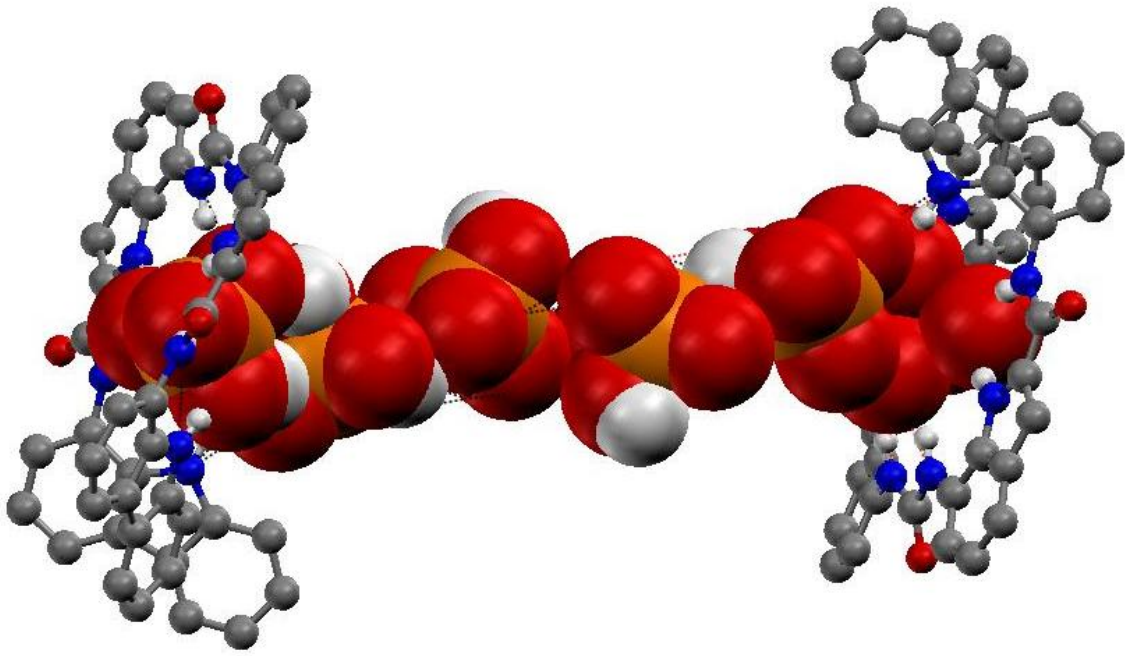

Figure 3.3.3.4b The hydrogen phosphate complex of receptor **222**, showing the dihydrogen phophate and hydrogen phosphate chain. The CH hydrogen atoms, some dissorder in the centre of the dihydrogen phosphate chains and the TBA counter ions have been omitted for clarity.

3.4 Spontaneous crystallisation with sulfate

During the ^{1}H NMR titration experiments in DMSO-d_6/10% H_2O with TBA sulfate and receptors **220-222**, the formation of a crystalline material was noted (Figure 3.4.1). This was shown to be the receptor/anion complex by single crystal X-ray diffraction, as illustrated in Figure 3.4.2. This prevented binding constants from being calculated for the anion/receptor complexes for receptors **220** and **221** as this process happened within 20 minutes of addition of the anion to the solution of the receptor. This process occurred over a longer period of time with receptor **222**, which allowed a full titration experiment to be carried out but the crystallisation process was still complete within an hour. The binding of this anion and the removal from solution of the complex is of great importance because of the roles of the anion in disease and biological systems[122,123,171,172], environmental pollution[173] and hydrometallurgy[174-176]..

The limited data gathered from the ^{1}H NMR titrations is shown in Graph 3.4.1. This shows a change in chemical shift of the urea NH of all three receptors upon the addition of TBA sulfate. Up to one equivalent of sulfate was added to the DMSO-d_6/10% H_2O receptor solutions before the crystallisation was observed. The binding strength and interaction of the urea NHs are practically identical for all three receptors. Photographic evidence for the formation of crystals during the titration process is shown in Figure 3.4.1.

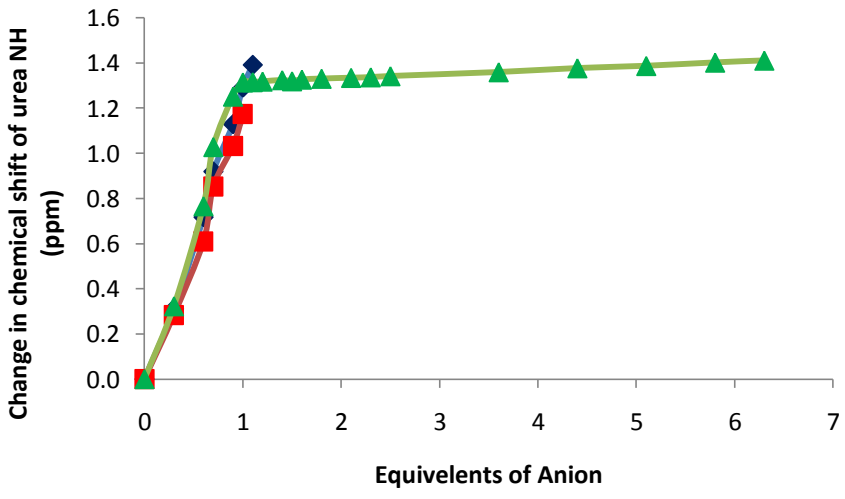

Graph 3.4.1 Change in chemical shift of the urea NH resonances of receptor **220** (blue diamonds), **221** (red squares) and **222** (green triangles) with TBA sulphate, illustrating the interaction between the urea NH functionalities of the different receptors and the sulfate anion before the spontaneous crystallisation process occurs in a DMSO-d_6/10% H_2O solution.

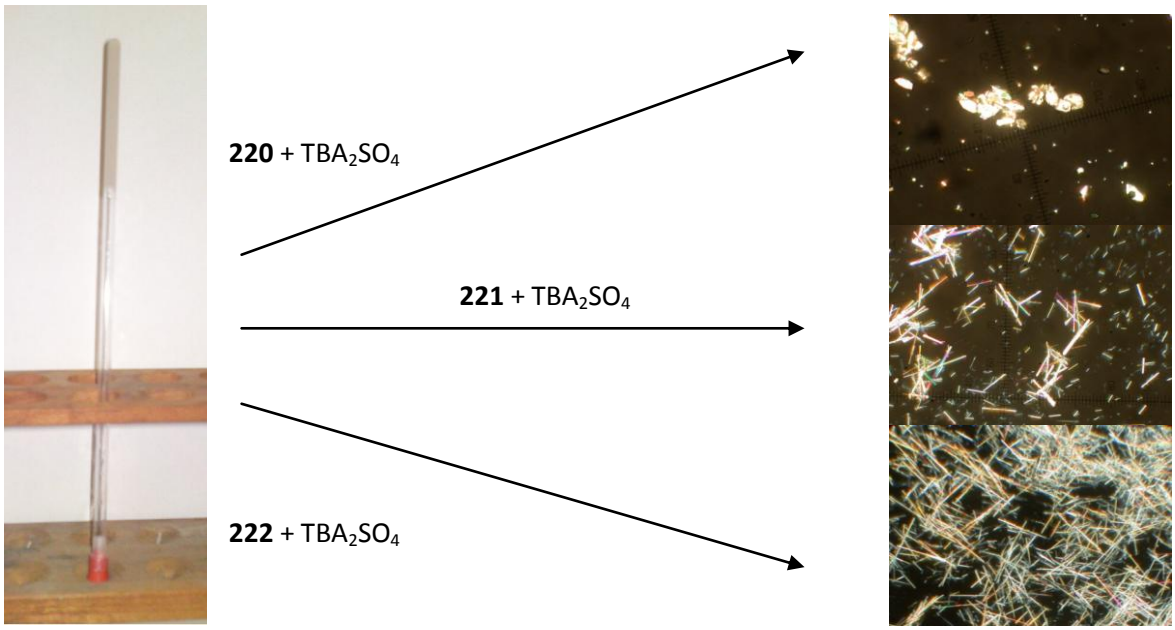

Figure 3.4.1 Left - Photographic evidence of the formation of crystals during the ^{1}H NMR titration of TBA sulfate to solutions of receptors **220**, **221** and **222** in DMSO-d_6/10% H_2O solutions. **Right** – Micrographs of the crystals formed with 15 equivalents of anion to receptor in DMSO-d_6/10% H_2O solutions.

From the crystals formed during the ^{1}H NMR DMSO-d_6/10% H_2O titration experiments, a crystal structure was obtained from a sample of receptor **221**. This showed a single sulfate anion, bound by one receptor through all eight hydrogen bond donor groups as was observed in the solution state with receptor **222**. The crystal structure shown in Figure 3.4.2 is almost identical to that shown in Figure 3.3.3.2. The hydrogen bonding interactions and hydrogen bond angles for the complex shown in Figure 3.4.2 are shown in Table 3.4.1. The hydrogen bonds from the nitrogen atoms of the receptor to the oxygen atoms of the anion range from N···O = 2.785(4) – 3.289(4) Å and the bonds angles range from N–H···O = 136.5°-177.8°.

Table 3.4.1 Hydrogen bonding table for the crystal structure of receptor **221** and TBA sulfate shown in Figure 3.4.2, obtained by single crystal X-ray diffraction at 120K. *D* – hydrogen bond donor atom. *A* – hydrogen bond acceptor atom. *d* – distance in Å. ∠ - bond angle in °. H – hydrogen atom.

D–H···*A*	*d*(*D*–H) (Å)	*d*(H···*A*) (Å)	*d*(*D*···*A*) (Å)	∠(*DHA*) (°)
N1–H1···O7	0.88	2.15	2.855(4)	136.5
N1–H1···O4	0.88	2.59	3.289(4)	137.0
N2–H2···O4	0.88	2.01	2.892(3)	177.8
N3–H3···O4	0.88	2.04	2.856(3)	153.7
N4–H4···O5	0.88	2.10	2.897(4)	151.0
N5–H5···O5	0.88	1.95	2.785(4)	158.1
N6–H6···O6	0.88	1.93	2.794(3)	168.8
N7–H7···O6	0.88	2.08	2.956(4)	170.7
N8–H8···O7	0.88	2.06	2.923(4)	165.1

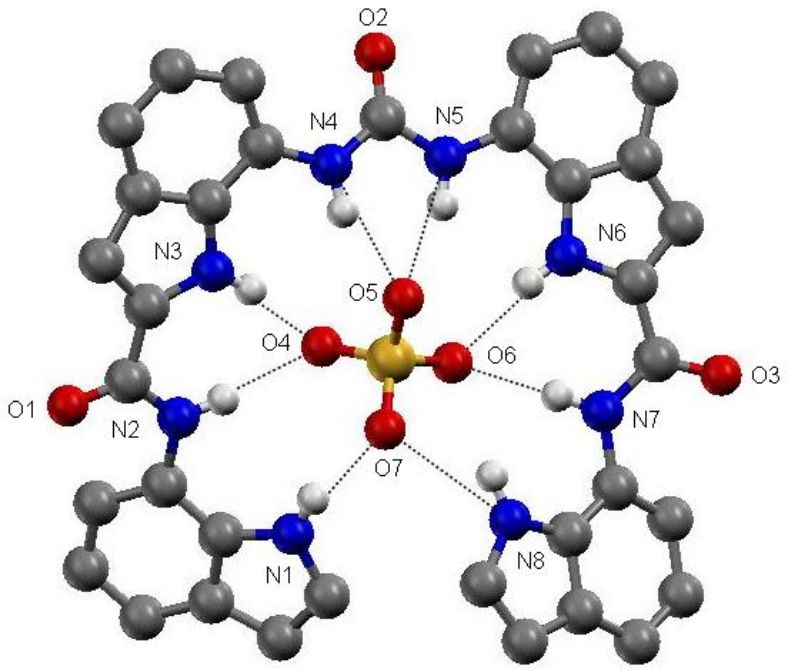

Figure 3.4.2. The sulfate complex of receptor **221**. Single X-ray crystal structure with TBA sulfate. The CH hydrogen atoms and the TBA counter ion have been omitted for clarity.

3.5 Conclusion

A set of amide-functionalised, diindolylurea-based receptors have been synthesised and the solution state anion binding properties explored using ^{1}H NMR titration and Job plot experiments. The solid state anion binding properties have been investigated by X-ray crystallography.

All these receptors were found to bind oxo-anions, with receptors **220**, **221** and **222** exhibiting preference for the sulfate anion. High binding constants were still observed with dihydrogen phosphate and receptor **219** in higher concentrations of water. Two different binding modes were observed with receptors **219** and **220**, based on anion geometry, with the first equivalent of anion binding through either four or six NH bond donor groups. Receptors **221** and **222** exhibited even more complex binding modes, which meant that only a limited idea of anion binding stoichiometry and anion affinity could be obtained in the solution state. Receptors **220-222** only show two main binding modes in the solid state; the first with a single anion bound in the centre of the anion binding pocket and the second with an anion bound in the central cleft and a second/third anion bound on the outside of the receptor's binding cleft.

Receptors **219**, **221** and **222** all exhibited deprotonation of the bound dihydrogen phosphate anion to excess anion in a DMSO-d_6/0.5% H_2O solution. This process was not observed with receptor **220** due to the low affinity observed with dihydrogen phosphate. The process was observed with receptors **220-222** in the solid state in the absence of solvent effects. Receptors **221** and **222** also showed deprotonation of bound bicarbonate in both DMSO-d_6/0.5% and 10% H_2O solutions but not in 25% H_2O solutions.

Spontaneous crystallisation of the sulfate anion with receptors **220**, **221** and **222** from a DMSO-d_6/10% H_2O was observed and verified by single X-ray diffraction.

Chapter 4 - Tripodal Indole Based Anion Receptors

4.1 Introduction

Following the study of the two dimensional simple cleft receptors **209-222**, the next step is to move into three dimensions. The synthesis of these receptors is based on a tripodal scaffold, functionalised with amide/urea/indole groups that provide greater numbers of hydrogen bond groups. The design of these receptors predisposes them to bind the larger trigonal planar or tetrahedral anions instead of the Y-shaped anions or the halide anions. Although there has been much investigation into the amide/urea/thiourea functionalised tripodal anion receptors, little work has been done to functionalise with aromatic NH bond donor groups, such as pyrrole, indole or carbazole groups. This chapter will discuss the synthesis and anion binding properties of indole-functionalised tripodal anion receptors.

4.2 Symmetrical TREN based anion receptors

The tri-amine based tripodal scaffolding unit, TREN, offers a small yet flexible structure on which to base anion receptor design. The first tripodal anion receptor based on the TREN scaffold was published in 1993 by Reinhoudt and co-workers[13] and inspired other research groups such as Bowmann-James and co-workers. There are now many examples of TREN-based anion receptors.[179,180] Based on work by Bowman-James and co-workers[181], Ghosh and co-workers have synthesised sets of tripodal receptors containing three to six hydrogen bond donating groups from amide or urea functionalities.[63,182] These receptors have been shown to bind phosphate anions selectively in DMSO-d_6. This research group has also shown that this type of receptor is capable of encapsulation of the halide anions.[183] Receptor **223** is similar to those synthesised by Ghosh and co-workers which are based on the urea functionalised TREN, synthesised by Das and Ganguly. It showed selective binding for dihydrogen phosphate and sulfate in acetonitrile/water (95:5) solution.[184]

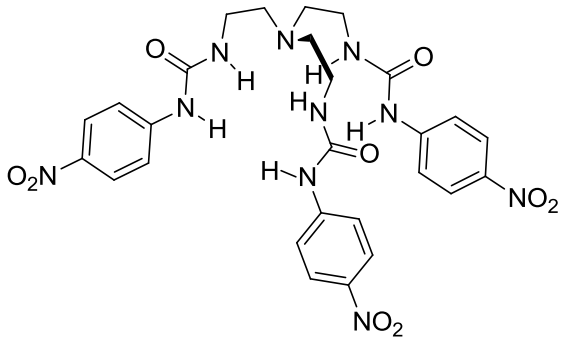

223

TREN-based anion receptors show promise in several areas; in ion extraction[185], in particular oxo-anion extraction[186], as luminescent sensors for anions[187] and in the transport of anions across bilipid membranes[14,15].

4.2.1 Synthesis

Receptors **224** and **225** were synthesised by a simple one-step reaction (illustrated in Scheme 4.2.1.1) by an amide coupling reaction with TREN, using PyBOP as the amide coupling agent and reacting with either indole-2-carboxylic acid (**224**) or 7-nitroindole-2-carboxylic acid (**225**). HOBt was used to catalyse the reaction in a dry DMF solution, with a few drops of NEt_3 to activate the amine. The reaction mixture was reduced to an oil and the protonated product was isolated by dissolving the oil in DCM and washing with water to remove DMF impurities, preventing precipitation if necessary. The neutral receptor was then obtained by the suspension of the product in a potassium hydroxide solution. Receptors **224** and **225** were isolated in 47 and 89 % yields respectively.

Receptor **226** was synthesised by the more lengthy three-step reaction process, *via* the formation of the N-(1H-indol-7-yl)-1H-imidazole-1-carboxamide intermediate (Scheme 4.2.1.2). The intermediate was synthesised by the reduction of 7-nitroindole in ethanol to 7-aminoindole, using a Pd/C 10% catalyst under a hydrogen atmosphere. The amine was then reacted with CDI in DCM and a white precipitate isolated from the reaction mixture. The N-(1H-indol-7-yl)-1H-imidazole-1-carboxamide intermediate was used, without purification, to give receptor **226** by reacting the intermediate with TREN in DMF. The reaction solution was then taken to dryness, dissolved in DCM and washed with

water to remove the CDI and DMF traces. The product was precipitated from the DCM solution with hexane, giving a 89 % yield. (Scheme 4.2.1.3)

The largest receptor (**227**) was synthesised by a two-step reaction from receptor **225** and the N-(1H-indol-7-yl)-1H-imidazole-1-carboxamide intermediate. Receptor **225** was first reduced to form the tri-amine, using Pd/C 10% suspended in DMF under a hydrogen atmosphere. The tri-amine was then reacted with the N-(1H-indol-7-yl)-1H-imidazole-1-carboxamide intermediate in DMF. The solution was then taken to dryness and the resultant oil sonicated in chloroform to give a precipitate that was then washed with water to give the final product in a 69 % yield. (Scheme 4.2.1.4)

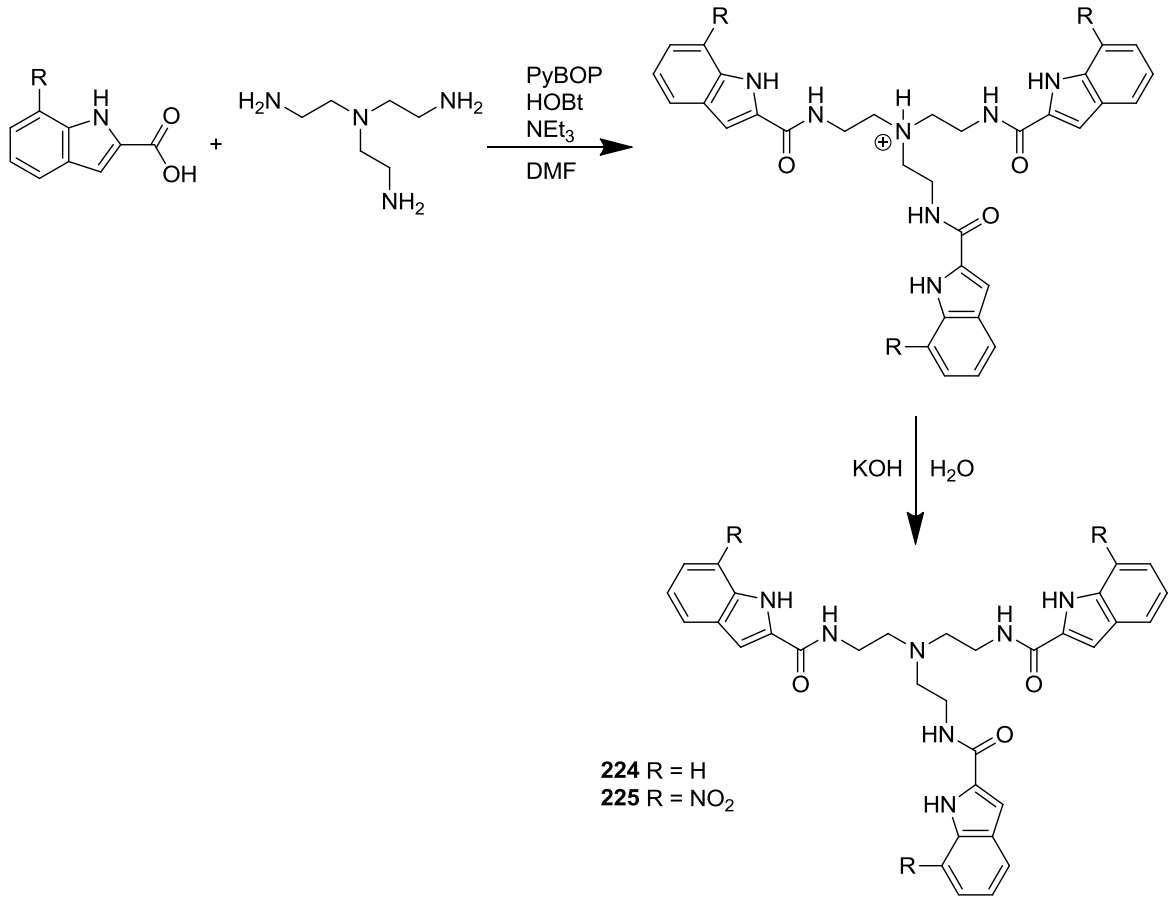

Scheme 4.2.1.1

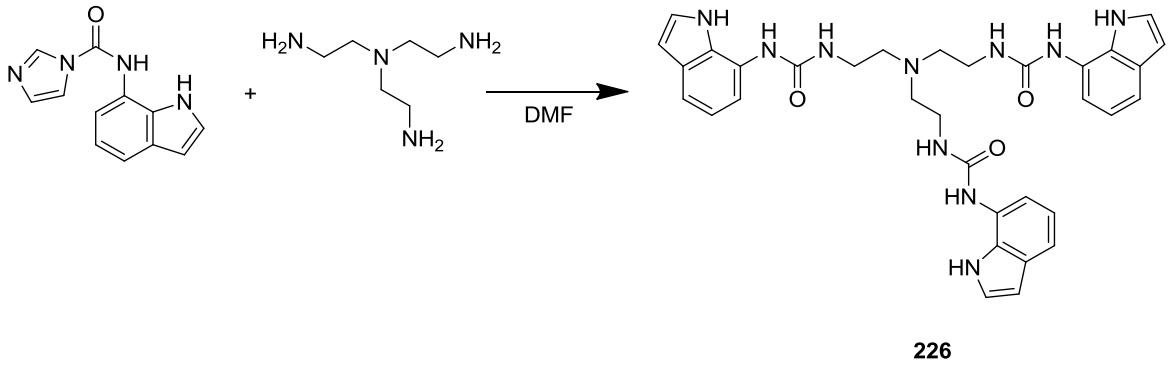

226

Scheme 4.2.1.2

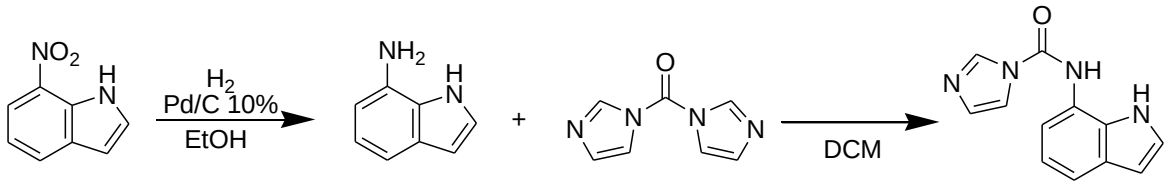

Scheme 4.2.1.3

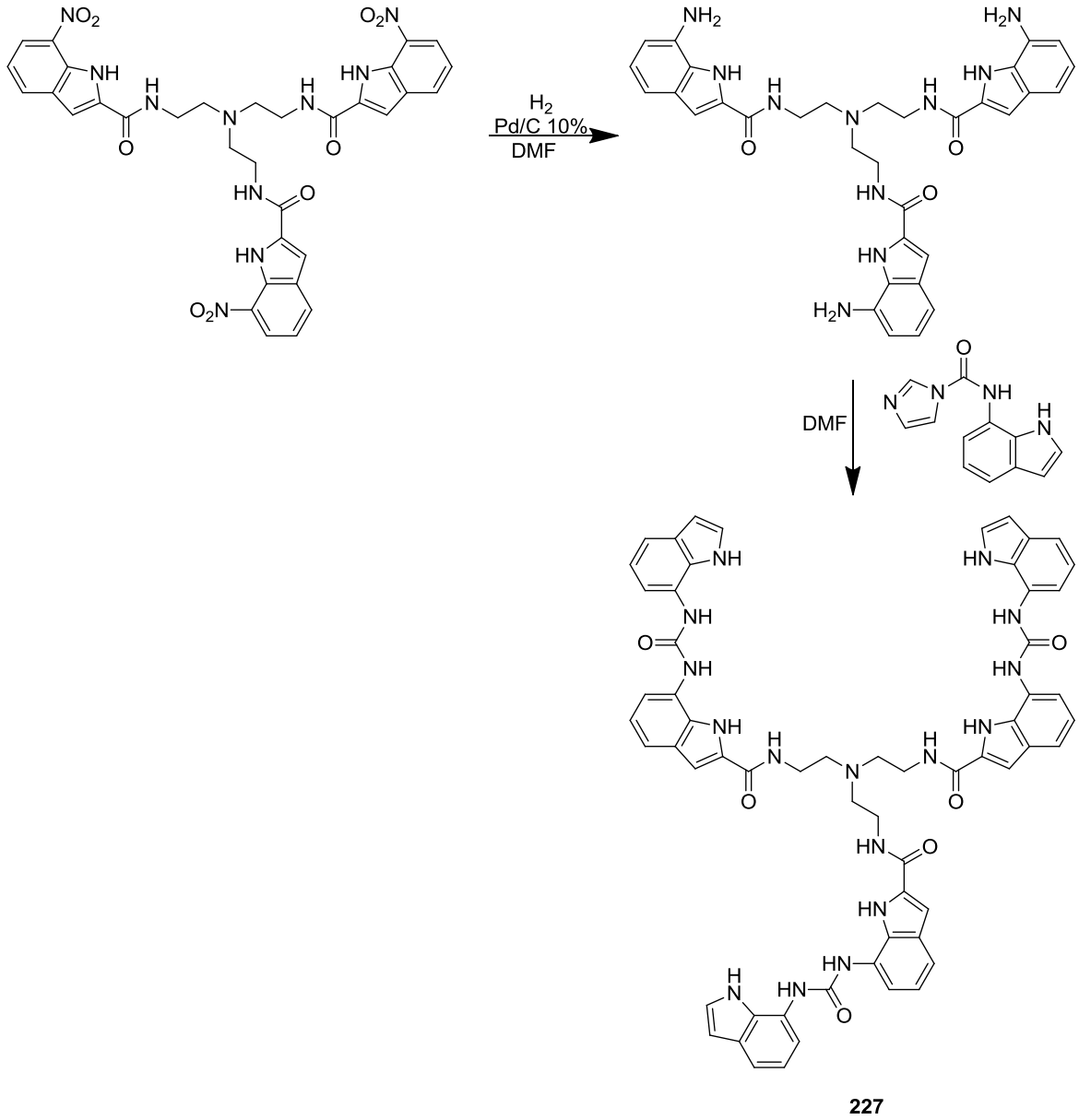

Scheme 4.2.1.4

4.2.2 Solution phase analysis

4.2.2.1 Proton NMR titration data

Anion binding constants were determined for receptors **224-227** with a wide range anions by ^{1}H NMR titration with the TBA salt of the anion in various DMSO-d_6/H_2O solutions, except for the bicarbonate anion, which was added as the TEA salt. The binding constants were calculated by the computer program WINEQNMR[153] and fitted to a 1:1 or 2:1

anion:receptor binding model. More complex 3:1 anion:receptor binding events were not fitted to binding modes because of complex equilibria and conformational events that would make the calculation of binding constants inaccurate.[153,188] Job plots[154] were produced to check the binding stoichiometry of receptors **224**, **226** and **227**. Binding stoichometries for receptor **225** were inferred from the ^{1}H NMR titration data and binding stoichiometries of the analogous receptor **224**.

Binding stoichometries for receptors **224** and **225** were determined by following the downfield shift of the indole and amide NH resonances. The binding constants and information derived from the ^{1}H NMR titration for receptor **224** and receptor **225** are shown in Tables 4.2.2.1 and 4.2.2.2 respectively. In a DMSO-d_6/0.5% H_2O solution, only moderate binding affinities were observed for the anions tested but all six hydrogen bond donor groups were shown to bind the anion, forming a 1:1 complex.

The binding constants calculated for receptor **224** were all found to be below 100 M^{-1}, with only a slight preference for the carboxylate anions over the chloride anion. Binding constants calculated for acetate and chloride were 69 M^{-1} and 12 M^{-1} respectively. The addition of electron withdrawing nitro groups to the structure of receptor **255,** which increased the acidity of the hydrogen bond donor groups, did cause an increase in anion affinity. The binding constants are not as large as those seen in Chapters Two and Three, but they do show selectivity for dihydrogen phosphate over the other anions tested, with binding constants of 197 M^{-1}, 144 M^{-1} and 59 M^{-1} being calculated for dihydrogen phosphate, acetate and benzoate respectively. As with receptor **224**, there is little affinity for chloride.

Table 4.2.2.1 Anion binding constants (M^{-1}) and percentage error for receptor **224**, measured in DMSO-d_6/0.5% H_2O at 298 K. Anionic guests were added as the TBA salt of the anion apart from bicarbonate, which was added as the TEA salt of the anion. Binding constants were determined by ^1H NMR titration following the amide NH, fitting data to a 1:1 binding model using WINEQNMR[153].

Anion	Binding Mode	224	E (%)
$CH_3CO_2^-$	1:1	69	5
$H_2PO_4^-$	a	a	-
$C_6H_5CO_2^-$	1:1	41	4
Cl^-	1:1	12	10
F^-	b	b	-
[c]HCO_3^-	1:1	81	6

a – Conformational change prevents binding mode or binding constant being obtained. b – Slow exchange. [c] Added as the TEA salt of the anion.

Table 4.2.2.2 Anion binding constants (M^{-1}) and percentage error for receptor **225**, measured in DMSO-d_6/0.5% H_2O at 298 K. Anionic guests were added as the TBA salt of the anion apart from bicarbonate, which was added as the TEA salt of the anion. Binding constants were determined by ^1H NMR titration following the amide NH, fitting data to a 1:1 binding model using WINEQNMR[153].

Anion	Binding Mode[a]	225	E (%)
$CH_3CO_2^-$	1:1	144	7
$H_2PO_4^-$	1:1	197	7
$C_6H_5CO_2^-$	1:1	59	2
Cl^-	1:1	11	9
F^-	b	b	-
[d]HCO_3^-	c	c	-

a – Assumed binding mode based on ^1H NMR titration data and evidence from analogous receptor X. b – Slow exchange. c – Peak broadening prevented a binding constant from being calculated. [d] –Added as the TEA salt of the anion.

The binding affinity of receptors **224** and **225** with fluoride could not be tested due to a slow exchange process on the NMR time scale. This is illustrated in Stack plots 4.2.2.1 and 4.2.2.2. Receptor **224** showed a straightforward slow exchange anion binding process with fluoride but receptor **225** shows more complex binding processes. A conformational change is observed between 0.9 and 1.5 equivalents of anion as a set of double peaks are observed for both the amide and indole NH resonances. This shows that not all the amide and indole NHs are chemically equivalent but there is no indication of deprotonation of the receptor at this point. It is probable that deprotonation of the receptor is observed after 4.7 equivalents of anion have been added because there is extreme peak broadening of the amide and indole NH resonances and the multiple new peaks and peak broadening occurring in the aromatic CH region.

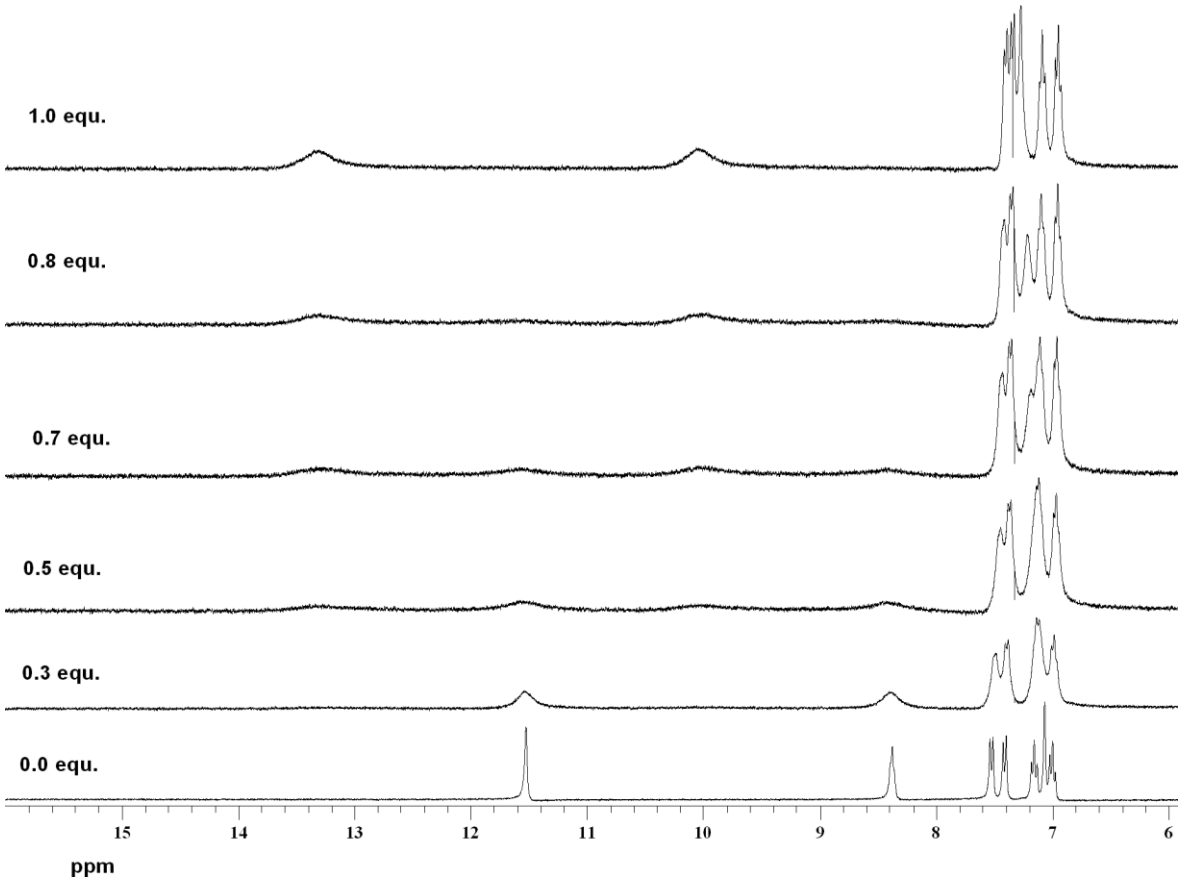

Stack plot 4.2.2.1 Receptor **224** with TBA fluoride, illustrating the slow exchange binding event of the anion to the receptor in a DMSO-d_6/0.5% H_2O solution.

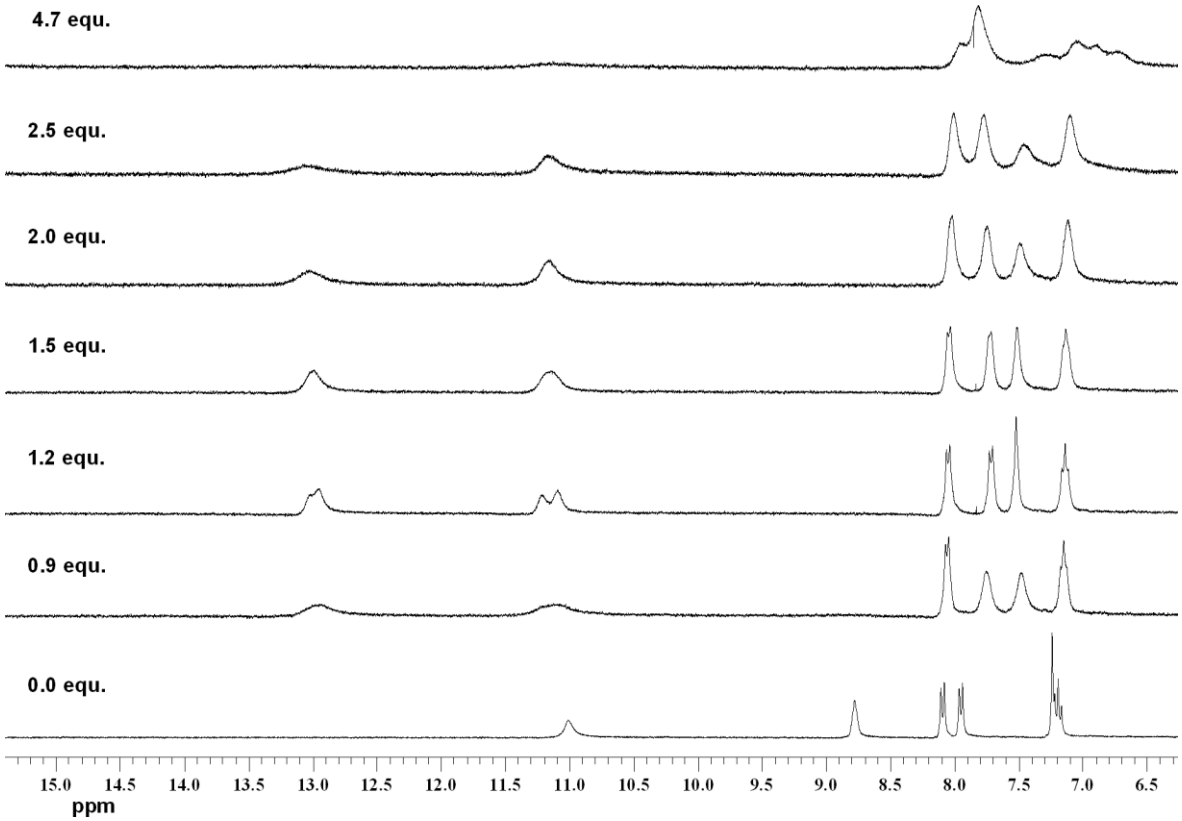

Stack plot 4.2.2.2 Receptor **225** with TBA fluoride, illustrating the slow exchange binding event of the anion to the receptor in a DMSO-d_6/0.5% H_2O solution. A conformational change is observed between 0.9 and 1.5 equivalents of anion. Deprotonation of the receptor is observed after 4.7 equivalents of anion.

Binding stoichometries for receptor **226** were determined by Job plot, following the downfield shift of a urea NH resonance. Binding constants calculated by following the downfield shift of a urea NH resonance, as observed from the ^{1}H NMR titration, are shown in Table 4.2.2.3. In a DMSO-d_6/0.5% H_2O solution, stronger anion binding affinities were observed than those observed with receptors **224** and **225**. All nine hydrogen bond donor groups were shown to bind the anions in a variety of binding stoichometries, as demonstrated by the downfield shift of all the NH resonances during the ^{1}H NMR titration process.

The binding constants for receptor **226** could only be calculated with chloride and acetate because of the complex binding events that were observed for everyother anion tested. Chloride was the only anion to form a 1:1 complex with the receptor, with a binding constant of 141 M^{-1}; over ten times greater in magnitude than that observed for receptors **224** and **225**. Acetate was found to form a 2:1 anion:receptor complex with the receptor, with K_1 (499 M^{-1}) > K_2 (100 M^{-1}). Dihydrogen phosphate was found to form a 3:1

anion:receptor binding stoichiometry in solution. The complex binding equilibria involved in the formation of a 3:1 complex could not be accurately modelled and therefore no binding constants could be calculated.[153,188] Binding constants could not be calculated for benzoate as the binding stoichiometry was not clear from Job plot analysis. It appears that there is a mixture of 1:1 and 2:1 complex formation with this anion.

Table 4.2.2.3 Anion binding constants (M^{-1}) and percentage error for receptor **226**, measured in DMSO-d_6/0.5% H_2O at 298 K. Anionic guests were added as the TBA salt of the anion apart from bicarbonate, which was added as the TEA salt of the anion. Binding constants determined by ^1H NMR titration following the urea NH, fitting data to a 1:1 binding model using WINEQNMR[153].

Anion	Binding Mode	226	E (%)
$CH_3CO_2^-$	2:1	K_1 = 499	9
		K_2 = 100	>50
$H_2PO_4^-$	3:1	a	-
$C_6H_5CO_2^-$	b	b	-
Cl^-	1:1	141	13
F^-	c	c	-
$^eHCO_3^-$	d	d	-

a – Complex binding equilibria prevents the calculation of accurate binding constants. b – Mixture of 1:1 and 2:1 binding modes prevents the calculation of binding constants. c – Slow exchange/conformational change/complex binding event. d – Deprotonation of bound anion. ^{e} –Added as the TEA salt of the anion.

The ^1H NMR studies in a DMSO-d_6/0.5% H_2O solution with fluoride illustrated complex anion binding events. The ^1H NMR spectra for this binding event are shown in Stack plot 4.2.2.3. Between the addition of 0 and 1.5 equivalents of anion, a normal fast exhange anion binding event is observed, with the steady downfield shift of both the amide and indole NH resonances. Between 1.5 and 2.5 equivalents of anion, there is a large upfield shift of both these resonaces that could be attributed to the formation of a 2:1 anion:receptor complex. With equivalents of anion greater than 2.5, there is a slow exchange event, with peaks appearing at approximatly 13.4 ppm, 11.4 ppm and 11.3 ppm. This could be due to a comformational change or a more complex anion binding event but the exact cause is not clear.

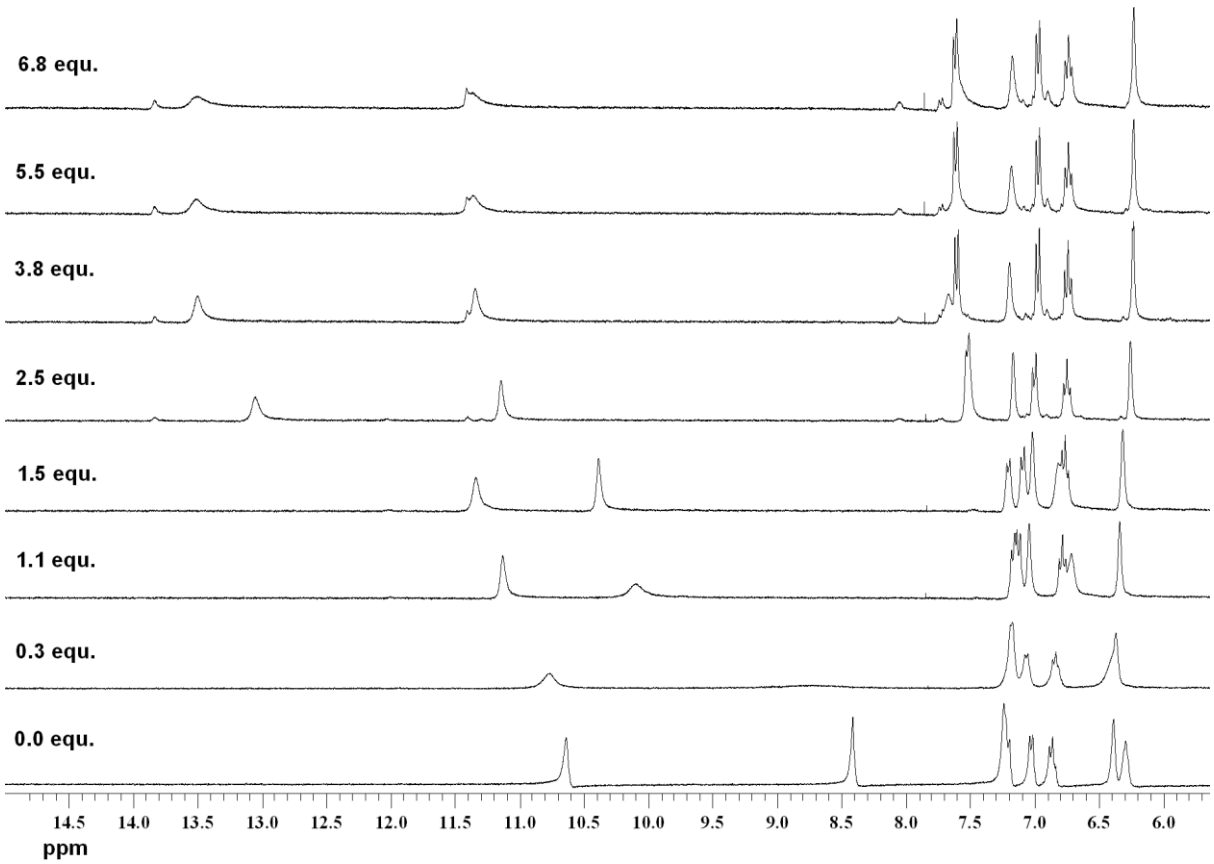

Stack plot 4.2.2.3 Receptor **226** with TBA fluoride, illustrating the fast exchange binding event of the anion to the receptor in a DMSO-d_6/0.5% H_2O solution. A conformational change/complex binding event is observed in slow exchange between 2.5 and 6.8 equivalents of anion.

As with receptors **219**, **221** and **222**, receptor **226** shows the deprotonation of the bound anion in excess anion solution. In this case, as with receptor **219**, we see this event in a DMSO-d_6/0.5% H_2O solution in slow exchange. The slow exchange deprotonation of the bound bicarbonate anion is shown in Stack plot 4.2.2.4. When 0 to 1 equivalents of bicarbonate are added, the anion is bound to the receptor. With further additions of anion, a second set of peaks are seen at approximately 13.8 ppm and 11.4 ppm, indicative of the bound carbonate complex. Small sets of peaks, also in slow exchange, are seen at 12.0 ppm and 9.7 ppm from when 0.6 to 2.5 equivalents of anion are added. The intensity of these peaks decreases with the addition of further aliquots of anion. It is most likely that these peaks are due to a minor conformational change.

.

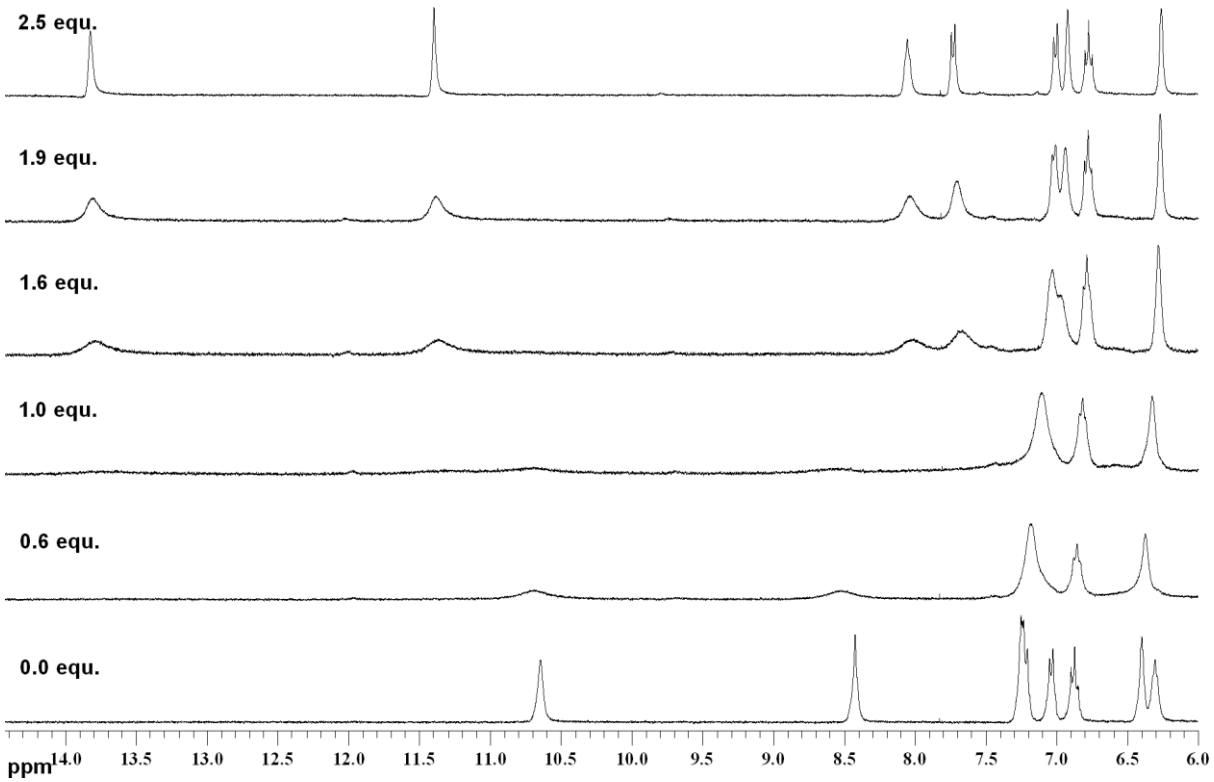

Stack plot 4.2.2.4 Receptor **226** with 0-2.5 equivalents TEA bicarbonate, illustrating the slow exchange deprotonation of the bound bicarbonate anion and binding of the carbonate anion to the receptor in a DMSO-d_6/0.5% H_2O solution.

As with receptors **219**, **221** and **222**, where deprotonation of the bound anion to excess anion in solution is suspected, the theory of deprotonation of the anion was verified with a combined bicarbonate/hydroxide ^{1}H NMR experiment, (Stack plot 4.2.2.5). Approximately one equivalent of bicarbonate was titrated into a DMSO-d_6/0.5% H_20 solution of receptor to give the bicarbonate/receptor complex. Hydroxide was then added to force the deprotonation of the bound anion. The spectra were then compared to those shown in Stack plot 4.2.2.4 and were found to be identical.

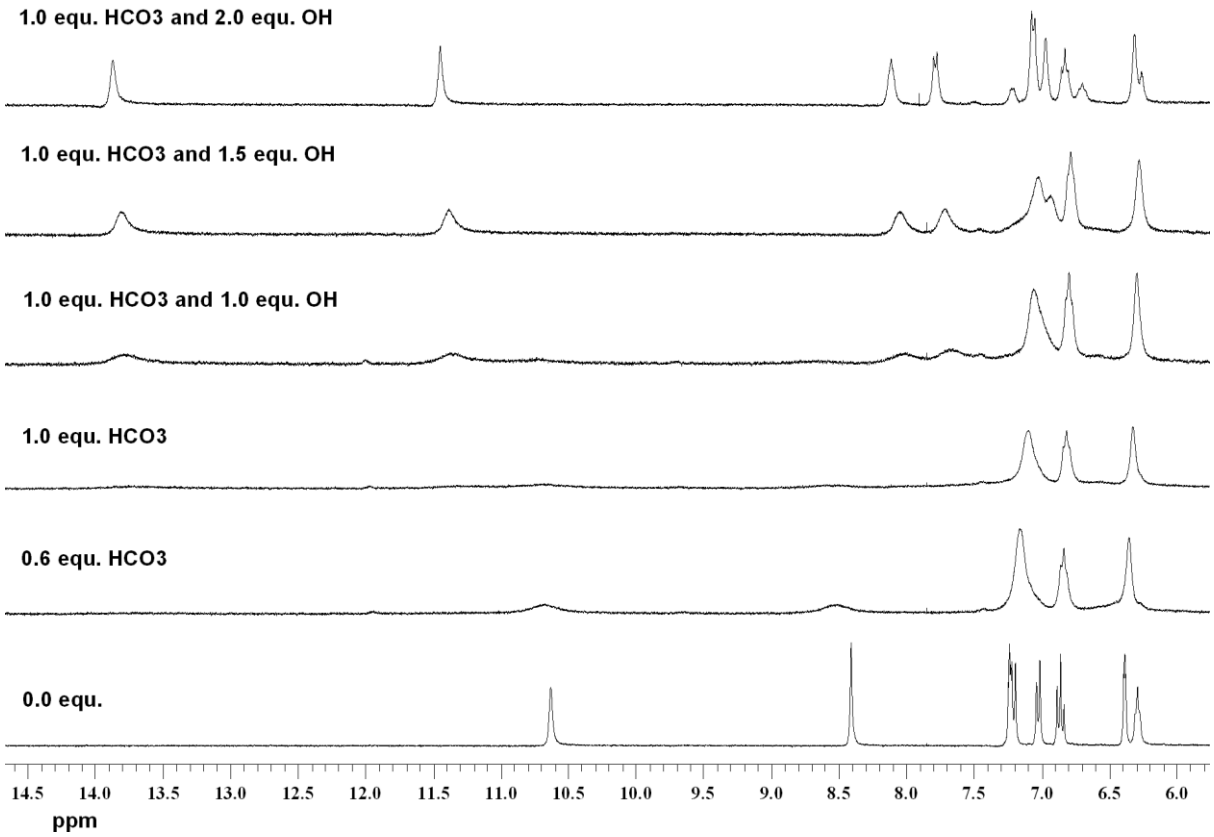

Stack plot 4.2.2.5 Receptor **226** with 0-1.0 equivalents TEA bicarbonate, followed by the addition of TBA hydroxide to deprotonate the bound bicarbonate anion in a DMSO-d_6/0.5% H_2O solution.

For completeness, receptor **226** was titrated with hydroxide to force the deprotonation of the receptor. The results of the ^{1}H NMR titration are shown in Stack plot 4.2.2.6. This produced NMR spectra completely different to those observed with the presence of the bicarbonate anion; no resonances were observed in the region of 8 ppm to 15 ppm after the addition of 0.5 equivalents of hydroxide.

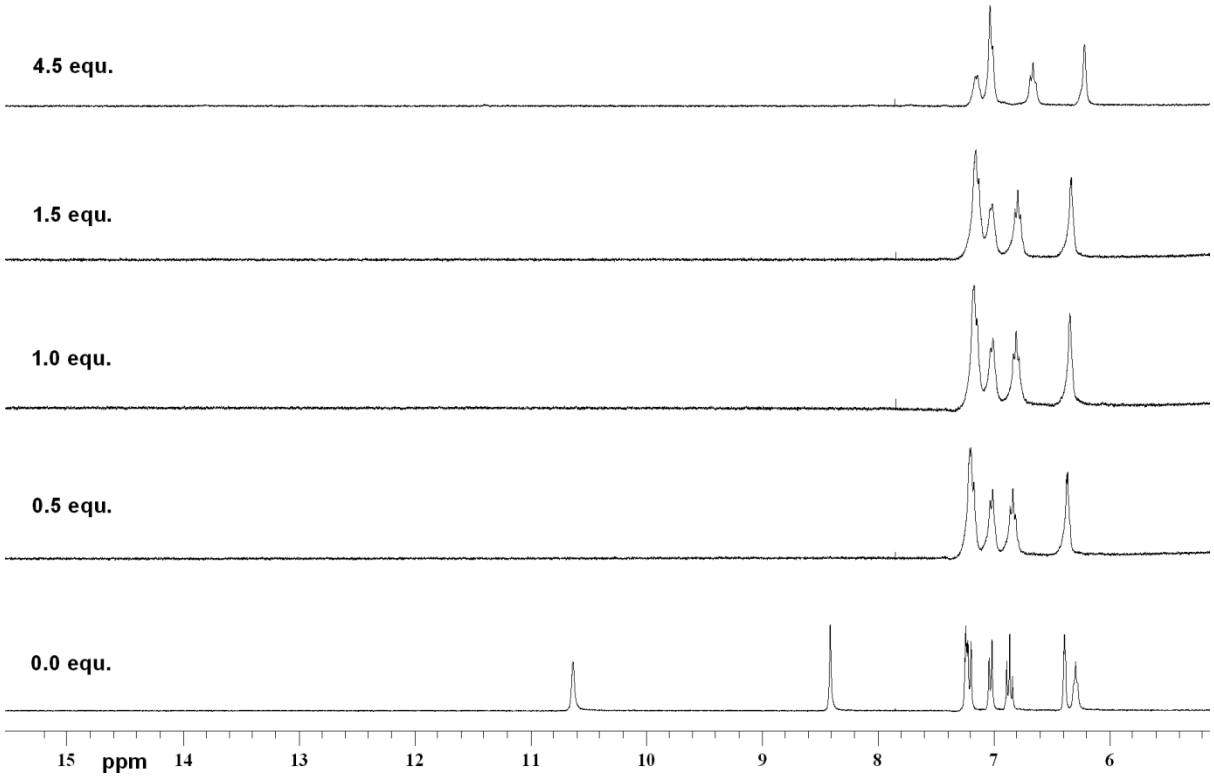

Stack plot 4.2.2.6 Receptor **226** with 0-4.5 equivalents TBA hydroxide, illustrating the deprotonation of the receptor in a DMSO-d_6/0.5% H_2O solution.

Binding stoichometries for receptors **227** were determined by following the downfield shift of the indole, urea and amide NH resonances. The results of the Job plots and ^{1}H NMR titration studies in a DMSO-d_6/0.5% H_2O solution are shown in Table 4.2.2.4. No binding constants could be calculated but, in some cases, the binding stoichiometry could be determined, together with the extent of the participation of different NH bond donor groups in the highly complex anion binding events. This could be deduced by monitoring the change in chemical shift of the different NH bond donor groups after the addition of anion equivalents (Graphs 4.2.2.1-4.2.2.4). From Job plot analysis, sulfate, acetate and benzoate were found to form 3:1 anion:receptor complexes. Dihydrogen phosphate and chloride were shown to exhibit mixed binding stoichometries, while the peak broadening shown with bicarbonate prevented any information being obtained.

Table 4.2.2.4 Anion binding constants (M^{-1}) and percentage error for receptor **227**, measured in DMSO-d_6/0.5% H_2O at 298 K. Anionic guests were added as the TBA salt of the anion apart from bicarbonate, which was added as the TEA salt of the anion. Binding constants were determined by ^1H NMR titration following the amide NH, fitting data to a 1:1 binding model using WINEQNMR[153].

Anion	Binding Mode	227	E (%)
$CH_3CO_2^-$	3:1	d	-
$H_2PO_4^-$	b	b	-
$C_6H_5CO_2^-$	3:1[a]	d	-
Cl^-	b	b	-
SO_4^{2-}	3:1	d	-
[e]HCO_3^-	c	c	-

a – Assumed binding mode based on ^1H NMR titration data and previous evidence from receptor **227** and acetate. b – Mixed binding modes prevented the calculation of binding constants. c – Peak broadening prevented calculation of binding mode or binding constant. d – Complex binding equilibria prevents the calculation of accurate binding constants. [e] –Added as the TEA salt of the anion.

Changes observed in chemical shift of the five different NH resonances of receptor **227**, with the addition of sulfate in a DMSO-d_6/0.5% H_2O solution, clearly indicate that this receptor has a strong affinity for this anion. All fifteen NH bond donor groups are involved in binding each of the three equivalents of anion to a similar degree. The evidence for this is shown in Graph 4.2.2.1. The shape of the curves created for each NH resonance indicates a strong affinity for the anion by all five different NH resonances.

Dihydrogen phosphate is also found to bind through all five different NH bond donor groups, although with a lower affinity when compared to the sulfate anion as seen by the shape of the curves (Graph 4.2.2.2). Although the indole and urea NHs appear to be effective in binding three equivalents of anion, the amide NH moiety does not appear to be as involved in the binding process.

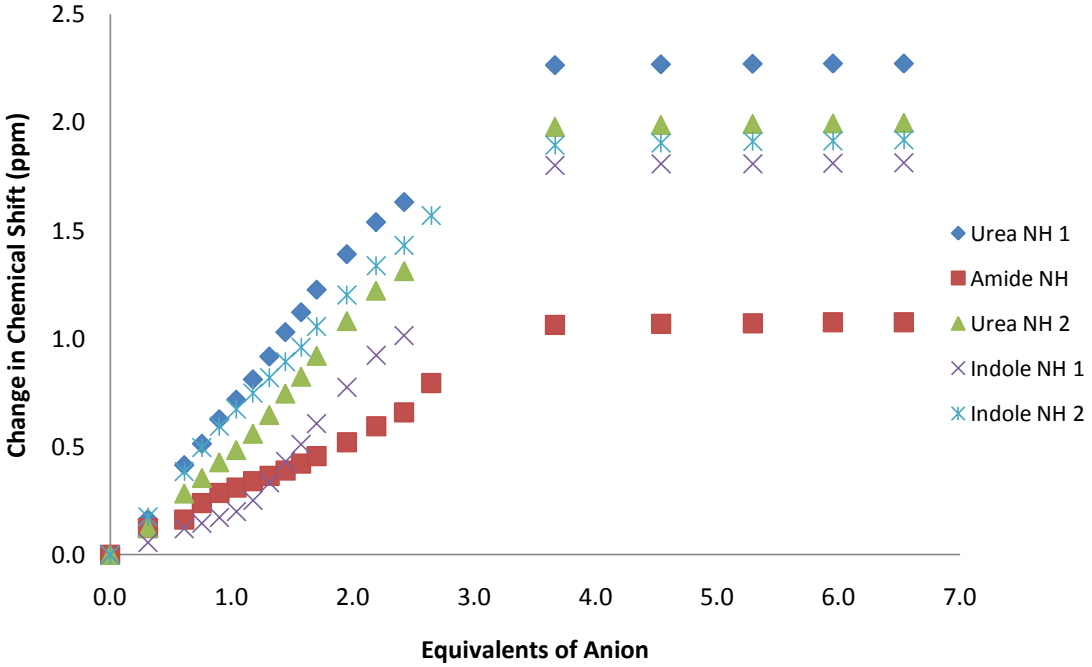

Graph 4.2.2.1 Change in chemical shift of the five different NH resonances of receptor **227** with TBA sulfate, illustrating the interaction of the different NH functionalities with the anion in a DMSO-d_6/0.5% H_2O solution.

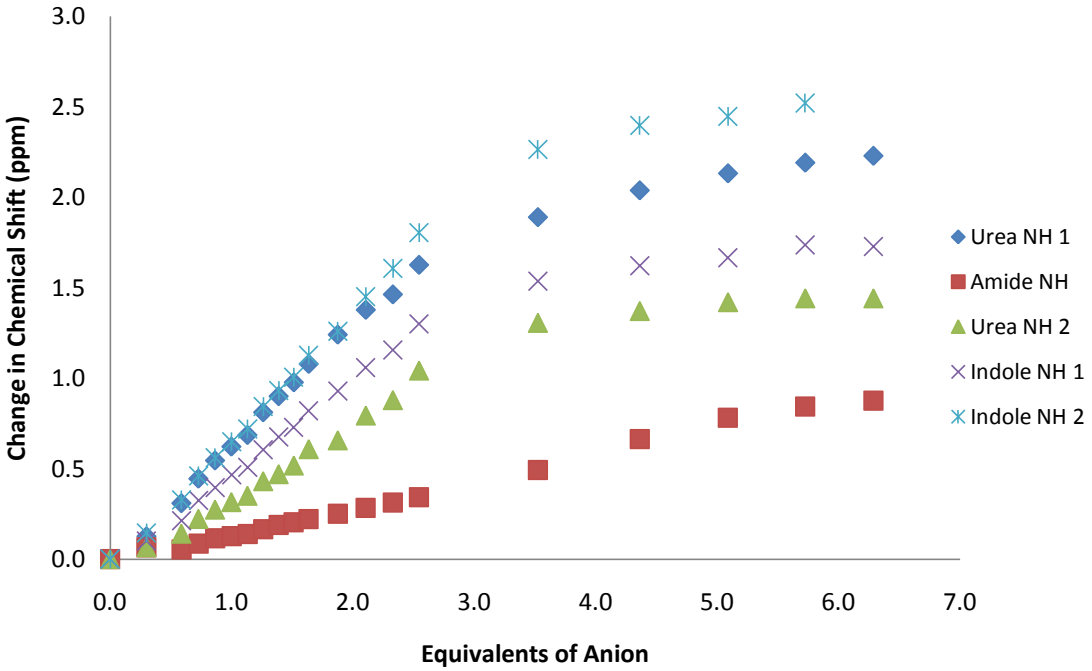

Graph 4.2.2.2 Change in chemical shift of the five different NH resonances of receptor **227** with TBA dihydrogen phosphate, illustrating the interaction of the different NH functionalities with the anion in a DMSO-d_6/0.5% H_2O solution.

Graph 4.2.2.3 shows the change in chemical shift of the five different NH bond donor groups of receptor **227** with acetate in a DMSO-d_6/0.5% H_2O solution. Graphs produced for the benzoate and bicarbonate anions show very similar results. The receptor binds three of the trigonal planar and Y-shaped carbonate anions with a high affinity through the two indole and two urea NH bond donor groups. There is no interaction from amide NH.

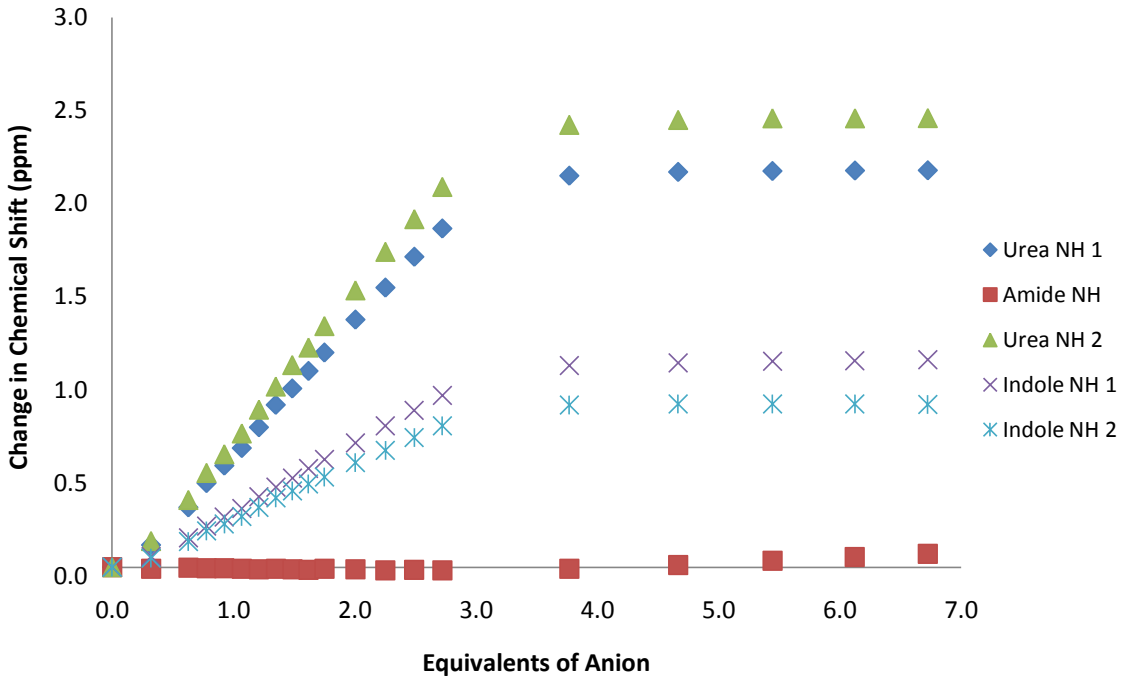

Graph 4.2.2.3 Change in chemical shift of the five different NH resonances of receptor **227** with TBA acetate, illustrating the interaction of the different NH functionalities with the anion in a DMSO-d_6/0.5% H_2O solution.

Graph 4.2.2.4 illustrates the change in chemical shift of the five different NH bond donor groups of receptor **227** with chloride in a DMSO-d_6/0.5% H_2O solution. This receptor shows a weak affinity for chloride. It is only the two urea NH bond donor groups that appear to interact with the anion. The amide and indole NH resonances do not show a large enough change in chemical shift for them to be considered as contributing to the binding of the anions.

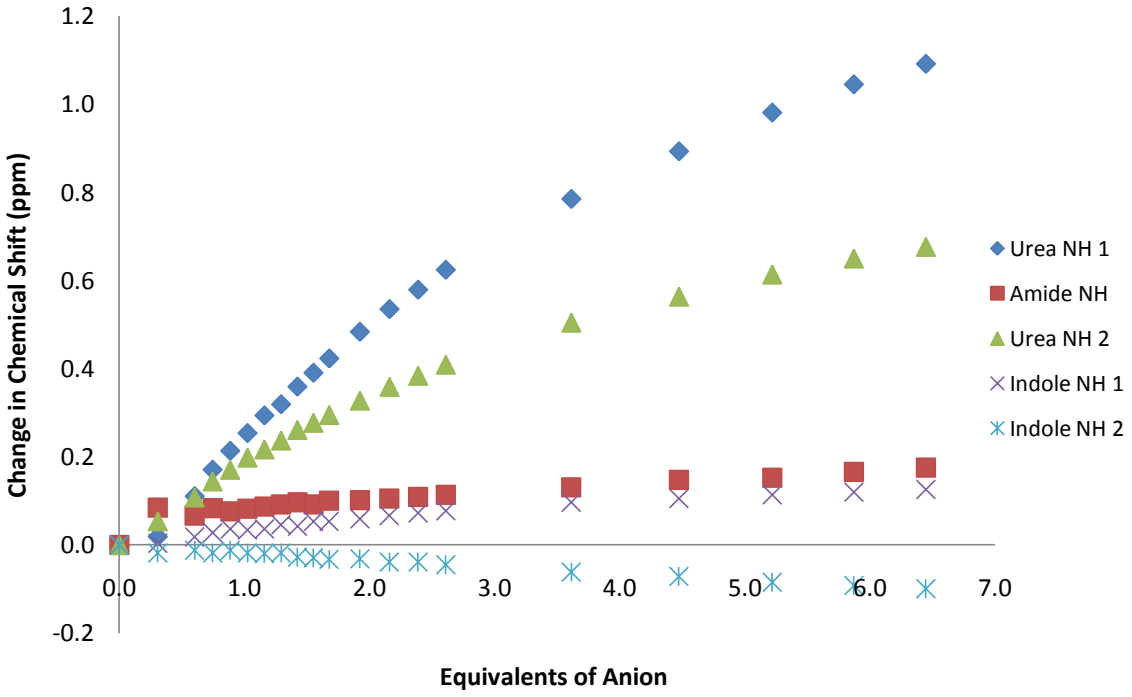

Graph 4.2.2.4 Change in chemical shift of the five different NH resonances of receptor **227** with TBA chloride, illustrating the interaction of the different NH functionalities with the anion in a DMSO-d_6/0.5% H_2O solution.

4.3 Symmetrical 'Pin-wheel' based anion receptors

The tri-amino pin-wheel scaffold offers a slightly larger, less flexible base unit for tripodal receptor design. This scaffold was first used in anion receptor design by Anslyn and co-workers in 1997. Citrate was bound with receptor **228** in an aqueous solution and a binding constant of 7.0 x 10^3 M^{-1} was calculated.[189]

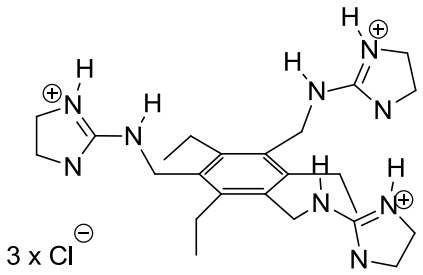

228

The pendent arms of receptor **228** are pre-organised so the anion binding units sit in the same direction above or below the central phenyl ring. Anslyn and co-workers went on to use this receptor in the first example of the use of competitive binding events to indicate the presence of an anion (citrate) in solution. An indicator was first bound to the free receptor but was known to be less favourably bound than the anion to be detected. In the presence of the anion, the anion becomes bound to the receptor, releasing the indicator, which results in a change in λ_{max} of the UV-Vis spectrum.[190] Since this scaffold was first used in anion receptor design, a great variety of anion receptors have been synthesised, based on the original pin-wheel scaffold or its analogues.[179,191]

Anzenbacher and co-workers have synthesised similar receptors to those that I have synthesised and discussed in this chapter. They produced a set of eight, anion binding receptors, based on the same pin-wheel unit and functionalised with amide or thiourea hydrogen bond donating linker groups attached to a variety of aromatic moieties. Of this set Of eight receptors, receptors **229** and **230** are the closest analogues to the receptors synthesised and discussed by myself. Other members in the set of eight receptors act in fluorescence-turn-on sensor arrays sensing phosphate, pyrophosphate, AMP and ATP from blood serum to enable the identification of these biological phosphate groups. These receptors contain NH bond donor groups and fluorescent functionalities instead of the pyrrole/benzyl groups of receptors **229** and **230** thus enabling the receptors to act as anion sensors. [192]

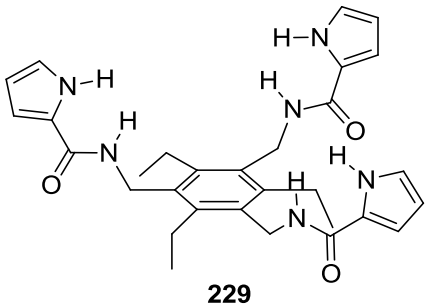

229

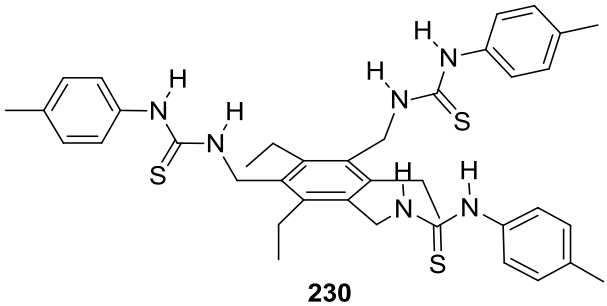

230

Cryptand receptors, based on this tripodal scaffold, have been synthesised by Delgado and co-workers and these also show selectivity for dihydrogen phosphate in methanol:water 1:1 solution.[193] Schmuck and Merschky have also used the pin-wheel scaffold as the basis of their low molecular weight organocatalysts for the breakdown of phosphates in an aqueous solution.[194]

4.3.1 Synthesis

Receptor **231** was synthesised by a one step reaction, analogous to that of receptor **224** and **225** and shown in Scheme 4.3.1.1. 7-nitroindole-2-carboxylic acid was amide-coupled to the pin-wheel scaffold, using PyBOP as the amide coupling agent in a dry DMF solution, with HOBt and NEt_3 to further catalyse the reaction. The reaction solution was then taken to dryness and the resultant oil dissolved in DCM and washed with water to precipitate the receptor in a 75% yield.

Receptor **232** was synthesised in the analogous reaction to receptor **226**, in a one step reaction shown in Scheme 4.3.1.2. The N-(1H-indol-7-yl)-1H-imidazole-1-carboxamide intermediate was reacted with the tri-amino pin-wheel in DMF (Scheme 4.2.1.3). The DMF was then removed and the crude product titrated in ethyl acetate, followed by water, to give the receptor in a 79% yield.

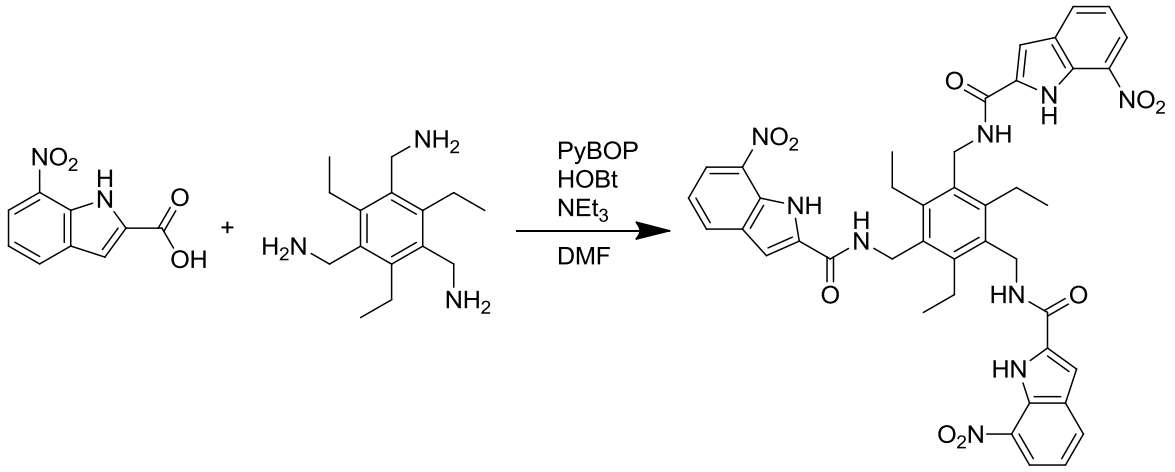

231

Scheme 4.3.1.1

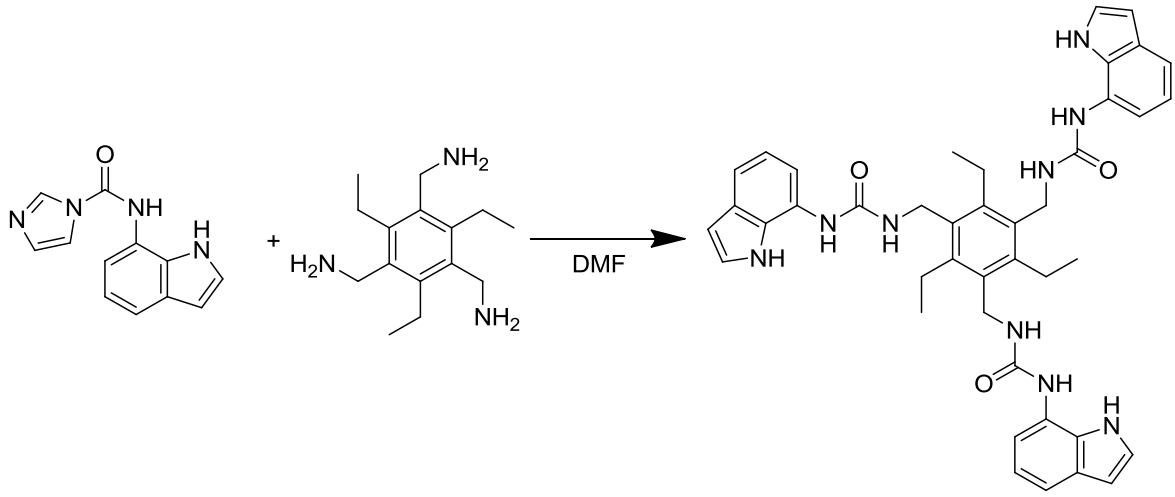

232

Scheme 4.3.1.2

4.3.2 Solution phase analysis

4.3.2.1 Proton NMR titration data

Anion binding constants were determined for receptors **231** and **232** with wide range anions. The binding constants were determined by ^{1}H NMR titration with the TBA salt of the anion in various DMSO-d_6/H_2O solutions, apart from bicarbonate, which was added as the TEA salt of the anion. The binding constants were calculated by the computer program

WINEQNMR[153] and fitted to a 1:1 or 2:1 anion:receptor binding model. Job plots[154] were produced to check the binding stoichiometry of receptors **231** and **232**.

Binding stoichometries of receptor **231** and chloride were inferred as 1:1 from the ^{1}H NMR titration data as the Job plot experiments were inconclusive, due to the small change in chemical shift of the NH resonances in the ^{1}H NMR spectra. The dihydrogen phosphate and benzoate binding stoichometries for receptor **231** were determined by following the downfield shift of the indole NH and amide NH resonances. Only the amide NH shift could be followed with acetate because there was peak broadening with the indole NH. No binding stoichometries/constants could be elucidated for sulfate and bicarbonate due to peak broadening events and conformational changes respectively. Binding constants were calculated by following the downfield shift of the amide NH resonance. The binding constants, binding stoichometries and information derived from the ^{1}H NMR titration data for receptor **231** are shown in Table 4.3.2.1. In a DMSO-d_6/0.5% H_2O solution, stronger binding affinities were observed for the Y-shaped carboxylate anions and the oxo-anion, dihydrogen phosphate, to the pin-wheel scaffold (**231**) than to the TREN scaffold (**225**). All six hydrogen bond donor groups of receptor **231** were shown to bind to the anion, forming a 1:1 complex. As with the TREN analogue, this receptor shows selectivity for dihydrogen phosphate (2240 M^{-1}) over the carboxylate anions, acetate (908 M^{-1}) and benzoate (321 M^{-1}) and the halide anion chloride (<10 M^{-1}). The larger but more rigid tripodal pin-wheel scaffold not only increases the binding affinity of the receptor for dihydrogen phosphate by more than ten times but also increases the degree of selectivity for dihydrogen phosphate over the carboxylate anions when compared to the smaller, more flexible TREN-based receptor **225**. This is because the pin-wheel scaffold is more pre-organised towards anion binding than the TREN scaffold and its larger size increases the affinity for the receptor of the tetrahedral anion, dihydrogen phosphate, over the Y-shaped carboxylate anions.

Table 4.3.2.1 Anion binding constants (M^{-1}) and percentage error for receptor **231**, measured in DMSO-d_6/0.5% H_2O at 298 K. Anionic guests were added as the TBA salt of the anion apart from bicarbonate, which was added as the TEA salt of the anion. Binding constants were determined by ^1H NMR titration following the amide NH, fitting data to a 1:1 binding model using WINEQNMR[153].

Anion	Binding Mode	231	E (%)
$CH_3CO_2^-$	1:1	908	10
$H_2PO_4^-$	1:1	2240	16
$C_6H_5CO_2^-$	1:1	321	7
Cl^-	1:1[a]	<10	-
SO_4^{2-}	b	b	-
[d]HCO_3^-	c	c	-

a – Assumed binding mode based on ^1H NMR titration data. b – Peak broadening prevented the calculation of binding constants and ascertainment of binding modes. c – Conformational change prevented the ascertainment of binding mode or binding constant. [d] –Added as the TEA salt of the anion.

Binding stoichometries for receptor **232** were determined by following the downfield shift of a urea NH and indole NH resonance. Binding constants were calculated by following the downfield shift of a urea NH resonance. The binding constants and information derived from the ^1H NMR titration experiments for receptor **232** are shown in Table 4.3.2.2. In a DMSO-d_6/0.5% H_2O solution, no simple 1:1 anion:receptor binding stoichometries were observed. All nine hydrogen bond donor groups were shown to bind the anion in a variety of binding stoichometries, as illustrated by the downfield shift of all the NH resonances during the ^1H MNR titration process.

Benzoate, chloride and bicarbonate all exhibited a combination of 1:1 and 2:1 binding stoichometries from Job plot analysis. This prevented the calculation of binding constants. The peak broadening events in the ^1H NMR spectrum of receptor **232** and dihydrogen phosphate also prevented the calculation of any binding constants. A straightforward 2:1 anion:receptor binding stoichiometry was observed with both acetate and sulfate, with selectivity being shown for sufate over acetate; a K_1 of 2250 M^{-1} was calculated for sulphate but the K_1 calculated for acetate was approximately only one eighth of this value. Receptor **232** shows a decreased affinity for acetate when compared to the

binding constants calculated for the TREN based analogue (**226**). The larger size and extra rigidity of the pin-wheel scaffold has lowered the affinity of the receptor for this anion.

Table 4.3.2.2 Anion binding constants (M^{-1}) and percentage error for receptor **232**, measured in DMSO-d_6/0.5% H_2O at 298 K. Anionic guests were added as the TBA salt of the anion apart from bicarbonate, which was added as the TEA salt of the anion. Binding constants determined by ^1H NMR titration following the amide NH, fitting data to a 1:1 binding model using WINEQNMR[153].

Anion	Binding Mode	232	E (%)
$CH_3CO_2^-$	2:1	$K_1 = 285$	7
		$K_2 = 63$	>50
$H_2PO_4^-$	a	a	-
$C_6H_5CO_2^-$	b	b	-
Cl^-	b	b	-
SO_4^{2-}	2:1	$K_1 = 2250$	26
		$K_1K_2>10^6$	-
$^cHCO_3^-$	b	b	-

a – Peak broadening prevented the ascertation of binding mode or binding constant. b – Mixed 1:1 and 2:1 anion:receptor binding modes prevented the calculation of binding constants. ^{c} –Added as the TEA salt of the anion.

4.3.3 Solid phase analysis

X-ray quality crystals of receptor **232** and TBA benzoate were obtained from a DMSO solution of receptor **232** with excess TBA benzoate.

The crystal structure of receptor **232**, produced by single crystal X-ray diffraction, is shown in Figure 4.3.3.1. This complex shows a 3:1 anion:receptor binding stoichiometry, with all nine NH bond donor groups coordinating to the six oxygen atoms of three benzoate anions. The binding stoichiometry is different from the mixture of 1:1 and 2:1 anion:receptor binding stoichometries observed in the DMSO-d_6/0.5% H_2O solution.

The nine hydrogen bond donor groups of the receptor form single hydrogen bonds to the oxygen atoms of the anions. Each benzoate anion is bound by one arm of the receptor

through three hydrogen bonds, two from urea NHs and one from an indole NH. Two similar receptor/anion complexes are contained within each unit cell but only one is shown in Figure 4.3.3.1 for clarity. The hydrogen bonding interactions and hydrogen bond angles for both anion/receptor complexes in the unit cell illustrated in Figure 4.3.3.1 are shown in Table 4.3.3.1. The hydrogen bonds from the nitrogen atoms of the receptor to the oxygen atoms of the anion range from N···O = 2.706(6) – 3.308(6) Å and the bond angles range from N–H···O = 132.1°-174.1°.

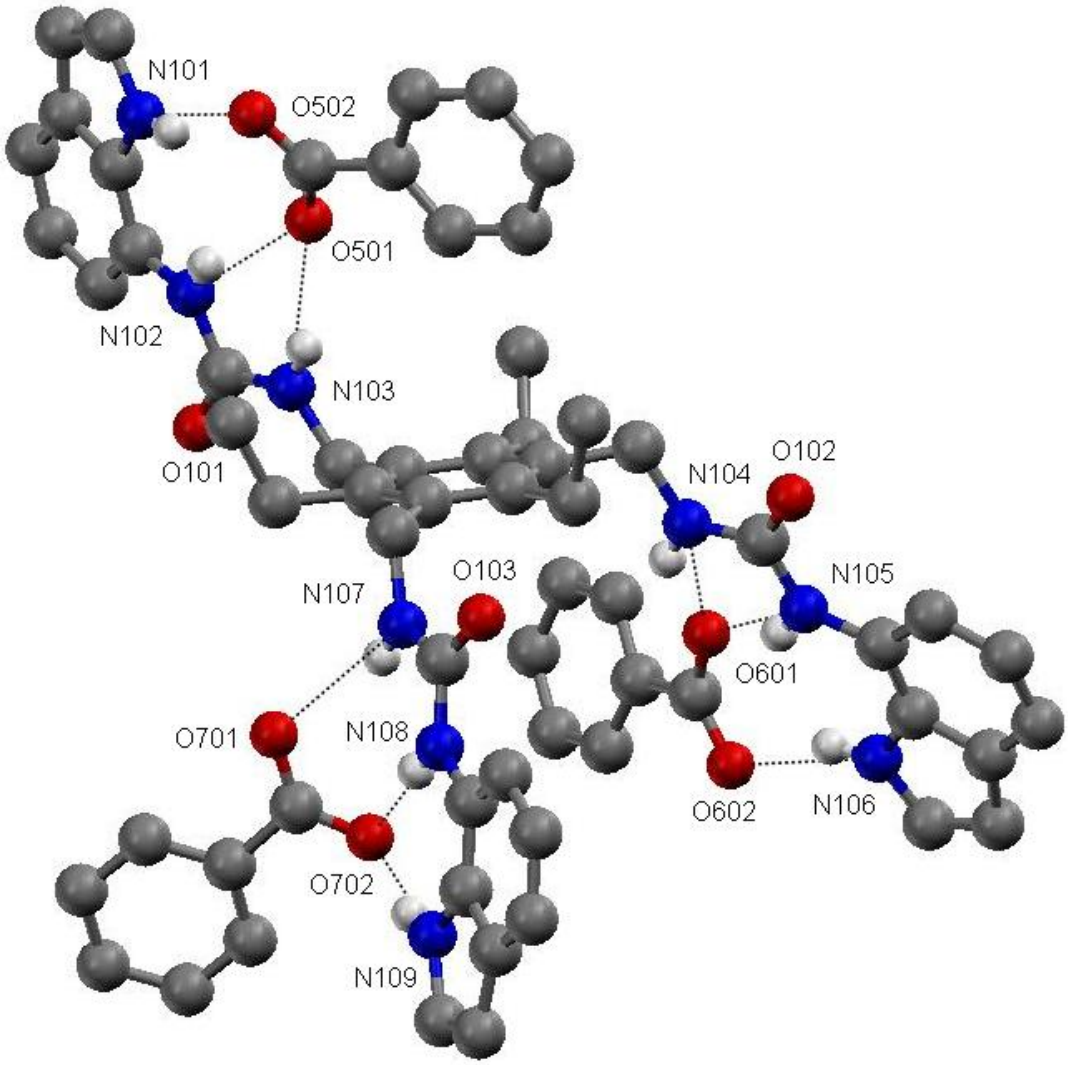

Figure 4.3.3.1 The benzoate complex of receptor **232**. Single X-ray crystal structure with TBA benzoate. The CH hydrogen atoms, solvent molecules, second receptor anion complex and the TBA counter ions have been omitted for clarity.

Table 4.3.3.1 Hydrogen bonding table for crystal structure of receptor **232** and TBA benzoate anion/receptor complex illustrated in Figure 4.3.3.1. Obtained by single crystal X-ray diffraction at 120K. *D* – hydrogen bond donor atom. *A* – hydrogen bond acceptor atom. *d* – distance in Å. ∠ - bond angle in °. H – hydrogen atom. Symmetry transformations used to generate equivalent atoms: (i) –x,–y,–z+1 (ii) –x+1,–y,–z+1 (iii) –x+1,–y+1,–z+1

D–H···*A*	*d*(*D*–H) (Å)	*d*(H···*A*) (Å)	*d*(*D*···*A*) (Å)	∠(*D*H*A*) (°)
N104–H997···O601	0.88	2.06	2.820(7)	143.4
N105–H996···O601	0.88	2.04	2.833(7)	148.8
N106–H888···O602	0.88	1.92	2.746(8)	155.3
N107–H107···O701	0.88	2.13	2.835(6)	137.2
N108–H108···O702	0.88	2.12	2.994(6)	174.1
N109–H109···O702	0.88	1.91	2.770(6)	164.7
N204–H993···O301	0.88	2.10	2.837(6)	140.2
N205–H992···O301	0.88	1.95	2.764(6)	152.8
N206–H991···O302	0.88	2.00	2.826(6)	155.5
N101–H999···O502^{i}	0.88	2.01	2.851(6)	160.3
N102–H998···O501^{i}	0.88	1.95	2.735(6)	147.8
N103–H103···O501^{i}	0.88	2.02	2.804(6)	147.3
N201–H995···O802^{ii}	0.88	2.10	2.924(6)	154.7
N201–H995···O801^{ii}	0.88	2.59	3.304(6)	139.2
N202–H994···O801^{ii}	0.88	1.96	2.706(6)	141.0
N203–H203···O801^{ii}	0.88	2.05	2.800(6)	142.7
N207–H207···O402^{iii}	0.88	2.10	2.834(6)	140.2
N208–H208···O401^{iii}	0.88	2.03	2.908(6)	173.2
N208–H208···O402^{iii}	0.88	2.65	3.308(6)	132.1
N209–H209···O401^{iii}	0.88	1.87	2.731(6)	163.8

4.4 Future work

These preliminary studies of the use of the tripodal scaffolds in indole-based receptor chemistry shows promise that this type of receptor can demonstrate selective, high affinity binding of anions in competitive solvent environments. The example of the deprotonation of bound bicarbonate with receptor **226** in a DMSO-d_6/0.5% H_2O solution also indicates properties that could be used for the basis of organocatalyst design.

We have already synthesised the cage receptor **233** in a moderate yield but the product still contains impurities. The formation of this TREN-based cage should permit some flexibility, allowing anions into and out of the cavity and allowing the cavity to alter shape slightly to better accommodate the anion in the cavity, while still pre-organising the eighteen NH bond donor groups for binding the anion within the cavity. The cavity restricts the space the anions can inhabit, which limits the number of anions that can be bound by a single receptor and reduces the complex nature of the anion binding events so that the receptor can be fully studied in the solution state. This receptor should be able to adopt a similar conformation to that seen in the crystal structure obtained by Claudia Caltagirone (Chapter Two – Figure 2.2.3.3a and b), where three diindolylurea receptors complex to a single dihydrogen phosphate anion, resulting in the double deprotonation of the anion. If this effect could be achieved in the solution state, it is possible that the receptor could act as a very powerful organocatalyst. An analogous receptor could also be synthesised by replacing the TREN-based scaffold with the pin-wheel.

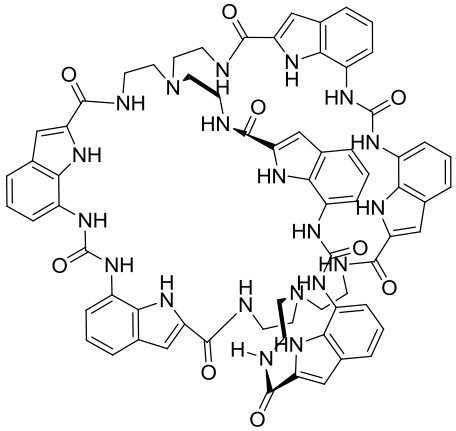

233

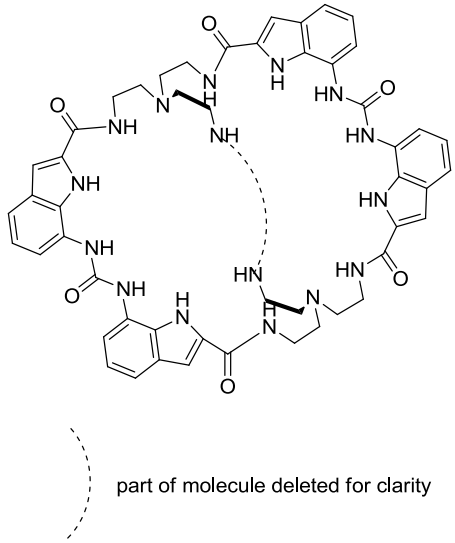

part of molecule deleted for clarity

It is also possible that the larger, multiple hydrogen bond donor receptors, such as receptor **233**, could be used to bind negatively-charged nano-particles such as $Mo_6O_{19}^{2-}$. The TBA salt of this receptor has already been synthesised in accordance with known literature procedure[195] and characterised by single crystal X-ray diffraction, giving the crystal structure shown in Figure 4.4.1. It has also been charicterised by elemental analysis, which matches the literature results. Preliminary ^{1}H NMR investigations have been carried out with several different receptors but further investigation is needed to fully understand the results.

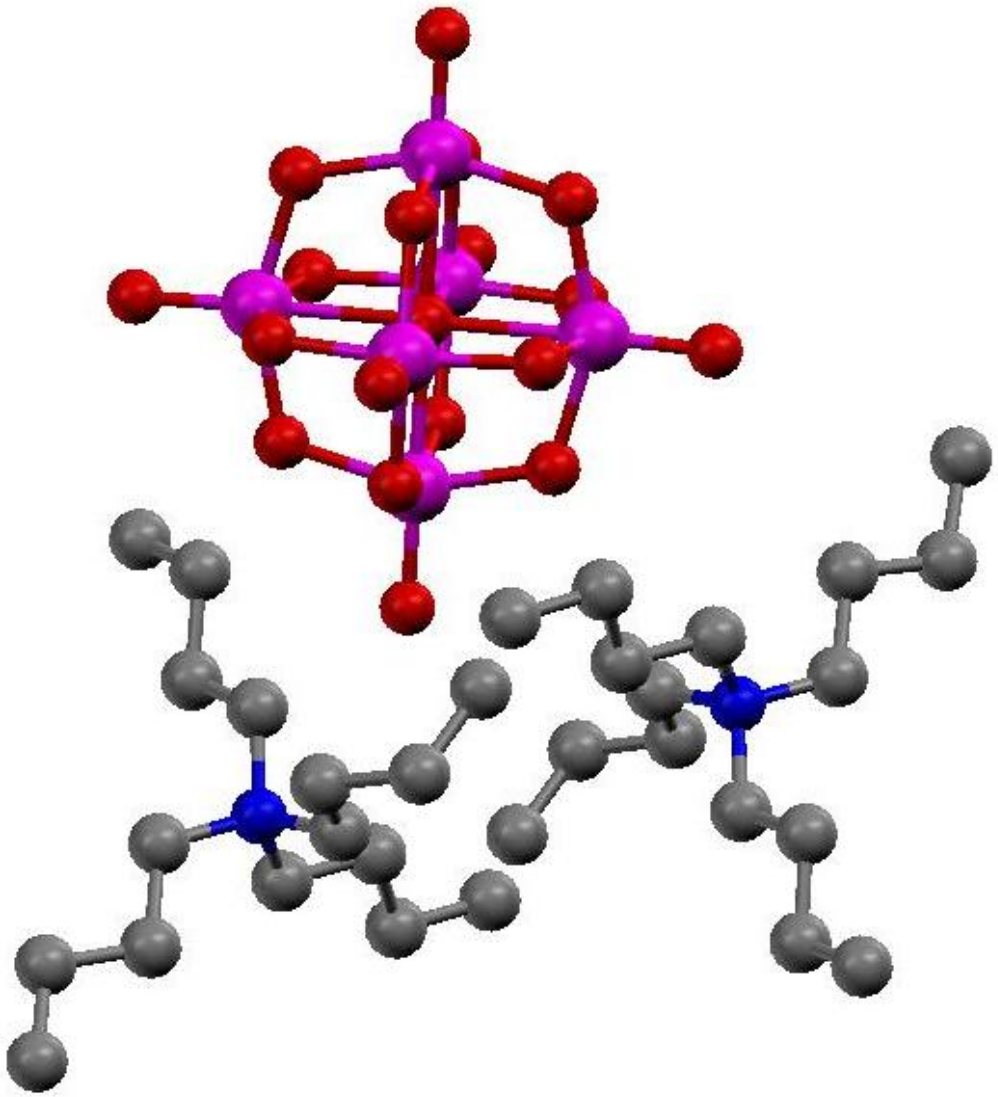

Figure 4.4.1 The single X-ray crystal structure $Mo_6O_{19}^{2-}$ TBA_2 complex. The CH hydrogen atoms have been omitted for clarity.

4.5 Conclusion

A set of six new tripodal-based anion receptors have been synthesised, utilising the TREN scaffold and the more rigid, slightly larger pin-wheel scaffold. The solution state anion binding properties were explored in DMSO-d_6/0.5% H_2O. Receptors **224**, **225** and **231** were found to form simple 1:1 complexes with all anions tested. Receptor **224** was found to have little affinity with any of the anions tested. The introduction ot electron withdrawing nitro groups (receptor **225**) did increase the affinity of the receptor for the oxo-anions and showed slight selectively for dihydrogen phosphate over the carboxylate anions. The increase rigidity and size of the binding cleft of receptor **231** increased the affinity of the receptor for the oxo-anions but also increased the degree of selectivity towards dihydrogen phosphate over the carboxylate anions, due to the combination of increased preorganisation and size exclusion effects.

Receptor **226** showed a variety of complex binding stoichometries in the DMSO-d_6/0.5% H_2O solution that made comparison of anion affinities impossible. Deprotonation of bound bicarbonate to excess basic species occurred in solution. Slow exchange binding events were exhibited, similar to those observed with receptors **224** and **225** when studied with fluoride. The pin-wheel analogue of **226**, receptor **232**, did not show the same variety of complex binding stoichometries as the TREN analogue but was able to show selectivity for sulfate over acetate, the binding affinity of which was reduced when compared to TREN analogue. This could be attributed to the reduction in flexibility of the receptor and the increase in size of the binding cavity. These same properties reverse the binding affinity when compared to the amide-based receptors **224**, **225** and **231**.

Receptor **227** also showed complex binding stoichometries that prevented the calculation of any binding constants. However, comparisons of change in chemical shift, plotted against equivalents of anion, did show the extent to which the five different NH bond donor groups were involved in the anion binding events. These comparisons also indicated the degree of affinity of the receptor for the different anions. Oxo-anions were shown to have strong affinities with the receptor. The carboxylate anions, acetate, benzoate and bicarbonate were shown not to utilise the amide NH in the binding events, unlike the tetrahedral anions, sulfate and dihydrogen phosphate. Chloride was shown to bind predominantly through the urea NH bond donor groups.

Binding constants observed for this set of six complex, three-dimensional receptors are smaller than those observed for the simpler, two-dimensional sets of cleft receptors, discussed in Chapters Two and Three. There are many possible reasons that may contribute to this. The two main reasons for consideration are the increased flexibility, causing the loss in pre-organisation and the increased amount of intramolecular hydrogen bonding that occurs within the three dimensional receptors (**224-227**, **231-232**), making anion binding less favourable.

Chapter 5 - Amide Based Anion Receptors

5.1 Introduction

As with the previous diindole/dicarbazole urea/thiourea based receptors described in Chapters Two and Three, this group of symmetrical receptors were synthesised as an extension to the previous work by Gale, Albrecht and co-workers[1,2]. These groups of receptors explore the diindole diamide and dicarbazole diamide-based symmetrical clefts that contain between four and five hydrogen bond donor groups. This more cleft-like approach to receptor design will cause all available hydrogen bonds to be utilised in the anion binding events. The more effective hydrogen bond formation (through the specific arrangement of the hydrogen bond donor groups along the cleft) and the incorporation of the more acidic carbazole group instead of the indole group will alter the affinity of the anions for the different receptors. The anion complexation effects were monitored in the solution state by ^{1}H NMR spectroscopy and in the solid state by single crystal X-ray diffraction.

5.2 Symmetrical indolylamide hydrogen bond donating clefts containing four to five hydrogen bond donating groups

This group of receptors are specifically based on the 2,7-indole functionalised receptors by Gale and co-workers in collaboration with Albrecht and co-workers[2]. Receptors **176-178** were originally inspired by a combination of work by Gale and co-workers, using of 2,5-dicarboxamidopyrroles in anion receptor design [44,45,81,82] and by Albrecht and co-workers, who used functionalised quinoline [196,197]. Receptors **176-178** were found to selectively bind acetate over the other anions tested, which included chloride and dihydrogen phosphate. The analogous receptors (**234-238**) synthesised by Claudia Caltagirone and myself were found to change this trend by binding dihydrogen phosphate selectively over acetate. This group of five receptors were synthesised by the reaction of indole-2-carboxylic acid with a diamino compound. Receptors **234-237** have been published previously.[198] The effects of

rigidifying the system with different diamino-appended scaffold groups was explored, as well as the effect of the addition of electron withdrawing groups and the addition of extra NH bond donor groups.

5.2.1 Synthesis

Receptors **234-237** were synthesised by a simple one step process. Receptors **234** and **236** were originally synthesised by Claudia Caltagirone, while analogues **235** and **237** were synthesised by myself in a one step simple synthesis. Indole-2-carboxylic acid (**234-235**) or 7-nitroindole-2-carboxylic acid (**236-237**) was first activated with CDI in chloroform, heated to reflux. The amines, either 1,5-diaminopentane (**234** or **236**)or 1,3-phenylenediamine (**235** or **237**), could then be added to the activated carboxylic acid solution in either chloroform or DMF, depending on the solubility of the diamine.

Receptor **234** precipitated directly from the chloroform solution. Minor impurities were removed by washing with ether to give a yield of 73%. The reaction is summarised in Scheme 5.2.1.1. Receptor **235** was isolated in two crops. The first crop precipitated directly from the solution. The second crop was obtained by removing the solvent and re-suspending the solid in DCM. The solid was then isolated and washed with ether to give a combined yield of 70%. The reaction is summarised in Scheme 5.2.1.2. Receptor **236** was obtained by washing the organic phase with water, taking the solution to dryness and obtaining the product by flash chromatography DCM:MeOH 9:1 to give a yield of 47 %. The reaction is summarised in Scheme 5.2.1.3. Receptor **237** was precipitated directly from the reactant mixture with ether, washed with dilute HCl to remove the CDI biproducts and washed further with aliquots of ether. This gave a yield of 72%. The reaction is summarised in Scheme 5.2.1.4.

Receptor **238** was synthesised by a lengthier, four step synthesis, shown in Scheme 5.2.1.5. The first three steps to synthise 1,8-diamino-3,6-dichlorocarbazole from carbazole is known in the literature.[114] The amide coupling with 7-nitroindole-2-carboxylic acid was achieved using PyBOP, HOBt and NEt_3 in DMF. The crude product precipitated directly from the reaction mixture and was purified by titration in methanol; the isolated solid was then washed with ether, giving a yield of 52%.

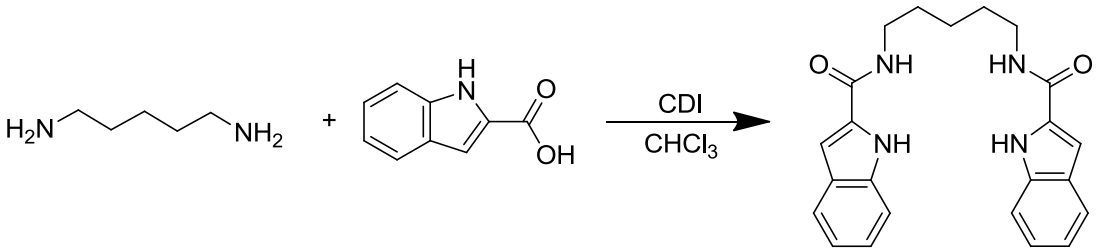

234

Scheme 5.2.1.1

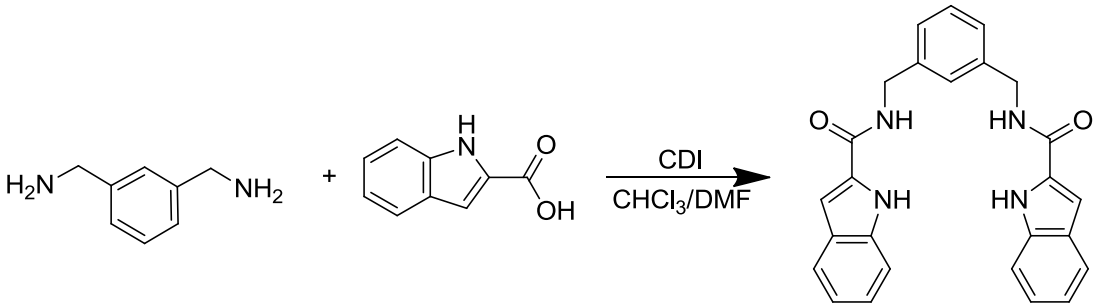

235

Scheme 5.2.1.2

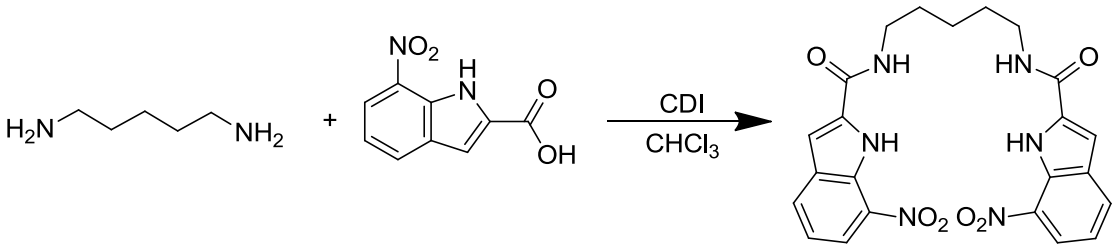

236

Scheme 5.2.1.3

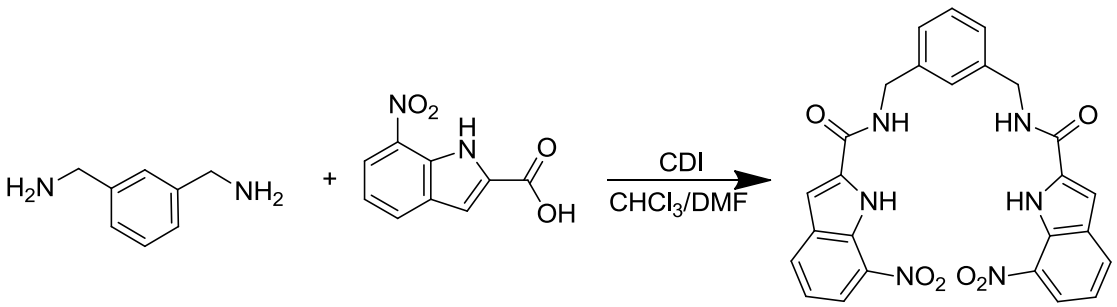

237

Scheme 5.2.1.4

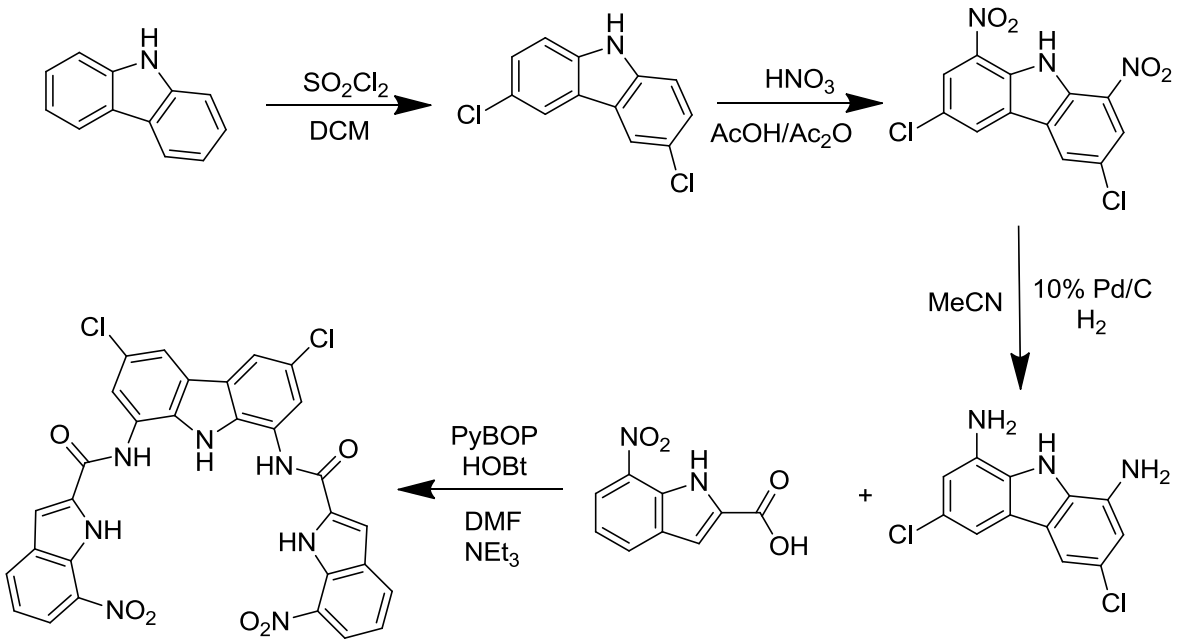

Scheme 5.2.1.5

5.2.2 Solution phase analysis

5.2.2.1 Proton NMR titration data

Anion binding constants were determined for receptors **234**-**238** with a wide range anions. The binding constants were determined by ^{1}H NMR titration with the TBA salt of the anion in DMSO-d_6/0.5% H_2O solutions. The binding constants were calculated by the computer program WINEQNMR[153] and fitted to 1:1 or 2:1 anion:receptor binding models. Job plots[154] were produced to check the binding modes that were strongly suggested by the titration data. The binding constants for receptors **234** and **236** were generated by Claudia Caltagirone. The binding constants for receptors **235**, **237** and **238** were generated by myself, with some help from Claudia Caltagirone. The majority of the binding stoichometries for the five receptors were determined by myself, with some help from Claudia Caltagirone. Binding constants and Job plots were determined by following the downfield shift of the amide NHs, except in the case of receptor **238**, where the carbazole NHs were also investigated. All the NH bond donor groups contained within each of the cleft receptors are shown to be involved in the anion binding process as they all experience a downfield shift upon introduction of anions to a solution of receptor.

The results of the anion binding studies performed with receptors **234** and **235** are shown in Table 5.2.2.1. In a DMSO-d_6/0.5% H_2O solution, both receptors were shown to form 1:1 complexes with the various anions through Job plot analysis. Both receptors **234** and **235** exhibit a moderate affinity for dihydrogen phosphate, with binding constants calculated as 260 M^{-1} and 176 M^{-1} respectively. There is little affinity shown for any of the other oxo- or halide anions tested. Therefore the receptors show selectivity for the dihydrogen phosphate anion, which is a change to the trend shown by the original amide-functionalised indole receptors synthesised by Gale, Albrecht and co-workers[2]. Receptors **234** and **235** exhibit a trend more similar to that of the diindolylurea receptors **209** and **210**. Although the binding constants are not large as those calculated for the diindolylurea compounds or the original indolylamide receptors (**181** and **182**), good selectivity is still shown. In general, slightly higher binding constants are observed for receptor **234**, which may be because the added flexibility of the pentyl chain allows the receptor to wrap around the anion. This would then allow the NH bond donor groups to complex with a greater affinity to the anion, causing a slightly higher binding constant when compared to those of receptor **235**.

Table 5.2.2.1 Anion binding constants (M^{-1}) and percentage error for receptors **234** and **235**, measured in DMSO-d_6/0.5% H_2O at 298 K. Anionic guests were added as the TBA salt of the anion. Binding constants determined by ^{1}H NMR titration following the amide NH, fitting data to a 1:1 binding model using WINEQNMR[153].

Anion	**234**	**E (%)**	**235**	**E (%)**
$CH_3CO_2^-$	46	2	38	12
$H_2PO_4^-$	260	2	176	2
F^-	83	9	<10	-
$C_6H_5CO_2^-$	25	4	18	8
Cl^-	<10	-	<10	-

Table 5.2.2.2 Anion binding constants (M^{-1}) and percentage error for receptors **236** and **237**, measured in DMSO-d_6/0.5% H_2O at 298 K. Anionic guests were added as the TBA salt of the anion. Binding constants determined by ^1H NMR titration following the amide NH, fitting data to a 1:1 and, in the case of dihydrogen phosphate, a 2:1 anion:receptor binding model using WINEQNMR[153].

Anion	**236**	**E (%)**	**237**	**E (%)**
$CH_3CO_2^-$	149	5	97	8
$H_2PO_4^-$	99	7	K_1 = 108	20
			K_2 = 216	>50
F^-	a	-	a	-
$C_6H_5CO_2^-$	24	3	11	28
Cl^-	<10	-	<10	-

a – No binding constant could be calculated due to the peak broadening of the receptor/anion complex.

In most examples, the addition of an electron withdrawing group to a receptor template often increases the affinity of an anion for the receptor because the acidic nature of the hydrogen bond donor groups is increased. This is not the case with receptors **236** and **237** as the binding constants observed are slightly higher with the pentyl analogue of the receptor **236** for similar reasons of molecule flexibility as previously mentioned. Overall, there is a decrease in affinity of the various anions for receptors **236** and **237** when compared to receptors **234** and **235** except with acetate, which experiences enhanced binding affinity. This could be attributed to steric hindrance effects; as the receptors wrap around the anion, the interaction between the two nitro groups may cause the destabilisation of the anion:receptor complex, resulting in lower binding constants. The results of the anion binding studies performed with receptors **236** and **237** are shown in Table 5.2.2.2. In a DMSO-d_6/0.5% H_2O solution, both receptors were shown to form 1:1 complexes with the various anions through Job plot analysis. The exception is the receptor **237**/dihydrogen phosphate combination, which now shows 2:1 anion:receptor binding stoichiometry, with binding constants of 108 M^{-1} and 216 M^{-1} calculated for K_1 and K_2 respectively. Dihydrogen phosphate has been shown to oligomerise on many occasions. If the 1:1 complex is disfavoured because there are steric interactions between the two nitro

groups when wrapped around a single anion, the formation of the 2:1 anion:receptor complex would be more favourable. This theory is supported by K_2 being larger than K_1, indicating that the formation of the 2:1 anion:receptor complex is promoted.

Receptor **238** has two additional nitro and two additional chloro electron withdrawing groups when compared to receptors **234** and **235**. It also contains an extra NH bond donor group from the carbazole scaffold. This receptor should show an increased affinity for the various anions because of three main factors;

1. The use of the carbazole scaffold increases the rigidity of the receptor, pre-organising receptor **238** for optimal anion binding.
2. The presence of the nitro and chloro electron withdrawing groups causes the NH bond donor groups to increase in acidity, increasing the favourability of hydrogen bond formation.
3. The extra NH bond donor group in the carbazole functionality increases the overall number of hydrogen bonds, therefore increasing the anion affinity for the receptor.

The results of the anion binding studies performed with receptor **238** are shown in Table 5.2.2.3. In a DMSO-d_6/0.5% H_2O solution, binding constants were calculated for both the amide and carbazole NH because more complex binding events were suspected. As expected, the binding constants calculated for chloride and dihydrogen phosphate are far larger than those calculated for receptors **234-237**.

Table 5.2.2.3 Anion binding constants (M^{-1}) and percentage error for receptor **238**, measured in DMSO-d_6/0.5% H_2O at 298 K. Anionic guests were added as the TBA salt of the anion. Binding constants determined by ^1H NMR titration following the amide and carbazole NH, fitting data to a 1:1 binding model using WINEQNMR[153].

Anion	Carbazole NH	E (%)	Amide NH	E (%)
$CH_3CO_2^-$	a	-	a	-
$H_2PO_4^-$	$>10^4$	-	599	7
F^-	a	-	a	-
$C_6H_5CO_2^-$	b	-	b	-
Cl^-	3250	11	2940	7

a – No binding constant could be calculated due to the peak broadening of the receptor/anion complex. b – Peak splitting the NH group prevented a binding constant from being calculated.

Binding constants could not be calculated for acetate or fluoride because of peak broadening events during the titration but Job plot analysis was able to indicate a 1:1 binding mode for both anions. Chloride was also shown to adopt this mode of anion binding, with binding constants calculated as 3250 M^{-1} and 2940 M^{-1} for the carbazole and amide NHs respectively. The ^1H NMR titration results were not so clear with benzoate and dihydrogen phosphate. Peak splitting was observed with benzoate through the carbazole and amide NH signals. This could be attributed to a more complex binding event or conformational change but there is not enough evidence to allow a full explanation. Although no peak splitting was observed with dihydrogen phosphate, substantially different binding constants were calculated for the carbazole ($>10^4$ M^{-1}) and amide (599 M^{-1}) NH groups. This again points to more complex binding events. Job plot analysis appears to indicate a 1:1 binding but, because of the shape of the curve, there is the possibility that 2:1 anion:receptor complex may also be suspected although this is unclear. Graphs 5.2.2.1 and 5.2.2.2 compare the change in chemical shift of the amide and carbazole NH groups with the addition of chloride and dihydrogen phosphate. With chloride, the shape of curves for the different NH groups is similar, resulting in similar binding constants. It is clear that this is not the case with dihydrogen phosphate. The curve of the carbazole NH is much steeper than that of the amide NH.

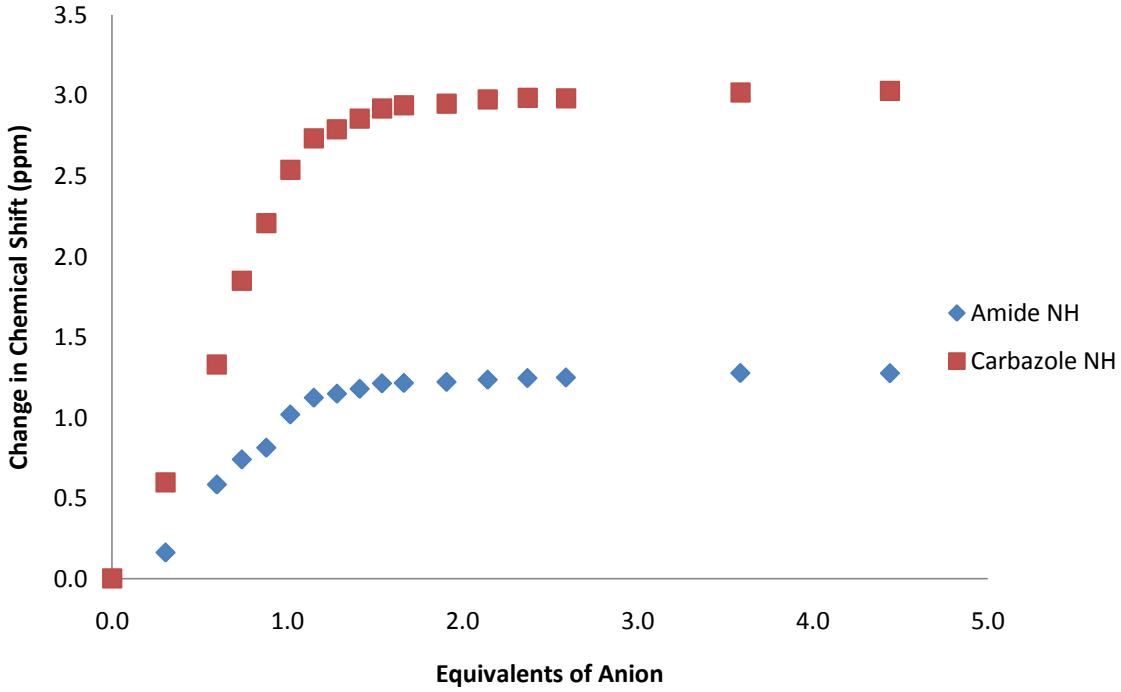

Graph 5.2.2.1 Change in chemical shift of receptor **234** with TBA chloride, illustrating the interaction of the carbazole NH and amide NH and functionalities with the anion in a DMSO-d_6/0.5% H_2O solution.

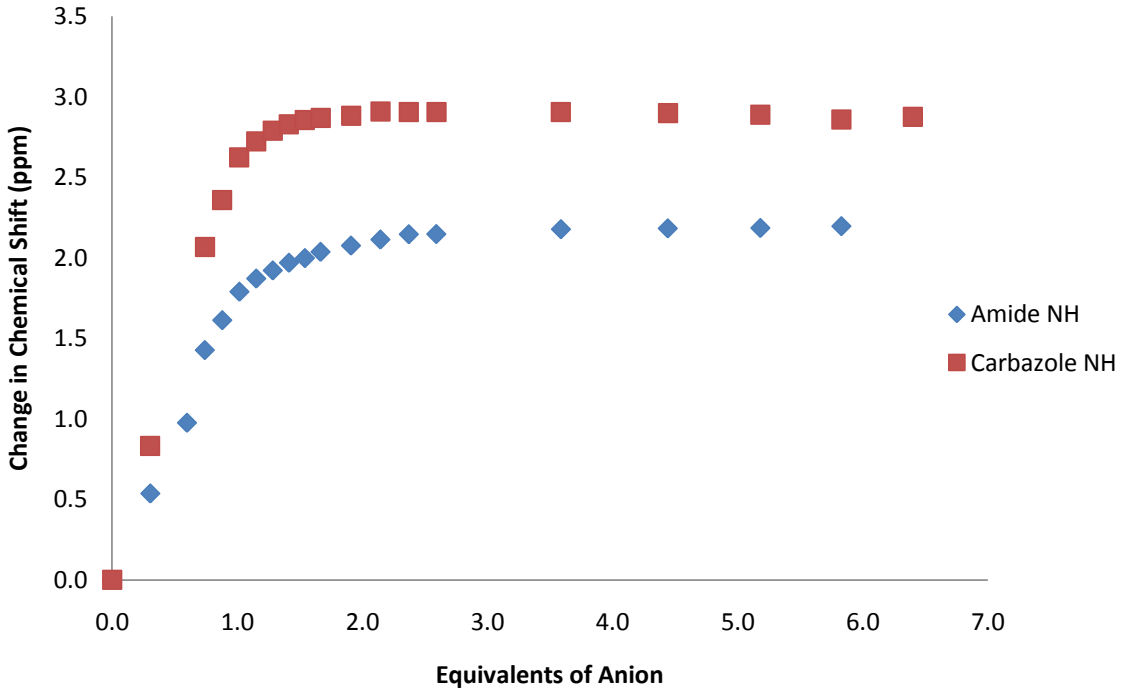

Graph 5.2.2.2 Change in chemical shift of receptor **234** with TBA dihydrogen phosphate, illustrating the interaction of the carbazole NH and amide NH and functionalities with the anion in a DMSO-d_6/0.5% H_2O solution.

5.2.3 Solid phase analysis

X-ray quality crystals of receptor **234** and TBA dihydrogen phosphate were obtained by Claudia Caltagirone by slow evaporation of excess TBA dihydrogen phosphate and receptor from acetonitrile.

The crystal structure produced by single crystal X-ray diffraction is shown in Figure 5.2.3.1a. The crystal structure shows a 2:1 anion:receptor binding stoichiometry, which is unlike the 1:1 binding stoichiometry observed in the DMSO-d_6/0.5 % H_2O solution state. Each anion is coordinated to the receptor by two hydrogen bonds, one from the amide and one from the indole NH bond donor groups. N3 and N4 both form one hydrogen bond each to one oxygen atom of a dihydrogen phosphate anion. N1 and N2 both form a single hydrogen bond to two different oxygen atoms of the second dihydrogen phosphate anion. The two dihydrogen phosphate anions oligermerise through the formation of two hydrogen bonds between the two anions. The extended crystal structure, shown in Figure 5.2.3.1b, shows a chain of oligemerised dihydrogen phosphate anions, encased by the hydrogen-bound receptors. The hydrogen bonding interactions and hydrogen bond angles for the complex shown in Figures 5.2.3.1a and b are shown in Table 5.2.3.1. The hydrogen bonds from the nitrogen atoms of the receptor to the oxygen atoms of the anion range from N···O = 2.659(8)-2.948(8) Å and the bond angles range from N–H···O = 154.4°-179.1°.

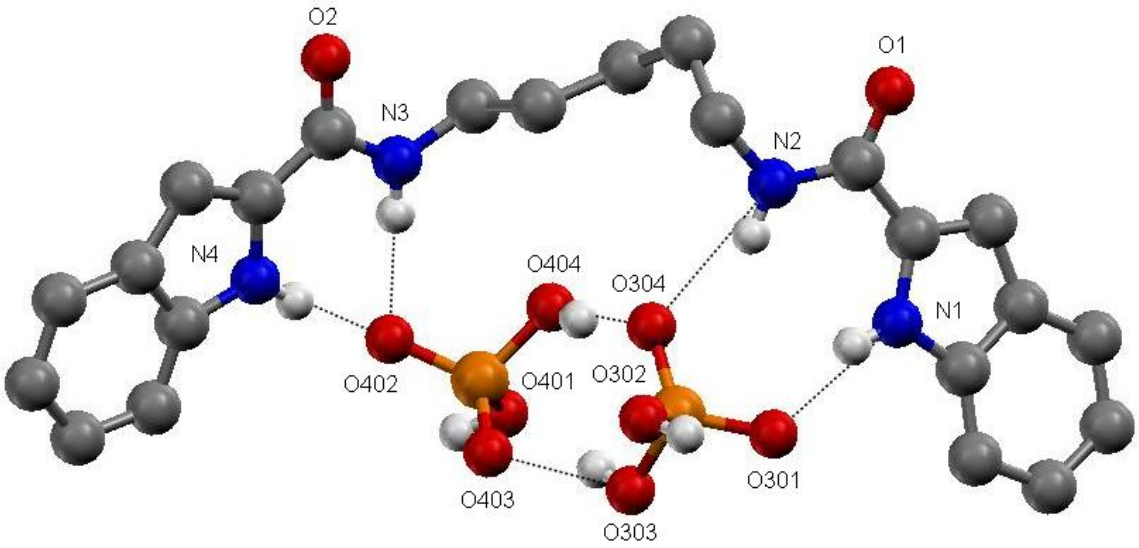

Figure 5.2.3.1a The dihydrogen phosphate complex of receptor **234**. Single X-ray crystal structure with TBA dihydrogen phosphate. The CH hydrogen atoms, some solvent molecules and the TBA counter ions have been omitted for clarity.

Table 5.2.3.1 Hydrogen bonding table for crystal structure of receptor **234** and TBA dihydrogen phosphate for the complexes shown in Figures 5.2.3.1a and b, obtained by single crystal X-ray diffraction at 120K. *D* – hydrogen bond donor atom. *A* – hydrogen bond acceptor atom. *d* – distance in Å. ∠ - bond angle in °. H – hydrogen atom. Symmetry transformations used to generate equivalent atoms: (i) –x+1,–y+1,–z (ii) –x+1,–y+1,–z+1

D–H···*A*	*d*(*D*–H) (Å)	*d*(H···*A*) (Å)	*d*(*D*···*A*) (Å)	∠(*DHA*) (°)
N1–H1···O301^{i}	0.88	1.84	2.659(8)	154.4
N2–H2···O304^{i}	0.88	2.08	2.901(8)	154.7
N3–H3···O402^{i}	0.88	2.07	2.948(8)	179.1
N4–H4···O402^{i}	0.88	1.85	2.719(8)	171.0
O302–H302···O301^{i}	0.84	1.85	2.596(7)	147.2
O303–H303···O403	0.84	1.75	2.510(8)	148.9
O401–H401···O402^{ii}	0.84	1.81	2.641(7)	171.4
O404–H404···O304	0.84	1.75	2.578(7)	168.3

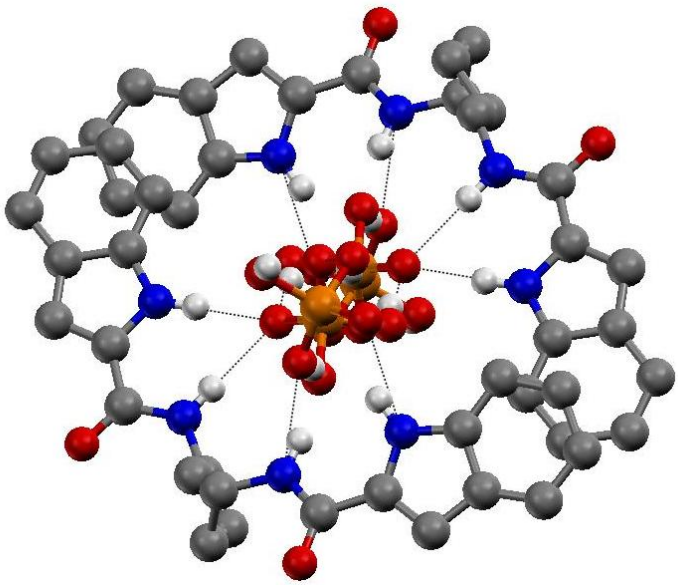

Figure 5.2.3.1b The extended dihydrogen phosphate complex of receptor **234**. Single X-ray crystal structure with TBA dihydrogen phosphate. The CH hydrogen atoms, some solvent molecules and the TBA counter ions have been omitted for clarity.

X-ray quality crystals of receptor **236** and TBA fluoride were obtained by Claudia Caltagirone by slow evaporation of an excess of the TBA salt and receptor from acetonitrile, producing an oil that was then recrystallised from DCM.
The crystal structure produced by single crystal X-ray diffraction is shown in Figure 5.2.3.2. The crystal structure shows a 2:1 anion:receptor binding stoichiometry that was not observed in DMSO-d_6/0.5 % H_2O, with each anion coordinated to the receptor by two hydrogen bonds, one from the amide and one from the indole NH bond donor groups. Each fluoride anion is also coordinated by water molecules. The water molecules interacting with F801 and F901 have been omitted for clarity. The hydrogen bonding interactions and hydrogen bond angles for the complex shown in Figure 5.2.3.2 are shown in Table 5.2.3.2. The hydrogen bonds from the nitrogen atoms of the receptor to the fluoride anions range from N···F = 2.560(11)-2.650(13) Å and the bonds angles range from N–H···F = 153.4°-176.6°.

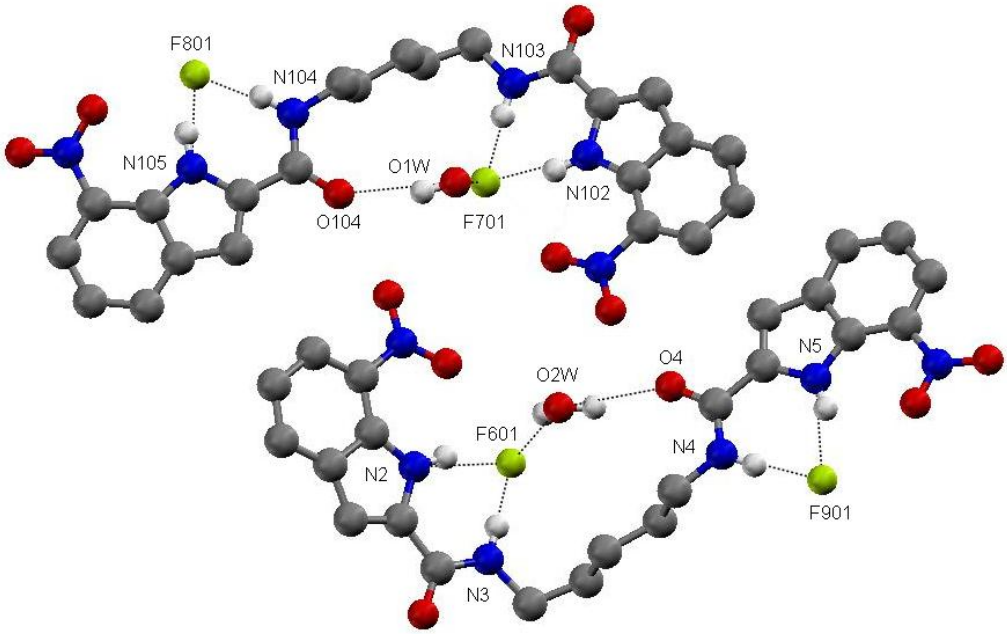

Figure 5.2.3.2 The fluoride complex of receptor **236**. Single X-ray crystal structure with TBA fluoride. The CH hydrogen atoms, some solvent molecules and the TBA counter ions have been omitted for clarity.

Table 5.2.3.2 Hydrogen bonding table for crystal structure of receptor **236** and TBA fluoride complex shown in Figure 5.2.3.2, obtained by single crystal X-ray diffraction at 120K. *D* – hydrogen bond donor atom. *A* – hydrogen bond acceptor atom. *d* – distance in Å. ∠ - bond angle in °. H – hydrogen atom.

D–H···*A*	*d*(*D*–H) (Å)	*d*(H···*A*) (Å)	*d*(*D*···*A*) (Å)	∠(*DHA*) (°)
N2–H2···F601	0.88	1.78	2.627(11)	159.7
N3–H3···F601	0.88	1.74	2.619(11)	174.8
N4–H4···F901	0.88	1.75	2.624(12)	173.5
N5–H5···F901	0.88	1.78	2.608(11)	155.3
N102–H102···F701	0.88	1.77	2.613(10)	160.8
N103–H103···F701	0.88	1.77	2.650(13)	176.6
N104–H104···F801	0.88	1.79	2.634(11)	158.9
N105–H105···F801	0.88	1.74	2.560(11)	153.4
O1W–H11W···F701	0.86(2)	1.85(3)	2.690(11)	164(11)
O2W–H22W···F601	0.85(2)	1.87(7)	2.642(10)	149(13)
O1W–H12W···O104	0.85(2)	2.07(4)	2.906(11)	166(13)
O2W–H21W···O4	0.85(2)	1.98(4)	2.776(12)	156(10)

.

X-ray quality crystals of receptor **238** and TBA fluoride were obtained by slow evaporation of excess TBA salt and receptor from DMSO.

The crystal structure produced by single crystal X-ray diffraction is shown in Figure 5.2.3.3a. The crystal structure shows a 2:1 anion:receptor binding stoichiometry that is unlike the 1:1 binding stoichiometry observed in the DMSO-d_6/0.5 % H_2O solution state. Although there has been previous examples of the two fluoride anions bound as HF_2^- in the solid state there is no evidence for the presence of the HF_2^- ion in this structure. Each anion is coordinated to the receptor by three hydrogen bonds, one from the amide, one from the carbazole and one from the indole NH bond donor group. N4 of the carbazole group forms two hydrogen bonds, one to each of the anions. The receptor is slightly twisted, allowing space for both anions. This twisted conformation and the close proximity of the two

fluoride anions is shown in Figure 5.2.3.3b. There is a distance of only 2.726 Å between the centre of each fluoride anion. The space-filling view of these anions shows the extreme close proximity the two anions. The hydrogen bonding interactions and hydrogen bond angles for the complex shown in Figures 5.2.3.3a and b are shown in Table 5.2.3.3. The hydrogen bonds from the nitrogen atoms of the receptor to the fluoride anions range from N···F = 2.625(7)-3.159(8) Å and the bond angles range from N–H···F = 120.6°-159.7°.

Table 5.2.3.3 Hydrogen bonding table for crystal structure of receptor **238** and TBA fluoride complex shown in Figures 5.2.3.3a and b, obtained by single crystal X-ray diffraction at 120K. *D* – hydrogen bond donor atom. *A* – hydrogen bond acceptor atom. *d* – distance in Å. ∠ - bond angle in °. H – hydrogen atom.

D–H···*A*	*d*(*D*–H) (Å)	*d*(H···*A*) (Å)	*d*(*D*···*A*) (Å)	∠(*DHA*) (°)
N2–H902···F1	0.88	1.96	2.800(8)	159.7
N3–H903···F1	0.88	1.99	2.812(8)	155.4
N4–H904···F2	0.88	1.79	2.625(7)	157.8
N4–H904···F1	0.88	2.62	3.159(7)	120.6
N5–H905···F2	0.88	1.77	2.644(8)	169.4
N6–H906···F2	0.88	1.88	2.708(7)	156.9

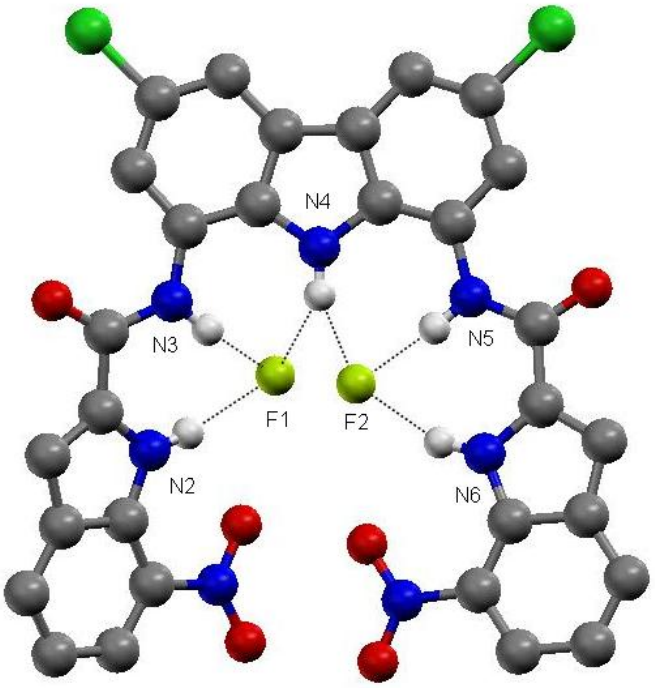

Figure 5.2.3.3a The fluoride complex of receptor **238**. Single X-ray crystal structure with TBA fluoride. The CH hydrogen atoms and the TBA counter ions have been omitted for clarity.

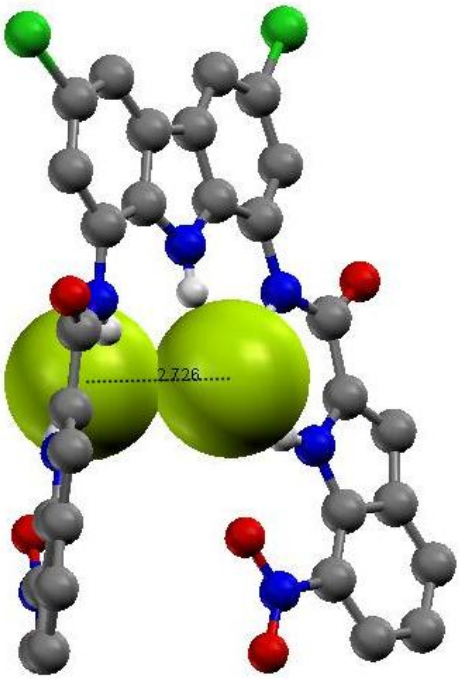

Figure 5.2.3.3b The space-filling fluoride complex of receptor **238**. Single X-ray crystal structure with TBA fluoride. The CH hydrogen atoms and the TBA counter ions have been omitted for clarity.

5.3 Symmetrical carbazolylamide hydrogen bond donating clefts containing four hydrogen bond donating groups

This group of receptors is specifically based on the isophthalamide- and the 2.6-dicarboxamidopyridine-based receptors synthesised by Gale and co-workers [1] and similar receptors synthesised by Jurczak and co-workers [3]. This work was originally inspired by Crabtree[16], Smith[23] and Gale and co-workers [18,22,199]. Gale and co-workers also synthesised a group of receptors that included receptor **239** and was published in 2003. This receptor was shown to form a 2:2 anion:receptor complex with TBA fluoride in the solid state. The receptor was found to organise into a double helix around the fluoride anions. This was the first reported example of a neutral receptor forming double helices. The crystal structures obtained of receptor **239** and fluoride are shown in Figures 5.3.1a and b.[200]

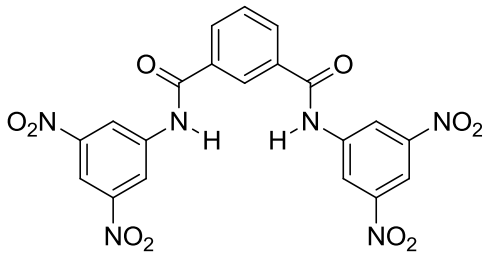

239

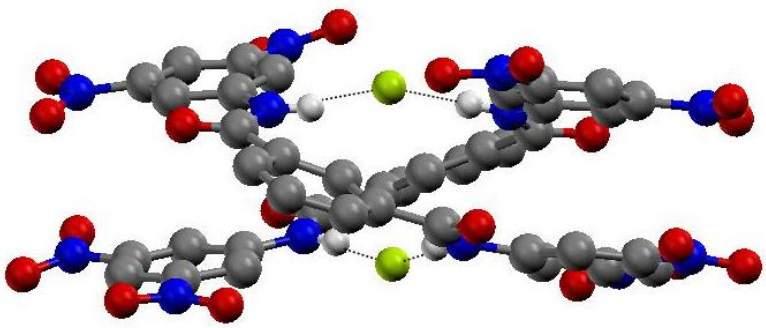

Figure 5.3.1a Side view of the 1:1 complex of receptor **239**, forming a double helix around the fluoride anions. The crystal structure was obtained by Gale and co-workers.

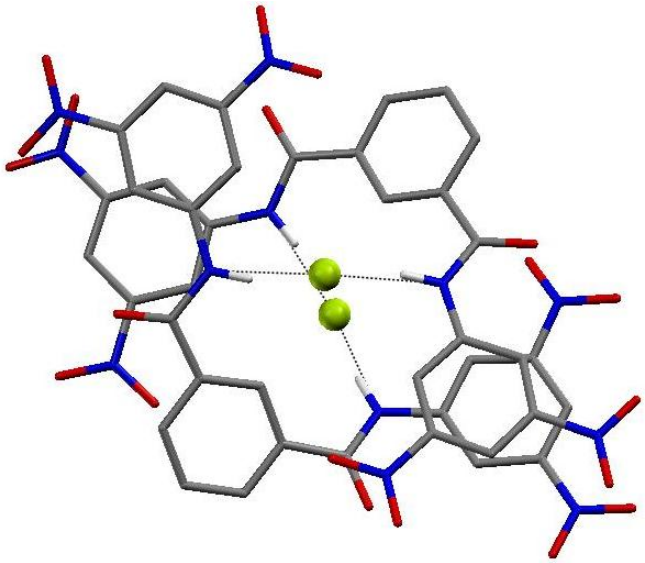

Figure 5.3.1b Top view of the 1:1 complex of receptor **239**, forming a double helix around the fluoride anions. The crystal structure was obtained by Gale and co-workers.

Other helical structures have also been observed in solid and solutions states with neutral molecules. Jeong and co-workers have observed this phenomenon many times with their foldmer receptors.[116,138,139,141-143] Sessler and co-workers[201] also observed helix formation with neutral receptors in the solid state, using longer, more complex receptors (**240**). The helical crystal structure is shown in Figure 5.3.2.[201]

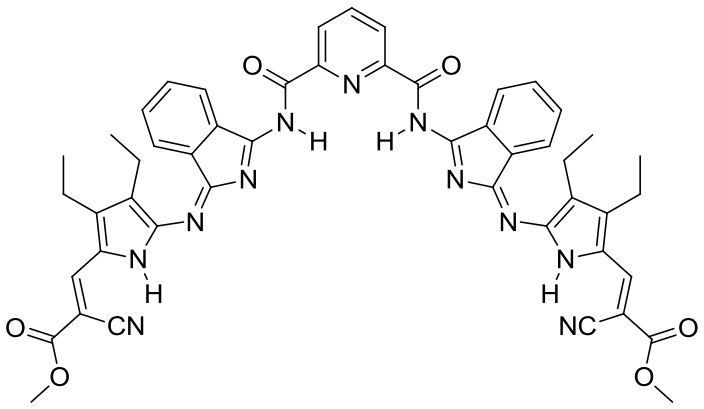

240

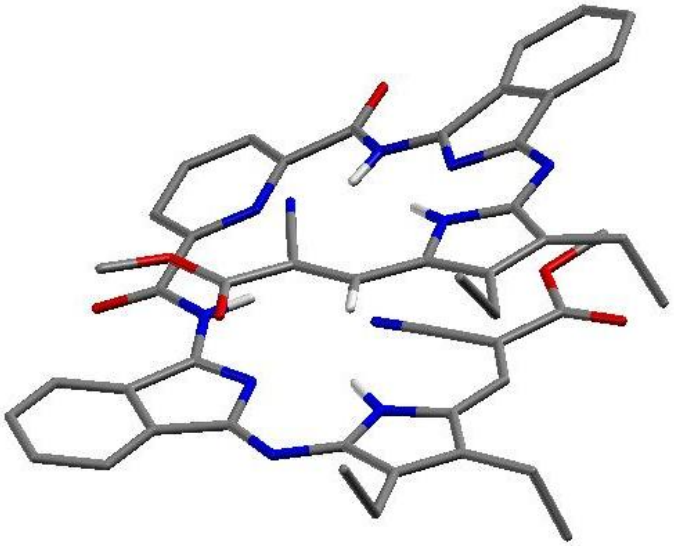

Figure 5.3.2 Receptor **240**, forming a helix without the presence of any anion template. The crystal structure was obtained by Jeong and co-workers.

With the more recent indole based receptors **182** and **183,** a selectivity of fluoride is shown over other anion guests, with the isophthalamide based receptor twisting and almost forming a helix around the fluoride anion, while the chloride anion is seen to balance on top, as shown in Figures 1.3.4.2.3a and b.[1] Receptors **241** and **242** look at the effect of the incorporating the bulky (but also more acidic) hydrogen bond-donating carbazole group onto the isophthalamide or 2,6-dicarboxamidopyridine scaffolds. The binding constants obtained for the indole based receptors **182** and **183** by Gale and co-workers[1] in a DMSO-d_6/0.5% and 5% H_2O solution are shown in Table 5.2.1.

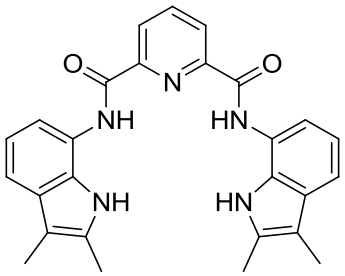

183

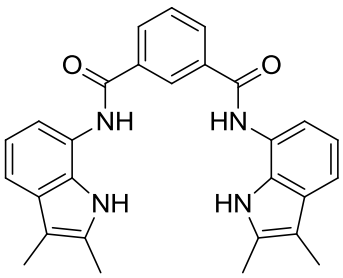

182

Table 5.2.1[1] Anion binding constants (M^{-1}) and percentage error for receptor **183** and **182**, measured in DMSO-d_6 and varying concentrations of water at 298 K. Anionic guests were added as the TBA salt of the anion. Binding constants determined by ^{1}H NMR titration following the urea NH, fitting data to a 1:1 or 2:1 binding model using WINEQNMR[153].

Anion	DMSO-d_6 0.5% H_2O		DMSO-d_6 5% H_2O	
	183	**182**	**183**	**182**
$CH_3CO_2^-$	250	880	14	110
$H_2PO_4^-$	70	1140	26	260
$C_6H_5CO_2^-$	17	120	<10	35
Cl^-	<10	17	<10	15
F^-	>10^4	a	1360	K1 = 940 K2 = 21
Br^-	b	b		

a – Binding constants could not be calculated as data could not be fitted to a 1:1 or 2:1 binding model. b – No interaction between anion and receptor.

5.3.1 Synthesis

The two receptors were synthesised by a four step synthesis, summarised in Scheme 5.3.1.1. The synthesis of 1-nirocarbazole was achieved by a slight alteration to a literature procedure, using nitric and acetic acid to convert carbazole to 1-nitrocarbazole. The crude product, obtained after precipitation with water, was purified by flash chromatography in chloroform.[158] 1-nitrocabazole was then reduced to 1-aminocarbazole in ethanol, with a Pd/C 10% catalyst under a hydrogen atmosphere. Characterisation data agreed with previously published data.[159]

Receptors **241** and **242** were produced *via* two different amide coupling reactions with 1-aminocarbazole and the appropriate dicarboxylic acid. Receptor **241** was synthesised by the activation of 2,6-pyridinedicarboxylic acid with CDI in a chloroform/DMF solution. The solution was then heated to reflux and, after washing the organic phase with water, the solid that precipitated was isolated and washed with ether, giving a yield of 43%. Receptor **242** was synthesised from 1-aminocarbazole and isophthalic acid, with the slightly more complex amide coupling reaction using PyBOP, HOBt and NEt_3 in DMF/DCM. After

washing the organic phase with water, the precipitate formed was isolated and washed with further aliquots of DCM giving a yield of 50 %.

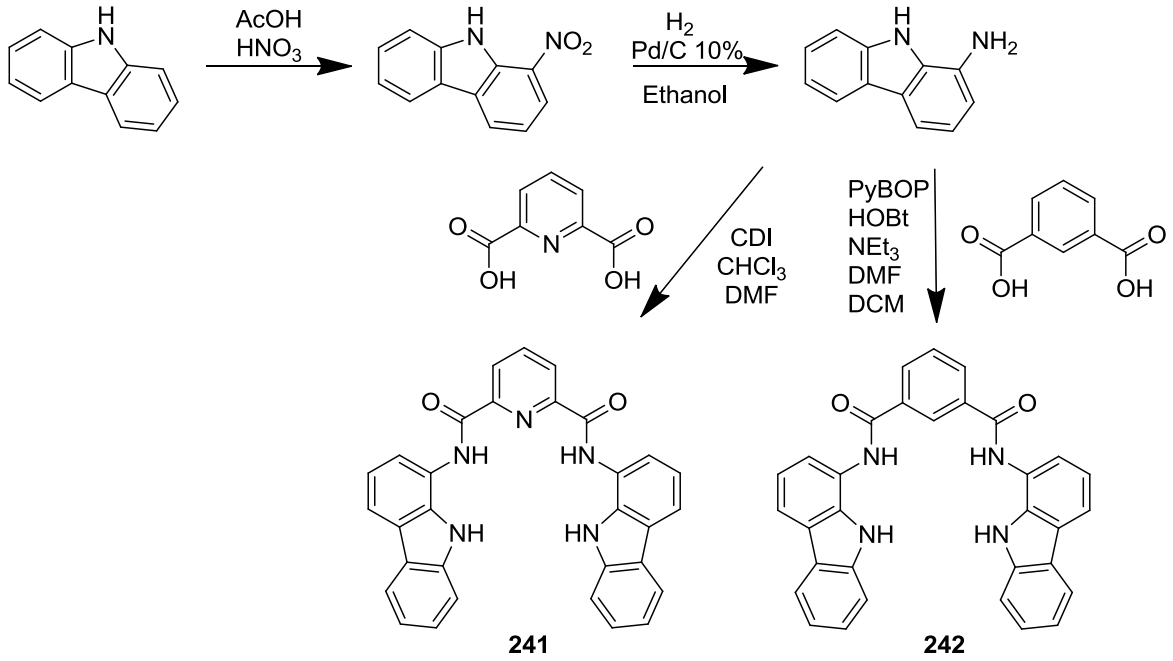

Scheme 5.3.1.1

5.3.2 Solution phase analysis

5.3.2.1 Proton NMR titration data

Anion binding constants were determined for receptors **241** and **242** with wide range anions. The binding constants were determined by ^{1}H NMR titration and calculated by the computer program WINEQNMR[153] with the TBA salt of the anion in DMSO-d_6/0.5% H_2O solutions. The data was fitted to a 1:1 or 2:1 anion:receptor binding model on the strength of titration evidence and past titration evidence with analogous compounds **182** and **183**. All four hydrogen bond donor groups are involved in binding a single anion. This can be seen by the downfield shifts of all NH bond donor signals upon the addition of the anion. The binding constants calculated for these two receptors are shown in Table 5.3.2.1.

Table 5.3.2.1 Anion binding constants (M^{-1}) and percentage error for receptors **241** and **242**, measured in DMSO-d_6/0.5% H_2O at 298 K. Anionic guests were added as the TBA salt of the anion. Binding constants determined by ^1H NMR titration following the carbazole NH, fitting data to a 1:1 binding model using WINEQNMR[153].

Anion	241	E (%)	242	E (%)
$CH_3CO_2^-$	210	1	682	9
$H_2PO_4^-$	63	8	803	9
F^-	8510	8	a	-
$C_6H_5CO_2^-$	32	7	191	8
Cl^-	<10	-	28	9

a – No full binding constant could be calculated, 2:1 anion:receptor binding with $K_1 > 10^4$.

As seen with the analogous receptors **182** and **183**, synthesised by Gale and co-workers[1], receptor **241** shows selectivity for fluoride (8510 M^{-1}) over all the other oxo- and halide anions tested. Chloride (<10 M^{-1}), benzoate (32 M^{-1}), dihydrogen phosphate (63 M^{-1}) and acetate (210 M^{-1}) all exhibit similar binding constants to the analogous indole receptor. Although receptor **241** is selective for fluoride, the binding constant calculated is lower than that of the analogous indole receptor **183**. This is unexpected as the more acidic carbazole NH bond donor groups for receptor **241** were thought to bind the various anions with a higher affinity. The reason for this lowered affinity towards the fluoride anion could be due to the extra phenyl ring on the carbazole skeleton, which may cause steric hindrance when wrapping around the small spherical anion. This would lower the affinity of the receptor for the anion, making the anion binding process less favourable.

Unlike the analogous receptor **182**, synthesised by Gale and co-workers[1], receptor **242** binds fluoride to form a 2:1 anion:receptor complex with $K_1 > 10^4$ M^{-1}. This high K_1 value means that no K_2 value could be calculated due to experimental limitations. Similar binding constants, binding trends and conformations were found for chloride, acetate, benzoate and dihydrogen phosphate and were ascertained for both the carbazole- (**242**) and indole- (**182**) based analogues. As expected, the binding constants for chloride and benzoate are slightly higher for the carbazole-based receptor **242** than receptor **182**, whereas the calculated binding constants for dihydrogen phosphate and acetate are slightly

lower, probably due to steric hindrance as previously explained in the case of the receptor **241**/fluoride complex. The binding constants calculated for receptor **242** with chloride (28 M^{-1}), benzoate (191 M^{-1}), acetate (682 M^{-1}) and dihydrogen phosphate (803 M^{-1}) are slightly higher across the board than those of receptor **241**. This may be due to the lack of intramolecular hydrogen bond formation, although the receptor is less pre-organised and the NH bond donor groups are free to interact with the anion. This trend was also noted with the indole analogues, **182** and **183**.

As with the indole based receptors **182** and **183**, receptor **241** exhibits a higher binding constant for fluoride over chloride for similar reasons; all three receptors adopt a twisted conformation in the DMSO-d_6/0.5% H_2O solution, effectively encapsulating the small spherical fluoride anion. The larger anions cannot be so effectively encapsulated and the affinity of the anion to the receptor is lowered.

5.3.3 Solid phase analysis

X-ray quality crystals of receptor **242** and TBA acetate were obtained by slow evaporation of excess TBA salt and receptor from DMSO.

The crystal structure was produced by single crystal X-ray diffraction and is shown in Figure 5.3.3.1. It shows a 2:1 anion:receptor binding stoichiometry, which is unlike the 1:1 binding stoichiometry observed in the DMSO-d_6/0.5 % H_2O solution state. Each anion is co-ordinated to the receptor by two hydrogen bonds, one from the amide and one from the carbazole NH bond donor groups. Each NH bond donor group forms a single hydrogen bond to a different oxygen of the acetate anions, giving a structure which contains four hydrogen bonds in total. The hydrogen bonding interactions and hydrogen bond angles for the complex shown in Figure 5.3.3.1 are shown in Table 5.3.3.1. The hydrogen bonds from the nitrogen atoms of the receptor to the oxygen atoms of the anion range from N···O = 2.707(5)-2.812(5) Å and the bond angles range from N–H···O = 153.8°-164.9°.

Table 5.3.3.1 Hydrogen bonding table for crystal structure of receptor **242** and TBA acetate, obtained by single crystal X-ray diffraction at 120K. *D* – hydrogen bond donor atom. *A* – hydrogen bond acceptor atom. *d* – distance in Å. ∠ - bond angle in °. H – hydrogen atom.

D–H···*A*	*d*(*D*–H) (Å)	*d*(H···*A*) (Å)	*d*(*D*···*A*) (Å)	∠(*DHA*) (°)
N5–H5···O7	0.86	1.87	2.707(5)	164.9
N3–H3···O6	0.86	2.00	2.812(5)	157.1
N6–H6···O4	0.86	1.89	2.725(5)	164.0
N4–H4···O3	0.86	2.00	2.797(5)	153.8

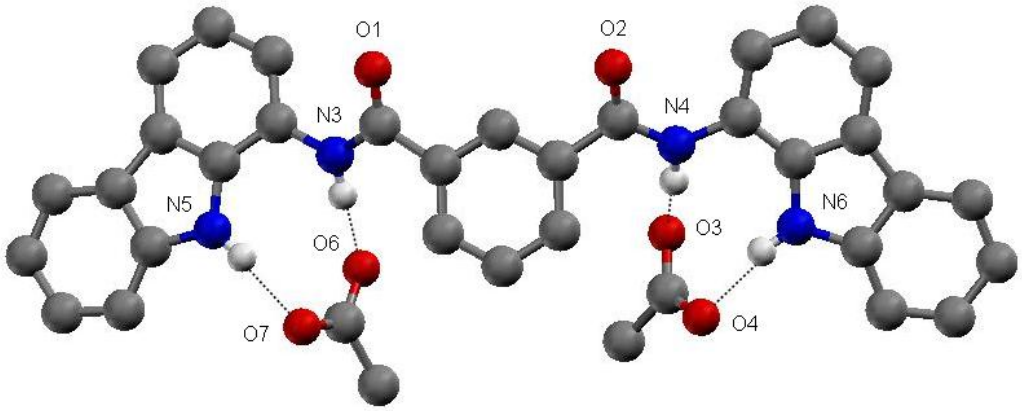

Figure 5.3.3.1 The acetate complex of receptor **242**. Single X-ray crystal structure with TBA acetate. The CH hydrogen atoms and the TBA counter ions have been omitted for clarity.

5.4 Conclusion

A set of seven new receptors have been synthesised and the majority of anion:receptor complexes showed 1:1 binding modes in a DMSO-d_6/0.5 % H_2O solution . The first five of these receptors (**234-238**) continue the work started by Gale, Albrecht and co-workers[2]. The remaining two receptors, **241** and **242**, evolve from work originally started by Gale and co-workers[1] and Jurczak and co-workers[3].

Receptors **234** and **235** showed a lower affinity for the oxo-anions in a DMSO-d_6/0.5 % H_2O solution and a change in the trend in selectivity for the anions when

compared to the parent receptors **176-178**. The previous indole amide receptors showed selectivity for acetate over dihydrogen phosphate but this trend was reversed with receptors **234** and **235**. The slightly more flexible receptor **234** was shown to be more effective in binding anions due to its ability to wrap around the anion. Solid state experiments with single crystal X-ray diffraction showed receptor **234** adopting a 2:1 anion:receptor binding stoichiometry with dihydrogen phosphate, which differs from the 1:1 binding mode observed in the solution state.

Receptors **236** and **237** were synthesised with additional nitro electron withdrawing groups to increase the affinity of the anion for the receptor. This was not the case however, as binding constants were lowered with every anion apart from acetate in a DMSO-d_6/0.5 % H_2O solution. The binding mode for receptor **237** and dihydrogen phosphate was also altered from a 1:1 to a 2:1 anion:receptor complex. This was attributed to unforeseen steric hindrance between the nitro groups when wrapping around the anion. Solid state experiments with single crystal X-ray diffraction showed receptor **236** adopting a 2:1 anion:receptor binding stoichiometry with fluoride, different to that observed in the solution state.

The introduction of a fifth NH bond donor group and increased rigidity from the carbazole scaffold was also meant to increase the receptors affinity for various anions. Although this was achieved with chloride, complex binding events took place which could not be fully explained in a DMSO-d_6/0.5 % H_2O solution. Solid state analysis of receptor **238** with fluoride, using single crystal X-ray diffraction, showed a different 2:1 anion:receptor binding mode to that observed in the solution state, with the fluoride anions held in incredibly close proximity.

The last two receptors of the set of seven (**241** and **242**) see the extension of work started by Gale and co-workers[1] and Jurczak and co-workers[3]. The replacement of the indole group in these symmetrical cleft receptors with a carbazole group does not see an increase in affinity of the receptors for any particular anion. Similar trends were observed with these two receptors as with the indole analogues **182** and **183** synthesised by Gale and co-workers[1] . The decrease in anion affinity can be attributed to steric interaction of the carbazole groups as they wrap around the anion. Solid state experiments with receptor **241** and acetate by single crystal X-ray diffraction see a 2:1 anion:receptor binding mode, different to the 1:1 binding mode observed in the solution state.

Chapter 6 – Conclusions

During the course of these investigations into the synthesis, design and properties of simple neutral anion receptors, we have synthesised a range of twenty eight new anion receptors that bind the anions in both competitive solution states (DMSO and water mixtures) and in the solid state through hydrogen bond donating NH groups. We have seen the first examples of the deprotonation of bound anions (dihydrogen phosphate and bicarbonate) in the solid and solution state.

The first set of ten urea/thiourea linked indole/carbazole groups were found to have varying affinities for the oxo-anions. Receptors **209** and **210** have shown a high affinity and selectivity towards dihydrogen phosphate, while receptors **213-215** were shown to have a high affinity and selectivity towards acetate and bicarbonate anions. These receptors also show selective quenching effects upon the addition of benzoate. X-ray analysis showed unusual 1:2 and 1:3 anion:receptor complexes with carbonate and phosphate, illustrating the first solid state examples of bound anion deprotonation due to the contribution of many acidic hydrogen bonds in the case of receptors **209** and **210** respectivly.

This receptor design was then modified by the introduction of amide fictionalisation to the diindolylurea skeleton (**219-222**). These receptors showed high affinities for the oxo-anions and molecules **219**, **221** and **222** were the first receptors to enable deprotonation of bound dihydrogen phosphate and bicarbonate in solution. Different binding modes were observed that depended on the geometry of the bound anion. Deprotonation of the dihydrogen phosphate anion was also observed in the solid state with receptors **220-222**. These compounds also showed rapid, spontaneous crystallisation with sulfate in as little as 20 minutes under DMSO-d_6/10% H_2O solution conditions.

The two dimensional planar receptor design was then further modified to produce a set of six tripodal receptors, based on the TREN and pin-wheel scaffolds to attempt to bind the anion through three dimensions. An example of the deprotonation of bound bicarbonate was observed in the solution state with receptor **226**. A variety of binding modes observed with in this set of receptors from 1:1 to 3:1 anion:receptor complexes. The complex

binding motif made it difficult to ascertain the binding constants for many of the anion/receptor complexes. The introduction of electron withdrawing groups to the structure of receptor **224**, which gave rise to receptor **225**, did increase binding affinity for the oxo-anions but the exchange of the smaller, more flexible TREN scaffold for the larger, rigid pin-wheel scaffold (**231**) had mixed results. Low binding constants are observed for this set of three dimensional receptors compared to simpler urea/thiourea sets of cleft receptor. The main reasons for this behaviour are the increased flexibility of the receptor, causing the loss in pre-organisation, and the increased degree of intramolecular hydrogen bonding, which makes anion binding less favourable.

Original work published by Gale and co-workers[1,2] and Jurczak and co-workers[3] was extended in Chapter five by the synthesis and the investigation of seven new anion receptors (**234-238**). Receptors **234-237** showed a decreased affinity for the oxo-anions when compared to the receptors synthesised by Gale, Albrecht and co-workers. This was due to steric hindrance, following the addition of electron withdrawing nitro groups. They also showed a change in anion binding trend.

The introduction of the carbazole scaffold in receptor **238** was also meant to increase the receptor's affinity for various anions; although this was achieved with chloride complex binding events took place in the solution state that could not be fully explained. Continuing the work of Gale, Jurczak and co-workers, the indole moieties were replaced with the more acidic carbazole groups in receptors **241** and **242** . The expected increase in anion affinity was not observed and this was attributed to steric interaction of the carbazole groups as they wrap around the bound anion.

Chapter 7 – Experimental Methods

7.1 General information

Where necessary, solvents were purified prior to use. Anhydrous DMF puriss, over molecular sieves, was purchased from Fluka. Anhydrous DCM was distilled over calcium hydride. NEt_3 and analine was distilled over KOH. NEt_3 was stored over KOH pellets under an argon or nitrogen atmosphere, while analine was used directly after distillation. Thionyl chloride was distilled from 10% (w/w) triphenyl phosphate and stored under argon or nitrogen or used directly after distillation. All solvents and starting materials are commercial grade and used as purchased from chemical sources when available. Reagents obtained *via* literature procedures have been referenced accordingly. All reactions were performed using oven-dried glassware under a slight positive pressure of nitrogen or argon unless otherwise specified. TBA and TEA salts of the anions used for ^{1}H NMR, fluorescence and UV-Vis titration studies were dried thoroughly overnight on a high vacuum line. Dry TBA sulfate was obtained from a 50% (w/w) water solution. The water was removed by distillation; the TBA sulfate crystals were then stored on a high vacuum line.

Claudia Caltagirone was responsible for the majority of the synthesis and characterisation of receptors **209**, **210**, **234** and **236**. Claudia was also responsible for conducting the fluorescence titrations.

7.2 Instrumental methods

The ^{1}H NMR (300 MHz) and ^{13}C{^{1}H} NMR (75 MHz) spectra were determined on Bruker AV300 and AC300 spectrometers. ^{1}H NMR (400 MHz) and ^{13}C NMR (100 MHz) spectra were determined on a Bruker AV400 spectrometer. Chemical shifts for ^{1}H NMR are reported in parts per million (ppm), calibrated to the solvent peak set. The following abbreviations are used for spin multiplicity: s = singlet, d = doublet, t = triplet, m = multiplet, q = quartet. Chemical shifts for ^{13}C{^{1}H} NMR are reported in ppm, calibrated to the solvent peak set. Infra-red (IR) spectra were recorded on a Matterson Satellite (ATR).

FTIR are reported in wavenumbers (cm^{-1}). Low resolution mass spectra were recorded on a Micromass Platform II Single Quadrupole mass spectrometer. High resolution mass spectra were recorded on a VG 70-250-SE normal geometry double focusing mass spectrometer by the Mass Spectrometry Service at the University of Southampton. Melting points were recorded in open capillaries on a Gellenkamp melting point apparatus and are uncorrected. UV-Vis and fluorescence spectra were recorded on a Thermo Nicolet Evolution 300 spectrophotometer and a Varian Cary Eclipse fluorescence spectrophotometer respectively. Elemental analyses were performed by Medac Ltd.

7.3 Titration and Job plot methods

7.3.1 ^{1}H NMR titrations

1.5 mL of a 0.01 M solution of receptor was prepared. Of this solution, 0.5 mL was added to an NMR tube, which was then sealed with an air tight suber seal. The remaining 1 mL of the receptor solution was used to make a 0.15 M solution of the TBA/TEA salt of the anion. The anion/receptor solution was titrated into the NMR tube in small aliquots and a ^{1}H NMR taken after each addition. This allows the concentration of the anion in the NMR tube to increase whilst the concentration of receptor to remain constant. Chemical shifts for each ^{1}H NMR spectra were recorded in ppm and calibrated to the solvent peak set. The computer program WINEQNMR[153] is then used to interpret the data to solve the binding constant(s).

7.3.2 ^{1}H NMR Job plots

Two solutions were prepared; the first was a 3 mL, 0.01M solution of receptor and the second was a 3 mL, 0.01M solution of TBA/TEA salt of the anion. Of the receptor solution, 0.5 mL was added to an NMR tube. The amount of the receptor solution was then decreased by 0.05 mL and the amount of anion solution increased by 0.05 mL for each successive NMR tube until a 9:1 anion:receptor ratio was reached. A ^{1}H NMR spectra was then taken in ppm for each of the ten NMR tubes and calibrated to the solvent peak set.

This data was then used to produce a Job plot in accordance with the methods described by Job[154]. Plotting the molar fraction of the receptor against the values given by the formula; $\frac{\delta_{obs}-\delta_{int}}{\delta_{fin}-\delta_{int}} \times x_r$ where δ_{obs} is the observed chemical shift, $\delta_{int}$is the initial chemical shift, $\delta_{fin}$is the final chemical shift and x_r is the molar fraction of the receptor.

7.3.3 Fluorescence and UV-Vis titrations

Fluorescence and UV-Vis titrations were both conducted in the same manner. Two solutions are prepared; the first was a 1.0 x 10^{-5} M solution of receptor and the second was a 1.0 x 10^{-3} M solution of TBA/TEA salt of the anion. The anion solution was then titrated into the receptor solution in suitable aliquots and a reading taken and recorded after each addition of anion. Luminescence quantum yields were determined using quinine sulfate in a 1 M H_2SO_4 aqueous solution (Φ = 0.546) as a reference.

7.4 Synthetic procedures

7.4.1 General synthetic procedures

7-Aminoindole: The reduction of 7-nitroindole with Pd/C 10% catalyst and hydrazine hydrate was based on the literature procedure by Gale and co-workers, replacing 2, 3-dimethyl-7-nitroindole with 7-nitroindole. A 100 % yield was assumed. This reagent was used immediately without purification in the next step of the reaction.[1]

7-Aminoindole: 7-Nitroindole (0.26 g, 1.58 mM) and a Pd/C 10% catalyst (0.03 g) were suspended in EtOH (40 mL). The flask was then evacuated and the mixture placed under a hydrogen atmosphere and stirred vigorously for 2 hrs. After this time, the palladium catalyst was removed by filtration through cellite and the filtrate taken to dryness and placed under reduced pressure. A 100 % yield was assumed. This reagent was used immediately, without purification, in the next step of the reaction.

1-Nitrocarbzole: This reagent was synthesised via an adapted literature procedure, alterating the separation of 1 and 3-nitrocarbazole by using $CHCl_3$ flash chromatography. ^{1}H NMR values agree with previously published data.[158]

1-Aminocarbazole: 1-Nitrocarbazole (0.27 g, 1.28 mM) and a Pd/C 10% catalyst (0.02 g) were suspended in EtOH (25 mL). The flask was evacuated and the mixture placed under a hydrogen atmosphere and stirred vigorously for 45 mins. After this time, the palladium catalyst was removed by filtration through cellite and the filtrate taken to dryness and placed under reduced pressure. This gave a white solid. ^{1}H NMR values agree with previously published data.[159]

7.4.2 Synthetic procedures for schemes in Chapter Two

2,3-Dimethyl-7-amino indole: The reduction of 2, 3-dimethyl-7-nitroindole with a Pd/C 10% catalyst and hydrazine hydrate is a literature procedure by Gale and co-workers. A 100% yield was assumed.[1] This reagent was used immediately, without purification, in the next step of the reaction.

2,3-Dimethyl-7-amino indole: 2, 3-Dimethyl-7-nitroindole (0.30 g, 1.58mM) and a Pd/C 10% catalyst (0.03 g) were suspended in EtOH (40mL). The flask was then evacuated and the mixture placed under a hydrogen atmosphere and stirred vigorously for 2 hrs. After this time, the palladium catalyst was removed by filtration through cellite and the filtrate taken to dryness and placed under reduced pressure. A 100% yield was assumed. This reagent was used immediately, without purification, in the next step of the reaction.

1,3-Bis (2,3-dimethyl-1*H*-indol-7-yl)urea (209): 2,3-Dimethyl-7-aminoindole (0.25 g, 1.58 mmol) was dissolved in a two phase solution of DCM (30 mL) and sat. aqueous $NaHCO_3$ (30 mL). Triphosgene (0.47 g, 1.58 mmol) was added in two portions and the reaction mixture left to stir at room temperature overnight. The organic layer was washed with water (250 mL), dried over $MgSO_4$, filtered and concentrated in vacuo. The pure product was obtained by recrystallisation from the minimum amount of hot MeOH and isolated as a white solid. Yield 78 %, 0.21 g; m.p. 259 °C; ^{1}H NMR (300 MHz, DMSO-

d_6): δ: 2.15 (s, 6 H), 2.33 (s, 6 H), 6.88 (t, J = 7.53 Hz, 2 ArH), 7.03 (d, J = 7.53 Hz, 2 ArH), 7.12 (d, J = 7.53 Hz, 2 ArH), 8.44 (s, NH urea, 2 ArH), 10.31 (s, NH indole, 2 H); ^{13}C NMR (75 MHz, DMSO-*d_6*): δ: 8.5 (CH_3), 11.3 (CH_3), 105.6 (ArC), 113.1 (ArCH), 113.1 (ArCH), 118.2 (ArCH), 123.1 (ArC), 128.1 (ArC), 130.5 (ArC), 131.1 (ArC), 153.6 (CO); IR (film): ν = 3392 (indole NH stretching), 3247 (urea NH stetching), 1617 (urea CO stretching); LRMS (ES^-):m/z: 345 $[M-H]^-$; HRMS (ES^+): m/z: Act.: 347.1866 $[M+H]^+$ Calcd.: 347.1870 $[M+H]^+$

1,3-Di(1*H*-indol-7-yl)urea (210): 7-Aminoindole (0.21 g, 1.58 mmol) was dissolved in a mixture of DCM (20 mL) and a sat. aqueous solution of $NaHCO_3$ (20 mL). Triphosgene (0.47 g, 1.58 mmol) was added in portions and the reaction mixture was left stirring at room temperature overnight. The organic layer was washed with water, dried over $MgSO_4$, filtered and concentrated in vacuo. The pure product was obtained by recrystallisation from the minimum of hot MeOH and isolated as a pale grey solid. Yield 50 %, 0.15 g; m.p. 252 °C; ^{1}H NMR (300 MHz, DMSO-*d_6*): δ: 6.44 (t, J = 2.64 Hz, 2 ArH), 6.94 (t, J = 7.92, 2 ArH), 7.08 (d, J = 7.14 Hz, 2 ArH), 7.31 (d, J = 7.92, 2 ArH), 7.34 (t, J = 2.64 Hz, 2 ArH), 8.63 (s, NH urea, 2 H), 10.77 (s, NH indole, 2 H); ^{13}C NMR (75 MHz, DMSO-*d_6*): δ: 101.4 (ArCH), 113.7 (ArCH), 115.9 (ArCH), 119.0 (ArCH), 124.1 (ArC), 125.1 (ArCH), 129.0 (ArC), 129.4 (ArC), 153.6 (ArCO); IR (film): ν = 3383 (indole NH stretching), 3255 (urea NH stretching), 1620 (urea CO stretching); LRMS (ES^-):m/z: 289 $[M-H]^-$; HRMS (ES^+): m/z: Act.: 291.1240 $[M+H]^+$ Calcd.: 291.1236 $[M+H]^+$

7-Isothiocyanato-2,3-dimethyl-1H-indole: 2, 3-Dimethyl-7-aminoindole (0.20 g, 1.25 mM) was dissolved in a two phase solution of DCM (20 mL) and sat. aqueous $NaHCO_3$ (20 mL). Thiophosgene (0.09 mL, 1.25 mM) was dissolved in DCM (5 mL) and added drop-wise to the reaction. The mixture was left at room temperature overnight. The organic layer was washed with water (250 mL), dried over $MgSO_4$, and the organic phase taken to dryness. This produces a cream solid that, because of stability issues, was used immediately, without purification, in the next step of the reaction. Yield 62 %, 0.16 g; ^{1}H NMR (300 MHz, DMSO-*d_6*): δ: 2.15 (s,CH_3 ,3 H), 2.33 (s,CH_3 ,3 H), 6.96 (t, J = 7.68, 1 ArH), 7.13 (d, J = 7.68, 1 ArH), 7.39 (d, J = 7.68 Hz, 1 ArH), 11.32 (s, NH indole, 1 H);

^{13}C NMR (75 MHz, DMSO-d_6): δ: 8.3 (CH_3), 11.1 (CH_3), 106.5 (ArC), 112.6 (ArC), 117.7 (ArCH), 118.5 (ArCH), 118.6 (ArCH), 129.6 (ArC), 130.9 (ArC), 132.6 (ArC), 133.4 (CS) LRMS (ES^-):m/z: 201 $[M-H]^-$

1,3-Bis (2,3-dimethyl-1*H*-indol-7-yl)thiourea (211): A solution of the 7-isothiocyanato-2,3-dimethyl-1H-indole (0.16 g, 0.77 mM) in DCM (20 mL) was then added drop-wise to a solution of 2, 3-dimethyl-7-aminoindole (0.12 g, 0.77 mM) in DCM (20 mL). The solution was then heated at reflux overnight. The solution was then taken to dryness and the mixture purified by flash chromatography (49(DCM):1(MeOH)). This produces a slightly off-white solid. Yield 29 %, 0.08 g; decomp. 205°C; ^{1}H NMR (300 MHz, DMSO-d_6): δ: 2.15 (s, CH_3, 6 H), 2.34 (s, CH_3, 6 H), 6.93-6.86 (m, J = 7.92, 4 ArH), 7.25 (dd, J_1 = 2.25 Hz, J_2 = 6.39 Hz, 2 ArH), 9.26 (s, NH thiourea, 2 H), 10.61 (s, NH indole, 2 H); ^{13}C NMR (75 MHz, DMSO-d_6): δ: 8.46 (CH_3), 11.28 (CH_3), 105.63 (ArC), 115.80 (ArCH), 118.02 (ArCH), 118.46 (ArCH), 122.46 (ArC), 130.58 (ArC), 131.08 (ArC), 131.63 (ArC), 180.33 (CS); IR (film): ν = 3396 (indole NH stretching), 3290 (thiourea NH stetching), 1152 (thiourea CS stretching); LRMS (ES^-):m/z: 361 $[M-H]^-$; HRMS (ES^+): m/z: Act.: 363.1638 $[M+H]^+$ Calcd.: 363.1633 $[M+H]^+$

7-Isothiocyanato-1H-indole: 7-Aminoindole (0.32 g, 2.39 mM) was dissolved in a two phase solution of DCM (20 mL) and sat. aqueous $NaHCO_3$ (20 mL). Thiophosgene (0.18 mL, 2.39 mM) was dissolved in DCM (5 mL) and added drop-wise to the reaction. The mixture was left stirring at room temperature overnight. The organic layer was washed with water (250 mL), dried over $MgSO_4$, and the organic phase taken to dryness. The oil obtained was dissolved in ether (20 mL) and a brown solid removed by filtration. The filtrate was then taken to dryness, leaving a brown oil. Because of stability issues, this compound was used immediately, without purification, in the next step of the reaction. Yield 79 %, 0.33 g; ^{1}H NMR (300 MHz, DMSO-d_6): δ: 6.55 (s, 1 ArH), 7.02 (t, J = 8.07, 1 ArH), 7.22 (d, J = 7.68 Hz, 1 ArH), 7.42 (d, J = 2.19 Hz, 1 ArH), 7.58 (d, J = 8.04 Hz, 2 ArH), 11.78 (s, NH indole, 1 H); ^{13}C NMR (75 MHz, DMSO-d_6): δ: 102.4 (ArCH), 113.9 (ArC), 119.4 (ArCH), 119.6 (ArCH), 120.4 (ArCH), 126.8 (ArCH), 129.8 (ArC), 130.3 (ArC), 133.5 (CS); LRMS (ES^-):m/z: 173 $[M-H]^-$

1,3-Di(1*H*-indol-7-yl)thiourea (212): A solution of the 7-isothiocyanato-1H-indole (0.33 g, 1.88 mM) in DCM (20 mL) was then added drop-wise to a solution of 7-aminoindole (0.25g, 1.88 mM) in DCM (20 mL). The solution was then heated at reflux overnight. A light brown solid was then removed from the solution by filtration and dried under reduced pressure. Yield 83 %, 0.48 g; ^{1}H NMR (300 MHz, DMSO-d_6): δ: 6.47 (dd , J_1 = 2.94 Hz, J_2 = 1.83 Hz, 2 ArH), 6.98 (t, J = 7.68 Hz, 2 ArH), 7.06 (d, J = 6.93 Hz, 2 ArH), 7.37 (t, J = 2.94 Hz, 2 ArH), 7.45 (d, J = 7.32 Hz, 2 ArH), 9.51 (s, NH thiourea, 2 H), 11.04 (s, NH indole, 2 H); ^{13}C NMR (75 MHz, DMSO-d_6): δ: 101.51 (ArCH), 118.44 (ArCH), 118.78 (ArCH), 119.18 (ArCH), 115.85 (ArC), 123.71 (ArCH), 125.30 (ArC), 125.30 (ArCH), 129.27 (ArC), 131.96 (ArC), 180.69 (CS); IR (film): ν = 3365 (indole NH stretching), 3300 (thiourea NH stretching), 1102 (thiourea CS stretching); LRMS (ES^+):m/z: 307 $[M+H]^+$; HRMS (ES^+): m/z: Act.: 307.1013 $[M+H]^+$ Calcd.: 307.1012 $[M+H]^+$

1-Isocyanato-9H-carbazole: A solution of 1-amino carbazole (0.17 g, 0.94 mM) in DCM (20 mL) was added drop-wise over a period of 2 mins to a stirring solution of triphosgene (0.28 g, 0.94 mM) in a two phase DCM (20 mL) and sat. aqueous $NaHCO_3$ (40 mL) solution. The solution was stirred vigorously overnight. The organic phase was then washed with water (250 mL), dried with $MgSO_4$, and taken to dryness, leaving a white solid (the isocyanate), which was used immediately due to its high reactivity. A of yield 100 % was assumed.

1,3-Di(9H-carbazol-1-yl)urea (213): A solution of 1-isocyanato-9H-carbazole (0.24 g, 1.16 mM) in $CHCl_3$ (25 mL) was added drop-wise to a solution of 1-aminocarbazole (0.21g, 1.16 mM) in $CHCl_3$ (25 mL). NEt_3 (2 mL) was then added and the solution heated at reflux for 2 hrs. The product was isolated as a white precipitate that was removed by filtration. Yield 41 %, 0.19 g; decomp. 260 ºC; ^{1}H NMR (300 MHz, DMSO-d_6): δ: ^{1}H NMR (300 MHz, DMSO-d_6): δ: 7.13-7.20 (m, 4 ArH), 7.38-7.46 (m, 4 ArH), 7.61 (d, J = 8.04 Hz, 2 ArH), 7.92 (d, J = 7.68 Hz, 2 ArH), 8.12 (d, J = 8.04 Hz, 2 ArH), 8.84 (s, NH urea, 2 H), 10.94 (s, NH carbazole, 2 H); ^{13}C NMR (75 MHz, DMSO-d_6): δ: 111.4 (ArCH), 116.1 (ArCH), 118.7 (ArCH), 118.8 (ArCH), 119.1 (ArCH), 120.2 (ArCH), 122.7 (ArC), 123.5 (ArC), 123.9 (ArC), 125.6 (ArCH), 133.3 (ArC), 139.6 (ArC), 153.7 (CO);

IR (film): ν = 3391 (indole NH stretching) , 3240 (urea NH stretching), 1614 (urea CO stretching); LRMS (ES^-): m/z: 389 $[M-H]^-$; HRMS (ES^+): m/z: Act.: 391.1554 $[M+H]^+$ Calcd.: 391.1553 $[M+H]^+$

1-(9H-carbazol-1-yl)-3-(1H-indol-7-yl)urea (214): A solution of 1-isocyanato-9H-carbazole in $CHCl_3$ (25 mL) was added drop-wise to a stirring solution of 7-aminoindole (0.12 g, 0.94 mM) and NEt_3 (2 mL) in $CHCl_3$ (25 mL). The solution was heated to reflux overnight. The product was isolated as a white precipitate, which was removed by filtration and washed with hexane (20 mL). Yield 26 %, 0.08 g; decomp. 275 ºC; ^{1}H NMR (300 MHz, DMSO-d_6): δ: 6.46 (dd, J_1 = 2.64 Hz, J_2 = 1.89 Hz, 1 ArH), 6.97 (t, J = 7.68 Hz, 1 ArH), 7.11-7.19 (m, 3 ArH), 7.31-7.45 (m, 4 ArH), 7.58 (d, J = 7.92 Hz, 1 ArH), 7.90 (d, J = 7.68 Hz, 1 ArH), 8.11 (d, J = 7.68 Hz, 1 ArH), 8.81 (s, NH urea, 1 H), 8.84 (s, NH urea, 1 H), 10.84 (s, NH, 1 H), 10.91 (s, NH, 1 H); ^{13}C NMR (75 MHz, DMSO-d_6): δ: 79.7 (ArCH), 101.5 (ArCH), 111.4 (ArCH), 113.4 (ArCH), 115.8 (ArCH), 115.9 (ArCH), 118.7 (ArCH), 118.8 (ArCH), 119.0 (ArCH), 120.2 (ArCH), 122.7 (ArC), 123.6 (ArC), 123.9 (ArC), 124.2 (ArC), 125.1 (ArCH), 125.6 (ArCH), 128.9 (ArC), 129.3 (ArC), 133.3 (ArC), 139.5 (ArC), 153.6 (CO); IR (film): ν = 3390 (indole NH stretching) , 3249 (urea NH stretching), 1616 (urea CO stretching); LRMS (ES^-): m/z: 339 $[M-H]^-$; HRMS (ES^+): m/z: Act.: 341.1395 $[M+H]^+$ Calcd.: 341.1397 $[M+H]^+$

1-(9H-carbazol-1-yl)-3-phenylurea (215): A solution of phenylisocyanate (0.10 mL, 0.94 mM) in DCM (10 mL) was added drop-wise to a stirring solution of 1-aminocarbazole (0.12 g, 0.94 mM), in DCM (30 mL). The solution was heated at reflux overnight and a white precipitate was removed by filtration and washed with DCM (10 mL) and dried under vacuum. Yield 69 %, 0.20 g; decomp. 238 ºC; ^{1}H NMR (300 MHz, DMSO-d_6): δ: 6.98 (t, J = 7.32 Hz, 1 ArH), 7.10-7.19 (m, 2 ArH), 7.30 (t, 7.68 Hz, 2 ArH), 7.36-7.42 (m, 2 ArH), 7.52-7.59 (m, 3 ArH), 7.89 (d, J = 7.68 Hz, 1 ArH), 8.10 (d, J = 7.68 Hz, 1 ArH), 8.53 (s, NH urea, 1H), 8.87 (s, NH urea, 1H), 10.81 (s, NH carbazole, 1H); ^{13}C NMR (75 MHz, DMSO-d_6): δ: 111.4 (ArCH), 116.0 (ArCH), 118.4 (ArCH), 118.8 (ArCH), 119.3 (ArCH), 120.2 (ArCH), 121.8 (ArCH), 122.7 (ArC), 123.2 (ArC), 123.9 (ArC), 125.6 (ArCH), 128.8 (ArCH), 133.5 (ArC), 139.6 (ArC), 140.0 (ArC), 153.2 (CO) (there are overlapping ^{13}C signals that result in fewer than expected carbon

resonances); IR (film): ν = 3389 (indole NH stretching) , 3257 (urea NH stretching), 1626 (urea CO stretching); LRMS (ES^-): m/z: 300 $[M-H]^-$; HRMS (ES^+): m/z: Act.: 302.1285 $[M+H]^+$ Calcd.: 302.1288 $[M+H]^+$

1-Isothiocyanato-9H-carbazole: 1-Aminocarbazole (0.43 g, 2.36 mM) was dissolved in a two phase solution of DCM (20 mL) and sat. aqueous $NaHCO_3$ (40 mL). Thiophosgene (0.11 mL, 2.36 mM) was added drop-wise in DCM (20 mL) and the reaction mixture was left stirring at room temperature overnight. The organic layer was washed with water, dried over $MgSO_4$, filtered and concentrated in vacuo. The crude product was purified by recrystallisation from hot MeOH. The isothiocyanate was isolated as a white solid, which was used immediately due to its high reactivity. A yield of 89-100 % was assumed.

1,3-Di(9H-carbazol-1-yl)thiourea (216): A solution of the isothiocyanate (0.23 g, 1.04 mM) in $CHCl_3$ (20 mL) was then added drop-wise to a solution of 1-aminocarbazole (0.19g, 1.04 mM) in $CHCl_3$ (20 mL). The solution was then heated at reflux overnight with NEt_3 (2 mL). The solution was then taken to dryness and the product isolated from a recrystallisation from an ether/MeOH solution to give a light green solid. Yield 36 %, 0.15 g; m.p. 221 ºC; ^{1}H NMR (300 MHz, DMSO-d_6): δ: 7.13-7.20 (m, 4 ArH), 7.33 (d, J = 7.68 Hz, 2 ArH), 7.40-7.45 (m , 2 ArH), 7.61 (d, J = 8.04 Hz, 2 ArH), 8.03 (d, J = 7.69 Hz, 2 ArH), 8.21 (d, J = 7.69 Hz, 2 ArH), 9.71 (s, NH thiourea, 2 H), 11.27 (s, NH carbazole, 2 H); ^{13}C NMR (75 MHz, DMSO-d_6): δ: 111.2 (ArCH), 118.6 (ArCH), 118.6 (ArCH), 118.7 (ArCH), 120.2 (ArCH), 122.7 (ArC), 123.1 (ArC), 124.0 (ArC), 124.2 (ArCH), 125.7 (ArCH), 136.3 (ArC), 139.8 (ArC), 180.8 (CS); IR (film): ν = 3389 (indole NH stretching) , 3281 (thiourea NH stretching), 1148 (thiourea CS stretching); LRMS (ES^-):m/z: 405 $[M-H]^-$; HRMS (ES^+): m/z: Act.: 407.1332 $[M+H]^+$ Calcd.: 407.1325 $[M+H]^+$

1-(9H-carbazol-1-yl)-3-(1H-indol-7-yl)thiourea (217): A solution of 7-aminoindole (0.31 g, 2.35 mM) and 1-isothiocyanatocarbazole (0.53 g, 2.35 mM) was stirred in dry pyridine (20 mL) at room temperature over the weekend. The solution was washed with hexane and taken to dryness. The oil obtained was dissolved in hot MeOH (2 mL) and left to cool to room temperature. White crystals were removed after 24 hrs, washed with

hexane (25 mL) and dried under reduced pressure. Yield 48 %, 0.41 g; m.p. 144 ºC; ^{1}H NMR (300 MHz, DMSO-d_6): δ: 6.48 (dd, J_1 = 1.83 Hz, J_2 = 2.55 Hz, 1 ArH), 6.99 (t, J = 7.68 Hz, 1 ArH), 7.06-7.20 (m, 3 ArH), 7.29 (d, J = 7.68 Hz, 1 ArH), 7.38-7.47 (m, 3 ArH), 7.57 (d, J = 8.07 Hz, 1 ArH), 8.00 (d, J = 7.68 Hz, 1 ArH), 8.12 (d, J = 7.68 Hz, 1 ArH), 9.59 (s, NH thiourea, 1 H), 9.61 (s, NH thiourea, 1 H), 11.11 (s, NH, 1 H), 11.19 (s, NH, 1 H); ^{13}C NMR (75 MHz, DMSO-d_6): δ: 101.6 (ArCH), 111.2 (ArCH), 118.4 (ArCH), 118.6 (ArCH), 118.6 (ArCH), 118.6 (ArCH), 118.8 (ArCH), 119.3 (ArCH), 120.2 (ArCH), 122.7 (ArC), 123.2 (ArC), 123.6 (ArC), 123.9 (ArC), 124.0 (ArCH), 125.4 (ArCH), 125.7 (ArCH), 129.3 (ArC), 132.0 (ArC), 136.2 (ArC), 139.7 (ArC), 180.7 (CS); IR (film): ν = 3380 (indole/carbazole NH stretching), 3280 (thiourea NH stretching), 1210 (thiourea CS stretching); LRMS (ES^-): m/z: 355 $[M-H]^-$; HRMS (ES^+): m/z: Act.: 357.1168 $[M+H]^+$ Calcd.: 357.1166 $[M+H]^+$

1-(9H-carbazol-1-yl)-3-phenylthiourea (218): A solution of phenylisothiocyanate (0.41 g, 3.00 mM) in $CHCl_3$ (20 mL) was added drop-wise to a stirring solution of 1-aminocarbazole (0.21 g, 1.18 mM) in $CHCl_3$ (20 mL). The solution was then heated to reflux over the weekend. The solution was then reduced in volume to 2mL and a mixture of DCM (10 mL) and hexane (20 mL) added. The solution was then sonicated for 5 min and a dark green semi-solid removed and a white precipitate collected, washed with hexane (10 mL) and dried under reduced pressure. Yield 41 %, 0.16 g; m.p. 169 ºC; ^{1}H NMR (300 MHz, DMSO-d_6): δ: 7.11-7.19 (m, 3 ArH), 7.28-7.41 (m, 4 ArH), 7.53-7.60 (m, 3 ArH), 8.01 (d, J = 7.68 Hz, 1 ArH), 8.11 (d, J = 7.68 Hz, 1 ArH), 9.65 (s, NH thiourea, 1H), 9.83 (s, NH thiourea, 1H), 11.14 (s, NH carbazole, 1H); ^{13}C NMR (75 MHz, DMSO-d_6): δ: 111.3 (ArCH), 118.3 (ArCH), 118.5 (ArCH), 118.7 (ArCH), 120.2 (ArCH), 122.6 (ArC), 123.2 (ArCH), 123.9 (ArC), 124.5 (ArCH), 125.7 (ArCH), 128.4 (ArCH), 136.0 (ArC), 139.6 (ArC), 139.8 (ArC), 180.4 (CS) (there are overlapping ^{13}C signals that result in fewer than expected carbon resonances); IR (film): ν = 3300 (carbazole NH stretching), 3320 (thiourea NH stretching), 1220 (thiourea CS stretching); LRMS (ES^-): m/z: 316 $[M-H]^-$; HRMS (ES^+): m/z: Act.: 318.1059 $[M+H]^+$ Calcd.: 318.1031 $[M+H]^+$

7.4.3 Synthetic procedures for schemes in Chapter Three

N-butyl-7-nitro-1H-indole-2-carboxamide: A dry solution of 7-nitroindole-2-carboxylic acid (1.00 g, 4.88 mM), PyBOP (3.17 g, 6.10 mM) and a catalytic amount of HOBt was stirred in DMF (10 mL) for 30 mins. A dry solution of butylamine (0.48 mL, 4.88 mM) and NEt_3 (0.5 mL) was stirred in DMF (5 mL) for 30 mins. The amine solution was added drop-wise to the acid solution and allowed to stir for three days at room temperature. The solution was then taken to dryness, dissolved in $CHCl_3$ (20 mL), washed with water (250 mL) and dried over $MgSO_4$. The filtrate was then taken to dryness, leaving orange oil. This oil was suspended in diethyl ether (5 mL) and a white solid removed. The filtrate was taken to dryness and the oil dissolved in a hexane:$CHCl_3$ solution 5:1 (40 mL) and refrigerated for 1 hr. A brown precipitate formed, which was then removed by filtration. The filtrate was reduced then in volume (10 mL) and a yellow solid removed by filtration. Yield 25 %, 0.33 g, ^{1}H NMR values agree with previously published data.[2]

N-butyl-7-nitro-1H-indole-2-carboxamide: A solution of 7-nitroindole-2-carboxylic acid (1.5 g, 7.28 mM) and CDI (2.36 g, 14.56 mM) was heated at reflux in $CHCl_3$ (150 mL) for 2 hrs. The solution was then washed with water (2 x 250 mL), dried with $MgSO_4$ and taken to dryness, leaving an orange solid. A solution of butylamine (4 mL, 40.47 mM) in $CHCl_3$ (5 mL) was then added to the orange solid and the solution heated at reflux overnight. The solution was then washed with water (250 mL), dried with $MgSO_4$ and taken to dryness to leave an orange oil. This crude product was purified by flash chromatography DCM:MeOH 1:49. Yield 74 %, 1.41 g, ^{1}H NMR values agree with previously published data.[2]

7-Amino-N-butyl-1H-indole-2-carboxamide: N-butyl-7-nitro-1H-indole-2-carboxamide (0.60 g, 2.30 mM) and a Pd/C 10% catalyst (0.07 g) were suspended in EtOH (30 mL). The flask was evacuated and the mixture placed under a hydrogen atmosphere and stirred vigorously for 3 hrs. After this time, the palladium catalyst was removed by filtration through cellite and the filtrate taken to dryness and placed under reduced pressure. This gives a white solid that was used, without purification, in the next step of the reaction. A yield of 100 % was assumed.

7,7'-Carbonylbis(azanediyl)bis(N-butyl-1H-indole-2-carboxamide) (219): 7-Amino-N-butyl-1H-indole-2-carboxamide was dissolved in a two phase solution of sat. aqueous $NaHCO_3$ (60 mL) and DCM (60 mL). This solution was stirred vigorously at room temperature and triphosgene (0.68 g, 2.30 mM) added in two equal aliquots. The solution was then allowed to stir overnight at room temperature. The two phase solution was filtered and the white precipitate sonicated in water (250 mL) for 30 mins. The white solid was then collected by filtration and washed with DCM (20 mL) and diethyl ether (20 mL). Yield 77 %, 0.43 g; m.p. 138 ºC; ^{1}H NMR (300 MHz, DMSO-d_6): δ: 0.92 (t, J = 7.32 Hz, 6 H), 1.36 (dd, J_1 = 6.93 Hz, J_2 = 13.53 Hz, 4 H), 1.54 (t, J = 6.96 Hz, 4 H), 3.33 (m, 2 H) (obscured by water peak), 7.01 (t, J = 7.68 Hz, 2 ArH), 7.16 (s, 2 ArH), 7.32 (d, J = 8.04 Hz, 2 ArH), 7.51 (d, J = 7.32 Hz, 4 ArH), 8.51 (s, NH amide, 2 H), 8.88 (s, NH urea, 2 H), 11.37 (s, NH indole, 2 H); ^{13}C NMR (75 MHz, DMSO-d_6): δ: 13.7 (CH_3), 19.6 (CH_2), 31.3 (CH_2), 38.4 (CH_2), 102.8 (ArCH), 113.7 (ArCH), 116.0 (ArCH), 120.2 (ArCH), 124.9 (ArC), 128.0 (ArC), 128.6 (ArC), 131.7 (ArC), 153.1 (CO), 160.8 (CO); IR (film): ν = 3340 (indole NH stretching), 3270 (urea NH stretching), 1640 (urea CO stretching), 1560 (amide CO stretching); LRMS (ES^-):m/z: 487 $[M-H]^-$; HRMS (ES^+): m/z: Act.: 489.2604 $[M+H]^+$ Calcd.: 489.2609 $[M+H]^+$.

7-Nitro-N-phenyl-1H-indole-2-carboxamide: The synthesis of 7-nitro-N-phenyl-1H-indole-2-carboxamide is taken from a method described by Gale *et. al*.. ^{1}H NMR values agree with previously published data.[2]

7-Nitro-N-phenyl-1H-indole-2-carboxamide: A dry solution of 7-nitroindole-2-carboxylic acid (1.00 g, 4.88 mM), PyBOP (3.20 g, 6.15 mM) and a catalytic amount of HOBt was stirred in DMF (10 mL) for 30 mins. A dry solution of aniline (0.18 mL, 4.88 mM) and NEt_3 (0.6 mL) was stirred in DMF (5 mL) for 30 mins. The amine solution was added drop-wise to the acid solution and allowed to stir for three days at room temperature. The solution was then taken to dryness, dissolved in $CHCl_3$ (15 mL) and cooled in the freezer for 1 hr. This gives the first crop of product. The remaining solution was then washed with water (250 mL) and dried over $MgSO_4$. Hexane was then added until the second crop of yellow solid had precipitated. Both crops of product were collected by

filtration and washed with hexane (20 mL). Yield 47 %, 0.65 g, ^{1}H NMR values agree with previously published data.[2]

7-Nitro-N-phenyl-1H-indole-2-carboxamide: A solution of 7-nitroindole-2-carboxylic acid (0.25 g, 1.22 mM) and CDI (0.20 g, 1.22 mM) was heated at reflux in $CHCl_3$ (20 mL) for 2 1/2 hrs. A solution of aniline (0.05 mL, 1.22 mM) in $CHCl_3$ (20 mL) was then added to the reaction mixture, which was then heated at reflux overnight. The solution was then washed with water (250 mL), dried over $MgSO_4$ and reduced in volume (2 mL). Hexane was then added until a yellow precipitate had formed. This was collected by filtration and allowed to dry. Yield 43 %, 0.15 g, ^{1}H NMR values agree with previously published data.[2]

7-amino-N-phenyl-1H-indole-2-carboxamide: 7-Nitro-N-phenyl-1H-indole-2-carboxamide (0.20 g, 0.73 mM) and a Pd/C 10% catalyst (0.07 g) were suspended in EtOH (20 mL). The flask was then evacuated and the mixture placed under a hydrogen atmosphere and stirred vigorously for 3 hrs. After this time, the Palladium catalyst was removed by filtration through cellite and the filtrate taken to dryness and placed under reduced pressure. This gives a white solid that was used without purification in the next step of the reaction. A yield of 100 % was assumed.

7,7'-Carbonylbis(azanediyl)bis(N-phenyl-1H-indole-2-carboxamide (220): 7-Amino-N-phenyl-1H-indole-2 carboxamide (0.18 g, 0.73 mM) was dissolved in a two phase solution of $CHCl_3$ (40 mL) and sat. aqueous $NaHCO_3$ (40 mL). Triphosgene (0.22 g, 0.73 mM) was added in two equal portions and the mixture was left stirring overnight. The organic layer was washed with water, dried over $MgSO_4$, filtered and concentrated in vacuo. The solid was sonicated in water 500 mL for 30 mins, then filtered and dried with ether (20 mL). The product was isolated as a white solid. Yield 88 %, 0.17 g; m.p. 174 °C; ^{1}H NMR (300 MHz, DMSO-d_6): δ: 7.05-7.15 (m, 4 ArH), 7.36-7.43 (m, 6 ArH), 7.51 (d, J = 1.83 Hz, 2 ArH), 7.60 (d, J = 7.68 Hz, 2 ArH), 7.84 (d, J = 7.68 Hz, 4 ArH), 8.97 (s, NH urea, 2 H), 10.30 (s, NH amide, 2 H), 11.62 (s, NH indole, 2 H); ^{13}C NMR (75 MHz, DMSO-d_6): δ: 104.5 (ArCH), 114.3 (ArCH), 116.3 (ArCH), 120.3 (ArCH), 120.5 (ArCH), 123.7 (ArCH), 125.0 (ArC), 128.6 (ArC), 128.8 (ArCH), 131.3 (ArC),138.9 (ArC), 153.2

(CO), 159.7 (CO) (there are overlapping ^{13}C signals that result in fewer than expected carbon resonances); IR (film): ν = 3289 (urea NH stretching), 1661 (urea CO stretching); LRMS (ES^-):m/z: 527.5 $[M-H]^-$; HRMS (ES^+): m/z: Act.: 551.1794 $[M+Na]^+$ Calcd.: 551.1802 $[M+Na]^+$

N-(1H-indol-7-yl)-7-nitro-1H-indole-2-carboxamide: A dry solution of 7-nitroindole-2-carboxylic acid (0.38 g, 1.85 mM), PyBOP (1.20 g, 2.31 mM) and a catalytic amount of HOBt was stirred in DMF (5 mL) for 30 mins. A dry solution of 7-aminoindole (0.24 g, 1.85 mM) and NEt_3 (0.3 mL) was stirred in DMF (5 mL) for 30 mins. The amine solution was added drop-wise to the acid solution and allowed to stir for three days at room temperature. The solution was then taken to dryness, dissolved in DCM (15 mL) and washed with water (250 mL), then dried over $MgSO_4$. The filtrate was then reduced to half original volume and hexane added drop-wise until a brown precipitate appeared, which was removed by filtration. The filtrate was then taken to dryness, leaving orange oil. This oil was dissolved in MeOH (30 mL) and a yellow solid removed by filtration and washed with ether (25 mL). Yield 89 %, 0.35 g; decomp. 212 ºC; ^1H NMR (300 MHz, DMSO-d_6): δ: 6.51 (dd, J_1 = 1.83 Hz, J_2 = 2.94 Hz, 1 ArH), 7.05 (t, J = 7.68 Hz, 1 ArH),7.31 (d, J = 7.32 Hz, 1 ArH), 7.35-7.40 (m, 2 ArH), 7.48 (d, J = 7.68 Hz, 1 ArH), 7.64 (d, J = 1.83 Hz, 1 ArH), 8.27 (d, J = 2.55 Hz, 1H), 8.30 (d, J = 2.94 Hz, 1 ArH), 10.66 (s, NH, 1 H), 10.90 (s, NH, 1 H), 11.53 (s, NH, 1 H); ^{13}C NMR (75 MHz, DMSO-d_6): δ: 101.6 (ArCH), 107.2 (ArCH), 116.2 (ArCH), 117.9 (ArCH), 118.8 (ArCH), 120.1 (ArCH), 121.3 (ArCH), 122.1 (ArC), 125.5 (ArCH), 128.9 (ArC), 129.4 (ArC), 130.0 (ArC), 130.8 (ArCH), 131.0 (ArC), 133.1 (ArC), 1304.7 (ArC), 158.3 (CO); IR (film): ν = 3470 and 3370 (indole NH stretching), 3290 (amide NH stretching), 1660 and 1550 (amide CO stretching); LRMS (ES^+):m/z: 343 $[M+Na]^+$; HRMS (ES^+): m/z: Act.: 321.0979 $[M+H]^+$ Calcd.: 321.0982 $[M+H]^+$.

7-Amino-N-(1H-indol-7-yl)-1H-indole-2-carboxamide: N-(1H-indol-7-yl)-7-nitro-1H-indole-2-carboxamide (0.5 g, 1.56 mM) and a Pd/C 10% catalyst (0.05 g) were suspended in DMF (3 mL). The flask was then evacuated and the mixture placed under a hydrogen atmosphere and stirred vigorously overnight. After this time, the palladium

catalyst was removed by filtration through cellite and the filtrate taken on to the next step. A yield of 100 % was assumed.

7,7'-Carbonylbis(azanediyl)bis(N-(1H-indol-7-yl)-1H-indole-2-carboxamide) (221): The filtrate was dissolved in a two phase solution of sat. $NaHCO_3$ (40 mL) and $CHCl_3$ (40 mL). This solution was stirred vigorously at room temperature and triphosgene (0.28 g, 0.94 mM) added in two equal aliquots. The solution was then allowed to stir for two days. The two phase solution was then filtered and a white solid sonicated in water (250 mL) for 30 mins. The white solid was then collected by filtration and washed with ether (100 mL). Yield 71 %, 0.20 g; m.p. 204 ºC; ^{1}H NMR (400 MHz, DMSO-d_6): δ: 6.49 (s, 2 ArH), 7.03 (t, J = 8.04 Hz, 2 ArH), 7.09 (t, J = 8.04 Hz, 2 ArH), 7.37-7.45 (m, 8 ArH), 7.54 (s, 2 ArH), 7.60 (d, J = 8.04 Hz, 2 ArH), 9.01 (s, NH urea, 2 H), 10.17 (s, NH amide, 2 H), 10.99 (s, NH indole, 2 H), 11.59 (s, NH indole, 2 H); ^{13}C NMR (100 MHz, DMSO-d_6): δ: 101.6 (ArCH), 104.6 (ArCH), 114.2 (ArCH), 115.9 (ArCH), 116.3 (ArCH), 117.4 (ArCH), 118.9 (ArCH), 120.5 (ArCH), 122.6 (ArC), 125.0 (ArC), 125.3 (ArCH), 128.5 (ArC), 128.7 (ArC), 129.3 (ArC), 129.7 (ArC), 131.4 (ArC), 153.3 (CO), 159.8 (CO); IR (film): ν = 3350 (indole NH stretching), 3250 (urea NH stretching), 1620 (urea CO stretching), 1550 (amide CO stretching); LRMS (ES^-):m/z: 605 $[M-H]^-$; HRMS (ES^+): m/z: Act.: 629.2008 $[M+Na]^+$ Calcd.: 629.2020 $[M+Na]^+$.

N-(9H-carbazol-1-yl)-7-nitro-1H-indole-2-carboxamide: A dry solution of 7-nitroindole-2-carboxylic acid (0.29 g, 1.41 mM), PyBOP (0.92 g, 1.77 mM) and a catalytic amount of HOBt was stirred in DMF (15 mL) for 30 mins. A dry solution of 1-aminocarbazole (0.26 g, 1.41 mM) and NEt_3 (0.3 mL) was stirred in DMF (5 mL) for 30 mins. The amine solution was added drop-wise to the acid solution and allowed to stir for three days at room temperature. The solution was then taken to dryness, dissolved in DCM (20 mL) and washed with water (150 mL) and the organic layer was placed in the freezer for 1 ½ hr. A yellow precipitate was then removed by filtration. Yield 70 %, 0.36 g; m.p. > 250 ºC; ^{1}H NMR (300 MHz, DMSO-d_6): δ: 7.17-7.25 (m, 2 ArH), 7.37-7.44 (m, 2 ArH), 7.53-7.59 (m, 2 ArH), 7.68 (d, J = 1.83 Hz, 1 ArH), 8.06 (d, J = 7.68 Hz, 1 ArH), 8.15 (d, J = 7.68 Hz, 1 ArH), 8.30-8.32 (m, 2 ArH), 10.84 (s, NH, 1 H), 11.01 (s, NH, 1H), 11.57 (s, NH, 1H); ^{13}C NMR (75 MHz, DMSO-d_6): δ: 107.3 (ArCH), 111.3 (ArCH), 118.0

(ArCH), 118.6 (ArCH), 118.8 (ArCH), 120.2 (ArCH), 120.3 (ArCH), 121.3 (ArCH), 122.5 (ArC), 124.1 (ArC), 125.9 (ArCH), 128.9 (ArC), 130.9 (ArCH), 131.0 (ArC), 133.1 (ArC), 134.4 (ArC), 134.6 (ArC), 139.7 (ArCH), 158.4 (CO) (there are overlapping ^{13}C signals that result in fewer than expected carbon resonances); IR (film): ν = 3370 (indole/carbazole NH stretching), 3250 (amide NH stretching), 1650 and 1550 (amide CO stretching); LRMS (ES^-):m/z: 369 $[M-H]^-$; HRMS (ES^+): m/z: Act.: 371.1134 $[M+H]^+$ Calcd.: 371.1139 $[M+H]^+$.

7-Amino-N-(9H-carbazol-1-yl)-1H-indole-2-carboxamide: N-(9H-carbazol-1-yl)-7-nitro-1H-indole-2-carboxamide (0.5 g, 1.35 mM) and a Pd/C 10% catalyst (0.05 g) were suspended in DMF (3 mL). The flask was then evacuated and the mixture placed under a hydrogen atmosphere and stirred vigorously overnight. After this time the palladium catalyst was removed by filtration through cellite and the filtrate reduced in volume (1 mL) and placed under reduced pressure, producing light brown oil, which was taken on to the next step. A yield of 100 % was assumed.

7,7'-Carbonylbis(azanediyl)bis(N-(9H-carbazol-1-yl)-1H-indole-2-carboxamide) (222): The light brown oil was dissolved in a two phase solution of sat. $NaHCO_3$ (40 mL), $CHCl_3$ (35 mL) and DMF (5 mL). This solution was stirred vigorously at room temperature and triphosgene (0.40 g, 1.35 mM) added in two equal aliquots. The solution was allowed to stir overnight. The two phase solution was then filtered and a white solid sonicated in water (250 mL) for 30 mins. The white solid was then collected by filtration and washed with ether (100 mL). Yield 79 %, 0.38g; m.p. > 250 ºC; ^1H NMR (300 MHz, DMSO-d_6): δ: 7.10 (t, J = 6.96 Hz, 2 ArH), 7.16-7.23 (m, 4 ArH), 7.38-7.46 (m, 4 ArH), 7.54-7.60 (m, 8 ArH), 8.03 (d, J = 7.32 Hz, 2 ArH), 8.14 (d, J = 7.32 Hz, 2 ArH), 9.01 (s, NH urea, 2 H), 10.38 (s, NH amide, 2 H), 11.10 (s, NH carbazole, 2 H), 11.65 (s, NH indole, 2 H); ^{13}C NMR (75 MHz, DMSO-d_6): δ: 104.6 (ArCH), 111.3 (ArCH), 114.2 (ArCH), 116.3 (ArCH), 117.6 (ArCH), 118.5 (ArCH), 118.8 (ArCH), 120.3 (ArCH), 120.5 (ArCH), 121.2 (ArCH), 121.9 (ArC), 122.5 (ArC), 123.9 (ArC), 125.0 (ArC), 125.8 (ArCH), 128.5 (ArC), 128.7 (ArC), 131.3 (ArC), 134.2 (ArC), 139.7 (ArC), 153.3 (CO), 159.9 (CO); IR (film): ν = 3410 (carbazole NH stretching), 3370 (indole NH stretching), 3300 (urea NH stretching), 3220 (amide NH stretching), 1640 (urea CO stretching), 1540

(amide CO stretching); LRMS (ES^-):m/z: 705.5 $[M-H]^-$; HRMS (ES^+): m/z: Act.: 707.2497 $[M+H]^+$ Calcd.: 707.2514 $[M+H]^+$.

7.4.4 Synthetic procedures for schemes in Chapter Four

N-(1H-indol-7-yl)-1H-imidazole-1-carboxamide: A solution of CDI (1.50 g, 9.25 mM) and DCM (50 mL) was stirred until the solution was clear. 7-aminoindole (0.41 g, 3.08 mM) was then added in DCM (5 mL) and allowed to stir overnight at room temperature. A white precipitate was then collected by filtration. It was not purified but used impure in further reactions. Approximate yield 72 - 82 %.

N,N',N''-(2,2',2''-Nitrilotris(ethane-2,1-diyl))tris(1H-indole-2-carboxamide) (224): A dry solution of indole-2-carboxylic acid (0.50 g, 3.10 mM), PyBOP (2.02 g, 3.88 mM) and a catalytic amount of HOBt was stirred in DMF (5 mL) for 30 mins. A dry solution of Tris(2-aminoethyl)amine (0.15 mL, 1.03 mM) and NEt_3 (0.3 mL) was stirred in DMF (5 mL) for 30 mins. The amine solution was added drop-wise to the acid solution and allowed to stir for three days at room temperature. The solution was then taken to dryness, dissolved in DCM (20 mL) and washed with water (250 mL). A precipitate was then collected and sonicated in a weak NaOH solution (0.01 M, 100 mL) for 1 hr. The solid was then collected by filtration, washed with water (100 mL) and dried with ether (25 mL). The ether filtrate was taken to dryness, producing further white precipitate. Yield 47 %, 0.28 g; m.p. > 250 ºC; ^{1}H NMR (300 MHz, DMSO-d_6): δ: 2.79 (s, 6 H), 3.44 (d, J_1 = 2.37 Hz, 6 H), 7.00 (t, J = 7.29 Hz, 3 ArH), 7.08 (s, 3 ArH), 7.16 (t, J = 8.07 Hz, 3 ArH), 7.41 (d, J = 8.04 Hz, 3 ArH), 7.53 (d, J = 7.68 Hz, 3 ArH), 8.39 (s, NH amide, 3 H), 11.55 (s, NH indole, 3 H); ^{13}C NMR (75 MHz, DMSO-d_6): δ: 37.3 (CH_2), 53.4 (CH_2), 102.3 (ArCH), 112.3 (ArCH), 119.6 (ArCH), 121.5 (ArCH), 123.2 (ArCH), 127.1 (ArC), 131.8 (ArC), 136.4 (ArC), 161.2 (CO); IR (film): ν = 3310 (indole NH stretching), 3220 (amide NH stretching), 1620 and 1540 (amide CO stretching); LRMS (ES^-):m/z: 574.5 $[M-H]^-$; HRMS (ES^+): m/z: Act.: 576.2719 $[M+H]^+$ Calcd.: 576.2718 $[M+H]^+$.

N,N',N''-(2,2',2''-Nitrilotris(ethane-2,1-diyl))tris(7-nitro-1H-indole-2-carboxamide) (225): A dry solution of PyBOP (3.16 g, 6.07 mM), HOBt (catalytic amount), NEt_3 (0.3 mL), 7-nitroindole-2-carboxylic acid (1.0 g, 4.85 mM) and TREN (0.24

g, 1.62 mM) in DMF (12 mL) was stirred at room temperature for three days. The solution was then taken to dryness and DCM (20 mL) was added. A yellow precipitate was then removed by filtration and sonicated for one hour in a 6 M KOH solution (100 mL). The yellow solid was then filtered and dried with ether (50 mL). Yield 89%, 1.02 g ; decomp. 153 ºC; ^{1}H NMR (300 MHz, DMSO-d_6): δ: 2.80 (s, 6 H), 3.48 (s, 6 H), 7.18 (t, J = 7.68 Hz, 3 ArH), 7.23 (s, 3 ArH), 7.94 (d, J = 7.32 Hz, 3 ArH), 8.08 (d, J = 8.04 Hz, 3 ArH), 8.78 (s, NH amide, 3 H), 11.00 (s, NH indole, 3 H); ^{13}C NMR (75 MHz, DMSO-d_6): δ: 37.4 (CH_2), 53.1 (CH_2), 105.7 (ArCH), 119.7 (ArCH), 120.8 (ArCH), 128.4 (ArC), 130.3 (ArCH), 130.8 (ArC), 132.7 (ArC), 134.4 (ArC), 159.7 (CO); IR (film): ν =3460 (amide NH stretching), 3390 (indole NH stretching), 3100 (amide NH stretching), 1630 and 1560 (amide CO stretching), 1500 and 1310 (nitro NO stretching); LRMS (ES^-):m/z: 709 $[M-H]^-$; HRMS (ES^+): m/z: Act.: 711.2282 $[M+H]^+$ Calcd.: 711.2270 $[M+H]^+$.

1,1',1''-(2,2',2''-Nitrilotris(ethane-2,1-diyl))tris(3-(1H-indol-7-yl)urea) (226): A dry solution of N-(1H-indol-7-yl)-1H-imidazole-1-carboxamide (0.50 g, 2.21 mM) in DMF (10 mL) was heated to 42 °C. TREN (0.10 g, 0.71 mM) was then added and the heated mixture allowed to stir overnight. The DMF was then removed, leaving a clear oil, which was dissolved in DCM (100 mL). The organic phase was washed with water (250 mL), dried over $MgSO_4$ and concentrated (20 mL). Hexane (approximately 30 mL) was then added and a white precipitate removed by filtration and dried under reduced pressure. Yield 89%, 0.40 g; m.p. 171 ºC; ^{1}H NMR (300 MHz, DMSO-d_6): δ: 2.69 (t, J = 6.57 Hz, 6 H), 3.29 (dd, J_1 = 5.85 Hz, J_2 = 12.09 Hz, 6 H), 6.31 (t, J = 5.13 Hz, NH urea, 3 H), 6.39 (dd, J_1 = 1.83 Hz, J_2 = 2.91 Hz, 3 ArH), 6.87 (t, J = 7.68 Hz, 3 ArH), 7.04 (d, J = 7.32 Hz, 3 ArH), 7.21 (d, J = 7.68 Hz, 3 ArH), 7.25 (t, J = 7.55 Hz, 3 ArH), 8.44 (s, NH urea, 3 H), 10.66 (s, NH indole, 3 H); ^{13}C NMR (75 MHz, DMSO-d_6): δ: 38.0 (CH_2), 54.1 (CH_2), 101.5 (ArCH), 112.3 (ArCH), 114.9 (ArCH), 119.1 (ArCH), 124.8 (ArC), 124.9 (ArCH), 128.1 (ArC), 129.2 (ArC), 155.9 (CO); IR (film): ν = 3300 (indole NH stretching), 3260 (urea NH stretching), 1630 (urea CO stretching); LRMS (ES^+):m/z: 621.5 $[M+H]^+$; HRMS (ES^+): m/z: Act.: 621.3036 $[M+H]^+$ Calcd.: 621.3045 $[M+H]^+$.

N,N',N''-(2,2',2''-Nitrilotris(ethane-2,1-diyl))tris(7-(3-1H-indol-7-ylureido)-1H-indole-2-carboxamide) (227): A solution of **225** (0.20 g, 0.28 mM) and a Pd/C 10%

catalyst (0.05 g) in DMF (5 mL) was stirred under a hydrogen atmosphere at room temperature for three hours. The solution was then filtered through cellite and a microfiber filter and taken to dryness. A dry solution of N-(1H-indol-7-yl)-1H-imidazole-1-carboxamide (0.21 g, 0.91 mM) in DMF (10 mL) was added to the off-white solid and allowed to stir at 45°C overnight. The solution was then taken to dryness and the resultant oil sonicated in $CHCl_3$ (50 mL). The green solid was suspended in water (250 mL) at 80 °C overnight. It was then removed by filtration and dried under reduced pressure. Yield 69 %, 0.19 g; decomp. 207 ºC; ^{1}H NMR (400 MHz, DMSO-d_6): δ: 2.84 (s, 6 H), 3.47 (s, 6 H), 6.44 (s, 3 ArH), 6.93-7.01 (m, 6 ArH), 7.13-7.17 (m, 6 ArH), 7.26 (d, J = 8.04 Hz, 3 ArH), 7.30-7.32 (m, 6 ArH), 7.50 (d, J = 7.52 Hz, 3 ArH), 8.44 (s, NH amide, 3 H), 8.50 (s, NH urea, 3 H), 9.02 (s, NH urea, 3 H), 10.80 (s, NH indole, 3 H), 11.26 (s, NH indole, 3 H); ^{13}C NMR (100 MHz, DMSO-d_6): δ: 37.4 (CH_2), 53.3 (CH_2), 101.6 (ArCH), 103.0 (ArCH), 113.6 (ArCH), 114.0 (ArCH), 115.0 (ArCH), 116.0 (ArCH), 119.1 (ArCH), 120.3 (ArCH), 123.8 (ArCH), 125.1 (ArC), 125.2 (ArC), 128.0 (ArC), 128.7 (ArC), 129.1 (ArC), 129.3 (ArC), 131.4 (ArC), 153.4 (CO), 161.1 (CO); IR (film): ν =3470-3140 broad (amide, indole, urea NH stretching), 1620 (urea CO stretching), 1550 (amide CO stretching); LRMS (ES^+):m/z: 1118 $[M+Na]^+$; Anal. Calcd. for "$C_{60}H_{54}N_{16}O_6$": C= 65.80 %, H= 4.97 %, N= 20.45 % Found: C= 65.68 %, H= 5.08 %, N= 20.55 %.

N,N',N''- (2,4,6-triethylbenzene-1,3,5-triyl)tris(methylene)tris(7-nitro-1H-indole-2-carboxamide) (231): A dry solution of PyBOP (1.96 g, 3.76 mM), 7-nitroindole-2-carboxylic acid (0.62 g, 3.01 mM) and HOBt (catalytic amount) in DMF (9 mL) was stirred at room temperature for 30 mins. A dry solution of NEt_3 (0.3 mL) and (2,4,6-triethylbenzene-1,3,5-triyl)trimethanamine (0.25 g, 1.00 mM) in DMF (3 mL)/ DCM (5 mL) was stirred at room temperature for 30 mins. The amine solution was then added to the acid solution and the mixture stirred at room temperature for three days. The solution was then taken to dryness and DCM (50 mL) and water (50 mL) were added and stirred vigorously for 1 hr the yellow precipitate formed was then removed by filtration, suspended in water (100 mL) and heated to 90 ºC overnight. The yellow solid was then filtered and dried under reduced pressure. Yield 75 %, 0.62 g; decomp. 182 ºC; ^{1}H NMR (300 MHz, DMSO-d_6): δ: 1.18 (t, J = 6.96 Hz, 6 H), 2.92 (d, J = 6.93 Hz, 4 H), 4.66 (s, 4 H), 7.31 (t, J = 8.04 Hz, 3 ArH), 7.46 (s, 3 ArH), 8.16-8.23 (m, 6 ArH), 9.08 (s, NH

amide, 3 H), 11.61 (s, NH indole, 3 H); ^{13}C NMR (75 MHz, DMSO-d_6): δ: 16.3 (CH_3), 23.0 (CH_2), 37.8 (CH_2), 107.7 (ArCH), 120.0 (ArCH), 121.2 (ArCH), 128.9 (ArC), 130.7 (ArCH), 130.9 (ArC), 132.0 (ArC), 133.1 (ArC), 134.6 (ArC), 144.2 (ArC), 159.2 (CO); IR (film): ν =3440 (amide NH stretching), 3270 (indole NH stretching), 3080 (amide NH stretching), 1620 and 1550 (amide CO stretching), 1510 and 1340 (nitro NO stretching); LRMS (ES^+):m/z: 836 $[M+Na]^+$; HRMS (ES^+): m/z: Act.: 836.2759 $[M+Na]^+$ Calcd.: 836.2763 $[M+Na]^+$.

1,1',1''-(2,4,6-Triethylbenzene-1,3,5-triyl)tris(methylene)tris(3-(1H-indol-7-yl)urea) (232): A dry solution of (2,4,6-triethylbenzene-1,3,5-triyl)trimethanamine (0.20 g, 0.80 mM) and N-(1H-indol-7-yl)-1H-imidazole-1-carboxamide (0.59 g, 2.61 mM) in DMF (15 mL) was heated to 50 °C overnight. The solution was then taken to dryness, leaving a white solid which was suspended in ethyl acetate (200 mL) and heated to reflux overnight. The white solid, was then removed by filtration and suspended in water (200 mL) and heated to reflux overnight. It was then removed by filtration and dried under reduced pressure. Yield 79 %, 0.46 g; decomp. >250 ºC; ^{1}H NMR (400 MHz, DMSO-d_6): δ: 1.23 (t, J = 7.28 Hz, 6 H), 2.89 (q, J = 7.04 Hz, 4 H), 4.45 (d, J = 4.28 Hz, 4 H), 6.17 (t, J = 4.76 Hz, NH urea, 3 H), 6.40 (dd, J_1 = 2.76 Hz, J_2 = 2.00 Hz, 3 ArH), 6.89 (t, J = 7.80 Hz, 3 ArH), 6.99 (d, J = 7.00 Hz, 3 ArH), 7.22 (d, J = 7.76 Hz, 3 ArH), 7.32 (t, J = 3 Hz, 3 ArH), 8.27 (s, NH urea, 3 H), 10.57 (s, NH indole, 3 H); ^{13}C NMR (100 MHz, DMSO-d_6): δ: 16.6 (CH_3), 22.4 (CH_2), 37.6 (CH_2), 101.5 (ArCH), 111.9 (ArCH), 114.9 (ArCH), 119.1 (ArCH), 124.6 (ArC), 125.1 (ArCH), 127.9 (ArC), 129.3 (ArC), 133.1 (ArC), 142.9 (ArC), 155.3 (CO); IR (film): ν = 3300 (indole NH stretching), 3270 (urea NH stretching), 1620 (urea CO stretching); LRMS (ES^-):m/z: 722.5 $[M-H]^-$; HRMS (ES^+): m/z: Act.: 746.3528 $[M+Na]^+$ Calcd.: 746.3538 $[M+Na]^+$.

Diindole urea based cage (233): A solution of compound **225** (0.10 g, 0.14 mM) and a Pd/C 10% catalyst (0.05 g) in DMF (5 mL) was stirred under a hydrogen atmosphere at room temperature for two hours. The solution was then filtered through a microfiber filter and taken to dryness. The off-white solid was then dissolved in DCM (30 mL) and a sat. solution of sodium hydrogen carbonate (30 mL) was added. The biphasic solution was

stirred rapidly and triphosgene (0.04 g, 0.14 mM) was added. The solution was allowed to stir overnight and then filtered and the precipitate washed with water (40 mL).

7.4.5 Synthetic procedures for schemes in Chapter Five

N,N'-(pentane-1,5-diyl)bis(1H-indole-2-carboxamide) (234): A solution of indole-2-carboxylic acid (0.63 g, 3.91 mM) and CDI (0.8 g, 5.00 mM) in $CHCl_3$ (30mL) was heated at reflux of 11/2 hrs. After this time, 1,5-diaminopentane (0.20 g, 1.96 mM) in $CHCl_3$ (5 mL) was added drop-wise and the solution was left at reflux over night. The reaction mixture was then left to cool to room temperature and the precipitate that had formed was removed by filtration, washed with ether (10 mL) and left to dry. Yield 73 %, 0.56 g; m.p. 270-272 ºC; ^{1}H NMR (300 MHz, DMSO-d_6): δ: 1.40-1.42 (br. m, 2 H), 1.55-1.62 (br. m, 4 H), 3.33 (m, 4 H) (obscured by water peak), 7.02 (t, J = 7.41 Hz, 2 ArH), 7.09 (s, 2 ArH), 7.16 (t, J = 7.89 Hz, 2 ArH), 7.42 (d, J = 7.92Hz, 2 ArH), 7.58 (d, J = 7.80Hz, 2 ArH), 8.44 (s, NH amide, 2 H), 11.51 (s, NH indole, 2 H); ^{13}C{^{1}H} NMR (75 MHz, DMSO-d_6): δ: 24.0 (CH_2), 29.0 (CH_2), 38.7 (CH_2), 102.2 (ArCH), 112.3 (ArCH), 119.7 (ArCH), 121.4 (ArCH), 123.2 (ArCH), 127.1 (ArC), 131.9 (ArC), 136.4 (ArC), 161.0 (CO); IR (film): ν = 3270 (indole NH stretching), 2940 (amide NH stretching), 1610 (amide CO stretching), 1550 (amide CO stretching); LRMS (ESI$^+$): m/z: 389 $(M+H)^+$; Anal. Calcd. for "$C_{23}H_{24}N_4O_2$": C= 71.11%, H= 6.23%, N= 14.42% Found: C= 70.89%, H= 6.11%, N= 14.69%

N,N'-(1,3-phenylenebis(methylene))bis(1*H*-indole-2-carboxamide) (235): A $CHCl_3$ (30 mL) solution of CDI (0.60 g, 3.70 mM) and indole-2-carboxylic acid (0.48 g, 2.94 mM) was heated at reflux for 11/4 hrs. A solution of 1,3-bis(aminomethyl)benzene (0.20 g, 1.47 mM) in DMF (5mL) was added drop-wise to the solution, which was then heated at reflux overnight. The solution was then left to cool to room temperature and ether (20 mL) added. The white precipitate that had formed was removed by suction filtration (ptt 1) and the filtrate was taken to dryness by evaporation under reduced pressure. The yellow solid produced was suspended in DCM (20 mL) and the solid isolated by suction filtration (ptt 2) and then washed with ether (10mL). Yeild 70 %, 0.44 g; m.p. 257-258 ºC; ^{1}H NMR (300 MHz, DMSO-d_6): δ: 4.52 (d, J = 5.85 Hz, 4 H), 7.04 (t, J = 6.96 Hz, 2 ArH), 7.16–7.30 (m, 4 ArH), 7.32-7.35 (m, 2 ArH), 7.43–7.62 (m, 2 ArH), 7.42 (d, J = 6.39 Hz, 2

ArH), 7.59 (d, J = 6.00 Hz, 2 ArH), 9.06 (s, NH amide, 2 H), 11.60 (s, NH indole, 2 H); $^{13}C\{^{1}H\}$ NMR (75 MHz, DMSO-d_6): δ: 42.2 (CH_2), 102.7 (ArCH), 112.3 (ArCH), 119.8 (ArCH), 121.5 (ArCH), 123.3 (ArCH), 125.9 (ArCH) , 126.3 (ArC), 127.1 (ArC), 128.4 (ArCH), 131.7 (ArC), 136.5 (ArC), 139.8 (ArC), 161.2 (CO); IR (film): ν = 3290 (indole NH stretching), 1620 (amide CO stretching), 1540 (amide CO stretching); LRMS (ES^-): m/z: Calcd: 421 $(M-H)^-$; Anal. Calcd. for "$C_{26}H_{22}N_4O_2$": C= 73.92%, H= 5.25%, N= 13.25% Found: C= 73.62%, H= 5.32%, N= 13.46%

N,N'-(pentane-1,5-diyl)bis(7-nitro-1*H*-indole-2-carboxamide (236): A solution of 7-nitro-1-indole carboxylic acid (0.63 g, 3.91 mM) and CDI (0.4g) in $CHCl_3$ (20mL) was heated at reflux for 11/2 hrs. After this time, 1,5-diaminopentane (0.1 g, 0.98 mM) in $CHCl_3$ (2 mL) was added drop-wise and heated at reflux over night. The reaction mixture was then left to cool to room temperature and the solution washed with water (3 x 50 mL). The organic phase was dried over $MgSO_4$. The solvent was then removed under reduced pressure and an orange solid was obtained. Flash chromatography DCM:MeOH 9:1 was then used to obtain the yellow product. Yield 47 %, 0.22 g; m.p. 200-202 ºC; ^{1}H NMR (300 MHz, DMSO-d_6): δ: 1.43 (m, 2 H), 1.63 (m, 4 H), 3.33 (m, 4 H) (obscured by water peak), 7.27-7.35 (m, 4 ArH), 8.14-8.22 (m, 4 ArH), 8.95 (s, NH amide, 2H), 10.70-10.81 (s, NH indole, 2 H); $^{13}C\{^{1}H\}$ NMR (75 MHz, DMSO-d_6): δ: 14.7 (CH_2), 24.0 (CH_2), 28.7 (CH_2), 106.04 (ArCH), 119.8 (ArCH), 120.9 (ArCH), 128.6 (ArCH), 130.5 (ArCH), 130.9 (ArC), 132.9 (ArC), 134.8 (ArC), 159.4 (CO); IR (film): ν = 3460 (amide NH stretching), 3370 (indole NH stretching), 2930 (amide NH stretching), 1630 (amide CO stretching), 1560 (amide CO stretching); LRMS (ES^-): m/z: 377 $(M-H)^-$; Anal. Calcd. for "$C_{23}H_{22}N_6O_6$": C= 57.74%, H= 4.63%, N= 17.56% Found: C= 57.41%, H= 4.71%, N= 17.82%

N,N'-(1,3-phenylenebis(methylene))bis(7-nitro-1H-indole-2-carboxamide) (237): A $CHCl_3$ (60 mL) solution of 7-nitroindole-2-carboxylic acid (0.61 g, 2.94 mM) and CDI (0.60 g, 3.70 mM) was stirred at reflux for 2 hrs. A DMF (5 mL) solution of bis(aminomethyl)benzene was then added drop-wise to the solution. This solution was then heated at reflux overnight and a yellow precipitate was removed by suction filtration. Ether (20 mL) was then added to the filtrate and the yellow precipitate produced was again

removed by suction filtration. The yellow precipitate was dried and then washed with a dilute HCL solution (100 mL) and dried with ether (15 mL). Yeild 72 %, 0.55 g; m.p. 268-269 ºC; ^{1}H NMR (400 MHz, DMSO-d_6): δ: 4.54 (d, J = 6.00 Hz, 4 H), 7.26–7.40 (m, 8 ArH), 8.11 (d, J = 7.52 Hz, 2 ArH), 8.17 (d, J = 8.04 Hz, 2 ArH), 9.55 (t, J = 6.00 Hz, NH amide, 2 H), 11.27 (s, NH amide, 2 H); ^{13}C{^{1}H} NMR (100 MHz, DMSO-d_6): δ: 42.8 (CH_2), 106.9 (ArCH), 120.3 (ArCH), 121.5 (ArCH), 126.6 (ArCH), 126.6 (ArCH), 128.9 (ArCH), 129.1 (ArC), 130.9 (ArCH), 131.3 (ArC), 133.4 (ArC), 134.9 (ArC), 139.8 (ArC), 159.9 (CO); IR (film): ν = 3460 (amide NH stretching), 3450 (indole NH stretching), 1640 (amide CO stretching), 1560 (amide CO stretching); LRMS (ES$^-$): m/z: 511 (M-H)$^-$; Anal. Calcd. for "$C_{26}H_{20}N_6O_6$": C= 60.94%, H= 3.93%, N= 16.40% Found: C= 61.05%, H= 3.97%, N= 16.32%

N-(1-(7-nitro-1H-indole-2-carboxamido)-3,6-dichloro-9H-carbazol-8-yl)-7-nitro-1H-indole-2-carboxamide (238): 7-Nitroindole-2carboxylic acid (0.31 g, 1.51 mM) was dissolved in dry DMF (15 mL) with PyBOP (0.99 g, 1.91 mM) and HOBt (catalytic amount). This solution was left to stir at room temperature for 30 mins. A solution of 1,8-Diamino-3,6-dichlorocarbazole[114] (0.20 g, 0.75 mM) and dry NEt_3 (0.3 mL) in dry DMF (5 mL) was also left to stir for 30 mins at room temperature. After this time, the amine solution was added acid solution drop-wise. The solution was then left stirring at room temperature over the weekend. The green/yellow precipitate formed was then removed by suction filtration and dried overnight under vacuum at 65 ºC. The solid was heated at reflux in MeOH (200 mL) overnight. The yellow solid formed was then removed by suction filtration, washed with ether (20 mL) and dried under vacuum. Yield 52 %, 0.48 g; decomp. 210 ºC; ^{1}H NMR (300 MHz, DMSO-d_6): δ: 7.34 (t, J = 7.92 Hz, 2 ArH), 7.67(d, J = 1.89Hz, 2 ArH), 7.83 (d, J = 1.89Hz, 2 ArH), 8.25-8.27 (m, 6 ArH), 10.96 (s, NH amide, 2 H), 11.06 (s, NH carbazole, 1 H), 11.61 (s, NH indole, 2 H); ^{13}C{^{1}H} NMR (75 MHz, DMSO-d_6): δ: 107.9 (ArCH), 117.7 (ArCH), 120.2 (ArCH), 121.1 (ArCH), 121.6 (ArC), 123.1 (ArCH), 123.4 (ArC), 124.4 (ArC), 128.9 (ArC), 130.7 (ArCH), 130.8 (ArC), 132.2 (ArC), 133.1 (ArC), 133.9 (ArC), 158.7 (CO); IR (film): ν = 3460 (amide NH stretching), 3210 (indole/carbazole NH stretching), 3080 (amide NH stretching), 1650 (amide CO stretching), 1550 (amide CO stretching); LRMS (ES$^-$): m/z: 640 (M-H)$^-$; Anal. Calcd. for

"$C_{30}H_{17}Cl_2N_7O_6$": C= 56.09%, H= 2.97%, N= 15.25% Found: C= 55.69%, H= 2.75%, N= 15.01%

N^2,N^6-di(9H-carbazol-1-yl)pyridine-2,6-dicarboxamide (241): A solution of 2, 6-pyridinedicarboxylic acid (0.10 g, 0.59 mM) and CDI (0.29 g, 1.77 mM) in $CHCl_3$ (20 mL) DMF (0.5 mL) was heated at reflux for 1 ½ hrs. A solution of 1-aminocarbazole (0.21 g, 1.77 mM) in $CHCl_3$ (20 mL) was then added drop-wise and the solution heated at reflux overnight. A solid was then removed by filtration and the filtrate washed with water (250 mL). A precipitate was then removed by filtration of the organic phase. The filtrate was then taken to dryness and the resultant oil sonicated for 5 min in ether (30 mL) and a green solid collected by filtation and washed with ether (10 mL). Yield 43 %, 0.13g; m.p. >250 ºC; ^{1}H NMR (300 MHz, DMSO-d_6): δ: 7.17-7.26 (m, 4 ArH), 7.43 (dt, J_1 = 0.72 Hz, J_2 = 7.32 Hz, 2 ArH), 8.09 (d, J = 7.68 Hz, 2 ArH), 8.16 (d, J = 7.68 Hz, 2 ArH), 8.40 (t, J = 24.12 Hz, 1 ArH), 8.52 (d, J = 1.08 Hz, 2 ArH), 11.18 (s, NH carbazole, 2 H), 11.37 (s, NH amide, 2 H); ^{13}C NMR (75 MHz, DMSO-d_6): δ: 111.2 (ArCH), 118.3 (ArCH), 118.4 (ArCH), 118.8 (ArCH), 120.3 (ArCH), 121.2 (ArC), 122.4 (ArC), 122.5 (ArCH), 123.8 (ArC), 125.2 (ArCH), 125.9 (ArCH), 135.2 (ArC), 139.7 (ArC), 139.9 (ArCH), 148.8 (ArC), 162.1 (CO); IR (film): ν = 3290 (indole/carbazole NH stretching), 3040 (amide NH stretching), 1650 (amide CO stretching), 1550 (amide CO stretching); LRMS (ES^-): m/z: 494 $[M-H]^-$; HRMS (ES^+): m/z: Act.: 518.1587 $[M+Na]^+$ Calcd.: 518.1580 $[M+Na]^+$.

N^1,N^3-di(9H-carbazol-1-yl)isophthalamide (242): A solution of isophthalic acid (0.08 g, 0.47 mM), PyBOP (0.62 g, 1.19 mM) and HOBt (catalytic amount) in DMF (3.5 mL) and DCM (30 mL) was stirred at room temperature under dry conditions for 30 mins. A solution of 1-aminocarbazole (0.17 g, 0.94 mM) and NEt_3 (0.2 mL) in DCM (10 mL) was also stirred at room temperature under dry conditions for 30 mins. The amine solution was then added drop-wise to the acidic solution. The mixture was then allowed to stir under dry conditions at room temperature for 3 days. After this time, the solution was washed with water (350 mL) and a white solid collected from the organic phase, which was washed with DCM (20 mL) and dried under reduced pressure. Yeild 50 %, 0.12g; m.p. >250 ºC; ^{1}H NMR (300 MHz, DMSO-d_6): δ: 7.16-7.24 (m, 4 ArH), 7.41 (dt, J_1 = 1.08 Hz, J_2 = 8.04 Hz, 2 ArH), 7.56-7.63 (m, 4 ArH), 7.81 (t, J = 7.68 Hz, 1 ArH), 8.06 (d, J = 7.32

Hz, 2 ArH), 8.15 (d, J = 7.32 Hz, 2 ArH), 8.37 (dd, J_1 = 1.44 Hz, J_2 = 8.04 Hz, 2 ArH), 8.83 (s, 1 ArH), 10.49 (s, indole NH, 2H), 11.03 (s, amide NH, 2H); ^{13}C NMR (75 MHz, DMSO-d_6): δ: 111.3 (ArCH), 117.6 (ArCH), 118.5 (ArCH), 118.8 (ArCH), 120.3 (ArCH), 121.1 (ArCH), 122.3 (ArC), 122.5 (ArC), 123.9 (ArC), 125.8 (ArCH), 127.8 (ArCH), 128.5 (ArCH), 131.0 (ArCH), 134.1 (ArC), 134.9 (ArC), 139.6 (ArC), 165.1 (CO); IR (film): ν = 3440 (amide NH stretching), 3340 (carbazole NH stretching), 3030 (amide NH stretching), 1630 (amide CO stretching), 1530 (amide CO stretching); LRMS (ES^-): m/z: 493 $[M-H]^-$; HRMS (ES^+): m/z: Act.: 517.1631 $[M+Na]^+$ Calcd.: 517.1635 $[M+Na]^+$.

References

(1) Bates, G. W.; Gale, P. A.; Light, M. E. *Chemical Communications* 2007, 2121-2123.

(2) Bates, G. W.; Triyanti; Light, M. E.; Albrecht, M.; Gale, P. A. *Journal of Organic Chemistry* 2007, *72*, 8921-8927.

(3) Zielinski, T.; Dydio, P.; Jurczak, J. *Tetrahedron* 2008, *64*, 568-574.

(4) Lehn, J. M. *Proceedings of the National Academy of Sciences* 2002, *99*, 4763–4768.

(5) Steed, J. W.; Atwood, J. L. *Supramolecular Chemistry second edition*; John Wiley & Sons: Chichester, 2009.

(6) Beer, P. D.; Gale, P. A.; Smith, D. K. *Supramolecular Chemistry*; Oxford Science Publications, 1999; Vol. 74.

(7) Desiraju, G. R. *Accounts of Chemical Research* 2002, *35*, 565-573.

(8) Emsley, J. *Progress in Inorganic Chemistry* 1968, *9*, 91-124.

(9) Sessler, J. L.; Gale, P. A.; Cho, W. S. *Anion Receptor Chemistry*; The Royal Society of Chemistry: Cambridge, 2006.

(10) Beer, P. D.; Gale, P. A. *Angewandte Chemie International Edition* 2001, *40*, 486-516.

(11) Bell, R. A.; Christoph, G. G.; Fronczek, F. R.; Marsh, R. E. *Science* 1975, *190*, 150-152.

(12) Pascal, R. A.; Spergel, J.; Vanengen, D. *Tetrahedron Letters* 1986, *27*, 4099-4102.

(13) Valiyayeettil, S.; Engbersen, J. F. J.; Verboom, W.; Reinhoudt, D. N. *Angewandte Chemie-International Edition in English* 1993, *32*, 900-901.

(14) Winstanley, K. J.; Allen, S. J.; Smith, D. K. *Chemical Communications* 2009, 4299-4301.

(15) Berezin, S. K.; Davis, J. T. *Journal of the American Chemical Society* 2009, *131*, 2458-2459.

(16) Kavallieratos, K.; deGala, S. R.; Austin, D. J.; Crabtree, R. H. *Journal of the American Chemical Society* 1997, *119*, 2325-2326.

(17) Kavallieratos, K.; Bertao, C. M.; Crabtree, R. H. *Journal of Organic Chemistry* 1999, *64*, 1675-1683.

(18) Brooks, S. L.; Garcia-Garrido, S. E.; Light, M. E.; Cole, P. A.; Gale, P. A. *Chemistry-a European Journal* 2007, *13*, 3320-3329.

(19) Chmielewski, M. J.; Jurczak, J. *Chemistry-a European Journal* 2005, *11*, 6080-6094.

(20) Chmielewski, M. J.; Jurczak, J. *Chemistry-a European Journal* 2006, *12*, 7652-7667.

(21) Hunter, C. A.; Purvis, D. H. *Angewandte Chemie-International Edition in English* 1992, *31*, 792-795.

(22) Santacroce, P. V.; Davis, J. T.; Light, M. E.; Gale, P. A.; Iglesias-Sanchez, J. C.; Prados, P.; Quesada, R. *Journal of the American Chemical Society* 2007, *129*, 1886-1887.

(23) Hughes, M. P.; Smith, B. D. *Journal of Organic Chemistry* 1997, *62*, 4492-4499.

(24) Ghosh, K.; Sarkar, A. R.; Masanta, G. *Tetrahedron Letters* 2007, *48*, 8725-8729.

(25) Dorazco-Gonzalez, A.; Hopfl, H.; Medrano, F.; Yatsimirsky, A. K. *Journal of Organic Chemistry* 2010, *75*, 2259-2273.

(26) Webb, J. E. A.; Crossley, M. J.; Turner, P.; Thordarson, P. *Journal of the American Chemical Society* 2007, *129*, 7155-7162.

(27) Prohens, R.; Tomas, S.; Morey, J.; Deya, P. M.; Ballester, P.; Costa, A. *Tetrahedron Letters* 1998, *39*, 1063-1066.

(28) Arunachalam, M.; Ghosh, P. *Chemical Communications* 2009, 5389-5391.

(29) Arunachalam, M.; Ghosh, P. *Inorganic Chemistry* 2010, *49*, 943-951.

(30) Arunachalam, M.; Ghosh, P. *Organic Letters* 2010, *12*, 328-331.

(31) Gong, W. T.; Hiratani, K. *Tetrahedron Letters* 2008, *49*, 5655-5657.

(32) Khatri, V. K.; Upreti, S.; Pandey, P. S. *Organic Letters* 2006, *8*, 1755-1758.

(33) Davis, A. P.; Perry, J. J.; Williams, R. P. *Journal of the American Chemical Society* 1997, *119*, 1793-1794.

(34) Choi, K. H.; Hamilton, A. D. *Journal of the American Chemical Society* 2001, *123*, 2456-2457.

(35) Choi, K. H.; Hamilton, A. D. *Journal of the American Chemical Society* 2003, *125*, 10241-10249.

(36) Kang, S. O.; Powell, D.; Bowman-James, K. *Journal of the American Chemical Society* 2005, *127*, 13478-13479.

(37) Kang, S. O.; Powell, D.; Day, V. W.; Bowman-James, K. *Angewandte Chemie-International Edition* 2006, *45*, 1921-1925.

(38) Kubik, S.; Goddard, R.; Kirchner, R.; Nolting, D.; Seidel, J. *Angewandte Chemie-International Edition* 2001, *40*, 2648-2651.

(39) Kubik, S.; Kirchner, R.; Nolting, D.; Seidel, J. *Journal of the American Chemical Society* 2002, *124*, 12752-12760.

(40) Sansone, F.; Baldini, L.; Casnati, A.; Lazzarotto, M.; Ugozzoli, F.; Ungaro, R. *Proceedings of the National Academy of Sciences of the United States of America* 2002, *99*, 4842-4847.

(41) Lankshear, M. D.; Cowley, A. R.; Beer, P. D. *Chemical Communications* 2006, 612-614.

(42) Gomez, D. E.; Fabbrizzi, L.; Licchelli, M.; Monzani, E. *Organic & Biomolecular Chemistry* 2005, *3*, 1495-1500.

(43) Hughes, M. P.; Shang, M. Y.; Smith, B. D. *Journal of Organic Chemistry* 1996, *61*, 4510-4511.

(44) Camiolo, S.; Gale, P. A.; Hursthouse, M. B.; Light, M. E. *Organic & Biomolecular Chemistry* 2003, *1*, 741-744.

(45) Camiolo, S.; Gale, P. A.; Hursthouse, M. B.; Light, M. E.; Shi, A. J. *Chemical Communications* 2002, 758-759.

(46) Amendola, V.; Esteban-Gomez, D.; Fabbrizzi, L.; Licchelli, M. *Accounts of Chemical Research* 2006, *39*, 343-353.

(47) Boiocchi, M.; Del Boca, L.; Gomez, D. E.; Fabbrizzi, L.; Licchelli, M.; Monzani, E. *Journal of the American Chemical Society* 2004, *126*, 16507-16514.

(48) Gunnlaugsson, T.; Davis, A. P.; Glynn, M. *Chemical Communications* 2001, 2556-2557.

(49) Gunnlaugsson, T.; Davis, A. P.; Hussey, G. M.; Tierney, J.; Glynn, M. *Organic & Biomolecular Chemistry* 2004, *2*, 1856-1863.

(50) Gunnlaugsson, T.; Kruger, P. E.; Jensen, P.; Pfeffer, F. M.; Hussey, G. M. *Tetrahedron Letters* 2003, *44*, 8909-8913.

(51) Gunnlaugsson, T.; Kruger, P. E.; Lee, T. C.; Parkesh, R.; Pfeffer, F. M.; Hussey, G. M. *Tetrahedron Letters* 2003, *44*, 6575-6578.

(52) Pfeffer, F. M.; Buschgens, A. M.; Barnett, N. W.; Gunnlaugsson, T.; Kruger, P. E. *Tetrahedron Letters* 2005, *46*, 6579-6584.

(53) Kondo, S.; Nagamine, M.; Yano, Y. *Tetrahedron Letters* 2003, *44*, 8801-8804.

(54) Kim, S. K.; Kim, H. N.; Xiaoru, Z.; Lee, H. N.; Soh, J. H.; Swamyand, K. M. K.; Yoon, J. *Supramolecular Chemistry* 2007, *19*, 221-227.

(55) Kwon, J. Y.; Jang, Y. J.; Kim, S. K.; Lee, K. H.; Kim, J. S.; Yoon, J. Y. *Journal of Organic Chemistry* 2004, *69*, 5155-5157.

(56) Kluciar, M.; Ferreira, R.; de Castro, B.; Pischel, U. *Journal of Organic Chemistry* 2008, *73*, 6079-6085.

(57) Pfeffer, F. M.; Gunnlaugsson, T.; Jensen, P.; Kruger, P. E. *Organic Letters* 2005, *7*, 5357-5360.

(58) Ayling, A. J.; Perez-Payan, M. N.; Davis, A. P. *Journal of the American Chemical Society* 2001, *123*, 12716-12717.

(59) Clare, J. P.; Ayling, A. J.; Joos, J. B.; Sisson, A. L.; Magro, G.; Perez-Payan, M. N.; Lambert, T. N.; Shukla, R.; Smith, B. D.; Davis, A. P. *Journal of the American Chemical Society* 2005, *127*, 10739-10746.

(60) Koulov, A. V.; Lambert, T. N.; Shukla, R.; Jain, M.; Boon, J. M.; Smith, B. D.; Li, H. Y.; Sheppard, D. N.; Joos, J. B.; Clare, J. P.; Davis, A. P. *Angewandte Chemie-International Edition* 2003, *42*, 4931-4933.

(61) Brooks, S. J.; Edwards, P. R.; Gale, P. A.; Light, M. E. *New Journal of Chemistry* 2006, *30*, 65-70.

(62) Brooks, S. J.; Gale, P. A.; Light, M. E. *Chemical Communications* 2005, 4696-4698.

(63) Lakshminarayanan, P. S.; Ravikumar, I.; Suresh, E.; Ghosh, P. *Chemical Communications* 2007, 5214-5216.

(64) Custelcean, R.; Moyer, B. A.; Hay, B. P. *Chemical Communications* 2005, 5971-5973.

(65) Custelcean, R.; Remy, P.; Bonnesen, P. V.; Jiang, D. E.; Moyer, B. A. *Angewandte Chemie-International Edition* 2008, *47*, 1866-1870.

(66) McCleskey, S. C.; Griffin, M. J.; Schneider, S. E.; McDevitt, J. T.; Anslyn, E. V. *Journal of the American Chemical Society* 2003, *125*, 1114-1115.

(67) Haino, T.; Nakamura, M.; Kato, N.; Hiraoka, M.; Fukazawa, Y. *Tetrahedron Letters* 2004, *45*, 2281-2284.

(68) Kyne, G. M.; Light, M. E.; Hursthouse, M. B.; de Mendoza, J.; Kilburn, J. D. *Journal of the Chemical Society-Perkin Transactions 1* 2001, 1258-1263.

(69) Rossi, S.; Kyne, G. M.; Turner, D. L.; Wells, N. J.; Kilburn, J. D. *Angewandte Chemie-International Edition* 2002, *41*, 4233-4236.

(70) Lee, K. H.; Hong, J. I. *Tetrahedron Letters* 2000, *41*, 6083-6087.

(71) Meshcheryakov, D.; Arnaud-Neu, F.; Bohmer, V.; Bolte, M.; Cavaleri, J.; Hubscher-Bruder, V.; Thondorf, I.; Werner, S. *Organic & Biomolecular Chemistry* 2008, *6*, 3244-3255.

(72) Snellink-Ruel, B. H. M.; Antonisse, M. M. G.; Engbersen, J. F. J.; Timmerman, P.; Reinhoudt, D. N. *European Journal of Organic Chemistry* 2000, 165-170.

(73) Hisaki, I.; Sasaki, S. I.; Hirose, K.; Tobe, Y. *European Journal of Organic Chemistry* 2007, 607-615.

(74) Vacca, A.; Nativi, C.; Cacciarini, M.; Pergoli, R.; Roelens, S. *Journal of the American Chemical Society* 2004, *126*, 16456-16465.

(75) Bordwell, F. G. *Accounts of Chemical Research* 1988, *21*, 456-463.

(76) Bordwell, F. G.; Drucker, G. E.; Fried, H. E. *Journal of Organic Chemistry* 1981, *46*, 632-635.

(77) Gale, P. A.; Anzenbacher, P.; Sessler, J. L. *Coordination Chemistry Reviews* 2001, *222*, 57-102.

(78) Sessler, J. L.; Camiolo, S.; Gale, P. A. *Coordination Chemistry Reviews* 2003, *240*, 17-55.

(79) Coles, S. J.; Gale, P. A.; Hursthouse, M. B. *Crystengcomm* 2001, art. no.-53.

(80) Camiolo, S.; Gale, P. A.; Hursthouse, M. B.; Light, M. E. *Tetrahedron Letters* 2002, *43*, 6995-6996.

(81) Gale, P. A.; Camiolo, S.; Tizzard, G. J.; Chapman, C. P.; Light, M. E.; Coles, S. J.; Hursthouse, M. B. *Journal of Organic Chemistry* 2001, *66*, 7849-7853.

(82) Gale, P. A.; Navakhun, K.; Camiolo, S.; Light, M. E.; Hursthouse, M. B. *Journal of the American Chemical Society* 2002, *124*, 11228-11229.

(83) Vega, I. E.; Camiolo, S.; Gale, P. A.; Hursthouse, M. B.; Light, M. E. *Chemical Communications* 2003, 1686-1687.

(84) Vega, I. E.; Gale, P. A.; Hursthouse, M. B.; Light, M. E. *Organic & Biomolecular Chemistry* 2004, *2*, 2935-2941.

(85) Sessler, J. L.; Barkey, N. M.; Pantos, G. D.; Lynch, V. M. *New Journal of Chemistry* 2007, *31*, 646-654.

(86) Black, C. B.; Andrioletti, B.; Try, A. C.; Ruiperez, C.; Sessler, J. L. *Journal of the American Chemical Society* 1999, *121*, 10438-10439.

(87) Shevchuk, S. V.; Lynch, V. M.; Sessler, J. L. *Tetrahedron* 2004, *60*, 11283-11291.

(88) Schmuck, C. *Journal of Organic Chemistry* 2000, *65*, 2432-2437.

(89) Schmuck, C.; Heil, M. *Organic Letters* 2001, *3*, 1253-1256.

(90) Schmuck, C.; Geiger, L. *Chemical Communications* 2004, 1698-1699.

(91) Schmuck, C.; Geiger, L. *Chemical Communications* 2005, 772-774.

(92) Sessler, J. L.; Cyr, M. J.; Lynch, V.; McGhee, E.; Ibers, J. A. *Journal of the American Chemical Society* 1990, *112*, 2810-2813.

(93) Bauer, V. J.; Clive, D. L. J.; Dolphin, D.; Paine, J. B.; Harris, F. L.; King, M. M.; Loder, J.; Wang, S. C.; Woodward, R. B. *Journal of the American Chemical Society* 1983, *105*, 6429-6436.

(94) Kral, V.; Furuta, H.; Shreder, K.; Lynch, V.; Sessler, J. L. *Journal of the American Chemical Society* 1996, *118*, 1595-1607.

(95) Sessler, J. L.; Katayev, E.; Pantos, G. D.; Ustynyuk, Y. A. *Chemical Communications* 2004, 1276-1277.

(96) Sessler, J. L.; Katayev, E.; Pantos, G. D.; Scherbakov, P.; Reshetova, M. D.; Khrustalev, V. N.; Lynch, V. M.; Ustynyuk, Y. A. *Journal of the American Chemical Society* 2005, *127*, 11442-11446.

(97) Troisi, F.; Gaeta, C.; Pierro, T.; Neri, P. *Tetrahedron Letters* 2009, *50*, 5113-5115.

(98) Baeyer, A. *Berichte der deutschen chemischen Gesellschaft* 1886, *19*, 2184-2185.

(99) Gale, P. A.; Sessler, J. L.; Kral, V.; Lynch, V. *Journal of the American Chemical Society* 1996, *118*, 5140-5141.

(100) Custelcean, R.; Delmau, L. H.; Moyer, B. A.; Sessler, J. L.; Cho, W. S.; Gross, D.; Bates, G. W.; Brooks, S. J.; Light, M. E.; Gale, P. A. *Angewandte Chemie-International Edition* 2005, *44*, 2537-2542.

(101) Schmidtchen, F. P. *Organic Letters* 2002, *4*, 431-434.

(102) Sessler, J. L.; Gross, D. E.; Cho, W. S.; Lynch, V. M.; Schmidtchen, F. P.; Bates, G. W.; Light, M. E.; Gale, P. A. *Journal of the American Chemical Society* 2006, *128*, 12281-12288.

(103) Bates, G. W.; Gale, P. A.; Light, M. E. *Crystengcomm* 2006, *8*, 300-302.

(104) Tong, C. C.; Quesada, R.; Sessler, J. L.; Gale, P. A. *Chemical Communications* 2008, 6321-6323.

(105) Sessler, J. L.; Cho, W. S.; Gross, D. E.; Shriver, J. A.; Lynch, V. M.; Marquez, M. *Journal of Organic Chemistry* 2005, *70*, 5982-5986.

(106) Gale, P. A.; Tong, C. C.; Haynes, C. J. E.; Adeosun, O.; Gross, D. E.; Karnas, E.; Sedenberg, E. M.; Quesada, R.; Sessler, J. L. *Journal of the American Chemical Society* 2010, *132*, 3240-+.

(107) Warriner, C. N.; Gale, P. A.; Light, M. E.; Hursthouse, M. B. *Chemical Communications* 2003, 1810-1811.

(108) Lee, C. H.; Miyaji, H.; Yoon, D. W.; Sessler, J. L. *Chemical Communications* 2008, 24-34.

(109) Yoon, D. W.; Hwang, H.; Lee, C. H. *Angewandte Chemie-International Edition* 2002, *41*, 1757-+.

(110) Lee, C. H.; Lee, J. S.; Na, H. K.; Yoon, D. W.; Miyaji, H.; Cho, W. S.; Sessler, J. L. *Journal of Organic Chemistry* 2005, *70*, 2067-2074.

(111) Miyaji, H.; Hong, S. J.; Jeong, S. D.; Yoon, D. W.; Na, H. K.; Hong, J.; Ham, S.; Sessler, J. L.; Lee, C. H. *Angewandte Chemie-International Edition* 2007, *46*, 2508-2511.

(112) Fisher, M. G.; Gale, P. A.; Hiscock, J. R.; Hursthouse, M. B.; Light, M. E.; Schmidtchen, F. P.; Tong, C. C. *Chemical Communications* 2009, 3017-3019.

(113) Black, D. S.; Craig, D. C.; Kumar, N.; McConnell, D. B. *Tetrahedron Letters* 1996, *37*, 241-244.

(114) Chmielewski, M. J.; Charon, M.; Jurczak, J. *Organic Letters* 2004, *6*, 3501-3504.

(115) Curiel, D.; Cowley, A.; Beer, P. D. *Chemical Communications* 2005, 236-238.

(116) Chang, K. J.; Moon, D.; Lah, M. S.; Jeong, K. S. *Angewandte Chemie-International Edition* 2005, *44*, 7926-7929.

(117) Gale, P. A. *Chemical Communications* 2008, 4525-4540.

(118) Suk, J. M.; Chae, M. K.; Kim, N. K.; Kim, U. I.; Jeong, K. S. *Pure and Applied Chemistry* 2008, *80*, 599-608.

(119) He, J. J.; Quiocho, F. A. *Protein Science* 1993, *2*, 1643-1647.

(120) Bartlett, G. J.; Porter, C. T.; Borkakoti, N.; Thornton, J. M. *Journal of Molecular Biology* 2002, *324*, 105-121.

(121) He, J. J.; Quiocho, F. A. *Science* 1991, *251*, 1479-1481.

(122) Pflugrath, J. W.; Quiocho, F. A. *Nature* 1985, *314*, 257-260.

(123) Pflugrath, J. W.; Quiocho, F. A. *Journal of Molecular Biology* 1988, *200*, 163-180.

(124) Verschueren, K. H. G.; Seljee, F.; Rozeboom, H. J.; Kalk, K. H.; Dijkstra, B. W. *Nature* 1993, *363*, 693-698.

(125) Qatsha, K. A.; Rudolph, C.; Marme, D.; Schachtele, C.; May, W. S. *Proceedings of the National Academy of Sciences of the United States of America* 1993, *90*, 4674-4678.

(126) Thangadurai, T. D.; Singh, N. J.; Hwang, I. C.; Lee, J. W.; Chandran, R. P.; Kim, K. S. *Journal of Organic Chemistry* 2007, *72*, 5461-5464.

(127) Yu, M.; Lin, H. *Supramolecular Chemistry* 2008, *20*, 357-361.

(128) Gross, D. E.; Mikkilineni, V.; Lynch, V. M.; Sessler, J. L. *Supramolecular Chemistry* 2009, *22*, 135-141.

(129) Piatek, P.; Lynch, V. M.; Sessler, J. L. *Journal of the American Chemical Society* 2004, *126*, 16073-16076.

(130) Sessler, J. L.; Cho, D. G.; Lynch, V. *Journal of the American Chemical Society* 2006, *128*, 16518-16519.

(131) Wang, T.; Bai, Y.; Ma, L.; Yan, X. P. *Organic & Biomolecular Chemistry* 2008, *6*, 1751-1755.

(132) He, X. M.; Hu, S. Z.; Liu, K.; Guo, Y.; Xu, J.; Shao, S. J. *Organic Letters* 2006, *8*, 333-336.

(133) Nishiki, M.; Oi, W.; Ito, K. *Journal of Inclusion Phenomena and Macrocyclic Chemistry* 2008, *61*, 61-69.

(134) Yu, J. O.; Browning, C. S.; Farrar, D. H. *Chemical Communications* 2008, 1020-1022.

(135) Pfeffer, F. M.; Lim, K. F.; Sedgwick, K. J. *Organic & Biomolecular Chemistry* 2007, *5*, 1795-1799.

(136) Qing, G. Y.; He, Y. B.; Wang, F.; Qin, H. J.; Hu, C. G.; Yang, X. *European Journal of Organic Chemistry* 2007, 1768-1778.

(137) Lee, J. Y.; Lee, M. H.; Jeong, K. S. *Supramolecular Chemistry* 2007, *19*, 257-263.

(138) Chang, K. J.; Chae, M. K.; Lee, C.; Lee, J. Y.; Jeong, K. S. *Tetrahedron Letters* 2006, *47*, 6385-6388.

(139) Kwon, T. H.; Jeong, K. S. *Tetrahedron Letters* 2006, *47*, 8539-8541.

(140) Ju, J.; Park, M.; Suk, J. M.; Lah, M. S.; Jeong, K. S. *Chemical Communications* 2008, 3546-3548.

(141) Chang, K. J.; Kang, B. N.; Lee, M. H.; Jeong, K. S. *Journal of the American Chemical Society* 2005, *127*, 12214-12215.

(142) Kim, U. I.; Suk, J. M.; Naidu, V. R.; Jeong, K. S. *Chemistry-a European Journal* 2008, *14*, 11406-11414.

(143) Kim, J. I.; Juwarker, H.; Liu, X.; Lah, M. S.; Jeong, K. S. *Chemical Communications* 2010, *46*, 764-766.

(144) Kim, N. K.; Chang, K. J.; Moon, D.; Lah, M. S.; Jeong, K. S. *Chemical Communications* 2007, 3401-3403.

(145) Chae, M. K.; Lee, J. I.; Kim, N. K.; Jeong, K. S. *Tetrahedron Letters* 2007, *48*, 6624-6627.

(146) Chmielewski, M. J.; Zhao, L. Y.; Brown, A.; Curiel, D.; Sambrook, M. R.; Thompson, A. L.; Santos, S. M.; Felix, V.; Davis, J. J.; Beer, P. D. *Chemical Communications* 2008, 3154-3156.

(147) Lin, C. I.; Selvi, S.; Fang, J. M.; Chou, P. T.; Lai, C. H.; Cheng, Y. M. *Journal of Organic Chemistry* 2007, *72*, 3537-3542.

(148) Nishizawa, S.; Buhlmann, P.; Iwao, M.; Umezawa, Y. *Tetrahedron Letters* 1995, *36*, 6483-6486.

(149) Smith, P. J.; Reddington, M. V.; Wilcox, C. S. *Tetrahedron Letters* 1992, *33*, 6085-6088.

(150) Caltagirone, C.; Gale, P. A.; Hiscock, J. R.; Brooks, S. J.; Hursthouse, M. B.; Light, M. E. *Chemical Communications* 2008, 3007-3009.

(151) Caltagirone, C.; Hiscock, J. R.; Hursthouse, M. B.; Light, M. E.; Gale, P. A. *Chemistry-a European Journal* 2008, *14*, 10236-10243.

(152) Sitzmann, M. E.; Gilligan, W. H. *Journal of Organic Chemistry* 1985, *50*, 5879-5881.

(153) Hynes, M. J. *Journal of the Chemical Society-Dalton Transactions* 1993, 311-312.

(154) Job, P. 1928, *9*, 113-203.

(155) Hamza, A.; Schubert, G.; Soos, T.; Papai, I. *Journal of the American Chemical Society* 2006, *128*, 13151-13160.

(156) Hiscock, J. R.; Caltagirone, C.; Light, M. E.; Hursthouse, M. B.; Gale, P. A. *Organic & Biomolecular Chemistry* 2009, *7*, 1781-1783.

(157) Hiscock, J. R.; Gale, P. A.; Caltagirone, C.; Hursthouse, M. B.; Light, M. E. *Supramolecular Chemistry* 2010.

(158) Merisor, E.; Beifuss, U. *Tetrahedron Letters* 2007, *48*, 8383-8387.

(159) Cadogan, J. I. G.; Hutchison, H. S.; McNab, H. *Journal of the Chemical Society-Perkin Transactions 1* 1987, 1407-1411.

(160) Light, M. E.; Gale, P. A.; Navakhun, K.; Maynard-Smith, M. *Acta Crystallographica Section E-Structure Reports Online* 2005, *61*, O1302-O1303.

(161) Gale, P. A. *Accounts of Chemical Research* 2006, *39*, 465-475.

(162) Evans, L. S.; Gale, P. A.; Light, M. E.; Quesada, R. *New Journal of Chemistry* 2006, *30*, 1019-1025.

(163) Evans, L. S.; Gale, P. A.; Light, M. E.; Quesada, R. *Chemical Communications* 2006, 965-967.

(164) Caltagirone, C.; Bates, G. W.; Gale, P. A.; Light, M. E. *Chemical Communications* 2008, 61-63.

(165) Duke, R. M.; O'Brien, J. E.; McCabe, T.; Gunnlaugsson, T. *Organic & Biomolecular Chemistry* 2008, *6*, 4089-4092.

(166) Ali, H. D. P.; Kruger, P. E.; Gunnlaugsson, T. *New Journal of Chemistry* 2008, *32*, 1153-1161.

(167) Arnendola, V.; Bonizzoni, M.; Esteban-Gomez, D.; Fabbrizzi, L.; Licchelli, M.; Sancenon, F.; Taglietti, A. *Coordination Chemistry Reviews* 2006, *250*, 1451-1470.

(168) Costero, A. M.; Banuls, M. J.; Aurell, M. J.; Ward, M. D.; Argent, S. *Tetrahedron* 2004, *60*, 9471-9478.

(169) Wu, B.; Liang, J. J.; Yang, J.; Jia, C. D.; Yang, X. J.; Zhang, H. R.; Tang, N.; Janiak, C. *Chemical Communications* 2008, 1762-1764.

(170) Zhuge, F. Y.; Wu, B. A.; Liang, J. J.; Yang, J.; Liu, Y. Y.; Jia, C. D.; Janiak, C.; Tang, N.; Yang, X. J. *Inorganic Chemistry* 2009, *48*, 10249-10256.

(171) Xu, H.; Strater, N.; Schroder, W.; Bottcher, C.; Ludwig, K.; Saenger, W. *Acta Crystallographica Section D-Biological Crystallography* 2003, *59*, 815-822.

(172) Freeman, R. M.; Richards, C. J. *Kidney International* 1979, *15*, 167-175.

(173) Moyer, B. A.; Delmau, L. H.; Fowler, C. J.; Ruas, A.; Bostick, D. A.; Sessler, J. L.; Katayev, E.; Pantos, G. D.; Llinares, J. M.; Hossain, A.; Kang, S. O.; Bowman-James, K. In *Advances in Inorganic Chemistry: Including Bioinorganic Studies, Vol 59 - Template Effects and Molecular Organization*; VanEldik, R., BowmanJames, K., Eds. 2007; Vol. 59, p 175-204.

(174) Galbraith, S. G.; Tasker, P. A. *Supramolecular Chemistry* 2005, *17*, 191-207.

(175) Galbraith, S. G.; Wang, Q.; Li, L.; Blake, A. J.; Wilson, C.; Collinson, S. R.; Lindoy, L. F.; Plieger, P. G.; Schroder, M.; Tasker, P. A. *Chemistry-a European Journal* 2007, *13*, 6091-6107.

(176) Plieger, P. G.; Tasker, P. A.; Galbraith, S. G. *Dalton Transactions* 2004, 313-318.

(177) Gale, P. A.; Hiscock, J. R.; Moore, S. J.; Caltagirone, C.; Hursthouse, M. B.; Light, M. E. *Chemistry-an Asian Journal* 2010, *5*, 555-561.

(178) Gale, P. A.; Hiscock, J. R.; Jie, C. Z.; Hursthouse, M. B.; Light, M. E. *Chemical Science* 2010, *1*, 215-220.

(179) Kubik, S.; Reyheller, C.; Stuwe, S. *Journal of Inclusion Phenomena and Macrocyclic Chemistry* 2005, *52*, 137-187.

(180) Llinares, J. M.; Powell, D.; Bowman-James, K. *Coordination Chemistry Reviews* 2003, *240*, 57-75.

(181) Hossain, A.; Liljegren, J. A.; Powell, D.; Bowman-James, K. *Inorganic Chemistry* 2004, *43*, 3751-3755.

(182) Ravikumar, I.; Lakshminarayanan, P. S.; Arunachalam, M.; Suresh, E.; Ghosh, P. *Dalton Transactions* 2009, 4160-4168.

(183) Lakshminarayanan, P. S.; Ravikumar, I.; Suresh, E.; Ghosh, P. *Inorganic Chemistry* 2007, *46*, 4769-4771.

(184) Jose, D. A.; Kumar, D. K.; Ganguly, B.; Das, A. *Inorganic Chemistry* 2007, *46*, 5817-5819.

(185) Wichmann, K.; Antonioli, B.; Sohnel, T.; Wenzel, M.; Gloe, K.; Price, J. R.; Lindoy, L. F.; Blake, A. J.; Schroder, M. *Coordination Chemistry Reviews* 2006, *250*, 2987-3003.

(186) Farrell, D.; Gloe, K.; Goretzki, G.; McKee, V.; Nelson, J.; Nieuwenhuyzen, M.; Pal, I.; Stephan, H.; Town, R. M.; Wichmann, K. *Dalton Transactions* 2003, 1961-1968.

(187) Fabbrizzi, L.; Licchelli, M.; Rabaioli, G.; Taglietti, A. *Coordination Chemistry Reviews* 2000, *205*, 85-108.

(188) Hynes, M. J.; National University of Ireland: Galway, 2001, p 1-19.

(189) Metzger, A.; Lynch, V. M.; Anslyn, E. V. *Angewandte Chemie-International Edition in English* 1997, *36*, 862-865.

(190) McCleskey, S. C.; Metzger, A.; Simmons, C. S.; Anslyn, E. V. *Tetrahedron* 2002, *58*, 621-628.

(191) Filby, M. H.; Steed, J. W. *Coordination Chemistry Reviews* 2006, *250*, 3200-3218.

(192) Zyryanov, G. V.; Palacios, M. A.; Anzenbacher, P. *Angewandte Chemie-International Edition* 2007, *46*, 7849-7852.

(193) Mateus, P.; Delgado, R.; Brandao, P.; Felix, V. *Journal of Organic Chemistry* 2009, *74*, 8638-8646.

(194) Merschky, M.; Schmuck, C. *Organic & Biomolecular Chemistry* 2009, *7*, 4895-4903.

(195) Klemperer, W. G. In *Inorganic syntheses*; Ginsberg, A. P., Ed.; John Wiley & Sons, Inc.: 1990; Vol. 27, p 71-85.

(196) Albrecht, M.; Triyanti; de Groot, M.; Bahr, M.; Weinhold, E. *Synlett* 2005, 2095-2097.

(197) Albrecht, M.; Triyanti; Schiffers, S.; Osetska, O.; Raabe, G.; Wieland, T.; Russo, L.; Rissanen, K. *European Journal of Organic Chemistry* 2007, 2850-2858.

(198) Caltagirone, C.; Gale, P. A.; Hiscock, J. R.; Hursthouse, M. B.; Light, M. E.; Tizzard, G. J. *Supramolecular Chemistry* 2009, *21*, 125-130.

(199) Gale, P. A.; Garric, J.; Light, M. E.; McNally, B. A.; Smith, B. D. *Chemical Communications* 2007, 1736-1738.

(200) Coles, S. J.; Frey, J. G.; Gale, P. A.; Hursthouse, M. B.; Light, M. E.; Navakhun, K.; Thomas, G. L. *Chemical Communications* 2003, 568-569.

(201) Pantos, G. D.; Rodriguez-Morgade, M. S.; Torres, T.; Lynch, V. M.; Sessler, J. L. *Chemical Communications* 2006, 2132-2134.

Appendix 1 – X-Ray Crystal Structure Data

The X-ray crystal structures that are reported in Chapters Two, Three, Four and Five were solved by myself and the ESPRC National Crystallography Service at the University of Southampton (Dr M. E. Light). The refinement of the structures and the fractional coordinates are reported for completeness so that the crystal structure may be regenerated from the text of this appendix if necessary.

Structures from Chapter Two

Benzoate complex of receptor 209

Table 1. Crystal data and structure refinement details.

Identification code	**2008sot0126r (Cl107^{+}BzO)**
Empirical formula	$C_{44}H_{63}N_5O_3$
Formula weight	709.99
Temperature	120(2) K
Wavelength	0.71073 Å
Crystal system	Monoclinic
Space group	$P2_1/c$
Unit cell dimensions	a = 8.5824(3) Å
	b = 19.9254(9) Å β = 95.659(3)°
	c = 24.1820(10) Å
Volume	4115.2(3) Å^3
Z	4
Density (calculated)	1.146 Mg / m^3
Absorption coefficient	0.072 mm^{-1}
F(000)	1544
Crystal	Fragment; Colourless
Crystal size	0.25 × 0.17 × 0.06 mm^3
θ range for data collection	2.97 – 25.03°
Index ranges	$-10 \le h \le 9$, $-23 \le k \le 23$, $-28 \le l \le 28$
Reflections collected	31851
Independent reflections	7193 [R_{int} = 0.1307]
Completeness to θ = 25.03°	98.9 %
Absorption correction	Semi–empirical from equivalents
Max. and min. transmission	0.9957 and 0.9793
Refinement method	Full-matrix least-squares on F^2
Data / restraints / parameters	7193 / 0 / 477
Goodness-of-fit on F^2	0.924
Final R indices [$F^2 > 2\sigma(F^2)$]	$R1$ = 0.1469, $wR2$ = 0.3562
R indices (all data)	$R1$ = 0.2215, $wR2$ = 0.4147
Largest diff. peak and hole	0.996 and –0.440 e Å^{-3}

Diffractometer: *Nonius KappaCCD* area detector (ϕ scans and ω scans to fill *asymmetric unit*). **Cell determination:** DirAx (Duisenberg, A.J.M.(1992). J. Appl. Cryst. 25, 92-96.) **Data collection:** Collect (Collect: Data collection software, R. Hooft, Nonius B.V., 1998). **Data reduction and cell refinement**: *Denzo* (Z. Otwinowski & W. Minor, *Methods in Enzymology* (1997) Vol. **276**: *Macromolecular Crystallography*, part A, pp. 307–326; C. W. Carter, Jr. & R. M. Sweet, Eds., Academic Press). **Absorption correction**: Sheldrick, G. M. SADABS - Bruker Nonius area detector scaling and absorption correction - V2.10 S**tructure solution**: *SHELXS97* (G. M. Sheldrick, Acta Cryst. (1990) A**46** 467–473). S**tructure refinement**: *SHELXL97* (G. M. Sheldrick (1997), University of Göttingen, Germany). **Graphics:** Cameron - A Molecular Graphics Package. (D. M. Watkin, L. Pearce and C. K. Prout, Chemical Crystallography Laboratory, University of Oxford, 1993).

Special details: All hydrogen atoms were placed in idealised positions and refined using a riding model.

Table 2. Atomic coordinates [$\times 10^4$], equivalent isotropic displacement parameters [$Å^2 \times 10^3$] and site occupancy factors. U_{eq} is defined as one third of the trace of the orthogonalized U^{ij} tensor.

Atom	*x*	*y*	*z*	U_{eq}	*S.o.f.*
O1	1938(6)	795(2)	612(2)	35(1)	1
N1	1345(7)	2658(3)	−851(2)	31(1)	1
N2	1549(6)	1784(3)	132(2)	27(1)	1
N3	2378(6)	1808(3)	1056(2)	28(1)	1
N4	2946(7)	2765(3)	1997(2)	32(1)	1
C1	1419(11)	3620(4)	−1518(4)	52(2)	1
C2	934(10)	2913(4)	−1373(3)	42(2)	1
C3	77(9)	2454(4)	−1690(3)	37(2)	1
C4	−610(11)	2532(5)	−2281(3)	51(2)	1
C5	−52(8)	1865(4)	−1354(3)	31(2)	1
C6	−760(9)	1237(4)	−1431(3)	35(2)	1
C7	−656(8)	785(4)	−1002(3)	34(2)	1
C8	124(7)	940(3)	−476(3)	29(2)	1
C9	817(8)	1561(4)	−382(3)	27(2)	1
C10	737(8)	2013(3)	−826(3)	29(2)	1
C11	1948(7)	1412(4)	593(3)	27(2)	1
C12	3167(8)	1615(4)	1561(3)	30(2)	1
C13	3751(8)	978(4)	1685(3)	33(2)	1
C14	4624(10)	845(4)	2202(3)	44(2)	1
C15	4919(10)	1328(4)	2596(3)	43(2)	1
C16	4308(8)	1971(4)	2492(3)	32(2)	1
C17	3448(8)	2111(4)	1983(3)	29(2)	1
C18	5063(12)	2657(5)	3402(3)	59(3)	1
C19	4305(9)	2573(4)	2817(3)	39(2)	1
C20	3441(9)	3032(4)	2507(3)	40(2)	1
C21	3034(11)	3737(4)	2638(4)	52(2)	1
O2	1375(6)	3177(3)	933(2)	38(1)	1
O3	2725(6)	3152(3)	188(2)	39(1)	1
C22	2262(10)	3424(4)	610(4)	41(2)	1
C23	3046(10)	4083(4)	803(3)	43(2)	1
C24	2611(11)	4426(5)	1262(4)	53(2)	1
C25	3407(13)	4996(5)	1464(4)	66(3)	1
C26	4670(13)	5227(5)	1210(4)	69(3)	1
C27	5105(13)	4892(5)	743(4)	67(3)	1
C28	4291(11)	4325(5)	538(4)	58(2)	1
N5	7070(6)	2825(3)	5612(2)	30(1)	1
C29	7864(8)	2439(4)	5180(3)	33(2)	1
C30	6828(10)	1970(5)	4818(3)	49(2)	1
C31	7730(11)	1569(5)	4416(3)	52(2)	1
C32	8638(18)	1016(7)	4732(6)	109(5)	1
C33	6363(8)	2347(4)	6019(3)	31(2)	1

C34	7505(9)	1833(4)	6292(3)	38(2)	1
C35	6697(10)	1426(5)	6725(3)	46(2)	1
C36	7734(12)	843(5)	6954(4)	64(3)	1
C37	8330(8)	3261(4)	5911(3)	31(2)	1
C38	7846(8)	3694(4)	6385(3)	37(2)	1
C39	9250(10)	4083(4)	6641(3)	44(2)	1
C40	8873(10)	4547(4)	7110(4)	50(2)	1
C41	5720(8)	3242(4)	5342(3)	33(2)	1
C42	6150(9)	3753(4)	4915(3)	41(2)	1
C43	4638(8)	4035(4)	4610(3)	33(2)	1
C44	4956(10)	4546(4)	4172(3)	46(2)	1

Carbonate complex of receptor 209

Table 1. Crystal data and structure refinement details.

Identification code	**2008sot0830 (MeUrea+HCO3–)**
Empirical formula	$C_{59}H_{84}N_{10}O_5$
Formula weight	1013.36
Temperature	120(2) K
Wavelength	0.71073 Å
Crystal system	Triclinic
Space group	*P*–1
Unit cell dimensions	a = 12.8866(8) Å α = 97.235(3)°
	b = 15.5411(7) Å β = 109.277(2)°
	c = 16.4858(10) Å γ = 108.363(3)°
Volume	2858.7(3) Å^3
Z	2
Density (calculated)	1.177 Mg / m^3
Absorption coefficient	0.076 mm^{-1}
F(000)	1096
Crystal	Prism; Colourless
Crystal size	0.4 × 0.25 × 0.04 mm^3
θ range for data collection	2.96 – 25.02°
Index ranges	$-15 \le h \le 15$, $-17 \le k \le 18$, $-19 \le l \le 19$
Reflections collected	44006
Independent reflections	10101 [R_{int} = 0.1315]
Completeness to θ = 25.02°	99.7 %
Absorption correction	Semi–empirical from equivalents
Max. and min. transmission	0.9970 and 0.9602
Refinement method	Full-matrix least-squares on F^2
Data / restraints / parameters	10101 / 155 / 737
Goodness-of-fit on F^2	1.008
Final *R* indices [$F^2 > 2\sigma(F^2)$]	*R1* = 0.0948, *wR2* = 0.2441
R indices (all data)	*R1* = 0.1753, *wR2* = 0.2962
Extinction coefficient	0.0128(8)
Largest diff. peak and hole	1.491 and –0.690 e Å^{-3}

Diffractometer: *Nonius KappaCCD* area detector (ϕ scans and ω scans to fill *asymmetric unit*). **Cell determination:** DirAx (Duisenberg, A.J.M.(1992). J. Appl. Cryst. 25, 92-96.) **Data collection:** Collect (Collect: Data collection software, R. Hooft, Nonius B.V., 1998). **Data reduction and cell refinement**: *Denzo* (Z. Otwinowski & W. Minor, *Methods in Enzymology* (1997) Vol. **276**: *Macromolecular Crystallography*, part A, pp. 307–326; C. W. Carter, Jr. & R. M. Sweet, Eds., Academic Press). **Absorption correction**: Sheldrick, G. M. SADABS - Bruker Nonius area detector scaling and absorption correction - V2.10 S**tructure solution**: *SHELXS97* (G. M. Sheldrick, Acta Cryst. (1990) A**46** 467–473). S**tructure refinement**: *SHELXL97* (G. M. Sheldrick (1997), University of Göttingen, Germany). **Graphics:** Cameron - A Molecular Graphics Package. (D. M. Watkin, L. Pearce and C. K. Prout, Chemical Crystallography Laboratory, University of Oxford, 1993).

Special details: All hydrogen atoms were placed in idealised positions and refined using a riding model, except those of the NH which were freely refined. One of the TEA molecules is disordered. It was refined with 2 conformations using geometric and thermal parameter restraints. All the CIF alerts related to this disorder.

Table 2. Atomic coordinates [$\times 10^4$], equivalent isotropic displacement parameters [$Å^2 \times 10^3$] and site occupancy factors. U_{eq} is defined as one third of the trace of the orthogonalized U^{ij} tensor.

Atom	*x*	*y*	*z*	U_{eq}	*S.o.f.*
O1	3741(1)	7376(1)	5024(1)	51(1)	1
N1	8173(1)	7863(1)	6076(1)	40(1)	1
N2	5637(1)	7528(1)	5196(1)	33(1)	1
N3	4260(1)	7258(1)	3822(1)	37(1)	1
N4	3852(1)	7564(1)	2022(1)	36(1)	1
C1	10301(2)	8103(2)	6444(2)	61(1)	1
C2	9295(2)	8112(1)	6715(1)	44(1)	1
C3	9299(2)	8352(1)	7541(1)	43(1)	1
C4	10334(2)	8666(2)	8424(2)	57(1)	1
C5	7430(1)	7953(1)	6498(1)	33(1)	1
C6	8114(2)	8265(1)	7421(1)	37(1)	1
C7	7566(2)	8426(1)	8000(1)	42(1)	1
C8	6374(2)	8267(1)	7641(1)	40(1)	1
C9	5696(2)	7952(1)	6721(1)	37(1)	1
C10	6216(1)	7802(1)	6128(1)	33(1)	1
C11	4478(1)	7380(1)	4706(1)	37(1)	1
C12	3121(1)	6892(1)	3136(1)	34(1)	1
C13	2087(1)	6340(1)	3208(1)	37(1)	1
C14	985(2)	5991(1)	2487(1)	41(1)	1
C15	874(2)	6175(1)	1678(1)	41(1)	1
C16	1901(1)	6725(1)	1572(1)	35(1)	1
C17	3002(1)	7057(1)	2298(1)	33(1)	1
C18	4029(2)	8027(1)	668(1)	54(1)	1
C19	3308(2)	7555(1)	1139(1)	39(1)	1
C20	2106(2)	7060(1)	846(1)	39(1)	1
C21	1148(2)	6910(1)	–31(1)	51(1)	1
O2	7367(1)	6860(1)	758(1)	57(1)	1
N5	6881(1)	9532(1)	2492(1)	40(1)	1
N6	7595(1)	8083(1)	1833(1)	44(1)	1
N7	7769(1)	6769(1)	2199(1)	39(1)	1
N8	7894(1)	5889(1)	3703(1)	42(1)	1
C22	6417(2)	10632(1)	3404(1)	54(1)	1
C23	6549(2)	10293(1)	2574(1)	39(1)	1
C24	6438(2)	10630(1)	1838(1)	39(1)	1
C25	6157(2)	11468(1)	1663(1)	47(1)	1
C26	6991(2)	9379(1)	1691(1)	38(1)	1
C27	6707(2)	10045(1)	1251(1)	38(1)	1
C28	6737(2)	10021(1)	411(1)	46(1)	1
C29	7067(2)	9361(1)	46(1)	49(1)	1
C30	7354(2)	8705(1)	485(1)	45(1)	1
C31	7319(2)	8695(1)	1316(1)	38(1)	1
C32	7568(2)	7206(1)	1528(1)	44(1)	1

C33	7828(2)	5868(1)	2162(1)	39(1)	1
C34	7805(2)	5316(1)	1414(1)	44(1)	1
C35	7912(2)	4442(1)	1451(2)	50(1)	1
C36	8054(2)	4119(1)	2190(1)	48(1)	1
C37	8052(1)	4654(1)	2946(1)	41(1)	1
C38	7915(2)	5519(1)	2906(1)	38(1)	1
C39	7965(2)	5471(1)	5137(1)	59(1)	1
C40	7992(2)	5270(1)	4238(1)	45(1)	1
C41	8102(2)	4513(1)	3798(1)	46(1)	1
C42	8278(2)	3700(1)	4148(2)	65(1)	1
N9	3975(1)	4551(1)	2043(1)	37(1)	1
C44	4491(2)	4352(1)	2917(1)	47(1)	1
C45	4653(2)	5024(1)	3730(1)	57(1)	1
C46	3730(1)	3740(1)	1289(1)	46(1)	1
C47	4835(1)	3601(1)	1269(1)	54(1)	1
C48	4838(2)	5479(1)	2010(1)	47(1)	1
C49	4504(2)	5722(1)	1121(1)	57(1)	1
C50	2785(1)	4668(1)	1908(1)	49(1)	1
C51	1863(2)	3856(1)	2026(1)	53(1)	1
N10A	1592(1)	9076(1)	3476(1)	69(1)	0.4079(15)
C52A	744(3)	8178(2)	3372(2)	58(1)	0.4079(15)
C53A	753(4)	7809(3)	4167(2)	50(1)	0.4079(15)
C54A	2880(2)	9065(3)	3887(2)	78(1)	0.4079(15)
C55A	3662(3)	9427(4)	3398(3)	133(2)	0.4079(15)
C56A	1412(4)	9516(2)	2688(2)	80(1)	0.4079(15)
C57A	650(7)	8879(5)	1752(3)	117(2)	0.4079(15)
C58A	1730(2)	9843(2)	4295(2)	50(1)	0.4079(15)
C59A	558(2)	9957(3)	4172(3)	67(1)	0.4079(15)
N10B	1592(1)	9076(1)	3476(1)	69(1)	0.5921(15)
C52B	1838(3)	8456(2)	4027(2)	58(1)	0.5921(15)
C53B	842(2)	7714(2)	4115(2)	50(1)	0.5921(15)
C54B	2603(2)	9764(2)	3346(2)	78(1)	0.5921(15)
C55B	3189(3)	9317(3)	2848(3)	133(2)	0.5921(15)
C56B	725(3)	8386(2)	2503(2)	80(1)	0.5921(15)
C57B	318(5)	8803(3)	1735(2)	117(2)	0.5921(15)
C58B	800(2)	9585(2)	3668(2)	50(1)	0.5921(15)
C59B	1349(3)	10084(3)	4653(2)	67(1)	0.5921(15)
O3	6980(1)	7263(1)	4233(1)	37(1)	1
O4	8021(1)	8138(1)	3584(1)	41(1)	1
O5	6231(1)	8149(1)	3431(1)	41(1)	1
C43	7078(2)	7852(1)	3746(1)	35(1)	1

Phosphate complex of receptor 210

Table 1. Crystal data and structure refinement details.

Identification code	**2008sot0409r**
Empirical formula	$C_{102}H_{159}N_{15}O_{8.50}PS_{1.50}$ $3C_{17}H_{14}N_4O$, $3C_{16}H_{36}N$, PO_4, $1.5C_2H_6SO$
Formula weight	1810.50
Temperature	120(2) K
Wavelength	0.71073 Å
Crystal system	Hexagonal
Space group	*R*–3
Unit cell dimensions	a = 24.0023(3) Å c = 32.4801(6) Å
Volume	16205.2(4) Å^3
Z	6
Density (calculated)	1.113 Mg / m^3
Absorption coefficient	0.113 mm^{-1}
F(000)	5898
Crystal	Block; Colourless
Crystal size	0.2 × 0.2 × 0.2 mm^3
θ range for data collection	2.94 – 25.03°
Index ranges	$-28 \le h \le 28$, $-28 \le k \le 26$, $-31 \le l \le 38$
Reflections collected	33495
Independent reflections	6352 [R_{int} = 0.1035]
Completeness to θ = 25.03°	99.7 %
Absorption correction	Semi–empirical from equivalents
Max. and min. transmission	0.9778 and 0.9678
Refinement method	Full-matrix least-squares on F^2
Data / restraints / parameters	6352 / 14 / 417
Goodness-of-fit on F^2	1.066
Final *R* indices [$F^2 > 2\sigma(F^2)$]	*R1* = 0.1057, *wR2* = 0.2929
R indices (all data)	*R1* = 0.1285, *wR2* = 0.3120
Largest diff. peak and hole	1.380 and –0.683 e Å^{-3}

Diffractometer: *Nonius KappaCCD* area detector (ϕ scans and ω scans to fill *asymmetric unit*). **Cell determination:** DirAx (Duisenberg, A.J.M.(1992). J. Appl. Cryst. 25, 92-96.) **Data collection:** Collect (Collect: Data collection software, R. Hooft, Nonius B.V., 1998). **Data reduction and cell refinement**: *Denzo* (Z. Otwinowski & W. Minor, *Methods in Enzymology* (1997) Vol. **276**: *Macromolecular Crystallography*, part A, pp. 307–326; C. W. Carter, Jr. & R. M. Sweet, Eds., Academic Press). **Absorption correction**: Sheldrick, G. M. SADABS - Bruker Nonius area detector scaling and absorption correction - V2.10 S**tructure solution**: *SHELXS97* (G. M. Sheldrick, Acta Cryst. (1990) A**46** 467–473). S**tructure refinement**: *SHELXL97* (G. M. Sheldrick (1997), University of Göttingen, Germany). **Graphics:** Cameron - A Molecular Graphics Package. (D. M. Watkin, L. Pearce and C. K. Prout, Chemical Crystallography Laboratory, University of Oxford, 1993).

Special details: All hydrogen atoms were placed in idealised positions and refined using a riding model. Hydrogens attached to the nitrogen atoms were located in the difference map and refined using distances restraints. The DMSO was modelled as half occupied and disordered 50/50 over 2 possible orientations. Its geometry and thermal parameters were restrained. The terminal atom of 1 TBA arm was modelled as disordered over 2 possible orientations and the occupancies constrained to total 1. These 2 disorders and partial occupancy of the DMSO explain the apparent close contacts in the structure. The crystal was a non-merohedral twin, but attempts to treat the data as such were unsuccessful. The resulting effect on the intensities has caused some parameters to misbehave, and the R-factors to be high.

Table 2. Atomic coordinates [$\times 10^4$], equivalent isotropic displacement parameters [$Å^2 \times 10^3$] and site occupancy factors. U_{eq} is defined as one third of the trace of the orthogonalized U^{ij} tensor.

Atom	*x*	*y*	*z*	U_{eq}	*S.o.f.*
O1	4448(1)	955(1)	174(1)	49(1)	1
N1	5545(1)	2805(1)	−808(1)	33(1)	1
N2	4983(1)	1995(1)	−77(1)	36(1)	1
N3	5387(1)	1732(1)	470(1)	37(1)	1
N4	6472(1)	2376(1)	1038(1)	34(1)	1
C1	5612(2)	3097(2)	−1181(1)	39(1)	1
C2	5030(2)	2841(2)	−1373(1)	45(1)	1
C3	4567(2)	2354(2)	−1107(1)	39(1)	1
C4	3903(2)	1921(2)	−1125(1)	51(1)	1
C5	3604(2)	1508(2)	−805(1)	53(1)	1
C6	3950(2)	1509(2)	−453(1)	44(1)	1
C7	4608(1)	1938(1)	−423(1)	36(1)	1
C8	4916(1)	2357(1)	−755(1)	34(1)	1
C9	4897(1)	1513(1)	186(1)	38(1)	1
C10	5400(2)	1435(1)	836(1)	37(1)	1
C11	4927(2)	835(2)	972(1)	50(1)	1
C12	4969(2)	616(2)	1364(1)	59(1)	1
C13	5458(2)	970(2)	1629(1)	59(1)	1
C14	5965(2)	1569(2)	1497(1)	46(1)	1
C15	6546(2)	2061(2)	1671(1)	57(1)	1
C16	6836(2)	2532(2)	1386(1)	46(1)	1
C17	5932(1)	1785(1)	1098(1)	35(1)	1
N5	4004(1)	3135(1)	356(1)	52(1)	1
C18	3456(2)	3116(2)	114(1)	57(1)	1
C19	3263(2)	2723(2)	−265(2)	66(1)	1
C20	2714(2)	2742(2)	−463(2)	80(1)	1
C21	2426(3)	2309(3)	−817(2)	98(2)	1
C22	4606(2)	3346(2)	91(1)	55(1)	1
C23	4862(2)	3986(2)	−135(1)	57(1)	1
C24	5320(2)	4024(2)	−463(1)	57(1)	1
C25	5623(2)	4649(2)	−704(1)	68(1)	1
C26	4182(2)	3624(2)	705(1)	54(1)	1
C27	3655(2)	3461(2)	1015(1)	56(1)	1
C28	3885(2)	3901(2)	1387(2)	77(2)	1
C29	3384(2)	3786(2)	1686(2)	69(1)	1
C30	3806(2)	2472(2)	523(2)	66(1)	1
C31	4234(2)	2425(2)	848(2)	82(2)	1
C32A	4058(6)	1734(5)	948(5)	73(2)	0.364(7)
C33A	3498(6)	1554(7)	1235(5)	92(2)	0.364(7)
C32B	3885(4)	1742(4)	1030(3)	73(2)	0.636(7)
C33B	4162(4)	1635(4)	1431(3)	92(2)	0.636(7)

P1	6667	3333	1	21(1)	23(1)	1
O2	6667	3333		–352(1)	29(1)	1
O3	6930(1)	2910(1)		286(1)	29(1)	1
S1A	5023(3)	1601(3)		2526(2)	92(1)	0.25
O4A	4554(6)	1558(7)		2816(5)	92(1)	0.25
C34A	5635(4)	2356(5)		2470(4)	92(1)	0.25
C35A	4665(5)	1679(5)		2074(3)	92(1)	0.25
S1B	4821(3)	1931(3)		2639(2)	92(1)	0.25
O4B	4691(7)	1365(6)		2858(5)	92(1)	0.25
C34B	5635(4)	2356(5)		2470(4)	92(1)	0.25
C35B	4665(5)	1679(5)		2074(3)	92(1)	0.25

Carbonate complex of receptor 211

Table 1. Crystal data and structure refinement details.

Identification code	**2008sot0763 (THIO+HCO3–)**
Empirical formula	$C_{26}H_{35}N_5O_3S$
Formula weight	497.65
Temperature	120(2) K
Wavelength	0.71073 Å
Crystal system	Monoclinic
Space group	$P2_1/n$
Unit cell dimensions	a = 7.9556(2) Å
	b = 16.0231(8) Å β = 95.842(3)°
	c = 19.7617(8) Å
Volume	2506.01(17) Å^3
Z	4
Density (calculated)	1.319 Mg / m^3
Absorption coefficient	0.167 mm^{-1}
F(000)	1064
Crystal	Fragment; Pale Yellow
Crystal size	0.2 × 0.2 × 0.2 mm^3
θ range for data collection	2.96 – 25.03°
Index ranges	$-9 \le h \le 9$, $-19 \le k \le 19$, $-23 \le l \le 23$
Reflections collected	25403
Independent reflections	4423 [R_{int} = 0.0679]
Completeness to θ = 25.03°	99.7 %
Absorption correction	Semi–empirical from equivalents
Max. and min. transmission	0.9673 and 0.9573
Refinement method	Full-matrix least-squares on F^2
Data / restraints / parameters	4423 / 0 / 337
Goodness-of-fit on F^2	1.075
Final R indices [$F^2 > 2\sigma(F^2)$]	*R1* = 0.0581, *wR2* = 0.1377
R indices (all data)	*R1* = 0.0822, *wR2* = 0.1540
Extinction coefficient	0.0156(16)
Largest diff. peak and hole	0.430 and –0.372 e Å^{-3}

Diffractometer: *Nonius KappaCCD* area detector (ϕ scans and ω scans to fill *asymmetric unit*). **Cell determination:** DirAx (Duisenberg, A.J.M.(1992). J. Appl. Cryst. 25, 92-96.) **Data collection:** Collect (Collect: Data collection software, R. Hooft, Nonius B.V., 1998). **Data reduction and cell refinement**: *Denzo* (Z. Otwinowski & W. Minor, *Methods in Enzymology* (1997) Vol. **276**: *Macromolecular Crystallography*, part A, pp. 307–326; C. W. Carter, Jr. & R. M. Sweet, Eds., Academic Press). **Absorption correction**: Sheldrick, G. M. SADABS - Bruker Nonius area detector scaling and absorption correction - V2.10 S**tructure solution**: *SHELXS97* (G. M. Sheldrick, Acta Cryst. (1990) A**46** 467–473). S**tructure refinement**: *SHELXL97* (G. M. Sheldrick (1997), University of Göttingen, Germany). **Graphics:** Cameron - A Molecular Graphics Package. (D. M. Watkin, L. Pearce and C. K. Prout, Chemical Crystallography Laboratory, University of Oxford, 1993).

Special details: All hydrogen atoms were placed in idealised positions and refined using a riding model, except for those of the NH which were freely refined. The hydrogen of the bicarbonate was not located and omitted from the refinement.

Table 2. Atomic coordinates [$\times 10^4$], equivalent isotropic displacement parameters [$Å^2 \times 10^3$] and site occupancy factors. U_{eq} is defined as one third of the trace of the orthogonalized U^{ij} tensor.

Atom	*x*	*y*	*z*	U_{eq}	*S.o.f.*
S1	710(1)	2527(1)	2171(1)	36(1)	1
N1	–3969(3)	4469(1)	1645(1)	37(1)	1
N2	–352(3)	3956(2)	1560(1)	39(1)	1
N3	958(3)	3064(2)	904(1)	39(1)	1
N4	4312(3)	2866(2)	354(1)	36(1)	1
C1	–5397(3)	4771(2)	1886(2)	41(1)	1
C2	–5052(3)	5031(2)	2539(1)	39(1)	1
C3	–3285(3)	4892(2)	2726(1)	32(1)	1
C4	–2187(3)	5011(2)	3321(1)	37(1)	1
C5	–525(4)	4793(2)	3317(1)	39(1)	1
C6	99(3)	4449(2)	2741(1)	36(1)	1
C7	–949(3)	4305(2)	2150(1)	32(1)	1
C8	–2639(3)	4538(1)	2149(1)	30(1)	1
C9	430(3)	3207(2)	1526(1)	32(1)	1
C10	1578(3)	2291(2)	683(1)	33(1)	1
C11	669(4)	1556(2)	711(1)	38(1)	1
C12	1325(4)	798(2)	495(1)	41(1)	1
C13	2865(4)	757(2)	241(1)	39(1)	1
C14	3823(3)	1491(2)	207(1)	34(1)	1
C15	5450(4)	1685(2)	8(1)	42(1)	1
C16	5690(4)	2518(2)	103(1)	42(1)	1
C17	3144(3)	2251(2)	422(1)	31(1)	1
C18	2440(14)	4934(3)	–16(2)	142(3)	1
O1	1213(7)	4570(2)	167(2)	137(2)	1
O2	2414(5)	5584(2)	–388(1)	110(1)	1
O3	3909(7)	4617(2)	209(1)	135(2)	1
N5	5685(2)	2221(1)	3265(1)	26(1)	1
C19	4662(3)	3022(2)	3202(1)	32(1)	1
C20	4551(4)	3486(2)	3862(1)	44(1)	1
C21	5123(3)	1657(2)	3815(1)	36(1)	1
C22	3258(4)	1478(2)	3754(2)	52(1)	1
C23	7535(3)	2445(2)	3445(1)	33(1)	1
C24	8721(3)	1710(2)	3527(2)	46(1)	1
C25	5414(3)	1755(2)	2586(1)	32(1)	1
C26	5934(4)	2220(2)	1980(1)	38(1)	1

Chloride complex of receptor 212

Table 1. Crystal data and structure refinement details.

Identification code	**2008sot0701 (THIO+Cl–)**
Empirical formula	$C_{33}H_{50}ClN_5S$
Formula weight	584.29
Temperature	120(2) K
Wavelength	0.71073 Å
Crystal system	Monoclinic
Space group	*Cc*
Unit cell dimensions	a = 14.4760(2) Å
	b = 14.0106(3) Å β = 93.8180(10)°
	c = 16.0360(3) Å
Volume	3245.16(10) Å^3
Z	4
Density (calculated)	1.196 Mg / m^3
Absorption coefficient	0.212 mm^{-1}
F(000)	1264
Crystal	Slab; Colourless
Crystal size	0.2 × 0.2 × 0.05 mm^3
θ range for data collection	3.17 – 27.48°
Index ranges	$-18 \le h \le 18$, $-18 \le k \le 16$, $-20 \le l \le 20$
Reflections collected	17419
Independent reflections	6742 [R_{int} = 0.0430]
Completeness to θ = 27.48°	99.6 %
Absorption correction	Semi–empirical from equivalents
Max. and min. transmission	0.9895 and 0.9489
Refinement method	Full-matrix least-squares on F^2
Data / restraints / parameters	6742 / 2 / 381
Goodness-of-fit on F^2	1.031
Final R indices [$F^2 > 2\sigma(F^2)$]	*R1* = 0.0460, *wR2* = 0.0887
R indices (all data)	*R1* = 0.0557, *wR2* = 0.0941
Absolute structure parameter	0.10(5)
Largest diff. peak and hole	0.208 and –0.228 e Å^{-3}

Diffractometer: *Nonius KappaCCD* area detector (ϕ scans and ω scans to fill *asymmetric unit*). **Cell determination:** DirAx (Duisenberg, A.J.M.(1992). J. Appl. Cryst. 25, 92-96.) **Data collection:** Collect (Collect: Data collection software, R. Hooft, Nonius B.V., 1998). **Data reduction and cell refinement**: *Denzo* (Z. Otwinowski & W. Minor, *Methods in Enzymology* (1997) Vol. **276**: *Macromolecular Crystallography*, part A, pp. 307–326; C. W. Carter, Jr. & R. M. Sweet, Eds., Academic Press). **Absorption correction**: Sheldrick, G. M. SADABS - Bruker Nonius area detector scaling and absorption correction - V2.10 S**tructure solution**: *SHELXS97* (G. M. Sheldrick, Acta Cryst. (1990) A**46** 467–473). S**tructure refinement**: *SHELXL97* (G. M. Sheldrick (1997), University of Göttingen, Germany). **Graphics:** Cameron - A Molecular Graphics Package. (D. M. Watkin, L. Pearce and C. K. Prout, Chemical Crystallography Laboratory, University of Oxford, 1993).

Special details: All hydrogen atoms were placed in idealised positions and refined using a riding model, except those of the NH which were located in the difference map and freely refined.

Table 2. Atomic coordinates [$\times 10^4$], equivalent isotropic displacement parameters [$Å^2 \times 10^3$] and site occupancy factors. U_{eq} is defined as one third of the trace of the orthogonalized U^{ij} tensor.

Atom	*x*	*y*	*z*	U_{eq}	*S.o.f.*
C1	6176(2)	6070(2)	2521(2)	30(1)	1
C2	5598(2)	5340(2)	2702(2)	31(1)	1
C3	4857(2)	5732(2)	3126(2)	23(1)	1
C4	4060(2)	5367(2)	3478(2)	24(1)	1
C5	3484(2)	5977(2)	3860(2)	26(1)	1
C6	3666(2)	6957(2)	3913(2)	24(1)	1
C7	4429(2)	7346(2)	3566(2)	22(1)	1
C8	5015(2)	6731(2)	3180(2)	20(1)	1
C9	4178(2)	9085(2)	3331(2)	19(1)	1
C10	5245(2)	11377(2)	2932(2)	18(1)	1
C11	4488(2)	10839(2)	3146(2)	19(1)	1
C12	3623(2)	11265(2)	3071(2)	22(1)	1
C13	3524(2)	12201(2)	2768(2)	25(1)	1
C14	4262(2)	12735(2)	2540(2)	25(1)	1
C15	5149(2)	12327(2)	2626(2)	20(1)	1
C16	6064(2)	12635(2)	2462(2)	23(1)	1
C17	6651(2)	11911(2)	2668(2)	23(1)	1
N1	5818(2)	6927(2)	2787(1)	24(1)	1
N2	4679(2)	8324(2)	3627(2)	24(1)	1
N3	4670(2)	9908(2)	3463(1)	20(1)	1
N4	6172(2)	11141(2)	2953(1)	20(1)	1
S1	3111(1)	9005(1)	2872(1)	23(1)	1
Cl1	6776(1)	8983(1)	3527(1)	27(1)	1
C18	8134(2)	7330(2)	4999(2)	23(1)	1
C19	7341(2)	6982(2)	5497(2)	28(1)	1
C20	6554(2)	6612(2)	4908(2)	31(1)	1
C21	5728(2)	6262(2)	5370(2)	34(1)	1
C22	8760(2)	8450(2)	6120(2)	23(1)	1
C23	8359(2)	9351(2)	5712(2)	25(1)	1
C24	7956(2)	9988(2)	6361(2)	29(1)	1
C25	7608(2)	10938(2)	6007(2)	35(1)	1
C26	9690(2)	8002(2)	4914(2)	24(1)	1
C27	10624(2)	8291(2)	5319(2)	27(1)	1
C28	11271(2)	8669(2)	4688(2)	34(1)	1
C29	12216(2)	8943(2)	5105(2)	39(1)	1
C30	9400(2)	6833(2)	6053(2)	23(1)	1
C31	9693(2)	5964(2)	5574(2)	26(1)	1
C32	10044(2)	5187(2)	6177(2)	30(1)	1
C33	10338(2)	4290(2)	5732(2)	35(1)	1
N5	8997(2)	7653(2)	5520(1)	21(1)	1

Complex of receptor 213

Table 1. Crystal data and structure refinement details.

Identification code	**2009jh0006**
Empirical formula	$C_{25}H_{18}N_4O$
Formula weight	390.43
Temperature	120(2) K
Wavelength	0.71073 Å
Crystal system	Monoclinic
Space group	*C*2/*c*
Unit cell dimensions	a = 36.5182(16) Å α = 90°
	b = 4.4881(2) Å β = 98.111(3)°
	c = 11.1125(5) Å γ = 90°
Volume	1803.09(14) Å^3
Z	4
Density (calculated)	1.438 Mg / m^3
Absorption coefficient	0.091 mm^{-1}
F(000)	816
Crystal	Plate; Colourless
Crystal size	0.20 × 0.20 × 0.01 mm^3
θ range for data collection	3.38 – 25.03°
Index ranges	$-42 \le h \le 42$, $-5 \le k \le 5$, $-13 \le l \le 13$
Reflections collected	8399
Independent reflections	1585 [R_{int} = 0.0723]
Completeness to θ = 25.03°	99.6 %
Absorption correction	Semi–empirical from equivalents
Max. and min. transmission	0.9991 and 0.9821
Refinement method	Full-matrix least-squares on F^2
Data / restraints / parameters	1585 / 0 / 137
Goodness-of-fit on F^2	1.119
Final *R* indices [$F^2 > 2\sigma(F^2)$]	*R1* = 0.1356, *wR2* = 0.3475
R indices (all data)	*R1* = 0.1541, *wR2* = 0.3571
Largest diff. peak and hole	0.574 and –0.514 e Å^{-3}

Diffractometer: *Nonius KappaCCD* area detector (ϕ scans and ω scans to fill *asymmetric unit*). **Cell determination:** DirAx (Duisenberg, A.J.M.(1992). J. Appl. Cryst. 25, 92-96.) **Data collection:** Collect (Collect: Data collection software, R. Hooft, Nonius B.V., 1998). **Data reduction and cell refinement**: *Denzo* (Z. Otwinowski & W. Minor, *Methods in Enzymology* (1997) Vol. **276**: *Macromolecular Crystallography*, part A, pp. 307–326; C. W. Carter, Jr. & R. M. Sweet, Eds., Academic Press). **Absorption correction**: Sheldrick, G. M. SADABS - Bruker Nonius area detector scaling and absorption correction - V2.10 S**tructure solution**: *SHELXS97* (G. M. Sheldrick, Acta Cryst. (1990) A**46** 467–473). S**tructure refinement**: *SHELXL97* (G. M. Sheldrick (1997), University of Göttingen, Germany). **Graphics:** Cameron - A Molecular Graphics Package. (D. M. Watkin, L. Pearce and C. K. Prout, Chemical Crystallography Laboratory, University of Oxford, 1993).

Special details:

Table 2. Atomic coordinates [$\times 10^4$], equivalent isotropic displacement parameters [$Å^2 \times 10^3$] and site occupancy factors. U_{eq} is defined as one third of the trace of the orthogonalized U^{ij} tensor.

Atom	*x*	*y*	*z*	U_{eq}	*S.o.f.*
O1	5000	822(17)	7500	29(2)	1
N1	3913(2)	4991(14)	6965(6)	24(2)	1
N2	4730(2)	5150(14)	7931(6)	22(2)	1
C7	4086(2)	3588(17)	7995(7)	22(2)	1
C6	3823(2)	1898(18)	8528(7)	26(2)	1
C8	3471(2)	2326(18)	7749(7)	25(2)	1
C4	4299(2)	306(17)	10098(7)	26(2)	1
C11	2903(2)	4170(20)	5964(8)	34(2)	1
C13	3539(2)	4286(19)	6805(7)	25(2)	1
C9	3107(2)	1300(20)	7800(8)	35(2)	1
C3	4553(2)	2061(19)	9567(7)	28(2)	1
C1	5000	3580(20)	7500	24(2)	1
C2	4461(2)	3641(17)	8513(7)	23(2)	1
C10	2831(2)	2250(20)	6896(8)	37(2)	1
C5	3931(2)	198(17)	9558(7)	26(2)	1
C12	3262(2)	5185(19)	5910(8)	31(2)	1

Benzoate complex of receptor 213

Table 1. Crystal data and structure refinement details.

Identification code	**2008jh0003**
Empirical formula	$C_{48}H_{59}N_5O_3$
Formula weight	754.00
Temperature	120(2) K
Wavelength	0.71069 Å
Crystal system	Triclinic
Space group	*P*1
Unit cell dimensions	a = 10.980(5) Å α = 68.760(5)°
	b = 13.774(5) Å β = 85.232(5)°
	c 15.173(5) Å γ = 81.541(5)°
Volume	2114.5(14) Å^3
Z	2
Density (calculated)	1.184 Mg / m^3
Absorption coefficient	0.074 mm^{-1}
F(000)	812
Crystal	Block; Colourless
Crystal size	0.4 × 0.2 × 0.05 mm^3
θ range for data collection	3.01 – 27.59°
Index ranges	$-14 \le h \le 14$, $-17 \le k \le 17$, $-19 \le l \le 19$
Reflections collected	44837
Independent reflections	9728 [R_{int} = 0.1052]
Completeness to θ = 27.50°	99.7 %
Absorption correction	Semi–empirical from equivalents
Max. and min. transmission	0.9963 and 0.9609
Refinement method	Full-matrix least-squares on F^2
Data / restraints / parameters	9728 / 3 / 1017
Goodness-of-fit on F^2	1.028
Final *R* indices [$F^2 > 2\sigma(F^2)$]	*R1* = 0.0661, *wR2* = 0.1368
R indices (all data)	*R1* = 0.1190, *wR2* = 0.1589
Largest diff. peak and hole	0.527 and –0.310 e Å^{-3}

Diffractometer: *Nonius KappaCCD* area detector (ϕ scans and ω scans to fill *asymmetric unit*). **Cell determination:** DirAx (Duisenberg, A.J.M.(1992). J. Appl. Cryst. 25, 92-96.) **Data collection:** Collect (Collect: Data collection software, R. Hooft, Nonius B.V., 1998). **Data reduction and cell refinement**: *Denzo* (Z. Otwinowski & W. Minor, *Methods in Enzymology* (1997) Vol. **276**: *Macromolecular Crystallography*, part A, pp. 307–326; C. W. Carter, Jr. & R. M. Sweet, Eds., Academic Press). **Absorption correction**: Sheldrick, G. M. SADABS - Bruker Nonius area detector scaling and absorption correction - V2.10 S**tructure solution**: *SHELXS97* (G. M. Sheldrick, Acta Cryst. (1990) A**46** 467–473). S**tructure refinement**: *SHELXL97* (G. M. Sheldrick (1997), University of Göttingen, Germany). **Graphics:** Cameron - A Molecular Graphics Package. (D. M. Watkin, L. Pearce and C. K. Prout, Chemical Crystallography Laboratory, University of Oxford, 1993).

Special details:

Table 2. Atomic coordinates [$\times 10^4$], equivalent isotropic displacement parameters [$Å^2 \times 10^3$] and site occupancy factors. U_{eq} is defined as one third of the trace of the orthogonalized U^{ij} tensor.

Atom	*x*	*y*	*z*	U_{eq}	*S.o.f.*
C1	7182(4)	5291(4)	3155(4)	31(1)	1
C2	7370(5)	6240(4)	2439(4)	37(1)	1
C3	8192(5)	6822(4)	2631(4)	44(1)	1
C4	8805(5)	6457(5)	3486(4)	47(2)	1
C5	8598(4)	5535(4)	4194(4)	36(1)	1
C6	7752(4)	4944(4)	4033(3)	29(1)	1
C7	7300(4)	3961(4)	4615(3)	26(1)	1
C8	7444(4)	3295(4)	5556(4)	31(1)	1
C9	6818(4)	2428(4)	5888(3)	30(1)	1
C10	6093(4)	2185(4)	5301(3)	31(1)	1
C11	5963(4)	2827(3)	4350(3)	25(1)	1
C12	6527(4)	3753(3)	4028(3)	25(1)	1
C13	5281(4)	1603(3)	3697(3)	24(1)	1
C14	3645(4)	981(3)	1953(3)	23(1)	1
C15	4475(4)	789(3)	2679(3)	24(1)	1
C16	5191(4)	−181(4)	2984(3)	28(1)	1
C17	5071(4)	−951(3)	2600(3)	30(1)	1
C18	4260(4)	−765(4)	1894(3)	30(1)	1
C19	3535(4)	216(3)	1566(3)	25(1)	1
C20	2686(4)	717(3)	799(3)	25(1)	1
C21	2221(5)	397(4)	139(3)	35(1)	1
C22	1444(5)	1102(4)	−540(4)	36(1)	1
C23	1108(4)	2130(4)	−552(3)	34(1)	1
C24	1537(4)	2472(4)	102(3)	30(1)	1
C25	2322(4)	1748(4)	777(3)	26(1)	1
C26	3559(4)	4378(3)	1889(3)	28(1)	1
C27	2847(4)	5451(3)	1466(3)	25(1)	1
C28	3463(4)	6321(3)	1058(3)	30(1)	1
C29	2813(5)	7316(4)	663(4)	39(1)	1
C30	1533(5)	7430(4)	684(4)	38(1)	1
C31	909(5)	6576(4)	1097(4)	37(1)	1
C32	1570(4)	5584(4)	1480(3)	31(1)	1
C33	−2902(4)	−6340(4)	9241(3)	29(1)	1
C34	−3674(4)	−6240(4)	9986(3)	33(1)	1
C35	−4108(5)	−7131(4)	10616(4)	38(1)	1
C36	−3792(5)	−8111(4)	10518(4)	39(1)	1
C37	−3037(4)	−8209(4)	9777(3)	33(1)	1
C38	−2579(4)	−7325(4)	9125(3)	27(1)	1
C39	−1738(4)	−7150(3)	8320(3)	26(1)	1
C40	−1059(4)	−7826(4)	7895(3)	30(1)	1
C41	−216(4)	−7400(4)	7170(3)	29(1)	1

C42	–26(4)	–6351(4)	6870(3)	29(1)	1
C43	–707(4)	–5662(3)	7265(3)	24(1)	1
C44	–1579(4)	–6079(4)	7994(3)	26(1)	1
C45	220(4)	–4027(3)	6331(3)	25(1)	1
C46	1710(4)	–1825(3)	6217(3)	29(1)	1
C47	1092(4)	–2356(3)	5789(3)	28(1)	1
C48	1323(4)	–2161(4)	4834(3)	31(1)	1
C49	2183(4)	–1489(4)	4323(3)	32(1)	1
C50	2842(4)	–1007(4)	4748(3)	34(1)	1
C51	2607(4)	–1174(3)	5703(3)	31(1)	1
C52	3087(4)	–818(4)	6378(3)	31(1)	1
C53	4023(5)	–188(4)	6322(4)	45(1)	1
C54	4247(6)	15(5)	7112(5)	56(2)	1
C55	3542(6)	–370(5)	7958(4)	57(2)	1
C56	2636(6)	–999(4)	8024(4)	47(1)	1
C57	2436(5)	–1217(4)	7233(4)	34(1)	1
C58	–1542(4)	–2883(4)	8333(3)	32(1)	1
C59	–2121(4)	–2300(3)	8968(3)	30(1)	1
C60	–1417(5)	–1734(4)	9266(4)	39(1)	1
C61	–1932(5)	–1179(4)	9851(4)	47(1)	1
C62	–3123(6)	–1215(5)	10144(5)	58(2)	1
C63	–3843(6)	–1794(5)	9869(6)	71(2)	1
C64	–3328(6)	–2322(5)	9270(5)	56(2)	1
C65	3902(4)	–4042(4)	7046(3)	31(1)	1
C66	4478(5)	–4373(4)	7998(3)	38(1)	1
C67	3648(5)	–3983(4)	8694(4)	40(1)	1
C68	2470(6)	–4476(6)	9000(5)	64(2)	1
C69	4707(4)	–5730(4)	6778(4)	33(1)	1
C70	3507(5)	–6194(4)	7134(4)	39(1)	1
C71	3734(5)	–7387(4)	7483(4)	42(1)	1
C72	4495(6)	–7879(5)	8361(4)	55(2)	1
C73	3844(4)	–4117(4)	5456(4)	34(1)	1
C74	4393(5)	–4480(5)	4652(4)	45(1)	1
C75	3768(5)	–3812(5)	3692(4)	49(1)	1
C76	2505(6)	–4093(6)	3658(5)	64(2)	1
C77	5877(4)	–4223(3)	6144(3)	27(1)	1
C78	5958(4)	–3077(4)	5570(4)	33(1)	1
C79	7273(4)	–2845(4)	5584(4)	32(1)	1
C80	7530(5)	–1799(4)	4826(4)	41(1)	1
C81	–1106(4)	1217(4)	4376(3)	31(1)	1
C82	–549(5)	158(4)	5035(4)	46(1)	1
C83	–1304(6)	–189(4)	5962(4)	49(1)	1
C84	–942(6)	241(5)	6633(5)	58(2)	1
C85	–129(5)	928(4)	2927(4)	37(1)	1
C86	–1281(5)	685(4)	2597(5)	48(1)	1

C87	–909(8)	83(6)	1889(7)	93(3)	1
C88	–33(8)	–841(7)	2208(7)	95(3)	1
C89	–1050(4)	2711(4)	2890(3)	29(1)	1
C90	–551(4)	3215(3)	1885(3)	29(1)	1
C91	–1269(5)	4287(4)	1398(3)	36(1)	1
C92	–855(5)	4788(4)	386(4)	43(1)	1
C93	920(4)	1826(4)	3702(3)	34(1)	1
C94	947(5)	2380(5)	4398(4)	42(1)	1
C95	2287(5)	2482(5)	4506(4)	45(1)	1
C96	2445(5)	2905(6)	5260(5)	58(2)	1
N1	6464(3)	4549(3)	3154(3)	28(1)	1
N2	5296(3)	2603(3)	3704(3)	27(1)	1
N3	4544(3)	1624(3)	3005(3)	24(1)	1
N4	2893(3)	1894(3)	1495(2)	22(1)	1
N5	1614(3)	–1848(3)	7140(3)	29(1)	1
N6	275(3)	–3063(3)	6372(3)	29(1)	1
N7	–548(3)	–4594(3)	7032(3)	29(1)	1
N8	–2310(3)	–5592(3)	8531(3)	28(1)	1
N9	4576(3)	–4534(3)	6364(3)	28(1)	1
N10	–342(3)	1677(3)	3473(3)	29(1)	1
O1	5854(3)	813(2)	4237(2)	30(1)	1
O2	799(3)	–4354(3)	5745(2)	34(1)	1
O3	2983(3)	3589(2)	2083(2)	30(1)	1
O4	4687(3)	4321(2)	2037(2)	33(1)	1
O5	–2178(3)	–3453(3)	8123(2)	36(1)	1
O6	–444(3)	–2770(3)	8055(3)	40(1)	1

Acetate complex of receptor 213

Table 1. Crystal data and structure refinement details.

Identification code	**2008jh0004**
Empirical formula	$C_{43}H_{57}N_5O_3$
Formula weight	691.94
Temperature	120(2) K
Wavelength	0.71073 Å
Crystal system	Monoclinic
Space group	$P2_1/n$
Unit cell dimensions	a = 11.0933(2) Å α = 90°
	b = 26.7833(6) Å β = 98.0560(10)°
	c 13.2013(3) Å γ = 90°
Volume	3883.60(14) Å^3
Z	4
Density (calculated)	1.183 Mg / m^3
Absorption coefficient	0.075 mm^{-1}
F(000)	1496
Crystal	Block; Colourless
Crystal size	0.1 × 0.1 × 0.1 mm^3
θ range for data collection	2.94 – 27.51°
Index ranges	$-14 \le h \le 14$, $-34 \le k \le 34$, $-16 \le l \le 17$
Reflections collected	40088
Independent reflections	8914 [R_{int} = 0.0815]
Completeness to θ = 27.50°	99.8 %
Absorption correction	Semi–empirical from equivalents
Max. and min. transmission	0.9926 and 0.9826
Refinement method	Full-matrix least-squares on F^2
Data / restraints / parameters	8914 / 0 / 465
Goodness-of-fit on F^2	1.040
Final R indices [$F^2 > 2\sigma(F^2)$]	*R1* = 0.0674, *wR2* = 0.1354
R indices (all data)	*R1* = 0.1274, *wR2* = 0.1613
Largest diff. peak and hole	0.251 and –0.330 e Å^{-3}

Diffractometer: *Nonius KappaCCD* area detector (ϕ scans and ω scans to fill *asymmetric unit*). **Cell determination:** DirAx (Duisenberg, A.J.M.(1992). J. Appl. Cryst. 25, 92-96.) **Data collection:** Collect (Collect: Data collection software, R. Hooft, Nonius B.V., 1998). **Data reduction and cell refinement**: *Denzo* (Z. Otwinowski & W. Minor, *Methods in Enzymology* (1997) Vol. **276**: *Macromolecular Crystallography*, part A, pp. 307–326; C. W. Carter, Jr. & R. M. Sweet, Eds., Academic Press). **Absorption correction**: Sheldrick, G. M. SADABS - Bruker Nonius area detector scaling and absorption correction - V2.10 S**tructure solution**: *SHELXS97* (G. M. Sheldrick, Acta Cryst. (1990) A**46** 467–473). S**tructure refinement**: *SHELXL97* (G. M. Sheldrick (1997), University of Göttingen, Germany). **Graphics:** Cameron - A Molecular Graphics Package. (D. M. Watkin, L. Pearce and C. K. Prout, Chemical Crystallography Laboratory, University of Oxford, 1993).

Special details:

Table 2. Atomic coordinates [$\times 10^4$], equivalent isotropic displacement parameters [$Å^2 \times 10^3$] and site occupancy factors. U_{eq} is defined as one third of the trace of the orthogonalized U^{ij} tensor.

Atom	*x*	*y*	*z*	U_{eq}	*S.o.f.*
C26	6302(2)	1256(1)	3297(2)	25(1)	1
C27	7470(2)	1089(1)	2939(2)	36(1)	1
C28	6301(2)	1789(1)	7793(2)	28(1)	1
C29	6912(2)	2123(1)	6160(2)	25(1)	1
C30	7759(2)	1321(1)	6936(2)	30(1)	1
C31	5592(2)	1397(1)	6092(2)	28(1)	1
C33	5333(2)	2187(1)	7798(2)	30(1)	1
C34	8264(2)	1146(1)	5987(2)	36(1)	1
C35	8000(2)	2427(1)	6626(2)	28(1)	1
C36	5175(2)	898(1)	6457(2)	37(1)	1
C37	4978(2)	2237(1)	8864(2)	31(1)	1
C38	7983(2)	2936(1)	6110(2)	30(1)	1
C39	9418(3)	837(1)	6299(2)	51(1)	1
C40	4082(3)	717(1)	5717(2)	43(1)	1
C41	10061(3)	712(1)	5396(3)	70(1)	1
C42	9205(2)	3201(1)	6311(2)	38(1)	1
C43	4151(2)	2686(1)	8947(2)	37(1)	1
C44	3600(3)	219(1)	6003(3)	62(1)	1
C1	11815(2)	1699(1)	−1828(2)	33(1)	1
C2	12287(2)	1227(1)	−1600(2)	38(1)	1
C3	11891(2)	933(1)	−836(2)	39(1)	1
C4	11007(2)	1102(1)	−286(2)	34(1)	1
C5	10505(2)	1577(1)	−508(2)	28(1)	1
C6	10926(2)	1870(1)	−1271(2)	29(1)	1
C7	9603(2)	1872(1)	−84(2)	27(1)	1
C8	9529(2)	2332(1)	−616(2)	24(1)	1
C9	8871(2)	1793(1)	679(2)	29(1)	1
C10	8068(2)	2164(1)	873(2)	31(1)	1
C11	7992(2)	2617(1)	335(2)	27(1)	1
C12	8724(2)	2709(1)	−414(2)	24(1)	1
C13	7685(2)	3428(1)	−1327(2)	26(1)	1
C14	7139(2)	4199(1)	−2349(2)	26(1)	1
C15	7627(2)	4577(1)	−2908(2)	24(1)	1
C16	6892(2)	4937(1)	−3475(2)	26(1)	1
C17	5627(2)	4922(1)	−3493(2)	31(1)	1
C18	5147(2)	4552(1)	−2942(2)	32(1)	1
C19	5882(2)	4194(1)	−2380(2)	30(1)	1
C20	7705(2)	5257(1)	−3943(2)	25(1)	1
C21	8897(2)	5077(1)	−3633(2)	24(1)	1
C22	7541(2)	5675(1)	−4584(2)	29(1)	1
C23	8544(2)	5901(1)	−4891(2)	30(1)	1

C24	9716(2)	5719(1)	–4570(2)	29(1)	1
C25	9912(2)	5304(1)	–3940(2)	27(1)	1
N1	8837(2)	4665(1)	–3012(2)	26(1)	1
N2	7953(2)	3858(1)	–1810(2)	26(1)	1
N3	8722(2)	3164(1)	–959(2)	25(1)	1
N4	10328(2)	2325(1)	–1334(2)	26(1)	1
O1	6662(2)	3290(1)	–1231(1)	37(1)	1
O2	5446(2)	941(1)	3242(1)	35(1)	1
O3	6224(2)	1691(1)	3633(1)	32(1)	1
N5	6645(2)	1656(1)	6745(1)	25(1)	1

Acetate complex of receptor 215

Table 1. Crystal data and structure refinement details.

Identification code	**2009jh001**
Empirical formula	$C_{55}H_{99}N_5O_8$
Formula weight	958.39
Temperature	120(2) K
Wavelength	0.71073 Å
Crystal system	Triclinic
Space group	*P*–1
Unit cell dimensions	a = 13.3317(7) Å α = 101.954(3)°
	b = 14.8340(6) Å β = 108.917(2)°
	c 16.8405(9) Å γ = 107.417(3)°
Volume	2830.3(2) Å^3
Z	2
Density (calculated)	1.125 Mg / m^3
Absorption coefficient	0.074 mm^{-1}
F(000)	1056
Crystal	Block; Colourless
Crystal size	0.4 × 0.3 × 0.1 mm^3
θ range for data collection	3.03 – 25.03°
Index ranges	$-15 \le h \le 15$, $-16 \le k \le 17$, $-20 \le l \le 20$
Reflections collected	48058
Independent reflections	9974 [R_{int} = 0.1009]
Completeness to θ = 25.03°	99.8 %
Absorption correction	Semi–empirical from equivalents
Max. and min. transmission	0.9926 and 0.9709
Refinement method	Full-matrix least-squares on F^2
Data / restraints / parameters	9974 / 66 / 626
Goodness-of-fit on F^2	1.021
Final *R* indices [$F^2 > 2\sigma(F^2)$]	*R1* = 0.1121, *wR2* = 0.2774
R indices (all data)	*R1* = 0.1719, *wR2* = 0.3183
Extinction coefficient	0.042(3)
Largest diff. peak and hole	1.225 and –0.791 e Å^{-3}

Diffractometer: *Nonius KappaCCD* area detector (ϕ scans and ω scans to fill *asymmetric unit*). **Cell determination:** DirAx (Duisenberg, A.J.M.(1992). J. Appl. Cryst. 25, 92-96.) **Data collection:** Collect (Collect: Data collection software, R. Hooft, Nonius B.V., 1998). **Data reduction and cell refinement**: *Denzo* (Z. Otwinowski & W. Minor, *Methods in Enzymology* (1997) Vol. **276**: *Macromolecular Crystallography*, part A, pp. 307–326; C. W. Carter, Jr. & R. M. Sweet, Eds., Academic Press). **Absorption correction**: Sheldrick, G. M. SADABS - Bruker Nonius area detector scaling and absorption correction - V2.10 S**tructure solution**: *SHELXS97* (G. M. Sheldrick, Acta Cryst. (1990) A**46** 467–473). S**tructure refinement**: *SHELXL97* (G. M. Sheldrick (1997), University of Göttingen, Germany). **Graphics:** Cameron - A Molecular Graphics Package. (D. M. Watkin, L. Pearce and C. K. Prout, Chemical Crystallography Laboratory, University of Oxford, 1993).

Special details:

Table 2. Atomic coordinates [$\times 10^4$], equivalent isotropic displacement parameters [$Å^2 \times 10^3$] and site occupancy factors. U_{eq} is defined as one third of the trace of the orthogonalized U^{ij} tensor.

Atom	*x*	*y*	*z*	U_{eq}	*S.o.f.*
O1	12178(2)	4665(2)	12267(2)	52(1)	1
N1	8204(2)	1719(2)	10544(2)	37(1)	1
N2	10262(2)	3576(2)	11609(2)	42(1)	1
N3	10870(3)	5008(2)	12757(2)	45(1)	1
C1	7444(3)	781(2)	9938(2)	36(1)	1
C2	6290(3)	268(2)	9729(2)	40(1)	1
C3	5720(3)	–681(3)	9101(2)	45(1)	1
C4	6288(3)	–1115(3)	8673(2)	47(1)	1
C5	7440(3)	–603(3)	8877(2)	45(1)	1
C6	8048(3)	355(2)	9521(2)	38(1)	1
C7	9212(3)	1080(2)	9900(2)	40(1)	1
C8	10204(3)	1101(3)	9768(2)	43(1)	1
C9	11200(3)	1943(3)	10245(2)	48(1)	1
C10	11256(3)	2774(3)	10861(2)	45(1)	1
C11	10293(3)	2783(2)	11012(2)	41(1)	1
C12	9269(3)	1920(2)	10524(2)	37(1)	1
C13	11194(3)	4448(3)	12222(2)	42(1)	1
C14	11571(3)	5980(3)	13387(2)	46(1)	1
C15	12774(3)	6368(3)	13776(2)	51(1)	1
C16	13383(4)	7323(3)	14385(3)	63(1)	1
C17	12822(4)	7904(3)	14622(3)	62(1)	1
C18	11633(4)	7527(3)	14269(3)	59(1)	1
C19	11000(4)	6547(3)	13636(2)	52(1)	1
N4	6230(2)	2633(2)	8337(2)	30(1)	1
C20	5891(3)	1932(2)	7407(2)	34(1)	1
C21	5971(3)	923(2)	7364(2)	37(1)	1
C22	5881(3)	390(3)	6453(2)	42(1)	1
C23	5889(3)	–642(3)	6362(3)	46(1)	1
C24	5533(3)	2118(2)	8791(2)	34(1)	1
C25	4236(3)	1840(2)	8359(2)	39(1)	1
C26	3661(3)	1252(3)	8845(2)	42(1)	1
C27	2370(3)	989(3)	8483(3)	56(1)	1
C28	6004(3)	3553(2)	8217(2)	35(1)	1
C29	6301(3)	4361(2)	9065(3)	44(1)	1
C30	5850(3)	5155(3)	8860(3)	54(1)	1
C31	6195(4)	6004(3)	9705(3)	68(1)	1
C32	7491(2)	2920(2)	8930(2)	31(1)	1
C33	8365(3)	3466(2)	8619(2)	35(1)	1
C34	9570(3)	3585(2)	9216(2)	34(1)	1
C35	10494(3)	4115(3)	8928(2)	43(1)	1
N5	11116(2)	2340(2)	13683(2)	32(1)	1
C36	9908(3)	2174(2)	13054(2)	34(1)	1

C37	8972(3)	1855(3)	13379(2)	38(1)	1
C38	7787(3)	1622(3)	12664(2)	40(1)	1
C39	6856(3)	1299(3)	12994(3)	53(1)	1
C40	11153(3)	1354(2)	13807(2)	33(1)	1
C41	10929(3)	545(2)	12977(2)	34(1)	1
C42	10972(3)	–391(2)	13214(2)	35(1)	1
C43	10809(3)	–1231(2)	12429(2)	41(1)	1
C44	11928(3)	2772(2)	13275(2)	36(1)	1
C45	13177(3)	2969(3)	13768(2)	44(1)	1
C46	13862(3)	3398(3)	13265(3)	56(1)	1
C47	15130(3)	3614(4)	13709(3)	68(1)	1
C48	11448(3)	3054(2)	14605(2)	33(1)	1
C49	11464(3)	4086(2)	14645(2)	38(1)	1
C50	11677(3)	4680(2)	15579(2)	39(1)	1
C51	11722(3)	5735(3)	15661(2)	47(1)	1
O2A	7820(5)	3381(4)	11121(4)	70(1)	0.361(3)
O3A	8542(5)	4455(5)	12479(4)	56(1)	0.361(3)
C52A	7709(5)	3877(3)	11755(4)	44(1)	0.361(3)
C53A	6512(5)	3780(9)	11651(7)	87(2)	0.361(3)
O2B	7083(4)	2925(3)	10870(3)	70(1)	0.639(3)
O3B	8579(3)	3877(3)	12152(3)	56(1)	0.639(3)
C52B	7559(4)	3609(3)	11602(3)	44(1)	0.639(3)
C53B	6836(5)	4140(5)	11833(5)	87(2)	0.639(3)
O4	11221(3)	1466(3)	16004(3)	99(1)	1
O5	13050(3)	2439(3)	16494(3)	112(1)	1
C54	12081(4)	2226(4)	16500(4)	82(2)	1
C55	11926(4)	2979(4)	17191(4)	88(2)	1
O6	8964(4)	444(4)	14686(3)	140(1)	1
O7	13312(4)	836(4)	15551(3)	140(1)	1
O8	14377(4)	3892(4)	16181(3)	140(1)	1

Structures from Chapter Three

Hydrogen phosphate complex of receptor 220

Table 1. Crystal data and structure refinement details.

Identification code	**2008jh0002**
Empirical formula	$C_{63}H_{101}N_8O_9P$
Formula weight	1145.49
Temperature	120(2) K
Wavelength	0.71073 Å
Crystal system	Triclinic
Space group	*P*–1
Unit cell dimensions	a = 13.9084(5) Å α = 65.864(2)°
	b = 16.5116(5) Å β = 72.349(2)°
	c 16.5971(4) Å γ = 71.014(2)°
Volume	3224.48(17) Å^3
Z	2
Density (calculated)	1.180 Mg / m^3
Absorption coefficient	0.102 mm^{-1}
F(000)	1244
Crystal	Block; Colourless
Crystal size	0.18 × 0.05 × 0.02 mm^3
θ range for data collection	2.96 – 25.00°
Index ranges	$-16 \le h \le 16$, $-19 \le k \le 19$, $-19 \le l \le 19$
Reflections collected	48032
Independent reflections	11275 [R_{int} = 0.0900]
Completeness to θ = 25.00°	99.3 %
Absorption correction	Semi–empirical from equivalents
Max. and min. transmission	0.9980 and 0.9818
Refinement method	Full-matrix least-squares on F^2
Data / restraints / parameters	11275 / 10 / 768
Goodness-of-fit on F^2	1.096
Final *R* indices [$F^2 > 2\sigma(F^2)$]	*R1* = 0.0931, *wR2* = 0.1597
R indices (all data)	*R1* = 0.1586, *wR2* = 0.1914
Largest diff. peak and hole	0.748 and –0.753 e Å^{-3}

Diffractometer: *Nonius KappaCCD* area detector (ϕ scans and ω scans to fill *asymmetric unit*). **Cell determination:** DirAx (Duisenberg, A.J.M.(1992). J. Appl. Cryst. 25, 92-96.) **Data collection:** Collect (Collect: Data collection software, R. Hooft, Nonius B.V., 1998). **Data reduction and cell refinement**: *Denzo* (Z. Otwinowski & W. Minor, *Methods in Enzymology* (1997) Vol. **276**: *Macromolecular Crystallography*, part A, pp. 307–326; C. W. Carter, Jr. & R. M. Sweet, Eds., Academic Press). **Absorption correction**: Sheldrick, G. M. SADABS - Bruker Nonius area detector scaling and absorption correction - V2.10 S**tructure solution**: *SHELXS97* (G. M. Sheldrick, Acta Cryst. (1990) A**46** 467–473). S**tructure refinement**: *SHELXL97* (G. M. Sheldrick (1997), University of Göttingen, Germany). **Graphics:** Cameron - A Molecular Graphics Package. (D. M. Watkin, L. Pearce and C. K. Prout, Chemical Crystallography Laboratory, University of Oxford, 1993).

Special details:

Table 2. Atomic coordinates [$\times 10^4$], equivalent isotropic displacement parameters [$Å^2 \times 10^3$] and site occupancy factors. U_{eq} is defined as one third of the trace of the orthogonalized U^{ij} tensor.

Atom	*x*	*y*	*z*	U_{eq}	*S.o.f.*
C48	4960(3)	12262(3)	558(3)	29(1)	1
C49	4095(3)	12657(3)	25(3)	32(1)	1
C50	3055(4)	12625(4)	661(3)	39(1)	1
C51	2155(4)	13020(4)	172(4)	48(1)	1
C52	6289(4)	11510(3)	–489(3)	28(1)	1
C53	6113(4)	10563(3)	118(3)	29(1)	1
C54	6538(4)	9875(3)	–381(3)	35(1)	1
C55	7710(4)	9613(3)	–604(3)	37(1)	1
C56	6758(3)	11799(3)	708(3) 2	8(1)	1
C57	7911(3)	11515(3)	356(3)	31(1)	1
C58	8511(4)	11312(3)	1071(3)	35(1)	1
C59	9675(4)	10999(4)	782(4)	52(2)	1
C60	6240(4)	13075(3)	–675(3)	29(1)	1
C61	6125(4)	13829(3)	–321(3)	32(1)	1
C62	7126(4)	13939(3)	–214(3)	40(1)	1
C63	6959(5)	14803(4)	–27(3)	49(2)	1
N8	6063(3)	12158(2)	25(2)	28(1)	1
O8	3588(6)	5540(5)	5398(5)	43(2)	0.50
O9	5755(6)	5295(5)	5176(5)	51(2)	0.50
O10	5263(3)	8414(2)	6973(2)	44(1)	1
C1	8583(4)	7377(3)	1681(3)	36(1)	1
C2	9235(4)	7870(3)	1661(3)	37(1)	1
C3	8795(4)	8688(3)	1820(3)	34(1)	1
C4	7733(4)	9016(3)	1989(3)	29(1)	1
C5	7084(3)	8506(3)	2022(3)	27(1)	1
C6	7524(4)	7681(3)	1860(3)	29(1)	1
C7	5366(3)	9497(3)	2423(3)	25(1)	1
C8	4235(3)	9579(3)	2627(3)	27(1)	1
C9	3462(4)	10322(3)	2719(3)	30(1)	1
C10	2491(4)	10110(3)	2860(3)	30(1)	1
C11	2748(3)	9208(3)	2858(3)	26(1)	1
C12	1440(4)	10581(3)	2961(3)	37(1)	1
C13	1996(4)	8747(3)	2987(3)	28(1)	1
C14	720(4)	10135(3)	3056(3)	39(1)	1
C15	973(4)	9236(3)	3074(3)	34(1)	1
C16	1885(4)	7372(3)	2797(3)	29(1)	1
C17	2158(4)	5830(3)	2763(3)	27(1)	1
C18	1164(4)	5854(3)	2737(3)	31(1)	1
C19	962(4)	5174(3)	2546(3)	35(1)	1
C20	1727(4)	4454(3)	2390(3)	32(1)	1
C21	2750(4)	4401(3)	2420(3)	27(1)	1
C22	2948(3)	5089(3)	2608(3)	26(1)	1

C23	3722(3)	3787(3)	2284(3)	27(1)	1
C24	4461(3)	4112(3)	2375(3)	25(1)	1
C25	5586(4)	3681(3)	2282(3)	26(1)	1
C26	7283(4)	3894(3)	2256(3)	30(1)	1
C27	7743(4)	4560(4)	2180(4)	46(1)	1
C28	7898(4)	3047(3)	2256(3)	39(1)	1
C29	8813(5)	4378(4)	2071(5)	63(2)	1
C30	8956(4)	2870(4)	2153(4)	46(1)	1
C31	9417(4)	3537(4)	2057(4)	55(2)	1
C32	7596(6)	10419(4)	3822(4)	82(2)	1
C33	6862(6)	9988(7)	4558(8)	144(5)	1
C34	6336(5)	9377(4)	4636(4)	69(2)	1
C35	6900(5)	8648(3)	4198(3)	49(2)	1
C36	7683(4)	7517(4)	5517(3)	39(1)	1
C37	8760(4)	7707(3)	5113(3)	43(1)	1
C38	9276(5)	7605(4)	5843(4)	56(2)	1
C39	10297(5)	7905(5)	5473(4)	66(2)	1
C40	7595(4)	7068(3)	4276(3)	35(1)	1
C41	7908(4)	6050(3)	4795(3)	39(1)	1
C42	8456(4)	5539(3)	4152(3)	43(1)	1
C43	8826(6)	4524(4)	4641(4)	77(2)	1
C44	6010(4)	7448(3)	5390(3)	37(1)	1
C45	5177(4)	7701(4)	4851(3)	41(1)	1
C46	4217(4)	7414(4)	5514(3)	54(2)	1
C47	3285(5)	7722(5)	5057(4)	67(2)	1
N1	6193(3)	4142(2)	2340(2)	27(1)	1
N2	3993(3)	4896(2)	2587(2)	25(1)	1
N3	2413(3)	6476(2)	2952(2)	27(1)	1
N4	2335(3)	7829(2)	3047(2)	29(1)	1
N5	3802(3)	8899(2)	2713(2)	24(1)	1
N6	5986(3)	8751(2)	2230(2)	24(1)	1
N7	7051(3)	7668(3)	4845(2)	35(1)	1
O1	5912(2)	2946(2)	2153(2)	32(1)	1
O2	1117(3)	7725(2)	2455(3)	53(1)	1
O3	5706(2)	10107(2)	2426(2)	29(1)	1
O4	6024(2)	6234(2)	3376(2)	32(1)	1
O5	5308(2)	5876(2)	2359(2)	33(1)	1
O6	5065(2)	7487(2)	2257(2)	28(1)	1
O7	4087(2)	6425(2)	3593(2)	32(1)	1
P1	5085(1)	6506(1)	2879(1)	26(1)	1

Chloride complex of receptor 220

Table 1. Crystal data and structure refinement details.

Identification code	**2008sot0833 (Ureaamide+Cl–)**
Empirical formula	$C_{67}H_{109.76}Cl_2N_8O_{5.88}S_2$
	$C_{31}H_{24}N_6O_3$. 2($C_{16}H_{36}N$) . 2(C_2H_6OS) . 2(Cl) . 0.88(H_2O)
Formula weight	1256.41
Temperature	120(2) K
Wavelength	0.71069 Å
Crystal system	Monoclinic
Space group	*C*2/*c*
Unit cell dimensions	a = 53.493(2) Å
	b = 7.8760(2) Å β = 100.3320(13)°
	c = 34.3220(12) Å
Volume	14225.8(8) Å^3
Z	8
Density (calculated)	1.173 Mg / m^3
Absorption coefficient	0.203 mm^{-1}
F(000)	5446
Crystal	Lath; Colourless
Crystal size	0.4 × 0.07 × 0.03 mm^3
θ range for data collection	2.94 – 25.02°
Index ranges	$-62 \le h \le 63$, $-9 \le k \le 8$, $-40 \le l \le 38$
Reflections collected	32498
Independent reflections	12299 [R_{int} = 0.1277]
Completeness to θ = 25.02°	97.7 %
Absorption correction	Semi–empirical from equivalents
Max. and min. transmission	0.9939 and 0.9133
Refinement method	Full-matrix least-squares on F^2
Data / restraints / parameters	12299 / 20 / 795
Goodness-of-fit on F^2	1.090
Final *R* indices [$F^2 > 2\sigma(F^2)$]	*R1* = 0.1624, *wR2* = 0.2463
R indices (all data)	*R1* = 0.3008, *wR2* = 0.3063
Largest diff. peak and hole	0.651 and –0.484 e Å^{-3}

Diffractometer: *Nonius KappaCCD* area detector (ϕ scans and ω scans to fill *asymmetric unit*). **Cell determination:** DirAx (Duisenberg, A.J.M.(1992). J. Appl. Cryst. 25, 92-96.) **Data collection:** Collect (Collect: Data collection software, R. Hooft, Nonius B.V., 1998). **Data reduction and cell refinement**: *Denzo* (Z. Otwinowski & W. Minor, *Methods in Enzymology* (1997) Vol. **276**: *Macromolecular Crystallography*, part A, pp. 307–326; C. W. Carter, Jr. & R. M. Sweet, Eds., Academic Press). **Absorption correction**: Sheldrick, G. M. SADABS - Bruker Nonius area detector scaling and absorption correction - V2.10 S**tructure solution**: *SHELXS97* (G. M. Sheldrick, Acta Cryst. (1990) A**46** 467–473). S**tructure refinement**: *SHELXL97* (G. M. Sheldrick (1997), University of Göttingen, Germany). **Graphics:** Cameron - A Molecular Graphics Package. (D. M. Watkin, L. Pearce and C. K. Prout, Chemical Crystallography Laboratory, University of Oxford, 1993).

Special details: All hydrogen atoms were placed in idealised positions and refined using a riding model. The hydrogens were on the waters were not located, but included in the UNIT instruction.

Table 2. Atomic coordinates [$\times 10^4$], equivalent isotropic displacement parameters [$Å^2 \times 10^3$] and site occupancy factors. U_{eq} is defined as one third of the trace of the orthogonalized U^{ij} tensor.

Atom	*x*	*y*	*z*	U_{eq}	*S.o.f.*
O1	5929(1)	25(3)	9350(1)	38(1)	1
O2	7134(1)	–2836(3)	8732(1)	42(1)	1
O3	5943(1)	146(3)	7404(1)	42(1)	1
N1	5945(1)	855(4)	9997(1)	24(1)	1
N2	6424(1)	–727(3)	9455(1)	24(1)	1
N3	6777(1)	–1908(4)	8953(1)	33(1)	1
N4	6758(1)	–2434(4)	8310(1)	35(1)	1
N5	6410(1)	–1315(3)	7591(1)	25(1)	1
N6	5950(1)	105(4)	6741(1)	29(1)	1
C1	5631(1)	2107(5)	10322(1)	33(1)	1
C2	5379(1)	2555(5)	10339(1)	45(1)	1
C3	5190(1)	2149(6)	10025(1)	51(2)	1
C4	5244(1)	1302(6)	9697(1)	48(1)	1
C5	5496(1)	866(5)	9680(1)	37(1)	1
C6	5688(1)	1281(4)	9989(1)	26(1)	1
C7	6048(1)	271(4)	9691(1)	26(1)	1
C8	6323(1)	–133(4)	9770(1)	22(1)	1
C9	6512(1)	–46(4)	10099(1)	24(1)	1
C10	6740(1)	–616(4)	9984(1)	25(1)	1
C11	6992(1)	–833(4)	10187(1)	31(1)	1
C12	7168(1)	–1414(4)	9971(1)	28(1)	1
C13	7108(1)	–1799(4)	9564(1)	27(1)	1
C14	6860(1)	–1596(4)	9359(1)	27(1)	1
C15	6681(1)	–1040(4)	9582(1)	28(1)	1
C16	6910(1)	–2406(5)	8670(1)	31(1)	1
C17	6828(1)	–2573(4)	7930(1)	28(1)	1
C18	7049(1)	–3266(5)	7854(1)	31(1)	1
C19	7095(1)	–3339(5)	7463(1)	32(1)	1
C20	6923(1)	–2786(5)	7146(1)	31(1)	1
C21	6693(1)	–2082(4)	7210(1)	24(1)	1
C22	6476(1)	–1390(4)	6963(1)	25(1)	1
C23	6308(1)	–936(4)	7200(1)	21(1)	1
C24	6650(1)	–1995(4)	7603(1)	23(1)	1
C25	6047(1)	–170(4)	7120(1)	27(1)	1
C26	5707(1)	811(4)	6590(1)	30(1)	1
C27	5631(1)	826(5)	6177(1)	34(1)	1
C28	5398(1)	1488(5)	6005(1)	37(1)	1
C29	5239(1)	2155(5)	6235(1)	49(1)	1
C30	5311(1)	2138(5)	6641(1)	44(1)	1
C31	5541(1)	1480(5)	6824(1)	38(1)	1
N7	5927(1)	3841(4)	8564(1)	32(1)	1

C32	6126(1)	3396(4)	8916(1)	31(1)	1
C33	6301(1)	4832(4)	9089(1)	31(1)	1
C34	6523(1)	4123(5)	9387(1)	42(1)	1
C35	6724(1)	3253(5)	9200(1)	54(2)	1
C36	5757(1)	5284(4)	8656(1)	37(1)	1
C37	5591(1)	4847(5)	8961(1)	42(1)	1
C38	5476(1)	6496(5)	9086(1)	51(1)	1
C39	5285(1)	6133(6)	9359(1)	63(2)	1
C40	6044(1)	4436(4)	8213(1)	34(1)	1
C41	6252(1)	3363(5)	8102(1)	42(1)	1
C42	6334(1)	4004(6)	7740(1)	62(2)	1
C43	6572(1)	3194(5)	7643(1)	57(1)	1
C44	5770(1)	2212(4)	8449(1)	29(1)	1
C45	5553(1)	2366(5)	8104(1)	44(1)	1
C46A	5366(1)	734(7)	8132(2)	38(2)	0.605(5)
C47A	5515(1)	−840(8)	8032(2)	61(2)	0.605(5)
C46B	5403(1)	924(14)	8012(2)	38(2)	0.395(5)
C47B	5164(2)	1057(14)	7687(3)	61(2)	0.395(5)
N8	6558(1)	4186(3)	5987(1)	26(1)	1
C48	6713(1)	2642(4)	6153(1)	31(1)	1
C49	6895(1)	2930(5)	6541(1)	38(1)	1
C50	7045(1)	1329(5)	6664(2)	56(2)	1
C51	7212(1)	1476(6)	7071(2)	68(2)	1
C52	6416(1)	4946(4)	6295(1)	28(1)	1
C53	6236(1)	3729(4)	6448(1)	29(1)	1
C54	6066(1)	4687(5)	6687(1)	34(1)	1
C55	5856(1)	5713(5)	6435(1)	50(1)	1
C56	6375(1)	3586(4)	5620(1)	28(1)	1
C57	6206(1)	4935(5)	5395(1)	36(1)	1
C58	6000(1)	4137(5)	5086(1)	42(1)	1
C59	5801(1)	3178(5)	5264(1)	50(2)	1
C60	6732(1)	5574(4)	5878(1)	32(1)	1
C61	6901(1)	5066(5)	5585(1)	32(1)	1
C62	7019(1)	6612(5)	5439(1)	41(1)	1
C63	7217(1)	6168(6)	5185(1)	48(1)	1
S1A	7477(1)	2479(2)	8408(1)	65(1)	0.8794(17)
O5A	7712(1)	1577(5)	8571(1)	75(1)	0.8794(17)
C66A	7227(1)	1016(8)	8241(2)	152(3)	0.8794(17)
C67A	7368(1)	3189(10)	8841(2)	152(3)	0.8794(17)
S1B	7489(1)	1312(8)	8617(2)	65(1)	0.1206(17)
O5B	7375(3)	605(17)	8214(2)	75(1)	0.1206(17)
C66B	7394(3)	−121(13)	8970(3)	152(3)	0.1206(17)
C67B	7251(2)	2879(12)	8666(5)	152(3)	0.1206(17)
O1W	7625(1)	−1979(13)	8957(3)	239(5)	0.8794(17)
S2	5096(1)	−3061(2)	6992(1)	66(1)	1
O4	4916(1)	−4523(4)	6912(1)	70(1)	1
C64	5392(1)	−3835(7)	7260(2)	80(2)	1
C65	5200(1)	−2648(6)	6536(1)	75(2)	1

Cl1	6226(1)	–1134(1)	8481(1)	29(1)	1
Cl2	6219(1)	–766(1)	5937(1)	26(1)	1

Benzoate complex of receptor 221

Table 1. Crystal data and structure refinement details.

Identification code	**2009jh0010**
Empirical formula	$C_{104}H_{151}N_{11}O_{10}$
Formula weight	1715.36
Temperature	120(2) K
Wavelength	0.71073 Å
Crystal system	Triclinic
Space group	*P*1
Unit cell dimensions	a = 8.93200(10) Å α = 93.6790(9)°
	b = 12.4500(2) Å β = 100.5490(12)°
	c 22.5830(4) Å γ = 98.6400(11)°
Volume	2429.96(6) Å^3
Z	1
Density (calculated)	1.172 Mg / m^3
Absorption coefficient	0.075 mm^{-1}
F(000)	932
Crystal	Plate; Colourless
Crystal size	0.5 × 0.2 × 0.05 mm^3
θ range for data collection	3.26 – 25.03°
Index ranges	$-10 \le h \le 10$, $-14 \le k \le 14$, $-26 \le l \le 26$
Reflections collected	38462
Independent reflections	8540 [R_{int} = 0.0637]
Completeness to θ = 25.03°	99.6 %
Absorption correction	Semi–empirical from equivalents
Max. and min. transmission	0.9962 and 0.9633
Refinement method	Full-matrix least-squares on F^2
Data / restraints / parameters	8540 / 1299 / 1136
Goodness-of-fit on F^2	1.229
Final *R* indices [$F^2 > 2\sigma(F^2)$]	*R1* = 0.0613, *wR2* = 0.1183
R indices (all data)	*R1* = 0.0811, *wR2* = 0.1288
Largest diff. peak and hole	0.454 and –0.365 e Å^{-3}

Diffractometer: *Nonius KappaCCD* area detector (ϕ scans and ω scans to fill *asymmetric unit*). **Cell determination:** DirAx (Duisenberg, A.J.M.(1992). J. Appl. Cryst. 25, 92-96.) **Data collection:** Collect (Collect: Data collection software, R. Hooft, Nonius B.V., 1998). **Data reduction and cell refinement**: *Denzo* (Z. Otwinowski & W. Minor, *Methods in Enzymology* (1997) Vol. **276**: *Macromolecular Crystallography*, part A, pp. 307–326; C. W. Carter, Jr. & R. M. Sweet, Eds., Academic Press). **Absorption correction**: Sheldrick, G. M. SADABS - Bruker Nonius area detector scaling and absorption correction - V2.10 S**tructure solution**: *SHELXS97* (G. M. Sheldrick, Acta Cryst. (1990) A**46** 467–473). S**tructure refinement**: *SHELXL97* (G. M. Sheldrick (1997), University of Göttingen, Germany). **Graphics:** Cameron - A Molecular Graphics Package. (D. M. Watkin, L. Pearce and C. K. Prout, Chemical Crystallography Laboratory, University of Oxford, 1993).

Special details:

Table 2. Atomic coordinates [$\times 10^4$], equivalent isotropic displacement parameters [$Å^2 \times 10^3$] and site occupancy factors. U_{eq} is defined as one third of the trace of the orthogonalized U^{ij} tensor.

Atom	*x*	*y*	*z*	U_{eq}	*S.o.f.*
O1	8934(3)	6823(2)	6237(1)	33(1)	1
O2	4966(3)	1896(2)	7583(1)	33(1)	1
O3	3972(3)	7150(2)	9259(1)	32(1)	1
N1	9562(4)	7167(3)	4173(1)	32(1)	1
N2	9679(4)	6293(3)	5351(1)	29(1)	1
N3	7554(3)	4720(2)	6351(1)	24(1)	1
N4	5936(3)	3455(2)	7201(1)	26(1)	1
N5	5347(3)	3538(2)	8151(1)	25(1)	1
N6	4246(3)	4995(2)	9038(1)	26(1)	1
N7	3380(3)	6863(3)	10181(2)	29(1)	1
N8	4800(4)	7854(3)	11435(2)	42(1)	1
C1	9824(5)	7838(3)	3715(2)	37(1)	1
C2	10859(5)	8747(4)	3967(2)	41(1)	1
C3	11276(4)	8647(3)	4593(2)	33(1)	1
C4	12289(5)	9291(3)	5082(2)	35(1)	1
C5	12422(5)	8934(3)	5645(2)	37(1)	1
C6	11557(5)	7945(3)	5758(2)	33(1)	1
C7	10553(4)	7295(3)	5287(2)	28(1)	1
C8	10442(4)	7647(3)	4703(2)	30(1)	1
C9	8966(4)	6108(3)	5845(2)	27(1)	1
C10	8203(4)	4972(3)	5854(2)	27(1)	1
C11	7932(4)	4072(3)	5447(2)	30(1)	1
C12	7041(4)	3221(3)	5680(2)	28(1)	1
C13	6392(5)	2134(3)	5462(2)	31(1)	1
C14	5570(5)	1530(3)	5810(2)	33(1)	1
C15	5391(4)	1940(3)	6386(2)	31(1)	1
C16	6038(4)	2995(3)	6625(2)	25(1)	1
C17	6832(4)	3643(3)	6250(2)	24(1)	1
C18	5386(4)	2882(3)	7639(2)	27(1)	1
C19	4753(4)	3155(3)	8650(2)	26(1)	1
C20	4641(4)	2079(3)	8792(2)	29(1)	1
C21	4034(5)	1741(3)	9297(2)	32(1)	1
C22	3529(5)	2443(3)	9672(2)	31(1)	1
C23	3618(4)	3538(3)	9540(2)	29(1)	1
C24	4244(4)	3890(3)	9042(2)	25(1)	1
C25	3248(4)	4488(3)	9841(2)	30(1)	1
C26	3663(4)	5358(3)	9526(2)	26(1)	1
C27	3669(4)	6528(3)	9635(2)	28(1)	1
C28	3364(4)	7964(3)	10381(2)	29(1)	1
C29	2671(4)	8674(3)	10010(2)	31(1)	1
C30	2653(5)	9748(3)	10227(2)	38(1)	1

C31	3342(5)	10158(4)	10810(2)	40(1)	1
C32	4059(5)	9466(4)	11198(2)	37(1)	1
C33	4034(4)	8373(3)	10974(2)	32(1)	1
C34	4877(6)	9577(4)	11814(2)	51(1)	1
C35	5295(6)	8599(4)	11937(2)	51(1)	1
O4	8055(3)	5045(2)	3622(1)	43(1)	1
O5	9768(3)	4727(2)	4410(1)	37(1)	1
C36	8868(5)	4439(3)	3910(2)	34(1)	1
C37	8735(5)	3277(3)	3650(2)	35(1)	1
C38	8162(6)	2948(4)	3050(2)	54(1)	1
C39	8077(7)	1859(5)	2821(3)	65(2)	1
C40	8521(8)	1112(4)	3200(3)	69(2)	1
C41	9096(8)	1414(4)	3802(3)	69(2)	1
C42	9229(6)	2507(4)	4032(2)	50(1)	1
O6	6856(4)	5652(2)	7366(1)	40(1)	1
O7	5809(3)	5833(2)	8173(1)	31(1)	1
C43	6268(4)	6196(3)	7723(2)	28(1)	1
C44	6125(4)	7353(3)	7601(2)	28(1)	1
C45	6433(5)	7736(3)	7063(2)	34(1)	1
C46	6213(5)	8788(4)	6941(2)	44(1)	1
C47	5762(5)	9466(3)	7361(2)	45(1)	1
C48	5494(5)	9090(4)	7903(2)	45(1)	1
C49	5672(5)	8034(3)	8022(2)	36(1)	1
O8	2534(3)	5478(2)	11059(1)	35(1)	1
O9	4918(3)	5685(2)	11603(1)	43(1)	1
C50	3593(5)	5154(3)	11416(2)	34(1)	1
C51	3227(5)	4026(4)	11632(2)	38(1)	1
C52	1839(6)	3360(4)	11395(3)	55(2)	1
C53	1513(7)	2326(5)	11591(3)	72(2)	1
C54	2573(7)	1961(4)	12011(3)	62(2)	1
C55	3977(7)	2606(4)	12235(2)	57(2)	1
C56	4300(6)	3638(4)	12052(2)	51(1)	1
N9	10386(4)	11673(3)	7322(2)	32(1)	1
C57	9583(5)	11439(4)	6662(2)	38(1)	1
C58	10661(5)	11325(4)	6224(2)	46(1)	1
C59	9853(7)	11135(5)	5576(2)	62(2)	1
C60	8730(7)	10058(5)	5430(3)	78(2)	1
C61	11293(5)	10757(3)	7508(2)	34(1)	1
C62	10347(5)	9614(4)	7392(2)	45(1)	1
C63	11292(6)	8758(4)	7627(2)	49(1)	1
C64	11733(6)	8837(4)	8311(2)	56(1)	1
C65	11542(4)	12721(3)	7424(2)	32(1)	1
C66	10882(4)	13751(3)	7252(2)	32(1)	1
C67	12171(5)	14730(3)	7398(2)	33(1)	1
C68	11688(5)	15764(3)	7152(2)	40(1)	1
C69	9158(5)	11744(4)	7703(2)	36(1)	1
C70	9784(5)	11972(4)	8384(2)	42(1)	1
C71	8472(5)	11981(4)	8729(2)	45(1)	1

C72	9035(6)	12179(4)	9405(2)	54(1)	1
N10	8510(4)	6527(3)	10338(2)	36(1)	1
C73	9399(5)	6068(4)	9893(2)	38(1)	1
C74	8422(5)	5395(4)	9328(2)	42(1)	1
C75	9416(5)	5120(4)	8879(2)	47(1)	1
C76	10100(6)	6097(4)	8599(2)	54(2)	1
C77	7420(5)	5623(4)	10538(2)	38(1)	1
C78	8139(5)	4677(4)	10792(2)	38(1)	1
C79	6879(6)	3815(4)	10930(3)	66(2)	1
C80	7439(6)	2817(4)	11168(3)	58(2)	1
C81	7518(5)	7307(4)	10044(2)	38(1)	1
C82	8340(5)	8275(4)	9788(2)	43(1)	1
C83	7327(5)	9157(4)	9673(2)	45(1)	1
C84	7210(6)	9836(4)	10232(2)	54(1)	1
C85	9724(5)	7102(4)	10872(2)	40(1)	1
C86	9131(5)	7713(4)	11361(2)	46(1)	1
C87	10464(6)	8484(5)	11763(2)	56(2)	1
C88	9930(8)	9141(5)	12237(2)	73(2)	1
N11	4157(4)	5788(3)	14233(2)	46(1)	1
C89A	2825(11)	5916(11)	13737(4)	57(1)	0.579(10)
C90A	3356(10)	5895(10)	13131(4)	57(1)	0.579(10)
C91A	2197(9)	6334(8)	12674(4)	57(1)	0.579(10)
C92A	647(10)	5620(9)	12520(4)	57(1)	0.579(10)
C89B	2897(16)	5984(17)	13704(5)	57(1)	0.421(10)
C90B	3085(13)	5932(14)	13043(5)	57(1)	0.421(10)
C91B	1683(13)	6115(11)	12606(5)	57(1)	0.421(10)
C92B	337(13)	5211(12)	12530(6)	57(1)	0.421(10)
C93	4756(5)	4747(4)	14099(2)	45(1)	1
C94	3608(6)	3705(4)	14011(2)	57(2)	1
C95	4448(8)	2750(5)	13914(3)	71(2)	1
C96	3415(11)	1657(6)	13828(4)	114(3)	1
C97A	5509(15)	6723(8)	14297(9)	82(1)	0.502(7)
C98A	4968(14)	7836(8)	14383(6)	82(1)	0.502(7)
C99A	5975(14)	8728(9)	14133(5)	82(1)	0.502(7)
C10A	5163(14)	8849(10)	13495(5)	82(1)	0.502(7)
C97B	5539(17)	6701(8)	14316(9)	82(1)	0.498(7)
C98B	5464(15)	7854(8)	14588(6)	82(1)	0.498(7)
C99B	5269(14)	8656(10)	14155(6)	82(1)	0.498(7)
C10B	6321(14)	8782(10)	13725(6)	82(1)	0.498(7)
C101	3461(5)	5756(4)	14798(2)	48(1)	1
C102	4553(5)	5596(5)	15379(2)	54(1)	1
C103	3640(5)	5335(4)	15874(2)	49(1)	1
C104	2668(6)	4201(4)	15763(2)	57(1)	1
O10	6936(4)	6417(3)	12718(2)	55(1)	1

Sulfate complex of receptor 221

Table 1. Crystal data and structure refinement details.

Identification code	**2009jh0011**
Empirical formula	$C_{67}H_{98}N_{10}O_7S$
Formula weight	1187.61
Temperature	120(2) K
Wavelength	0.71073 Å
Crystal system	Triclinic
Space group	*P*–1
Unit cell dimensions	a = 8.78000(10) Å α = 88.1700(11)°
	b = 16.9160(4) Å β = 85.7350(12)°
	c 22.1640(5) Å γ = 82.7650(13)°
Volume	3255.75(11) Å^3
Z	2
Density (calculated)	1.211 Mg / m^3
Absorption coefficient	0.110 mm^{-1}
F(000)	1284
Crystal	Block; Colourless
Crystal size	0.3 × 0.2 × 0.15 mm^3
θ range for data collection	2.96 – 25.03°
Index ranges	$-10 \le h \le 10$, $-20 \le k \le 20$, $-26 \le l \le 26$
Reflections collected	61520
Independent reflections	11472 [R_{int} = 0.0907]
Completeness to θ = 25.03°	99.7 %
Absorption correction	Semi–empirical from equivalents
Max. and min. transmission	0.9837 and 0.9678
Refinement method	Full-matrix least-squares on F^2
Data / restraints / parameters	11472 / 19 / 767
Goodness-of-fit on F^2	1.027
Final *R* indices [$F^2 > 2\sigma(F^2)$]	*R1* = 0.0731, *wR2* = 0.1518
R indices (all data)	*R1* = 0.1081, *wR2* = 0.1701
Largest diff. peak and hole	0.806 and –0.839 e Å^{-3}

Diffractometer: *Nonius KappaCCD* area detector (ϕ scans and ω scans to fill *asymmetric unit*). **Cell determination:** DirAx (Duisenberg, A.J.M.(1992). J. Appl. Cryst. 25, 92-96.) **Data collection:** Collect (Collect: Data collection software, R. Hooft, Nonius B.V., 1998). **Data reduction and cell refinement**: *Denzo* (Z. Otwinowski & W. Minor, *Methods in Enzymology* (1997) Vol. **276**: *Macromolecular Crystallography*, part A, pp. 307–326; C. W. Carter, Jr. & R. M. Sweet, Eds., Academic Press). **Absorption correction**: Sheldrick, G. M. SADABS - Bruker Nonius area detector scaling and absorption correction - V2.10 S**tructure solution**: *SHELXS97* (G. M. Sheldrick, Acta Cryst. (1990) A**46** 467–473). S**tructure refinement**: *SHELXL97* (G. M. Sheldrick (1997), University of Göttingen, Germany). **Graphics:** Cameron - A Molecular Graphics Package. (D. M. Watkin, L. Pearce and C. K. Prout, Chemical Crystallography Laboratory, University of Oxford, 1993).

Special details:

Table 2. Atomic coordinates [$\times 10^4$], equivalent isotropic displacement parameters [$Å^2 \times 10^3$] and site occupancy factors. U_{eq} is defined as one third of the trace of the orthogonalized U^{ij} tensor.

Atom	*x*	*y*	*z*	U_{eq}	*S.o.f.*
C1	6418(4)	881(2)	9433(2)	41(1)	1
C2	6962(4)	899(2)	9991(2)	45(1)	1
C3	6730(4)	1711(2)	10173(2)	37(1)	1
C4	7018(4)	2093(2)	10697(2)	42(1)	1
C5	6606(4)	2909(2)	10726(2)	43(1)	1
C6	5957(4)	3346(2)	10246(2)	37(1)	1
C7	5663(4)	2987(2)	9718(1)	32(1)	1
C8	6042(3)	2156(2)	9690(1)	32(1)	1
C9	4074(3)	4107(2)	9243(2)	33(1)	1
C10	3748(3)	4548(2)	8675(1)	29(1)	1
C11	2844(3)	5266(2)	8635(2)	32(1)	1
C12	2866(3)	5511(2)	8015(1)	29(1)	1
C13	3806(3)	4901(2)	7692(1)	25(1)	1
C14	2229(4)	6187(2)	7692(2)	34(1)	1
C15	2547(3)	6220(2)	7076(2)	35(1)	1
C16	3457(3)	5604(2)	6760(2)	30(1)	1
C17	4086(3)	4929(2)	7062(1)	27(1)	1
C18	5776(3)	4210(2)	6249(1)	28(1)	1
C19	7172(3)	3124(2)	5606(1)	27(1)	1
C20	7524(3)	3566(2)	5087(1)	30(1)	1
C21	8302(3)	3196(2)	4573(1)	29(1)	1
C22	8738(3)	2386(2)	4556(1)	28(1)	1
C23	8411(3)	1921(2)	5078(1)	26(1)	1
C24	7661(3)	2298(2)	5597(1)	25(1)	1
C25	8720(3)	1097(2)	5229(1)	30(1)	1
C26	8183(3)	997(2)	5819(1)	29(1)	1
C27	8300(3)	225(2)	6159(1)	31(1)	1
C28	7921(3)	–459(2)	7143(1)	29(1)	1
C29	8959(4)	–1144(2)	7049(2)	33(1)	1
C30	8910(4)	–1814(2)	7435(2)	39(1)	1
C31	7843(4)	–1837(2)	7919(2)	40(1)	1
C32	6788(4)	–1152(2)	8030(2)	34(1)	1
C33	6859(3)	–470(2)	7648(1)	28(1)	1
C34	5562(4)	–950(2)	8482(2)	41(1)	1
C35	4964(4)	–187(2)	8363(2)	38(1)	1
C36	5108(3)	2370(2)	3949(2)	39(1)	1
C37	5169(4)	1742(2)	3476(2)	47(1)	1
C38	6874(4)	1474(2)	3280(2)	54(1)	1
C39	7027(5)	928(3)	2768(2)	71(1)	1
C40	2902(3)	1921(2)	4591(2)	33(1)	1
C41	3877(4)	1520(2)	5077(2)	44(1)	1
C42	3118(4)	840(2)	5387(2)	46(1)	1

C43	3998(5)	467(3)	5908(2)	71(1)	1
C44	3694(4)	3280(2)	4690(2)	36(1)	1
C45	2197(4)	3684(2)	4985(2)	39(1)	1
C46	2483(4)	4155(2)	5535(2)	42(1)	1
C47	1020(5)	4615(2)	5804(2)	55(1)	1
C48	2392(3)	2928(2)	3788(2)	30(1)	1
C49	2831(4)	3629(2)	3401(2)	36(1)	1
C50	1512(4)	3968(2)	3024(2)	40(1)	1
C51	1791(5)	4740(2)	2697(2)	62(1)	1
C52	9538(3)	2010(2)	8573(2)	34(1)	1
C53	10592(4)	1235(2)	8547(2)	46(1)	1
C54	9748(4)	568(2)	8334(2)	44(1)	1
C55	10405(5)	–238(2)	8546(2)	62(1)	1
C56A	11423(10)	2939(6)	8131(3)	48(1)	0.670(5)
C57A	10834(7)	3018(4)	7504(3)	48(1)	0.670(5)
C58A	11036(6)	2260(3)	7142(2)	48(1)	0.670(5)
C59A	11081(7)	2376(4)	6513(3)	48(1)	0.670(5)
C56B	11160(20)	2915(13)	8031(7)	48(1)	0.330(5)
C57B	10048(14)	3100(7)	7497(4)	48(1)	0.330(5)
C58B	10944(12)	3048(7)	6901(4)	48(1)	0.330(5)
C59B	10393(14)	2545(7)	6484(5)	48(1)	0.330(5)
C60	9009(3)	3433(2)	8767(2)	33(1)	1
C61	9487(4)	4256(2)	8846(2)	35(1)	1
C62	8066(4)	4856(2)	8976(2)	41(1)	1
C63	8464(5)	5708(2)	9002(2)	57(1)	1
C64	11326(4)	2651(2)	9185(2)	41(1)	1
C65	10473(5)	2550(2)	9799(2)	50(1)	1
C66	11576(6)	2207(3)	10277(2)	69(1)	1
C67	12158(6)	1329(3)	10178(2)	78(2)	1
N1	5851(3)	1636(2)	9244(1)	33(1)	1
N2	5054(3)	3412(2)	9205(1)	31(1)	1
N3	4334(3)	4320(1)	8101(1)	26(1)	1
N4	4929(3)	4250(1)	6796(1)	29(1)	1
N5	6352(3)	3427(1)	6133(1)	31(1)	1
N6	7521(3)	1726(1)	6047(1)	27(1)	1
N7	7903(3)	230(1)	6764(1)	29(1)	1
N8	5721(3)	110(2)	7859(1)	31(1)	1
N9	10304(3)	2756(2)	8654(1)	32(1)	1
N10	3527(3)	2623(2)	4253(1)	31(1)	1
O1	3466(3)	4368(2)	9723(1)	49(1)	1
O2	6000(2)	4779(1)	5917(1)	35(1)	1
O3	8741(3)	–393(1)	5886(1)	44(1)	1
O4	6260(2)	2876(1)	7987(1)	31(1)	1
O5	4786(2)	2661(1)	7143(1)	31(1)	1
O6	4771(2)	1771(1)	8023(1)	35(1)	1
O7	7045(2)	1751(1)	7338(1)	32(1)	1
S1	5708(1)	2263(1)	7623(1)	27(1)	1

Sulfate complex of receptor 221 – from spontaneous crystallisation

Table 1. Crystal data and structure refinement details.

Identification code	ssj0294
Empirical formula	$C_{67}H_{98}N_{10}O_7S$
Formula weight	1187.61
Temperature	120(2) K
Wavelength	0.6889 Å
Crystal system	Triclinic
Space group	*P*–1
Unit cell dimensions	a = 8.764(2) Å α = 88.188(3)°
	b = 16.882(4) Å β = 85.747(3)°
	c 22.114(6) Å γ = 82.761(3)°
Volume	3236.0(14) Å^3
Z	2
Density (calculated)	1.219 Mg / m^3
Absorption coefficient	0.110 mm^{-1}
F(000)	1284
Crystal	Plate; colourless
Crystal size	0.04 × 0.03 × 0.01 mm^3
θ range for data collection	2.88 – 24.28°
Index ranges	$-10 \le h \le 10$, $-14 \le k \le 19$, $-26 \le l \le 26$
Reflections collected	25784
Independent reflections	11133 [R_{int} = 0.0709]
Completeness to θ = 24.28°	96.5 %
Absorption correction	Semi–empirical from equivalents
Max. and min. transmission	0.9989 and 0.9956
Refinement method	Full-matrix least-squares on F^2
Data / restraints / parameters	11133 / 0 / 774
Goodness-of-fit on F^2	1.049
Final *R* indices [$F^2 > 2\sigma(F^2)$]	*R1* = 0.0673, *wR2* = 0.1699
R indices (all data)	*R1* = 0.1153, *wR2* = 0.1938
Largest diff. peak and hole	1.240 and –0.602 e Å^{-3}

Diffractometer: *Nonius KappaCCD* area detector (ϕ scans and ω scans to fill *asymmetric unit*). **Cell determination:** DirAx (Duisenberg, A.J.M.(1992). J. Appl. Cryst. 25, 92-96.) **Data collection:** Collect (Collect: Data collection software, R. Hooft, Nonius B.V., 1998). **Data reduction and cell refinement:** *Denzo* (Z. Otwinowski & W. Minor, *Methods in Enzymology* (1997) Vol. 276: *Macromolecular Crystallography*, part A, pp. 307–326; C. W. Carter, Jr. & R. M. Sweet, Eds., Academic Press). **Absorption correction:** Sheldrick, G. M. SADABS - Bruker Nonius area detector scaling and absorption correction - V2.10 Structure solution: *SHELXS97* (G. M. Sheldrick, Acta Cryst. (1990) A**46** 467–473). **Structure refinement:** *SHELXL97* (G. M. Sheldrick (1997), University of Göttingen, Germany). Graphics: Cameron - A Molecular Graphics Package. (D. M. Watkin, L. Pearce and C. K. Prout, Chemical Crystallography Laboratory, University of Oxford, 1993).

Special details:

Table 2. Atomic coordinates [$\times 10^4$], equivalent isotropic displacement parameters [$Å^2 \times 10^3$] and site occupancy factors. U_{eq} is defined as one third of the trace of the orthogonalized U^{ij} tensor.

Atom	*x*	*y*	*z*	U_{eq}	*S.o.f.*
O1	6256(3)	5392(1)	4116(1)	45(1)	1
O2	9003(3)	220(1)	4083(1)	37(1)	1
O3	11534(3)	632(2)	278(1)	52(1)	1
N1	9282(3)	4891(2)	2141(1)	33(1)	1
N2	7097(3)	4769(2)	3236(1)	32(1)	1
N3	7480(3)	3274(2)	3954(1)	30(1)	1
N4	8652(3)	1571(2)	3870(1)	34(1)	1
N5	10073(3)	749(2)	3208(1)	32(1)	1
N6	10665(3)	679(2)	1900(1)	31(1)	1
N7	9947(3)	1585(2)	793(1)	33(1)	1
N8	9142(3)	3365(2)	753(1)	35(1)	1
C1	10046(4)	5180(2)	1638(2)	41(1)	1
C2	9452(4)	5949(2)	1521(2)	43(1)	1
C3	8224(4)	6152(2)	1969(2)	36(1)	1
C4	7167(5)	6835(2)	2082(2)	42(1)	1
C5	6094(4)	6815(2)	2568(2)	40(1)	1
C6	6045(4)	6142(2)	2950(2)	36(1)	1
C7	7088(4)	5463(2)	2855(2)	31(1)	1
C8	8151(4)	5466(2)	2355(2)	31(1)	1
C9	6703(4)	4775(2)	3842(2)	35(1)	1
C10	6813(4)	4006(2)	4180(2)	33(1)	1
C11	6275(4)	3903(2)	4771(2)	33(1)	1
C12	6575(4)	3078(2)	4921(1)	29(1)	1
C13	6260(4)	2609(2)	5444(1)	31(1)	1
C14	6687(4)	1805(2)	5426(1)	32(1)	1
C15	7474(4)	1436(2)	4913(1)	31(1)	1
C16	7831(4)	1875(2)	4395(1)	30(1)	1
C17	7337(4)	2702(2)	4402(1)	28(1)	1
C18	9230(4)	786(2)	3752(2)	30(1)	1
C19	10907(4)	64(2)	2939(2)	31(1)	1
C20	11547(4)	–604(2)	3242(2)	33(1)	1
C21	12455(4)	–1219(2)	2927(2)	35(1)	1
C22	12772(4)	–1185(2)	2310(2)	38(1)	1
C23	12134(4)	–512(2)	1986(2)	31(1)	1
C24	11193(4)	98(2)	2307(2)	29(1)	1
C25	12153(4)	–265(2)	1365(2)	36(1)	1
C26	11257(4)	449(2)	1325(2)	32(1)	1
C27	10925(4)	897(2)	756(2)	35(1)	1
C28	9339(4)	2013(2)	283(2)	35(1)	1
C29	9037(4)	1653(2)	–245(2)	40(1)	1
C30	8389(5)	2093(2)	–722(2)	44(1)	1
C31	7973(5)	2908(2)	–696(2)	45(1)	1

C32	8263(4)	3292(2)	–172(2)	38(1)	1
C33	8958(4)	2840(2)	307(2)	36(1)	1
C34	8030(5)	4103(2)	9(2)	46(1)	1
C35	8574(5)	4120(2)	564(2)	44(1)	1
N9	11470(3)	2375(2)	5744(1)	35(1)	1
C36	9886(4)	2624(2)	6047(2)	41(1)	1
C37	9816(4)	3252(2)	6529(2)	49(1)	1
C38	8121(5)	3523(3)	6724(2)	53(1)	1
C39	7959(5)	4079(3)	7232(2)	69(1)	1
C40	12599(4)	2071(2)	6210(2)	34(1)	1
C41	12170(4)	1369(2)	6597(2)	40(1)	1
C42	13494(4)	1032(2)	6976(2)	42(1)	1
C43	13214(6)	253(3)	7299(2)	62(1)	1
C44	12084(4)	3084(2)	5409(2)	36(1)	1
C45	11124(4)	3478(2)	4919(2)	46(1)	1
C46	11865(5)	4166(2)	4613(2)	49(1)	1
C47	11003(6)	4538(3)	4090(2)	72(1)	1
C48	11302(4)	1721(2)	5308(2)	38(1)	1
C49	12802(4)	1321(2)	5015(2)	42(1)	1
C50	12524(5)	843(2)	4466(2)	44(1)	1
C51	14001(5)	391(3)	4191(2)	57(1)	1
N10	4694(3)	2238(2)	1349(1)	34(1)	1
C52	3644(5)	2065(2)	1901(2)	51(1)	1
C53	4354(8)	1961(3)	2496(2)	82(2)	1
C54	3959(7)	2736(4)	2875(3)	93(2)	1
C55	4120(9)	2579(4)	3497(3)	113(2)	1
C56	5451(4)	2987(2)	1429(2)	36(1)	1
C57	4397(5)	3761(2)	1452(2)	48(1)	1
C58	5254(5)	4429(2)	1671(2)	47(1)	1
C59	4604(5)	5236(2)	1448(2)	60(1)	1
C60	5977(4)	1563(2)	1236(2)	37(1)	1
C61	5511(4)	741(2)	1156(2)	39(1)	1
C62	6926(5)	142(2)	1024(2)	44(1)	1
C63	6535(5)	–712(2)	999(2)	57(1)	1
C64	3688(4)	2345(2)	812(2)	42(1)	1
C65	4531(5)	2449(3)	199(2)	51(1)	1
C66	3440(6)	2788(3)	–281(2)	70(1)	1
C67	2834(6)	3669(3)	–182(2)	73(1)	1
S1	9287(1)	2735(1)	2377(1)	30(1)	1
O4	7953(3)	3246(1)	2662(1)	36(1)	1
O5	10217(3)	2338(1)	2856(1)	35(1)	1
O6	8731(3)	2122(1)	2014(1)	34(1)	1
O7	10225(3)	3226(1)	1975(1)	37(1)	1

Hydrogen phosphate complex of receptor 221

Table 1. Crystal data and structure refinement details.

Identification code	**2009jh0015**
Empirical formula	$C_{67}H_{99}N_{10}O_7P$
	$C_{35}H_{26}N_8O_3$, $2(C_{16}H_{36}N)$, HPO_4
Formula weight	1187.53
Temperature	120(2) K
Wavelength	0.71073 Å
Crystal system	Monoclinic
Space group	$P2_1/n$
Unit cell dimensions	a = 14.7860(6) Å
	b = 17.7836(6) Å β = 103.512(2)°
	c = 25.6491(10) Å
Volume	6557.7(4) Å^3
Z	4
Density (calculated)	1.203 Mg / m^3
Absorption coefficient	0.102 mm^{-1}
F(000)	2568
Crystal	Block; Colourless
Crystal size	0.20 × 0.20 × 0.15 mm^3
θ range for data collection	2.92 – 25.03°
Index ranges	$-16 \le h \le 17$, $-21 \le k \le 21$, $-30 \le l \le 30$
Reflections collected	63501
Independent reflections	11548 [R_{int} = 0.1856]
Completeness to θ = 25.03°	99.7 %
Absorption correction	Semi–empirical from equivalents
Max. and min. transmission	0.9849 and 0.9800
Refinement method	Full-matrix least-squares on F^2
Data / restraints / parameters	11548 / 845 / 789
Goodness-of-fit on F^2	1.191
Final R indices [$F^2 > 2\sigma(F^2)$]	*R1* = 0.1595, *wR2* = 0.2338
R indices (all data)	*R1* = 0.2672, *wR2* = 0.2775
Largest diff. peak and hole	0.366 and –0.320 e Å^{-3}

Diffractometer: *Nonius KappaCCD* area detector (ϕ scans and ω scans to fill *asymmetric unit*). **Cell determination:** DirAx (Duisenberg, A.J.M.(1992). J. Appl. Cryst. 25, 92-96.) **Data collection:** Collect (Collect: Data collection software, R. Hooft, Nonius B.V., 1998). **Data reduction and cell refinement**: *Denzo* (Z. Otwinowski & W. Minor, *Methods in Enzymology* (1997) Vol. **276**: *Macromolecular Crystallography*, part A, pp. 307–326; C. W. Carter, Jr. & R. M. Sweet, Eds., Academic Press). **Absorption correction**: Sheldrick, G. M. SADABS - Bruker Nonius area detector scaling and absorption correction - V2.10 S**tructure solution**: *SHELXS97* (G. M. Sheldrick, Acta Cryst. (1990) A**46** 467–473). S**tructure refinement**: *SHELXL97* (G. M. Sheldrick (1997), University of Göttingen, Germany). **Graphics:** Cameron - A Molecular Graphics Package. (D. M. Watkin, L. Pearce and C. K. Prout, Chemical Crystallography Laboratory, University of Oxford, 1993).

Special details: All hydrogen atoms were placed in idealised positions and refined using a riding model, except the H of the phosphate which was freely refined. One arm of one TBA is modelled as disordered over 2 positions.

Table 2. Atomic coordinates [$\times 10^4$], equivalent isotropic displacement parameters [$Å^2 \times 10^3$] and site occupancy factors. U_{eq} is defined as one third of the trace of the orthogonalized U^{ij} tensor.

Atom	*x*	*y*	*z*	U_{eq}	*S.o.f.*
O1	1716(4)	8185(3)	–1346(2)	49(2)	1
O2	1309(4)	3419(3)	–821(2)	39(1)	1
O3	3255(5)	4243(3)	2360(2)	73(2)	1
N1	4583(4)	7593(3)	55(2)	31(2)	1
N2	2676(4)	7619(3)	–630(2)	32(1)	1
N3	1943(4)	6188(3)	–1083(2)	31(1)	1
N4	2078(4)	4526(3)	–900(2)	35(2)	1
N5	2688(4)	3688(3)	–236(2)	30(1)	1
N6	3063(4)	3940(3)	947(2)	31(1)	1
N7	3390(4)	5129(3)	1738(3)	39(2)	1
N8	4077(4)	6558(3)	1407(2)	33(2)	1
C1	5421(6)	7812(5)	360(3)	43(2)	1
C2	5419(6)	8560(5)	461(3)	42(2)	1
C3	4519(6)	8837(4)	203(3)	37(2)	1
C4	4098(6)	9552(4)	143(4)	47(2)	1
C5	3219(6)	9603(4)	–165(4)	51(2)	1
C6	2712(6)	8988(4)	–418(3)	41(2)	1
C7	3110(5)	8274(4)	–372(3)	33(2)	1
C8	4012(5)	8213(4)	–54(3)	29(2)	1
C9	2023(6)	7620(4)	–1100(3)	37(2)	1
C10	1662(5)	6880(4)	–1313(3)	31(2)	1
C11	967(5)	6778(4)	–1759(3)	37(2)	1
C12	799(6)	5997(4)	–1819(3)	37(2)	1
C13	147(6)	5559(5)	–2193(3)	49(2)	1
C14	166(6)	4797(5)	–2119(4)	54(2)	1
C15	803(6)	4442(5)	–1700(3)	42(2)	1
C16	1436(5)	4857(4)	–1328(3)	32(2)	1
C17	1418(5)	5634(4)	–1394(3)	33(2)	1
C18	1970(5)	3851(4)	–669(3)	29(2)	1
C19	2678(5)	3106(4)	138(3)	31(2)	1
C20	2479(5)	2367(4)	–27(3)	37(2)	1
C21	2471(5)	1805(4)	352(4)	42(2)	1
C22	2634(6)	1957(4)	890(3)	41(2)	1
C23	2814(5)	2707(4)	1061(3)	35(2)	1
C24	2955(6)	3081(4)	1557(3)	40(2)	1
C25	3107(6)	3823(4)	1482(3)	36(2)	1
C26	2872(5)	3265(4)	682(3)	32(2)	1
C27	3260(6)	4410(5)	1899(3)	46(2)	1
C28	3497(6)	5781(4)	2075(3)	39(2)	1
C29	3293(6)	5825(5)	2573(3)	45(2)	1
C30	3444(6)	6495(5)	2870(3)	48(2)	1

C31	3786(6)	7124(5)	2688(3)	43(2)	1
C32	3988(5)	7108(4)	2174(3)	36(2)	1
C33	4346(5)	7633(4)	1860(3)	38(2)	1
C34	4368(5)	7286(4)	1393(3)	35(2)	1
C35	3836(5)	6431(4)	1880(3)	33(2)	1
N9	1557(4)	9377(3)	–2639(3)	39(2)	1
C36	1139(6)	9795(4)	–3153(3)	44(2)	1
C37	987(6)	10624(4)	–3131(3)	44(2)	1
C38	631(6)	10948(4)	–3697(3)	44(2)	1
C39	482(7)	11778(5)	–3691(4)	60(3)	1
C40	2540(6)	9634(5)	–2423(3)	45(2)	1
C41	3120(6)	9145(5)	–1968(4)	50(2)	1
C43	3982(6)	9558(5)	–1657(4)	55(2)	1
C44	4683(7)	9029(6)	–1316(4)	68(3)	1
C45	957(6)	9482(4)	–2232(3)	41(2)	1
C46	1183(6)	10123(4)	–1839(3)	41(2)	1
C47	470(7)	10154(5)	–1497(4)	56(2)	1
C48	757(7)	10675(6)	–1023(4)	70(3)	1
C49A	1523(6)	8533(4)	–2767(4)	51(2)	0.448(11)
C50A	2030(40)	8207(12)	–3153(19)	55(3)	0.448(11)
C51A	2110(20)	7351(11)	–3063(9)	57(4)	0.448(11)
C52A	2511(16)	6993(11)	–3473(8)	70(4)	0.448(11)
C49B	1523(6)	8533(4)	–2767(4)	51(2)	0.552(11)
C50B	2010(30)	8337(10)	–3198(15)	55(3)	0.552(11)
C51B	2015(18)	7494(9)	–3307(7)	57(4)	0.552(11)
C52B	2430(14)	7022(9)	–2839(7)	70(4)	0.552(11)
N10	3850(4)	2252(3)	4174(3)	35(2)	1
C53	4292(5)	2310(4)	3702(3)	36(2)	1
C54	3671(6)	2193(4)	3148(3)	44(2)	1
C55	4248(7)	2122(5)	2740(4)	65(3)	1
C56	4831(8)	2804(8)	2697(4)	103(5)	1
C57	3021(5)	2764(4)	4106(4)	40(2)	1
C58	3215(5)	3602(4)	4064(3)	41(2)	1
C59	2328(6)	4038(4)	3874(4)	51(2)	1
C60	2504(7)	4883(5)	3857(4)	65(3)	1
C61	3512(5)	1459(4)	4235(3)	36(2)	1
C62	4215(6)	832(4)	4245(3)	41(2)	1
C63	3810(6)	81(4)	4359(4)	50(2)	1
C64	4387(6)	–583(4)	4270(4)	56(3)	1
C65	4615(5)	2473(4)	4658(3)	35(2)	1
C66	4351(6)	2465(5)	5192(3)	43(2)	1
C67	5120(6)	2823(5)	5627(3)	53(2)	1
C68	5210(6)	3673(5)	5557(3)	52(2)	1
P1	3808(1)	5616(1)	152(1)	29(1)	1
O4	3195(4)	6253(3)	–112(2)	35(1)	1
O5	3790(3)	4946(3)	–220(2)	34(1)	1
O6	3593(3)	5383(2)	679(2)	31(1)	1

O7	4821(4)	5958(3)	285(2)	39(1)	1

Hydrogen phosphate and dihydrogen phosphate complex of receptor 222

Table 1. Crystal data and structure refinement details.

Identification code	**2009jh0012**
Empirical formula	$C_{107}H_{179}N_{12}O_{15}P_3$
	$C_{43}H_{30}N_8O_3$, 4($C_{16}H_{36}N$), 2(H_2PO_4), HPO_4
Formula weight	1966.53
Temperature	120(2) K
Wavelength	0.71073 Å
Crystal system	Triclinic
Space group	*P*–1
Unit cell dimensions	a = 15.5015(6) Å α = 92.802(2)°
	b = 18.5413(8) Å β = 106.805(2)°
	c = 19.9295(7) Å γ = 93.436(2)°
Volume	5460.5(4) Å^3
Z	2
Density (calculated)	1.196 Mg / m^3
Absorption coefficient	0.121 mm^{-1}
F(000)	2140
Crystal	Plate; Colourless
Crystal size	0.40 × 0.30 × 0.15 mm^3
θ range for data collection	2.92 – 25.03°
Index ranges	$-18 \le h \le 18$, $-22 \le k \le 22$, $-23 \le l \le 23$
Reflections collected	58813
Independent reflections	19035 [R_{int} = 0.1292]
Completeness to θ = 25.03°	98.6 %
Absorption correction	Semi–empirical from equivalents
Max. and min. transmission	0.9821 and 0.9533
Refinement method	Full-matrix least-squares on F^2
Data / restraints / parameters	19035 / 1856 / 1265
Goodness-of-fit on F^2	1.019
Final *R* indices [$F^2 > 2\sigma(F^2)$]	*R1* = 0.1815, *wR2* = 0.3618
R indices (all data)	*R1* = 0.3155, *wR2* = 0.4440
Largest diff. peak and hole	1.972 and –1.044 e Å^{-3}

Diffractometer: *Nonius KappaCCD* area detector (ϕ scans and ω scans to fill *asymmetric unit*). **Cell determination:** DirAx (Duisenberg, A.J.M.(1992). J. Appl. Cryst. 25, 92-96.) **Data collection:** Collect (Collect: Data collection software, R. Hooft, Nonius B.V., 1998). **Data reduction and cell refinement**: *Denzo* (Z. Otwinowski & W. Minor, *Methods in Enzymology* (1997) Vol. **276**: *Macromolecular Crystallography*, part A, pp. 307–326; C. W. Carter, Jr. & R. M. Sweet, Eds., Academic Press). **Absorption correction**: Sheldrick, G. M. SADABS - Bruker Nonius area detector scaling and absorption correction - V2.10 S**tructure solution**: *SHELXS97* (G. M. Sheldrick, Acta Cryst. (1990) A**46** 467–473). S**tructure refinement**: *SHELXL97* (G. M. Sheldrick (1997), University of Göttingen, Germany). **Graphics:** Cameron - A Molecular Graphics Package. (D. M. Watkin, L. Pearce and C. K. Prout, Chemical Crystallography Laboratory, University of Oxford, 1993).

Special details: All hydrogen atoms were placed in idealised positions and refined using a riding model.

Table 2. Atomic coordinates [$\times 10^4$], equivalent isotropic displacement parameters [$Å^2 \times 10^3$] and site occupancy factors. U_{eq} is defined as one third of the trace of the orthogonalized U^{ij} tensor.

Atom	*x*	*y*	*z*	U_{eq}	*S.o.f.*
O1	8085(1)	3525(1)	5297(1)	59(1)	1
O2	11772(1)	940(1)	3897(1)	58(1)	1
O3	7355(2)	–1818(1)	1484(1)	62(1)	1
N1	6387(2)	3304(1)	2937(1)	42(1)	1
N2	7565(2)	2800(1)	4291(1)	40(1)	1
N3	9457(2)	2487(1)	4477(1)	42(1)	1
N4	10614(2)	1685(1)	3830(1)	47(1)	1
N5	10484(2)	786(1)	2979(1)	49(1)	1
N6	9063(2)	–345(1)	2236(1)	50(1)	1
N7	7150(2)	–748(1)	2007(1)	49(1)	1
N8	5928(2)	422(1)	1957(1)	40(1)	1
C1	5674(2)	3568(2)	2449(2)	46(1)	1
C2	5612(2)	3741(2)	1764(2)	52(1)	1
C3	4798(2)	3982(2)	1372(2)	57(1)	1
C4	4086(2)	4056(2)	1662(2)	63(1)	1
C5	4157(2)	3870(2)	2330(2)	58(1)	1
C6	4949(2)	3618(2)	2729(2)	48(1)	1
C7	5251(2)	3392(2)	3429(2)	48(1)	1
C8	4858(2)	3337(2)	3974(2)	56(1)	1
C9	5340(2)	3112(2)	4611(2)	57(1)	1
C10	6235(2)	2919(2)	4703(2)	51(1)	1
C11	6657(2)	2969(2)	4181(2)	41(1)	1
C12	6150(2)	3205(2)	3539(2)	42(1)	1
C13	8233(2)	3110(2)	4849(2)	48(1)	1
C14	9157(2)	2950(2)	4910(2)	46(1)	1
C15	9893(2)	3265(2)	5397(2)	61(1)	1
C16	10690(2)	3037(2)	5271(2)	53(1)	1
C17	11623(2)	3173(2)	5588(2)	66(1)	1
C18	12193(2)	2820(2)	5326(2)	58(1)	1
C19	11900(2)	2302(2)	4737(2)	50(1)	1
C20	10999(2)	2164(2)	4426(2)	46(1)	1
C21	10397(2)	2527(2)	4687(2)	44(1)	1
C22	11024(2)	1123(2)	3591(2)	44(1)	1
C23	10669(2)	148(2)	2634(2)	57(1)	1
C24	11529(2)	10(2)	2619(2)	77(1)	1
C25	11642(2)	–636(2)	2245(2)	93(1)	1
C26	10940(3)	–1108(2)	1882(2)	98(1)	1
C27	10070(2)	–965(2)	1891(2)	72(1)	1
C28	9940(2)	–336(2)	2271(2)	58(1)	1
C29	9210(2)	–1358(2)	1632(2)	68(1)	1
C30	8601(2)	–962(2)	1844(2)	57(1)	1

C31	7663(2)	−1221(2)	1761(2)	57(1)	1
C32	6239(2)	−886(2)	1987(2)	48(1)	1
C33	5834(2)	−1580(2)	2003(2)	55(1)	1
C34	4931(2)	−1686(2)	1998(2)	58(1)	1
C35	4392(2)	−1101(2)	1967(2)	54(1)	1
C36	4783(2)	−399(2)	1955(1)	46(1)	1
C37	5709(2)	−308(2)	1975(1)	43(1)	1
C38	4445(2)	312(2)	1926(2)	41(1)	1
C39	3613(2)	564(2)	1885(2)	50(1)	1
C40	3525(2)	1291(2)	1886(2)	60(1)	1
C41	4265(2)	1780(2)	1903(2)	48(1)	1
C42	5097(2)	1538(2)	1938(1)	41(1)	1
C43	5192(2)	799(2)	1943(1)	40(1)	1
N9	7148(2)	64(1)	4457(1)	40(1)	1
C44	7548(2)	437(2)	5180(2)	44(1)	1
C45	8070(2)	1154(2)	5216(2)	50(1)	1
C46	8517(2)	1468(2)	5976(2)	55(1)	1
C47	7830(2)	1737(2)	6292(2)	98(2)	1
C48	6510(2)	533(2)	3979(1)	41(1)	1
C49	5708(2)	762(2)	4239(2)	50(1)	1
C50	5057(2)	1172(2)	3707(2)	50(1)	1
C51	4212(2)	1312(2)	3904(2)	61(1)	1
C52	6660(2)	−650(1)	4553(1)	39(1)	1
C53	6312(2)	−1162(2)	3905(2)	46(1)	1
C54	5645(2)	−1736(2)	3998(2)	50(1)	1
C55	4729(2)	−1479(2)	3975(2)	62(1)	1
C56	7891(2)	−81(2)	4110(1)	42(1)	1
C57	8668(2)	−498(2)	4537(1)	47(1)	1
C58	9260(2)	−746(2)	4099(1)	47(1)	1
C59	8853(2)	−1366(2)	3603(2)	59(1)	1
N10	11773(2)	4566(1)	3683(1)	45(1)	1
C60	12339(2)	4963(2)	3254(2)	55(1)	1
C61	12667(2)	5716(2)	3456(2)	58(1)	1
C62	13188(2)	6012(2)	2971(2)	66(1)	1
C63	13594(3)	6770(2)	3174(2)	78(2)	1
C64	12236(2)	4698(2)	4471(2)	41(1)	1
C65	13201(2)	4500(2)	4746(2)	48(1)	1
C66	13606(2)	4808(2)	5499(2)	55(1)	1
C67	14562(2)	4613(2)	5810(2)	61(1)	1
C68	11717(2)	3768(2)	3472(2)	57(1)	1
C69	11304(3)	3560(2)	2689(2)	60(1)	1
C70	11198(2)	2732(2)	2549(2)	65(1)	1
C71	12043(2)	2366(2)	2732(2)	61(1)	1
C72	10848(2)	4883(2)	3503(2)	58(1)	1
C73	10179(2)	4525(2)	3800(2)	47(1)	1
C74	9325(2)	4895(2)	3664(2)	64(1)	1
C75	8574(2)	4551(2)	3869(2)	64(1)	1

N11	7638(2)	1377(1)	127(1)	58(1)	1
C76	7029(2)	1778(1)	455(2)	61(1)	1
C77	6114(2)	1933(2)	–39(2)	58(1)	1
C78	5529(2)	2254(2)	383(2)	67(1)	1
C79	4654(3)	2497(2)	–68(2)	81(2)	1
C80	8534(2)	1363(2)	735(2)	73(1)	1
C81	9229(2)	946(2)	512(2)	89(2)	1
C82	10151(2)	1117(2)	1022(2)	83(2)	1
C83	10863(3)	714(3)	854(3)	107(2)	1
C84A	7266(3)	648(2)	–138(2)	59(1)	0.465(4)
C85A	7241(3)	123(2)	431(2)	76(1)	0.465(4)
C86A	6688(3)	–577(2)	169(4)	65(1)	0.465(4)
C87A	5774(2)	–499(2)	–104(3)	85(2)	0.465(4)
C84B	7234(4)	635(2)	–97(2)	59(1)	0.535(4)
C85B	6959(4)	135(2)	416(2)	76(1)	0.535(4)
C86B	6469(3)	–569(2)	71(3)	65(1)	0.535(4)
C87B	7089(3)	–1055(3)	–66(3)	85(2)	0.535(4)
C88A	7764(3)	1729(2)	–495(2)	80(1)	0.655(5)
C89A	8207(3)	2517(2)	–320(2)	99(1)	0.655(5)
C90A	8554(3)	2806(3)	–888(2)	107(2)	0.655(5)
C91A	7799(3)	2749(4)	–1492(2)	112(2)	0.655(5)
C88B	7722(4)	1744(2)	–480(3)	80(1)	0.345(5)
C89B	8058(6)	2548(2)	–448(2)	99(1)	0.345(5)
C90B	7655(2)	2943(3)	–1094(2)	107(2)	0.345(5)
C91B	8199(3)	2933(3)	–1561(2)	112(2)	0.345(5)
N12	7520(2)	5958(1)	1231(1)	48(1)	1
C92	6825(2)	6066(2)	1621(2)	54(1)	1
C93	6883(2)	5578(2)	2232(2)	55(1)	1
C94	6058(2)	5639(2)	2501(2)	70(1)	1
C95	5974(3)	6396(2)	2767(2)	81(1)	1
C96	7375(2)	6535(2)	700(2)	55(1)	1
C97	8002(3)	6558(2)	268(2)	80(1)	1
C98	7786(3)	7164(2)	–258(2)	81(1)	1
C99	8380(4)	7214(3)	–673(3)	152(2)	1
C10A	8414(3)	5942(2)	1690(3)	61(1)	0.363(4)
C11A	8850(2)	6604(3)	2200(4)	78(1)	0.363(4)
C12A	9845(3)	6516(3)	2533(5)	95(2)	0.363(4)
C13A	10308(3)	7195(2)	2818(5)	106(2)	0.363(4)
C10B	8443(3)	6041(2)	1720(2)	61(1)	0.637(4)
C11B	8729(3)	6769(2)	2166(3)	78(1)	0.637(4)
C12B	9640(2)	6770(3)	2709(2)	95(2)	0.637(4)
C13B	10365(2)	6759(4)	2405(3)	106(2)	0.637(4)
C104	7369(2)	5207(2)	864(1)	59(1)	1
C105	6512(3)	5027(2)	317(2)	95(2)	1
C106	6456(4)	4235(2)	9(2)	114(2)	1
C107	5984(4)	4109(2)	–680(2)	127(2)	1
P1	8137(1)	1386(1)	2808(1)	37(1)	1

O4	9027(1)	1654(1)	2691(1)	39(1)	1
O5	8096(1)	1642(1)	3527(1)	41(1)	1
O6	7962(1)	574(1)	2662(1)	51(1)	1
O7	7336(1)	1698(1)	2242(1)	47(1)	1
P2A	8432(1)	3358(1)	2007(1)	45(1)	0.5882(16)
O8A	9183(1)	3024(1)	2536(1)	61(1)	0.5882(16)
O9A	8424(2)	3130(1)	1281(1)	61(1)	0.5882(16)
O10A	8470(2)	4163(1)	2140(1)	61(1)	0.5882(16)
O11A	7514(13)	3087(1)	2122(1)	61(1)	0.5882(16)
P2B	8321(1)	3342(1)	1908(1)	45(1)	0.4118(16)
O8B	8929(2)	2742(2)	1870(2)	61(1)	0.4118(16)
O9B	7680(2)	3418(2)	1205(1)	61(1)	0.4118(16)
O10B	8847(2)	4037(1)	2236(2)	61(1)	0.4118(16)
O11B	7779(2)	3138(2)	2429(2)	61(1)	0.4118(16)
P3A	9875(1)	4619(1)	1009(1)	66(1)	0.6712(13)
O12A	9419(2)	3885(1)	705(2)	121(1)	0.6712(13)
O13A	9907(2)	4724(2)	1756(1)	121(1)	0.6712(13)
O14A	9460(2)	5214(1)	581(2)	121(1)	0.6712(13)
O15A	10855(1)	4652(2)	951(2)	121(1)	0.6712(13)
P3B	9122(2)	4390(1)	427(2)	66(1)	0.3288(13)
O12B	9877(3)	4060(3)	205(3)	121(1)	0.3288(13)
O13B	8318(3)	3861(3)	271(3)	121(1)	0.3288(13)
O14B	8909(4)	5103(2)	121(3)	121(1)	0.3288(13)
O15B	9471(4)	4590(3)	1237(2)	121(1)	0.3288(13)

Structures from Chapter Four

Benzoate complex of receptor 232

Table 1. Crystal data and structure refinement details.

Identification code	**2010jh0021**
Empirical formula	$C_{223}H_{340}N_{24}O_{19}$
Formula weight	3661.19
Temperature	120(2) K
Wavelength	0.71073 Å
Crystal system	Triclinic
Space group	*P*–1
Unit cell dimensions	a = 22.3858(4) Å α = 65.6980(10)°
	b = 22.4799(4) Å β = 86.6570(10)°
	c 23.8730(5) Å γ = 75.0560(10)°
Volume	10563.2(3) Å^3
Z	2
Density (calculated)	1.151 Mg / m^3
Absorption coefficient	0.073 mm^{-1}
F(000)	3996
Crystal	Slab; Colourless
Crystal size	0.2 × 0.1 × 0.03 mm^3
θ range for data collection	2.92 – 25.03°
Index ranges	$-26 \le h \le 26$, $-26 \le k \le 26$, $-28 \le l \le 28$
Reflections collected	134253
Independent reflections	37104 [R_{int} = 0.0954]
Completeness to θ = 25.03°	99.4 %
Absorption correction	Semi–empirical from equivalents
Max. and min. transmission	0.9978 and 0.9855
Refinement method	Full-matrix least-squares on F^2
Data / restraints / parameters	37104 / 2153 / 2358
Goodness-of-fit on F^2	1.111
Final R indices [$F^2 > 2\sigma(F^2)$]	*R1* = 0.1576, *wR2* = 0.2771
R indices (all data)	*R1* = 0.2619, *wR2* = 0.3312
Largest diff. peak and hole	1.563 and –1.433 e Å^{-3}

Diffractometer: *Nonius KappaCCD* area detector (ϕ scans and ω scans to fill *asymmetric unit*). **Cell determination:** DirAx (Duisenberg, A.J.M.(1992). J. Appl. Cryst. 25, 92-96.) **Data collection:** Collect (Collect: Data collection software, R. Hooft, Nonius B.V., 1998). **Data reduction and cell refinement**: *Denzo* (Z. Otwinowski & W. Minor, *Methods in Enzymology* (1997) Vol. **276**: *Macromolecular Crystallography*, part A, pp. 307–326; C. W. Carter, Jr. & R. M. Sweet, Eds., Academic Press). **Absorption correction**: Sheldrick, G. M. SADABS - Bruker Nonius area detector scaling and absorption correction - V2.10 S**tructure solution**: *SHELXS97* (G. M. Sheldrick, Acta Cryst. (1990) A**46** 467–473). S**tructure refinement**: *SHELXL97* (G. M. Sheldrick (1997), University of Göttingen, Germany). **Graphics:** Cameron - A Molecular Graphics Package. (D. M. Watkin, L. Pearce and C. K. Prout, Chemical Crystallography Laboratory, University of Oxford, 1993).

Special details:

Table 2. Atomic coordinates [$\times 10^4$], equivalent isotropic displacement parameters [$Å^2 \times 10^3$] and site occupancy factors. U_{eq} is defined as one third of the trace of the orthogonalized U^{ij} tensor.

Atom	*x*	*y*	*z*	U_{eq}	*S.o.f.*
O101	2576(2)	−1597(2)	8232(2)	46(1)	1
O102	−749(2)	2616(2)	5143(2)	62(1)	1
O103	−525(2)	2430(2)	8066(2)	48(1)	1
N101	1314(2)	−3375(2)	8953(2)	51(2)	1
N102	1867(2)	−2219(2)	8382(2)	39(1)	1
N103	1612(2)	−1088(2)	7779(2)	41(1)	1
N104	220(2)	1989(2)	5519(2)	47(1)	1
N105	86(3)	3034(2)	4731(2)	54(2)	1
N106	807(3)	3933(3)	3907(3)	76(2)	1
N107	399(2)	1686(2)	8102(2)	38(1)	1
N108	389(2)	2659(2)	8203(2)	40(1)	1
N109	1209(2)	3442(2)	8316(2)	45(1)	1
C101	1246(3)	−4020(3)	9255(3)	62(2)	1
C102	1815(3)	−4474(3)	9427(3)	66(2)	1
C103	2266(3)	−4095(3)	9226(3)	54(2)	1
C104	2917(3)	−4257(3)	9263(3)	62(2)	1
C105	3202(3)	−3751(3)	9000(3)	54(2)	1
C106	2877(3)	−3065(3)	8703(3)	44(2)	1
C107	2236(3)	−2880(3)	8669(2)	39(1)	1
C108	1934(3)	−3401(3)	8931(3)	45(2)	1
C109	2060(3)	−1628(3)	8133(2)	37(1)	1
C110	1747(2)	−446(2)	7455(2)	40(1)	1
C111	1157(2)	145(3)	7296(2)	33(1)	1
C112	891(2)	339(3)	7762(2)	33(1)	1
C113	386(2)	905(3)	7614(2)	35(1)	1
C114	121(2)	1265(3)	7009(2)	34(1)	1
C115	360(2)	1039(3)	6560(2)	37(1)	1
C116	893(2)	497(3)	6689(2)	36(1)	1
C117	19(2)	1389(3)	5925(3)	48(2)	1
C118	−188(3)	2554(3)	5126(3)	49(2)	1
C119	−203(3)	3654(3)	4253(3)	52(2)	1
C120	−823(3)	3922(3)	4121(3)	62(2)	1
C121	−1074(4)	4547(3)	3627(3)	71(2)	1
C122	−701(4)	4908(4)	3247(3)	83(2)	1
C123	−71(4)	4683(3)	3371(3)	75(2)	1
C124	453(5)	4916(4)	3101(3)	100(3)	1
C125	982(5)	4484(4)	3436(3)	94(3)	1
C126	172(4)	4048(3)	3877(3)	66(2)	1
C127	124(2)	1167(3)	8097(3)	43(2)	1
C128	46(3)	2267(3)	8121(2)	39(2)	1
C129	154(3)	3234(3)	8331(3)	42(2)	1

C130	–457(3)	3478(3)	8437(3)	49(2)	1
C131	–635(3)	4046(3)	8581(3)	59(2)	1
C132	–223(3)	4383(3)	8620(3)	59(2)	1
C133	395(3)	4157(3)	8511(3)	49(2)	1
C134	952(3)	4369(3)	8518(3)	61(2)	1
C135	1428(3)	3917(3)	8404(3)	52(2)	1
C136	577(3)	3576(3)	8381(3)	41(1)	1
C137	1140(2)	–67(3)	8439(2)	41(2)	1
C138	765(3)	–569(3)	8793(3)	52(2)	1
C139	1177(2)	309(3)	6159(2)	50(2)	1
C140	983(4)	–312(3)	6178(3)	65(2)	1
C141	–434(2)	1865(3)	6858(3)	43(2)	1
C142	–1043(3)	1646(3)	6972(3)	63(2)	1
O201	7676(2)	–2088(2)	8257(2)	37(1)	1
O202	4593(2)	2372(2)	5233(2)	45(1)	1
O203	4628(2)	2187(2)	7998(2)	45(1)	1
N201	6163(2)	–3624(2)	8863(2)	43(1)	1
N202	6868(2)	–2593(2)	8450(2)	36(1)	1
N203	6694(2)	–1452(2)	7934(2)	37(1)	1
N204	5523(2)	1625(2)	5627(2)	38(1)	1
N205	5500(2)	2665(2)	4870(2)	39(1)	1
N206	6326(2)	3490(2)	4138(2)	52(2)	1
N207	5547(2)	1393(2)	8155(2)	34(1)	1
N208	5541(2)	2423(2)	8119(2)	40(1)	1
N209	6370(2)	3258(2)	8132(2)	48(1)	1
C201	6008(3)	–4225(3)	9040(3)	46(2)	1
C202	6531(3)	–4734(3)	9130(3)	55(2)	1
C203	7039(3)	–4438(3)	9001(3)	47(2)	1
C204	7683(3)	–4691(3)	8995(3)	59(2)	1
C205	8044(3)	–4247(3)	8827(3)	55(2)	1
C206	7797(3)	–3544(3)	8652(3)	44(2)	1
C207	7166(2)	–3286(3)	8645(2)	37(1)	1
C208	6799(3)	–3741(3)	8825(2)	39(1)	1
C209	7127(2)	–2050(3)	8215(2)	32(1)	1
C210	6879(2)	–835(2)	7607(2)	34(1)	1
C211	6313(2)	–217(2)	7425(2)	29(1)	1
C212	6033(2)	–2(2)	7878(2)	33(1)	1
C213	5538(2)	572(2)	7709(2)	31(1)	1
C214	5296(2)	923(2)	7103(2)	31(1)	1
C215	5551(2)	697(3)	6655(2)	32(1)	1
C216	6074(2)	137(3)	6810(2)	34(1)	1
C217	5262(2)	1059(2)	5999(2)	38(1)	1
C218	5163(3)	2230(3)	5242(2)	39(2)	1
C219	5262(3)	3332(3)	4437(2)	40(1)	1
C220	4639(3)	3685(3)	4318(3)	43(2)	1
C221	4465(3)	4350(3)	3875(3)	49(2)	1
C222	4882(3)	4685(3)	3537(3)	52(2)	1

C223	5514(3)	4359(3)	3657(3)	47(2)	1
C224	6075(3)	4537(3)	3432(3)	61(2)	1
C225	6560(3)	4000(3)	3736(3)	63(2)	1
C226	5687(3)	3684(3)	4101(3)	40(1)	1
C227	5268(2)	858(2)	8184(2)	35(1)	1
C228	5196(3)	2007(3)	8090(2)	35(1)	1
C229	5308(3)	3077(3)	8102(2)	39(1)	1
C230	4692(3)	3385(3)	8104(3)	51(2)	1
C231	4508(3)	4035(3)	8086(3)	64(2)	1
C232	4915(4)	4396(3)	8077(3)	63(2)	1
C233	5542(3)	4099(3)	8098(3)	51(2)	1
C234	6095(4)	4304(3)	8109(3)	63(2)	1
C235	6578(3)	3784(3)	8131(3)	58(2)	1
C236	5737(3)	3441(3)	8105(2)	41(1)	1
C237	6264(2)	–393(3)	8553(2)	39(1)	1
C238	5871(3)	–866(3)	8936(3)	52(2)	1
C239	6399(2)	–36(3)	6279(2)	43(2)	1
C240	6195(3)	–609(3)	6242(3)	57(2)	1
C241	4761(2)	1553(2)	6917(2)	39(1)	1
C242	4114(3)	1413(3)	7016(3)	52(2)	1
O301	6666(2)	1785(2)	5084(2)	63(1)	1
O302	7336(2)	2405(2)	4808(3)	83(2)	1
C301	7205(3)	1854(3)	5013(3)	53(2)	1
C302	7727(3)	1222(3)	5166(3)	44(2)	1
C303	7610(3)	627(3)	5232(3)	54(2)	1
C304	8079(3)	48(3)	5372(3)	62(2)	1
C305	8676(3)	63(4)	5440(3)	63(2)	1
C306	8806(3)	651(3)	5378(3)	58(2)	1
C307	8336(3)	1236(3)	5237(3)	52(2)	1
N301	8640(2)	2941(2)	3037(2)	48(1)	1
C308	9142(2)	3056(2)	2576(2)	56(2)	1
C309	9549(2)	3481(3)	2615(3)	68(2)	1
C310	10118(3)	3414(4)	2256(4)	105(3)	1
C311	10595(3)	3721(4)	2367(4)	105(3)	1
C312	8937(2)	2527(2)	3690(2)	52(2)	1
C313	9285(3)	1802(2)	3832(2)	61(2)	1
C314	9816(2)	1550(3)	4304(3)	57(2)	1
C315	10384(3)	1794(4)	4058(3)	71(2)	1
C316	8238(3)	3614(2)	2997(2)	54(2)	1
C317	7879(3)	4055(2)	2383(3)	64(2)	1
C318	7607(3)	4774(2)	2331(3)	66(2)	1
C319	7276(3)	5233(3)	1700(3)	74(2)	1
C320	8252(2)	2555(2)	2892(2)	48(2)	1
C321	7743(2)	2380(3)	3314(2)	52(2)	1
C322	7364(2)	2021(3)	3127(2)	53(2)	1
C323	6854(3)	1835(4)	3550(3)	69(2)	1
O401	3114(2)	7992(2)	1849(2)	49(1)	1
O402	3321(2)	8941(2)	1177(2)	52(1)	1

C401	2979(3)	8551(3)	1385(3)	40(2)	1
C402	2352(2)	8748(3)	1059(2)	36(1)	1
C403	2229(2)	9295(3)	490(2)	37(1)	1
C404	1664(3)	9492(3)	171(3)	46(2)	1
C405	1216(3)	9151(3)	429(3)	49(2)	1
C406	1333(3)	8613(3)	995(3)	46(2)	1
C407	1898(3)	8410(3)	1314(2)	40(1)	1
N401	6302(2)	2203(2)	158(2)	33(1)	1
C408	5888(2)	2046(2)	–218(2)	38(1)	1
C409	5299(2)	1882(2)	65(2)	39(1)	1
C410	4974(2)	1657(2)	–324(2)	42(1)	1
C411	5308(3)	966(2)	–291(3)	49(2)	1
C412	6847(2)	2376(2)	–233(2)	38(1)	1
C413	7326(2)	2563(3)	41(2)	42(1)	1
C414	7856(2)	2672(3)	–380(3)	56(2)	1
C415	8347(2)	2883(3)	–150(3)	64(2)	1
C416	6516(2)	1610(2)	769(2)	33(1)	1
C417	6915(2)	970(2)	733(2)	40(1)	1
C418	6973(2)	373(2)	1360(2)	44(2)	1
C419	6385(2)	133(3)	1523(3)	53(2)	1
C420	5944(2)	2793(2)	298(2)	36(1)	1
C421	5631(3)	3428(2)	–235(2)	43(2)	1
C422	5244(3)	3936(3)	–9(3)	64(2)	1
C423	4854(3)	4562(3)	–503(3)	66(2)	1
O501	–696(2)	1758(2)	2153(2)	49(1)	1
O502	–151(2)	2402(2)	1467(2)	50(1)	1
C501	–193(3)	1889(3)	1943(2)	37(1)	1
C502	385(2)	1398(3)	2295(2)	34(1)	1
C503	385(3)	738(3)	2675(3)	41(1)	1
C504	913(3)	285(3)	3013(3)	54(2)	1
C505	1438(3)	499(3)	2999(3)	55(2)	1
C506	1445(3)	1152(3)	2636(3)	47(2)	1
C507	925(2)	1597(3)	2277(2)	38(1)	1
N501	1438(2)	2081(2)	367(2)	35(1)	1
C508	1967(2)	2267(3)	–38(2)	39(2)	1
C509	2468(2)	2437(3)	225(3)	40(1)	1
C510	2938(3)	2652(3)	–259(3)	50(2)	1
C511	3423(3)	2894(3)	–53(3)	56(2)	1
C512	990(2)	1993(2)	–29(2)	46(2)	1
C513	418(2)	1798(3)	277(2)	47(2)	1
C514	35(2)	1659(2)	–166(2)	50(2)	1
C515	344(3)	1045(3)	–241(3)	60(2)	1
C56A	1144(7)	2622(3)	585(5)	78(2)	0.624(7)
C57A	904(6)	3358(3)	166(4)	78(2)	0.624(7)
C58A	615(5)	3732(3)	612(4)	78(2)	0.624(7)
C59A	630(3)	4413(3)	294(5)	78(2)	0.624(7)
C56B	1111(8)	2629(3)	568(7)	78(2)	0.376(7)

C57B	765(5)	3253(3)	34(4)	78(2)	0.376(7)
C58B	543(4)	3849(4)	261(6)	78(2)	0.376(7)
C59B	1073(4)	4121(4)	190(5)	78(2)	0.376(7)
C520	1665(2)	1447(2)	941(2)	33(1)	1
C521	1995(3)	817(2)	858(2)	37(1)	1
C522	2040(3)	193(3)	1469(3)	39(1)	1
C523	1438(3)	–8(3)	1613(3)	47(2)	1
O601	1332(2)	2253(3)	4984(2)	89(2)	1
O602	1850(3)	3042(3)	4607(3)	98(2)	1
C601	1818(4)	2439(4)	4874(3)	65(2)	1
C602	2407(3)	1899(3)	5068(3)	53(2)	1
C603	2429(3)	1232(3)	5218(3)	57(2)	1
C604	2974(3)	738(4)	5371(3)	69(2)	1
C605	3541(3)	904(4)	5388(3)	69(2)	1
C606	3510(3)	1554(4)	5261(3)	66(2)	1
C607	2970(3)	2058(4)	5087(3)	65(2)	1
N601	3878(2)	3010(2)	3129(2)	47(1)	1
C608	4329(2)	3198(3)	2625(2)	51(2)	1
C609	4891(2)	3370(3)	2777(2)	56(2)	1
C610	5271(2)	3610(3)	2225(3)	70(2)	1
C611	5880(3)	3690(3)	2387(3)	68(2)	1
C612	3446(2)	2688(3)	2944(2)	50(2)	1
C613	2950(2)	2481(3)	3391(2)	49(2)	1
C614	2484(2)	2301(3)	3093(2)	54(2)	1
C615	1956(3)	2109(4)	3504(3)	70(2)	1
C616	3516(2)	3633(2)	3215(2)	50(2)	1
C617	3035(3)	4123(2)	2702(3)	56(2)	1
C618	2717(3)	4742(3)	2822(3)	66(2)	1
C619	2222(3)	5235(3)	2318(3)	77(2)	1
C620	4228(3)	2510(2)	3736(2)	50(2)	1
C621	4636(3)	1862(3)	3744(2)	60(2)	1
C622	5089(3)	1500(3)	4301(3)	69(2)	1
C623	5481(3)	820(3)	4369(3)	76(2)	1
O701	1566(2)	1264(2)	8739(2)	60(1)	1
O702	1771(2)	2259(2)	8184(2)	54(1)	1
C701	1915(3)	1650(3)	8578(3)	44(2)	1
C702	2555(2)	1377(3)	8885(2)	37(1)	1
C703	2677(2)	802(3)	9444(2)	38(1)	1
C704	3246(3)	548(3)	9754(3)	43(2)	1
C705	3718(3)	847(3)	9498(3)	48(2)	1
C706	3618(3)	1403(3)	8943(3)	48(2)	1
C707	3040(3)	1670(3)	8632(3)	41(1)	1
N701	3739(2)	6781(2)	3775(2)	57(2)	1
C708	3490(3)	7476(2)	3772(2)	55(2)	1
C709	3529(3)	8066(2)	3180(3)	59(2)	1
C710	3097(2)	8708(2)	3172(3)	57(2)	1
C711	2424(2)	8746(3)	3108(3)	70(2)	1
C712	4391(2)	6709(3)	3537(3)	60(2)	1

C713	4885(2)	6764(3)	3910(3)	64(2)	1
C714	5510(2)	6629(4)	3642(3)	72(2)	1
C715	6021(3)	6690(3)	3994(3)	75(2)	1
C716	3720(4)	6285(2)	4430(2)	74(2)	1
C717	3975(4)	5550(3)	4538(3)	91(3)	1
C718	3947(3)	5096(3)	5219(3)	92(3)	1
C719	3276(3)	5097(3)	5391(4)	108(3)	1
C720	3340(2)	6677(3)	3349(2)	63(2)	1
C721	2688(2)	6673(4)	3498(3)	83(2)	1
C722	2340(3)	6596(4)	3020(3)	82(2)	1
C723	1700(3)	6517(5)	3174(5)	129(4)	1
O801	4311(2)	1993(2)	2024(2)	63(1)	1
O802	4974(2)	2534(2)	1435(2)	52(1)	1
C801	4853(3)	2045(3)	1859(3)	39(1)	1
C802	5366(2)	1447(3)	2260(2)	35(1)	1
C803	5238(3)	847(3)	2651(3)	42(1)	1
C804	5701(3)	317(3)	3024(3)	53(2)	1
C805	6292(3)	373(3)	3027(3)	58(2)	1
C806	6423(3)	970(3)	2637(3)	51(2)	1
C807	5967(2)	1513(3)	2252(2)	40(1)	1
N801	1535(4)	3270(3)	6281(3)	92(2)	1
C88A	972(3)	3413(5)	6082(5)	138(3)	0.285(7)
C89A	606(3)	3254(12)	6646(5)	138(3)	0.285(7)
C80A	–116(4)	3492(5)	6456(10)	138(3)	0.285(7)
C81A	–277(6)	4199(5)	6065(5)	138(3)	0.285(7)
C88B	764(4)	3502(6)	6349(6)	138(3)	0.715(7)
C89B	406(3)	3402(6)	5896(6)	138(3)	0.715(7)
C80B	–312(4)	3734(4)	5895(6)	138(3)	0.715(7)
C81B	–443(4)	4441(4)	5501(4)	138(3)	0.715(7)
C812	1772(3)	3438(5)	6740(4)	120(3)	1
C813	2378(5)	3399(6)	6821(4)	130(4)	1
C814	2553(4)	3584(5)	7317(4)	94(3)	1
C815	3183(4)	3554(6)	7373(5)	126(4)	1
C16A	1793(5)	2501(3)	6424(5)	98(2)	0.586(8)
C17A	1555(4)	1953(4)	6911(6)	98(2)	0.586(8)
C18A	2126(5)	1323(5)	7266(4)	98(2)	0.586(8)
C19A	2424(6)	1076(4)	6828(5)	98(2)	0.586(8)
C16B	1618(7)	2623(4)	6244(6)	98(2)	0.414(8)
C17B	1538(6)	2099(4)	6863(6)	98(2)	0.414(8)
C18B	1901(4)	1380(5)	6876(8)	98(2)	0.414(8)
C19B	2534(5)	1237(9)	7083(10)	98(2)	0.414(8)
C820	1808(5)	3646(4)	5631(4)	299(5)	1
C821	1752(5)	4389(4)	5374(3)	299(5)	1
C822	2015(5)	4639(5)	4698(4)	299(5)	1
C823	2571(6)	4153(7)	4675(4)	299(5)	1
O901	7968(4)	2944(5)	5340(3)	253(6)	1
C901	7887(4)	3380(4)	4773(4)	253(6)	1

Molibdenium Tetrabutylammonium complex

Table 1. Crystal data and structure refinement details.

Identification code	**2010jh0024**
Empirical formula	$C_{32}H_{72}Mo_6N_2O_{19}$
Formula weight	1364.56
Temperature	120(2) K
Wavelength	0.71073 Å
Crystal system	Monoclinic
Space group	?
Unit cell dimensions	a = 15.9805(4) Å α = 90°
	b = 17.2997(4) Å β = 101.5780(10)°
	c 17.4706(2) Å γ = 90°
Volume	4731.61(17) Å^3
Z	4
Density (calculated)	1.916 Mg / m^3
Absorption coefficient	1.612 mm^{-1}
F(000)	2728
Crystal	Block; Yellow
Crystal size	0.30 × 0.18 × 0.04 mm^3
θ range for data collection	3.05 – 27.53°
Index ranges	$-20 \le h \le 20$, $-22 \le k \le 22$, $-22 \le l \le 22$
Reflections collected	64646
Independent reflections	10839 [R_{int} = 0.0488]
Completeness to θ = 27.50°	99.5 %
Absorption correction	Semi–empirical from equivalents
Max. and min. transmission	0.9383 and 0.6434
Refinement method	Full-matrix least-squares on F^2
Data / restraints / parameters	10839 / 0 / 540
Goodness-of-fit on F^2	1.062
Final R indices [$F^2 > 2\sigma(F^2)$]	$R1$ = 0.0381, $wR2$ = 0.0937
R indices (all data)	$R1$ = 0.0597, $wR2$ = 0.1074
Largest diff. peak and hole	1.005 and –1.230 e Å^{-3}

Diffractometer: *Nonius KappaCCD* area detector (ϕ scans and ω scans to fill *asymmetric unit*). **Cell determination:** DirAx (Duisenberg, A.J.M.(1992). J. Appl. Cryst. 25, 92-96.) **Data collection:** Collect (Collect: Data collection software, R. Hooft, Nonius B.V., 1998). **Data reduction and cell refinement**: *Denzo* (Z. Otwinowski & W. Minor, *Methods in Enzymology* (1997) Vol. **276**: *Macromolecular Crystallography*, part A, pp. 307–326; C. W. Carter, Jr. & R. M. Sweet, Eds., Academic Press). **Absorption correction**: Sheldrick, G. M. SADABS - Bruker Nonius area detector scaling and absorption correction - V2.10 S**tructure solution**: *SHELXS97* (G. M. Sheldrick, Acta Cryst. (1990) A**46** 467–473). S**tructure refinement**: *SHELXL97* (G. M. Sheldrick (1997), University of Göttingen, Germany). **Graphics:** Cameron - A Molecular Graphics Package. (D. M. Watkin, L. Pearce and C. K. Prout, Chemical Crystallography Laboratory, University of Oxford, 1993).

Special details:

Table 2. Atomic coordinates [$\times 10^4$], equivalent isotropic displacement parameters [$Å^2 \times 10^3$] and site occupancy factors. U_{eq} is defined as one third of the trace of the orthogonalized U^{ij} tensor.

Atom	*x*	*y*	*z*	U_{eq}	*S.o.f.*
Mo1	12536(1)	11753(1)	–7415(1)	23(1)	1
Mo2	13148(1)	10420(1)	–8521(1)	19(1)	1
Mo3	13856(1)	10387(1)	–6628(1)	19(1)	1
Mo4	11888(1)	10399(1)	–6350(1)	20(1)	1
Mo5	11181(1)	10428(1)	–8242(1)	19(1)	1
Mo6	12503(1)	9063(1)	–7455(1)	17(1)	1
O1	12541(2)	12726(2)	–7397(1)	31(1)	1
O2	11450(2)	11507(1)	–8089(1)	24(1)	1
O3	11994(2)	11484(1)	–6552(1)	24(1)	1
O4	13605(2)	11481(1)	–6732(1)	25(1)	1
O5	13051(2)	11513(1)	–8277(1)	23(1)	1
O6	12517(1)	10407(1)	–7436(1)	16(1)	1
O7	11444(2)	9336(1)	–8133(1)	20(1)	1
O8	11976(2)	9309(1)	–6593(1)	22(1)	1
O9	12498(2)	8085(1)	–7477(1)	25(1)	1
O10	13582(2)	9303(1)	–6785(1)	21(1)	1
O11	13043(2)	9339(1)	–8320(1)	21(1)	1
O12	13065(2)	10385(1)	–5904(1)	24(1)	1
O13	10923(2)	10408(1)	–7233(1)	23(1)	1
O14	11969(2)	10447(1)	–8969(1)	22(1)	1
O15	14113(2)	10416(1)	–7630(1)	23(1)	1
O16	13635(2)	10455(1)	–9288(1)	26(1)	1
O17	11399(2)	10403(1)	–5581(1)	28(1)	1
O18	10221(2)	10418(1)	–8849(1)	27(1)	1
O19	14817(2)	10348(1)	–6025(2)	28(1)	1
N1	9944(2)	7295(2)	–4391(2)	20(1)	1
C1	9005(2)	7116(2)	–4453(2)	24(1)	1
C2	8805(2)	6395(2)	–4030(2)	27(1)	1
C3	7836(2)	6286(3)	–4153(2)	32(1)	1
C4	7600(3)	5643(2)	–3647(2)	37(1)	1
C5	10407(2)	7345(2)	–3536(2)	21(1)	1
C6	9997(2)	7872(2)	–3016(2)	24(1)	1
C7	10670(2)	8084(2)	–2283(2)	26(1)	1
C8	11293(3)	8691(3)	–2444(2)	41(1)	1
C9	10025(2)	8067(2)	–4774(2)	23(1)	1
C10	9711(2)	8112(2)	–5648(2)	28(1)	1
C11	9857(2)	8915(2)	–5943(2)	29(1)	1
C12	9600(3)	8974(2)	–6828(2)	37(1)	1
C13	10352(2)	6652(2)	–4783(2)	19(1)	1

C14	11277(2)	6795(2)	–4842(2)	21(1)	1
C15	11647(2)	6095(2)	–5191(2)	20(1)	1
C16	12572(2)	6243(2)	–5247(2)	26(1)	1
N2	15001(2)	7610(2)	–5508(1)	17(1)	1
C17	14603(2)	8267(2)	–5125(2)	19(1)	1
C18	13673(2)	8135(2)	–5064(2)	22(1)	1
C19	13315(2)	8829(2)	–4696(2)	20(1)	1
C20	12396(2)	8679(2)	–4619(2)	28(1)	1
C21	14924(2)	6847(2)	–5096(2)	21(1)	1
C22	15237(2)	6845(2)	–4225(2)	26(1)	1
C23	15095(2)	6060(2)	–3882(2)	28(1)	1
C24	15360(3)	6060(2)	–2994(2)	33(1)	1
C25	15944(2)	7782(2)	–5455(2)	20(1)	1
C26	16147(2)	8517(2)	–5851(2)	23(1)	1
C27	17102(2)	8555(2)	–5836(2)	28(1)	1
C28	17346(3)	9281(2)	–6218(2)	33(1)	1
C29	14530(2)	7547(2)	–6356(2)	20(1)	1
C30	14941(2)	7017(2)	–6872(2)	24(1)	1
C31	14283(2)	6790(2)	–7597(2)	26(1)	1
C32	13658(3)	6189(3)	–7433(2)	43(1)	1

Structures from Chapter Five

Dihydrogen phosphate complex of receptor 234

Table 1. Crystal data and structure refinement.

Identification code	2007sot1221a
Empirical formula	$C_{55}H_{100}N_6O_{10}P_2$
Formula weight	1067.35
Temperature	120(2) K
Wavelength	0.71073 Å
Crystal system	Triclinic
Space group	*P*–1
Unit cell dimensions	a = 14.4568(8) Å α = 108.932(2)°
	b = 14.5325(8) Å β = 104.053(2)°
	c = 16.3506(8) Å γ = 98.051(2)°
Volume	3061.1(3) Å^3
Z	2
Density (calculated)	1.158 Mg / m^3
Absorption coefficient	0.128 mm^{-1}
F(000)	1164
Crystal	Block; Colourless
Crystal size	0.30 × 0.30 × 0.10 mm^3
θ range for data collection	2.99 – 25.00°
Index ranges	$-17 \le h \le 17$, $-17 \le k \le 17$, $-19 \le l \le 19$
Reflections collected	34256
Independent reflections	10399 [R_{int} = 0.0662]
Completeness to θ = 25.00°	96.4 %
Absorption correction	Semi–empirical from equivalents
Max. and min. transmission	0.9873 and 0.9626
Refinement method	Full-matrix least-squares on F^2
Data / restraints / parameters	10399 / 0 / 671
Goodness-of-fit on F^2	1.058
Final *R* indices [$F^2 > 2\sigma(F^2)$]	*R1* = 0.1248, *wR2* = 0.3162
R indices (all data)	*R1* = 0.1518, *wR2* = 0.3381
Largest diff. peak and hole	1.336 and –0.448 e Å^{-3}

Diffractometer: *Nonius KappaCCD* area detector (ϕ scans and ω scans to fill *asymmetric unit* sphere). **Cell determination:** DirAx (Duisenberg, A.J.M.(1992). J. Appl. Cryst. 25, 92-96.) **Data collection:** Collect (Collect: Data collection software, R. Hooft, Nonius B.V., 1998). **Data reduction and cell refinement**: *Denzo* (Z. Otwinowski & W. Minor, *Methods in Enzymology* (1997) Vol. **276**: *Macromolecular Crystallography*, part A, pp. 307–326; C. W. Carter, Jr. & R. M. Sweet, Eds., Academic Press). **Absorption correction**: *SORTAV* (R. H. Blessing, Acta Cryst. A**51** (1995) 33–37; R. H. Blessing, J. Appl. Cryst. **30** (1997) 421–426). S**tructure solution**: *SHELXS97* (G. M. Sheldrick, Acta Cryst. (1990) A**46** 467–473). S**tructure refinement**: *SHELXL97* (G. M. Sheldrick (1997), University of Göttingen, Germany). **Graphics:** Cameron - A Molecular Graphics Package. (D. M. Watkin, L. Pearce and C. K. Prout, Chemical Crystallography Laboratory, University of Oxford, 1993).

Special details:

Table 2. Atomic coordinates [$\times 10^4$], equivalent isotropic displacement parameters [$Å^2 \times 10^3$] and site occupancy factors. U_{eq} is defined as one third of the trace of the orthogonalized U^{ij} tensor.

Atom	*x*	*y*	*z*	U_{eq}	*S.o.f.*
O1	5967(5)	660(4)	−1305(4)	48(2)	1
O2	9310(4)	4085(5)	−3497(4)	50(2)	1
N1	4125(5)	2081(5)	−1267(4)	35(2)	1
N2	6088(5)	2152(5)	−1484(4)	36(2)	1
N3	7656(5)	3913(5)	−3858(4)	36(2)	1
N4	7916(4)	5896(5)	−3845(4)	33(1)	1
C1	3157(6)	1759(6)	−1353(5)	37(2)	1
C2	2466(6)	2307(6)	−1201(5)	40(2)	1
C3	1526(7)	1762(7)	−1348(6)	48(2)	1
C4	1300(8)	717(8)	−1638(6)	58(3)	1
C5	1997(8)	190(7)	−1775(7)	59(3)	1
C6	2957(7)	705(6)	−1629(6)	43(2)	1
C7	3838(7)	403(6)	−1694(6)	46(2)	1
C8	4534(6)	1267(6)	−1479(5)	37(2)	1
C9	5580(6)	1334(6)	−1423(5)	39(2)	1
C10	7138(6)	2298(7)	−1359(6)	44(2)	1
C11	7406(7)	1626(7)	−2148(7)	53(2)	1
C12	7091(7)	1817(7)	−3021(6)	48(2)	1
C13	7572(6)	2856(6)	−2951(6)	41(2)	1
C14	7426(6)	2896(6)	−3887(6)	40(2)	1
C15	8586(5)	4438(6)	−3663(6)	38(2)	1
C16	8698(5)	5478(6)	−3630(5)	36(2)	1
C17	9548(6)	6178(7)	−3364(6)	45(2)	1
C18	9301(6)	7073(7)	−3420(6)	45(2)	1
C19	9833(7)	8058(7)	−3233(7)	58(3)	1
C20	9330(7)	8764(7)	−3337(7)	56(3)	1
C21	8303(7)	8539(7)	−3645(6)	48(2)	1
C22	7764(6)	7580(6)	−3847(5)	37(2)	1
C23	8272(6)	6871(6)	−3724(5)	35(2)	1
N101	8132(4)	6455(5)	3351(4)	31(1)	1
C101	9035(5)	7087(6)	4140(5)	34(2)	1
C102	9613(6)	7952(6)	3995(6)	38(2)	1
C103	10526(6)	8497(6)	4802(6)	43(2)	1
C104	11140(7)	9369(7)	4690(8)	58(3)	1
C105	8442(6)	5948(6)	2520(5)	34(2)	1
C106	7665(6)	5101(6)	1735(5)	38(2)	1
C107	8058(7)	4741(7)	930(6)	53(2)	1
C108	8893(7)	4243(9)	1086(8)	80(4)	1
C109	7598(5)	5661(5)	3613(5)	31(2)	1
C110	8151(6)	4905(6)	3794(6)	40(2)	1

C111	7456(6)	4028(6)	3831(6)	40(2)	1
C112	7970(7)	3219(7)	3944(7)	55(2)	1
C113	7416(5)	7080(6)	3118(5)	32(2)	1
C114	7075(5)	7679(6)	3875(5)	32(2)	1
C115	6395(6)	8282(6)	3545(6)	38(2)	1
C116	5970(7)	8851(6)	4272(6)	47(2)	1
N201	3429(4)	1862(4)	1566(4)	28(1)	1
C201	2836(6)	2636(5)	1864(5)	31(2)	1
C202	2359(5)	3028(6)	1157(5)	31(2)	1
C203	1872(6)	3848(6)	1570(5)	39(2)	1
C204	1480(7)	4346(7)	925(7)	49(2)	1
C205	4250(5)	2347(5)	1301(5)	33(2)	1
C206	5016(6)	1746(6)	1125(6)	40(2)	1
C207	5876(6)	2402(6)	1024(6)	38(2)	1
C208	6738(7)	1907(7)	993(7)	54(2)	1
C209	3831(6)	1562(5)	2367(5)	33(2)	1
C210	4637(6)	2366(6)	3183(5)	42(2)	1
C211	4917(7)	2023(6)	3960(6)	48(2)	1
C212	5384(9)	1149(7)	3788(7)	69(3)	1
C213	2807(5)	934(5)	763(5)	32(2)	1
C214	1916(5)	380(6)	913(5)	34(2)	1
C215	1418(6)	–579(6)	89(6)	44(2)	1
C216	536(6)	–1194(7)	198(7)	49(2)	1
P301	4780(1)	5451(1)	1299(1)	28(1)	1
O301	5485(4)	5970(4)	954(3)	35(1)	1
O302	3933(4)	4670(4)	467(3)	40(1)	1
O303	5350(4)	4855(4)	1794(4)	39(1)	1
O304	4339(4)	6139(4)	1920(4)	35(1)	1
P401	4731(1)	5405(1)	3840(1)	26(1)	1
O401	5747(4)	5833(4)	4606(4)	35(1)	1
O402	3969(4)	5123(4)	4263(4)	41(1)	1
O403	4785(4)	4568(4)	3046(4)	42(1)	1
O404	4566(4)	6332(4)	3585(3)	33(1)	1

Fluoride complex of receptor 236

Table 1. Crystal data and structure refinement.

Identification code	2007sot1257a
Empirical formula	$C_{110}H_{199}F_4N_{16}O_{17.50}$
Formula weight	2101.85
Temperature	120(2) K
Wavelength	0.71073 Å
Crystal system	Triclinic
Space group	*P*–1
Unit cell dimensions	a = 18.2686(7) Å α = 67.912(2)°
	b = 19.4475(6) Å β = 83.791(2)°
	c = 20.3422(8) Å γ = 63.537(2)°
Volume	5979.7(4) Å^3
Z	2
Density (calculated)	1.167 Mg / m^3
Absorption coefficient	0.083 mm^{-1}
F(000)	2294
Crystal	Block; Yellow
Crystal size	0.08 × 0.08 × 0.05 mm^3
θ range for data collection	2.92 – 25.00°
Index ranges	$-21 \le h \le 21$, $-23 \le k \le 23$, $-24 \le l \le 24$
Reflections collected	80601
Independent reflections	20927 [R_{int} = 0.1711]
Completeness to θ = 25.00°	99.4 %
Absorption correction	Semi–empirical from equivalents
Max. and min. transmission	0.9959 and 0.9934
Refinement method	Full-matrix least-squares on F^2
Data / restraints / parameters	20927 / 18 / 1396
Goodness-of-fit on F^2	1.094
Final *R* indices [$F^2 > 2\sigma(F^2)$]	*R1* = 0.2023, *wR2* = 0.2828
R indices (all data)	*R1* = 0.3790, *wR2* = 0.3665
Largest diff. peak and hole	0.717 and –0.360 e Å^{-3}

Diffractometer: *Nonius KappaCCD* area detector (ϕ scans and ω scans to fill *asymmetric unit* sphere). **Cell determination:** DirAx (Duisenberg, A.J.M.(1992). J. Appl. Cryst. 25, 92-96.) **Data collection:** Collect (Collect: Data collection software, R. Hooft, Nonius B.V., 1998). **Data reduction and cell refinement**: *Denzo* (Z. Otwinowski & W. Minor, *Methods in Enzymology* (1997) Vol. **276**: *Macromolecular Crystallography*, part A, pp. 307–326; C. W. Carter, Jr. & R. M. Sweet, Eds., Academic Press). **Absorption correction**: *SORTAV* (R. H. Blessing, Acta Cryst. A**51** (1995) 33–37; R. H. Blessing, J. Appl. Cryst. **30** (1997) 421–426). S**tructure solution**: *SHELXS97* (G. M. Sheldrick, Acta Cryst. (1990) A**46** 467–473). S**tructure refinement**: *SHELXL97* (G. M. Sheldrick (1997), University of Göttingen, Germany). **Graphics:** Cameron - A Molecular Graphics Package. (D. M. Watkin, L. Pearce and C. K. Prout, Chemical Crystallography Laboratory, University of Oxford, 1993).

Special details:

Table 2. Atomic coordinates [$\times 10^4$], equivalent isotropic displacement parameters [$Å^2 \times 10^3$] and site occupancy factors. U_{eq} is defined as one third of the trace of the orthogonalized U^{ij} tensor.

Atom	*x*	*y*	*z*	U_{eq}	*S.o.f.*
O1	10577(5)	–529(5)	6050(4)	82(3)	1
O2	10846(5)	–1535(4)	7082(4)	62(2)	1
O3	11080(5)	–5129(5)	8073(5)	84(3)	1
O4	9847(7)	–1721(5)	9926(5)	107(4)	1
O5	8801(9)	–1811(8)	12993(5)	167(6)	1
O6	8880(6)	–1208(7)	13633(5)	115(4)	1
N1	10610(6)	–1206(6)	6451(6)	60(3)	1
N2	10828(5)	–2999(5)	7225(5)	58(3)	1
N3	11356(6)	–4392(5)	8555(6)	73(3)	1
N4	9621(7)	–2649(6)	10895(5)	87(4)	1
N5	9336(7)	–1534(6)	11647(5)	86(4)	1
N6	8935(8)	–1278(10)	13047(7)	111(5)	1
C1	10489(7)	–2466(7)	6560(7)	57(3)	1
C2	10358(7)	–1645(7)	6158(6)	55(3)	1
C3	9992(8)	–1264(8)	5480(7)	79(4)	1
C4	9736(8)	–1677(9)	5187(7)	81(4)	1
C5	9864(9)	–2488(9)	5556(9)	89(4)	1
C6	10253(8)	–2889(8)	6244(8)	70(4)	1
C7	10476(8)	–3695(8)	6751(8)	78(4)	1
C8	10834(7)	–3755(7)	7335(8)	64(3)	1
C9	11109(8)	–4480(8)	8008(8)	74(4)	1
C10	11594(8)	–5058(7)	9269(8)	87(4)	1
C11	11529(8)	–4716(7)	9828(7)	79(4)	1
C12	10660(8)	–4180(7)	9945(6)	70(4)	1
C13	10595(8)	–3738(7)	10449(6)	76(4)	1
C14	9708(9)	–3186(7)	10518(7)	76(4)	1
C15	9691(10)	–1960(8)	10571(8)	92(5)	1
C16	9558(10)	–1386(8)	10944(7)	93(5)	1
C17	9643(11)	–681(8)	10696(7)	116(6)	1
C18	9499(9)	–365(9)	11241(7)	87(4)	1
C19	9521(9)	315(8)	11287(7)	92(5)	1
C20	9373(9)	455(9)	11909(8)	88(4)	1
C21	9169(8)	–60(10)	12494(8)	86(5)	1
C22	9144(8)	–734(9)	12442(7)	79(4)	1
C23	9304(9)	–907(8)	11822(7)	81(4)	1
O101	5454(6)	–10(5)	9048(4)	84(3)	1
O102	5827(5)	685(4)	8109(4)	59(2)	1
O103	6183(6)	3997(5)	7147(6)	112(4)	1
O104	4479(6)	1783(5)	5255(5)	90(3)	1
O105	3867(6)	3067(6)	1914(5)	105(3)	1

O106	4414(9)	2385(6)	1245(6)	154(5)	1
N101	5603(6)	574(5)	8697(5)	54(2)	1
N102	5899(5)	2126(4)	7956(5)	46(2)	1
N103	6326(6)	3088(6)	6677(6)	85(4)	1
N104	4372(5)	2938(5)	4304(5)	63(3)	1
N105	4292(5)	2173(5)	3380(5)	56(2)	1
N106	4162(8)	2417(8)	1821(6)	96(4)	1
C101	5674(6)	1846(6)	8627(6)	45(3)	1
C102	5519(6)	1164(6)	9015(5)	43(3)	1
C103	5295(7)	1037(7)	9696(6)	69(4)	1
C104	5197(8)	1572(7)	10022(7)	85(4)	1
C105	5355(8)	2248(7)	9658(7)	73(4)	1
C106	5587(7)	2395(7)	8956(7)	60(3)	1
C107	5777(7)	3012(7)	8457(8)	75(4)	1
C108	5971(7)	2841(6)	7865(7)	63(3)	1
C109	6182(8)	3340(8)	7213(9)	89(5)	1
C110	6497(9)	3611(9)	6008(8)	102(5)	1
C111	6375(8)	3370(8)	5488(8)	85(4)	1
C112	5412(11)	3610(9)	5320(7)	116(6)	1
C113	5314(9)	3200(7)	4848(6)	76(4)	1
C114	4444(8)	3360(7)	4742(6)	68(4)	1
C115	4423(7)	2163(7)	4610(7)	57(3)	1
C116	4385(7)	1775(7)	4117(6)	65(3)	1
C117	4447(8)	1011(7)	4307(7)	75(4)	1
C118	4398(7)	883(8)	3669(7)	66(3)	1
C119	4508(8)	193(8)	3534(7)	80(4)	1
C120	4463(8)	266(8)	2834(8)	79(4)	1
C121	4344(8)	977(9)	2277(8)	82(4)	1
C122	4253(7)	1672(8)	2400(6)	67(3)	1
C123	4299(7)	1636(7)	3102(6)	62(3)	1
N201	8183(5)	–381(5)	7208(4)	49(2)	1
C201	8733(6)	–1304(6)	7484(5)	48(3)	1
C202	8334(6)	–1865(6)	7912(5)	52(3)	1
C203	8951(7)	–2757(6)	8053(5)	55(3)	1
C204	8656(8)	–3386(7)	8529(6)	83(4)	1
C205	7733(6)	–121(6)	7814(5)	51(3)	1
C206	8294(7)	–271(6)	8408(6)	61(3)	1
C207	7835(10)	–28(7)	9043(9)	122(7)	1
C208	7554(12)	–618(13)	9461(12)	192(10)	1
C209	8757(6)	25(5)	6909(5)	49(3)	1
C210	8341(7)	955(6)	6594(6)	67(3)	1
C211	8983(8)	1267(7)	6380(8)	100(5)	1
C212	8651(8)	2200(7)	6021(8)	118(6)	1
C213	7528(7)	–129(7)	6654(6)	65(3)	1
C214	7853(8)	–261(8)	5975(6)	76(4)	1
C26A	7175(10)	–59(10)	5459(8)	106(5)	0.53(3)
C27A	7350(20)	–70(20)	4800(14)	151(18)	0.53(3)

C26B	7175(10)	–59(10)	5459(8)	106(5)	0.47(3)
C27B	6654(19)	740(18)	5131(17)	112(15)	0.47(3)
N301	7843(7)	–5294(5)	7149(6)	77(3)	1
C301	8483(9)	–6185(7)	7507(8)	103(5)	1
C302	8128(11)	–6811(9)	7654(11)	168(9)	1
C303	8535(14)	–7547(11)	8034(12)	185(10)	1
C304	8265(9)	–8219(8)	8214(9)	127(6)	1
C305	7102(8)	–5074(7)	7586(7)	77(4)	1
C306	7248(8)	–5145(8)	8337(7)	87(4)	1
C307	6422(10)	–5024(10)	8689(7)	109(5)	1
C308	6468(11)	–5000(11)	9408(8)	148(7)	1
C309	8286(7)	–4773(6)	7080(6)	66(3)	1
C310	7770(7)	–3845(6)	6803(6)	61(3)	1
C311	8323(7)	–3421(6)	6682(6)	60(3)	1
C312	7853(7)	–2483(7)	6443(7)	77(4)	1
C313	7525(8)	–5135(7)	6419(7)	80(4)	1
C314	8142(9)	–5420(7)	5905(8)	91(5)	1
C315	7724(10)	–5149(8)	5180(7)	97(5)	1
C316	8342(10)	–5511(8)	4683(8)	120(6)	1
N401	2951(6)	2641(6)	7750(5)	63(3)	1
C401	3450(7)	1720(7)	7955(6)	67(3)	1
C402	2975(8)	1216(7)	8208(6)	76(4)	1
C403	3513(10)	298(8)	8436(9)	122(6)	1
C405	2497(7)	2847(6)	8369(6)	66(3)	1
C404	3027(11)	–202(8)	8699(9)	145(7)	1
C406	3036(7)	2560(8)	9021(6)	72(4)	1
C407	2509(8)	2673(8)	9635(7)	82(4)	1
C408	3030(11)	2425(11)	10277(9)	143(7)	1
C409	3551(8)	3027(8)	7512(7)	86(4)	1
C410	3173(10)	3946(9)	7276(10)	154(8)	1
C411	3814(11)	4277(11)	7131(11)	139(8)	1
C412	3889(18)	4620(20)	6521(12)	320(20)	1
C413	2318(7)	2971(7)	7154(5)	65(3)	1
C414	2643(8)	2781(8)	6502(6)	83(4)	1
C415	1958(8)	3188(8)	5935(7)	84(4)	1
C416	2220(10)	2979(9)	5271(7)	116(6)	1
N501	3271(6)	–2466(6)	7802(6)	73(3)	1
C501	3910(7)	–3331(8)	8121(7)	76(4)	1
C502	3593(8)	–3990(7)	8375(7)	86(4)	1
C503	4220(10)	–4855(9)	8732(9)	147(8)	1
C504	3875(11)	–5481(9)	8974(10)	163(9)	1
C505	2679(8)	–2245(7)	8360(7)	79(4)	1
C506	3075(9)	–2425(9)	9056(8)	104(5)	1
C507	2486(11)	–2072(11)	9605(13)	173(10)	1
C508	2032(13)	–2436(14)	9880(14)	231(13)	1
C509	3714(8)	–1897(8)	7547(7)	85(4)	1

C510	3166(8)	–969(7)	7138(7)	86(4)	1
C511	3651(9)	–494(8)	6855(8)	101(5)	1
C512	3172(10)	408(8)	6536(9)	128(6)	1
C513	2765(7)	–2358(7)	7204(7)	68(4)	1
C514	3256(8)	–2517(9)	6575(7)	95(5)	1
C515	2672(11)	–2365(13)	6000(10)	124(7)	1
C516	2572(12)	–3106(17)	6176(11)	200(12)	1
F601	11502(4)	–3042(3)	8325(3)	63(2)	1
F701	6280(4)	1687(3)	6853(3)	64(2)	1
F801	4535(4)	3468(4)	2925(3)	71(2)	1
F901	9344(4)	–2981(4)	12246(3)	83(2)	1
O1W	4769(5)	1905(6)	6575(4)	76(2)	1
O2W	10112(5)	–2058(5)	8687(4)	72(2)	1
O3W	4910(6)	–4483(6)	7020(6)	96(3)	1
O4W	10370(8)	–5468(5)	7120(6)	120(4)	1
O5W	9780(11)	–4901(14)	5715(10)	272(10)	1
O6W	9986(12)	–6769(12)	6488(11)	110(7)	0.50

Fluoride complex of receptor 238

Table 1. Crystal data and structure refinement details.

Identification code	2008sot0749 (JEN3+F–)
Empirical formula	$C_{62}H_{89}Cl_2F_2N_9O_6$
Formula weight	1165.32
Temperature	120(2) K
Wavelength	0.71073 Å
Crystal system	Triclinic
Space group	*P*–1
Unit cell dimensions	a = 9.1563(2) Å α = 93.973(2)°
	b = 17.1789(4) Å β = 90.7960(10)°
	c = 19.4856(5) Å γ = 93.8740(10)°
Volume	3050.11(12) Å^3
Z	2
Density (calculated)	1.269 Mg / m^3
Absorption coefficient	0.170 mm^{-1}
F(000)	1248
Crystal	Needle; Yellow
Crystal size	0.14 × 0.02 × 0.02 mm^3
θ range for data collection	3.03 – 25.03°
Index ranges	$-10 \le h \le 10$, $-20 \le k \le 20$, $-23 \le l \le 23$
Reflections collected	38482
Independent reflections	10683 [R_{int} = 0.1064]
Completeness to θ = 25.03°	99.3 %
Absorption correction	Semi–empirical from equivalents
Max. and min. transmission	0.9966 and 0.9665
Refinement method	Full-matrix least-squares on F^2
Data / restraints / parameters	10683 / 474 / 738
Goodness-of-fit on F^2	1.060
Final *R* indices [$F^2 > 2\sigma(F^2)$]	*R1* = 0.1464, *wR2* = 0.2479
R indices (all data)	*R1* = 0.2429, *wR2* = 0.2990
Largest diff. peak and hole	1.319 and –1.423 e Å^{-3}

Diffractometer: *Nonius KappaCCD* area detector (ϕ scans and ω scans to fill *asymmetric unit*). **Cell determination:** DirAx (Duisenberg, A.J.M.(1992). J. Appl. Cryst. 25, 92-96.) **Data collection:** Collect (Collect: Data collection software, R. Hooft, Nonius B.V., 1998). **Data reduction and cell refinement**: *Denzo* (Z. Otwinowski & W. Minor, *Methods in Enzymology* (1997) Vol. **276**: *Macromolecular Crystallography*, part A, pp. 307–326; C. W. Carter, Jr. & R. M. Sweet, Eds., Academic Press). **Absorption correction**: Sheldrick, G. M. SADABS - Bruker Nonius area detector scaling and absorption correction - V2.10 S**tructure solution**: *SHELXS97* (G. M. Sheldrick, Acta Cryst. (1990) A**46** 467–473). S**tructure refinement**: *SHELXL97* (G. M. Sheldrick (1997), University of Göttingen, Germany). **Graphics:** Cameron - A Molecular Graphics Package. (D. M. Watkin, L. Pearce and C. K. Prout, Chemical Crystallography Laboratory, University of Oxford, 1993).

Special details: All hydrogen atoms were placed in idealised positions and refined using a riding model.

Table 2. Atomic coordinates [$\times 10^4$], equivalent isotropic displacement parameters [$Å^2 \times 10^3$] and site occupancy factors. U_{eq} is defined as one third of the trace of the orthogonalized U^{ij} tensor.

Atom	*x*	*y*	*z*	U_{eq}	*S.o.f.*
Cl1	8615(3)	6625(2)	4703(1)	88(1)	1
Cl2	9405(4)	11478(2)	6038(2)	141(2)	1
O1	5114(7)	6650(4)	10534(3)	62(2)	1
O2	6284(7)	6864(4)	9607(3)	57(2)	1
O3	4999(8)	5761(5)	6488(3)	94(3)	1
O4	6193(7)	11415(3)	8010(3)	61(2)	1
O5	3431(6)	8479(3)	9403(3)	46(1)	1
O6	2104(7)	8356(4)	10315(3)	66(2)	1
N1	5307(8)	6522(4)	9917(4)	45(2)	1
N2	5145(6)	6272(4)	8319(3)	38(2)	1
N3	5975(6)	6916(4)	7039(3)	37(2)	1
N4	6554(6)	8602(4)	6997(3)	38(2)	1
N5	6142(7)	10094(4)	7784(3)	47(2)	1
N6	4312(6)	9937(3)	8982(3)	34(2)	1
N7	2710(8)	8753(4)	9891(4)	46(2)	1
C1	4361(8)	5936(4)	9512(4)	42(2)	1
C2	3429(9)	5456(5)	9870(5)	53(2)	1
C3	2472(10)	4890(5)	9517(6)	56(3)	1
C4	2462(9)	4804(5)	8815(5)	54(2)	1
C5	3382(9)	5291(5)	8442(5)	46(2)	1
C6	4376(8)	5876(4)	8787(4)	38(2)	1
C7	3627(8)	5354(4)	7739(4)	44(2)	1
C8	4669(8)	5941(5)	7675(4)	39(2)	1
C9	5255(8)	6201(5)	7009(4)	49(2)	1
C10	6661(8)	7228(6)	6469(4)	42(2)	1
C11	7151(9)	6817(6)	5887(4)	54(2)	1
C12	7971(9)	7212(8)	5405(4)	62(3)	1
C13	8326(10)	7992(8)	5441(5)	64(3)	1
C14	7795(8)	8442(6)	6009(4)	50(2)	1
C15	6975(8)	8044(6)	6507(4)	43(2)	1
C16	7892(9)	9258(6)	6211(4)	56(3)	1
C17	8611(10)	9923(7)	5957(5)	76(4)	1
C18	8474(11)	10624(7)	6318(6)	85(4)	1
C19	7699(10)	10708(6)	6923(6)	77(4)	1
C20	6979(9)	10060(5)	7181(5)	52(2)	1
C21	7122(8)	9330(5)	6828(4)	48(2)	1
C22	5797(8)	10752(5)	8150(4)	43(2)	1
C23	4840(8)	10639(4)	8753(4)	38(2)	1
C24	4363(9)	11246(5)	9166(4)	45(2)	1
C25	3471(8)	10911(4)	9664(4)	40(2)	1
C26	2680(9)	11221(5)	10214(4)	45(2)	1
C27	1912(9)	10730(5)	10624(4)	46(2)	1

C28	1890(9)	9917(5)	10506(4)	45(2)	1
C29	2692(8)	9600(4)	9972(4)	38(2)	1
C30	3477(8)	10078(4)	9534(4)	36(2)	1
N8	5002(7)	6933(4)	3063(3)	40(2)	1
C31	5012(9)	6355(5)	3622(5)	57(3)	1
C32	3643(11)	6278(7)	4040(5)	79(3)	1
C33	3924(12)	5783(7)	4642(5)	83(4)	1
C34	2587(14)	5667(8)	5086(6)	115(5)	1
C35	3676(8)	6745(4)	2577(4)	38(2)	1
C36	3505(9)	5927(5)	2236(4)	48(2)	1
C37	2147(10)	5827(5)	1782(5)	52(2)	1
C38	1810(10)	4976(5)	1507(5)	59(2)	1
C39	4878(9)	7758(5)	3371(4)	41(2)	1
C40	6075(11)	8094(6)	3874(5)	65(3)	1
C41	5943(13)	8963(7)	4043(5)	86(4)	1
C42	6639(16)	9412(8)	3521(8)	122(5)	1
C43	6433(8)	6876(5)	2682(5)	48(2)	1
C44	6743(9)	7454(5)	2147(4)	48(2)	1
C45	8147(16)	7395(7)	1707(9)	114(5)	1
C46	9300(20)	7369(9)	2119(8)	139(6)	1
C47	12406(8)	7747(5)	7048(5)	59(3)	1
C48	12022(11)	8032(9)	6362(5)	97(4)	1
C49	13359(11)	8136(8)	5939(6)	87(4)	1
C50	13060(20)	8330(13)	5328(9)	187(8)	1
C51	10024(9)	6967(5)	7174(5)	58(3)	1
C52	10619(10)	6165(5)	7086(4)	50(2)	1
C53	9621(10)	5589(5)	6626(5)	58(2)	1
C54	10207(11)	4781(6)	6575(5)	68(3)	1
C55	10280(8)	8341(5)	7609(5)	53(2)	1
C56	11148(9)	9037(5)	7950(6)	65(3)	1
C57	10332(12)	9758(5)	7840(6)	70(3)	1
C58	10980(11)	10474(6)	8184(6)	82(3)	1
C59	11680(8)	7373(5)	8187(5)	53(2)	1
C60	10521(9)	7275(5)	8733(5)	54(2)	1
C61	11063(10)	6809(4)	9310(5)	57(3)	1
C62	10015(11)	6777(6)	9897(6)	78(3)	1
N9	11088(7)	7598(4)	7505(4)	48(2)	1
F1	6947(5)	7654(3)	8313(2)	60(1)	1
F2	4949(4)	8723(2)	8100(2)	40(1)	1

Acetate complex of receptor 242

Table 1. Crystal data and structure refinement details.

Identification code	**2009jh0002**
Empirical formula	$C_{68}H_{100}N_6O_6$
Formula weight	1097.54
Temperature	120(2) K
Wavelength	0.71073 Å
Crystal system	Monoclinic
Space group	$P2_1/c$
Unit cell dimensions	a = 9.5797(3) Å α = 90°
	b = 34.5143(11) Å β = 95.2190(10)°
	c 19.6987(7) Å γ = 90°
Volume	6486.1(4) Å^3
Z	4
Density (calculated)	1.124 Mg / m^3
Absorption coefficient	0.071 mm^{-1}
F(000)	2392
Crystal	Plate; Colourless
Crystal size	0.1 × 0.05 × 0.01 mm^3
θ range for data collection	3.03 – 25.03°
Index ranges	$-11 \le h \le 11$, $-39 \le k \le 41$, $-23 \le l \le 23$
Reflections collected	40240
Independent reflections	11352 [R_{int} = 0.0799]
Completeness to θ = 25.03°	99.0 %
Absorption correction	Semi–empirical from equivalents
Max. and min. transmission	0.9993 and 0.9929
Refinement method	Full-matrix least-squares on F^2
Data / restraints / parameters	11352 / 0 / 731
Goodness-of-fit on F^2	1.110
Final R indices [$F^2 > 2\sigma(F^2)$]	*R1* = 0.1137, *wR2* = 0.2057
R indices (all data)	*R1* = 0.1713, *wR2* = 0.2340
Largest diff. peak and hole	0.685 and –0.333 e Å^{-3}

Diffractometer: *Nonius KappaCCD* area detector (ϕ scans and ω scans to fill *asymmetric unit*). **Cell determination:** DirAx (Duisenberg, A.J.M.(1992). J. Appl. Cryst. 25, 92-96.) **Data collection:** Collect (Collect: Data collection software, R. Hooft, Nonius B.V., 1998). **Data reduction and cell refinement**: *Denzo* (Z. Otwinowski & W. Minor, *Methods in Enzymology* (1997) Vol. **276**: *Macromolecular Crystallography*, part A, pp. 307–326; C. W. Carter, Jr. & R. M. Sweet, Eds., Academic Press). **Absorption correction**: Sheldrick, G. M. SADABS - Bruker Nonius area detector scaling and absorption correction - V2.10 S**tructure solution**: *SHELXS97* (G. M. Sheldrick, Acta Cryst. (1990) A**46** 467–473). S**tructure refinement**: *SHELXL97* (G. M. Sheldrick (1997), University of Göttingen, Germany). **Graphics:** Cameron - A Molecular Graphics Package. (D. M. Watkin, L. Pearce and C. K. Prout, Chemical Crystallography Laboratory, University of Oxford, 1993).

Special details:

Table 2. Atomic coordinates [$\times 10^4$], equivalent isotropic displacement parameters [$Å^2 \times 10^3$] and site occupancy factors. U_{eq} is defined as one third of the trace of the orthogonalized U^{ij} tensor.

Atom	*x*	*y*	*z*	U_{eq}	*S.o.f.*
O7	–3633(4)	1644(1)	3034(2)	47(1)	1
O6	–2465(3)	1098(1)	3267(2)	47(1)	1
C69	–3518(5)	1313(2)	3297(3)	43(1)	1
C70	–4680(6)	1168(2)	3702(4)	78(2)	1
N1	3998(4)	2623(1)	2954(2)	27(1)	1
C1	2912(5)	2906(1)	3186(2)	31(1)	1
C10	6372(5)	2636(1)	2432(3)	35(1)	1
C5	3371(5)	2366(1)	2381(2)	29(1)	1
C13	4531(5)	2351(1)	3534(2)	28(1)	1
C2	1683(5)	2717(1)	3494(2)	33(1)	1
C6	2843(5)	2566(1)	1725(2)	33(1)	1
C9	5188(5)	2866(1)	2717(2)	33(1)	1
C7	2186(5)	2261(1)	1232(2)	38(1)	1
C14	5166(5)	2542(1)	4180(2)	34(1)	1
C11	7496(5)	2907(2)	2226(3)	41(1)	1
C15	5552(5)	2232(2)	4708(2)	40(1)	1
C3	599(5)	3016(2)	3664(3)	41(1)	1
C16	6226(6)	2392(2)	5372(3)	53(2)	1
C8	1763(6)	2411(2)	525(3)	53(2)	1
C12	8719(5)	2690(2)	1976(3)	54(2)	1
C4	–672(5)	2825(2)	3942(3)	51(2)	1
O1	2170(3)	1708(1)	3334(2)	40(1)	1
O2	3795(3)	1639(1)	5827(2)	43(1)	1
N2	–584(4)	202(1)	2583(2)	34(1)	1
N5	–2303(4)	1592(1)	1883(2)	35(1)	1
O3	83(4)	769(1)	6250(2)	49(1)	1
N3	–13(4)	1490(1)	2981(2)	33(1)	1
N6	1342(4)	1066(1)	7752(2)	35(1)	1
O4	–1122(4)	1118(1)	6949(2)	54(1)	1
C45	1000(5)	1615(1)	3463(2)	32(1)	1
C46	607(5)	1619(1)	4180(2)	32(1)	1
C66	2737(5)	1086(1)	7627(2)	31(1)	1
C22	–1915(5)	248(1)	1394(2)	36(1)	1
C48	1690(5)	1570(1)	4694(2)	33(1)	1
N4	2367(4)	1275(1)	6447(2)	33(1)	1
C43	214(5)	1449(1)	2281(2)	33(1)	1
C29	17(5)	469(1)	3149(2)	38(1)	1
C51	1442(5)	1552(1)	5371(2)	32(1)	1
C52	2649(5)	1491(1)	5899(2)	34(1)	1
C50	70(5)	1600(1)	5548(3)	38(1)	1
C44	–929(5)	1505(1)	1787(3)	35(1)	1

C47	–744(5)	1675(1)	4366(3)	39(1)	1
C17	–1660(5)	–75(1)	2843(3)	37(1)	1
C21	–1257(5)	459(1)	2022(3)	36(1)	1
C30	796(6)	273(2)	3751(3)	46(1)	1
C39	–789(5)	1456(1)	1086(3)	36(1)	1
C42	1457(5)	1331(1)	2051(3)	38(1)	1
C25	560(5)	–46(1)	2330(3)	35(1)	1
C57	5053(5)	982(1)	8201(2)	37(1)	1
C64	1278(5)	943(1)	8418(3)	39(1)	1
C54	3297(5)	1187(1)	7025(2)	35(1)	1
C23	–2537(5)	536(1)	868(3)	42(1)	1
C40	505(6)	1346(1)	872(3)	42(1)	1
C58	3592(5)	975(1)	8217(2)	36(1)	1
C55	4746(5)	1194(1)	7026(3)	38(1)	1
C26	1761(5)	173(2)	2046(3)	41(1)	1
C41	1606(6)	1279(2)	1354(3)	42(1)	1
C49	–1005(5)	1670(2)	5046(3)	42(1)	1
C59	2650(5)	881(1)	8726(2)	37(1)	1
C63	104(6)	873(1)	8762(3)	41(1)	1
C35	–5050(6)	1568(2)	441(3)	47(1)	1
C33	–3072(5)	1583(1)	1258(3)	39(1)	1
C18	–2851(5)	121(2)	3165(3)	47(1)	1
C36	–4186(6)	1497(2)	–78(3)	48(1)	1
C34	–4527(6)	1610(2)	1109(3)	44(1)	1
C38	–2177(5)	1509(1)	742(3)	37(1)	1
C65	2838(5)	–107(2)	1813(3)	48(1)	1
C61	1671(6)	674(2)	9735(3)	48(1)	1
C56	5610(5)	1091(1)	7614(3)	40(1)	1
C37	–2764(6)	1469(1)	68(3)	42(1)	1
C60	2836(6)	748(2)	9397(3)	43(1)	1
C19	–3908(6)	–179(2)	3360(3)	49(1)	1
C24	–3179(6)	346(2)	217(3)	50(2)	1
C62	314(6)	736(2)	9421(3)	50(2)	1
C28	4072(6)	95(2)	1549(3)	60(2)	1
C31	1246(8)	573(2)	4299(3)	74(2)	1
C67	–1037(6)	899(2)	6436(3)	50(1)	1
C32	2104(10)	413(2)	4916(4)	108(3)	1
C20	–5029(8)	5(2)	3731(5)	94(3)	1
C68	–2389(6)	802(2)	6016(4)	74(2)	1

Appendix 2 – Proton NMR Titration Curves

Where reported, anion stability constants have been elucidated through ^{1}H NMR titration experiments, with the anions added as the tetraethylammonium or tetrabutylammonium salt at 298 K in the appropriate DMSO-d_6/H_2O mixtures.

The NMR data from the titration experiments have been fitted to either a 1:1 or 2:1 anion:receptor binding model as appropriate, with the resulting titration profiles reported for completeness.

Proton NMR titrations from Chapter Two

NMR titration for 209 *vs*. TBAOAc in DMSO-d_6/H_2O 0.5%

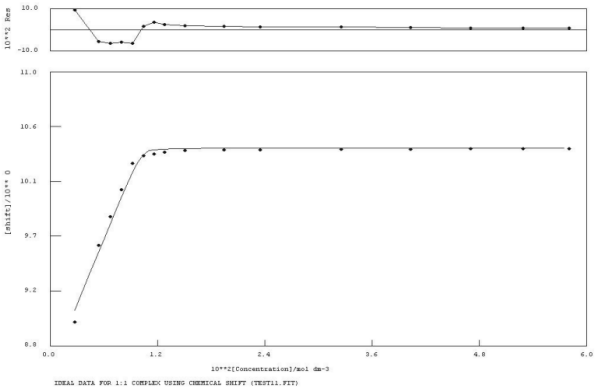

K_a = <10^4 M^{-1} Error = NA

NMR titration for 209 *vs*. $TBAH_2PO_4$ in DMSO-d_6/H_2O 0.5%

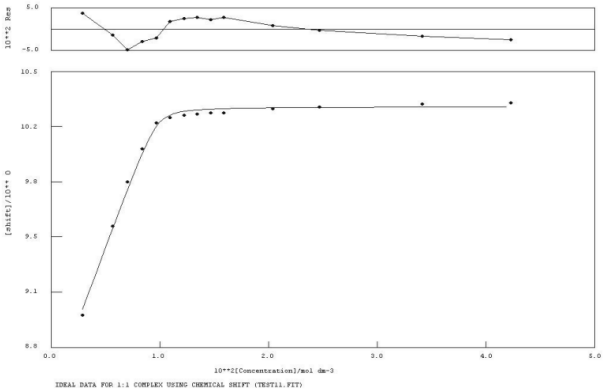

K_a = <10^4 M^{-1} Error = NA

NMR titration for 209 *vs*. $TBAHSO_4$ in DMSO-d_6/H_2O 0.5%

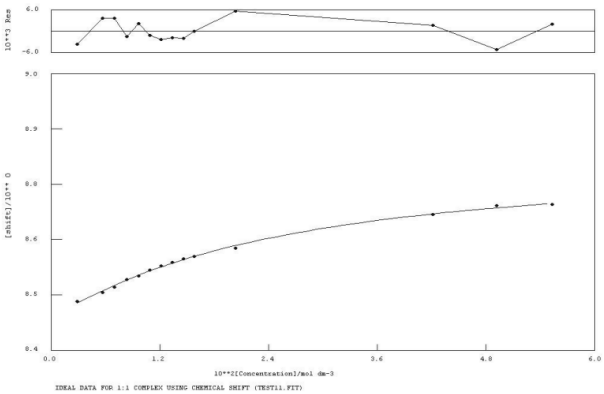

K_a = 50 M^{-1} Error = 10%

NMR titration for 209 *vs.* TBAOBz in DMSO-d_6/H_2O 0.5%

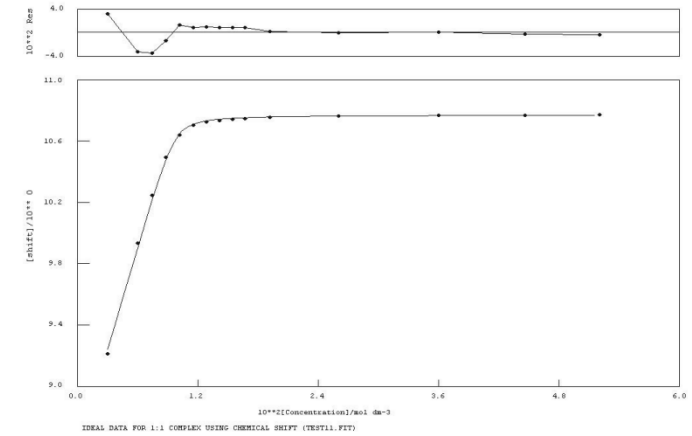

$K_a = <10^4\ M^{-1}$ Error = NA

NMR titration for 209 *vs.* TBACl in DMSO-d_6/H_2O 0.5%

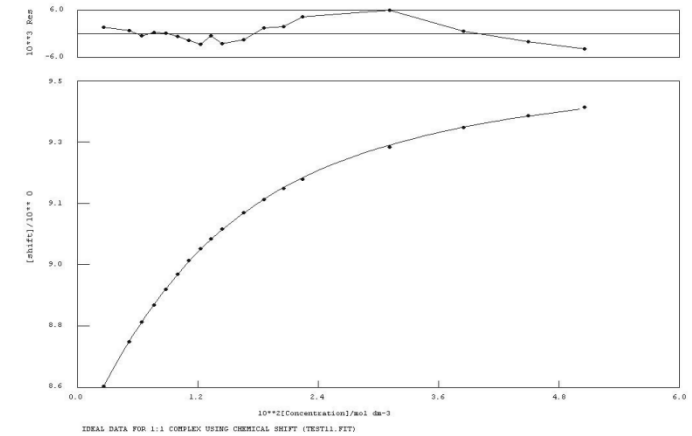

$K_a = 128\ M^{-1}$ Error = 1%

NMR titration for 209 *vs.* $TEAHCO_3$ in DMSO-d_6/H_2O 0.5%

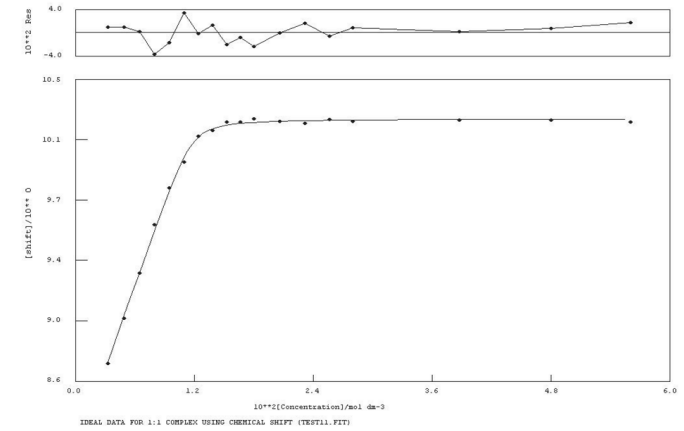

$K_a = >10^4\ M^{-1}$ Error = NA

NMR titration for 209 *vs*. TBAOAc in DMSO-d_6/H_2O 10%

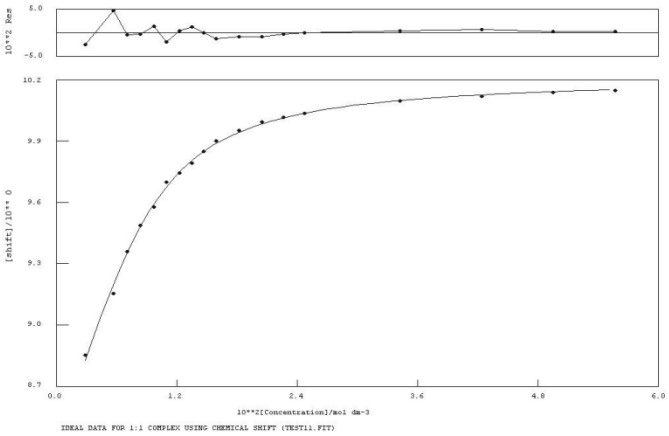

K_a = 567 M^{-1} Error = 6%

NMR titration for 209 *vs*. TBAOBz in DMSO-d_6/H_2O 10%

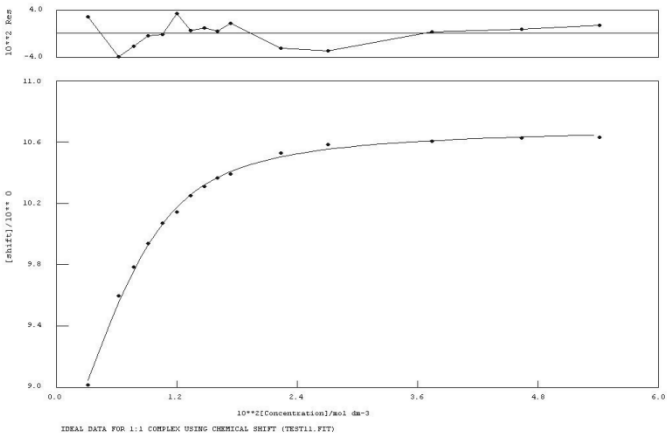

K_a = 763 M^{-1} Error = 7%

Figure S38 NMR titration for 209 *vs*. TBAH_2PO_4 in DMSO-d_6/H_2O 10%.

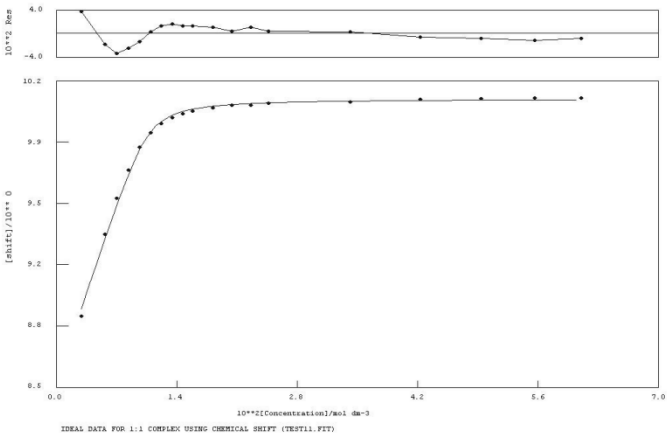

K_a = 4785 M^{-1} Error = 4%

NMR titration for 209 *vs.* TBACl in DMSO-d_6/H_2O 10%

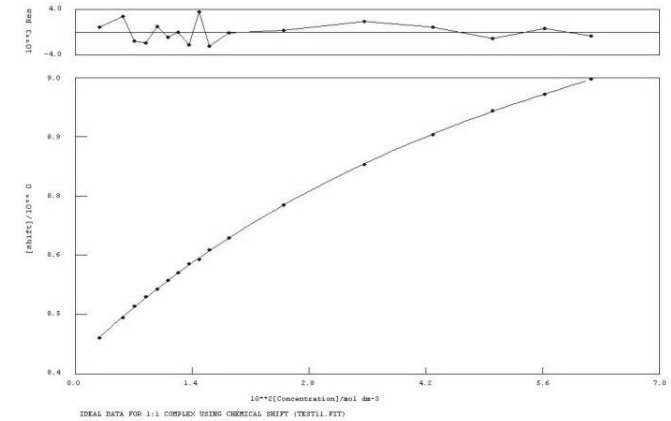

K_a = 16 M^{-1} Error = 3%

NMR titration for 209 *vs.* $TEAHCO_3$ in DMSO-d_6/H_2O 10%

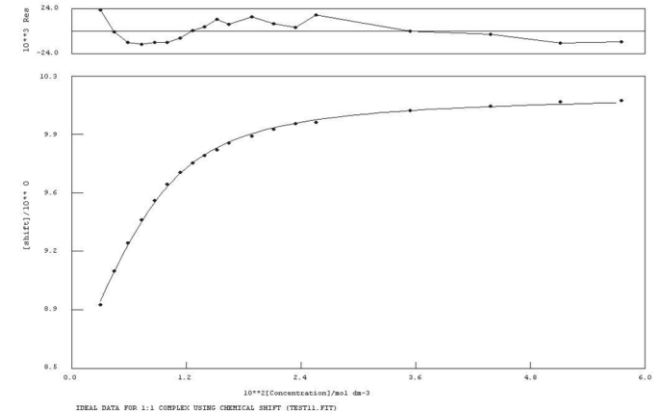

K_a = 545 M^{-1} Error = 4%

NMR titration for 210 *vs.* TBAOAc in DMSO-d_6/H_2O 0.5%

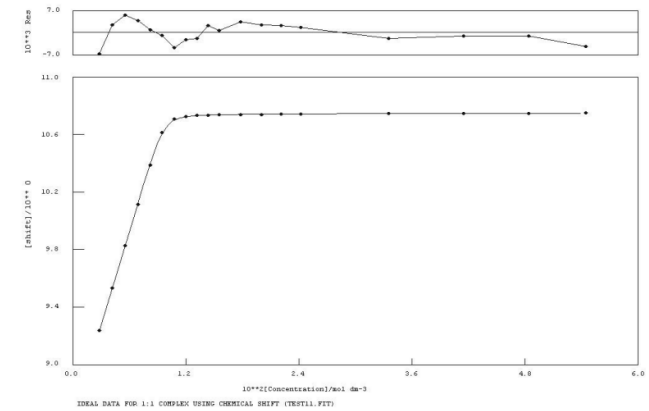

K_a = <10^4 M^{-1} Error = NA

NMR titration for 210 *vs*. TBAH_2PO_4 in DMSO-d_6/H_2O 0.5%

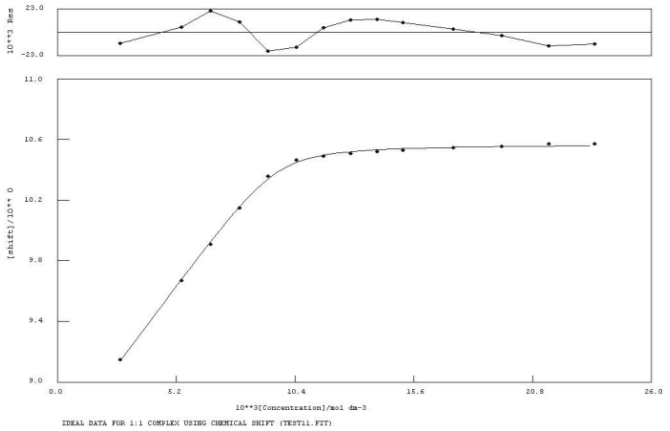

K_a = <10^4 M^{-1} Error = NA

NMR titration for 210 *vs*. TBAHSO_4 in DMSO-d_6/H_2O 0.5%

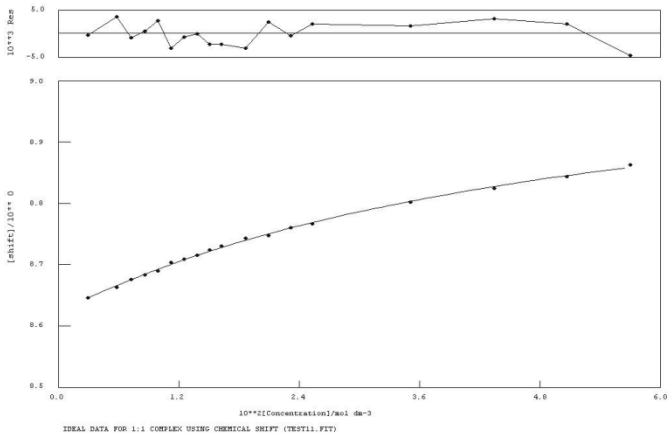

K_a = 23 M^{-1} Error = 9%

NMR titration for 210 *vs*. TBAOBz in DMSO-d_6/H_2O 0.5%

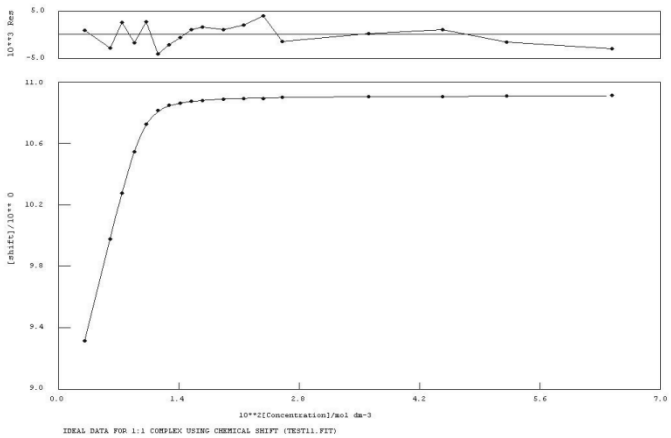

K_a = <10^4 M^{-1} Error = NA

NMR titration for 210 *vs.* TBACl in DMSO-d_6/H_2O 0.5%

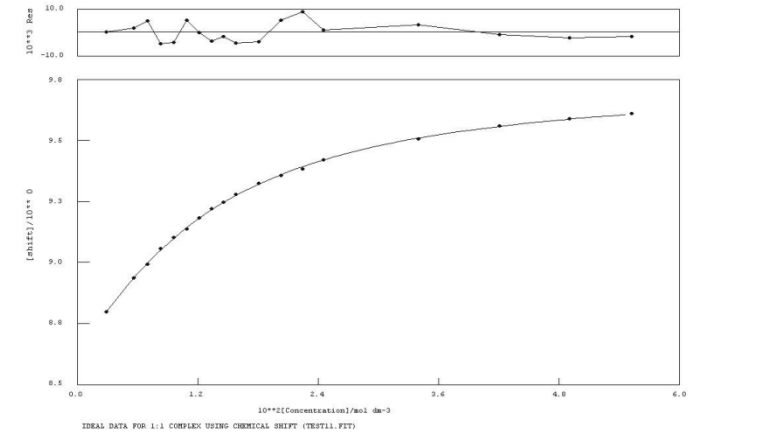

K_a = 128 M^{-1} Error = 3%

NMR titration for 210 *vs.* $TEAHCO_3$ in DMSO-d_6/H_2O 0.5%

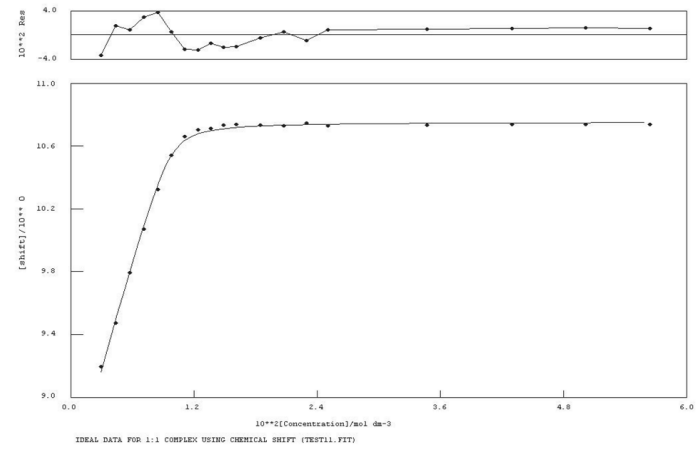

K_a = 9578 M^{-1} Error = 11%

NMR titration for 210 *vs.* TBAOAc in DMSO-d_6/H_2O 10%

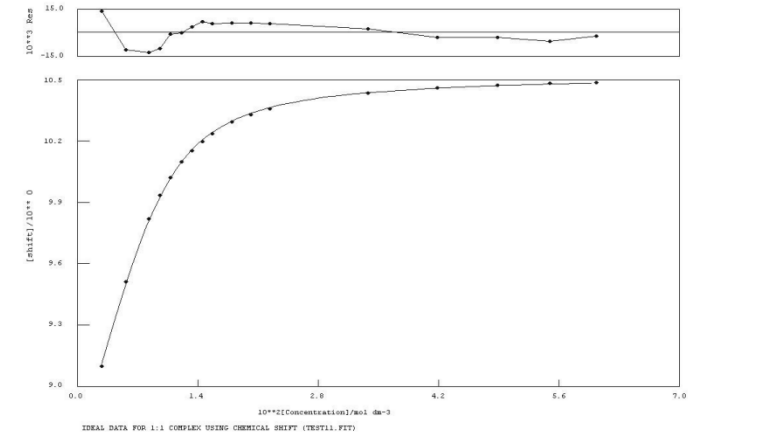

K_a = 774 M^{-1} Error = 3%

NMR titration for 210 *vs*. TBAH_2PO_4 in DMSO-d_6/H_2O 10%

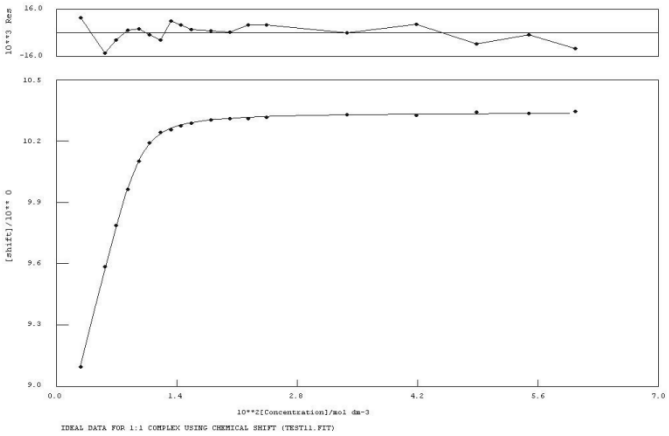

K_a = 5172 M^{-1} Error = 5%

NMR titration for 210 *vs*. TBAOBz in DMSO-d_6/H_2O 10%

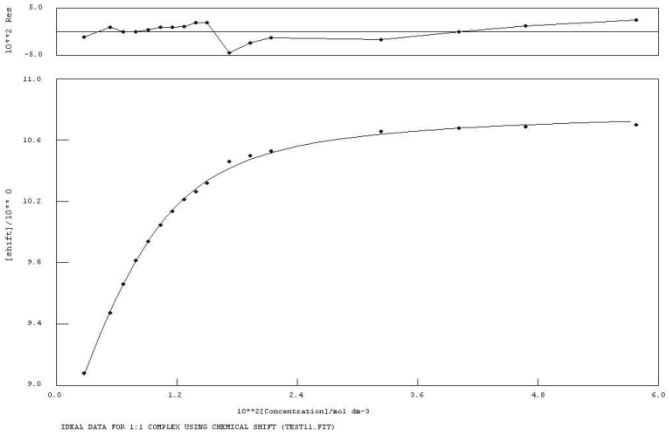

K_a = 521 M^{-1} Error = 6%

NMR titration for 210 *vs*. TBACl in DMSO-d_6/H_2O 10%

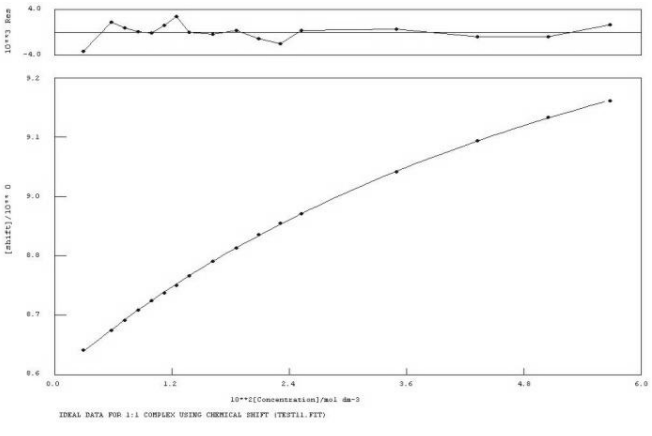

K_a = 17 M^{-1} Error = 3%

NMR titration for 210 *vs.* $TEAHCO_3$ in DMSO-d_6/H_2O 10%

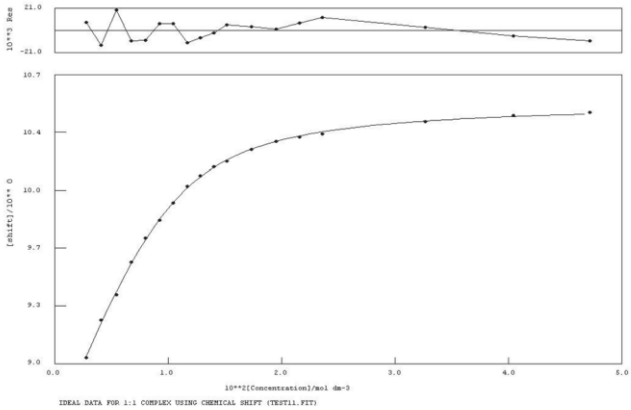

K_a = 699 M^{-1} Error = 4%

NMR titration for 210 *vs.* TBAOAc in DMSO-d_6/H_2O 25%

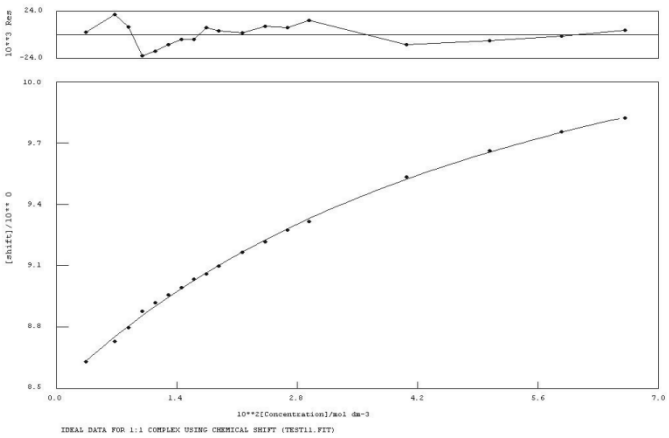

K_a = 20 M^{-1} Error = 7%

NMR titration for 210 *vs.* $TBAH_2PO_4$ in DMSO-d_6/H_2O 25%

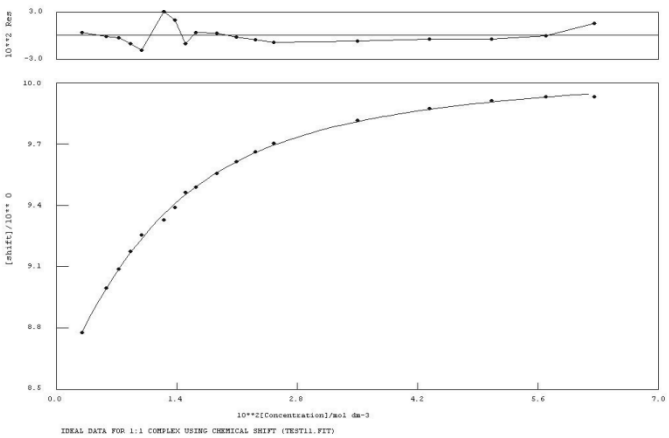

K_a = 160 M^{-1} Error = 5%

NMR titration for 210 *vs*. TBAH_2PO_4 in DMSO-d_6/H_2O 25%

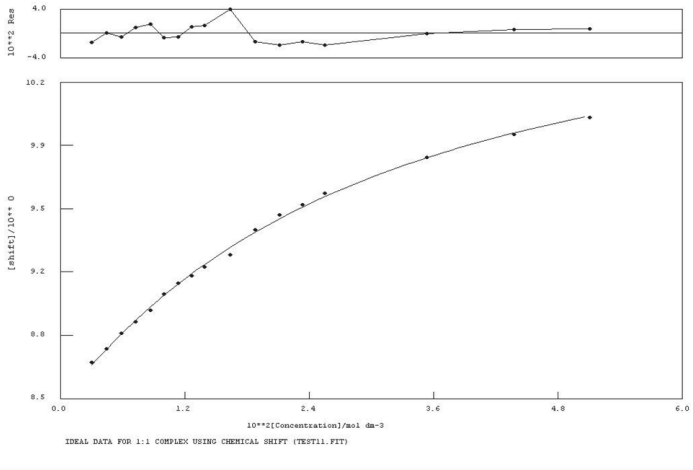

K_a = 42 M^{-1} Error = 8%

NMR titration for 211 *vs*. TBAH_2PO_4 in DMSO-d_6/H_2O 0.5%

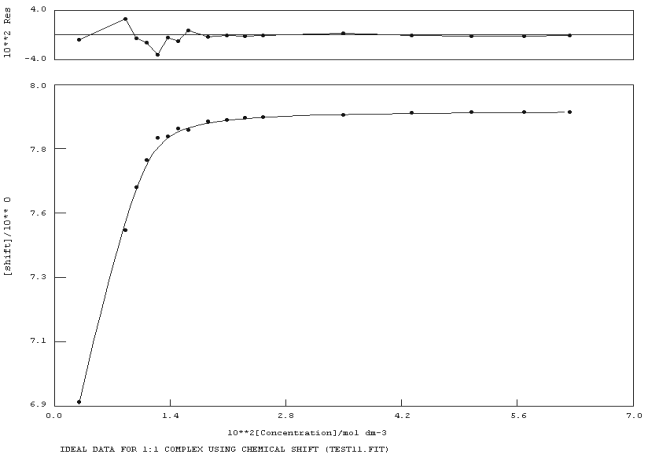

K_a = 3830 M^{-1} Error = 5%

NMR titration for 211 *vs*. TBAOBz in DMSO-d_6/H_2O 0.5%

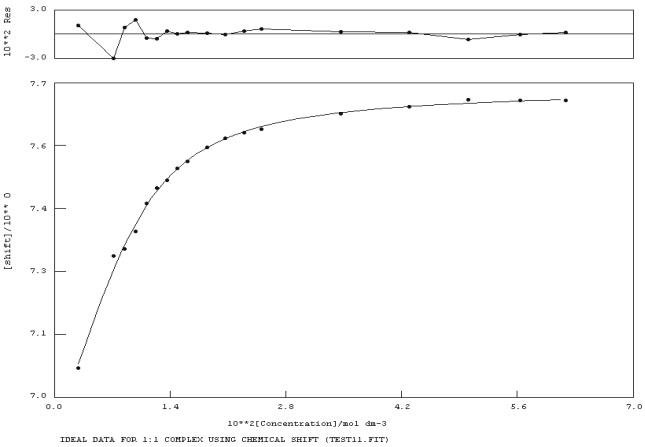

K_a = 514 M^{-1} Error = 8%

NMR titration for 211 *vs.* TBACl in DMSO-d_6/H_2O 0.5%

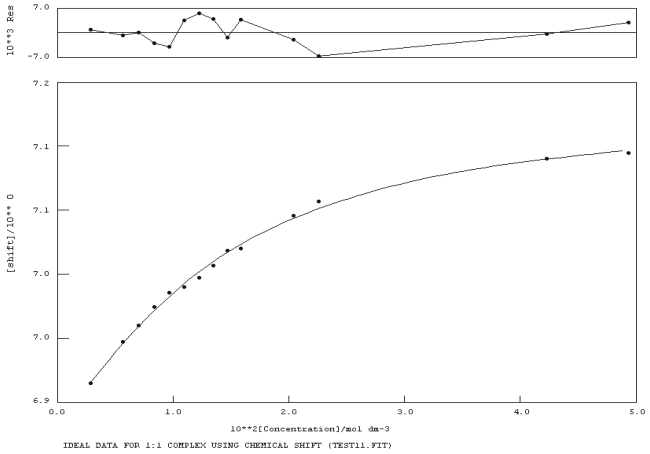

K_a = 128 M^{-1} Error = 10%

NMR titration for 211 *vs.* $TEAHCO_3$ in DMSO-d_6/H_2O 0.5%

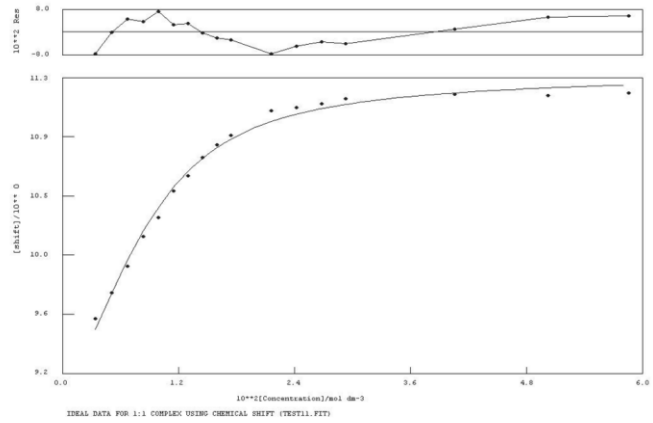

K_a = 477 M^{-1} Error = 14%

NMR titration for 211 *vs.* TBAOAc in DMSO-d_6/H_2O 0.5%

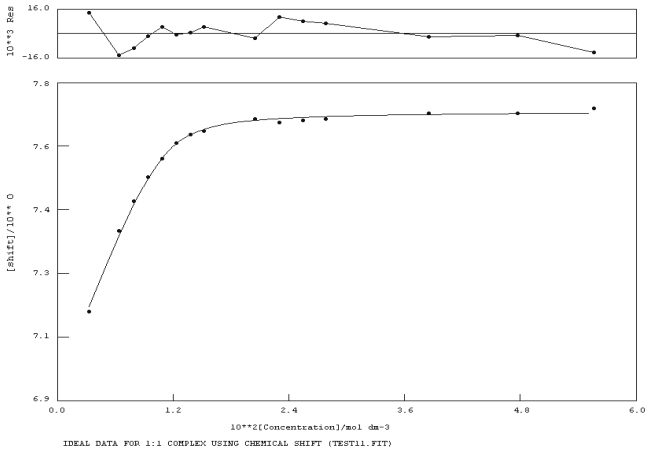

K_a = 2830 M^{-1} Error = 5%

NMR titration for 212 *vs*. $TBAH_2PO_4$ in DMSO-d_6/H_2O 0.5%

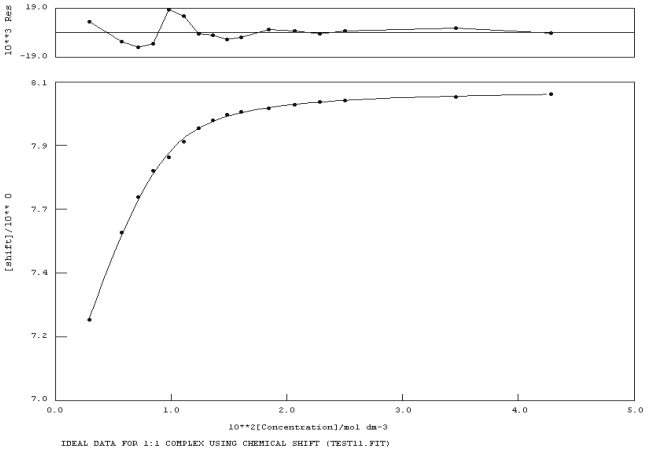

K_a = 1630 M^{-1} Error = 7%

NMR titration for 212 *vs*. TBABzO in DMSO-d_6/H_2O 0.5%

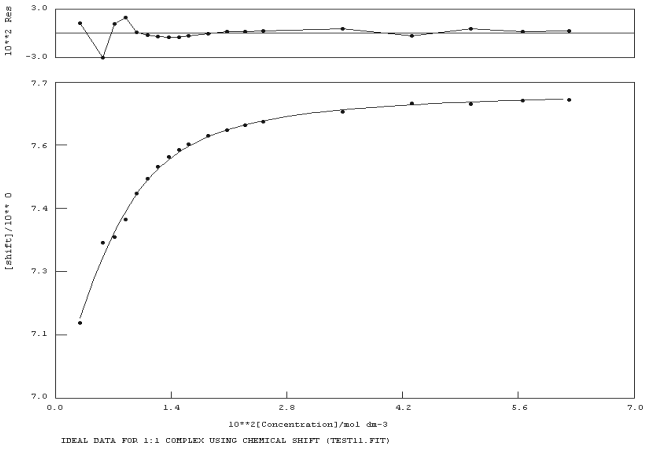

K_a = 477 M^{-1} Error = 8%

NMR titration for 212 *vs*. TBAF in DMSO-d_6/H_2O 0.5%

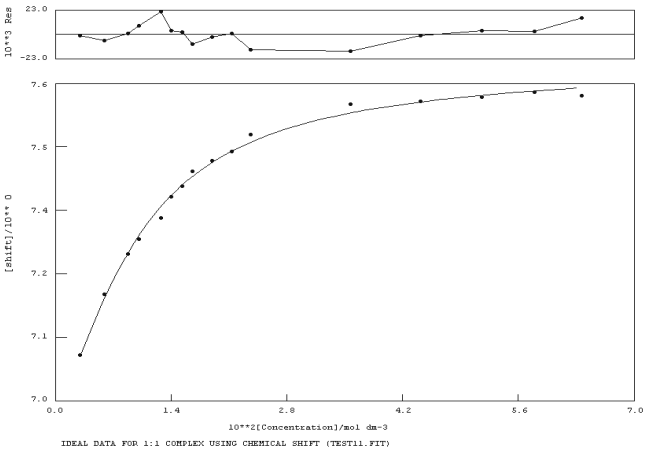

K_a = 205 M^{-1} Error = 9%

NMR titration for 212 *vs.* TBACl in DMSO-d_6/H_2O 0.5%

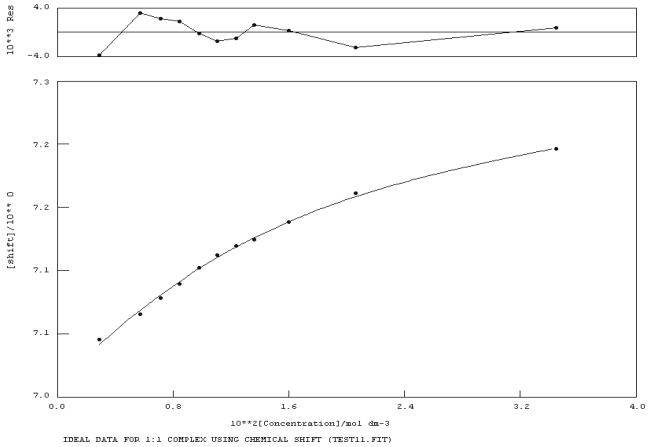

K_a = 74 M^{-1} Error = 8%

NMR titration for 212 *vs.* TBAAcO in DMSO-d_6/H_2O 0.5%

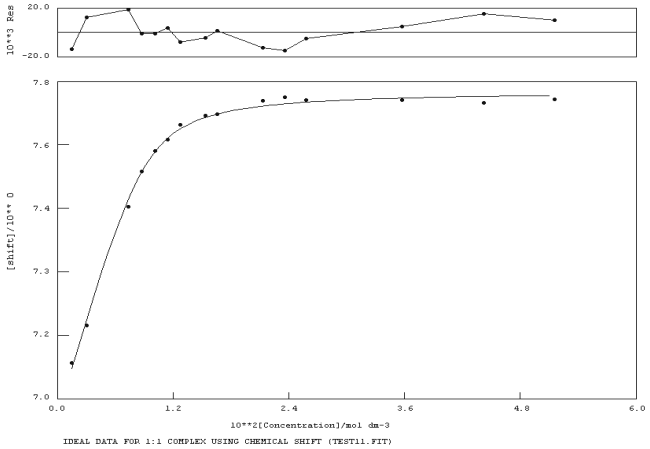

K_a = 1620 M^{-1} Error = 12%

NMR titration for 213 *vs.* TBAAcO in DMSO-d_6/H_2O 0.5%

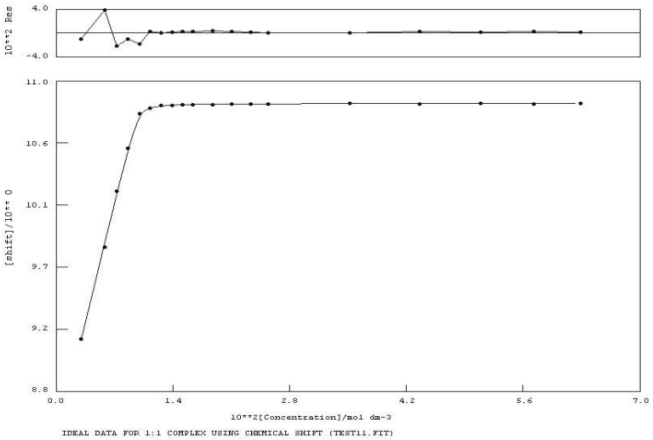

K_a = <10^4 M^{-1} Error = NA

NMR titration for 213 *vs*. TBABzO in DMSO-d_6/H_2O 0.5%

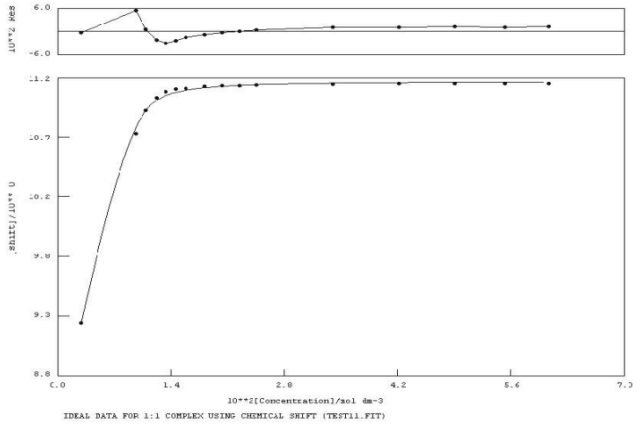

K_a = 5670 M^{-1} Error = 10%

NMR titration for 213 *vs*. TBACl in DMSO-d_6/H_2O 0.5%

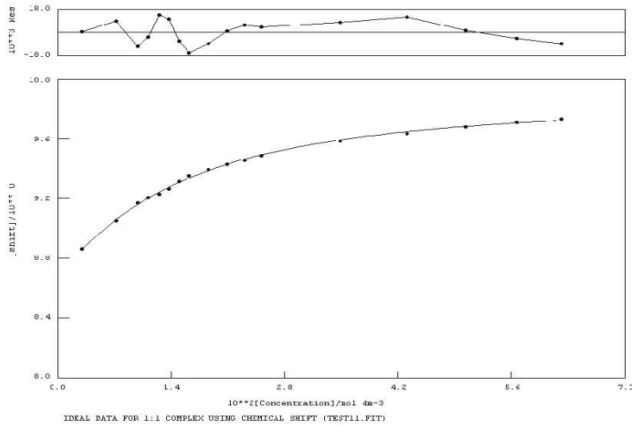

K_a = 102 M^{-1} Error = 5%

NMR titration for 213 *vs*. $TEAHCO_3$ in DMSO-d_6/H_2O 0.5%

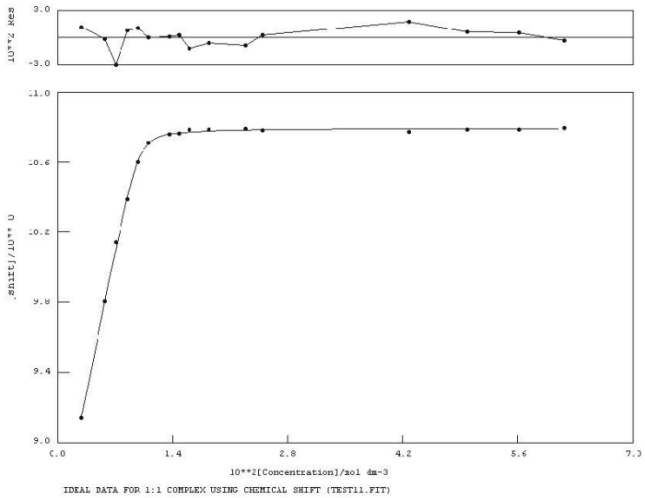

K_a = > 10^4 M^{-1} Error = NA

NMR titration for 214 *vs.* TBAOAc in DMSO-d_6/H_2O 0.5%

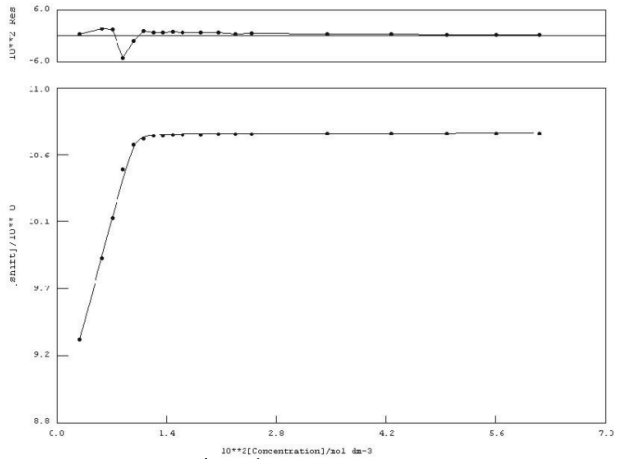

K_a = > 10^4 M^{-1} Error = NA

NMR titration for 214 *vs.* TBAOBz in DMSO-d_6/H_2O 0.5%

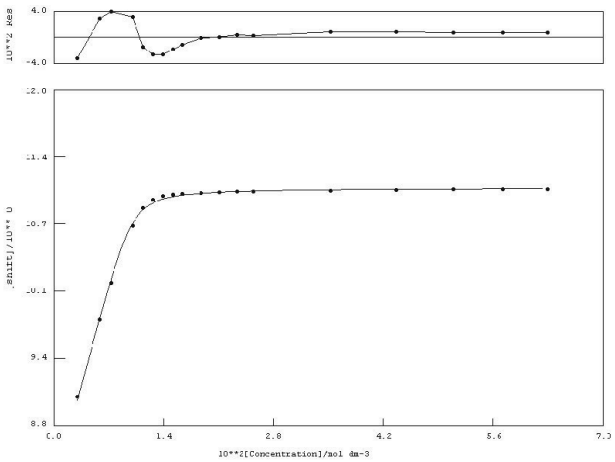

K_a = 5880 M^{-1} Error = 10%

NMR titration for 214 *vs.* TBACl in DMSO-d_6/H_2O 0.5%

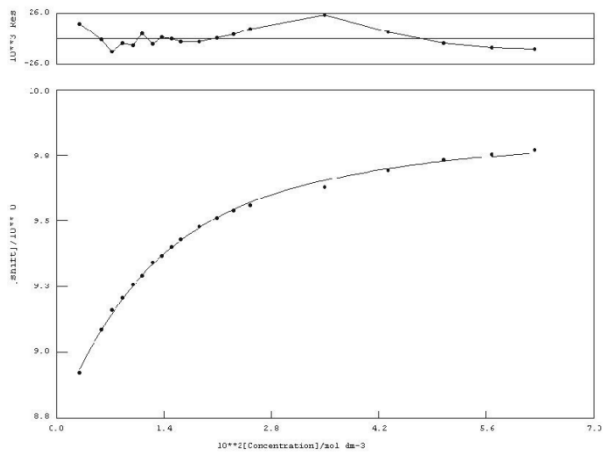

K_a = 139 M^{-1} Error = 6%

NMR titration for 214 *vs*. TBAF in DMSO-d_6/H_2O 0.5%

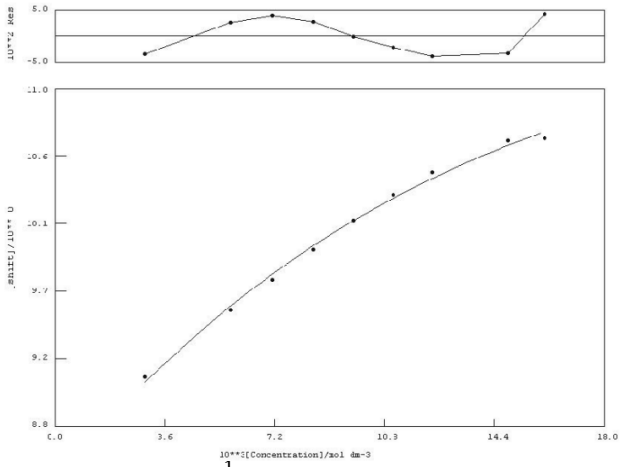

K_a = 154 M^{-1} Error = 46%

NMR titration for 214 *vs*. $TEAHCO_3$ in DMSO-d_6/H_2O 0.5%

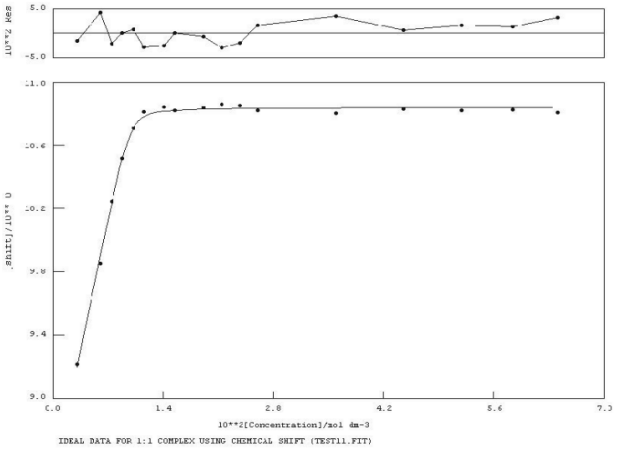

K_a = > 10^4 M^{-1} Error = NA

NMR titration for 215 *vs*. TBAOAc in DMSO-d_6/H_2O 0.5%

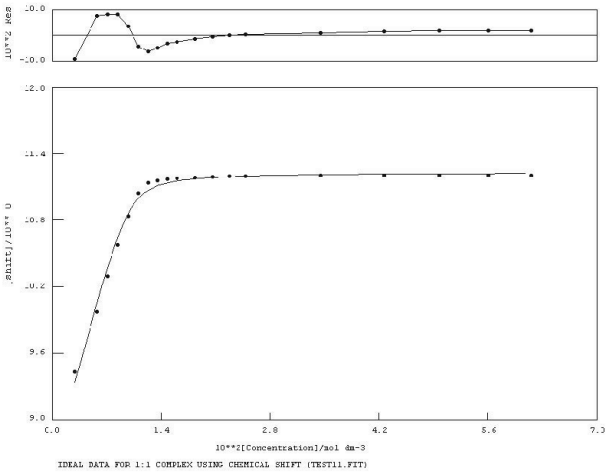

K_a = > 10^4 M^{-1} Error = NA

NMR titration for 215 *vs.* TBAOBz in DMSO-d_6/H_2O 0.5%

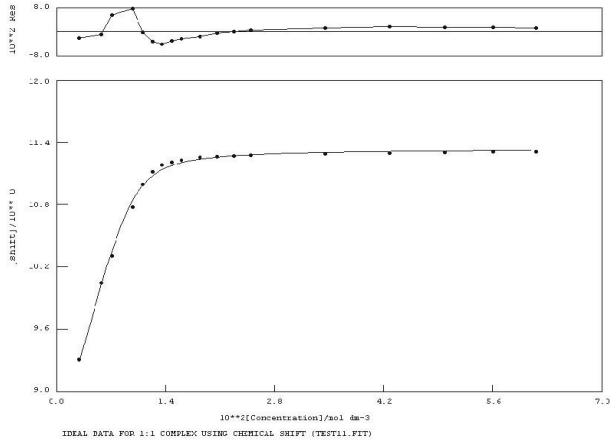

K_a = 3420 M^{-1} Error = 10%

NMR titration for 215 *vs.* TBACl in DMSO-d_6/H_2O 0.5%

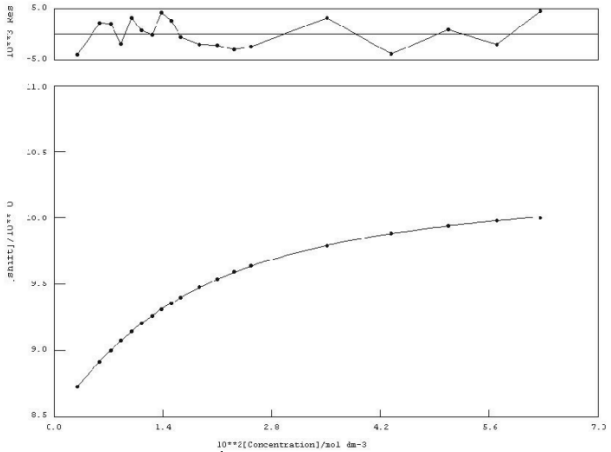

K_a = 85 M^{-1} Error = 1%

NMR titration for 215 *vs.* TBAH_2PO_4 in DMSO-d_6/H_2O 0.5%

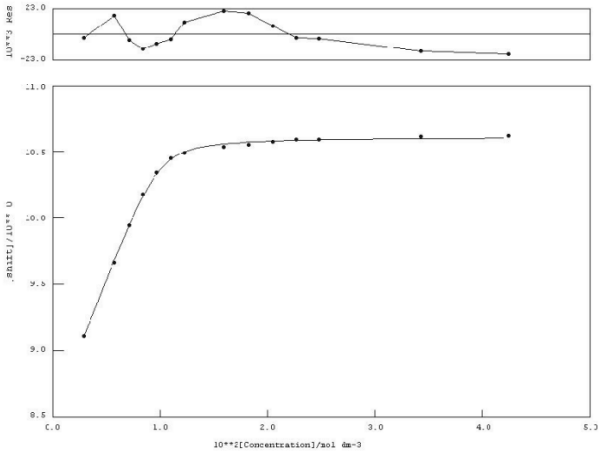

K_a = 6140 M^{-1} Error = 10%

NMR titration for 215 *vs*. TBAF in DMSO-d_6/H_2O 0.5%

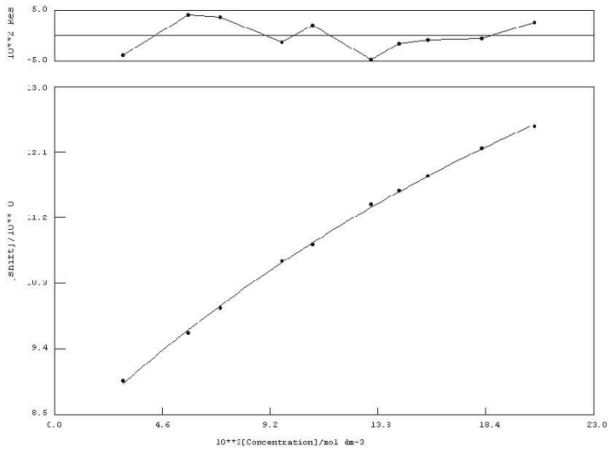

K_a = 36 M^{-1} Error = 19%

NMR titration for 215 *vs*. TBAOAc in DMSO-d_6/H_2O 0.5%

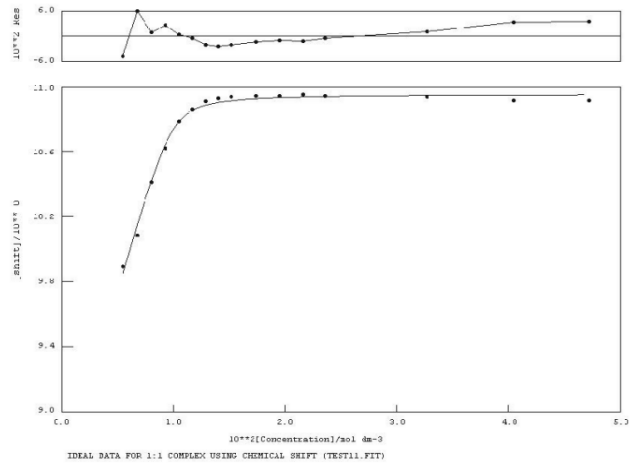

K_a = > 10^4 M^{-1} Error = NA

NMR titration for 216 *vs*. TBAAcO in DMSO-d_6/H_2O 0.5%

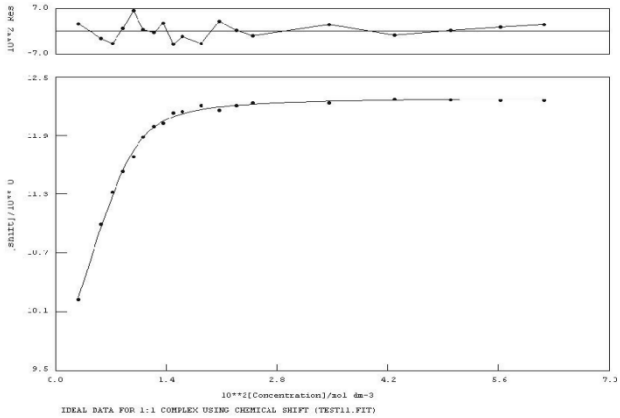

K_a = 2230 M^{-1} Error = 9%

NMR titration for 216 *vs.* TBABzO in DMSO-d_6/H_2O 0.5%

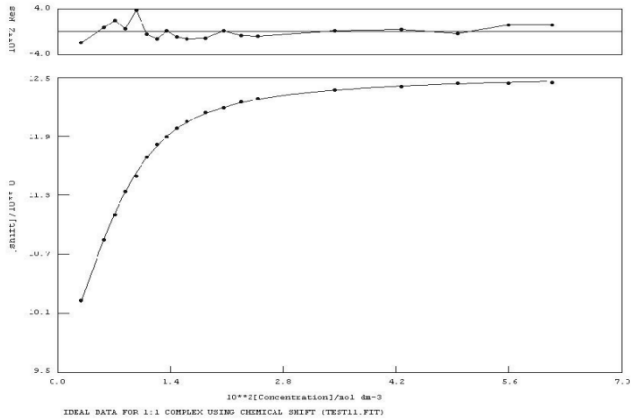

K_a = 658 M^{-1} Error = 3%

NMR titration for 216 *vs.* TBACl in DMSO-d_6/H_2O

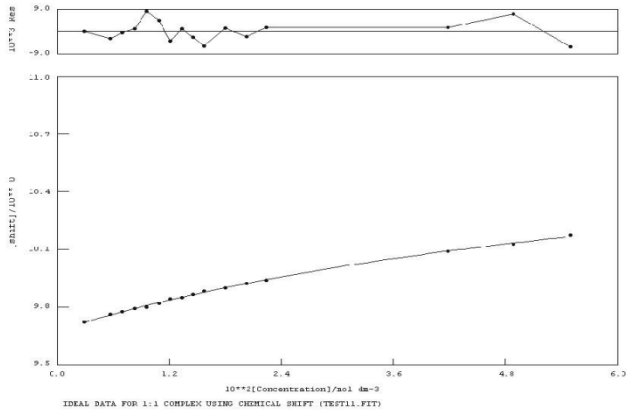

K_a = 15 M^{-1} Error = 10%

NMR titration for 216 *vs.* TBAH_2PO_4 in DMSO-d_6/H_2O 0.5%

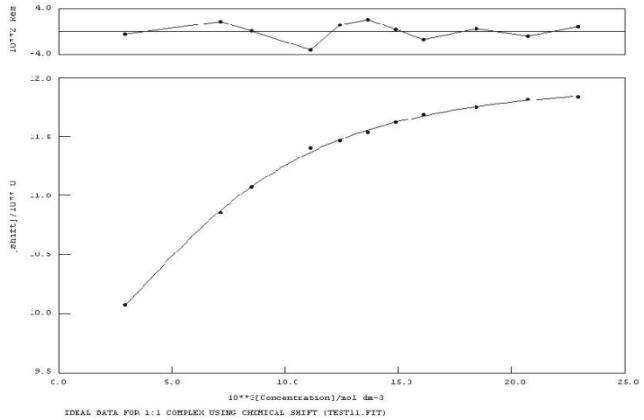

K_a = 687 M^{-1} Error = 8%

NMR titration for 217 *vs*. TBAH_2PO_4 in DMSO-d_6/H_2O 0.5%

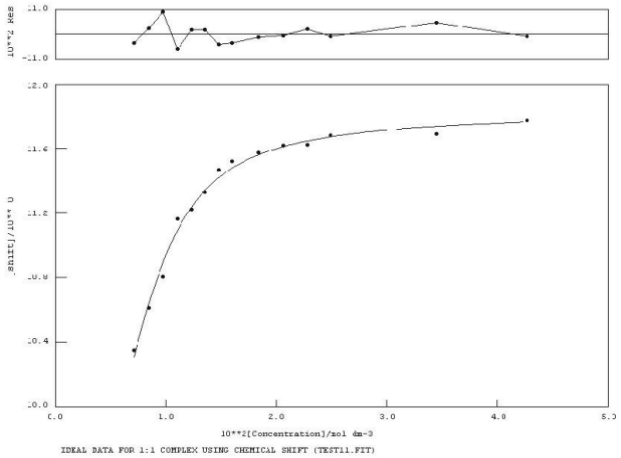

K_a = 1342 M^{-1} Error = 12%

NMR titration for 217 *vs*. TBAOAc in DMSO-d_6/H_2O 0.5%

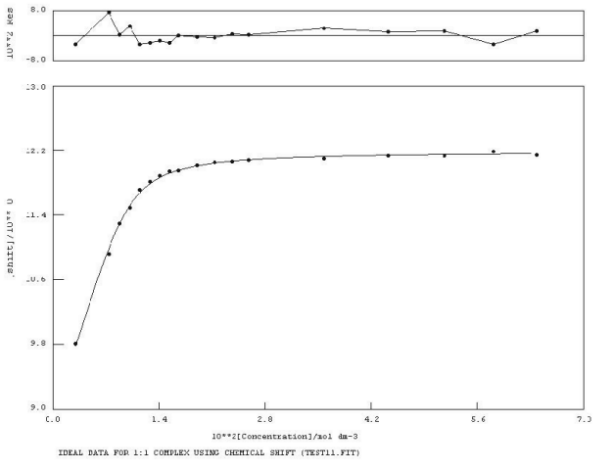

K_a = 1800 M^{-1} Error = 7%

NMR titration for 217 *vs*. TBAOBz in DMSO-d_6/H_2O 0.5%

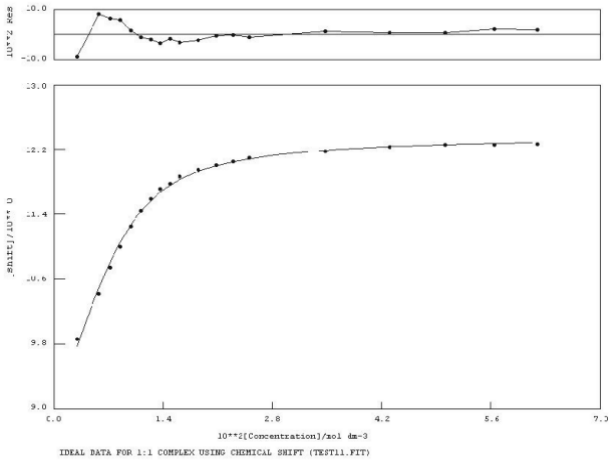

K_a = 675 M^{-1} Error = 7%

NMR titration for 217 *vs.* TBACl in DMSO-d_6/H_2O 0.5%

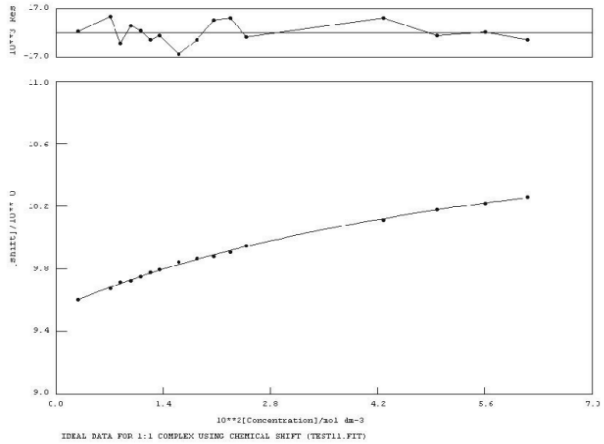

K_a = 17 M^{-1} Error = 10%

NMR titration for 218 *vs.* TBAOAc in DMSO-d_6/H_2O 0.5%

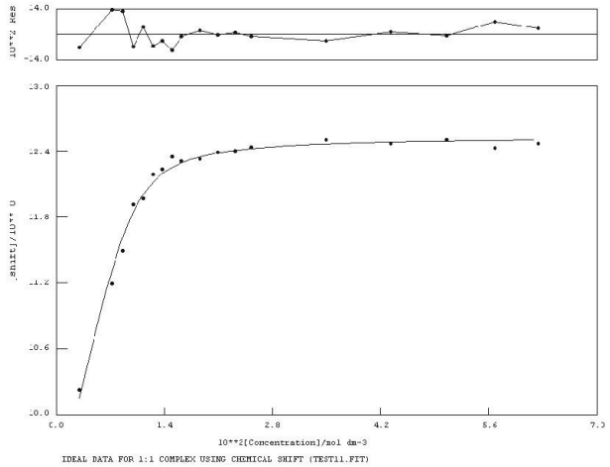

K_a = 1780 M^{-1} Error = 16%

NMR titration for 218 *vs.* TBAOBz in DMSO-d_6/H_2O 0.5%

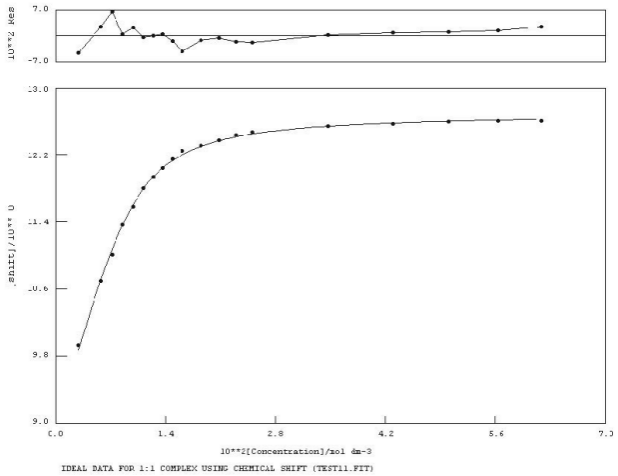

K_a = 870 M^{-1} Error = 5%

NMR titration for 218 *vs*. TBACl in DMSO-d_6/H_2O 0.5%

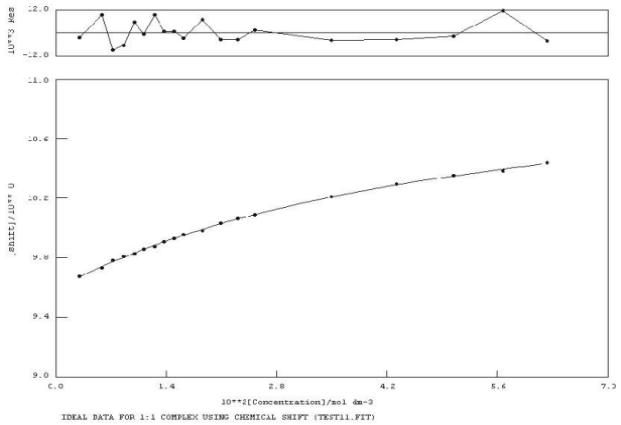

K_a = 23 M^{-1} Error = 6%

Proton NMR titrations from Chapter Three

NMR titration for 219 *vs*. TBAOAc in DMSO-d_6/H_2O 0.5% (aromatic CH)

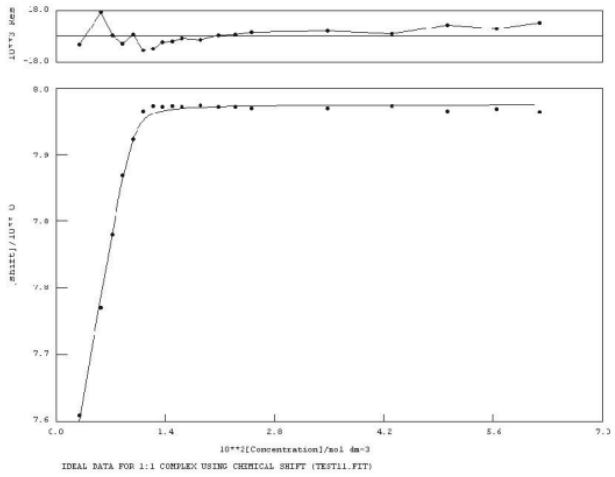

K_a = > 10^4 M^{-1} Error = NA

NMR titration for 219 *vs.* TBAOAc in DMSO-d_6/H_2O 0.5% (urea NH)

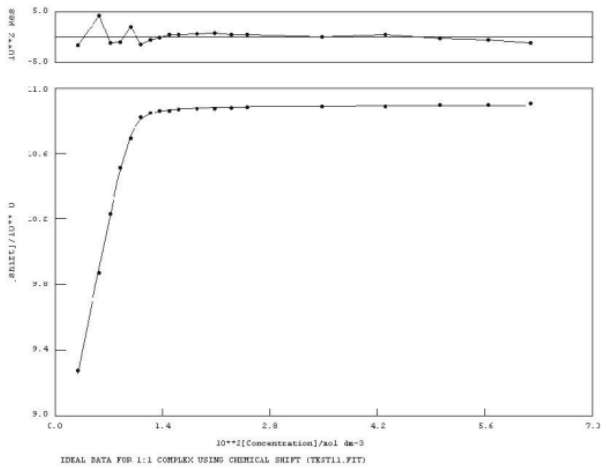

K_a = > 10^4 M^{-1} Error = NA

NMR titration for 219 *vs.* TBAOBz in DMSO-d_6/H_2O 0.5% (aromatic CH)

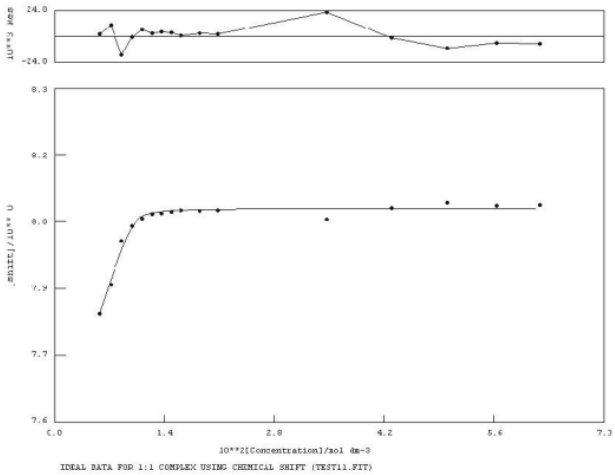

K_a = > 10^4 M^{-1} Error = NA

NMR titration for 219 *vs.* TBAOBz in DMSO-d_6/H_2O 0.5% (urea NH)

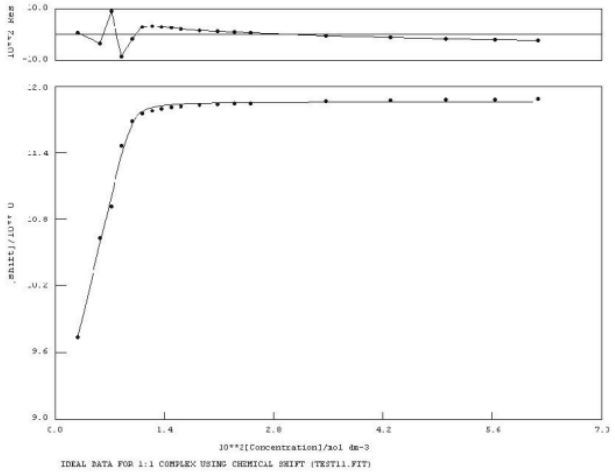

K_a = > 10^4 M^{-1} Error = NA

NMR titration for 219 *vs*. TBACl in DMSO-d_6/H_2O 0.5% (aromatic CH)

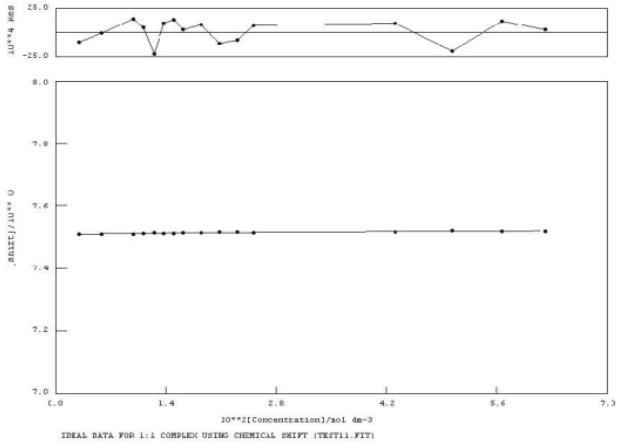

K_a = 166 M^{-1} Error = 1%

NMR titration for 219 *vs*. TBACl in DMSO-d_6/H_2O 0.5% (urea NH)

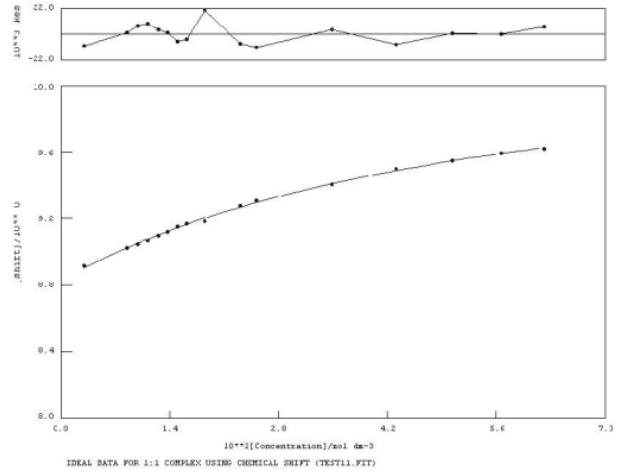

K_a = 22 M^{-1} Error = 9%

NMR titration for 219 *vs*. $TEAHCO_3$ in DMSO-d_6/H_2O 0.5% (aromatic CH)

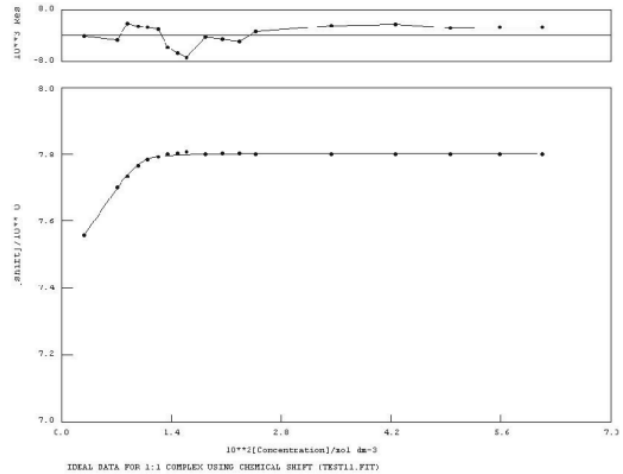

K_a = > 10^4 M^{-1} Error = NA

NMR titration for 219 *vs.* $TEAHCO_3$ in DMSO-d_6/H_2O 0.5% (urea NH)

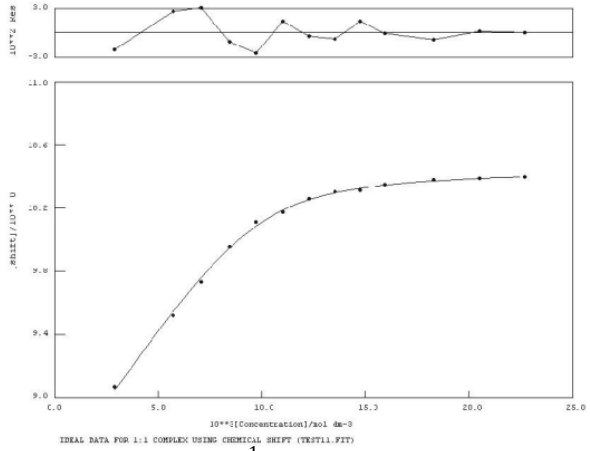

K_a = 2470 M^{-1} Error = 14%

NMR titration for 219 *vs.* $TBAH_2PO_4$ in DMSO-d_6/H_2O 10% (aromatic CH)

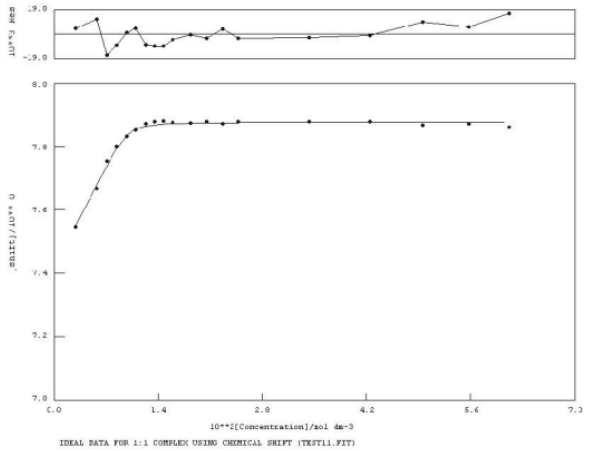

K_a = > 10^4 M^{-1} Error = NA

NMR titration for 219 *vs.* $TBAH_2PO_4$ in DMSO-d_6/H_2O 10% (urea NH)

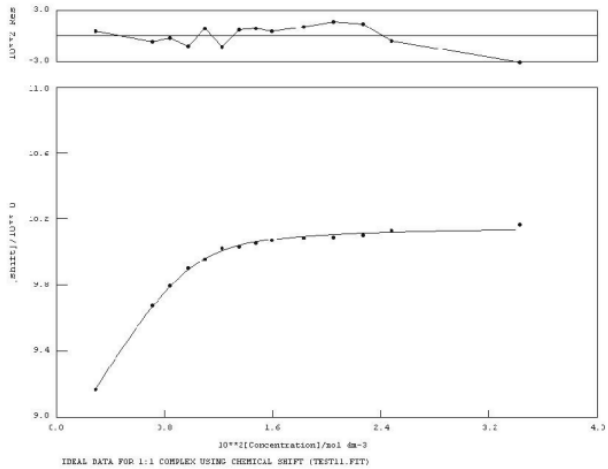

K_a = 2310 M^{-1} Error = 4%

NMR titration for 219 *vs*. TBAOAc in DMSO-d_6/H_2O 10% (aromatic CH)

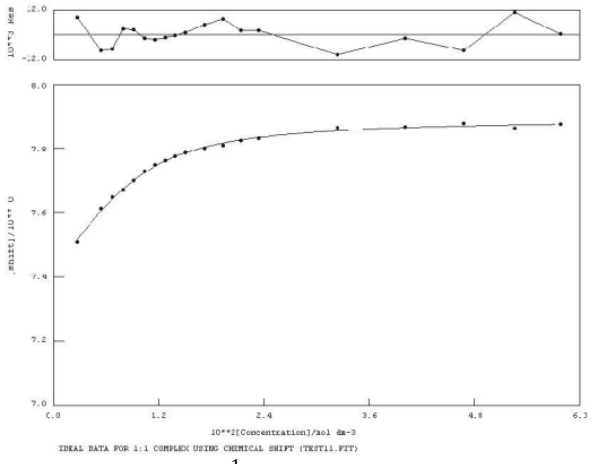

K_a = 462 M^{-1} Error = 7%

NMR titration for 219 *vs*. TBAOBz in DMSO-d_6/H_2O 10% (aromatic CH)

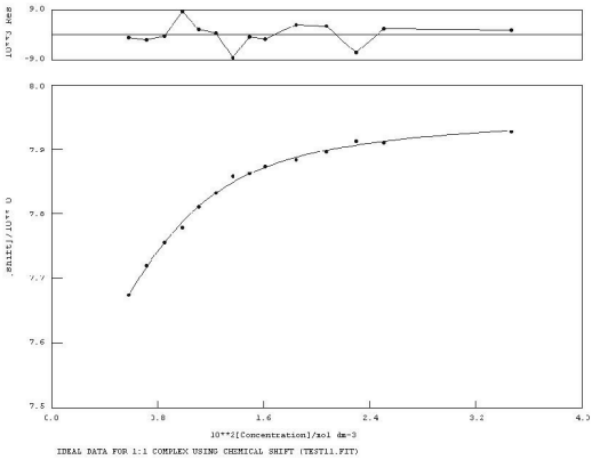

K_a = 1020 M^{-1} Error = 8%

NMR titration for 219 *vs*. TBAOBz in DMSO-d_6/H_2O 10% (urea NH)

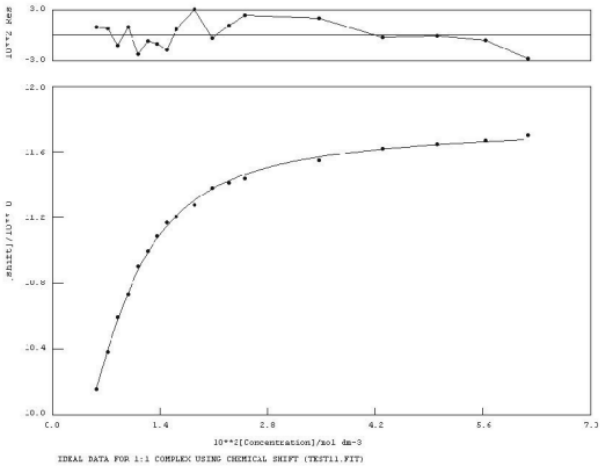

K_a = 1100 M^{-1} Error = 4%

NMR titration for 219 *vs.* $TEAHCO_3$ in DMSO-d_6/H_2O 10% (aromatic CH)

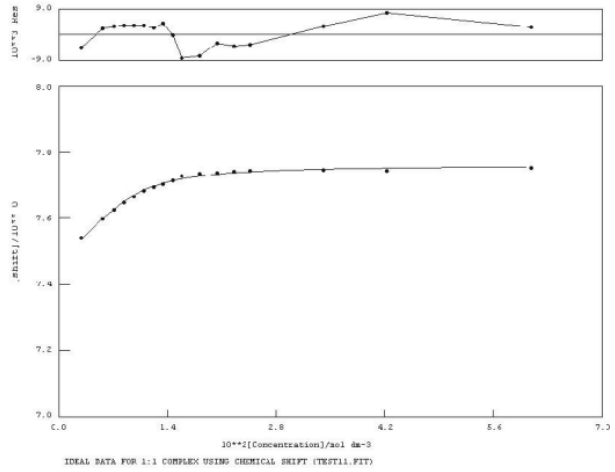

K_a = 809 M^{-1} Error = 3%

NMR titration for 219 *vs.* $TEAHCO_3$ in DMSO-d_6/H_2O 10% (urea NH)

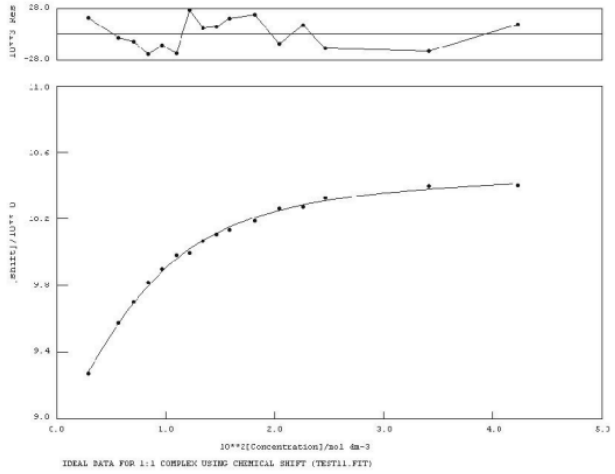

K_a = 395 M^{-1} Error = 9%

NMR titration for 220 *vs.* $TBAHSO_4$ in DMSO-d_6/H_2O 0.5% (urea NH)

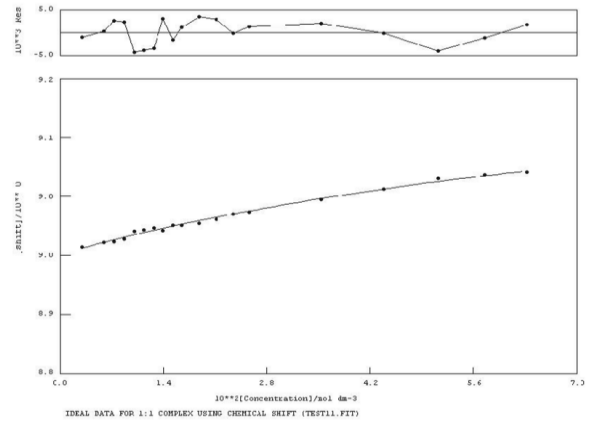

K_a = ≤10 M^{-1} Error = NA

NMR titration for 220 *vs*. $TBAHSO_4$ in DMSO-d_6/H_2O 0.5% (aromatic CH)

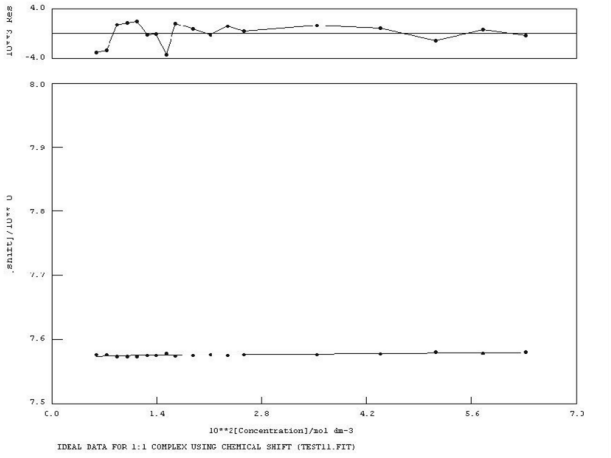

K_a = 18 M^{-1} Error = 14%

NMR titration for 220 *vs*. TBA_2SO4 in DMSO-d_6/H_2O 0.5% (urea NH)

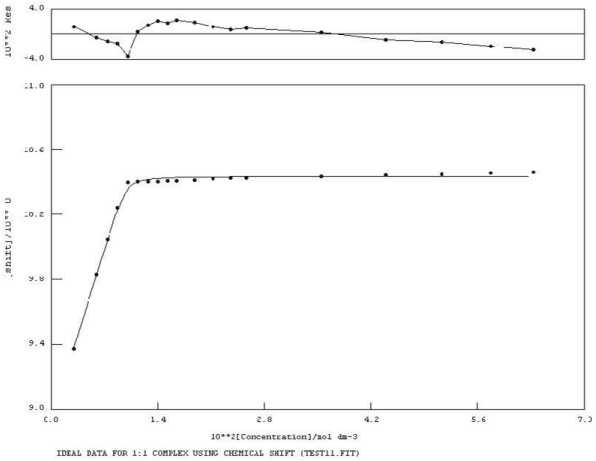

K_a = >10^4 M^{-1} Error = NA

NMR titration for 220 *vs*. TBA_2SO4 in DMSO-d_6/H_2O 0.5% (aromatic CH)

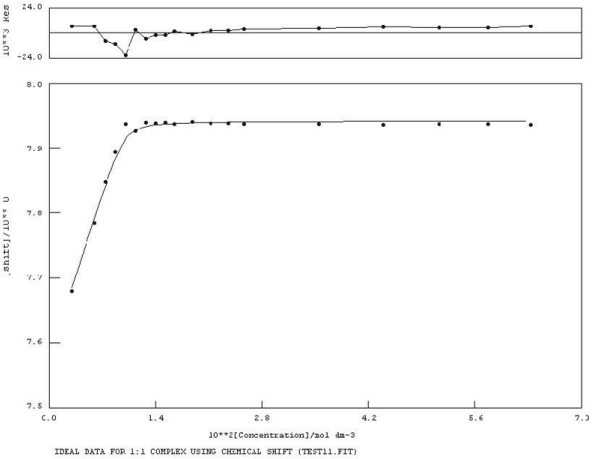

K_a = >10^4 M^{-1} Error = NA

NMR titration for 220 *vs.* TBAH_2PO_4 in DMSO-d_6/H_2O 0.5% (aromatic CH)

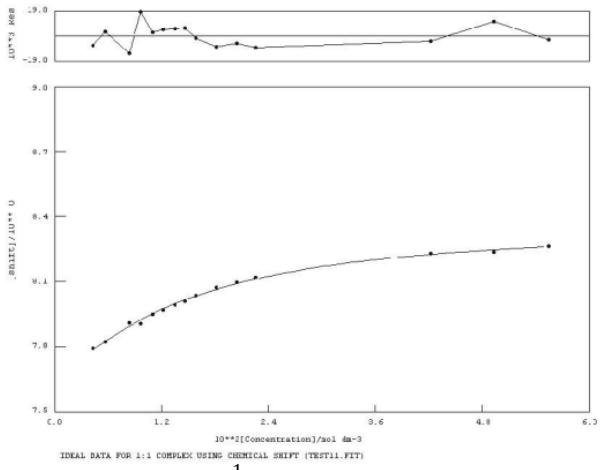

K_a = 107 M^{-1} Error = 8%

NMR titration for 220 *vs.* TBAOAc in DMSO-d_6/H_2O 0.5% (aromatic CH)

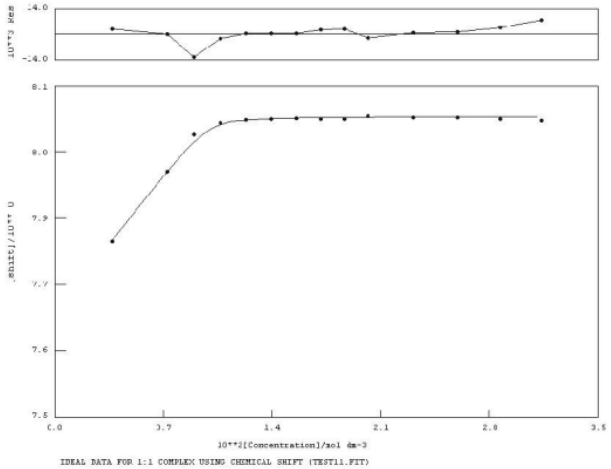

K_a = > 10^4 M^{-1} Error = NA

NMR titration for 220 *vs.* TBAOAc in DMSO-d_6/H_2O 0.5% (urea NH)

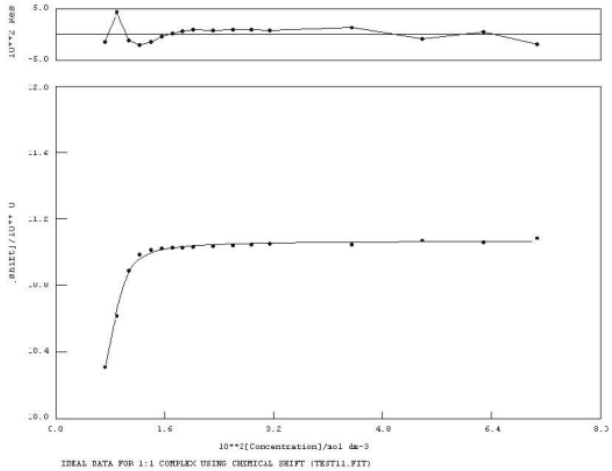

K_a = 8460 M^{-1} Error = 12%

NMR titration for 220 *vs*. TBAOBz in DMSO-d_6/H_2O 0.5% (aromatic CH)

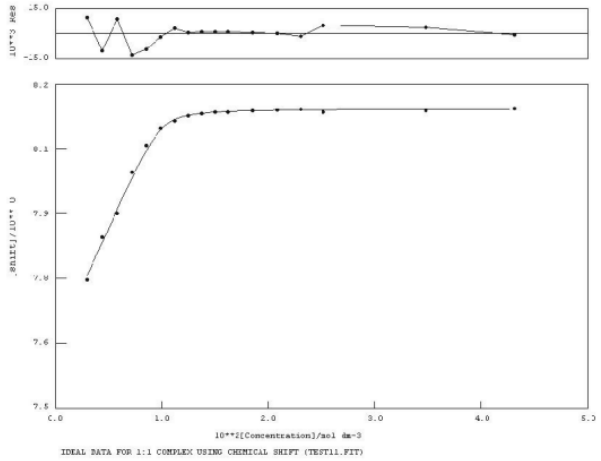

K_a = > 10^4 M^{-1} Error = NA

NMR titration for 220 *vs*. TBACl in DMSO-d_6/H_2O 0.5% (aromatic CH)

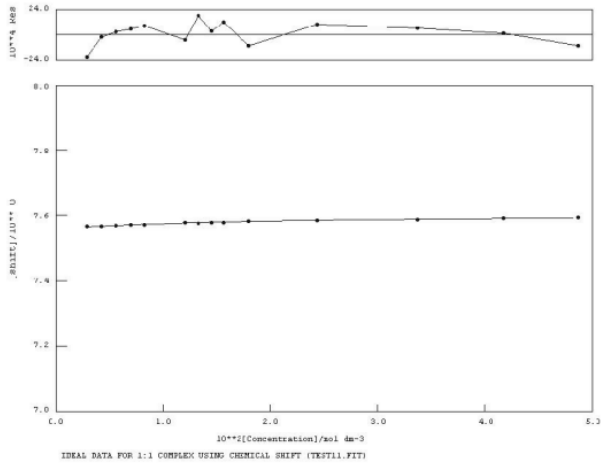

K_a = 79 M^{-1} Error = 5%

NMR titration for 220 *vs*. TBACl in DMSO-d_6/H_2O 0.5% (urea NH)

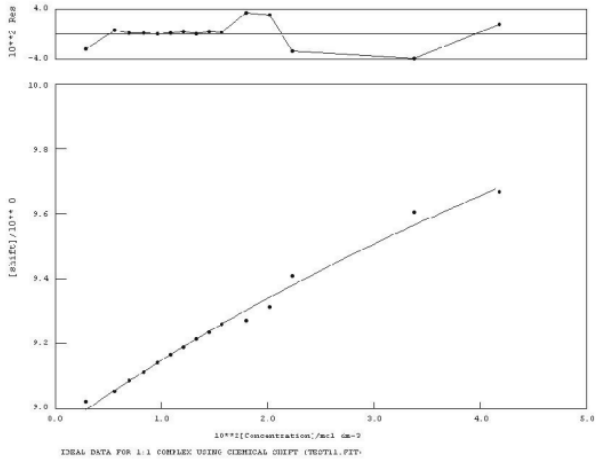

K_a = ≤ 10 M^{-1} Error = NA

NMR titration for 220 *vs.* $TEAHCO_3$ in DMSO-d_6/H_2O 0.5% (aromatic CH)

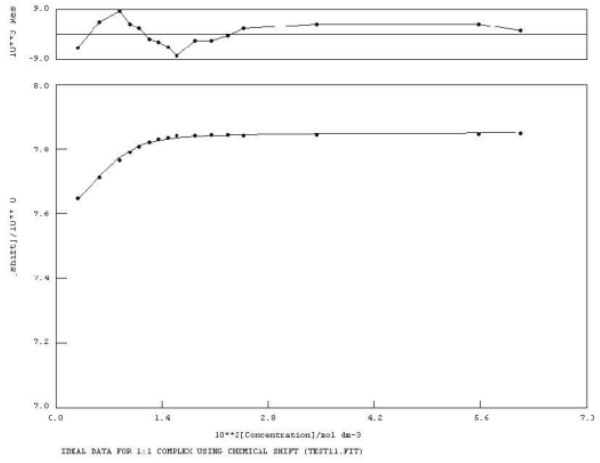

K_a = 2250 M^{-1} Error = 17%

NMR titration for 220 *vs.* TBAOAc in DMSO-d_6/H_2O 10% (urea NH)

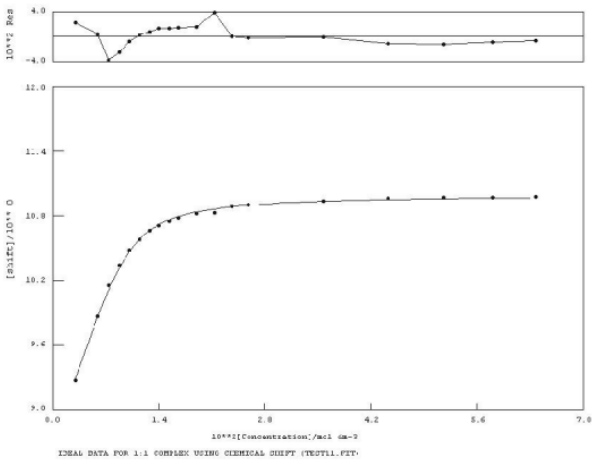

K_a = 1420 M^{-1} Error = 6%

NMR titration for 220 *vs.* TBAOBz in DMSO-d_6/H_2O 10% (aromatic CH)

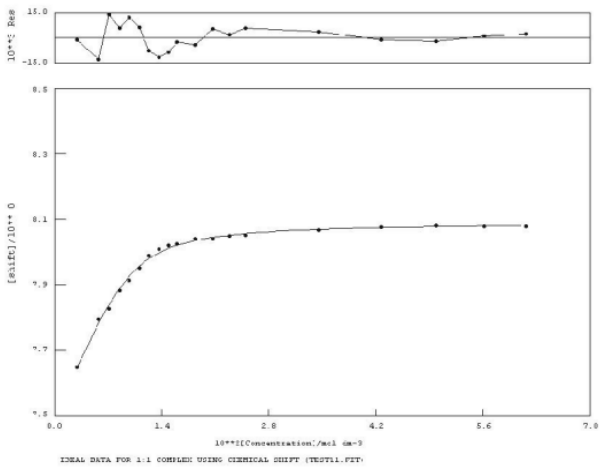

K_a = 639 M^{-1} Error = 3%

NMR titration for 220 *vs*. TBAOBz in DMSO-d_6/H_2O 10% (urea NH)

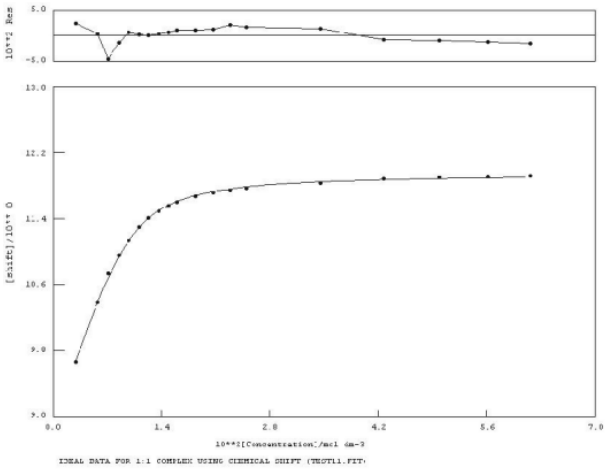

K_a = 481 M^{-1} Error = 5%

NMR titration for 220 *vs*. $TEAHCO_3$ in DMSO-d_6/H_2O 10% (aromatic CH)

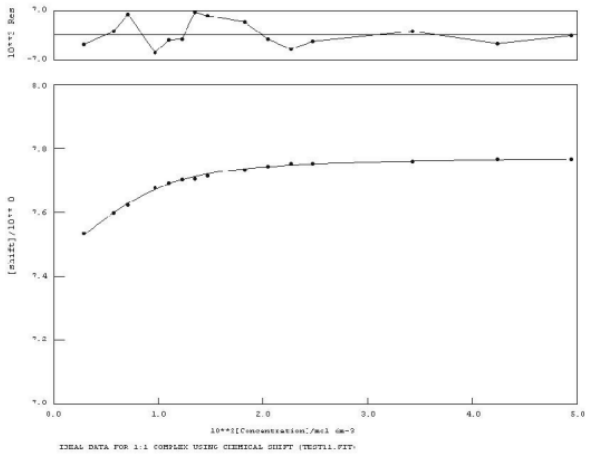

K_a = 728 M^{-1} Error = 7%

NMR titration for 221 *vs*. TBAOAc in DMSO-d_6/H_2O 10%

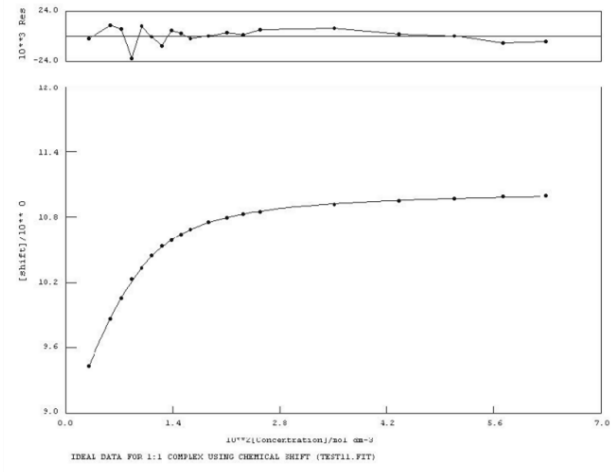

K_a = 602 M^{-1} Error = 2%

NMR titration for 221 *vs.* $TBAH_2PO_4$ in DMSO-d_6/H_2O 10%

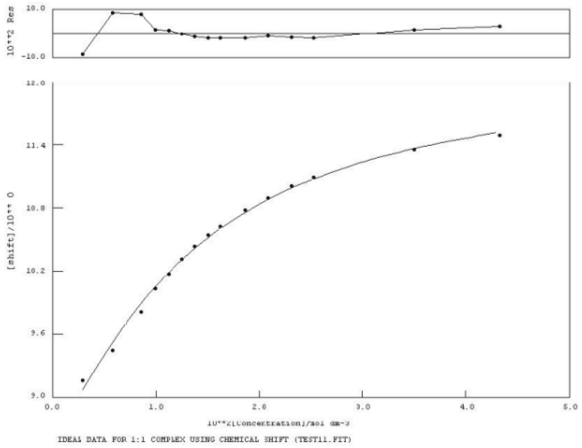

K_a = 122 M^{-1} Error = 11%

NMR titration for 222 *vs.* TBAOAc in DMSO-d_6/H_2O 10%

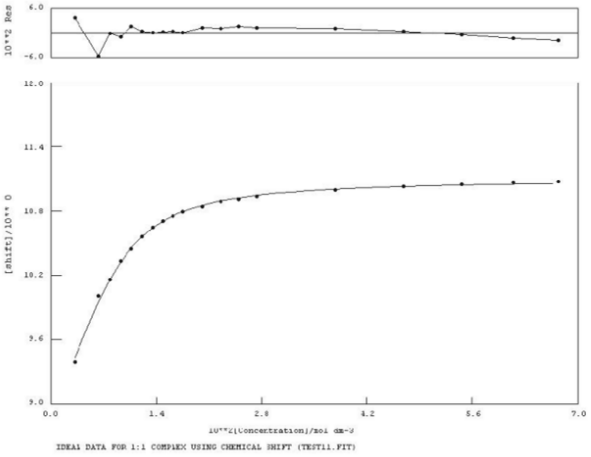

K_a = 691 M^{-1} Error = 5%

NMR titration for 222 *vs.* $TBAH_2PO_4$ in DMSO-d_6/H_2O 10%

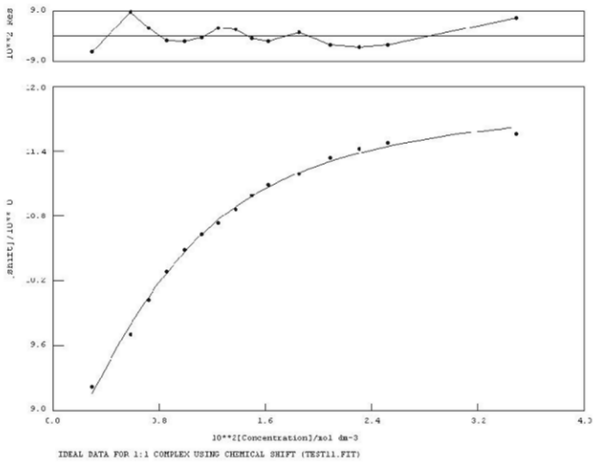

K_a = 315 M^{-1} Error = 11%

NMR titration for 222 *vs*. TBA_2SO_4 in DMSO-d_6/H_2O 10%

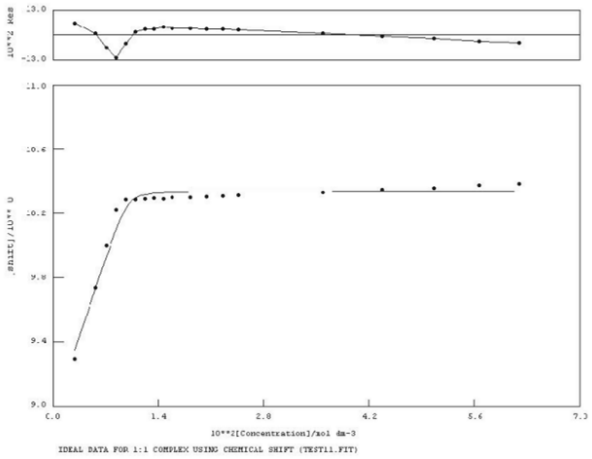

K_a = >10^4 M^{-1} Error = NA

Proton NMR titrations from Chapter Four

NMR titration for 224 *vs*. $TEAHCO_3$ in DMSO-d_6/H_2O 0.5%

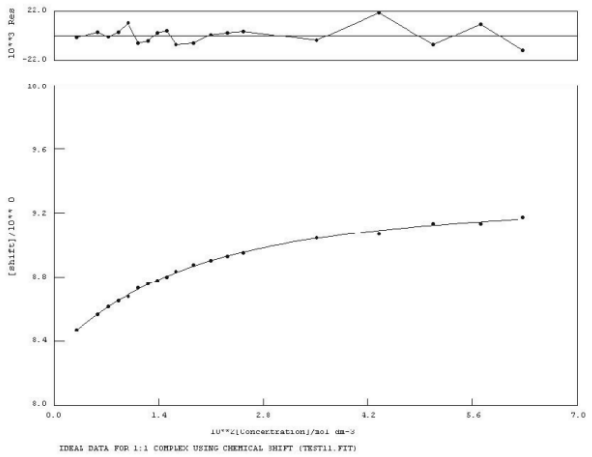

K_a = 81 M^{-1} Error = 6%

NMR titration for 224 *vs.* TBAOAc in DMSO-d_6/H_2O 0.5%

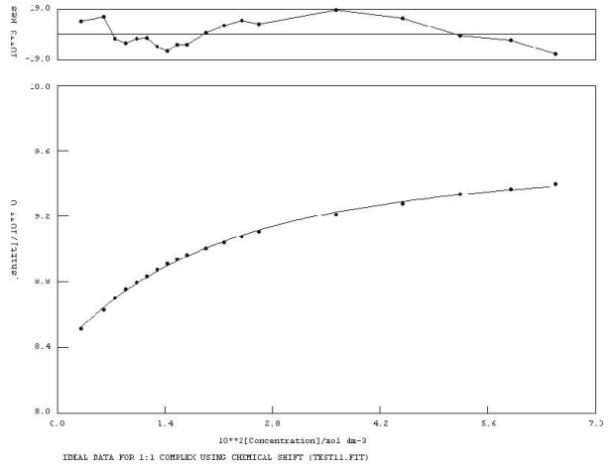

K_a = 69 M^{-1} Error = 5%

NMR titration for 224 *vs.* TBAOBz in DMSO-d_6/H_2O 0.5%

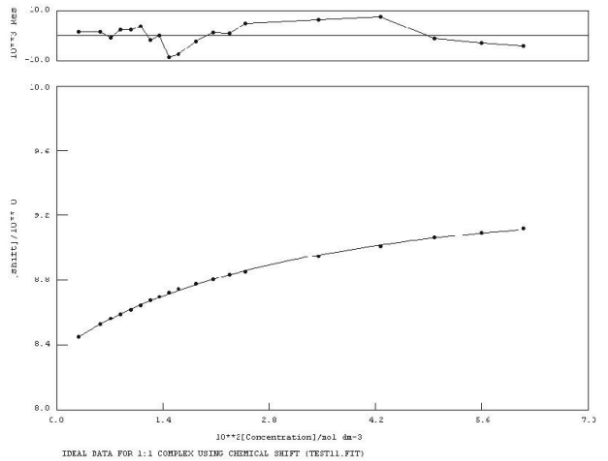

K_a = 41 M^{-1} Error = 4%

NMR titration for 224 *vs.* TBACl in DMSO-d_6/H_2O 0.5%

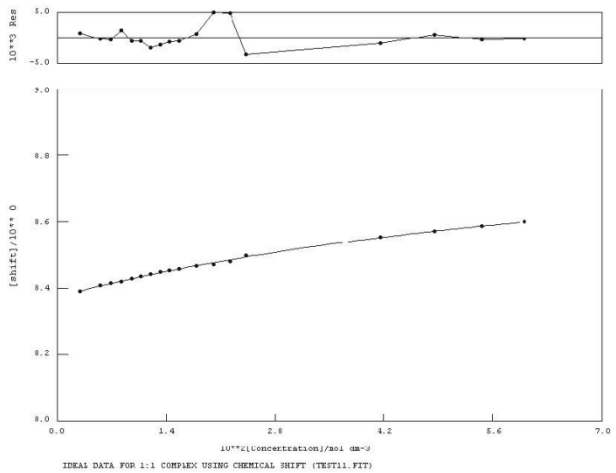

K_a = 12 M^{-1} Error = 10%

NMR titration for 225 *vs*. TBAH_2PO_4 in DMSO-d_6/H_2O 0.5%

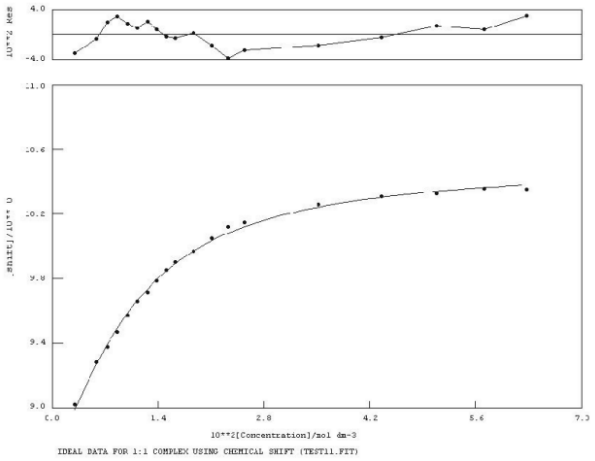

K_a = 197 M^{-1} Error = 7%

NMR titration for 225 *vs*. TBACl in DMSO-d_6/H_2O 0.5%

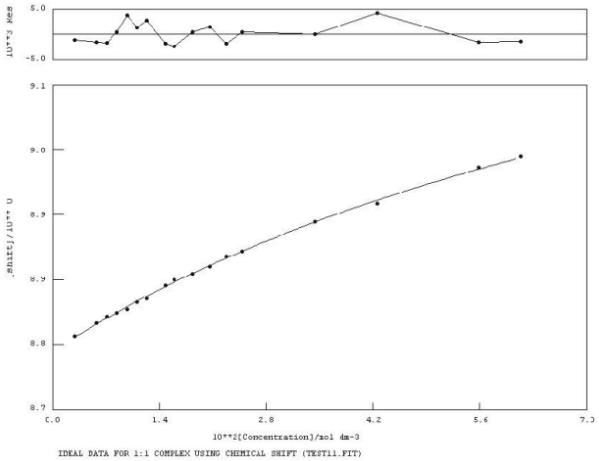

K_a = 11 M^{-1} Error = 9%

NMR titration for 225 *vs*. TBAOAc in DMSO-d_6/H_2O 0.5%

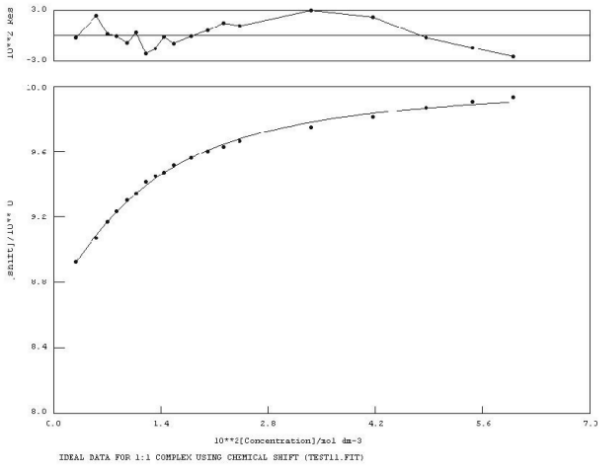

K_a = 144 M^{-1} Error = 7%

NMR titration for 225 *vs.* TBAOBz in DMSO-d_6/H_2O 0.5%

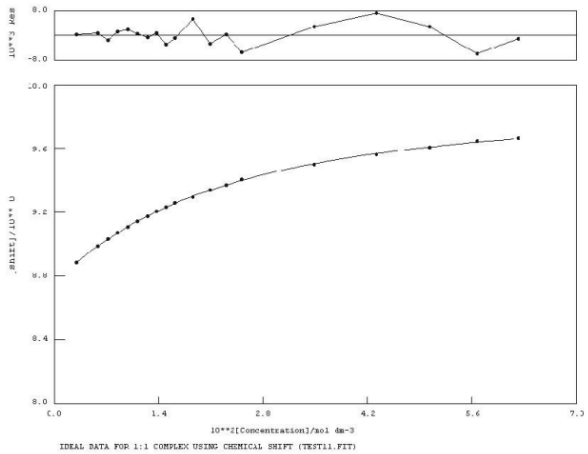

K_a = 59 M^{-1} Error = 2%

NMR titration for 226 *vs.* TBACl in DMSO-d_6/H_2O 0.5%

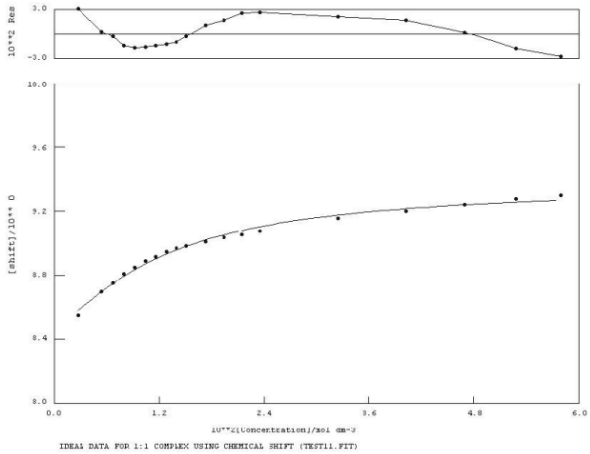

K_a = 141 M^{-1} Error = 13%

NMR titration for 226 *vs.* TBAOAc in DMSO-d_6/H_2O 0.5%

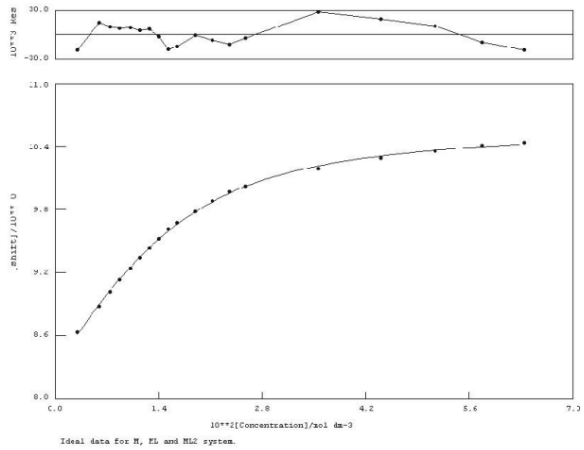

K_1 = 499 M^{-1} Error = 9%
K_2 = 100 M^{-1} Error = > 50%

NMR titration for 231 *vs*. TBACl in DMSO-d_6/H_2O 0.5%

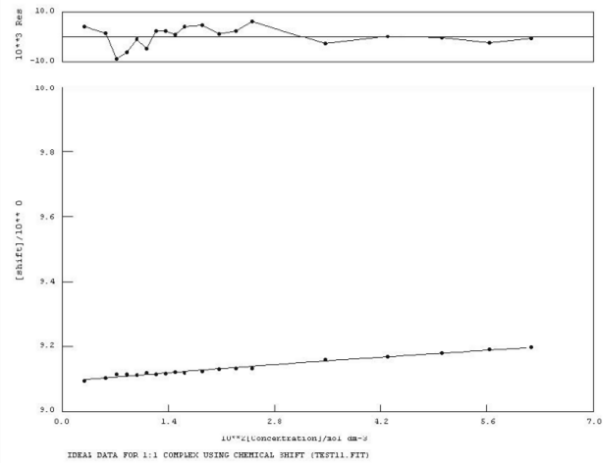

K_a = <10 M^{-1} Error = NA

NMR titration for 231 *vs*. TBAH_2PO_4 in DMSO-d_6/H_2O 0.5%

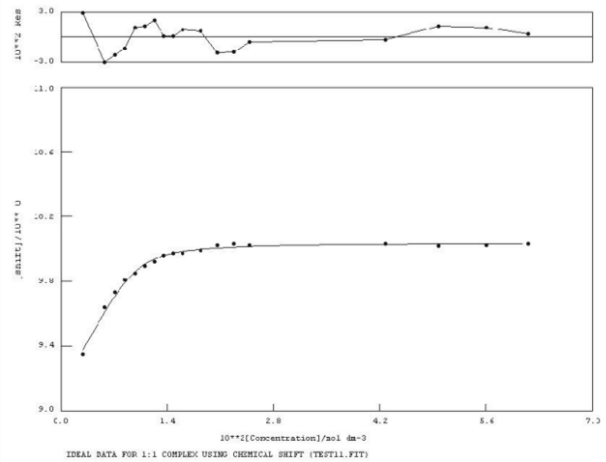

K_a = 2240 M^{-1} Error = 16%

NMR titration for 231 *vs*. TBAOAc in DMSO-d_6/H_2O 0.5%

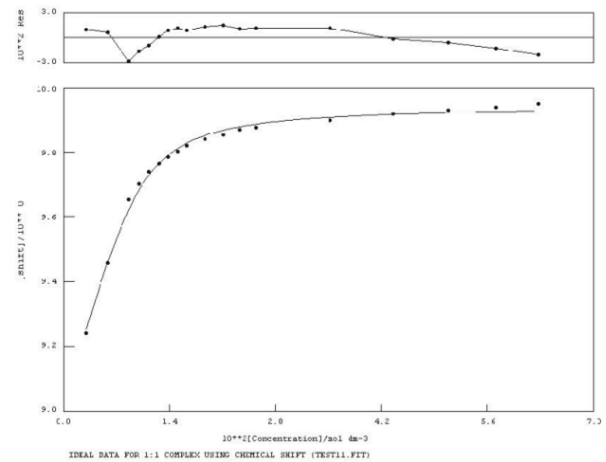

K_a = 908 M^{-1} Error = 10%

NMR titration for 231 *vs.* TBAOBz in DMSO-d_6/H_2O 0.5%

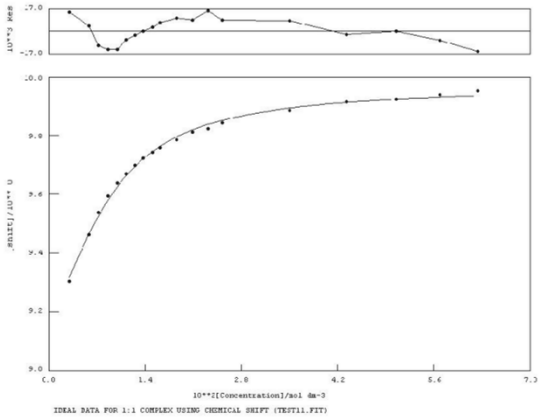

K_a = 321 M^{-1} Error = 7%

NMR titration for 232 *vs.* TBAOAc in DMSO-d_6/H_2O 0.5%

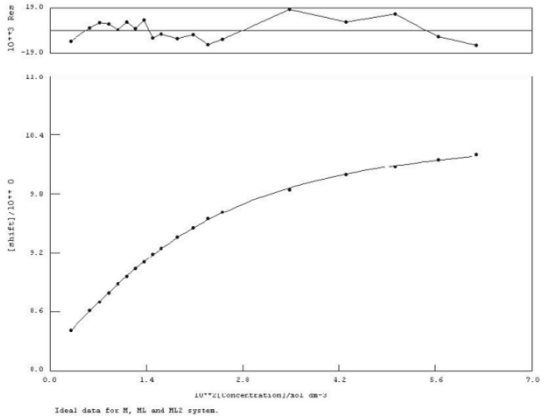

K_1 = 285 M^{-1} Error = 7%
K_2 = 63 M^{-1} Error = > 50%

Figure S15 NMR titration for 232 *vs.* TBA_2SO_4 in DMSO-d_6/H_2O 0.5%

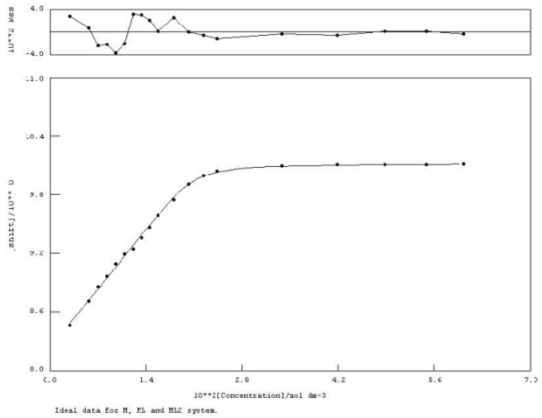

K_1 = 2250 M^{-1} Error = 26%
K_1K_2 = > 10^6 M^{-1}Error = NA

Proton NMR titrations from Chapter Five

NMR titration for 234 *vs*. TBABzO in DMSO-d_6/H_2O 0.5%

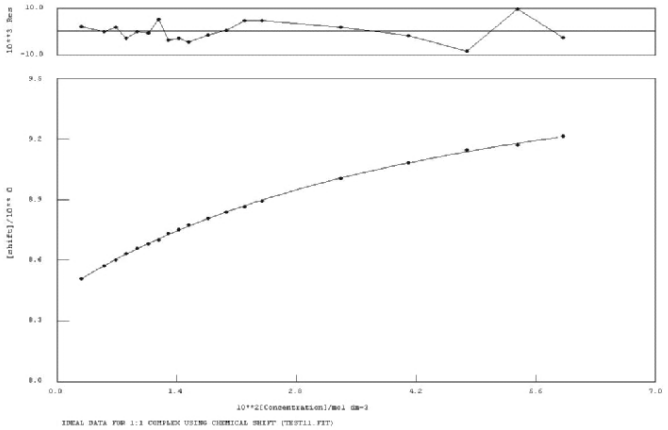

K_a = 25 M^{-1} Error = 4%

NMR titration for 234 *vs*. TBAAcO in DMSO-d_6/H_2O 0.5%

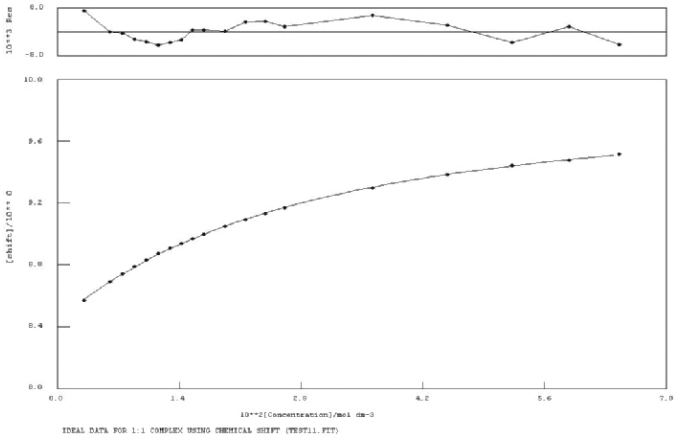

K_a = 46 M^{-1} Error = 2%

NMR titration for 234 *vs.* TBAF in DMSO-d_6/H_2O 0.5%

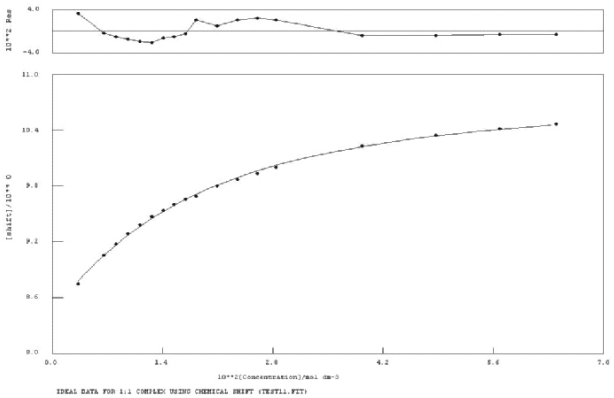

K_a = 83 M^{-1} Error = 9%

NMR titration for 234 *vs.* $TBAH_2PO_4$ in DMSO-d_6/H_2O 0.5%

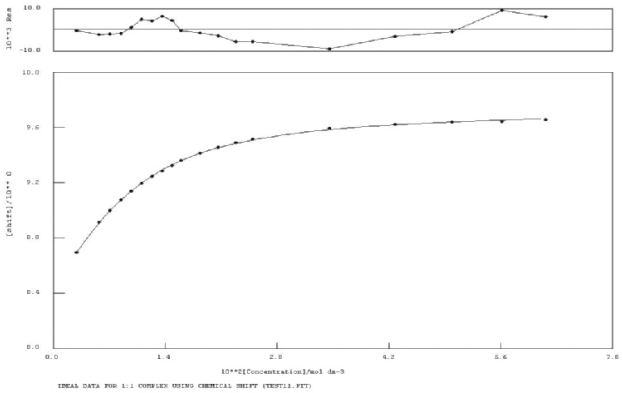

K_a = 260 M^{-1} Error = 2%

NMR titration for 234 *vs.* TBACl in DMSO-d_6/H_2O 0.5%

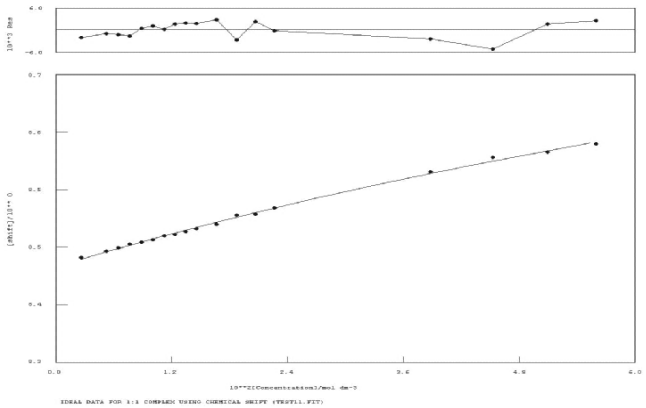

K_a = <10 M^{-1} Error = 22%

NMR titration for 235 *vs*. TBABzO in DMSO-d_6/H_2O 0.5%

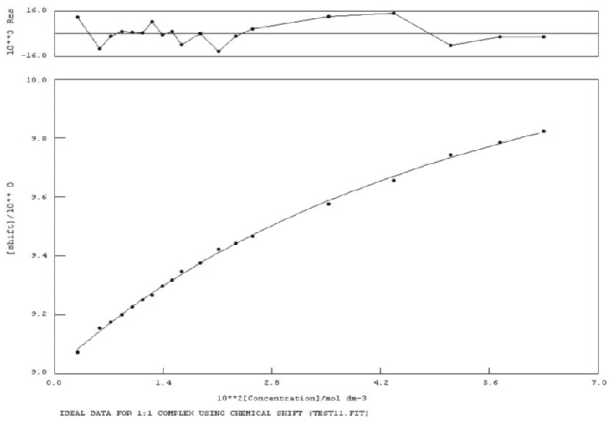

K_a = 18 M^{-1} Error = 8%

NMR titration for 235 *vs*. TBAF in DMSO-d_6/H_2O 0.5%

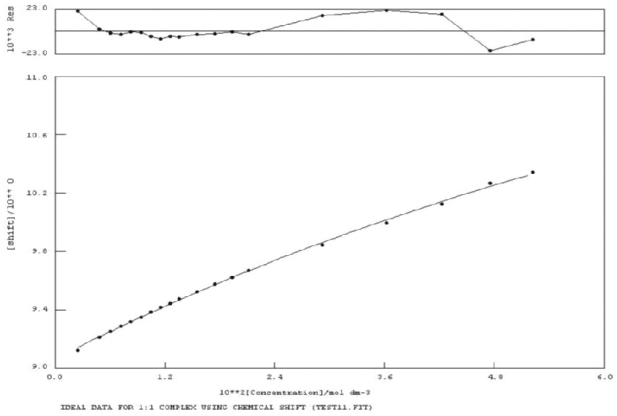

K_a = <10 M^{-1} Error = 14%

NMR titration for 235 *vs*. TBAH_2PO_4 in DMSO-d_6/H_2O 0.5%

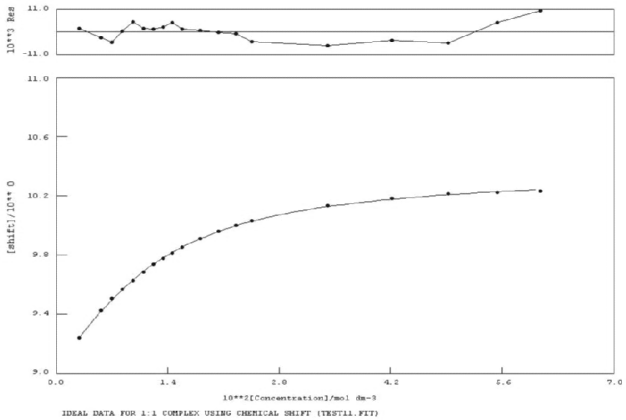

K_a = 176 M^{-1} Error = 2%

NMR titration for 235 *vs.* TBACl in DMSO-d_6/H_2O 0.5%

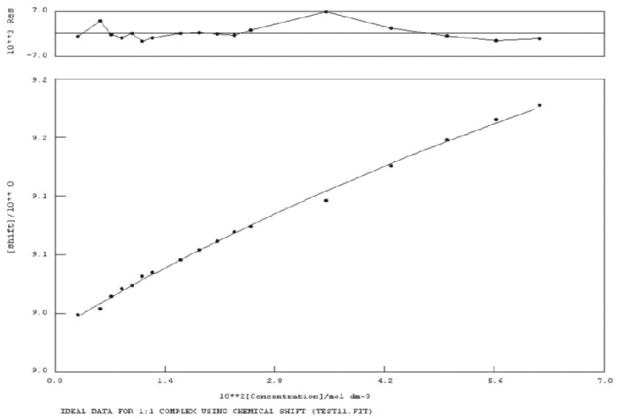

K_a = <10 M^{-1} Error = 23%

NMR titration for 235 *vs.* TBAAcO in DMSO-d_6/H_2O 0.5%

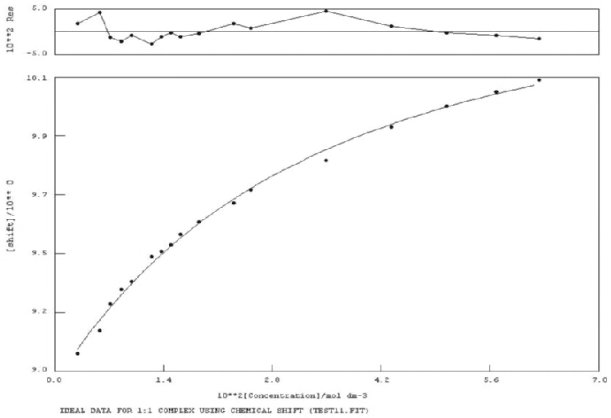

K_a = 38 M^{-1} Error = 12%

NMR titration for 236 *vs.* TBAAcO in DMSO-d_6/H_2O 0.5%

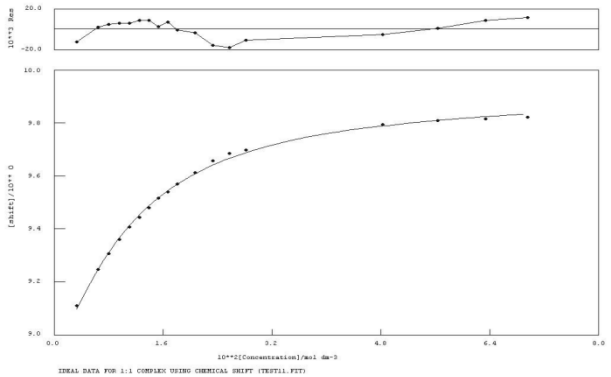

K_a = 149 M^{-1} Error = 5%

NMR titration for 236 *vs*. TBAH_2PO_4 in DMSO-d_6/H_2O 0.5%

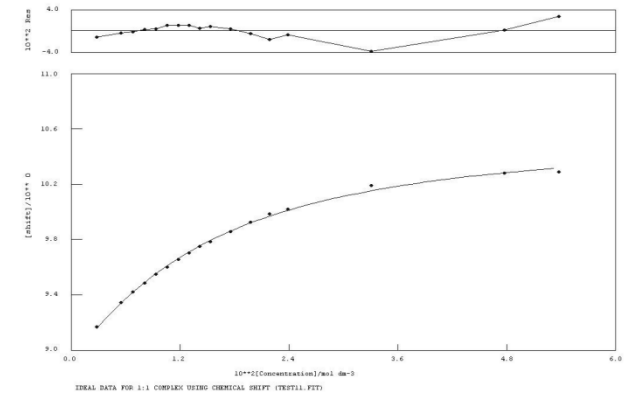

K_a = 99 M^{-1} Error = 7%

NMR titration for 236 *vs*. TBAOBz in DMSO-d_6/H_2O 0.5%

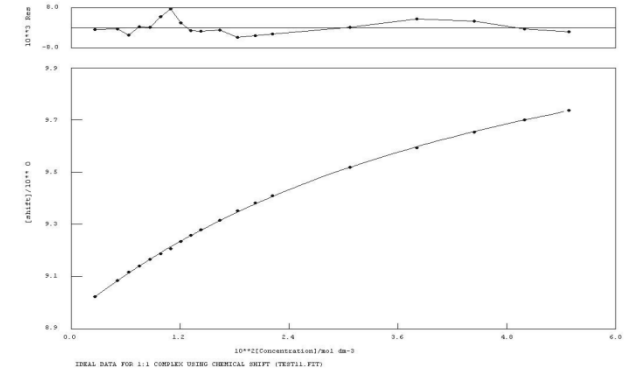

K_a = 24 M^{-1} Error = 3%

NMR titration for 236 *vs*. TBACl in DMSO-d_6/H_2O 0.5%

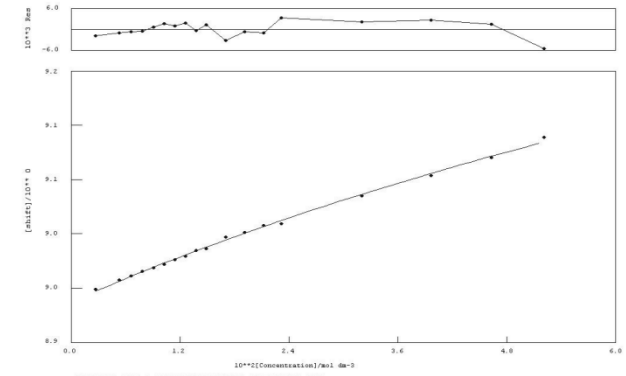

K_a = <10 M^{-1} Error = 22%

NMR titration for 237 *vs.* TBAAcO in DMSO-d_6/H_2O 0.5%

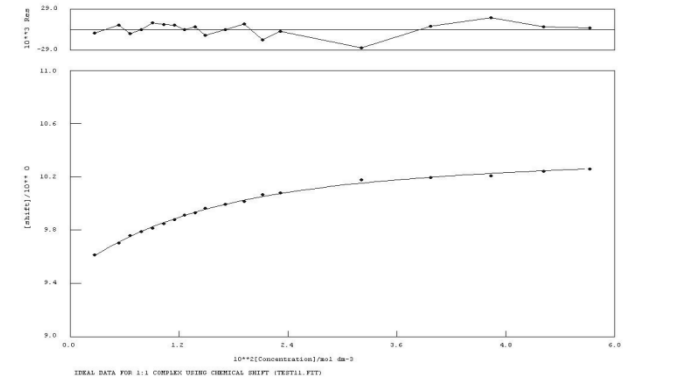

K_a = 97 M^{-1} Error = 8%

NMR titration for 237 *vs.* TBABzO in DMSO-d_6/H_2O 0.5%

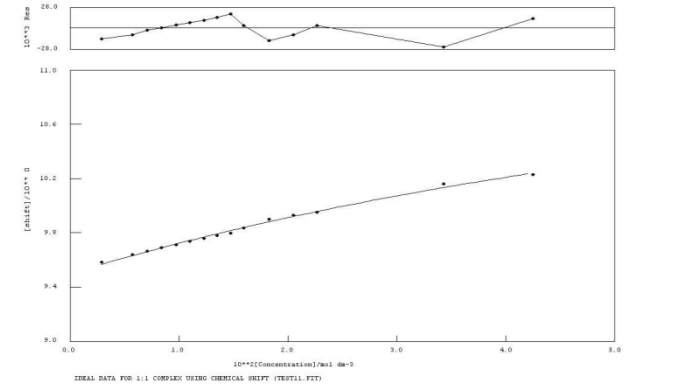

K_a = 11 M^{-1} Error = 28%

NMR titration for 237 *vs.* TBACl in DMSO-d_6/H_2O 0.5%

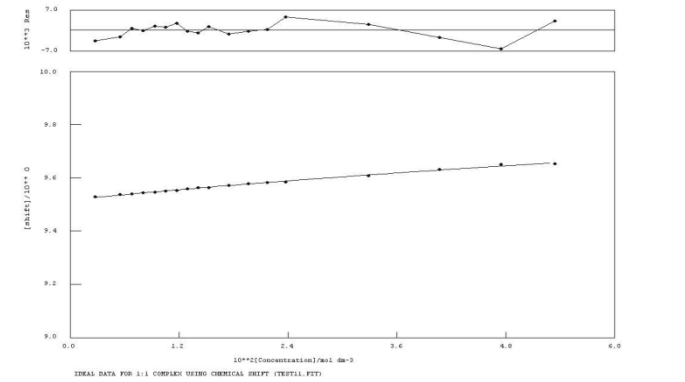

K_a = <10 M^{-1} Error = 26%

NMR titration for 237 *vs*. $TBAH_2PO_4$ in DMSO-d_6/H_2O 0.5%

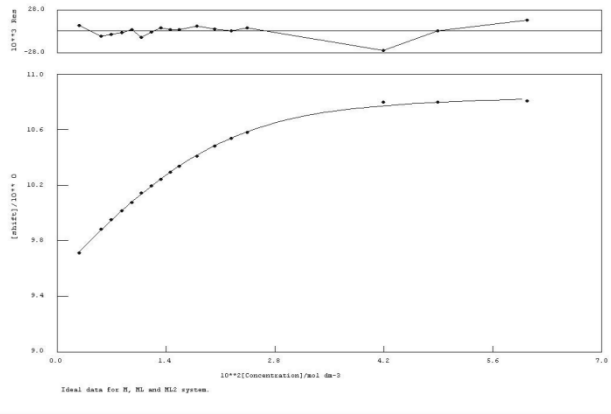

K_1 = 108 M^{-1} Error = 20%
K_2 = 216 M^{-1} Error = > 50%

NMR titration for 238 *vs*. $TBAH_2PO_4$ in DMSO-d_6/H_2O 0.5% (amide NH)

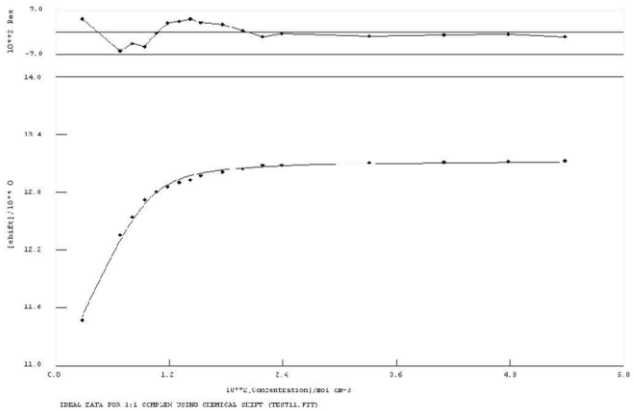

K_a = 599 M^{-1} Error = 7%

NMR titration for 238 *vs*. $TBAH_2PO_4$ in DMSO-d_6/H_2O 0.5% (carbazole NH)

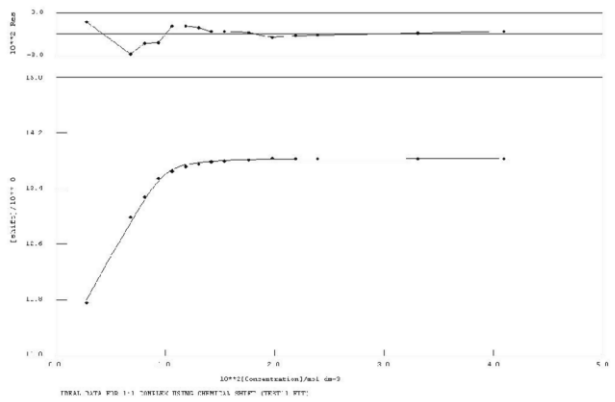

K_a = <10^4 M^{-1} Error = NA

NMR titration for 238 *vs.* TBACl in DMSO-d_6/H_2O 0.5% (amide NH)

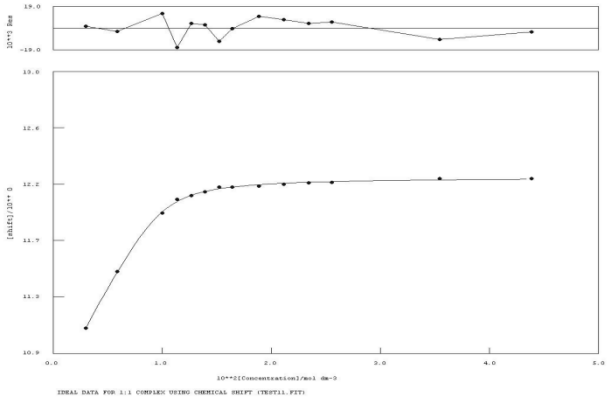

K_a = 2940 M^{-1} Error = 7%

NMR titration for 238 *vs.* TBACl in DMSO-d_6/H_2O 0.5% (carbazole NH)

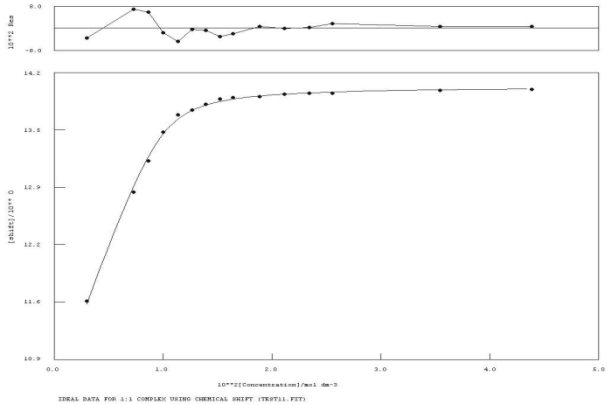

K_a = 3250 M^{-1} Error = 11%

NMR titration for 241 *vs.* TBAOAc in DMSO-d_6/H_2O 0.5%

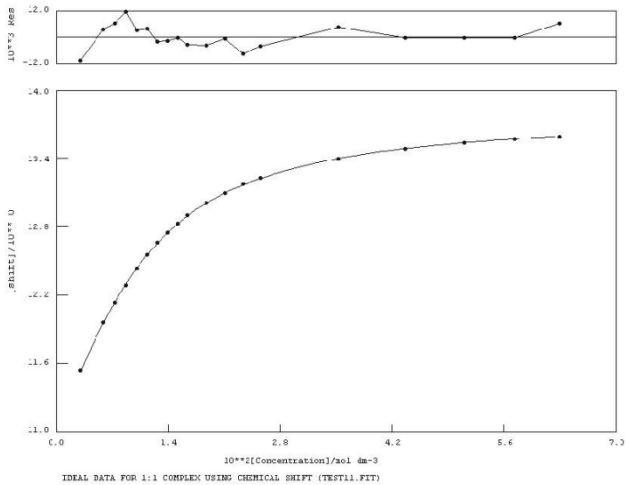

K_a = 210 M^{-1} Error = 1%

NMR titration for 241 *vs*. TBAOBz in DMSO-d_6/H_2O 0.5%

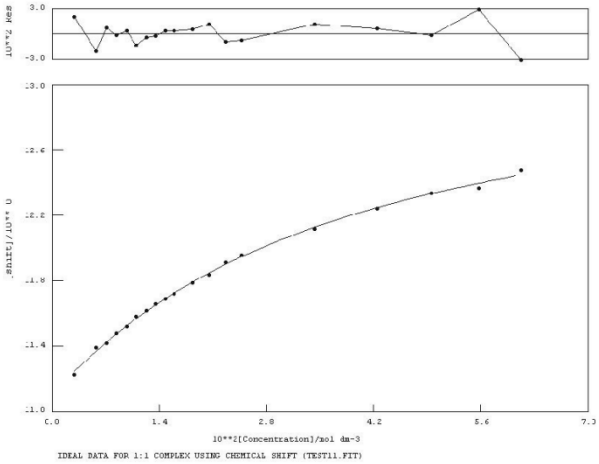

K_a = 32 M^{-1} Error = 7%

NMR titration for 241 *vs*. TBACl in DMSO-d_6/H_2O 0.5%

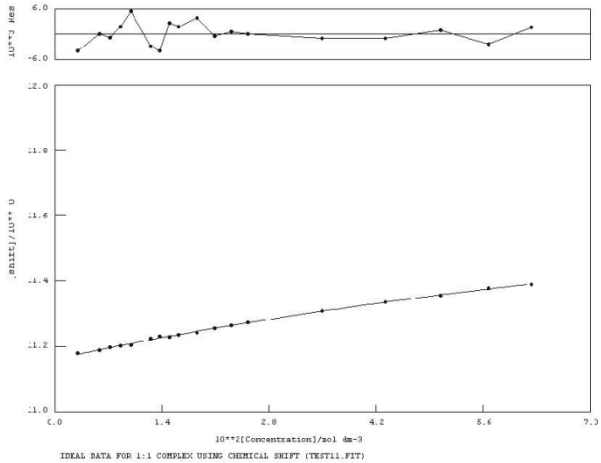

K_a = < 10 M^{-1} Error = NA

NMR titration for 241 *vs*. TBAH_2PO_4 in DMSO-d_6/H_2O 0.5%

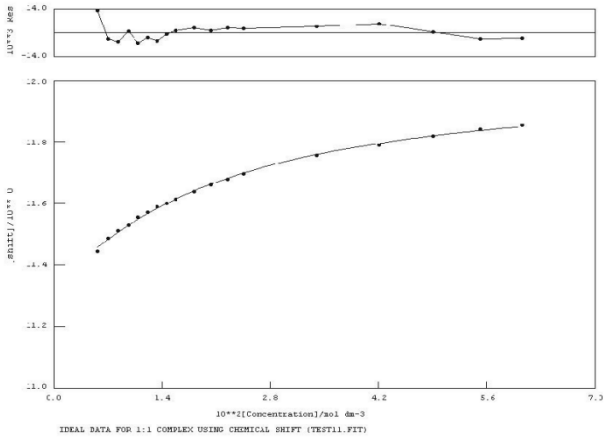

K_a = 63 M^{-1} Error = 8%

NMR titration for 241 *vs.* TBAF in DMSO-d_6/H_2O 0.5%

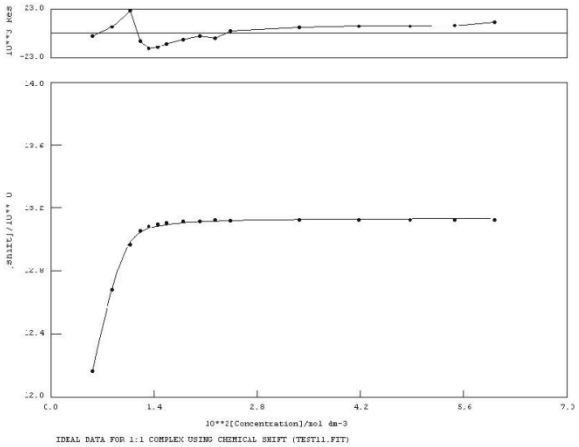

K_a = 8510 M^{-1} Error = 8%

NMR titration for 242 *vs.* TBAOAc in DMSO-d_6/H_2O 0.5%

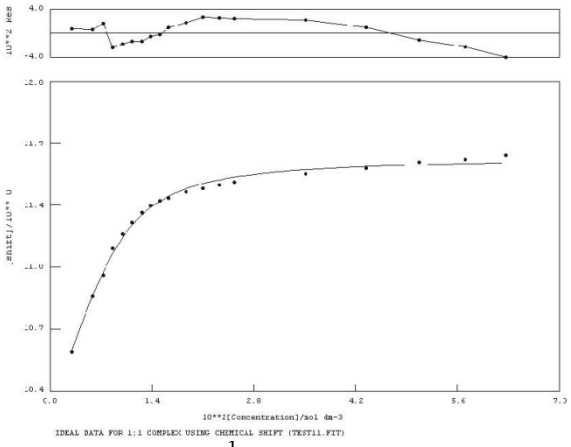

K_a = 682 M^{-1} Error = 9%

NMR titration for 242 *vs.* TBAOBz in DMSO-d_6/H_2O 0.5%

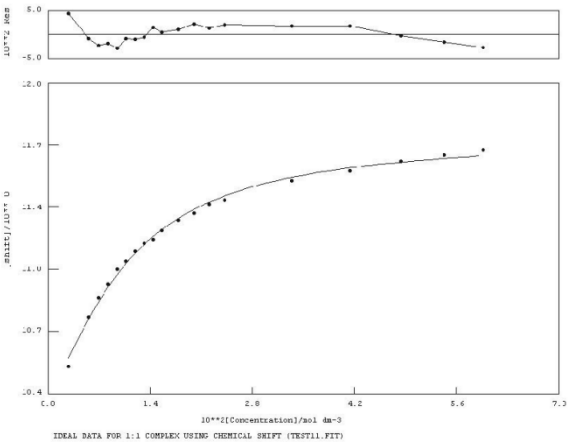

K_a = 191 M^{-1} Error = 8%

NMR titration for 242 *vs*. TBACl in DMSO-d_6/H_2O 0.5%

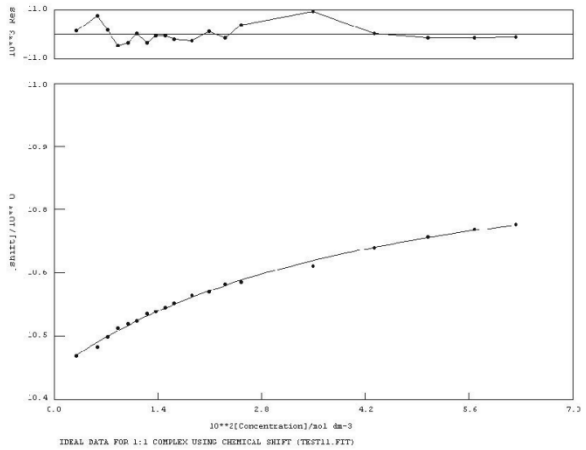

K_a = 28 M^{-1} Error = 9%

NMR titration for 242 *vs*. TBAH_2PO_4 in DMSO-d_6/H_2O 0.5%

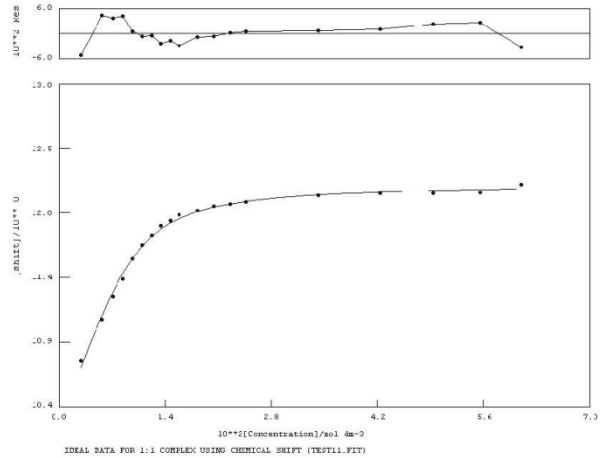

K_a = 803 M^{-1} Error = 9%

NMR titration for 242 *vs*. TBAF in DMSO-d_6/H_2O 0.5%

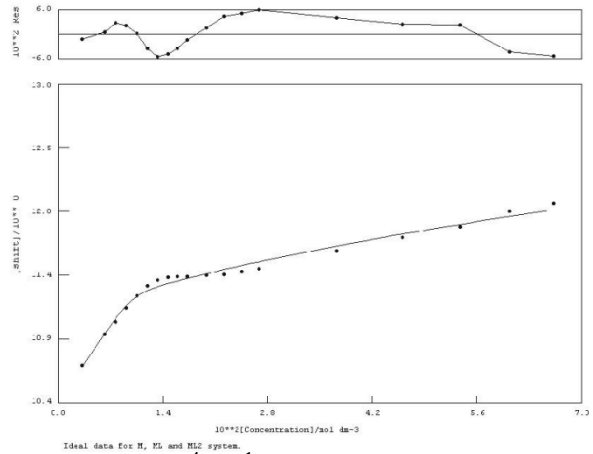

K_1 = >10^4 M^{-1} Error = NA
K_2 = NA M^{-1} Error = NA

Appendix 3 – Proton NMR Job Plots

Were reported, ^{1}H NMR Job plot experiments were conducted to allow solution state binding modes to be ascertained with the anions added as the tetraethylammonium or tetrabutylammonium salt at 298 K in the appropriate DMSO-d_6/H_2O mixtures. The results are given for completeness.

Job plots for Chapter Two

Receptor 209 *vs.* $TBAH_2PO_4$ in DMSO-d_6/H_2O 0.5% (urea NH)

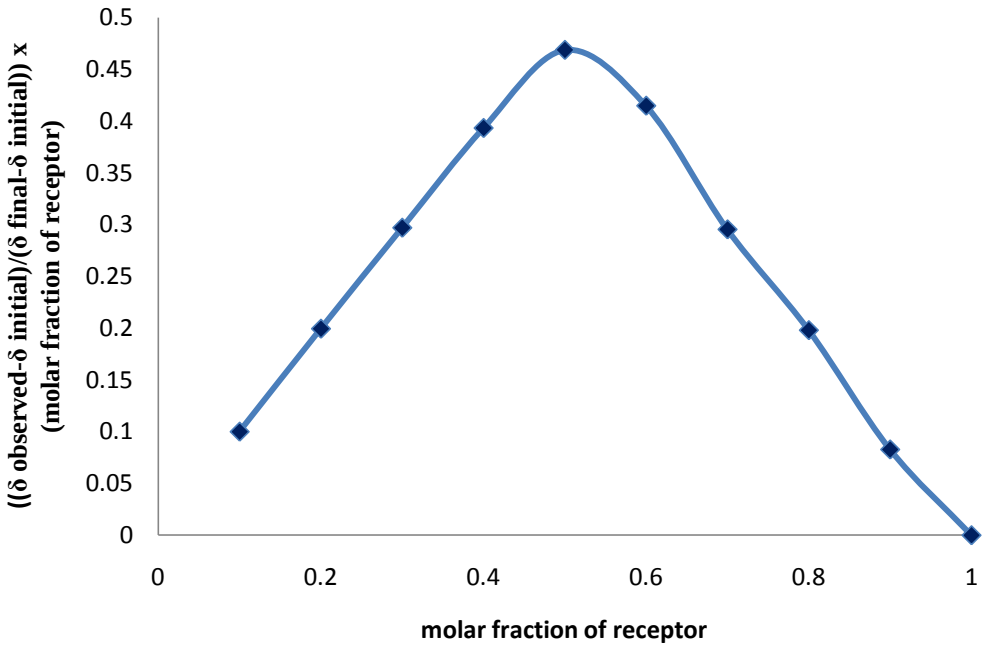

Receptor 210 *vs.* $TBAH_2PO_4$ in DMSO-d_6/H_2O 0.5% (urea NH)

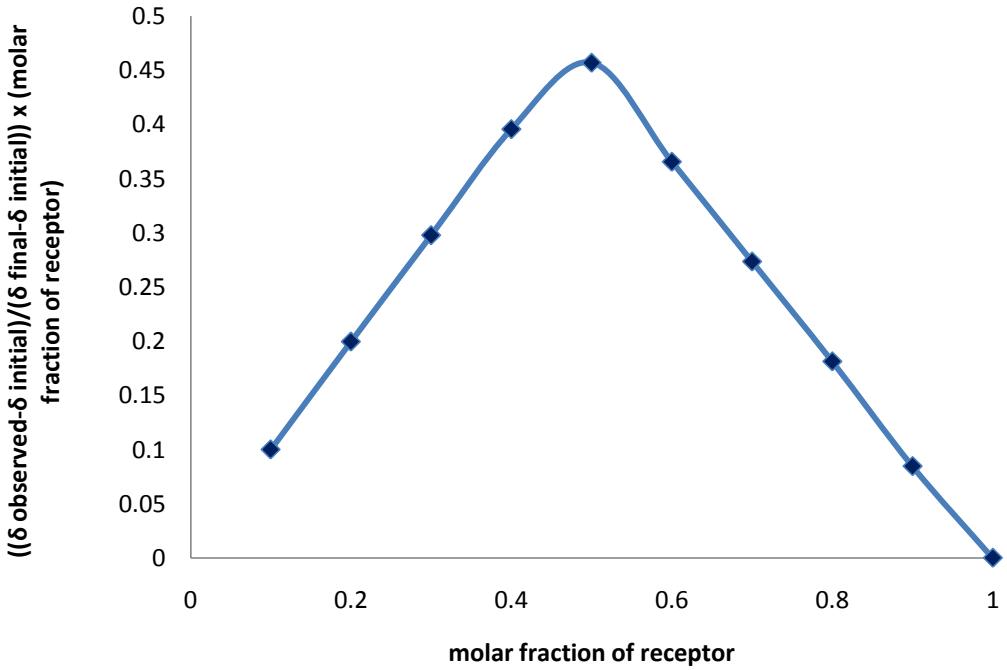

Receptor 210 *vs.* $TEAHCO_3$ in DMSO-d_6/H_2O 10% (urea NH)

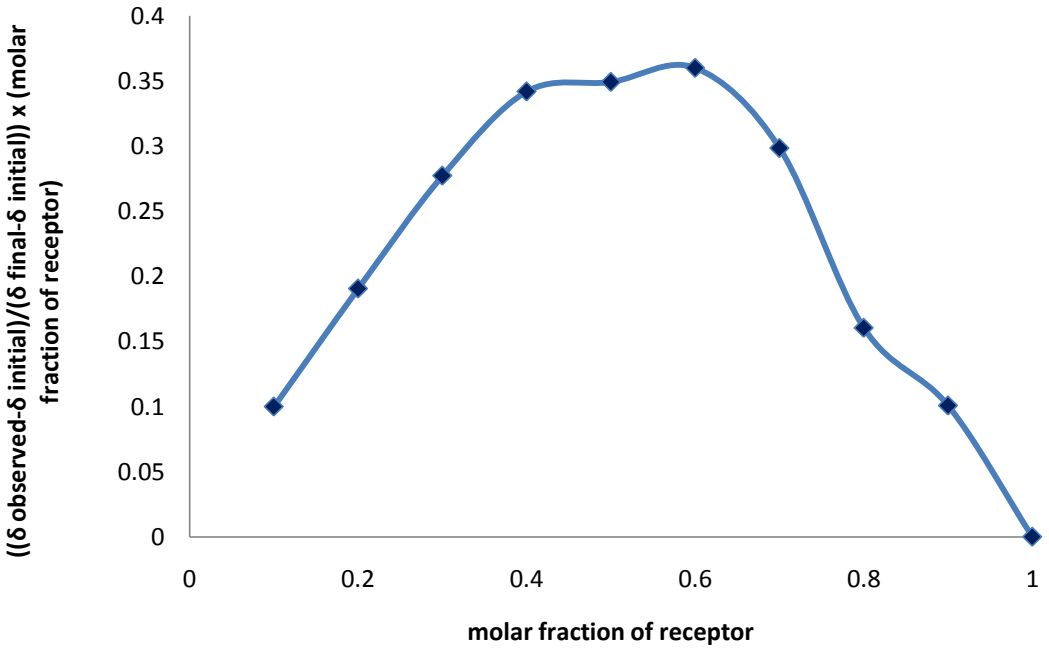

Receptor 212 *vs.* $TBAH_2PO_4$ in DMSO-d_6/H_2O 0.5% (aromatic CH)

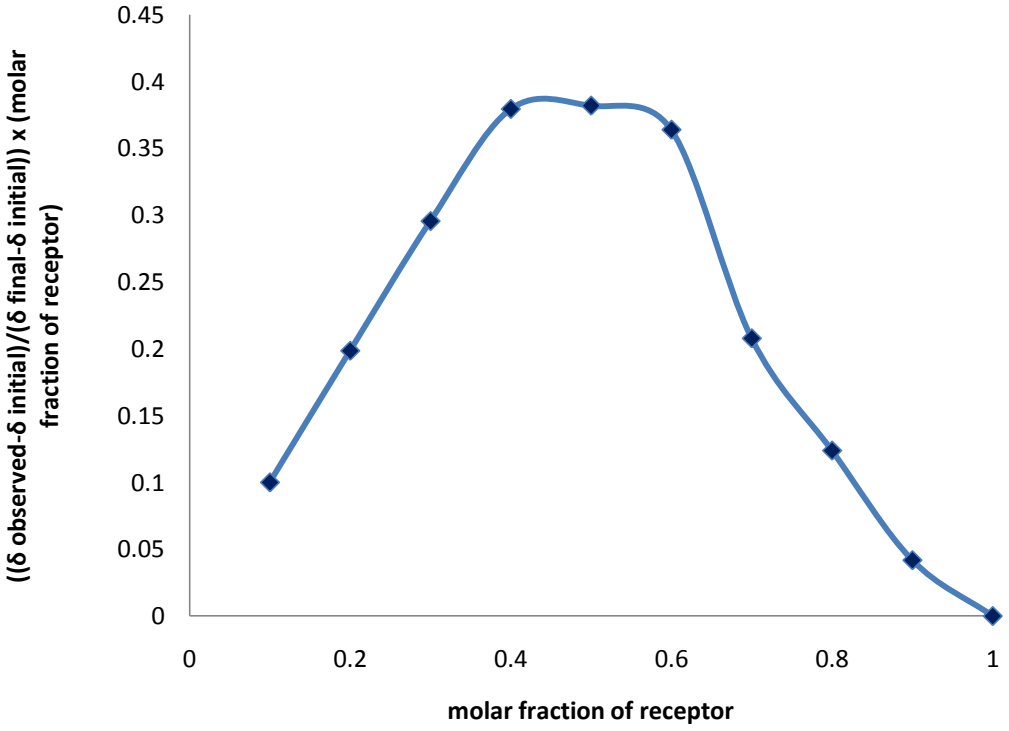

Receptor 213 *vs.* $TBAH_2PO_4$ in DMSO-d_6/H_2O 0.5% (aromatic CH)

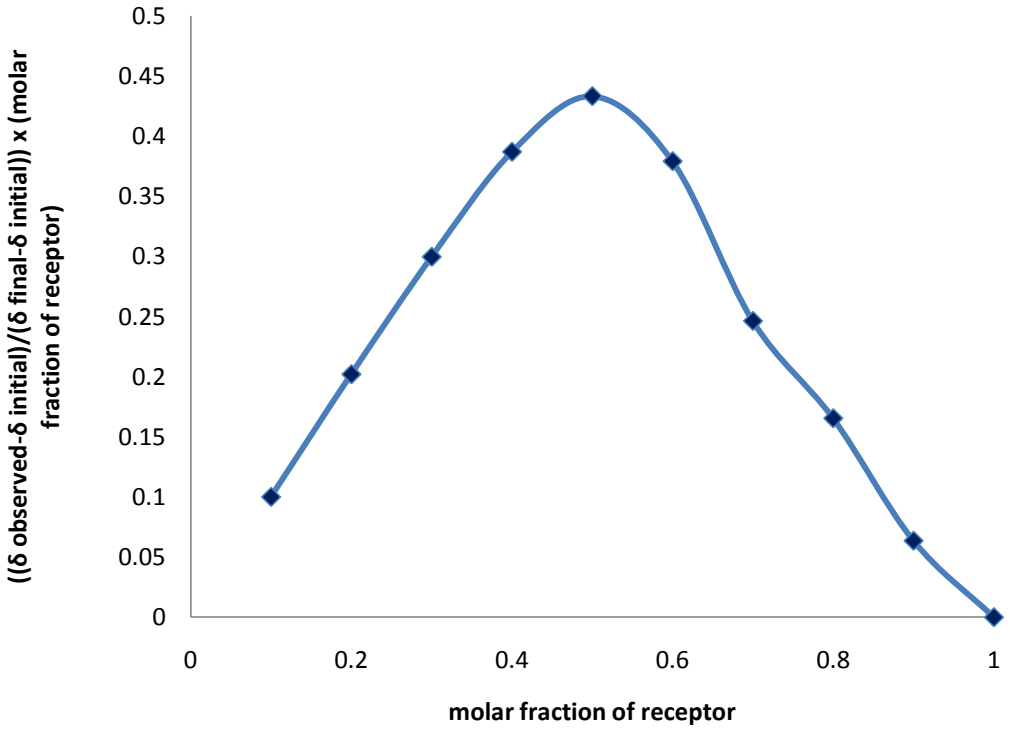

Job plots for Chapter Three

Receptor 220 *vs.* $TBAH_2PO_4$ in DMSO-d_6/H_2O 10% (urea NH)

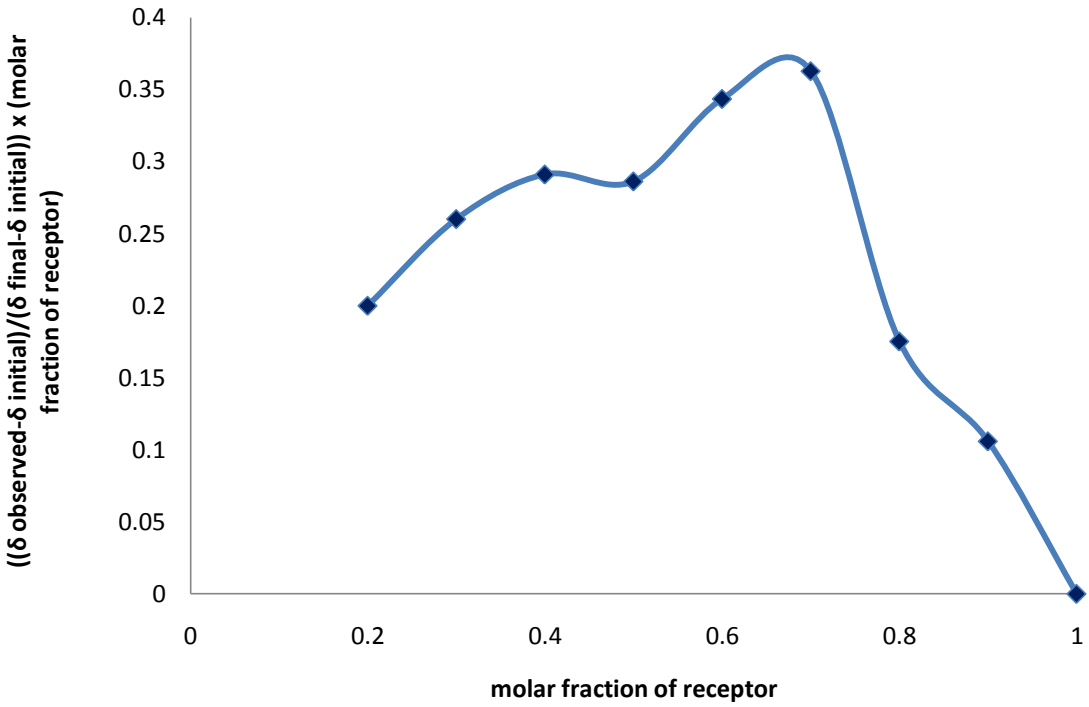

Receptor 221 *vs.* TBACl in DMSO-d_6/H_2O 0.5%

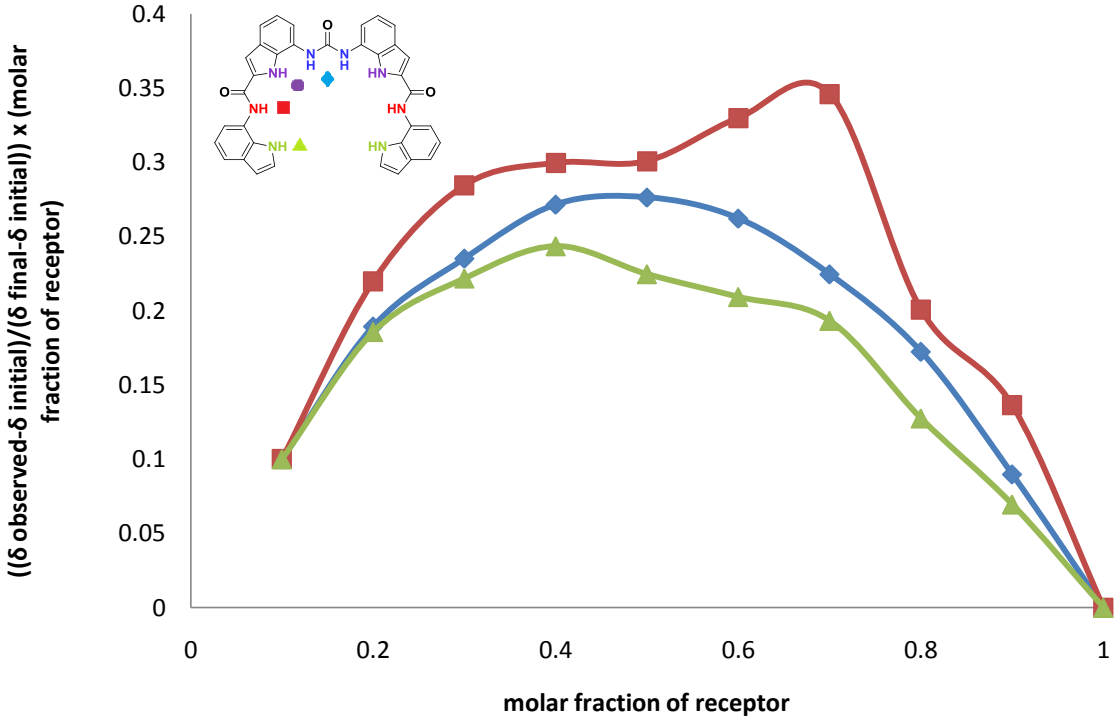

Receptor 221 *vs.* TBAOAc in DMSO-d_6/H_2O 0.5%

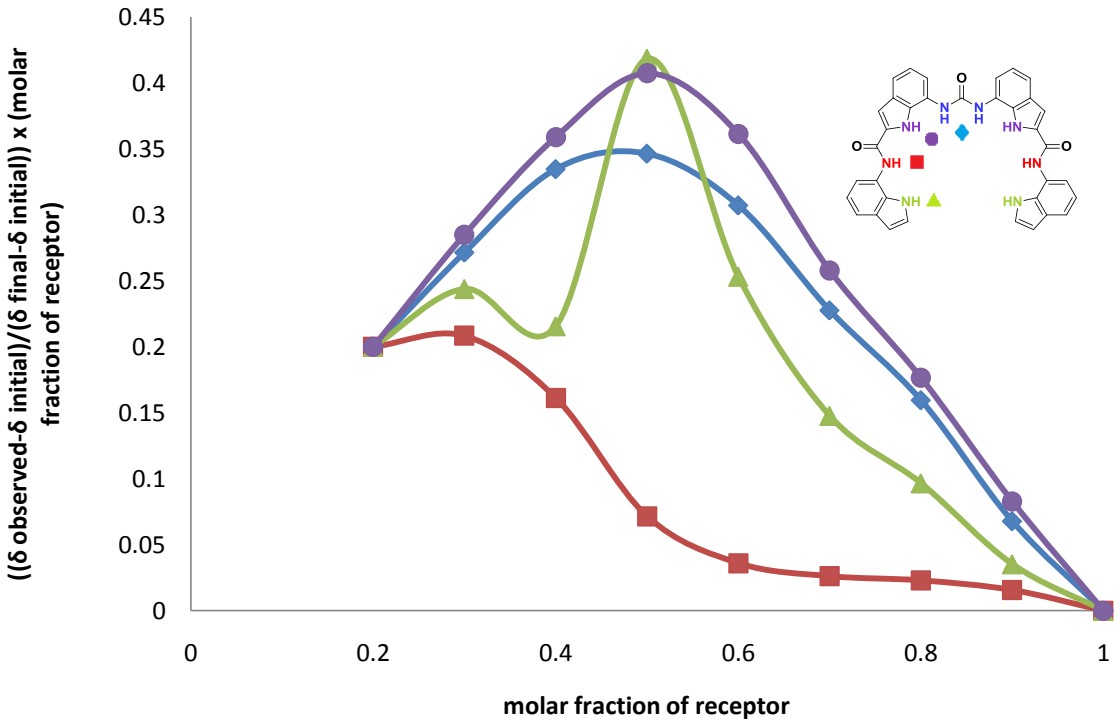

Receptor 221 *vs.* TBA_2SO_4 in DMSO-d_6/H_2O 0.5%

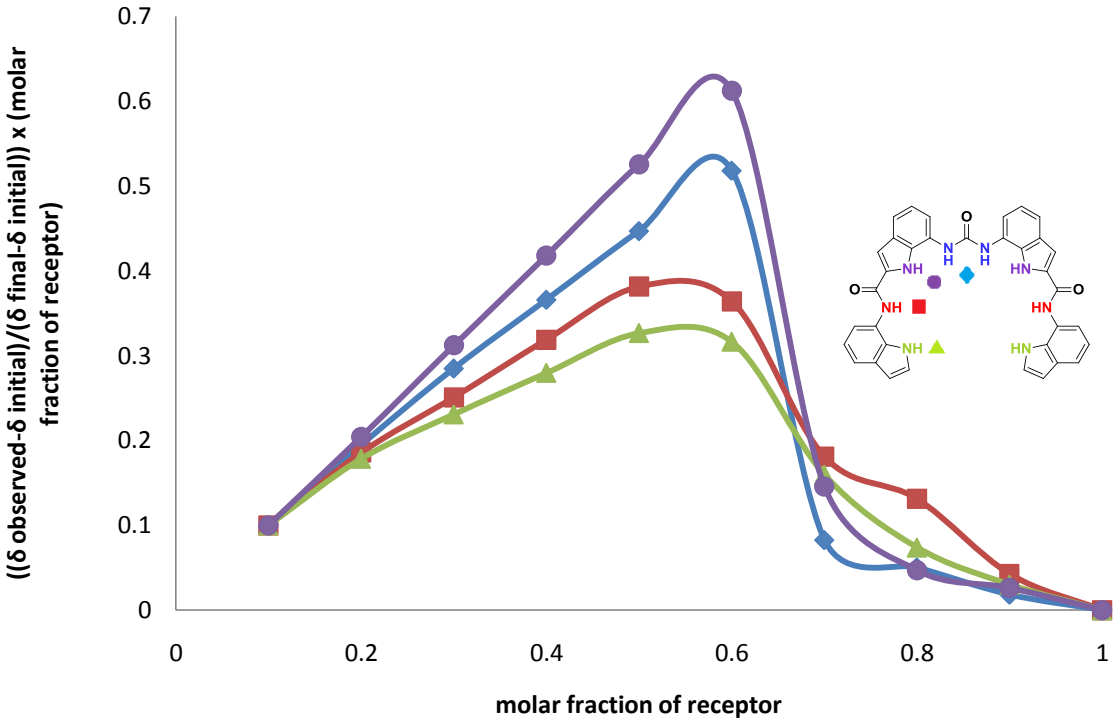

Receptor 222 *vs.* TBACl in DMSO-d_6/H_2O 0.5%

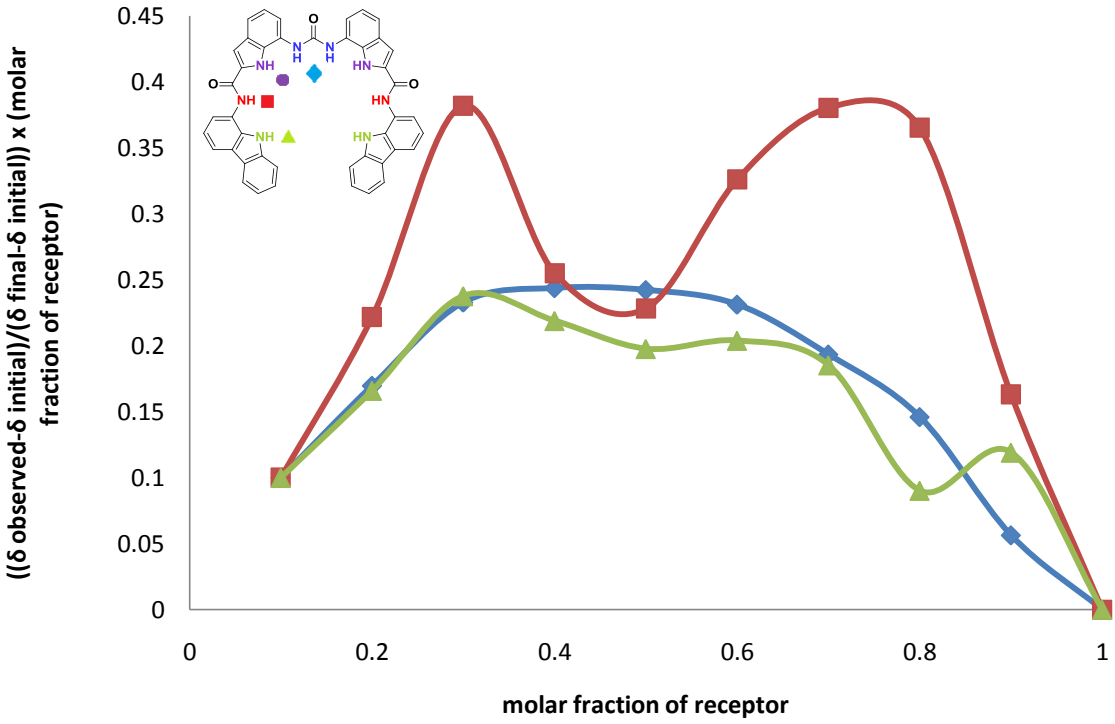

Receptor 222 *vs.* TBAOAc in DMSO-d_6/H_2O 0.5%

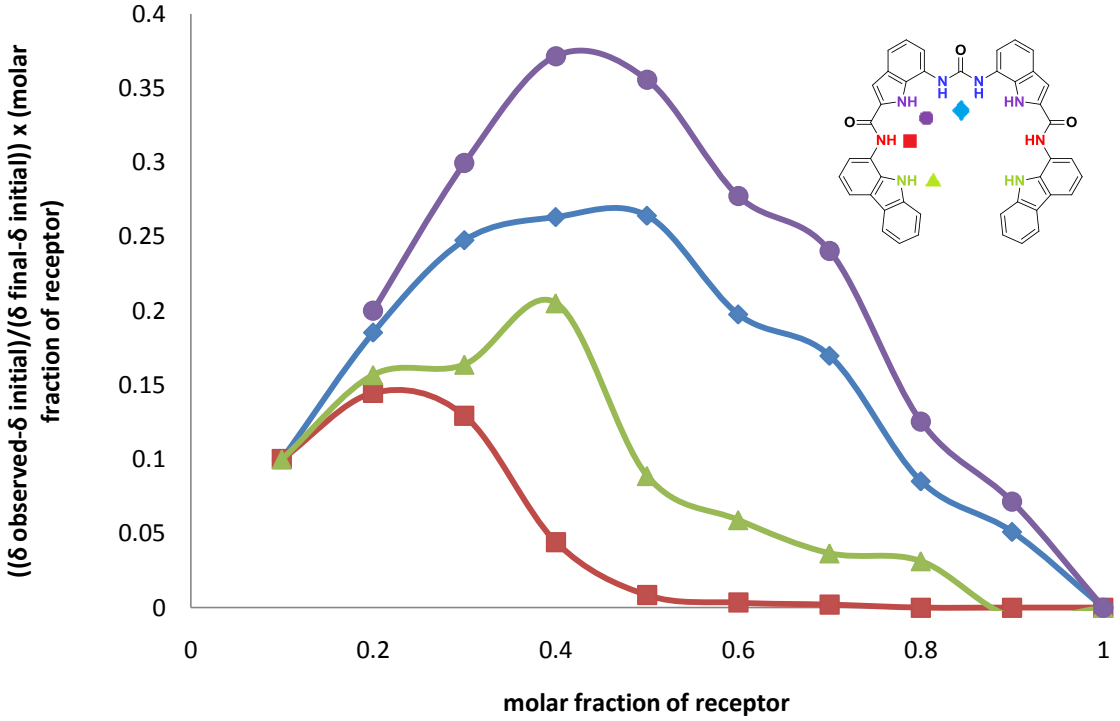

Receptor 222 *vs.* TBA_2SO_4 in DMSO-d_6/H_2O 0.5%

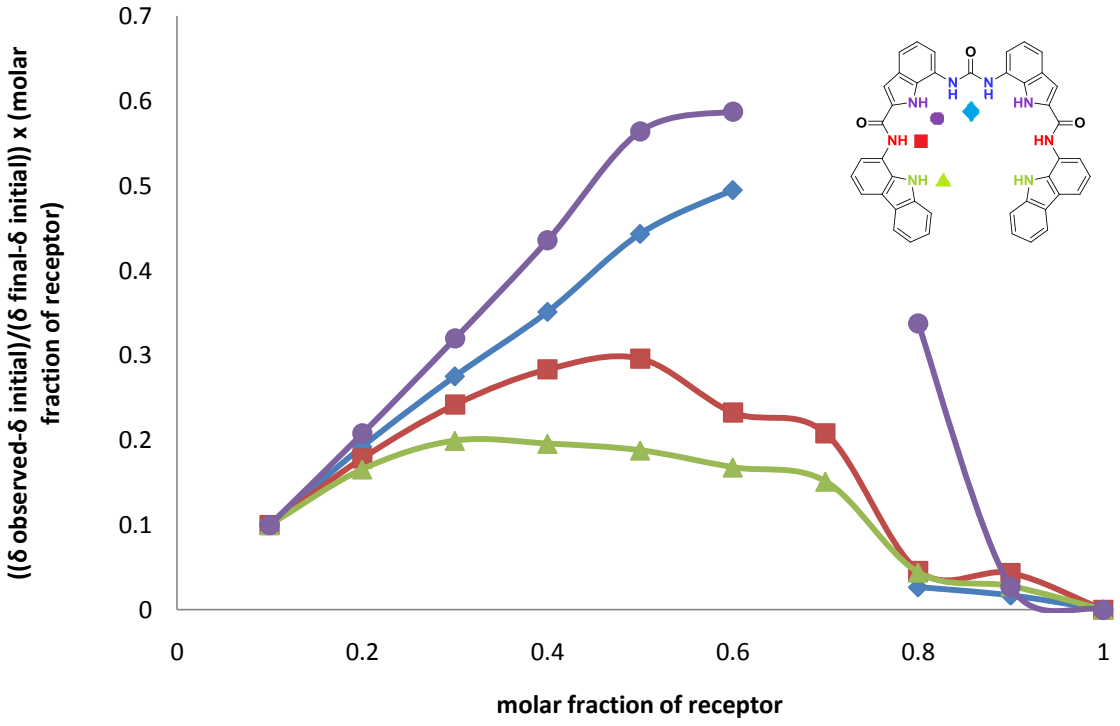

Job plots for Chapter Four

Receptor 224 *vs.* TBACl in DMSO-d_6/H_2O 0.5%

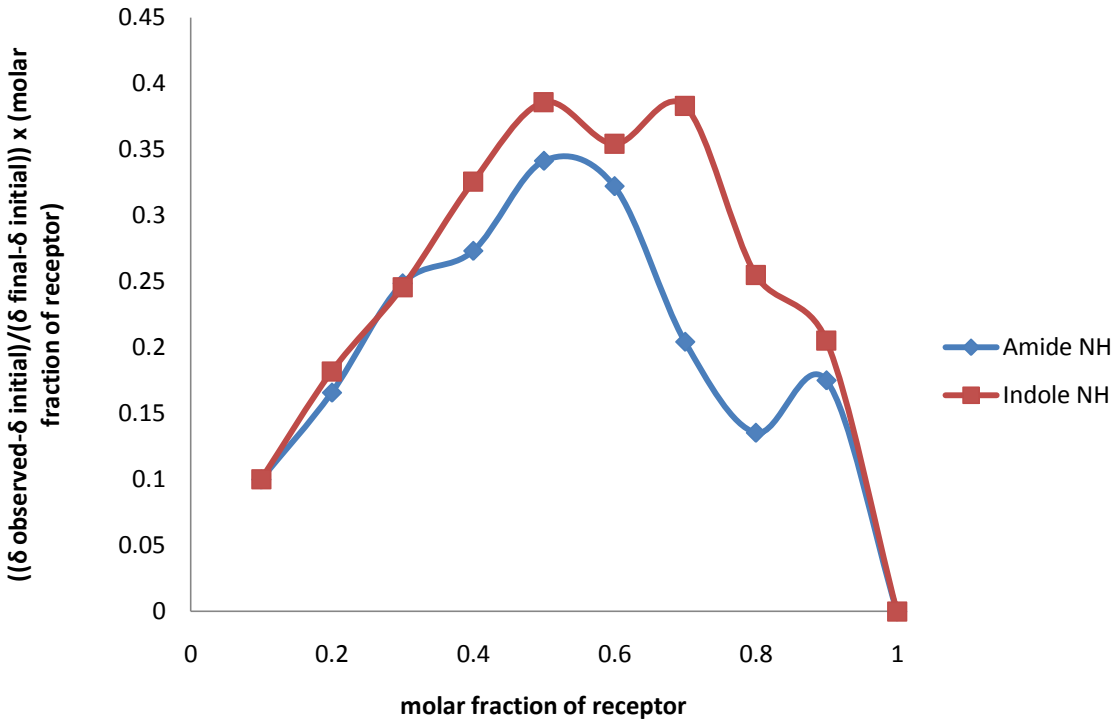

Receptor 224 *vs.* $TBAH_2PO_4$ in DMSO-d_6/H_2O 0.5%

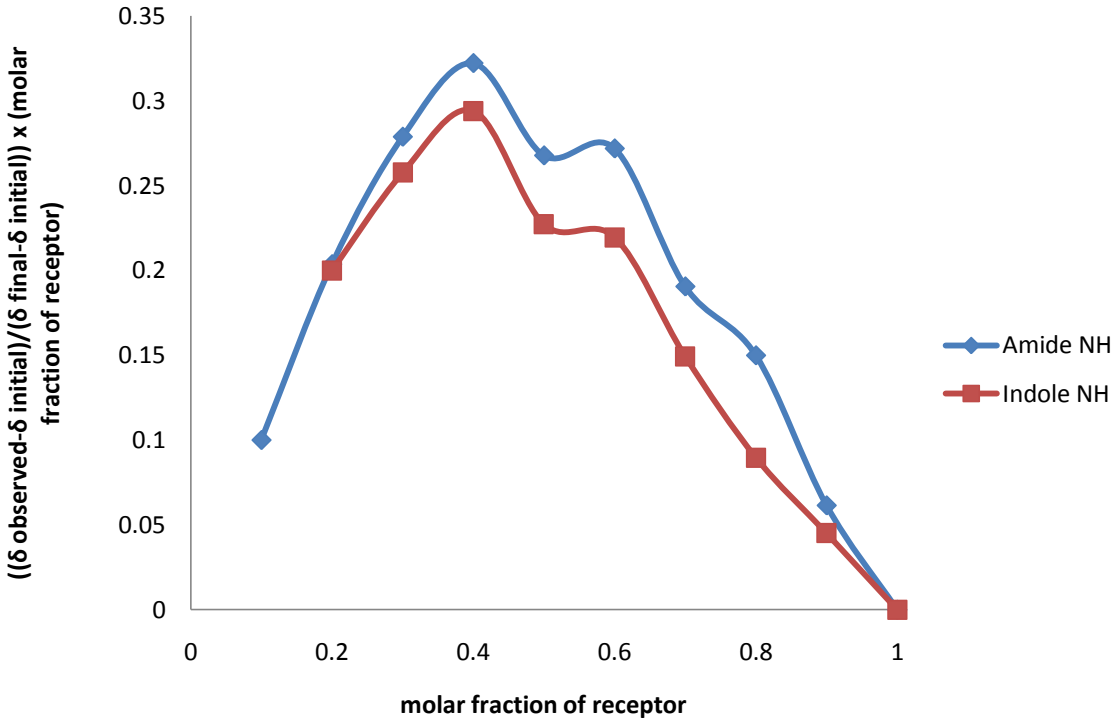

Receptor 224 *vs.* $TEAHCO_3$ in DMSO-d_6/H_2O 0.5%

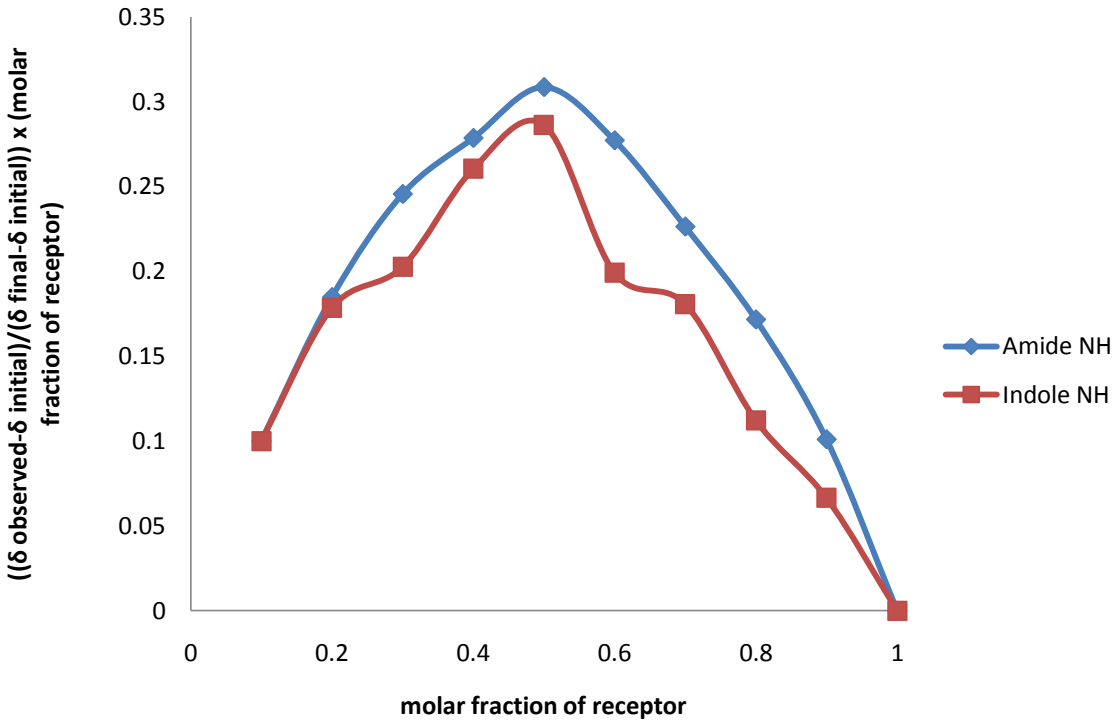

Receptor 224 *vs.* TBAOAc in DMSO-d_6/H_2O 0.5%

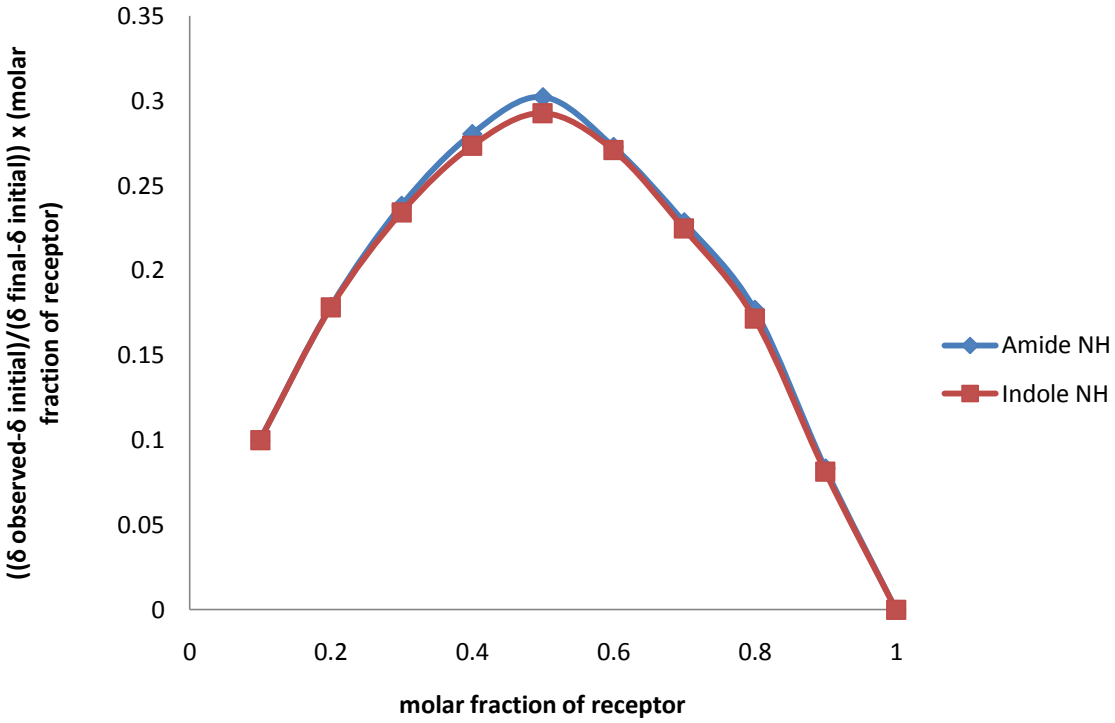

Receptor 224 *vs.* TBAOBz in DMSO-d_6/H_2O 0.5%

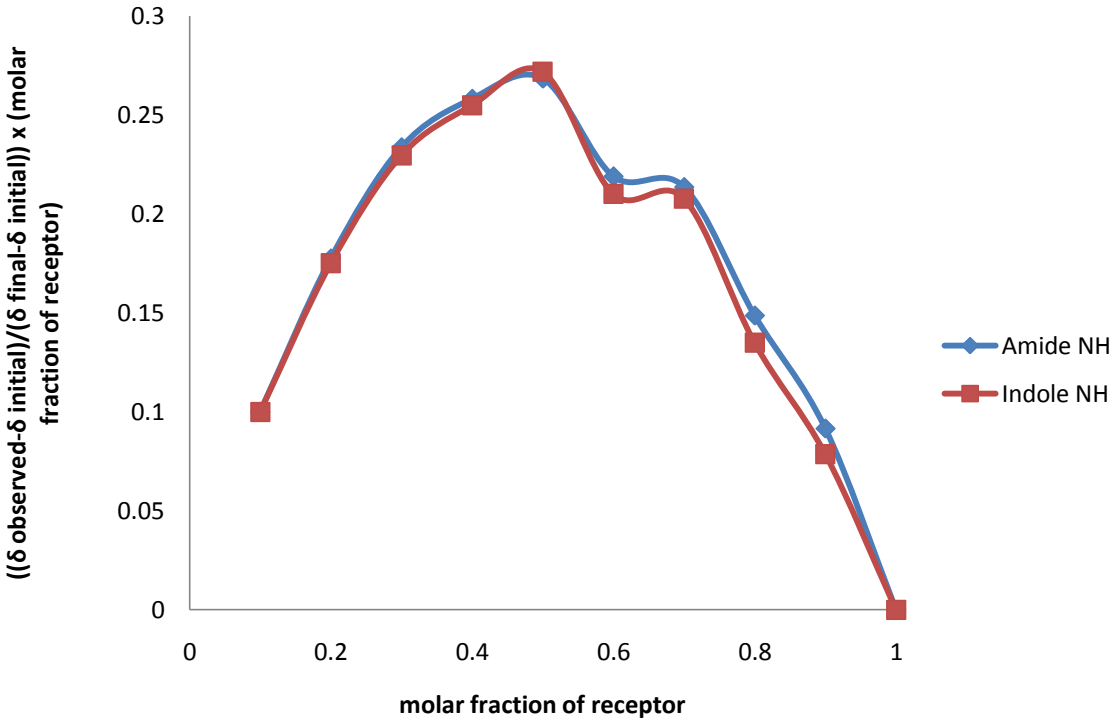

Receptor 226 *vs.* TBACl in DMSO-d_6/H_2O 0.5% (urea NH)

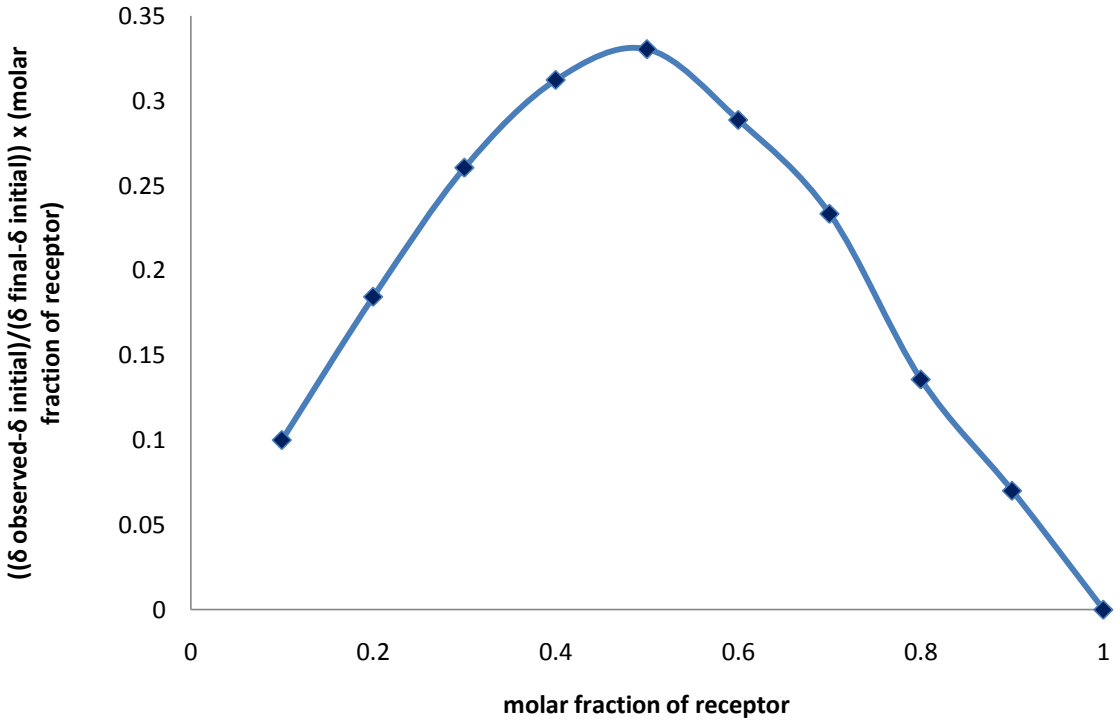

Receptor 226 *vs.* TBAH_2PO_4 in DMSO-d_6/H_2O 0.5% (urea NH)

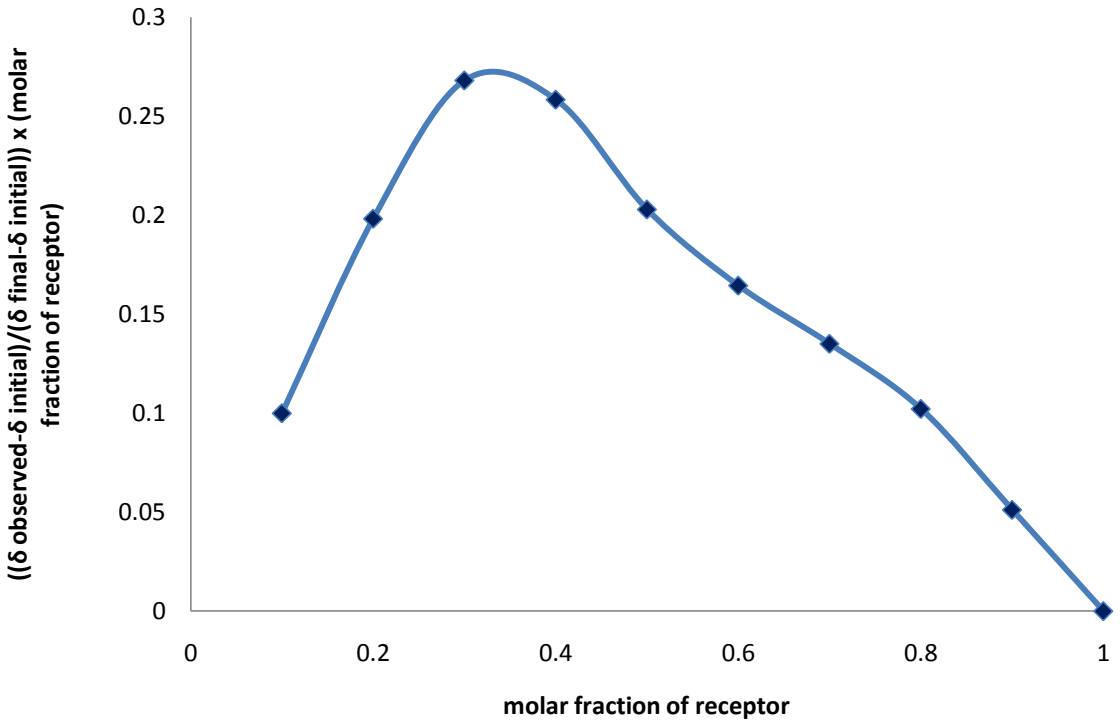

Receptor 226 *vs.* TBAOAc in DMSO-d_6/H_2O 0.5% (urea NH)

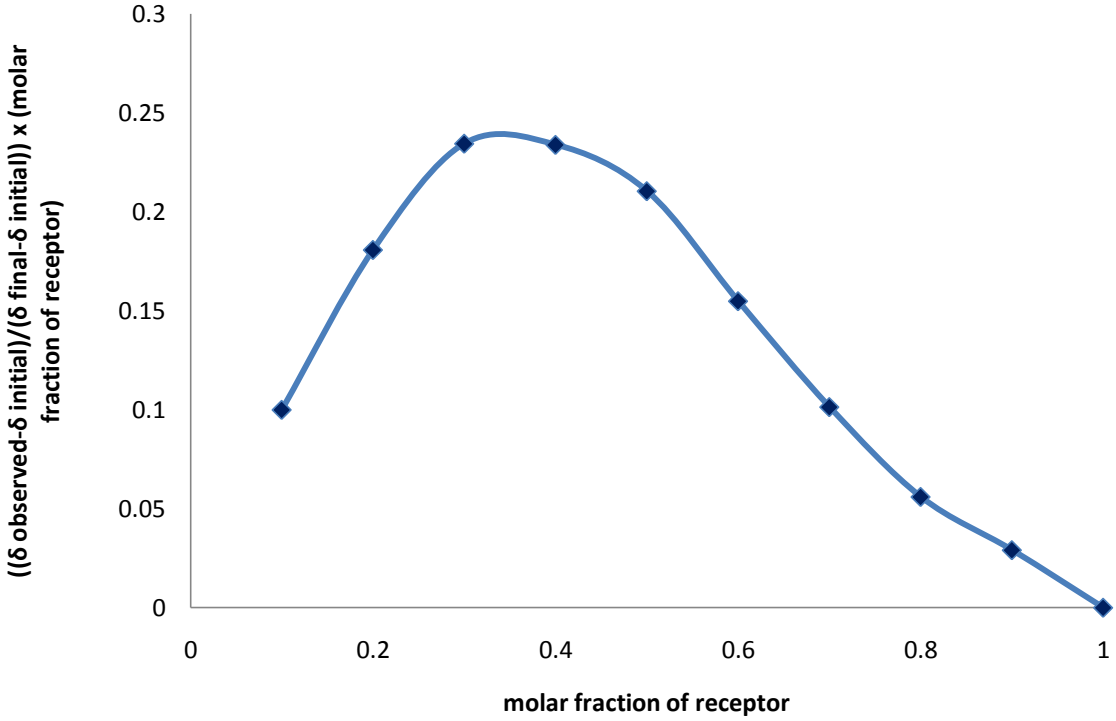

Receptor 226 *vs.* TBAOBz in DMSO-d_6/H_2O 0.5% (urea NH)

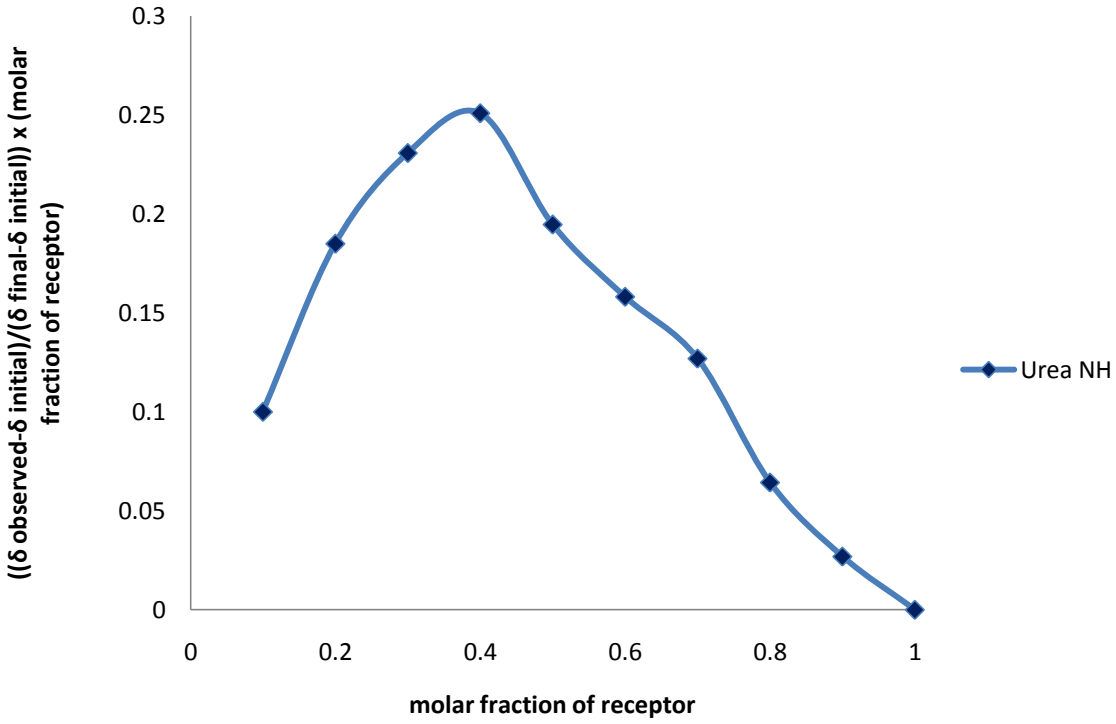

Receptor 227 *vs.* TBACl in DMSO-d_6/H_2O 0.5%

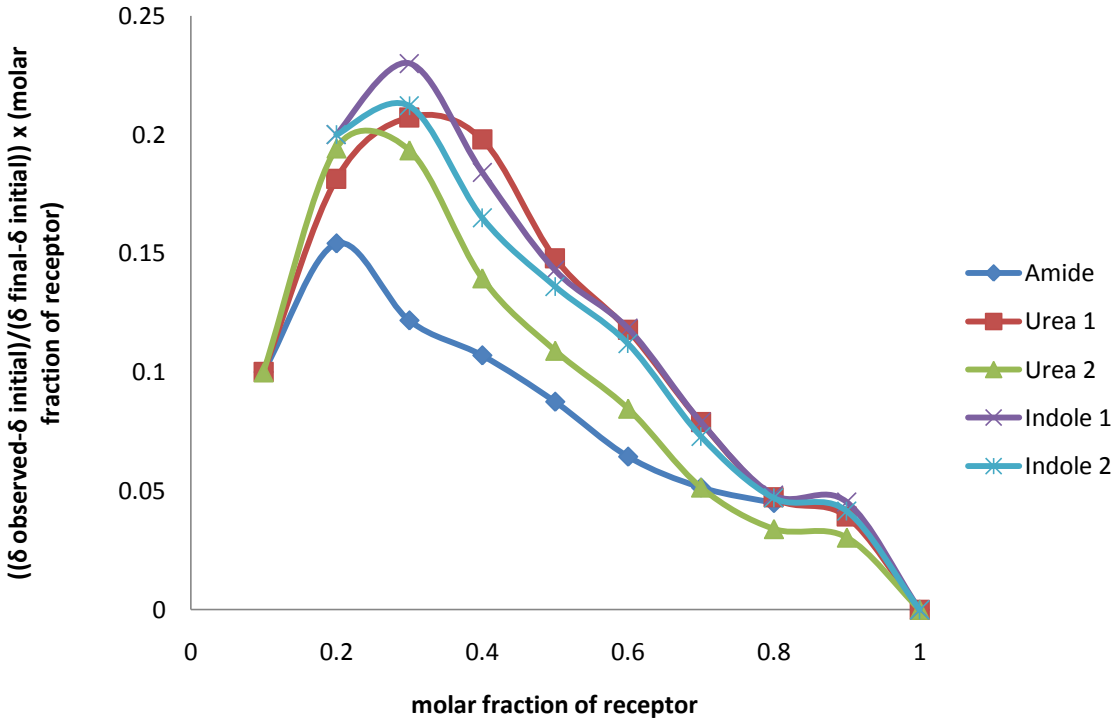

Receptor 227 *vs.* TBAH_2PO_4 in DMSO-d_6/H_2O 0.5%

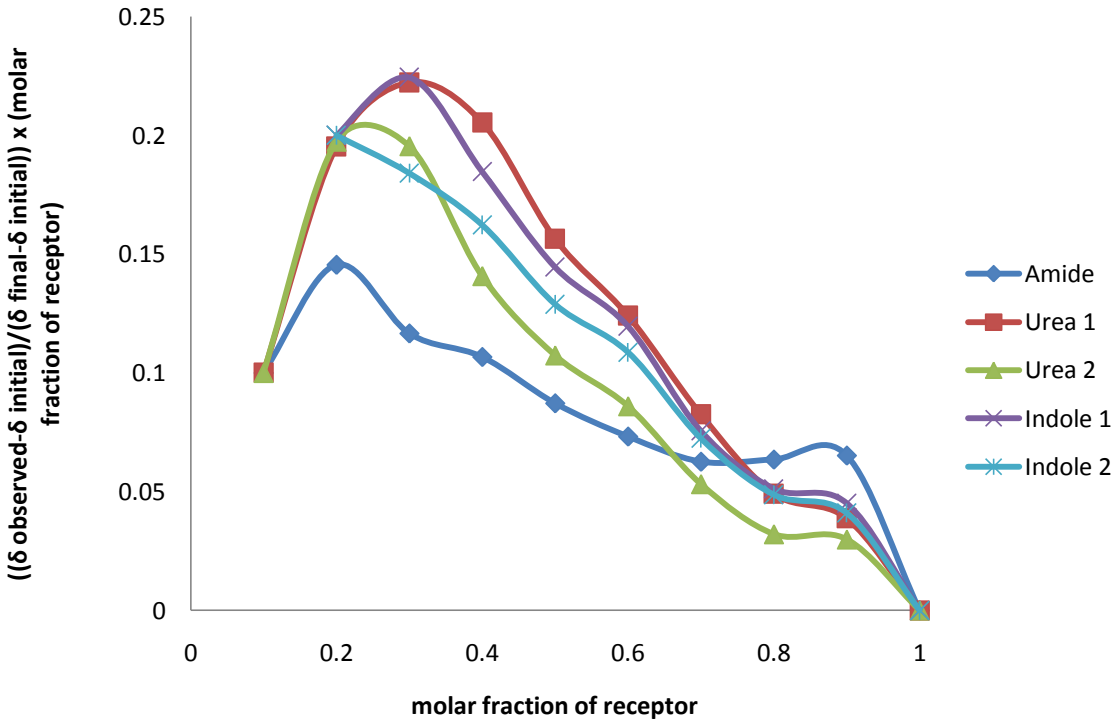

Receptor 227 *vs.* TBAOAc in DMSO-d_6/H_2O 0.5%

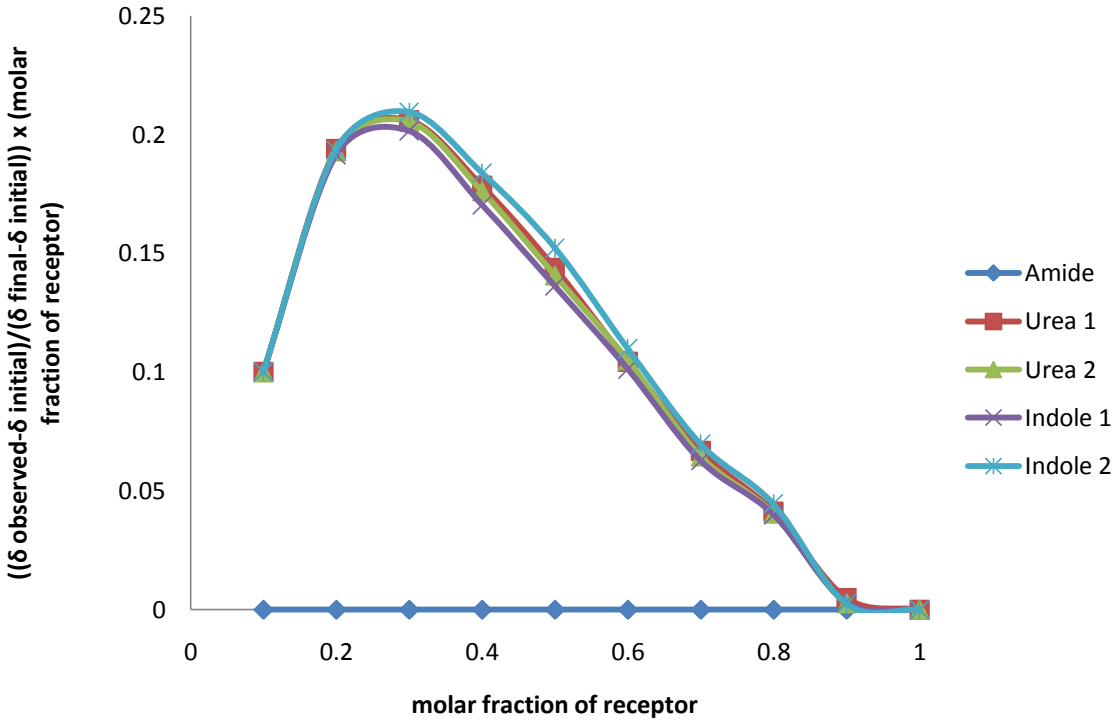

Receptor 227 *vs.* TBA_2SO_4 in DMSO-d_6/H_2O 0.5%

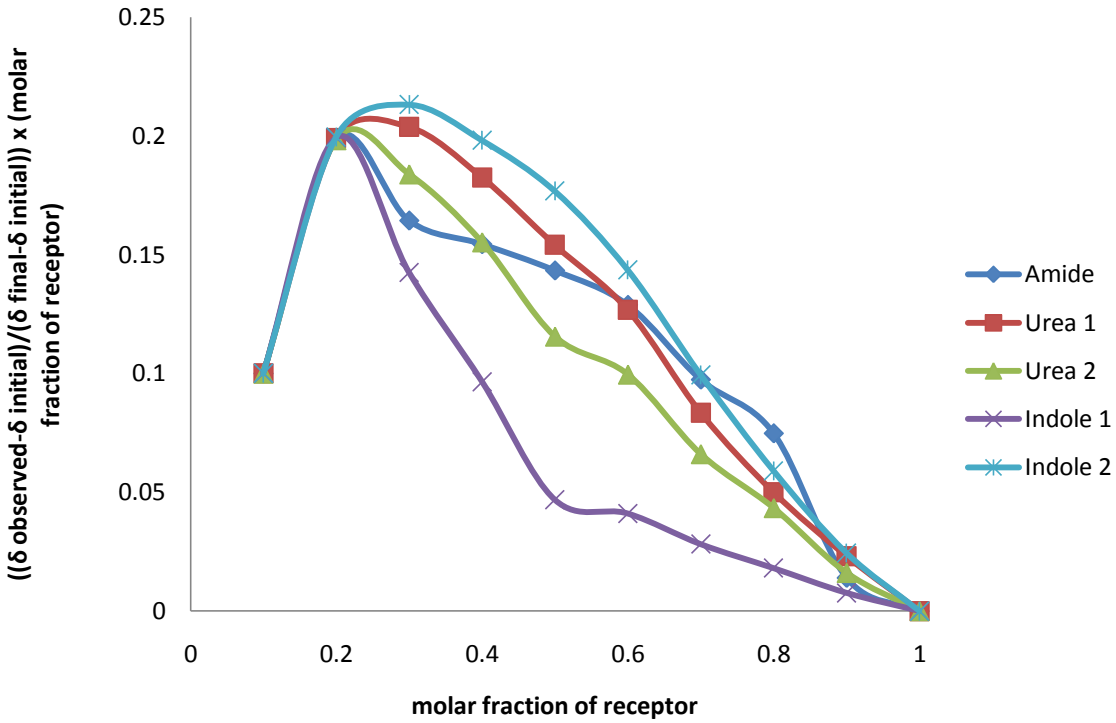

Receptor 231 *vs.* $TBAH_2PO_4$ in DMSO-d_6/H_2O 0.5%

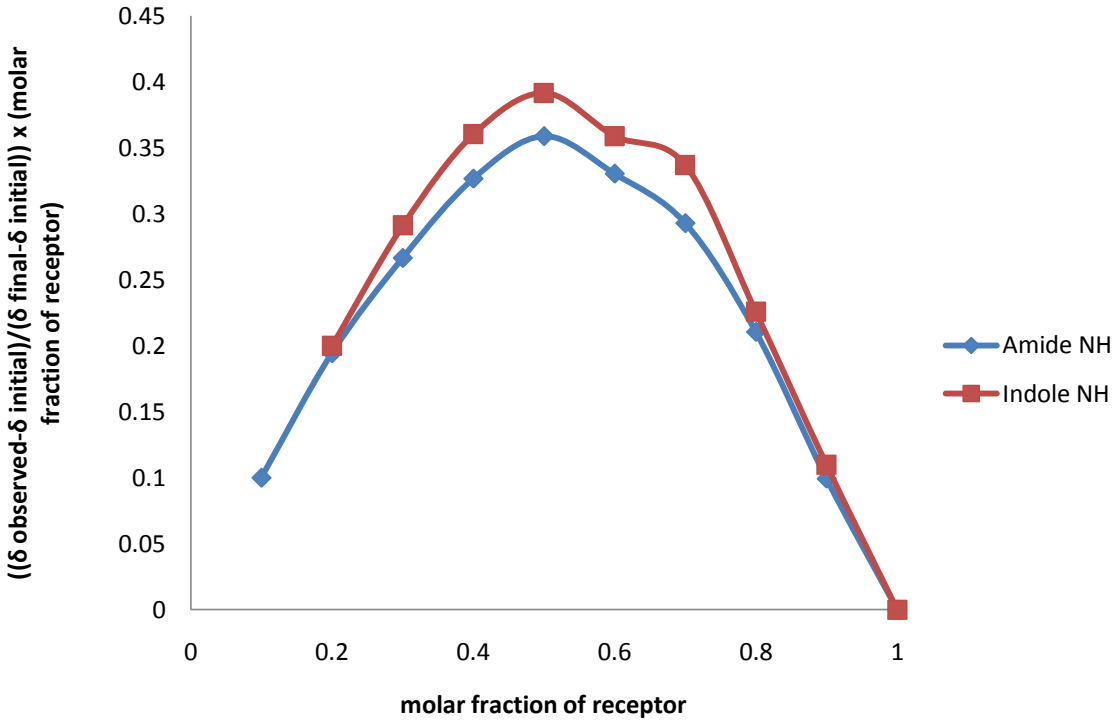

Receptor 231 *vs.* TBAOAc in DMSO-d_6/H_2O 0.5%

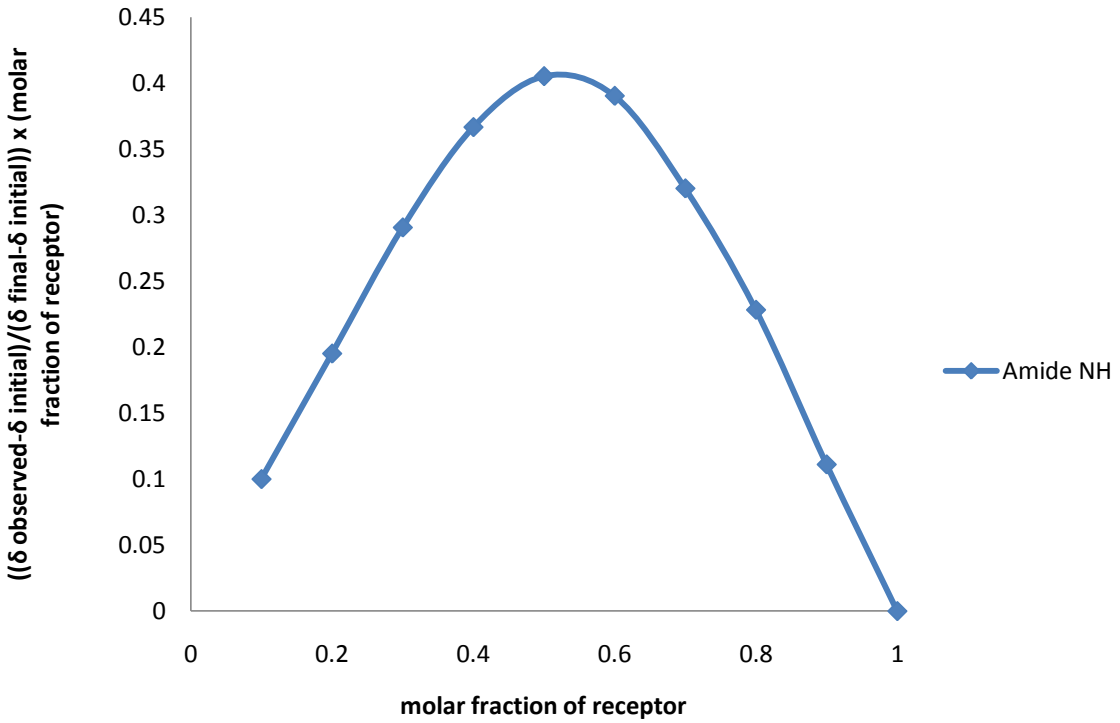

Receptor 231 *vs.* TBAOBz in DMSO-d_6/H_2O 0.5%

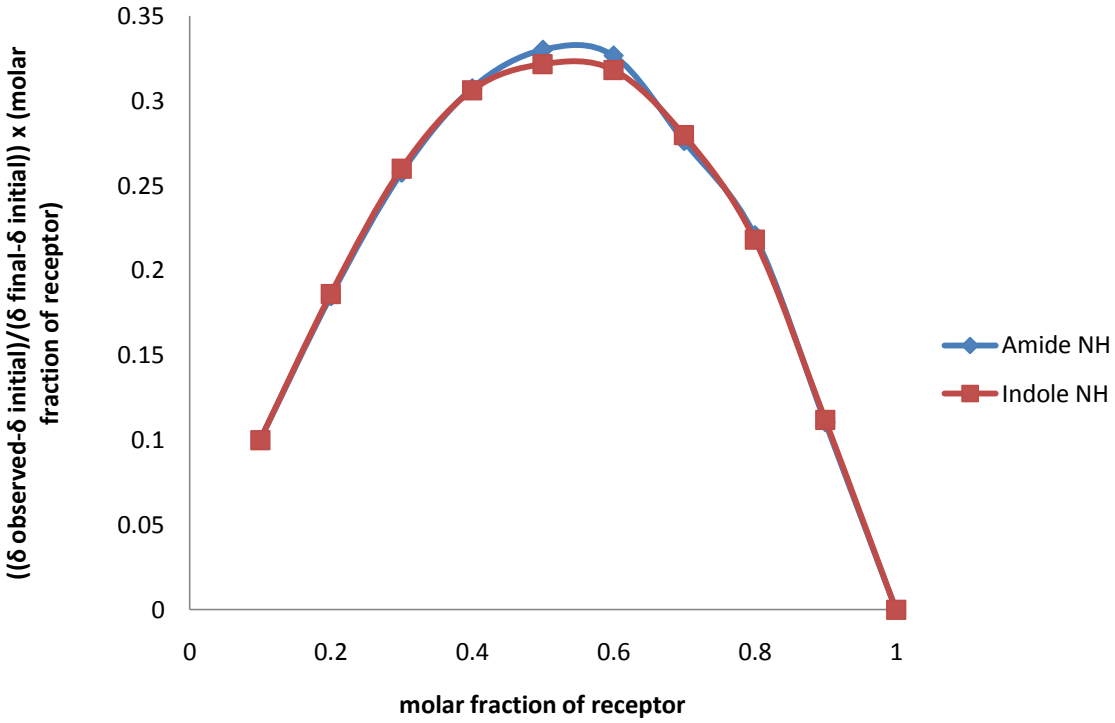

Receptor 232 *vs.* TBACl in DMSO-d_6/H_2O 0.5%

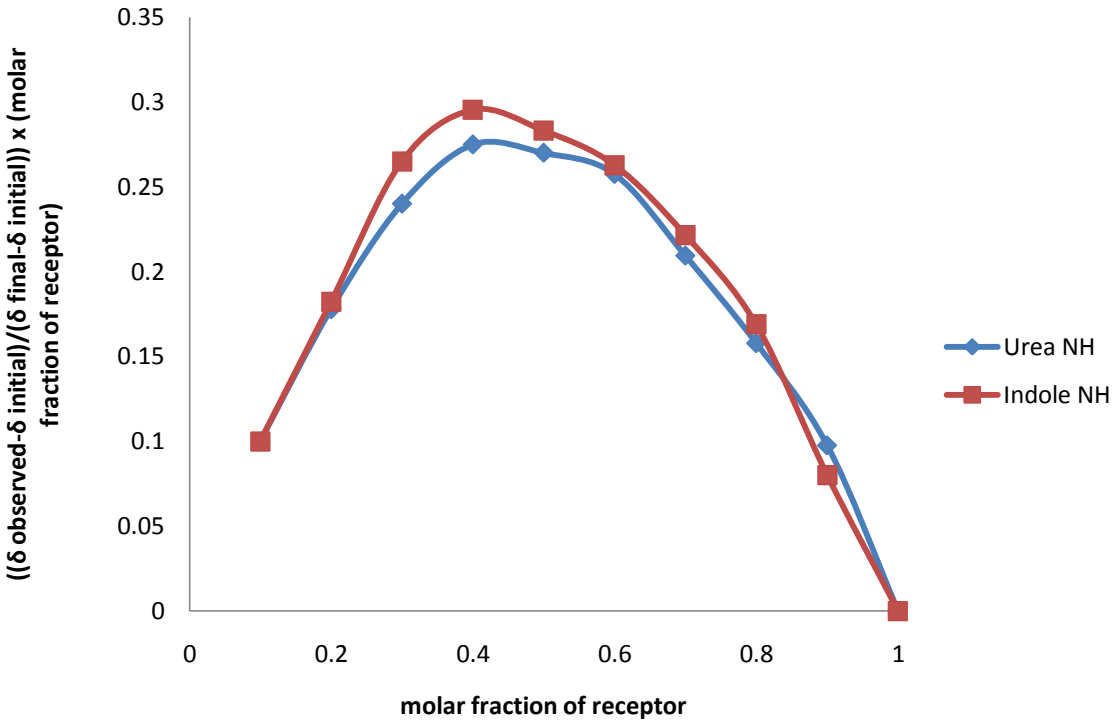

Receptor 232 *vs.* $TEAHCO_3$ in DMSO-d_6/H_2O 0.5%

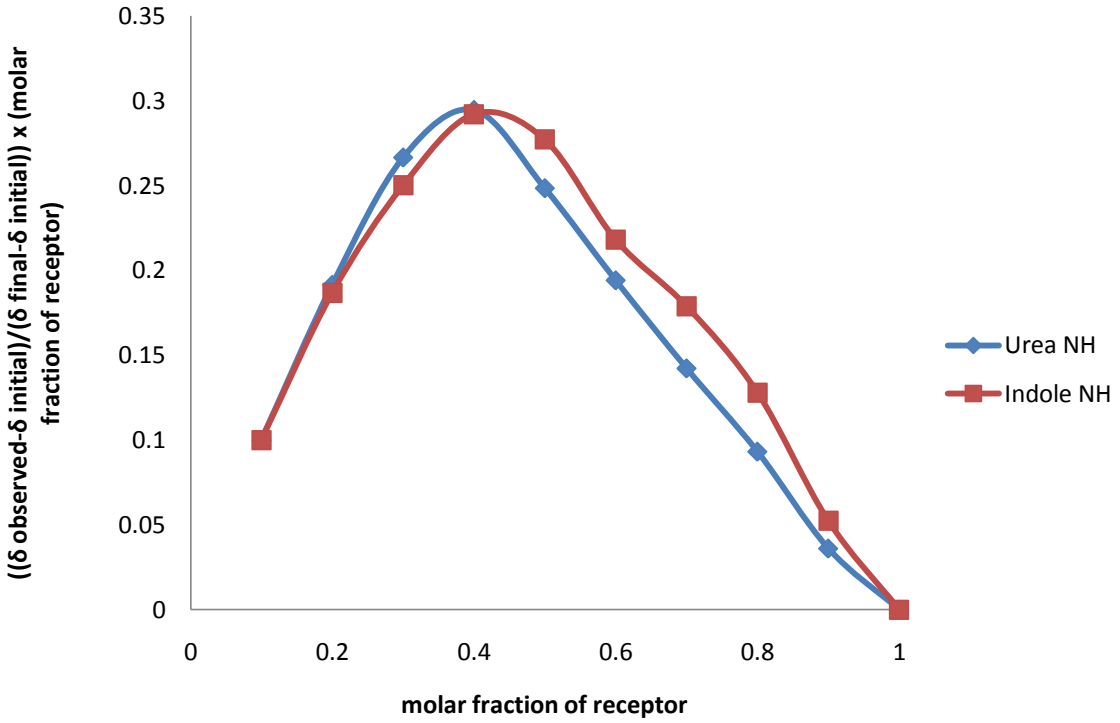

Receptor 232 *vs.* TBAOAc in DMSO-d_6/H_2O 0.5%

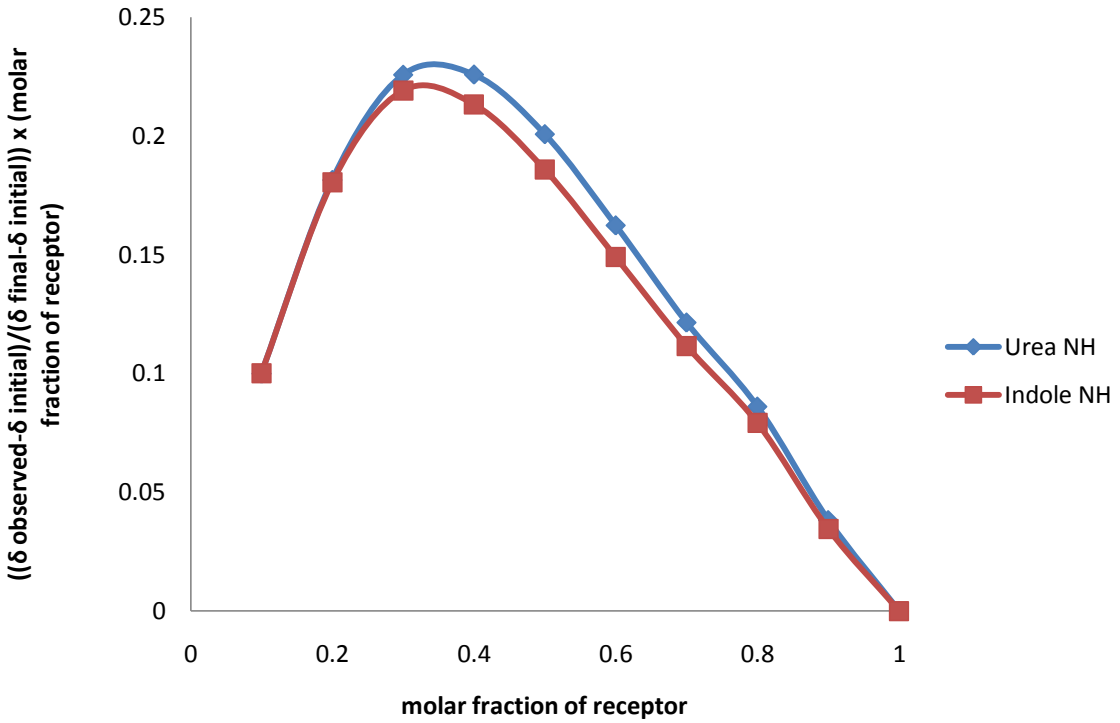

Receptor 232 *vs.* TBAOBz in DMSO-d_6/H_2O 0.5%

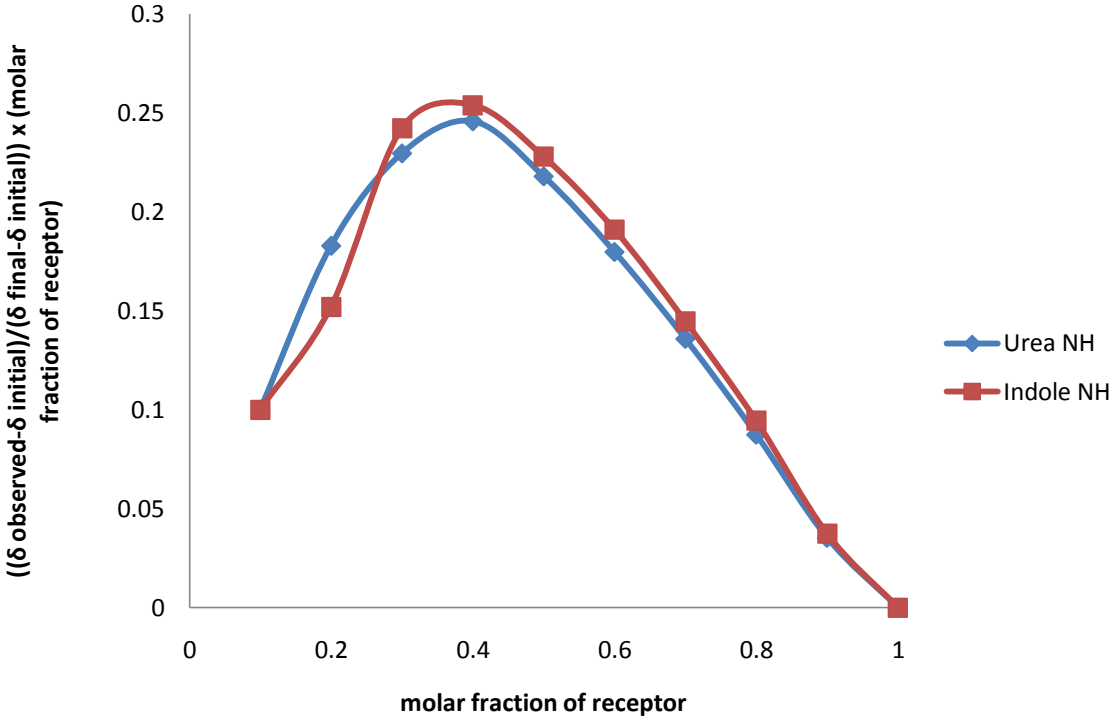

Receptor 232 *vs.* TBA_2SO_4 in DMSO-d_6/H_2O 0.5%

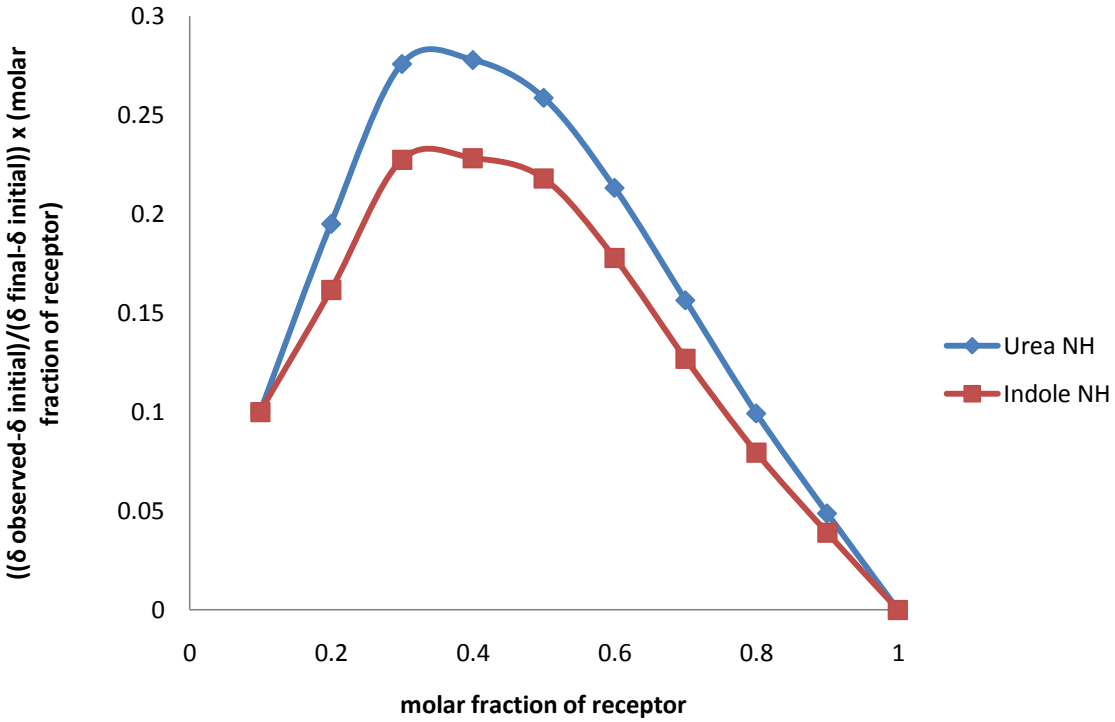

Job plots for Chapter Five

Receptor 234 *vs.* $TBAH_2PO_4$ in DMSO-d_6/H_2O 0.5% (amide NH)

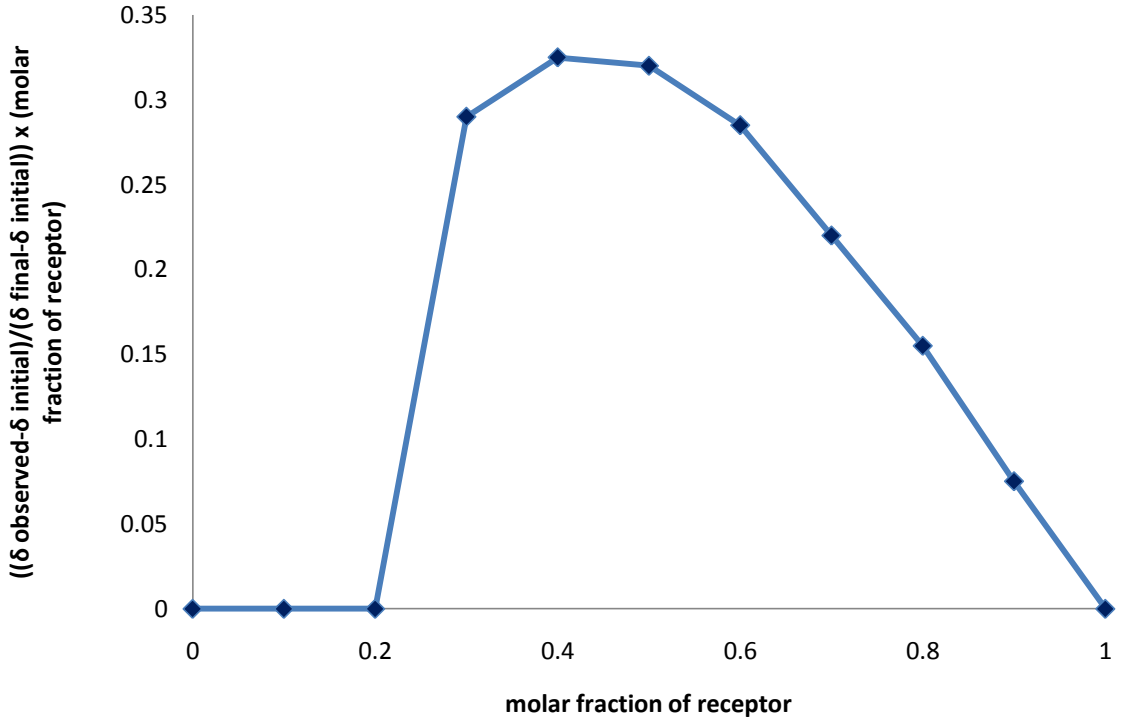

Receptor 234 *vs.* TBAOAc in DMSO-d_6/H_2O 0.5% (amide NH)

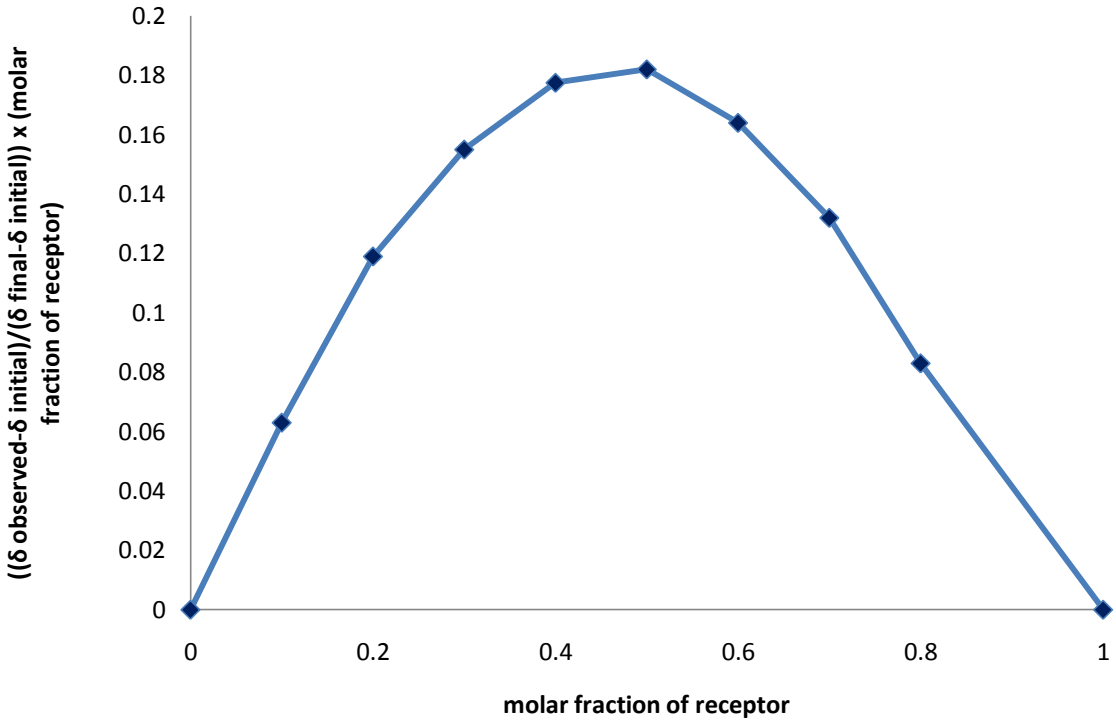

Receptor 234 vs. TBAOBz in DMSO-d6/H2O 0.5% (amide NH)

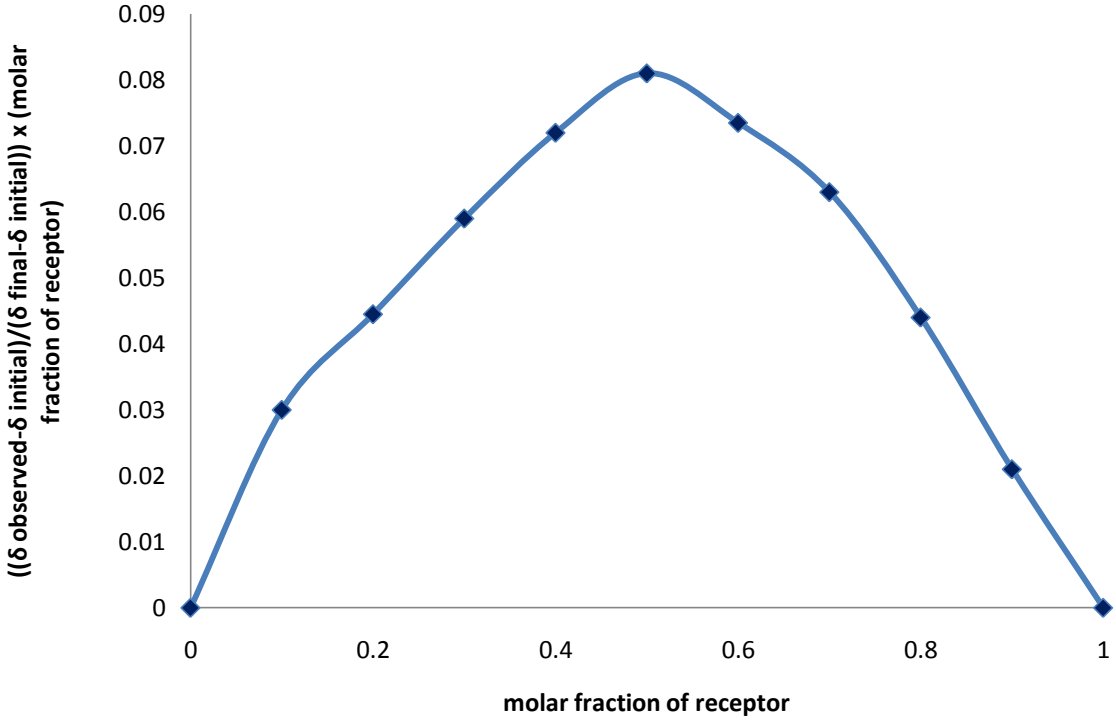

Receptor 234 *vs.* TBAF in DMSO-d_6/H_2O 0.5% (amide NH)

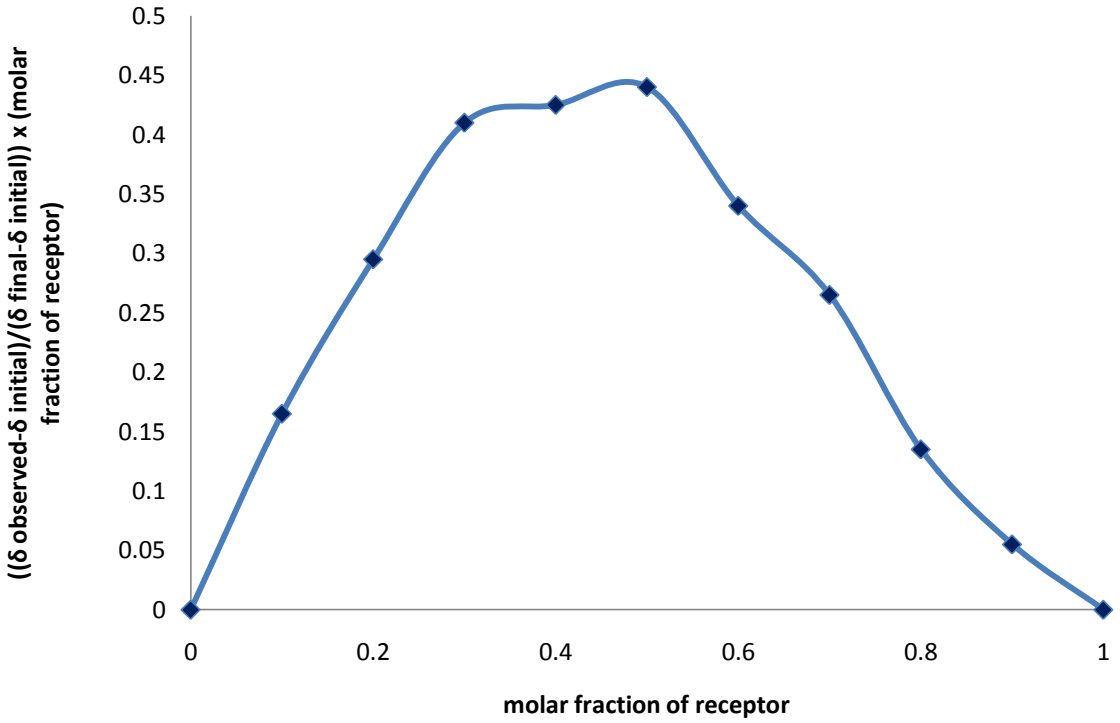

Receptor 235 *vs.* TBAH_2PO_4 in DMSO-d_6/H_2O 0.5% (amide NH)

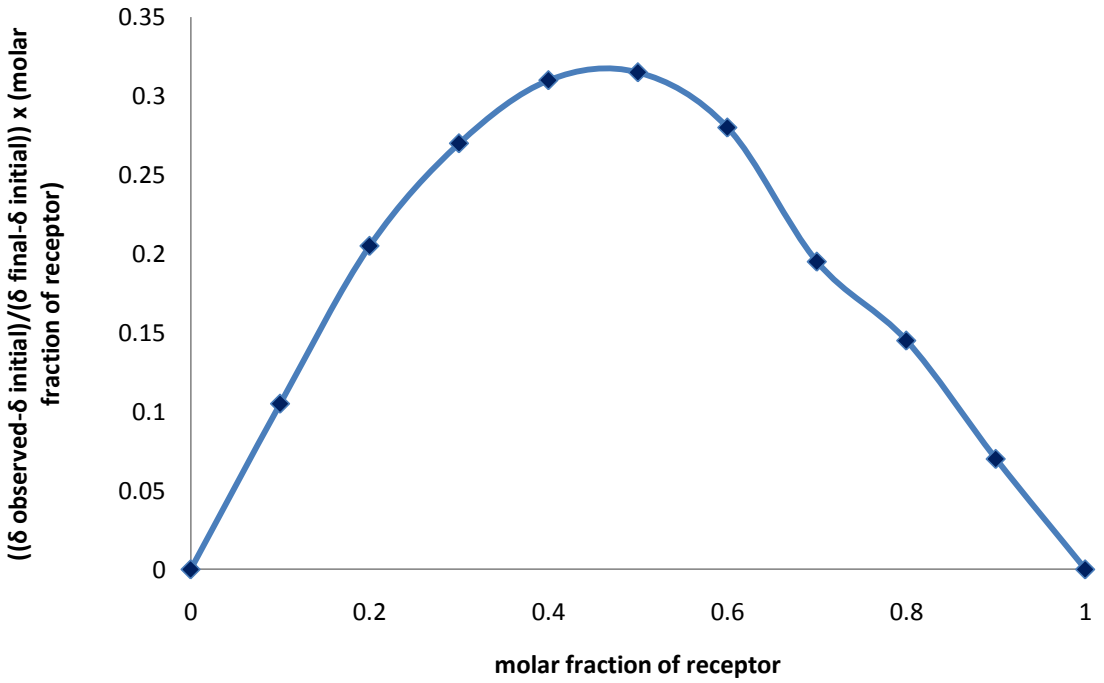

Receptor 235 *vs.* TBAOAc in DMSO-d_6/H_2O 0.5% (amide NH)

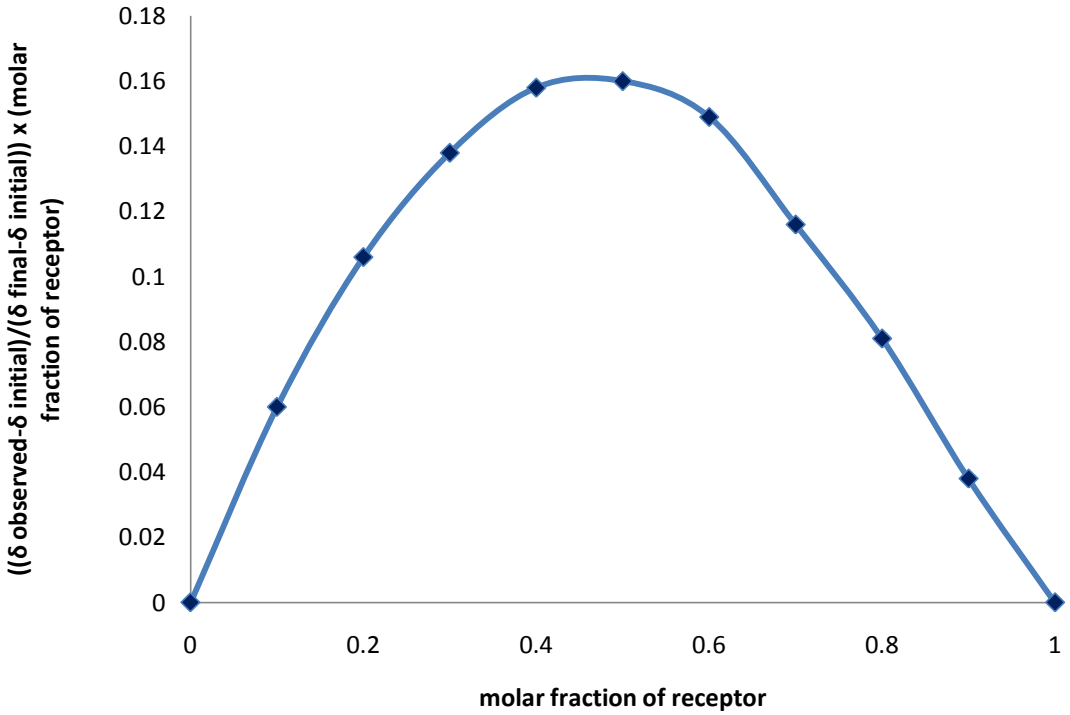

Receptor 235 vs. TBAOBz in DMSO-d6/H2O 0.5% (amide NH)

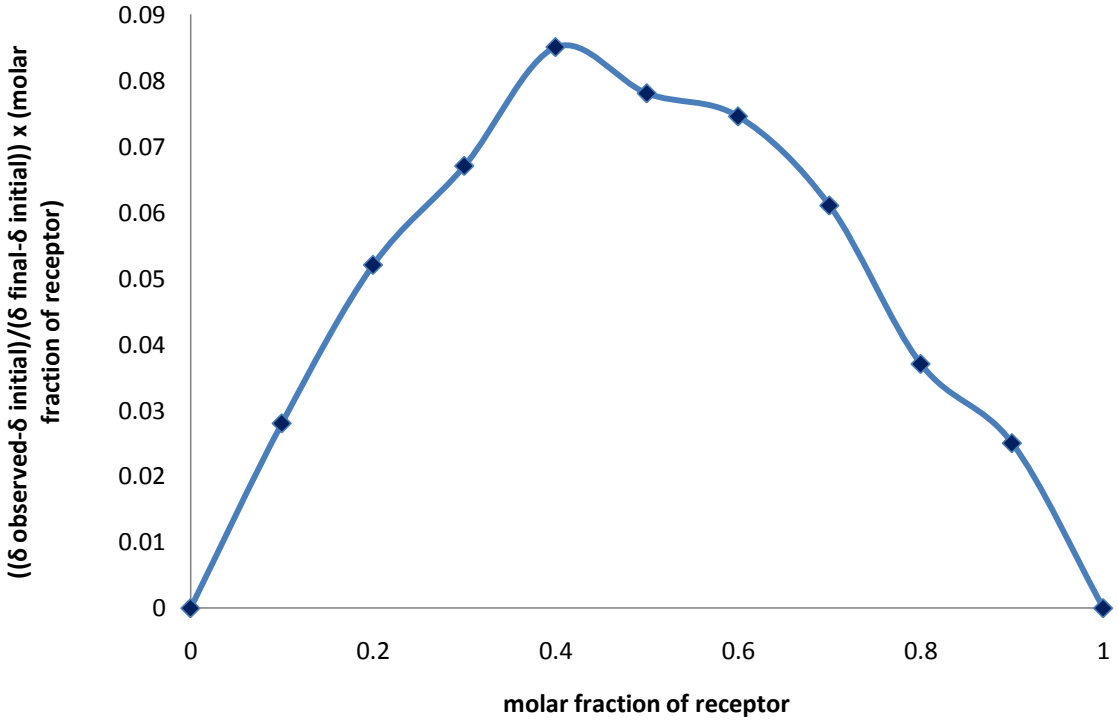

Receptor 236 *vs.* $TBAH_2PO_4$ in DMSO-d_6/H_2O 0.5% (amide NH)

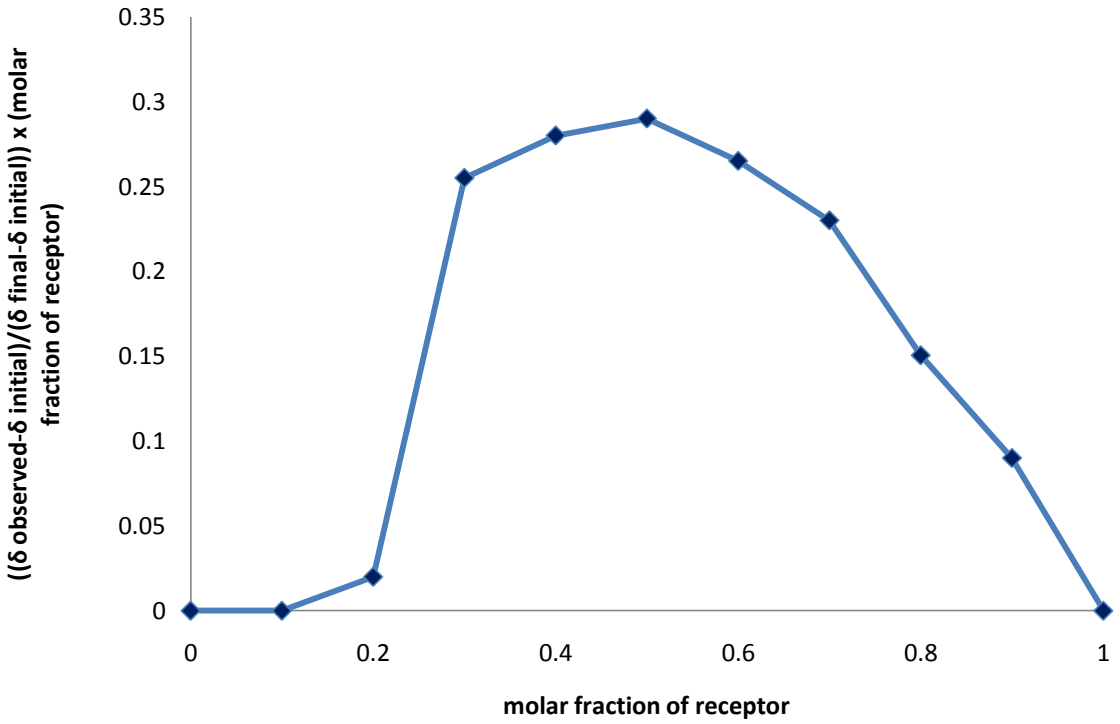

Receptor 236 *vs.* TBAOAc in DMSO-d_6/H_2O 0.5% (amide NH)

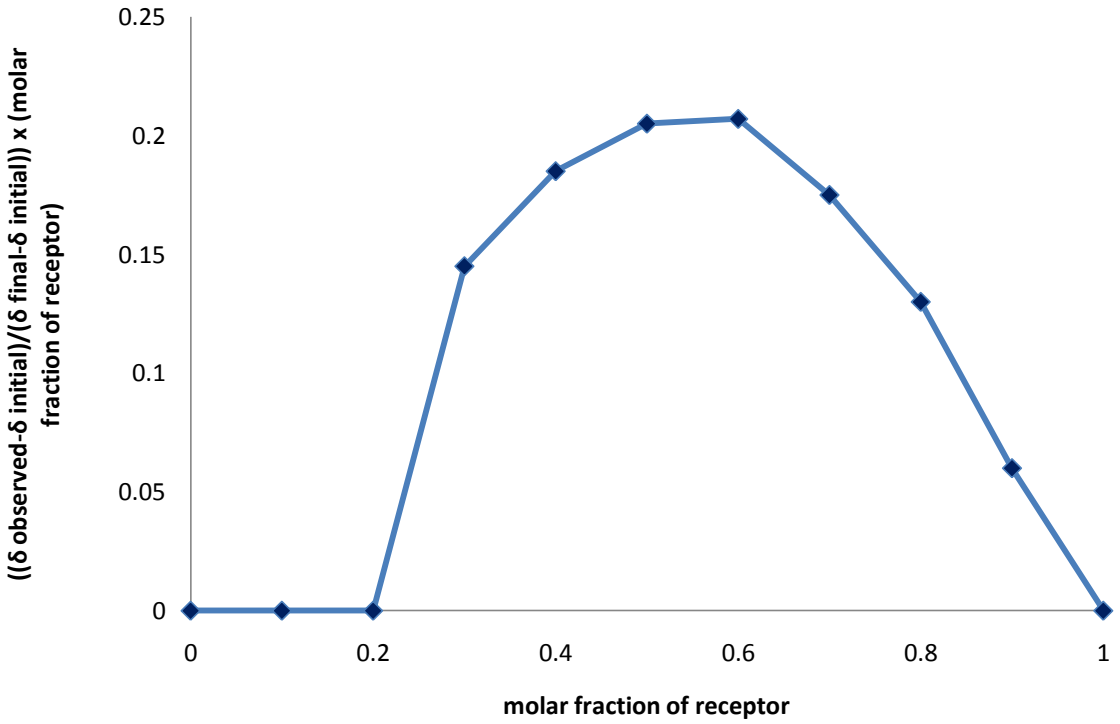

Receptor 236 *vs.* TBAOBz in DMSO-d_6/H_2O 0.5% (amide NH)

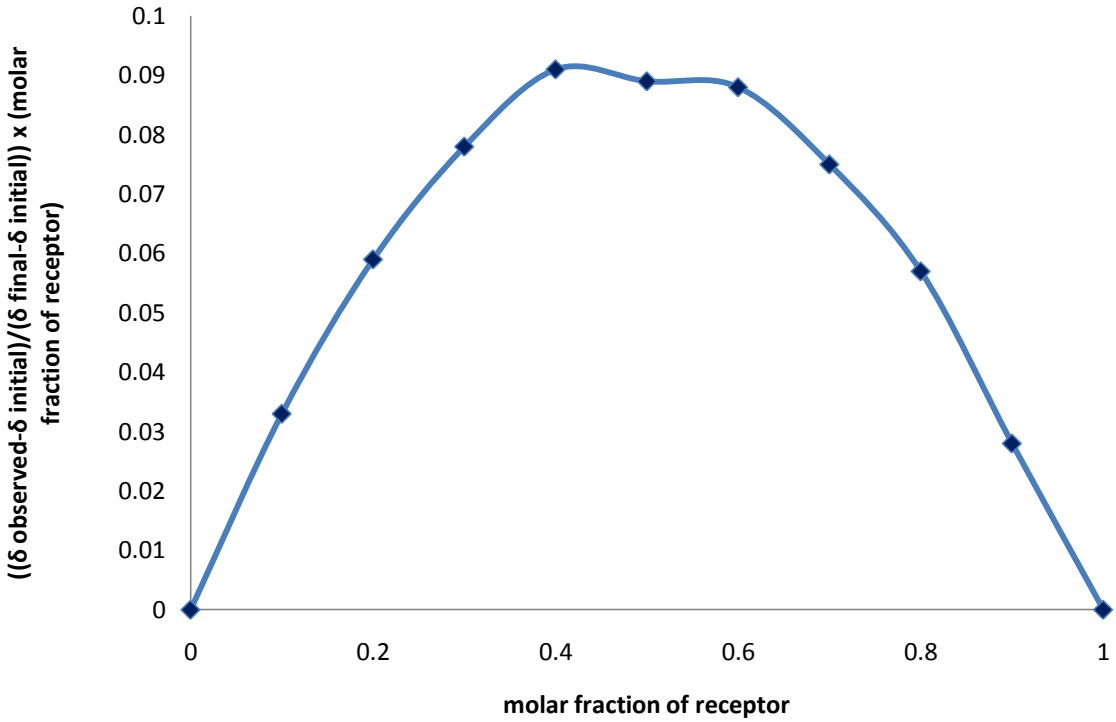

Receptor 237 vs. TBAH2PO4 in DMSO-d6/H2O 0.5% (amide NH)

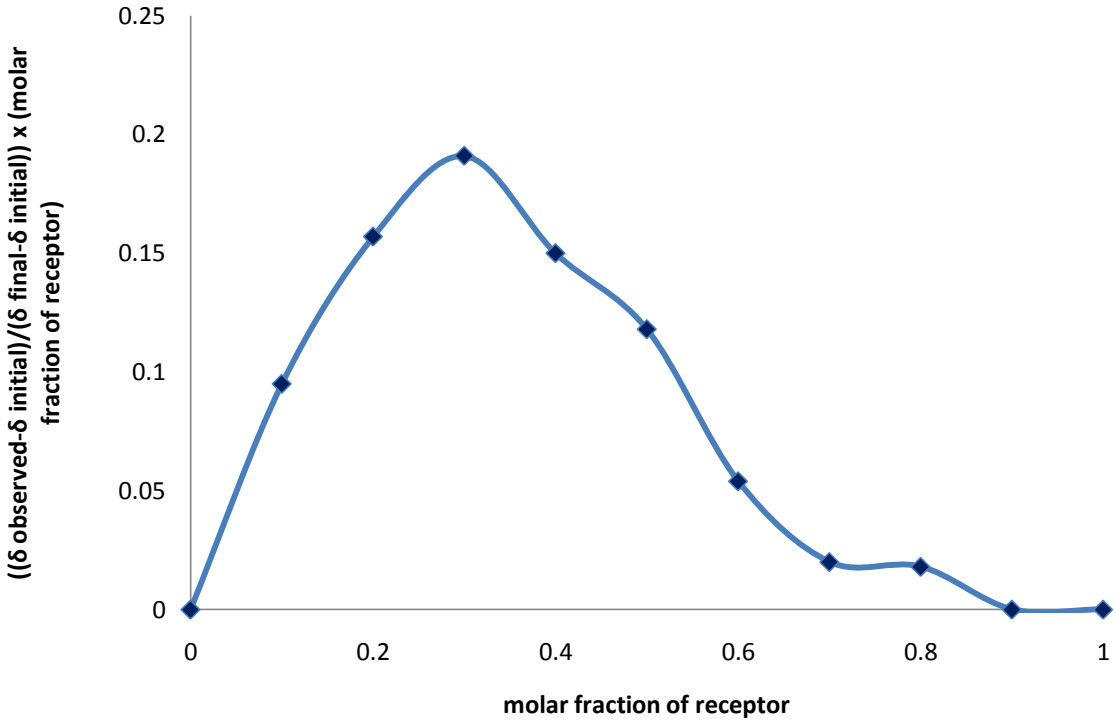

Receptor 237 *vs.* TBAOAc in DMSO-d_6/H_2O 0.5% (amide NH)

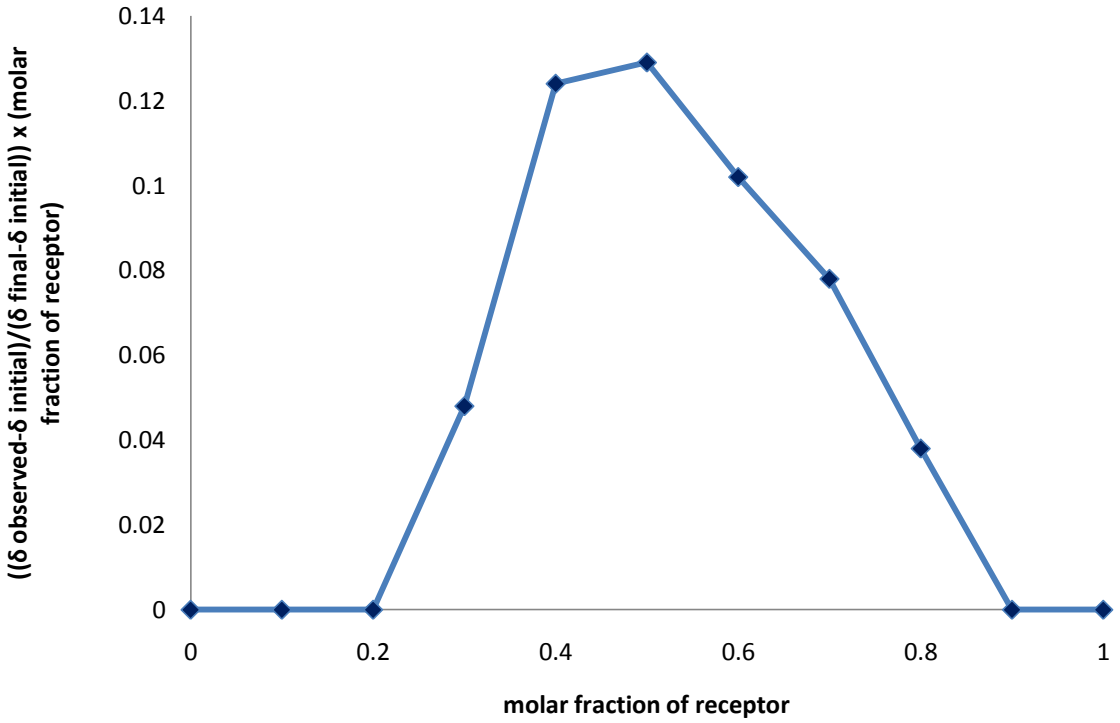

Receptor 237 *vs.* TBAOBz in DMSO-d_6/H_2O 0.5% (amide NH)

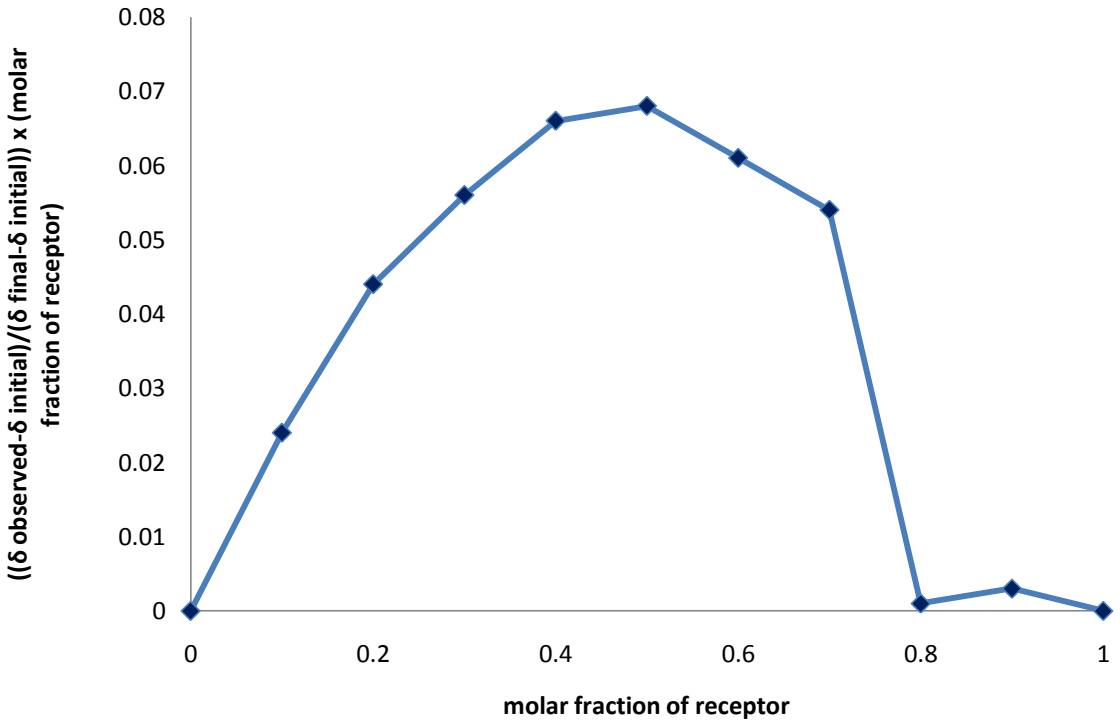

Receptor 238 *vs.* TBAOAc in DMSO-d_6/H_2O 0.5% (amide NH)

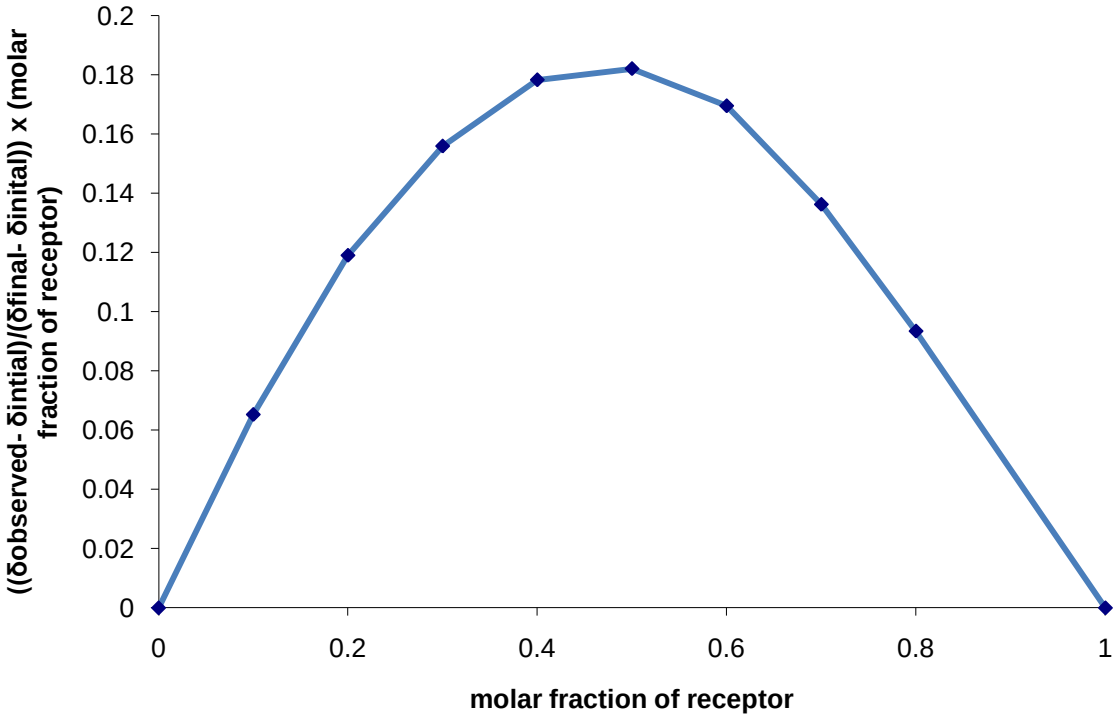

Receptor 238 *vs.* TBAF in DMSO-d_6/H_2O 0.5% (amide NH)

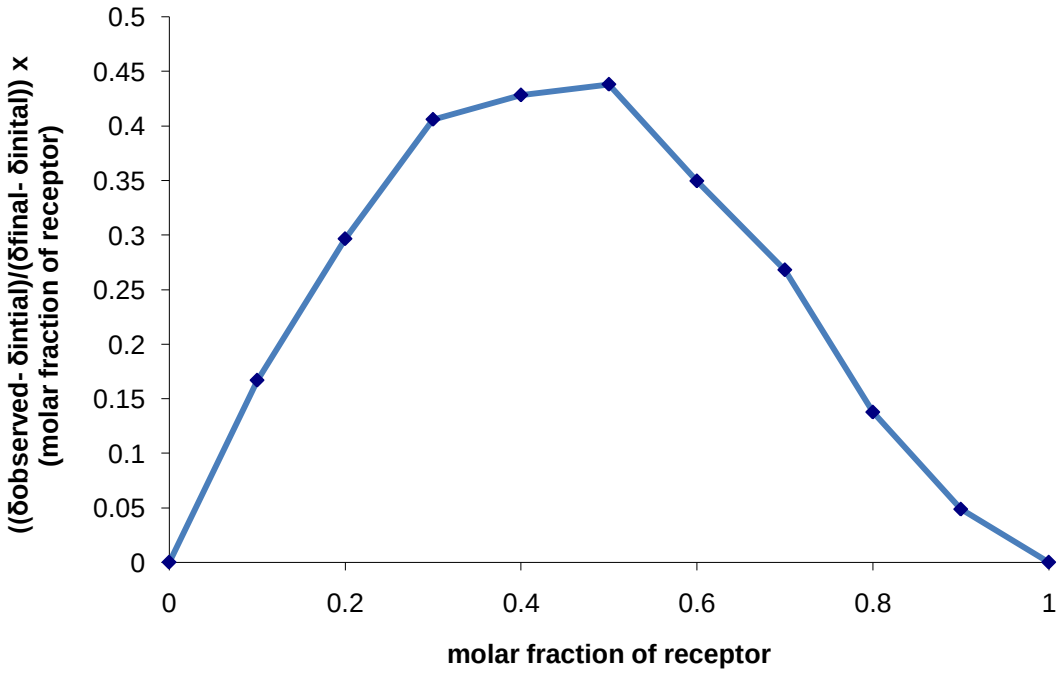

Receptor 238 *vs.* $TBAH_2PO_4$ in DMSO-d_6/H_2O 0.5% (amide NH)

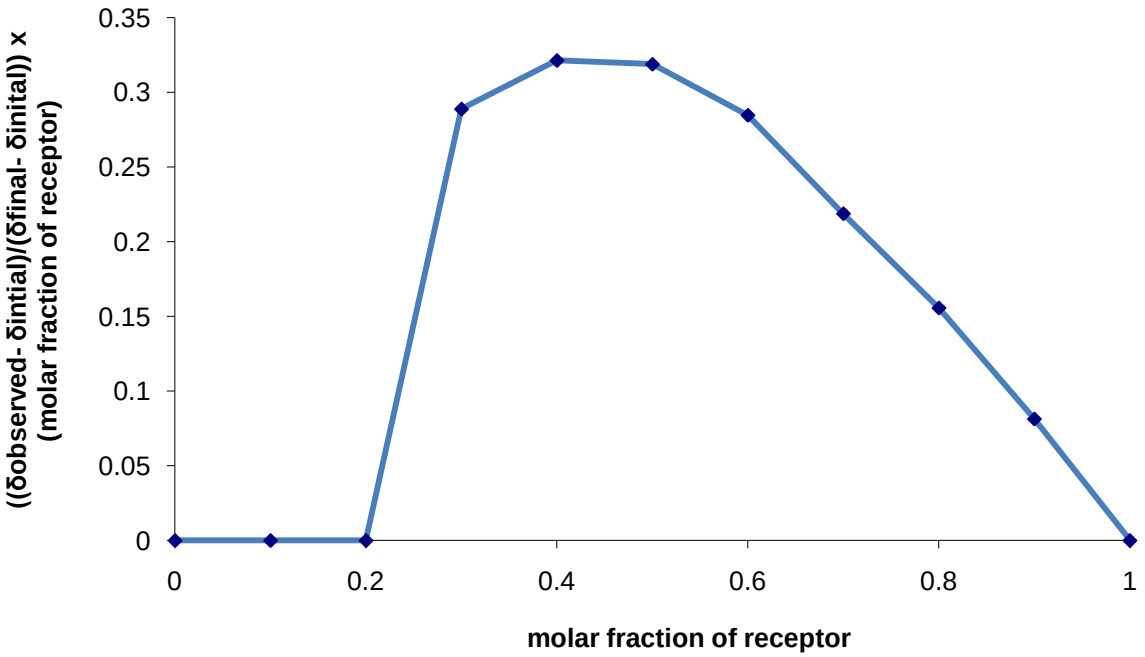

Appendix 4 – Proton NMR Change In Chemical Shift

Where complex binding events were observed in Chapters Three and Four, data collected from ^{1}H NMR titration experiments were used to compare the various binding modes observed of the receptor/anion complexes. The anions were added as the tetraethylammonium or tetrabutylammonium salt at 298 K in the appropriate DMSO-d_6/H_2O mixtures.

Graphs for Chapter Three

Receptor 219 *vs.* $TEAHCO_3$ in DMSO-d_6/H_2O 0.5%

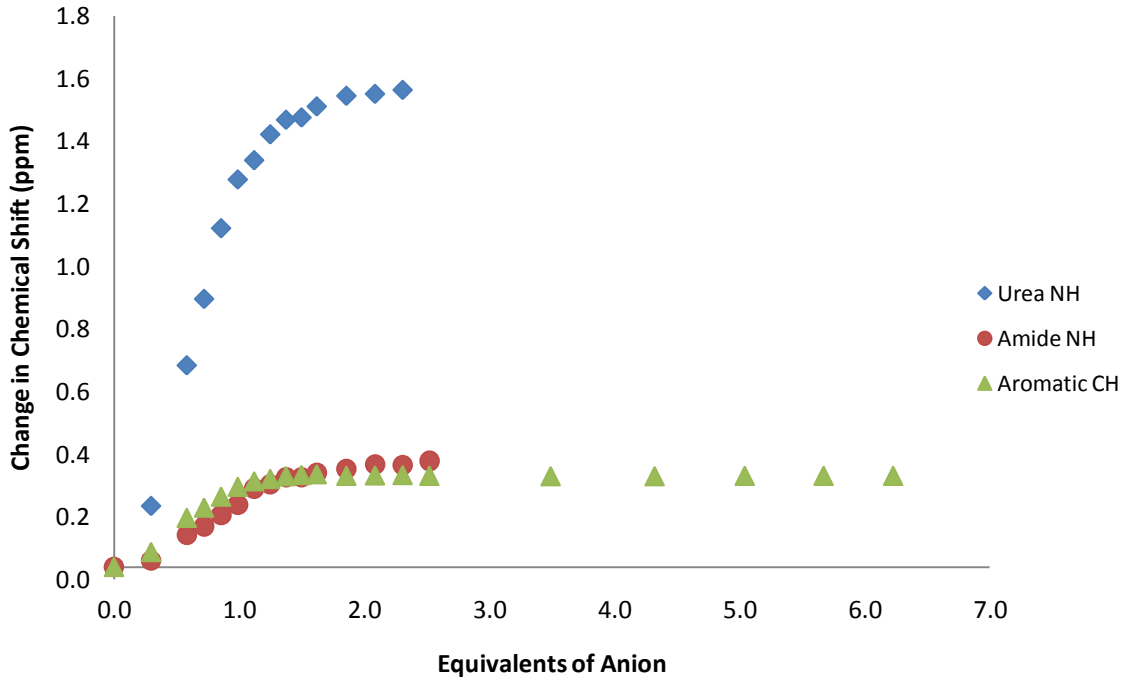

Receptor 219 *vs.* TBAOAc in DMSO-d_6/H_2O 0.5%

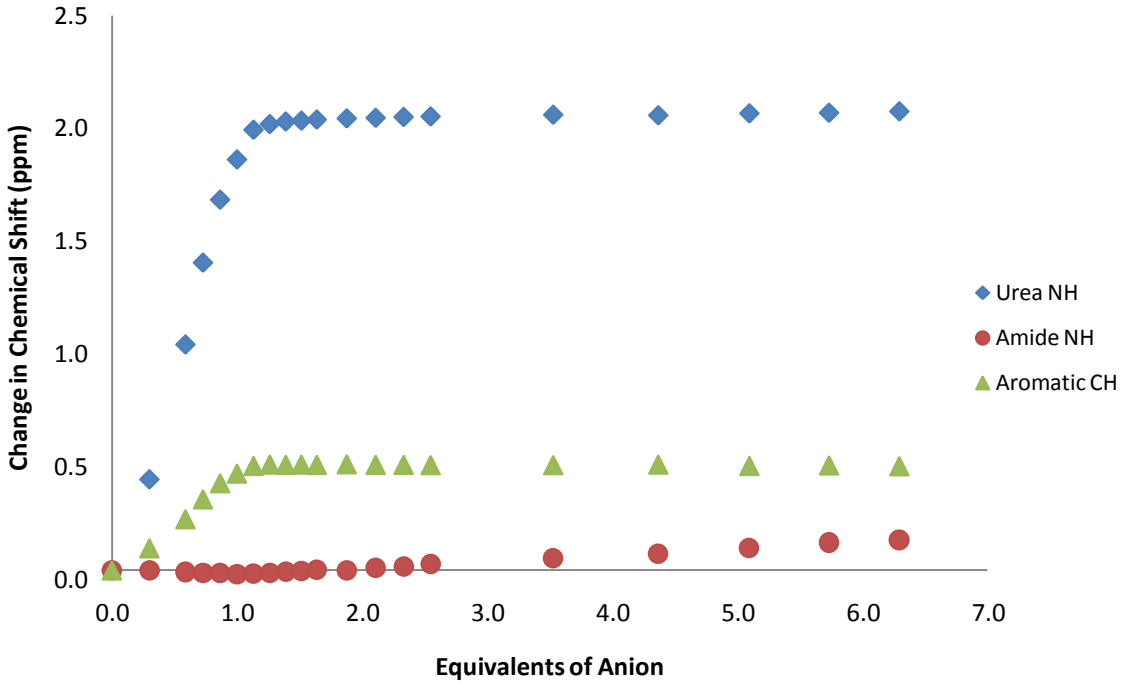

Receptor 219 *vs.* TBACl in DMSO-d_6/H_2O 0.5%

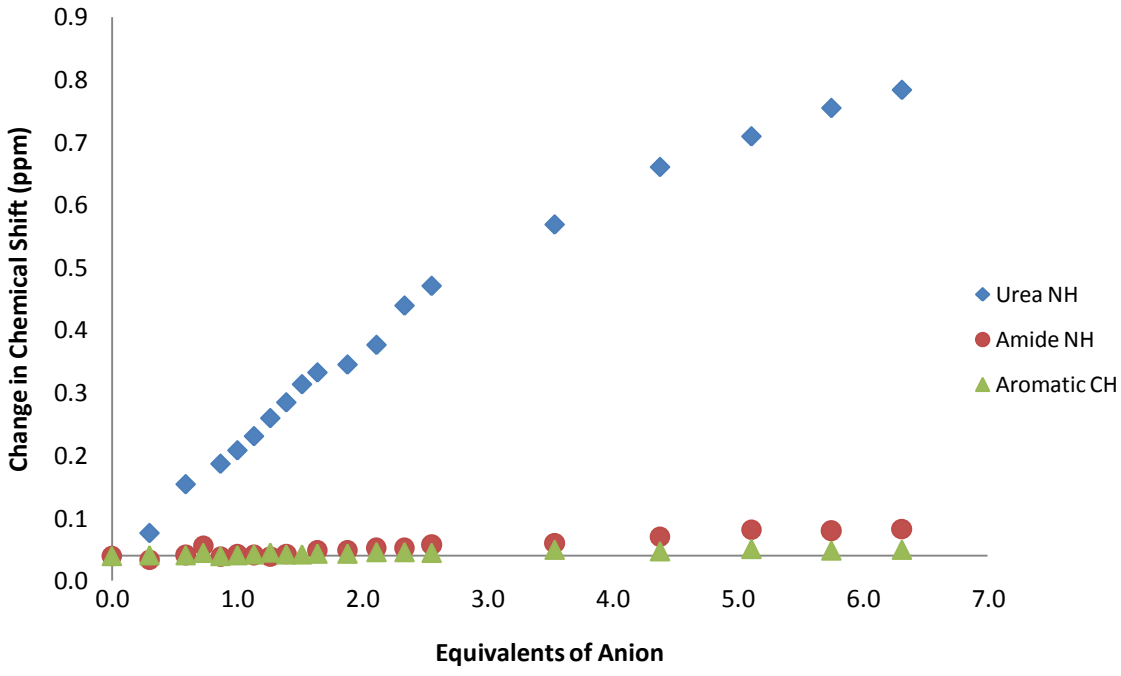

Receptor 219 *vs.* TBAOBz in DMSO-d_6/H_2O 10%

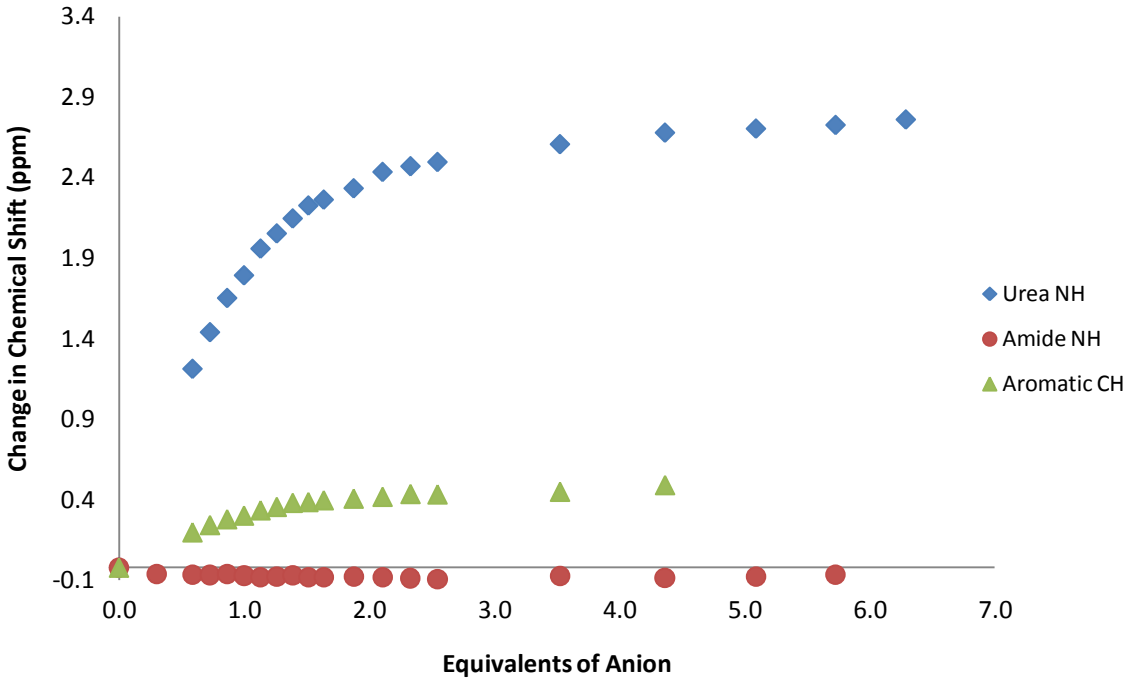

Receptor 219 *vs.* TBAOAc in DMSO-d_6/H_2O 10%

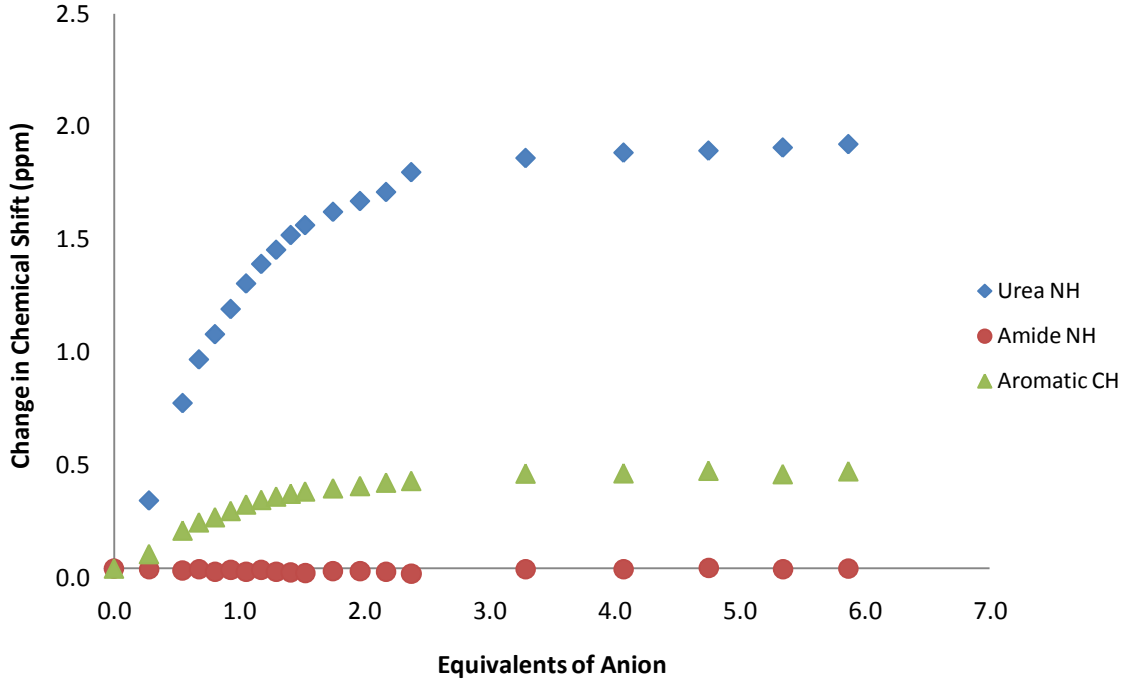

Receptor 219 *vs.* $TBAH_2PO_4$ in DMSO-d_6/H_2O 10%

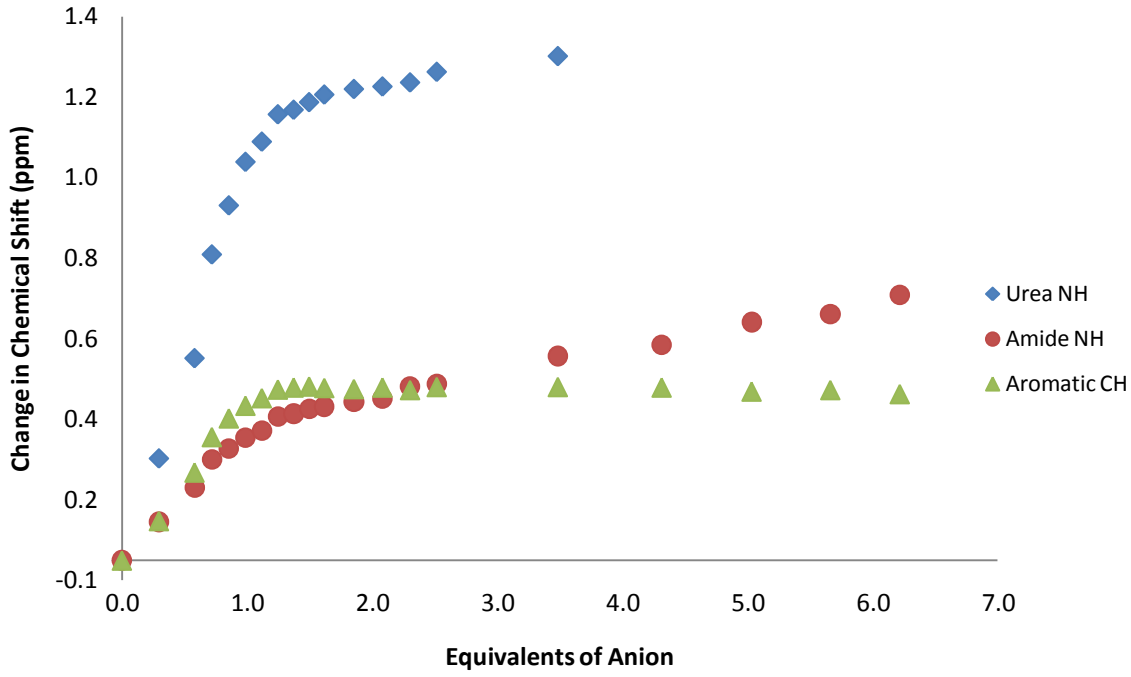

Receptor 220 *vs.* $TBAHSO_4$ in DMSO-d_6/H_2O 0.5%

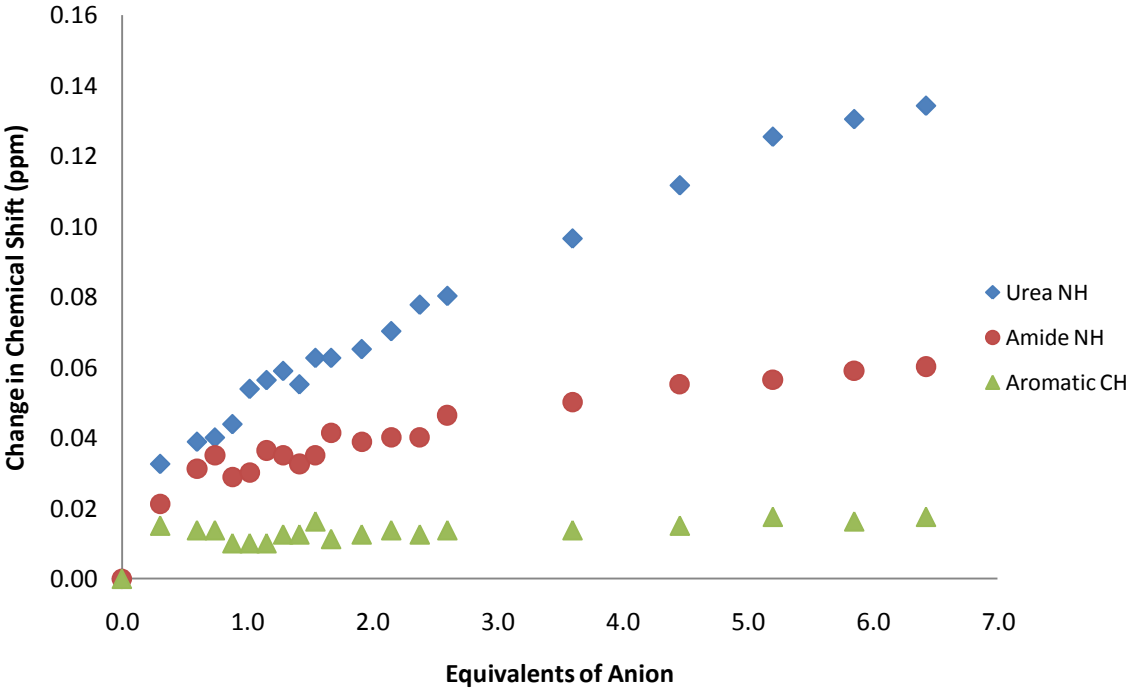

Receptor 220 *vs.* TBA_2SO_4 in DMSO-d_6/H_2O 0.5%

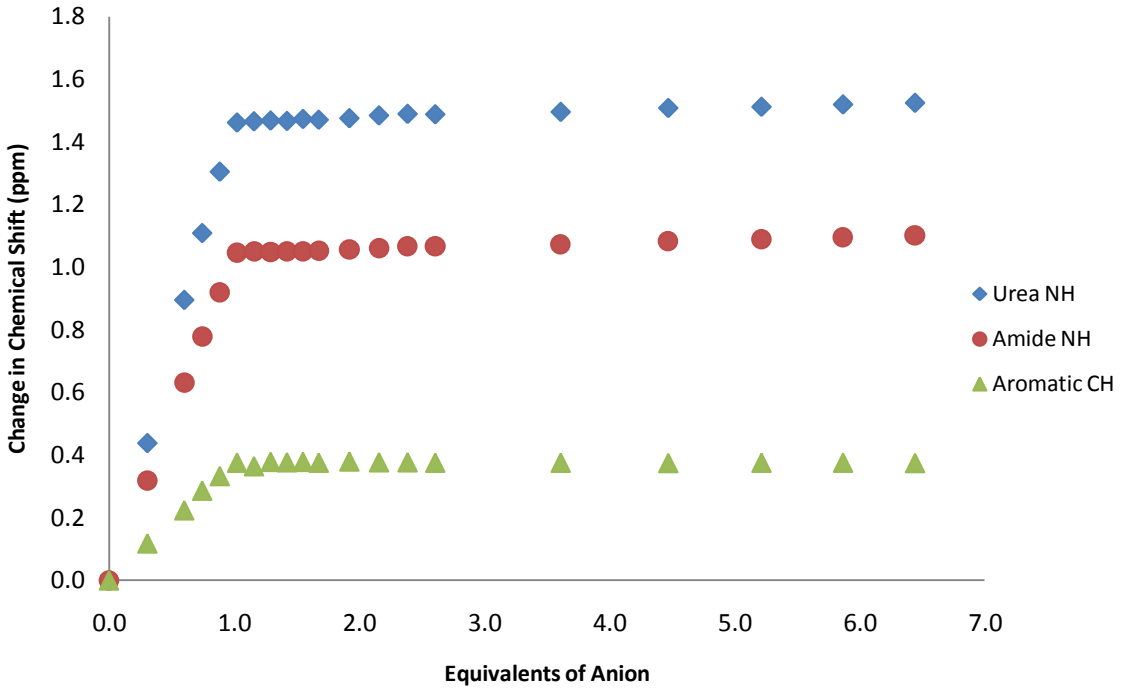

Receptor 220 *vs.* TBAOBz in DMSO-d_6/H_2O 0.5%

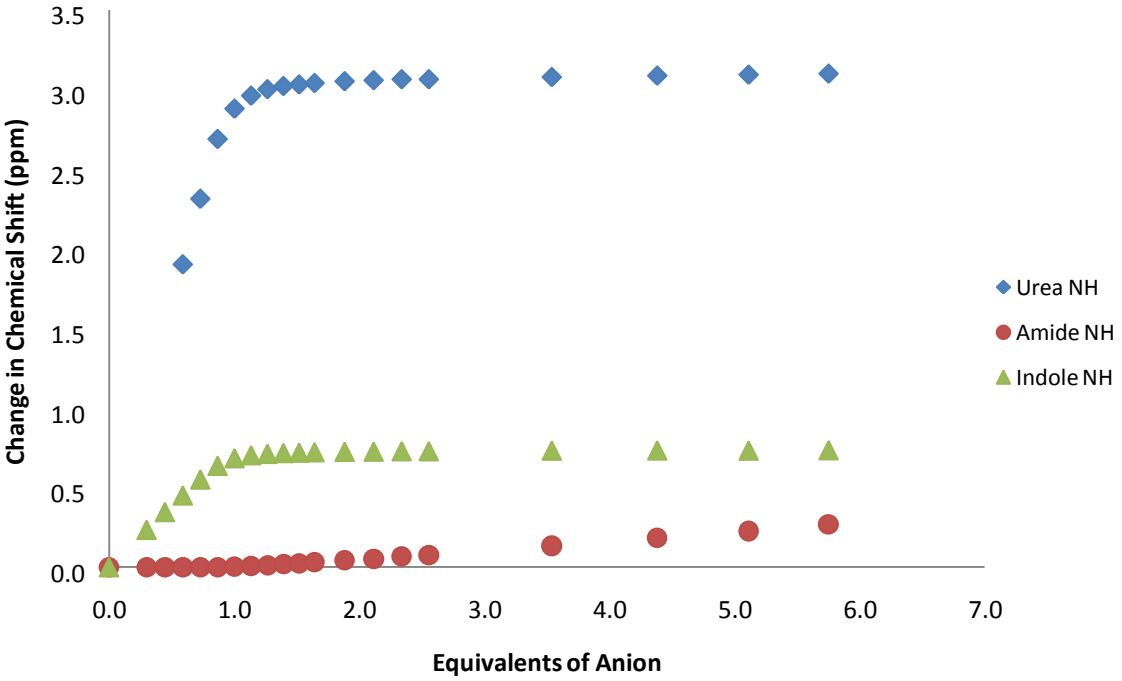

Receptor 220 *vs.* $TEAHCO_3$ in DMSO-d_6/H_2O 0.5%

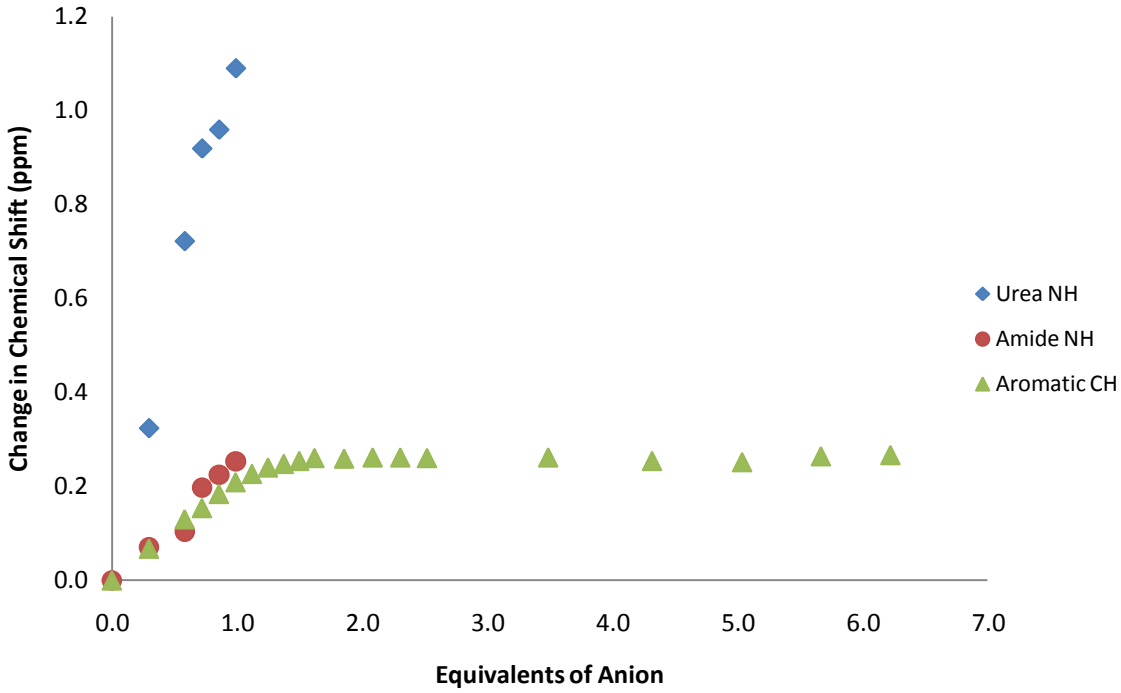

Receptor 220 *vs.* $TBAH_2PO_4$ in DMSO-d_6/H_2O 0.5%

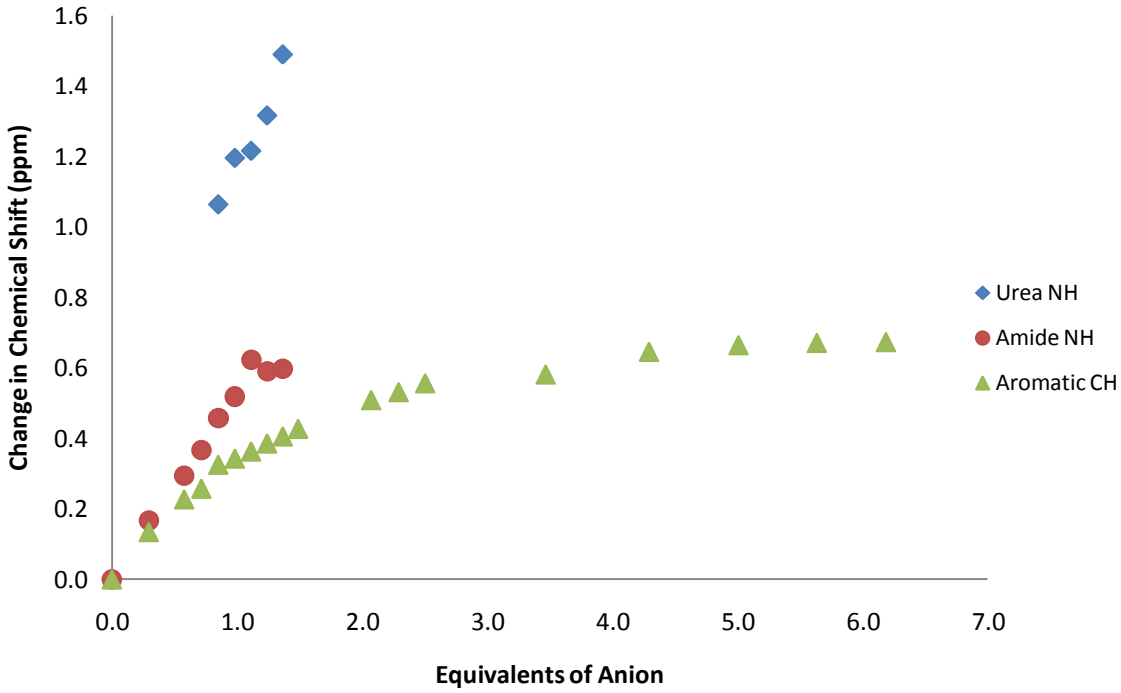

Receptor 220 *vs.* TBACl in DMSO-d_6/H_2O 0.5%

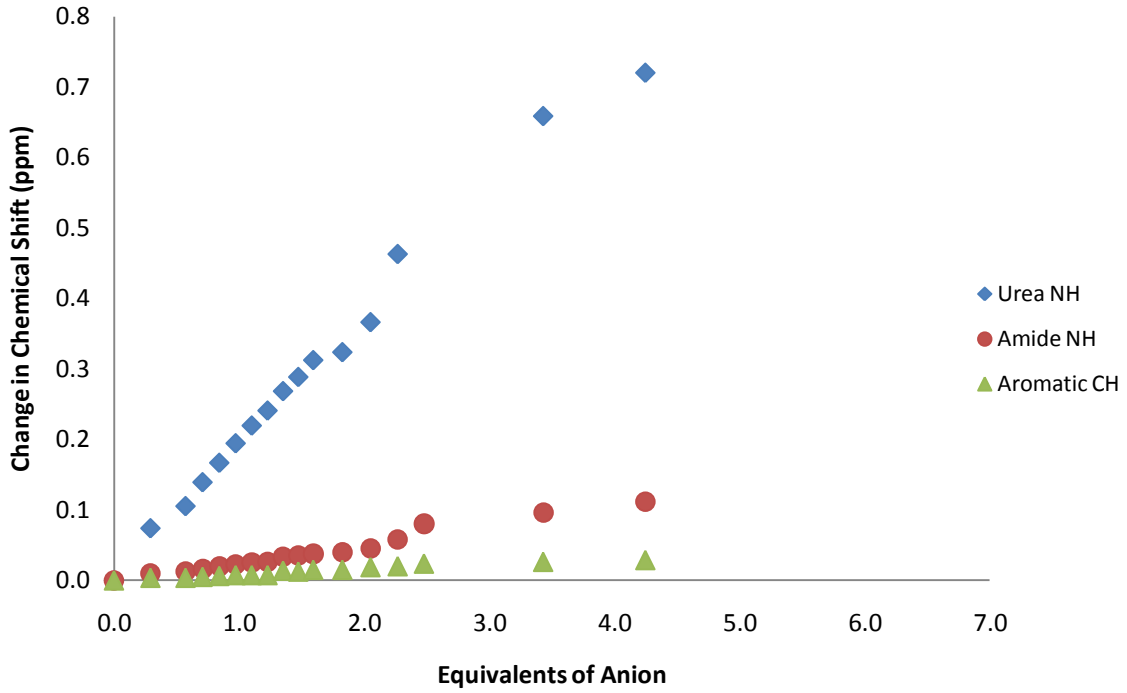

Receptor 220 *vs.* TBAOBz in DMSO-d_6/H_2O 10%

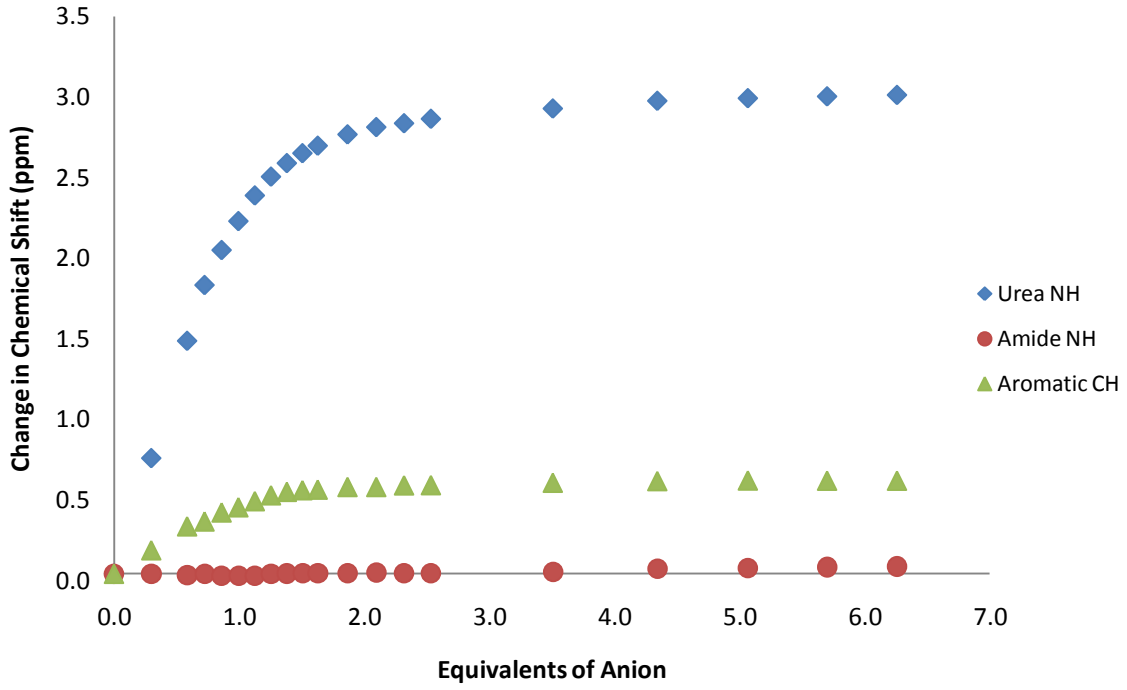

Receptor 220 *vs.* $TEAHCO_3$ in DMSO-d_6/H_2O 10%

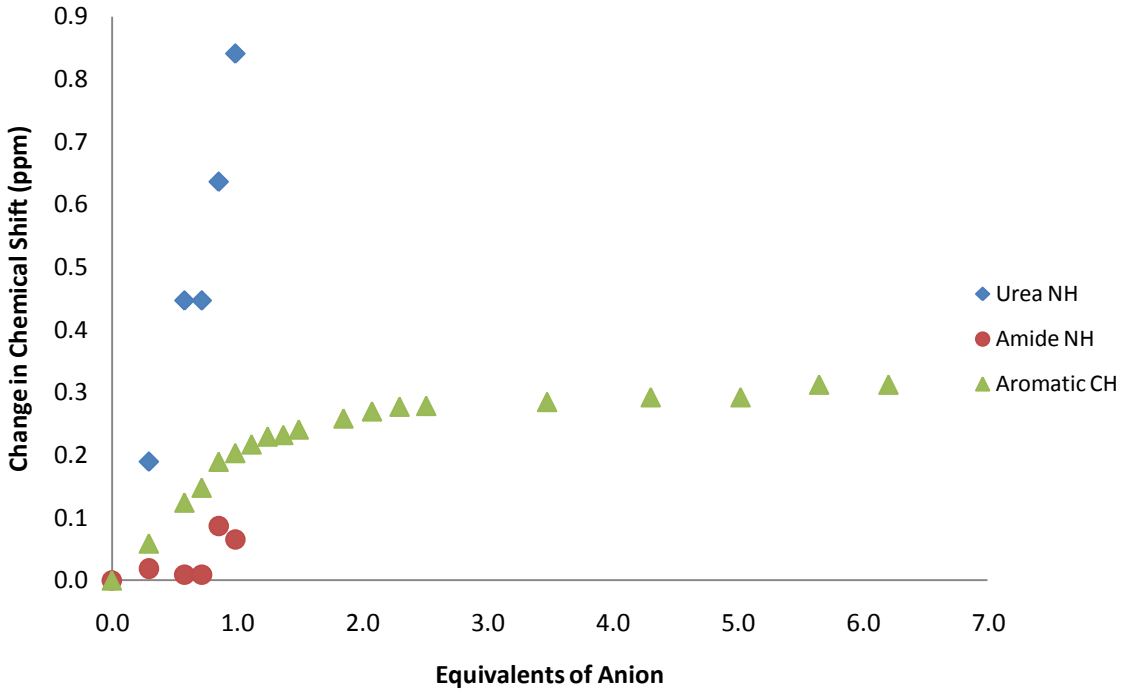

Receptor 220 *vs.* TBAOAc in DMSO-d_6/H_2O 10%

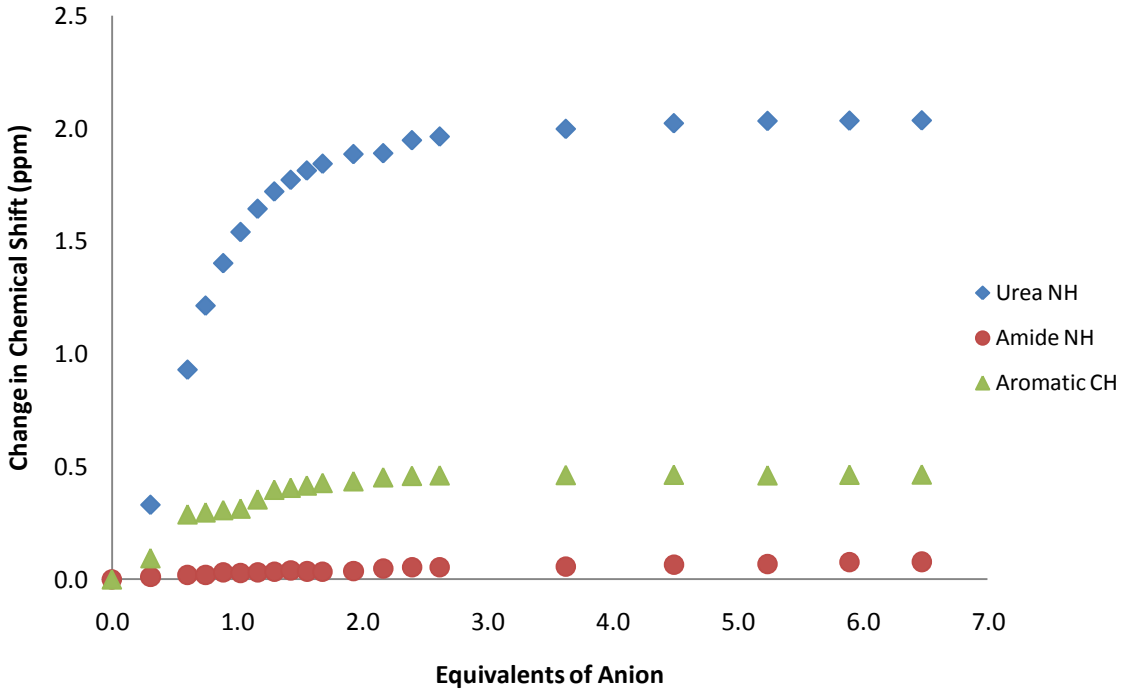

Receptor 220 *vs.* $TBAH_2PO_4$ in DMSO-d_6/H_2O 10%

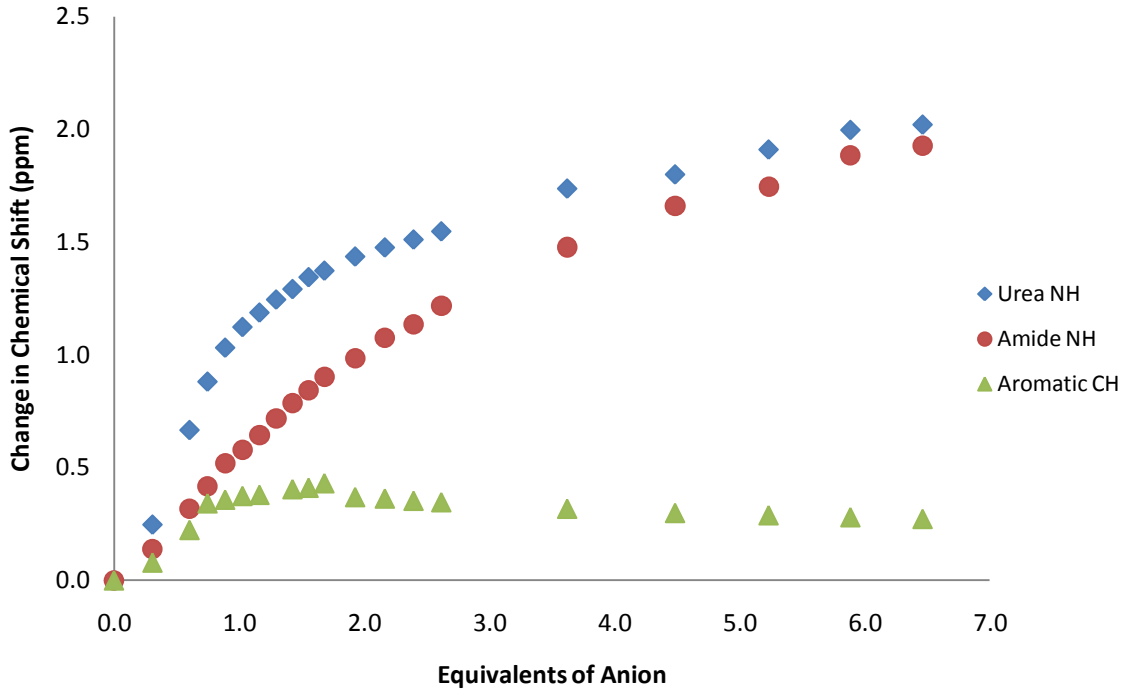

Receptor 220 *vs.* TBA_2SO_4 in DMSO-d_6/H_2O 10%

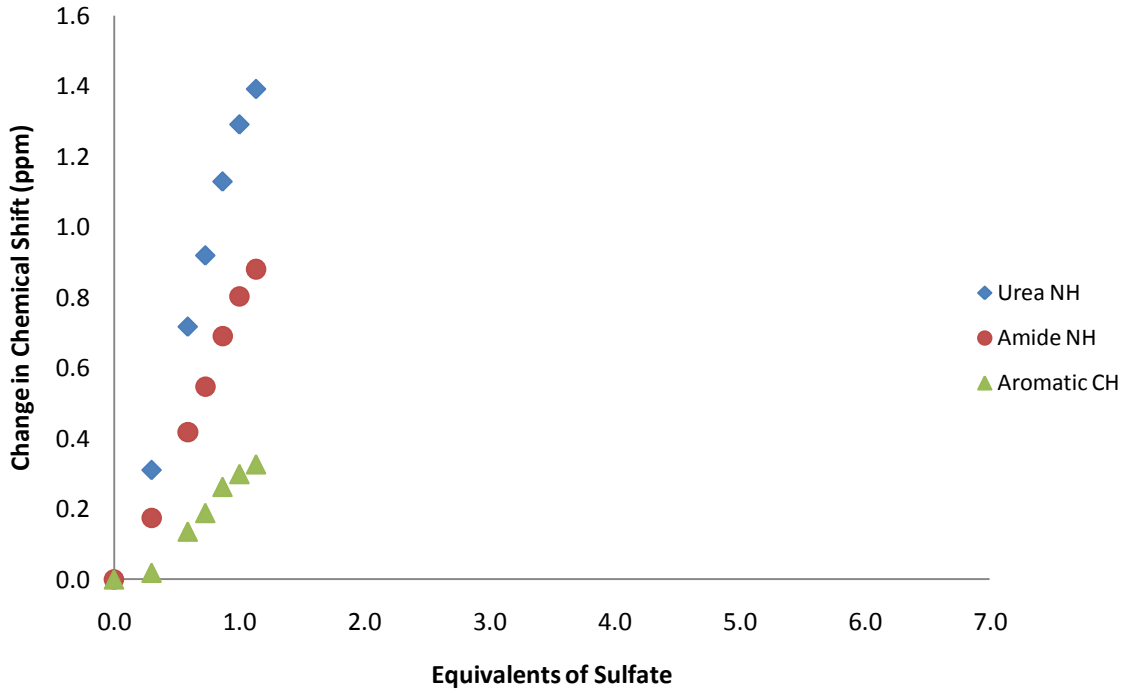

Receptor 221 *vs.* $TBAHSO_4$ in DMSO-d_6/H_2O 0.5%

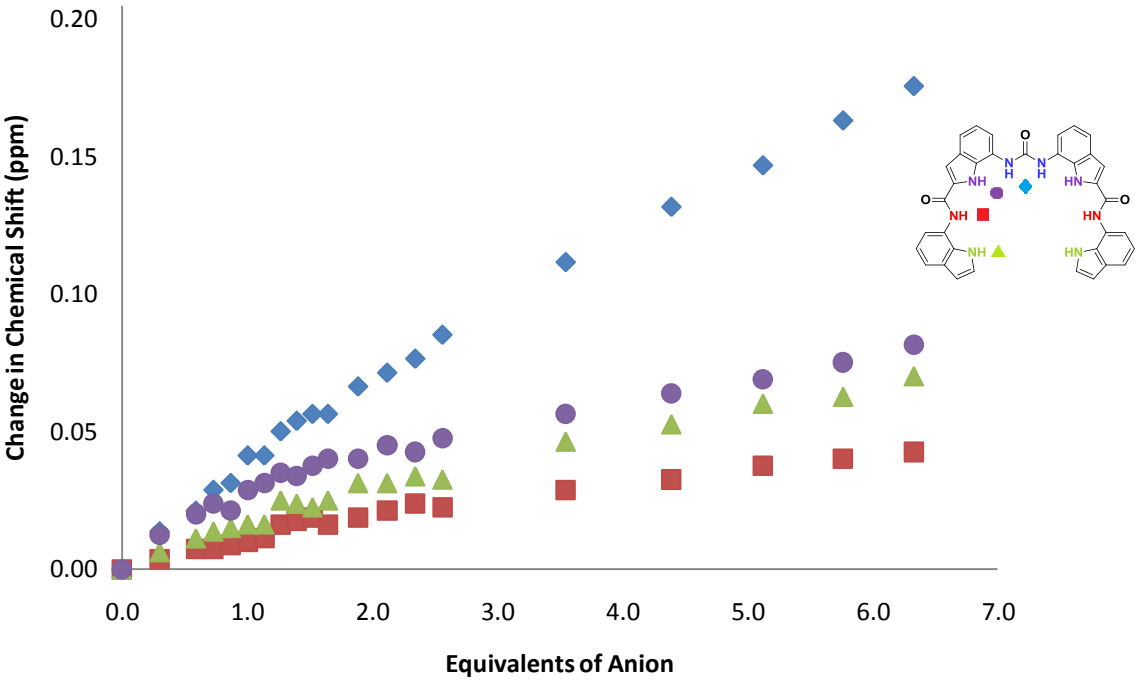

Receptor 221 *vs.* $TBAH_2PO_4$ in DMSO-d_6/H_2O 10%

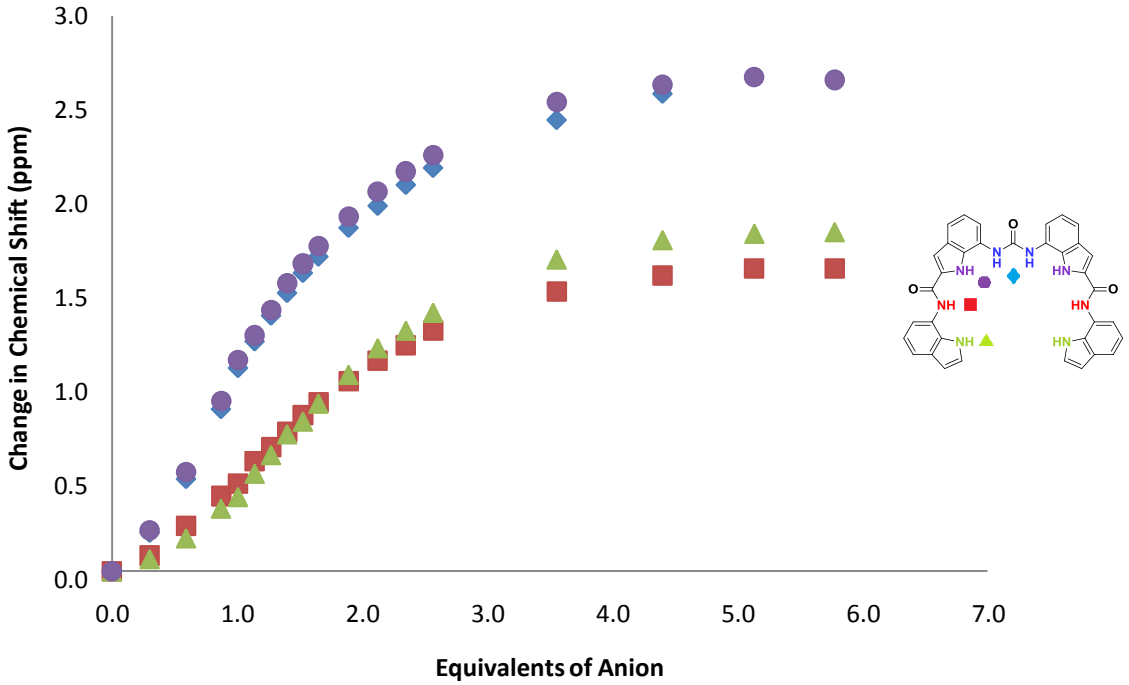

Receptor 221 *vs.* TBA_2SO_4 in DMSO-d_6/H_2O 10%

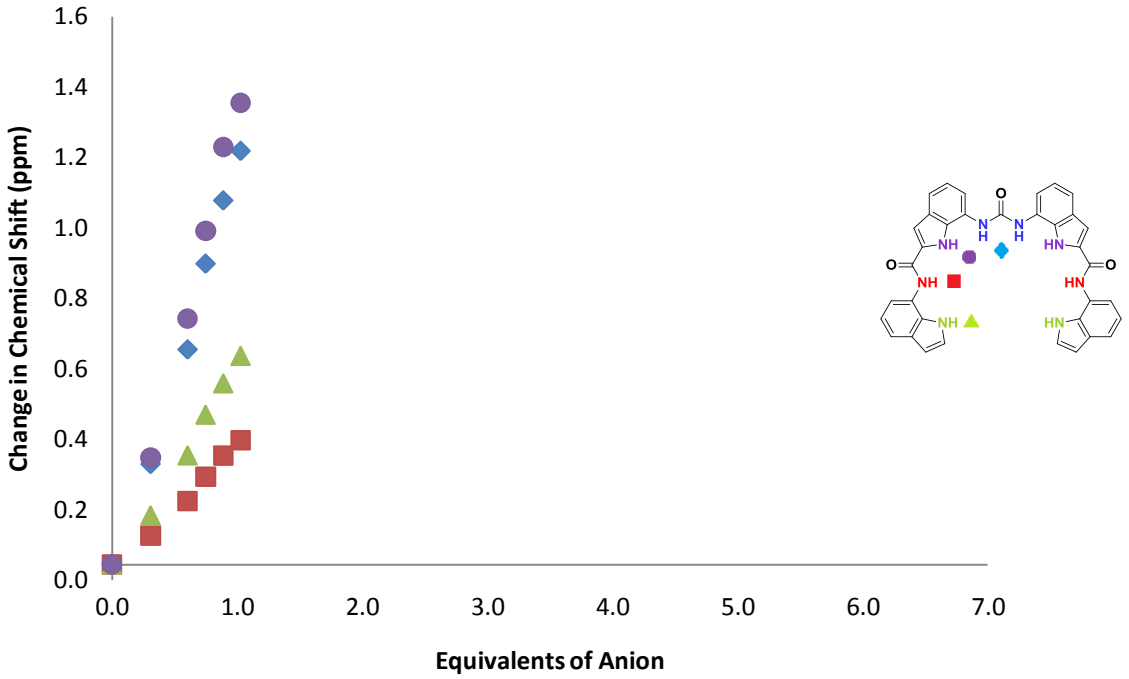

Receptor 221 *vs.* $TEAHCO_3$ in DMSO-d_6/H_2O 25%

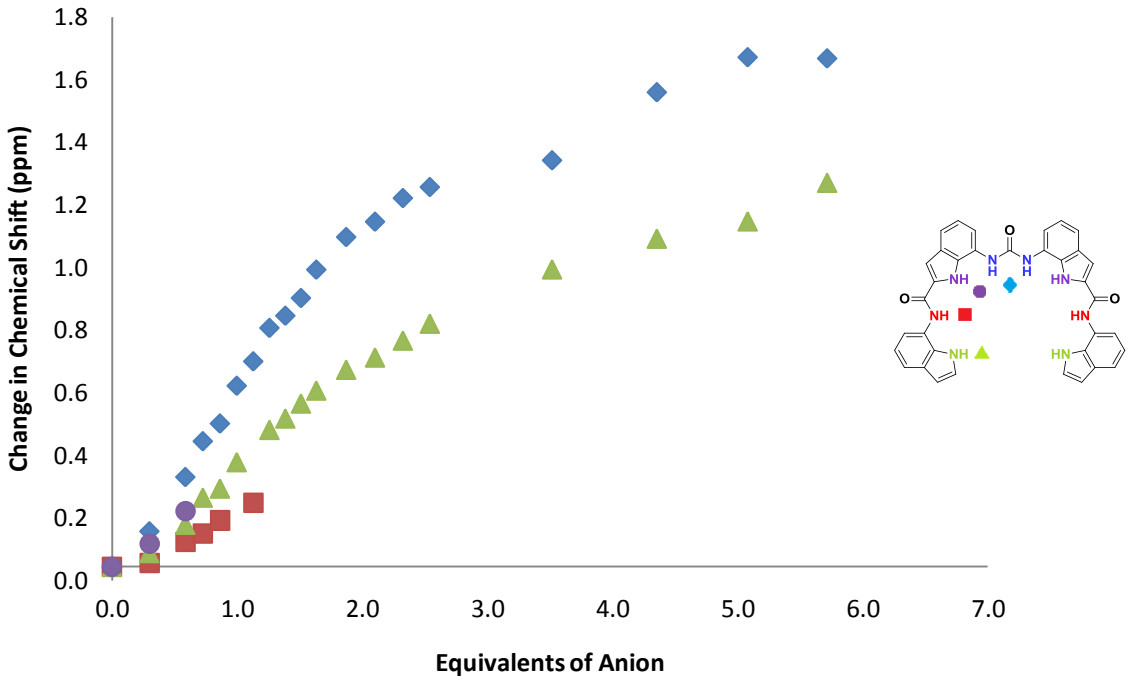

Receptor 222 *vs.* $TBAHSO_4$ in DMSO-d_6/H_2O 0.5%

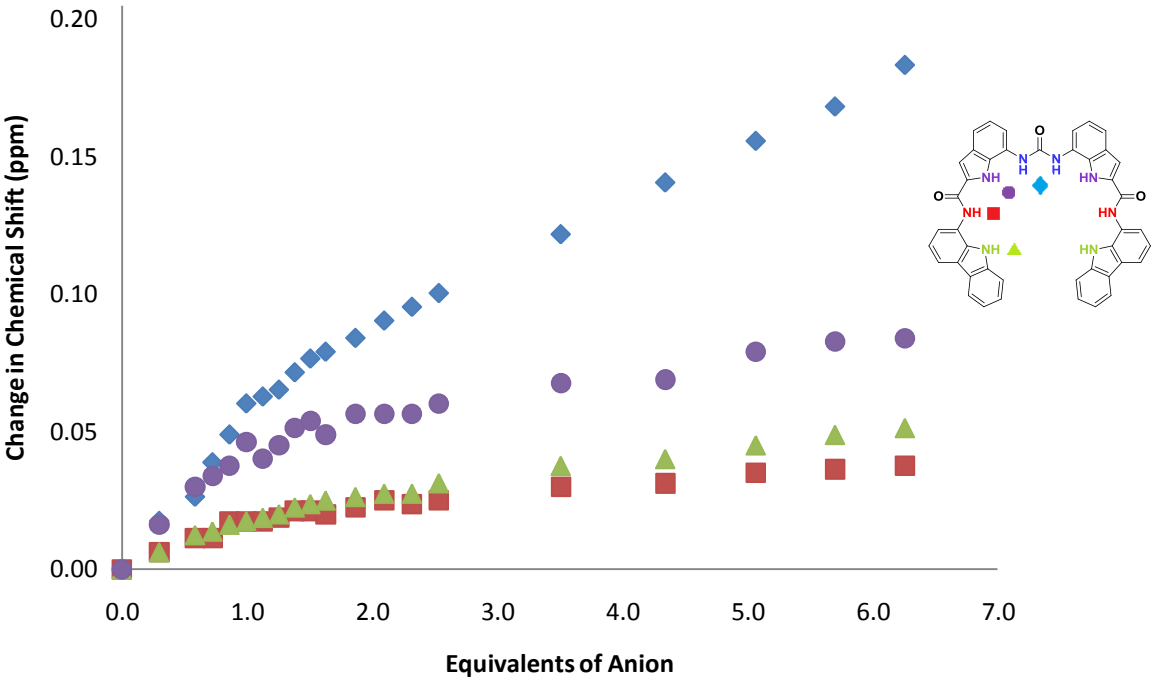

Receptor 222 *vs.* $TBAH_2PO_4$ in DMSO-d_6/H_2O 10%

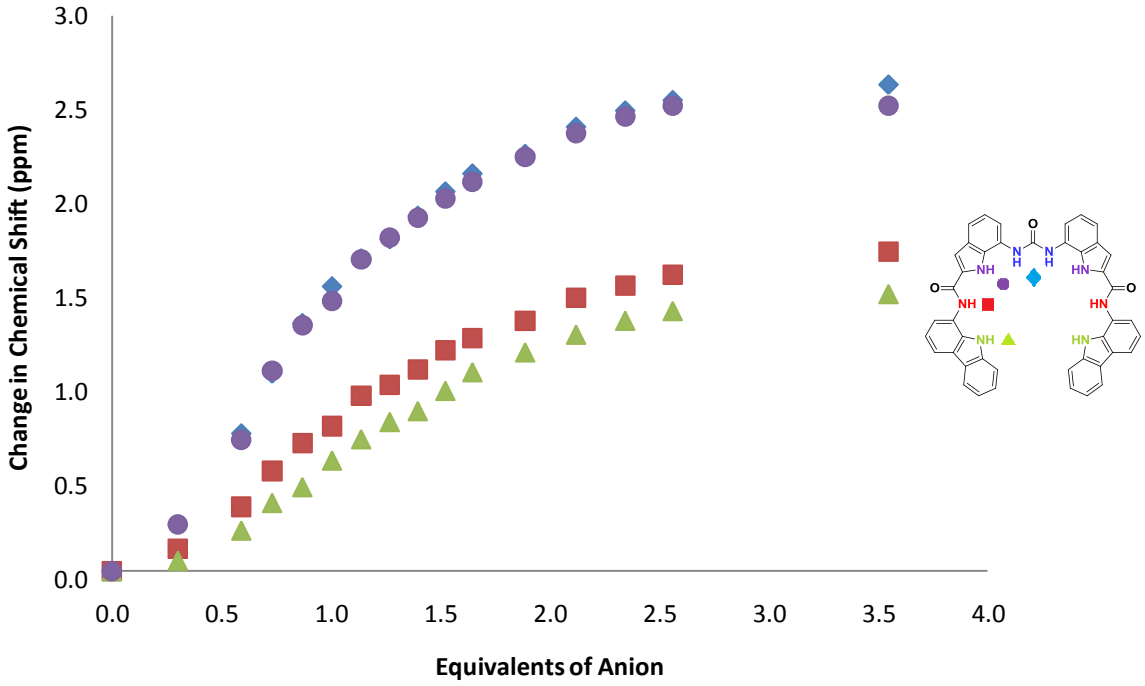

Receptor 222 *vs.* $TEAHCO_3$ in DMSO-d_6/H_2O 25%

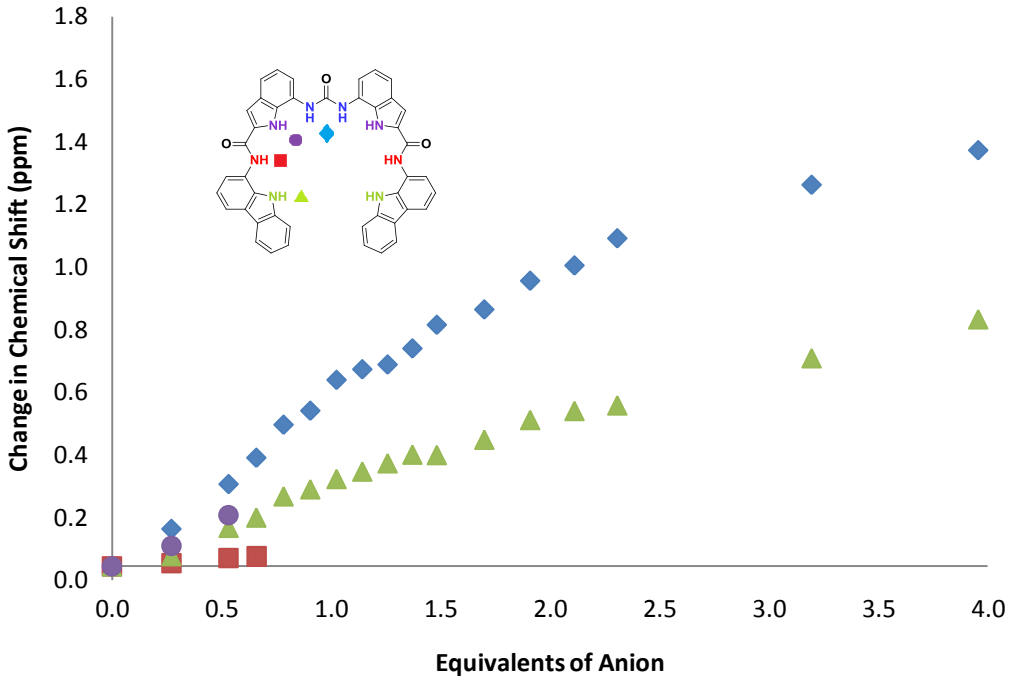

Graphs for Chapter Four

Receptor 227 *vs.* $TEAHCO_3$ in DMSO-d_6/H_2O 0.5%

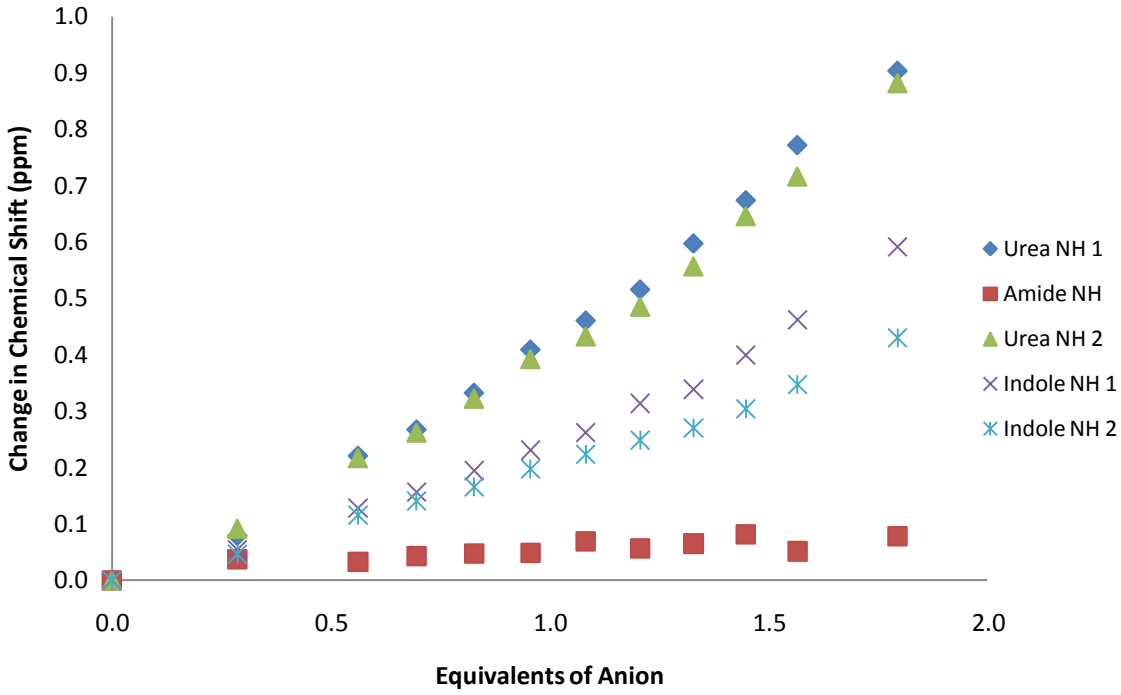

Receptor 227 *vs.* TBAOBz in DMSO-d_6/H_2O 0.5%

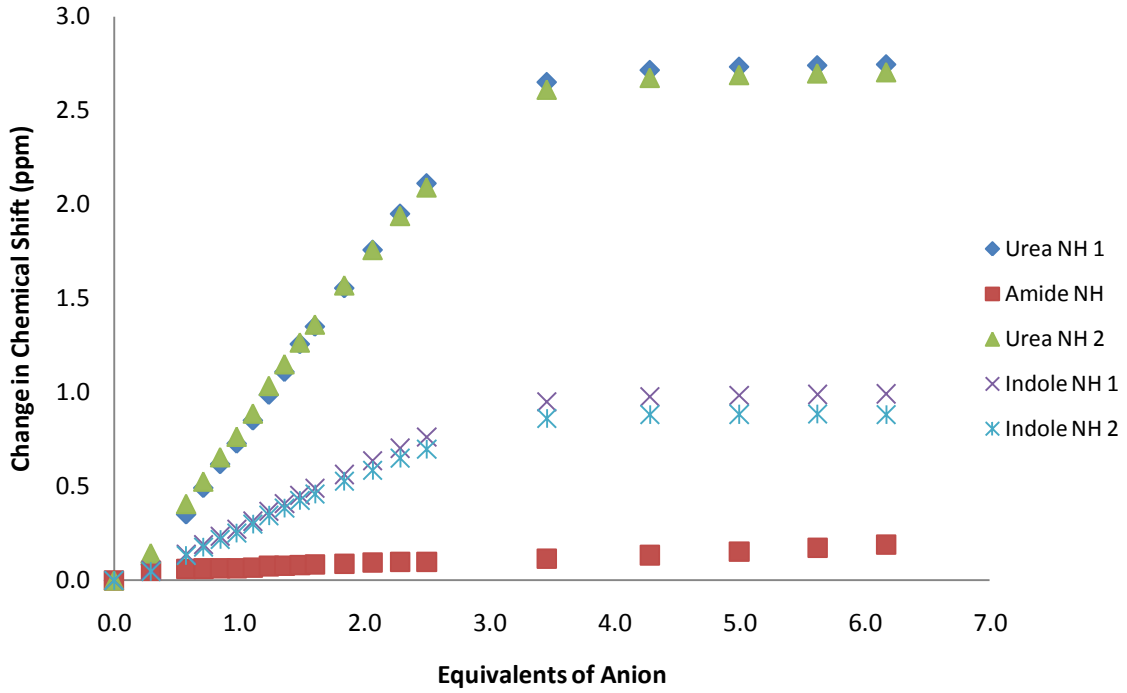

Receptor 232 *vs.* TBACl in DMSO-d_6/H_2O 0.5%

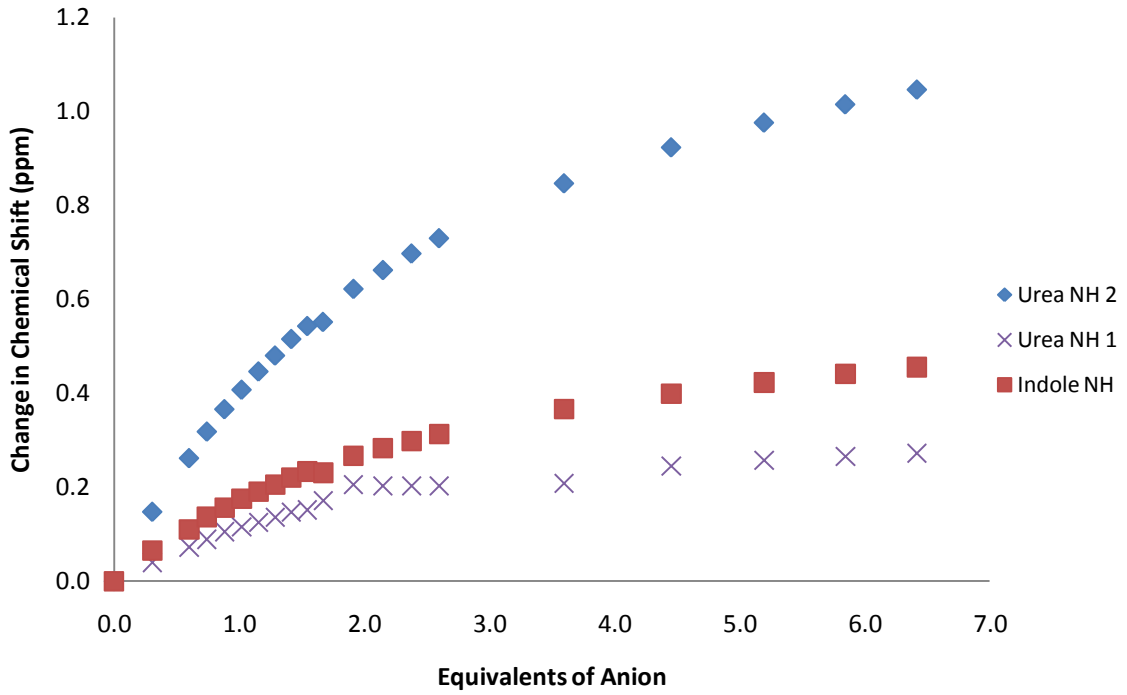

Receptor 232 *vs.* $TBAH_2PO_4$ in DMSO-d_6/H_2O 0.5%

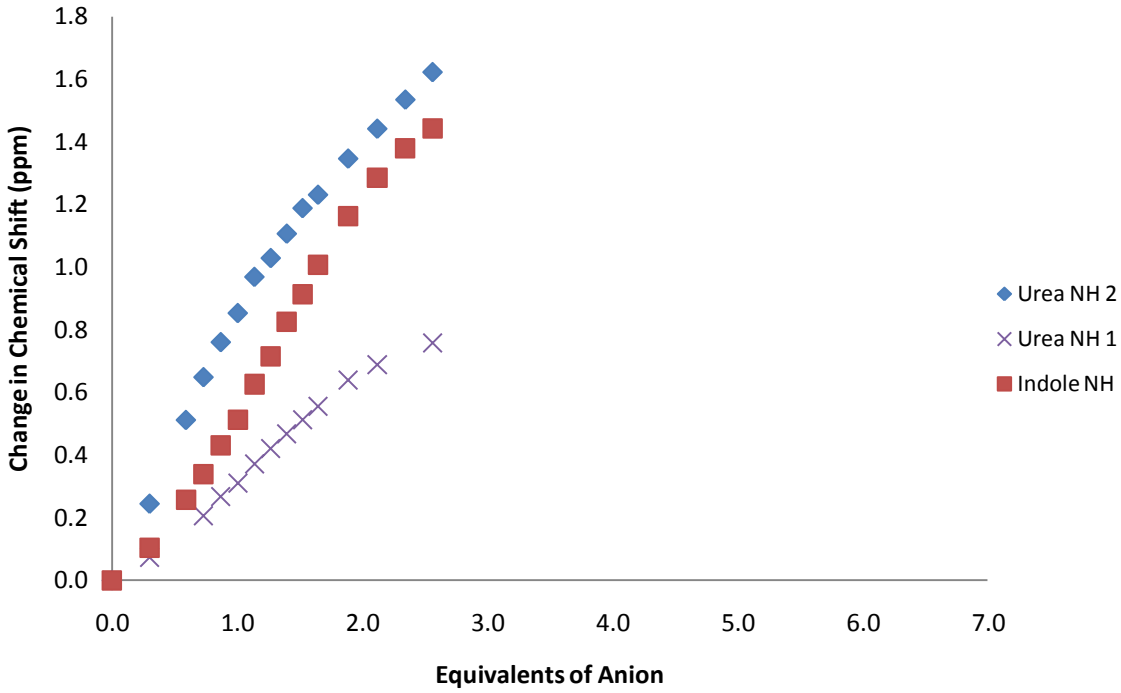

Receptor 232 *vs.* $TEAHCO_3$ in DMSO-d_6/H_2O 0.5%

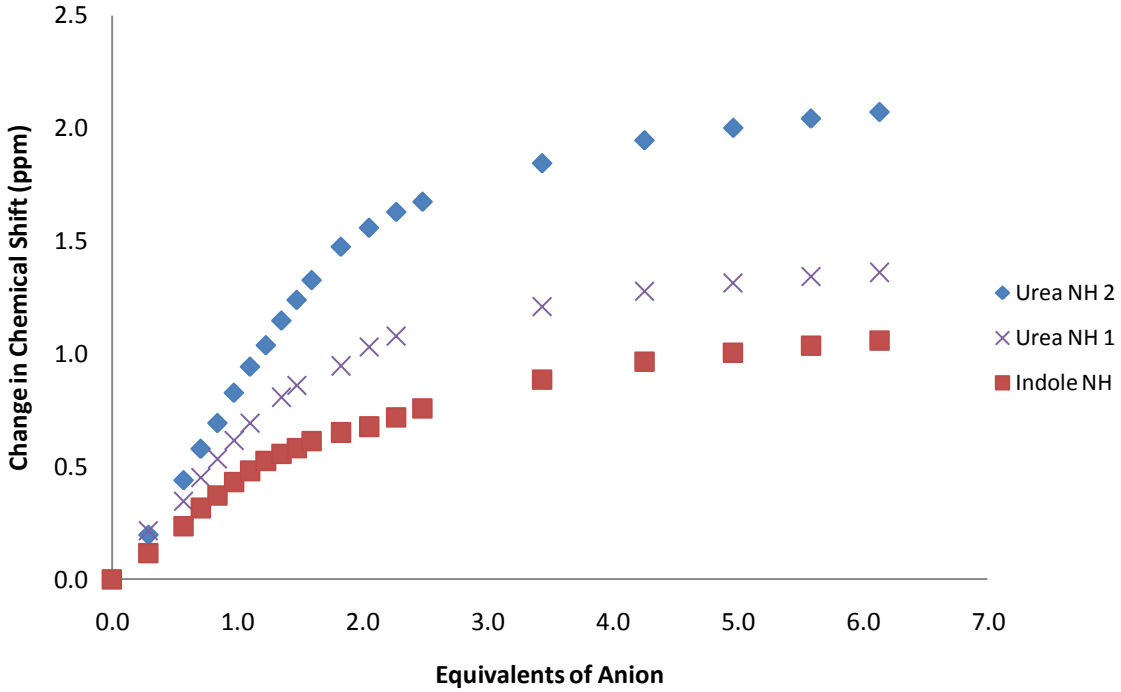

Receptor 232 *vs.* TBAOAc in DMSO-d_6/H_2O 0.5%

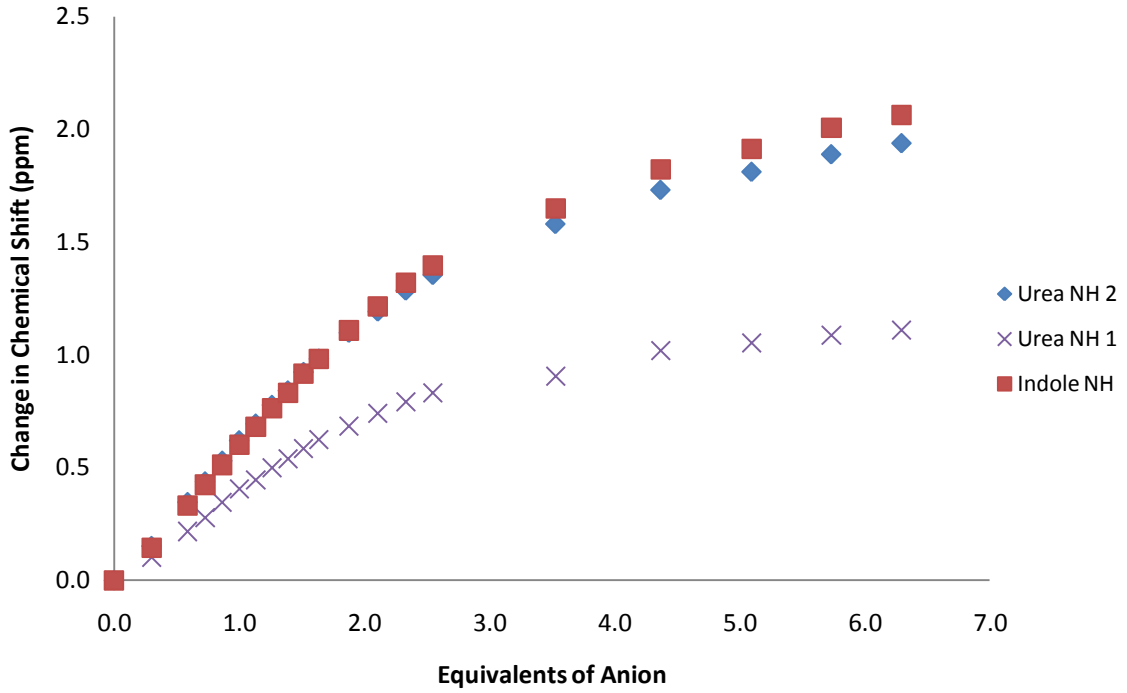

Receptor 232 *vs.* TBAOBz in DMSO-d_6/H_2O 0.5%

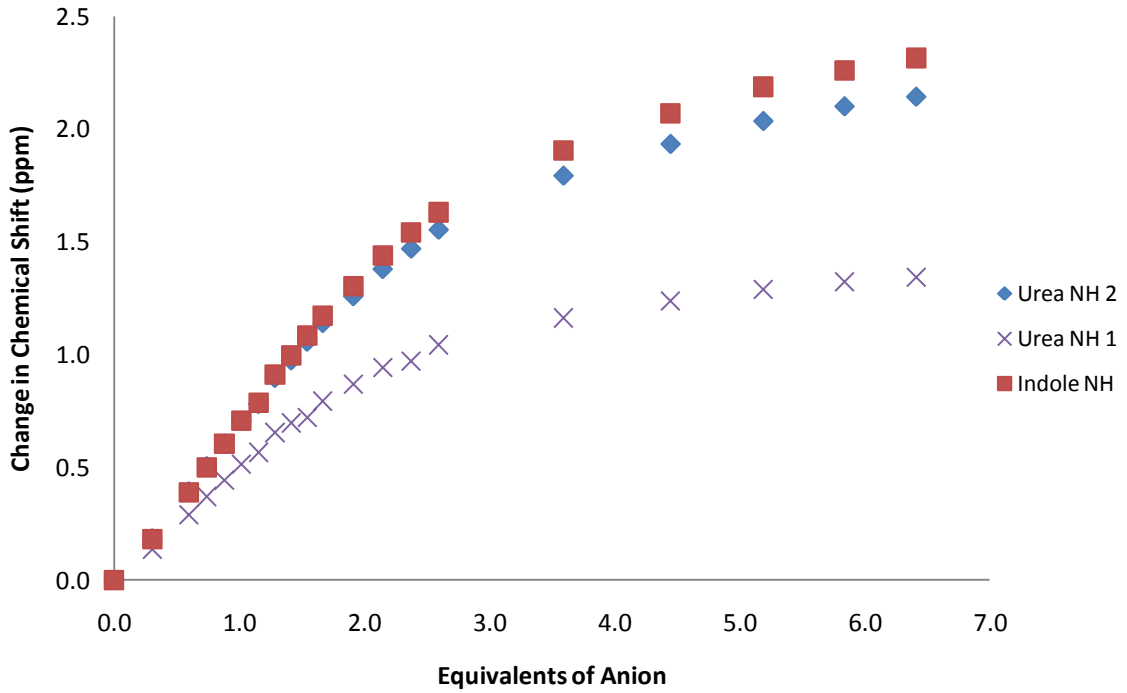

Receptor 232 *vs.* TBA_2SO_4 in DMSO-d_6/H_2O 0.5%

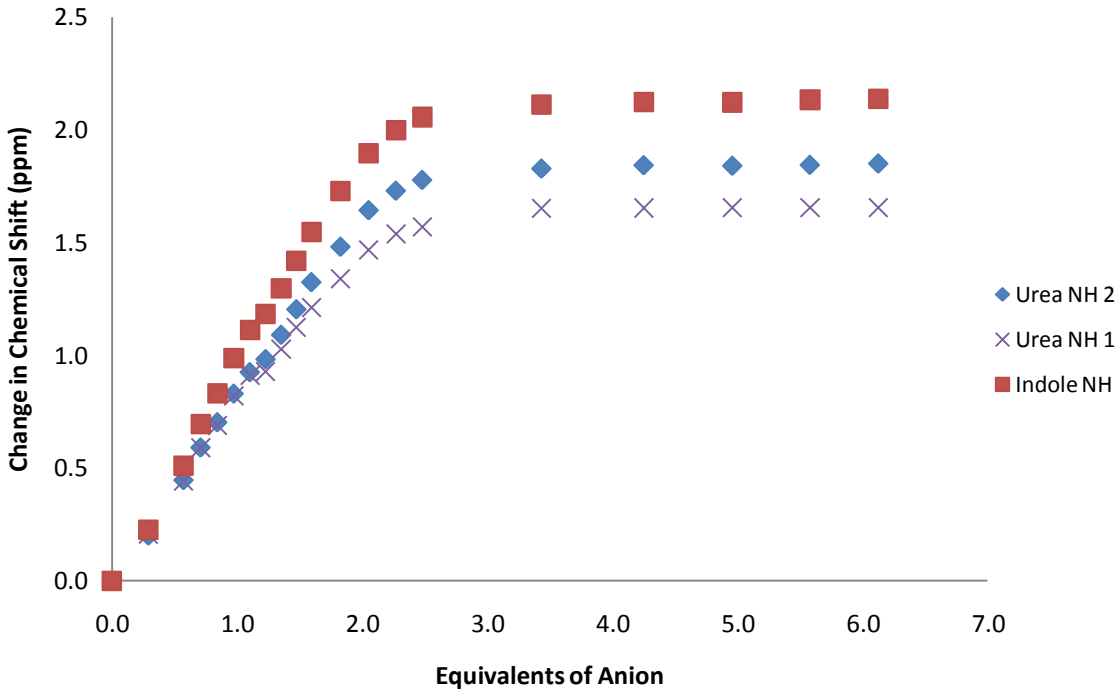

Appendix 5 – UV-Vis and Fluorescence Quenching Experiments

These fluorescence quenching experiments were conducted with compounds **213-215** in DMSO-0.5% H_2O, with the anions added as the tetraethylammonium or tetrabutylammonium salt at 298 K.

Graphs for Chapter Two

UV-Vis spectrum of 213 and $TEAHCO_3$ in DMSO-0.5% H_2O (0 to 9 equ. anion)

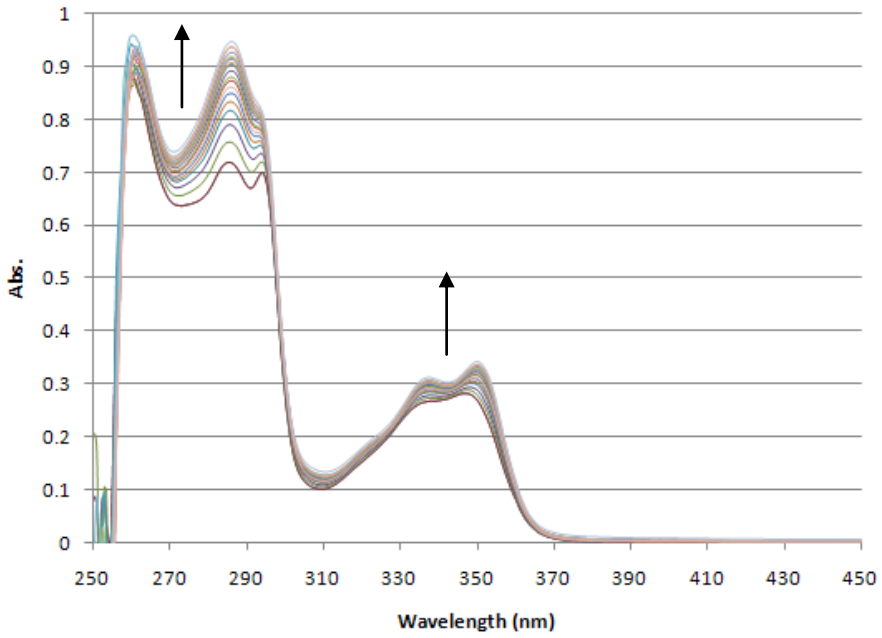

UV-Vis spectrum of 213 and TBAF in DMSO-0.5% H_2O (0 to 9 equ. anion)

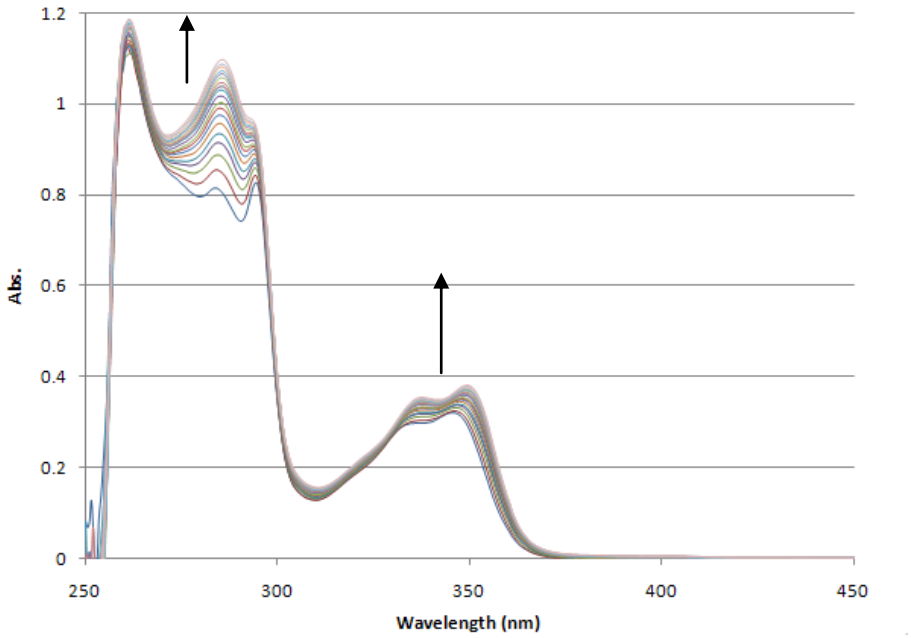

UV-Vis spectrum of 213 and TBAOBz in DMSO-0.5% H_2O (0 to 9 equ. anion)

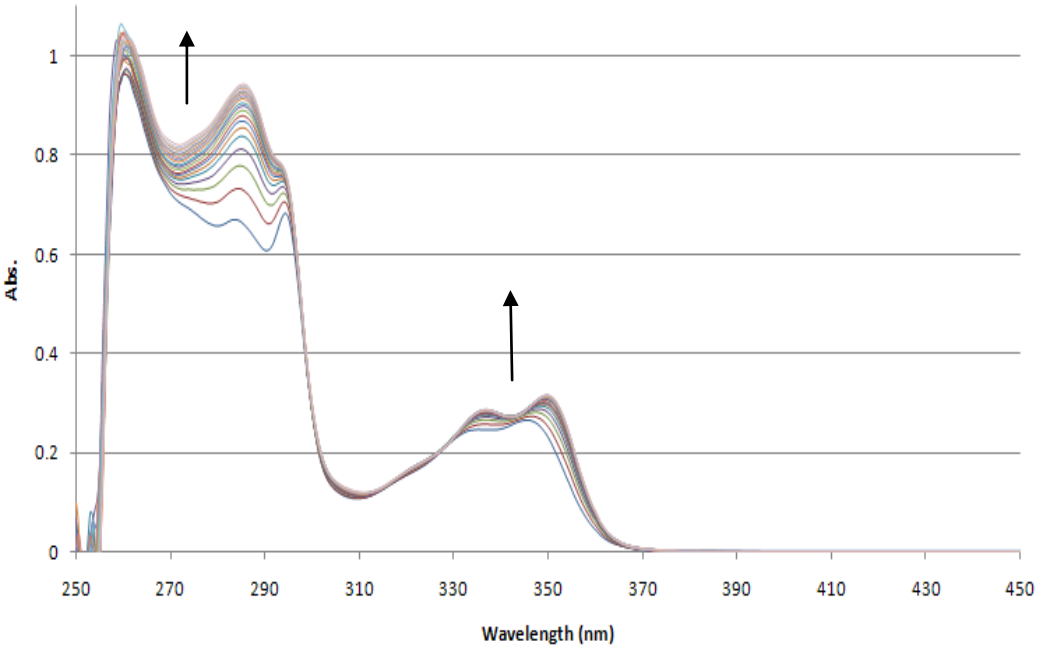

Fluorescence quenching of 213 in DMSO-0.5% H_2O with addition of TBAOAc

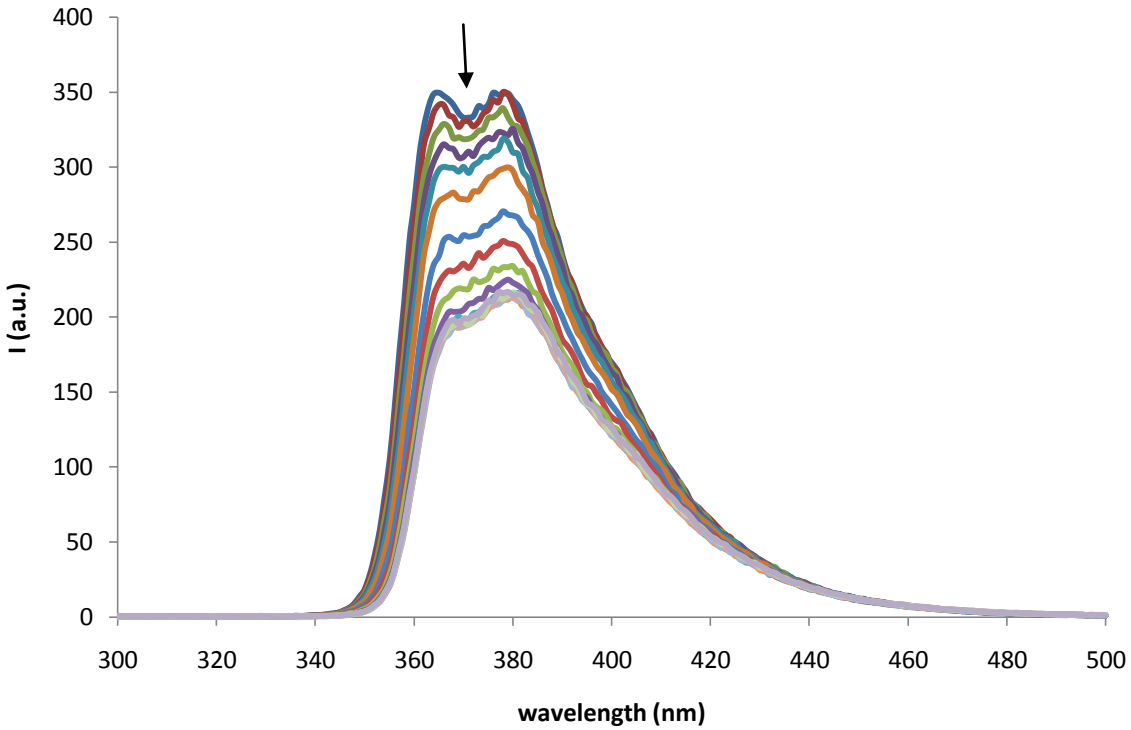

Fluorescence quenching of 213 in DMSO-0.5% H_2O with addition of TBACl

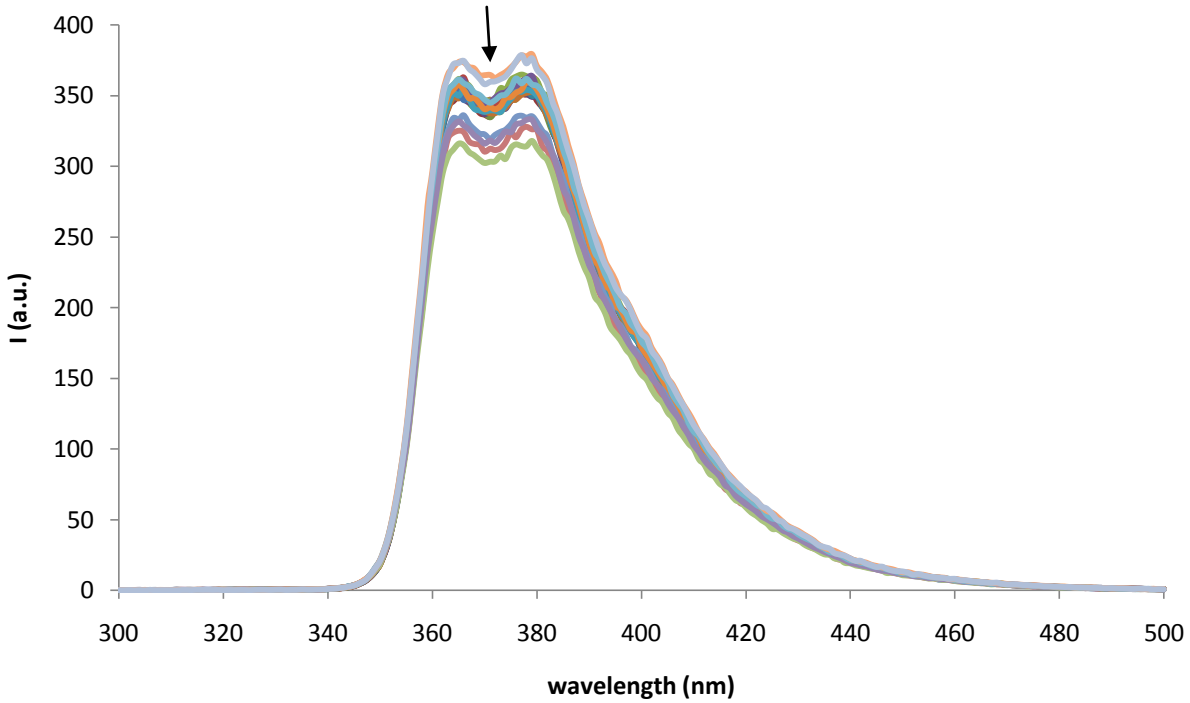

Fluorescence quenching of 213 in DMSO-0.5% H_2O with addition of TBAF

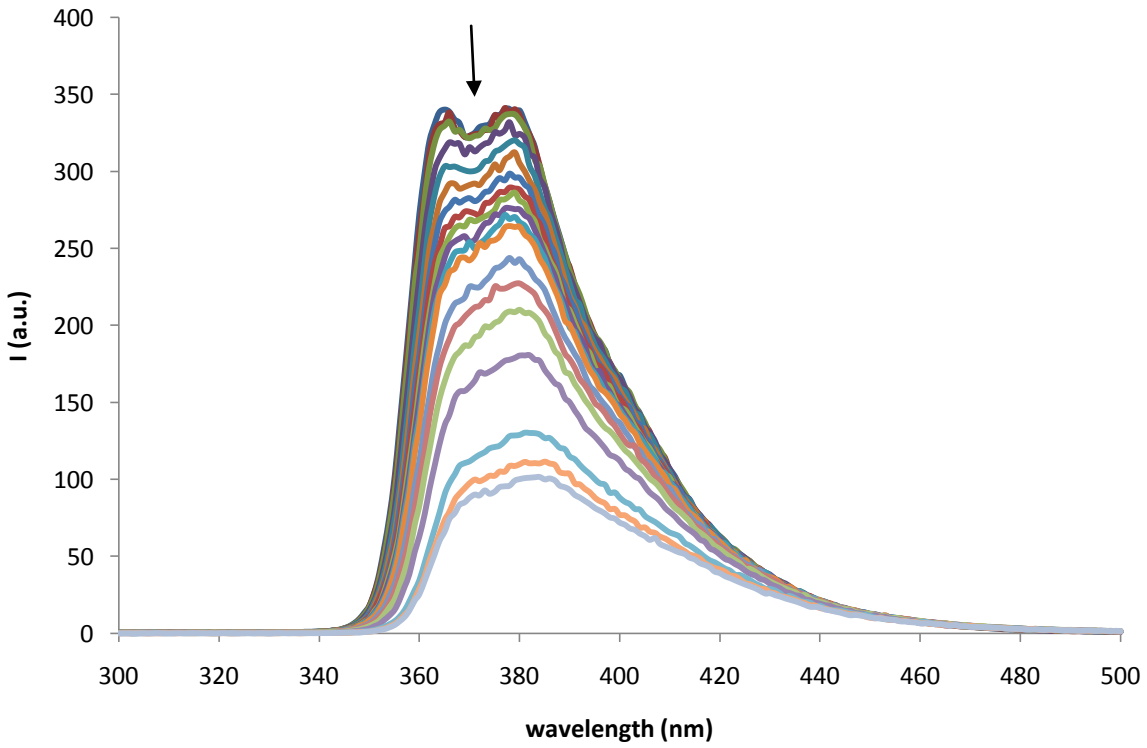

Fluorescence quenching of 213 in DMSO-0.5% H_2O with addition of $TBAH_2PO_4$

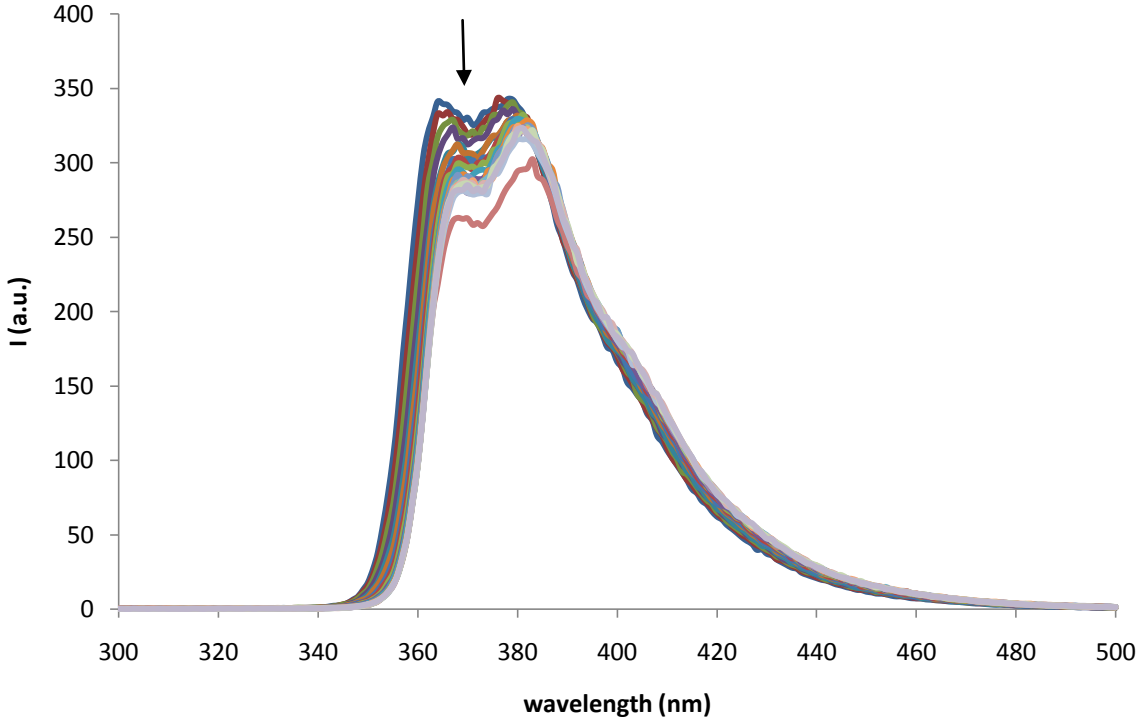

Fluorescence quenching of 213 in DMSO-0.5% H_2O with addition of $TEAHCO_3$

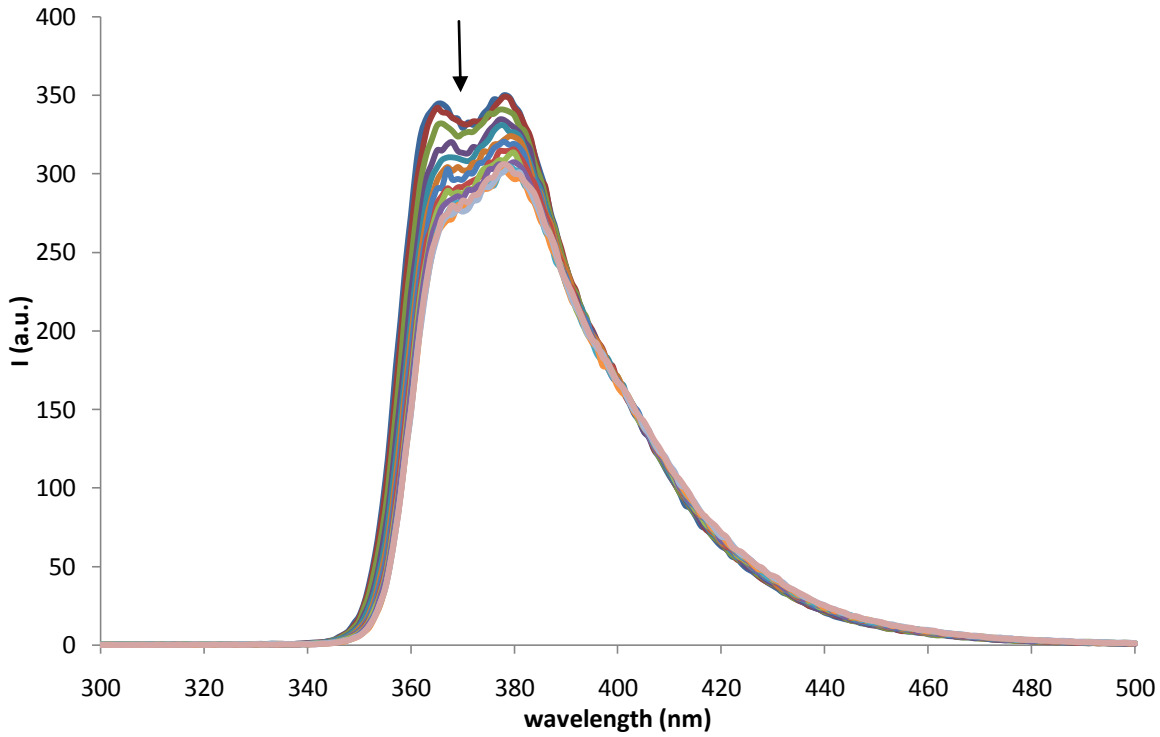

UV-Vis spectrum of 214 and $TEAHCO_3$ in DMSO-0.5% H_2O (0 to 9 equ. anion)

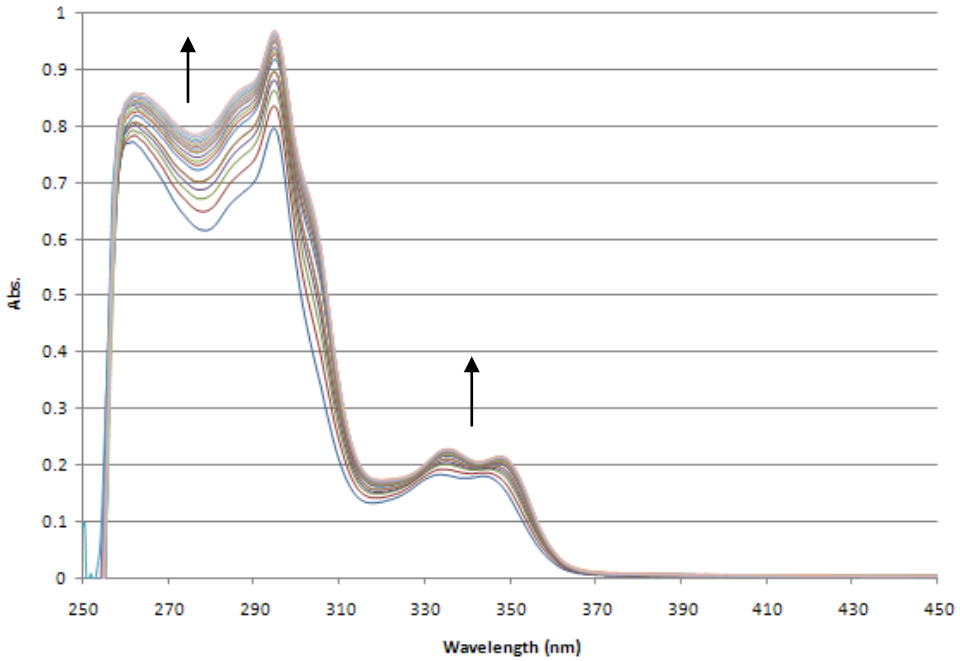

UV-Vis spectrum of 214 and TBAF in DMSO-0.5% H_2O (0 to 9 equ. anion)

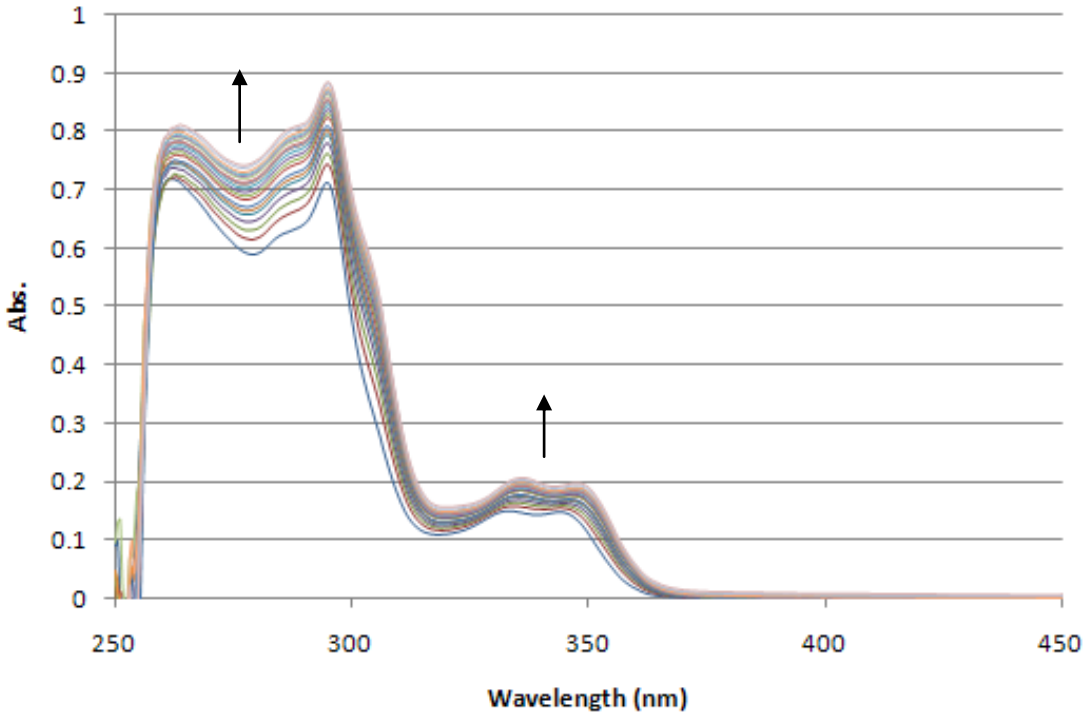

UV-Vis spectrum of 214 and TBAOBz in DMSO-0.5% H_2O (0 to 9 equ. anion)

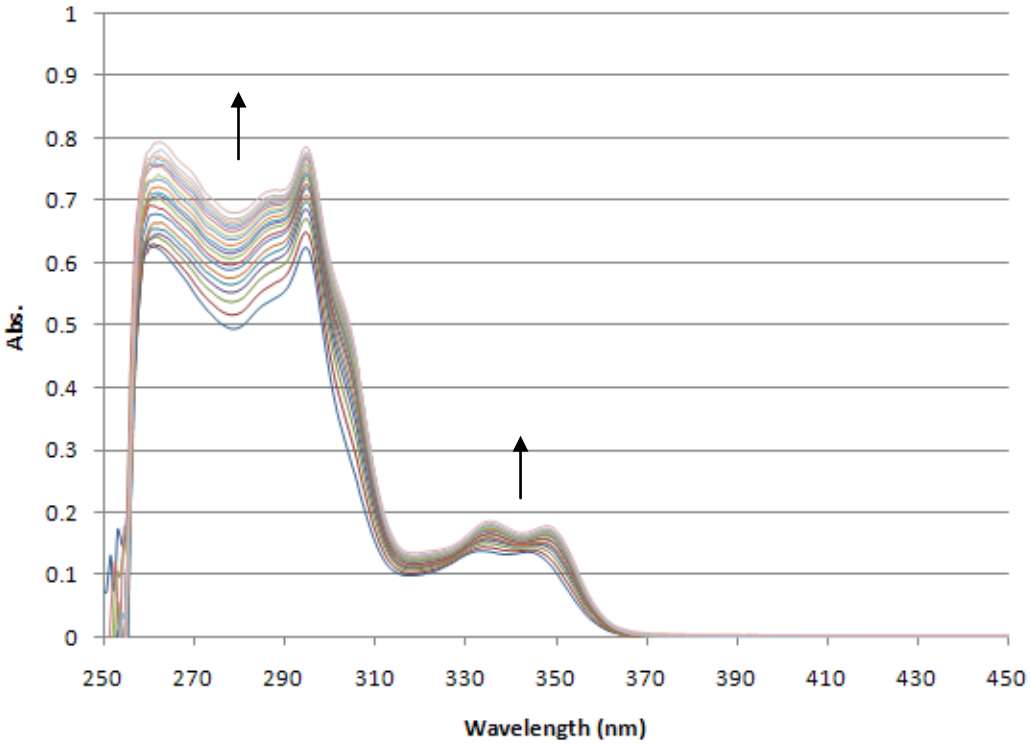

Fluorescence quenching of 214 in DMSO-0.5% H_2O with addition of TBAOAc

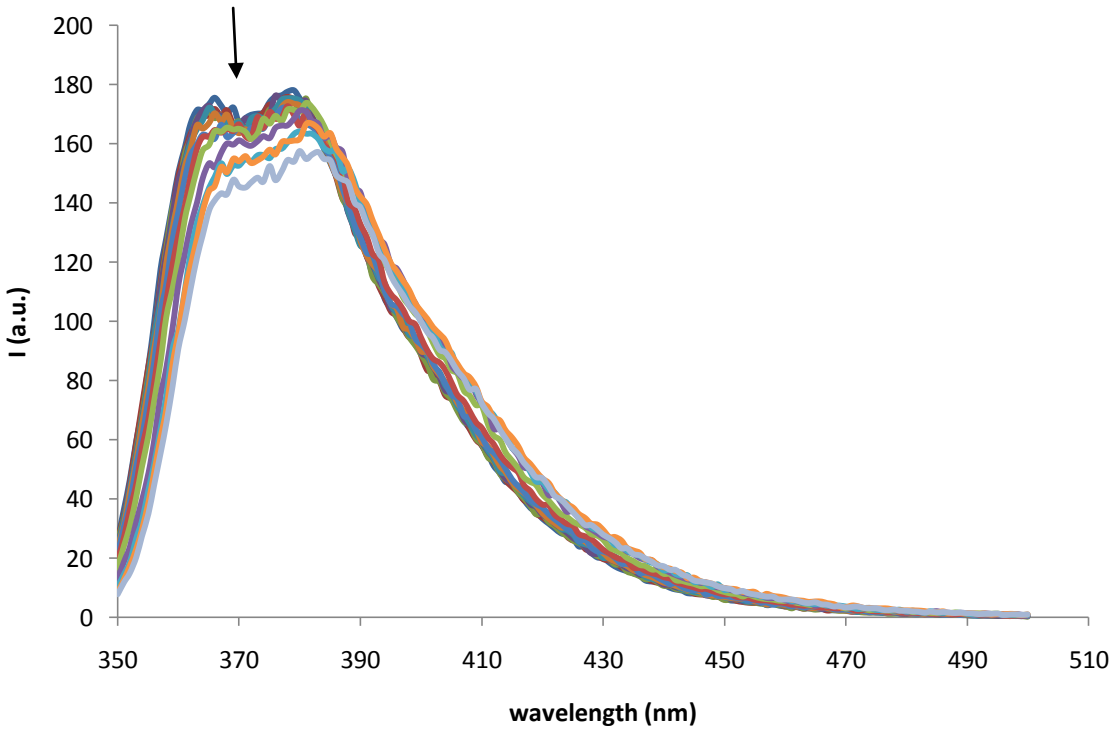

Fluorescence quenching of 214 in DMSO-0.5% H_2O with addition of TBAOBz

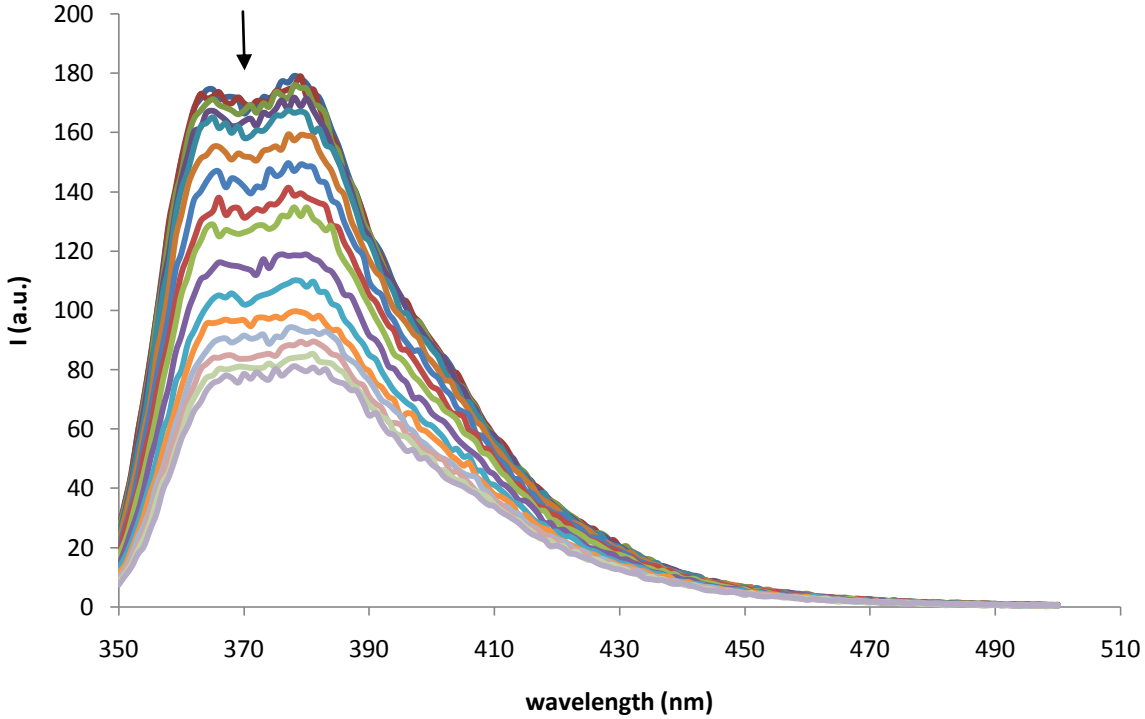

Fluorescence quenching of 214 in DMSO-0.5% H_2O with addition of TBACl

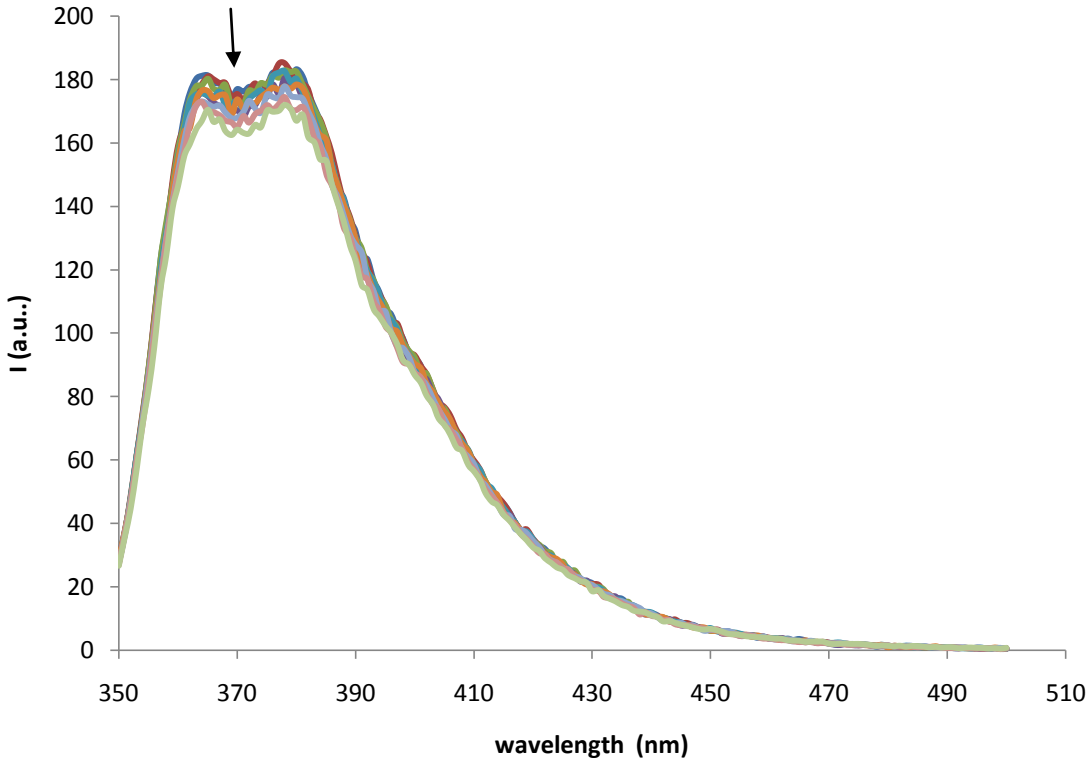

Fluorescence quenching of 214 in DMSO-0.5% H_2O with addition of TBAF

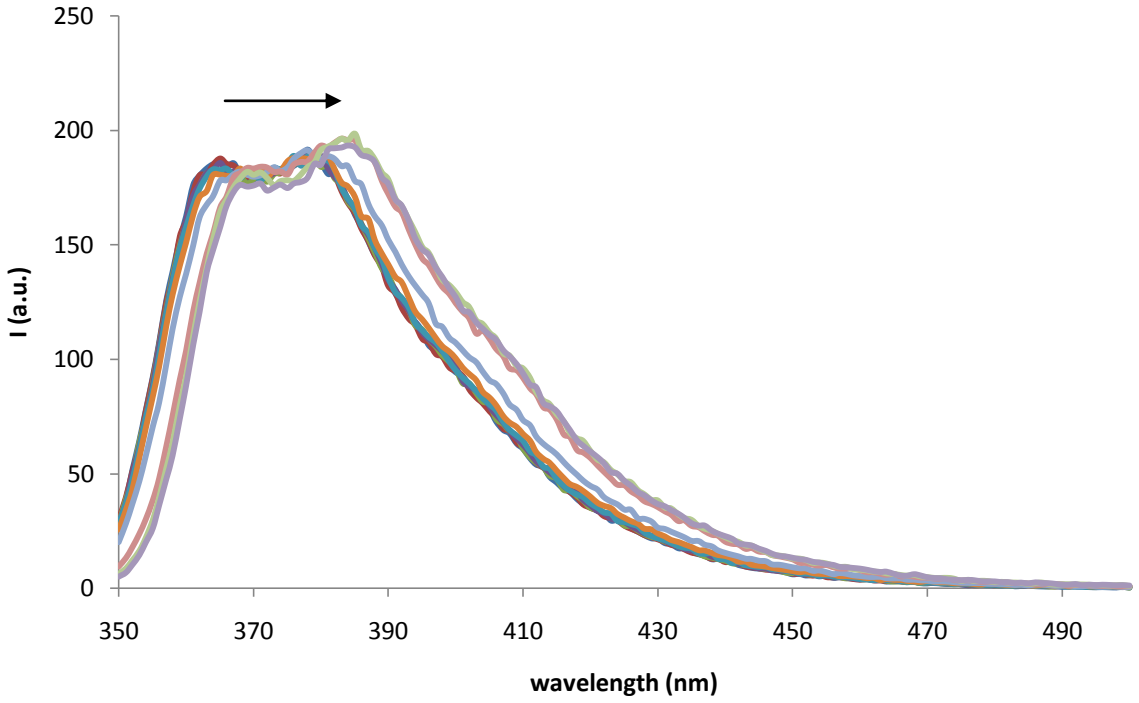

Fluorescence quenching of 214 in DMSO-0.5% H_2O with addition of $TBAH_2PO_4$

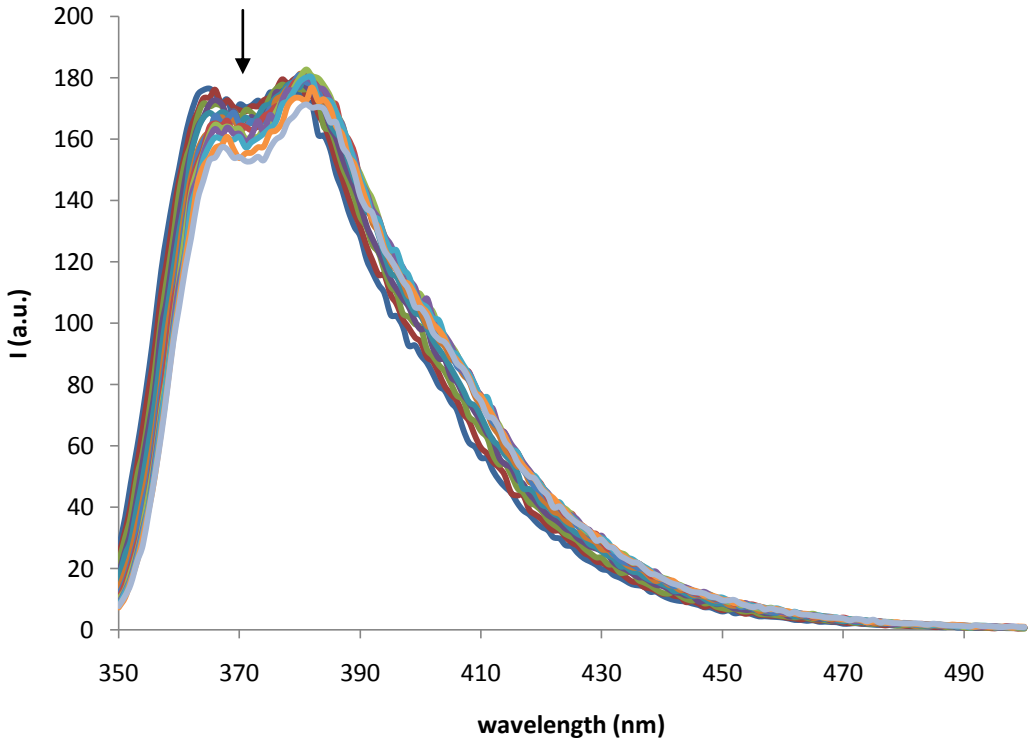

Fluorescence quenching of 214 in DMSO-0.5% H_2O with addition of $TEAHCO_3$

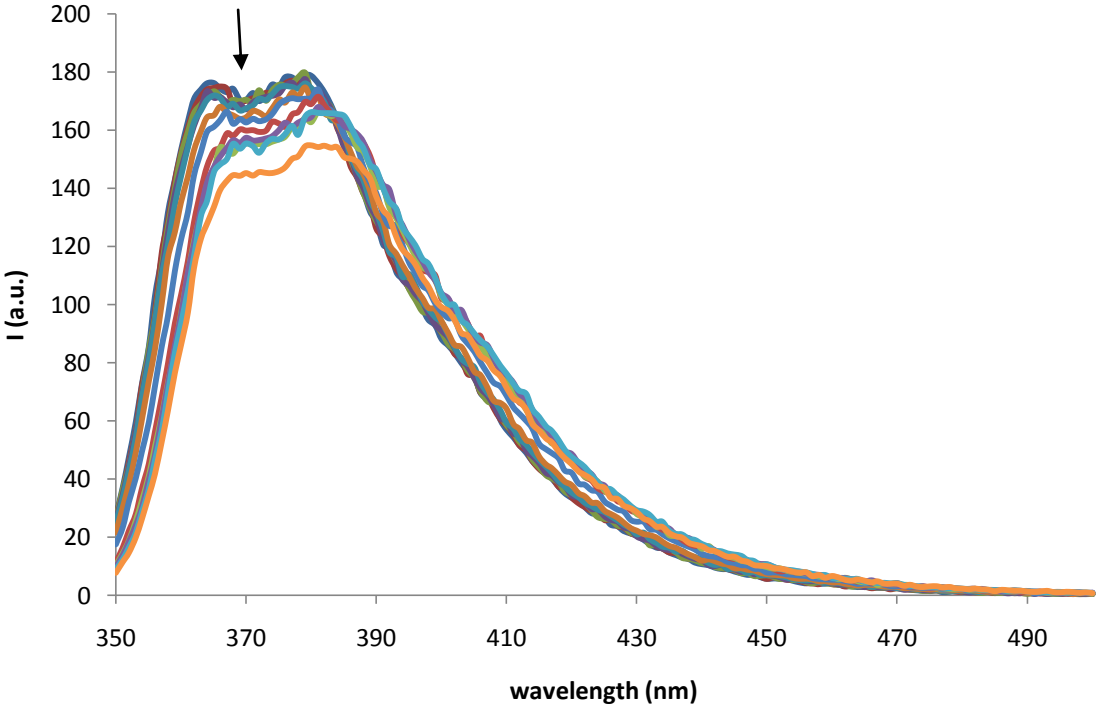

UV-Vis spectrum of 215 and $TEAHCO_3$ in DMSO-0.5% H_2O (0 to 9 equ. anion)

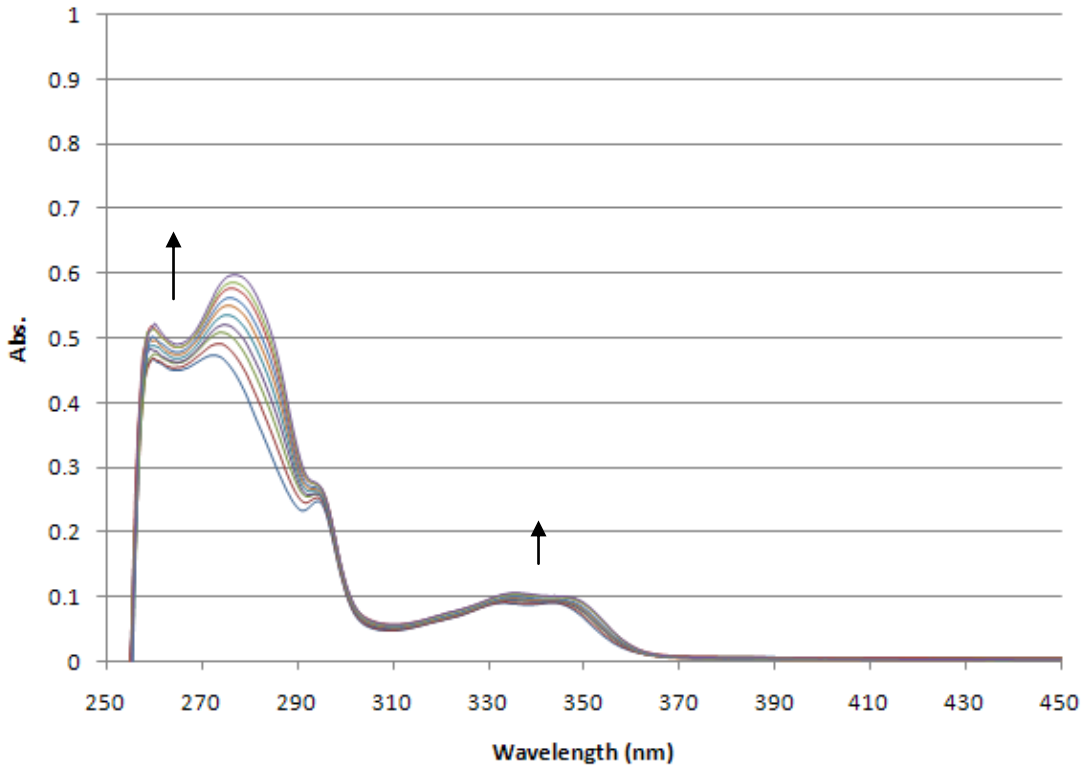

UV-Vis spectrum of 215 and TBAF in DMSO-0.5% H_2O (0 to 9 equ. anion)

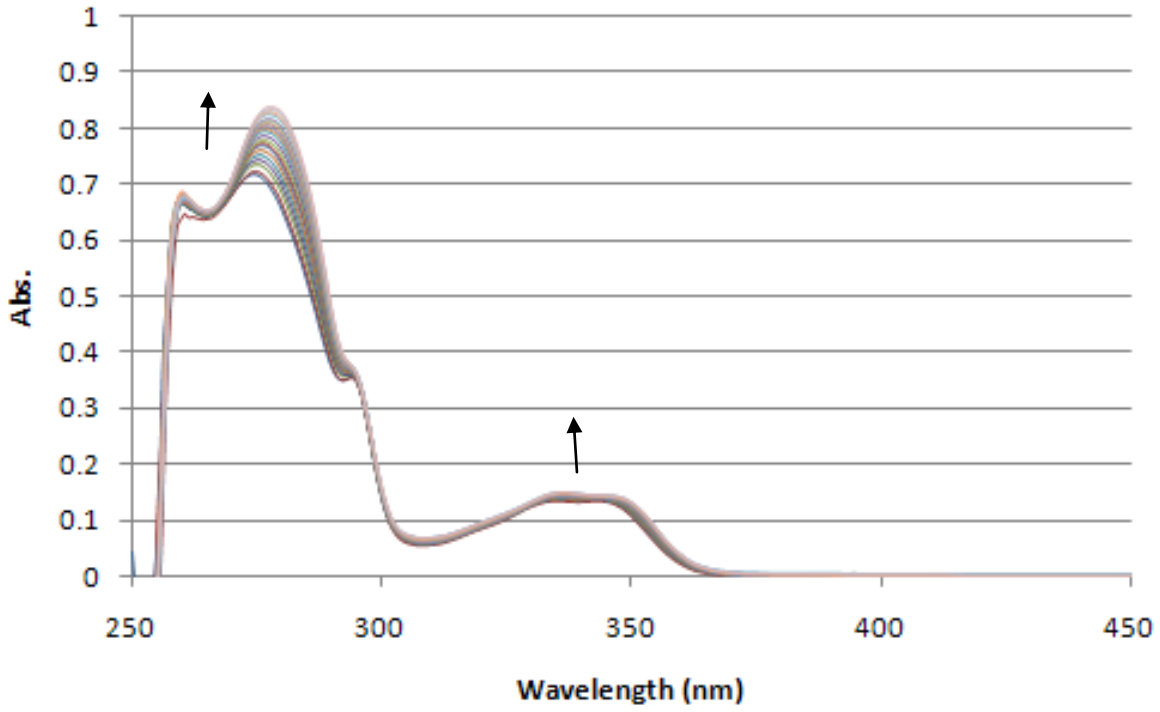

UV-Vis spectrum of 215 and TBAOBz in DMSO-0.5% H_2O (0 to 9 equ. anion)

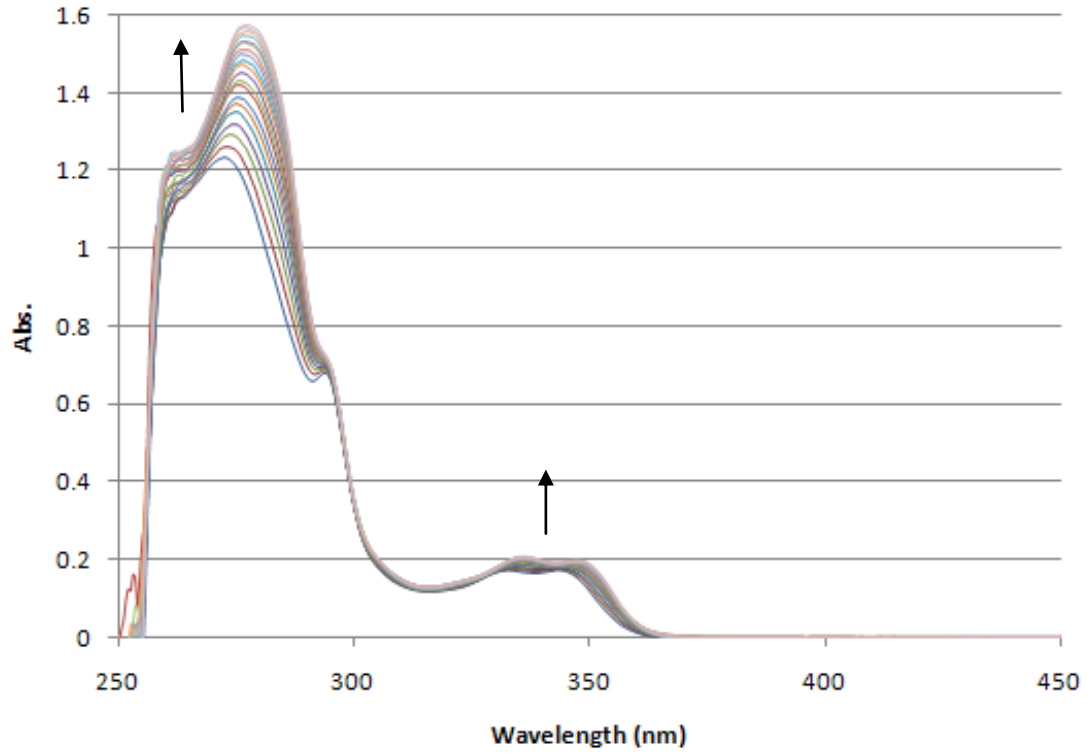

Fluorescence quenching of 215 in DMSO-0.5% H_2O with addition of TBAOAc

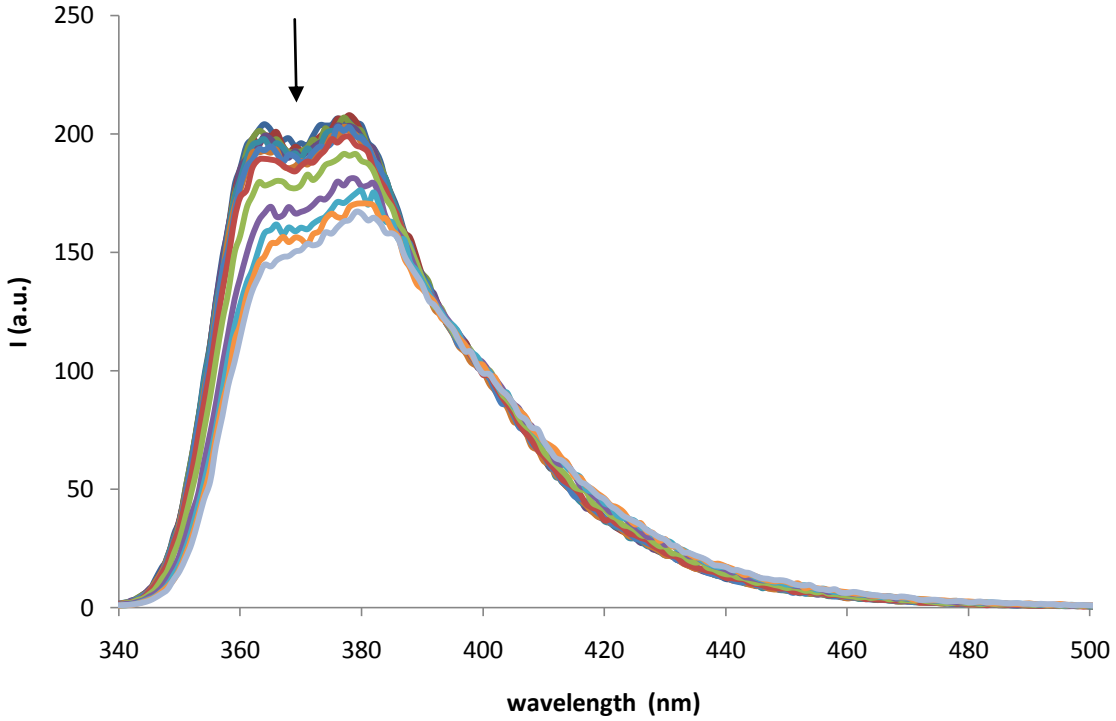

Fluorescence quenching of 215 in DMSO-0.5% H_2O with addition of TBAOBz

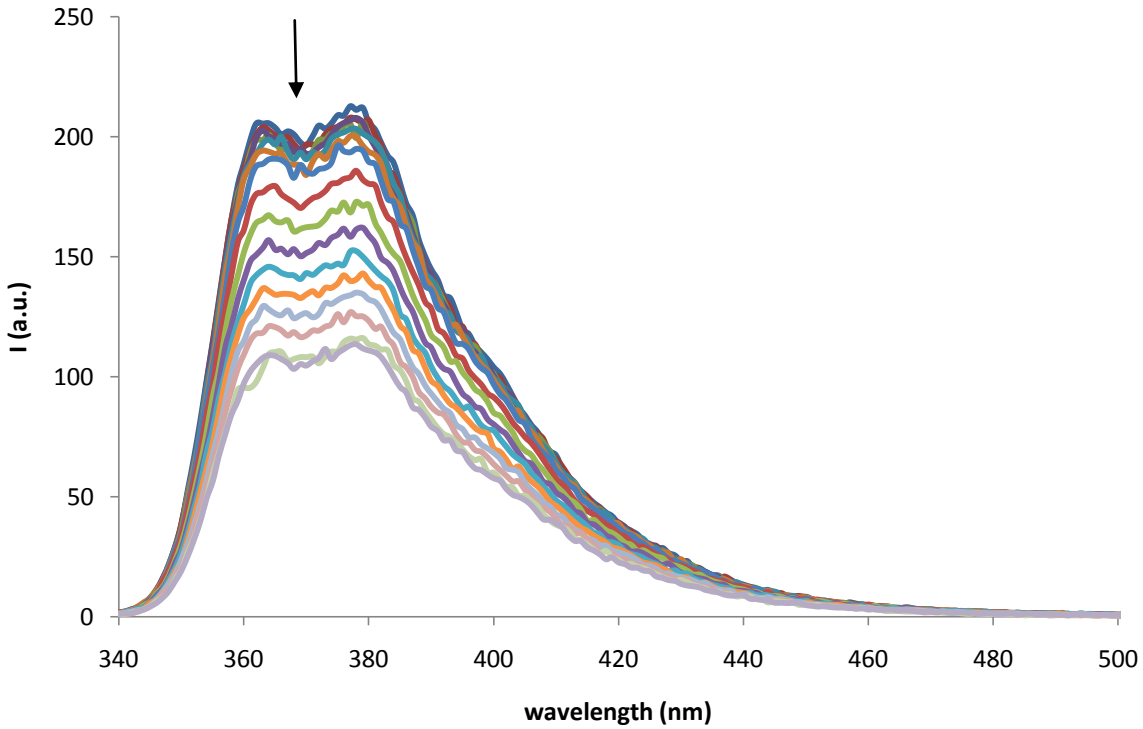

Fluorescence quenching of 213 in DMSO-0.5% H_2O with addition of TBACl

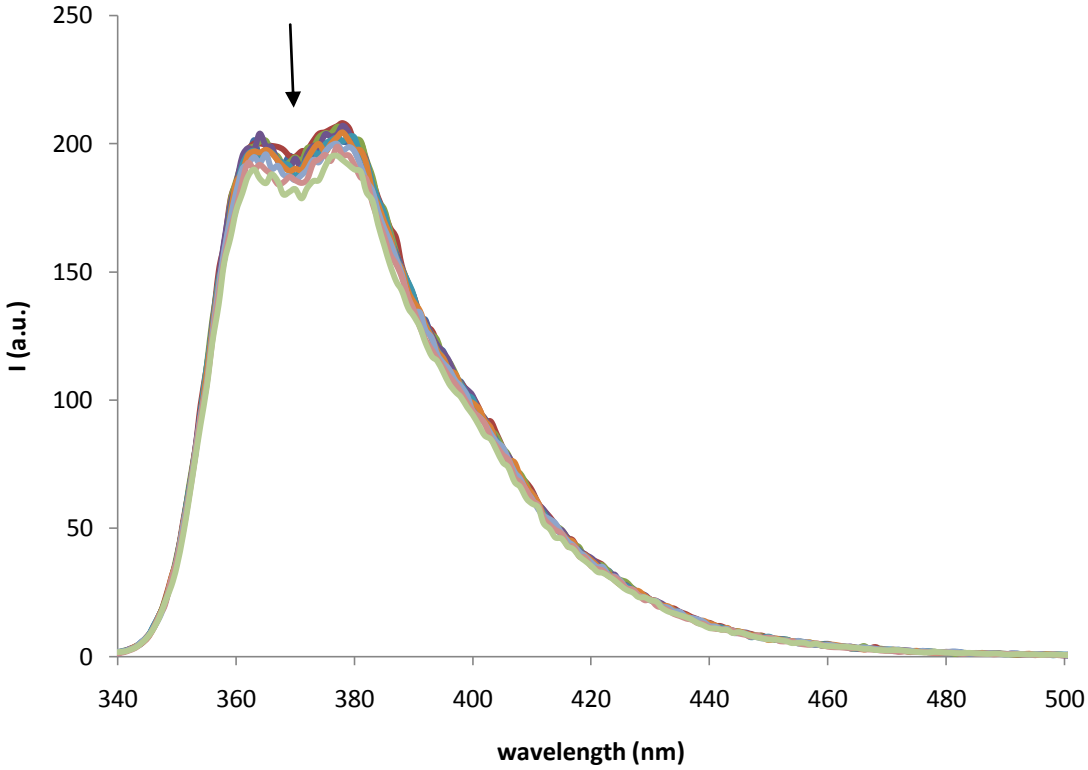

Fluorescence quenching of 213 in DMSO-0.5% H_2O with addition of TBAF

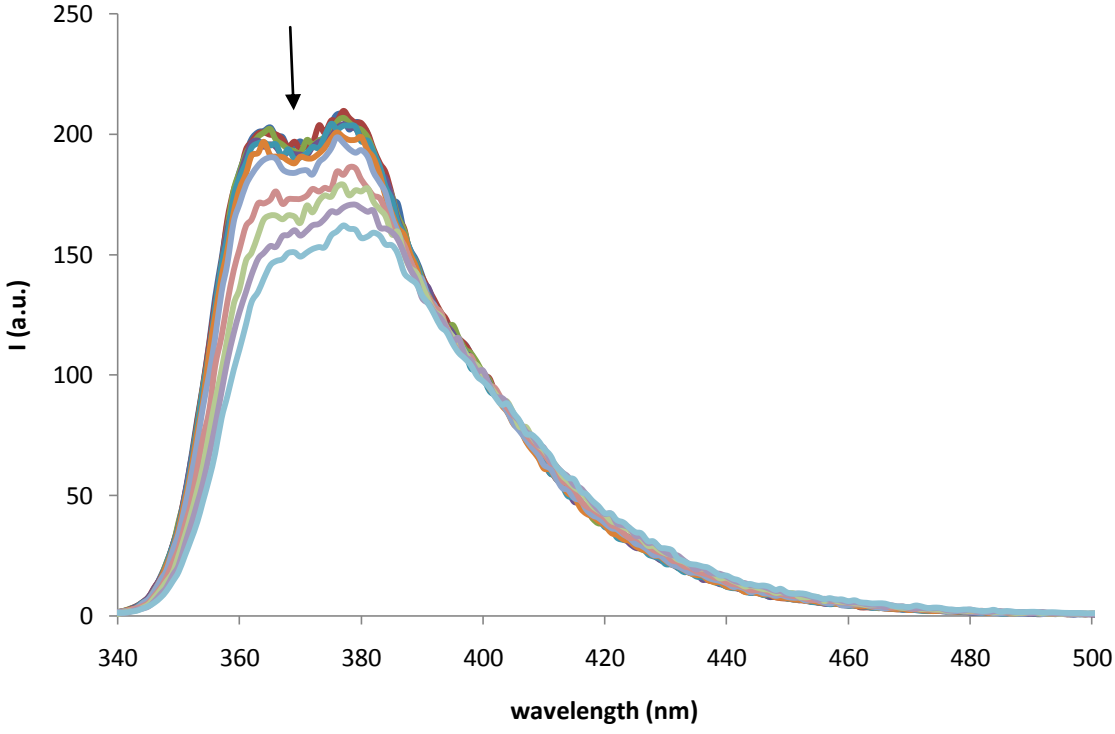

Fluorescence quenching of 213 in DMSO-0.5% H_2O with addition of $TBAH_2PO_4$

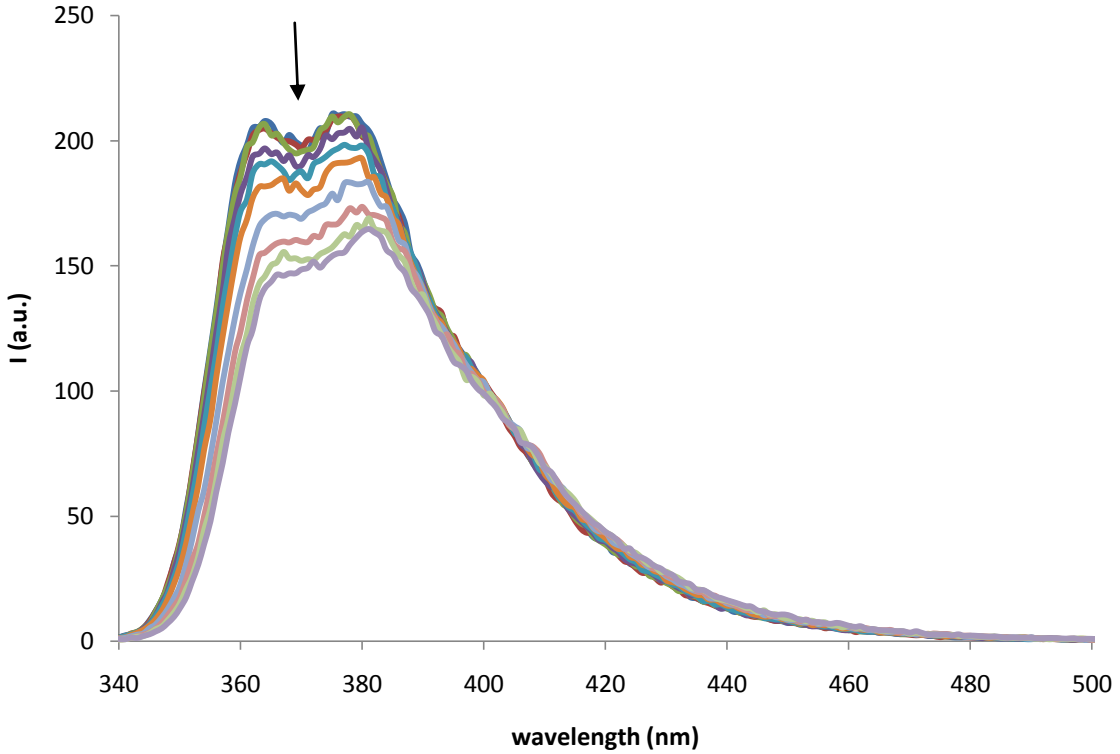

Fluorescence quenching of 213 in DMSO-0.5% H_2O with addition of $TEAHCO_3$

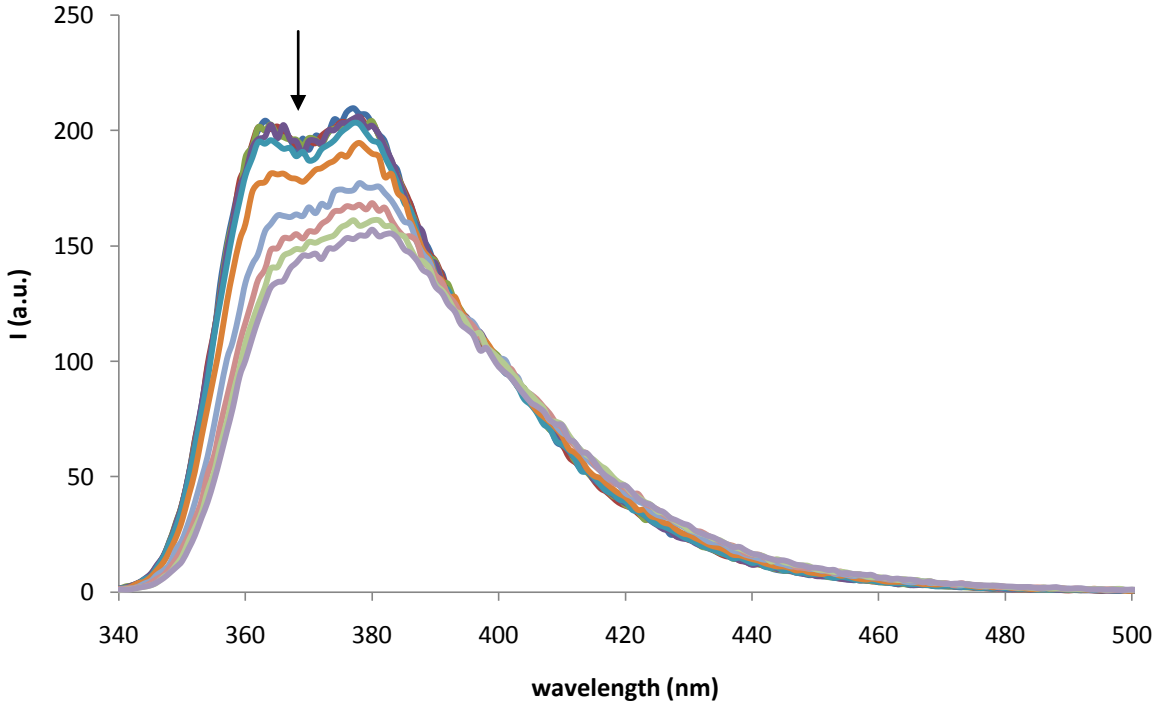

Appendix 6 – Proton NMR Titration Stack Plots

These graphs show data from the ^{1}H NMR titration experiments conducted in Chapters Two, Three, Four and Five, with the anions added as the tetraethylammonium or tetrabutylammonium salt at 298 K in the appropriate DMSO-d_6/H_2O mixtures. Only the regions of the spectra that are of interest have been shown.

Stack plots for receptors **211** and **212** marked with a * are taken from the pre-peer reviewed version of the supplementary information from the following article: Caltagirone, C.; Hiscock, J. R.; Hursthouse, M. B.; Light, M. E. and Gale, P. A, *Chem. Eur. J.*, **2008**, *14*, 10236-10243.

Stack plots for receptors **219** and **220** marked with a * are taken from the pre-peer reviewed version of the supplementary information from the following article: Gale, P. A.; Hiscock, J. R.; Moore, S. J.; Caltagirone, C.; Hursthouse, M. B. and Light, M. E. *Chem. Asian. J.*, **2010**, *5*, 555-561.

Stack plots for receptors **221** and **222** marked with a * are taken from the supplementary information of the following article: Gale, P. A.; Hiscock, J. R.; Jie, C. Z.; Hursthouse, M. B. and Light, M. E., *Chem. Sci.*, **2010**, *1*, 215-220.

NMR Stack plots from Chapter Two

Receptor 211 *vs* TBAF in DMSO-d_6/H_2O 0.5%

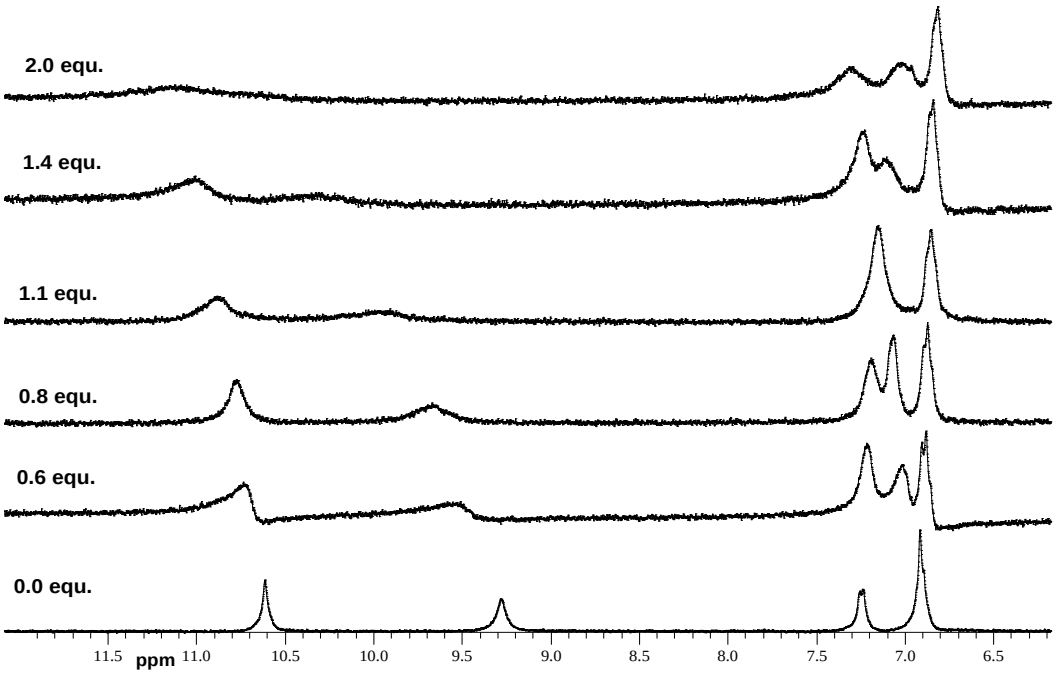

Receptor 211 *vs* TBAOBz in DMSO-d_6/H_2O 0.5% *

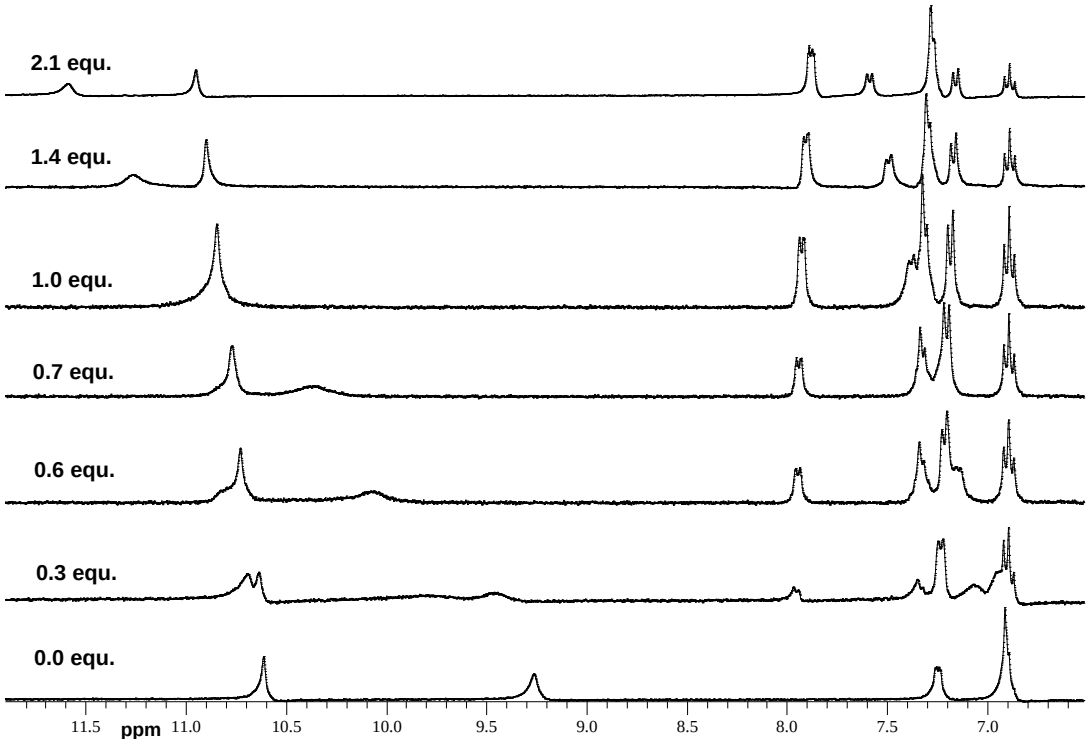

Receptor 211 *vs* TBACl in DMSO-d_6/H_2O 0.5% *

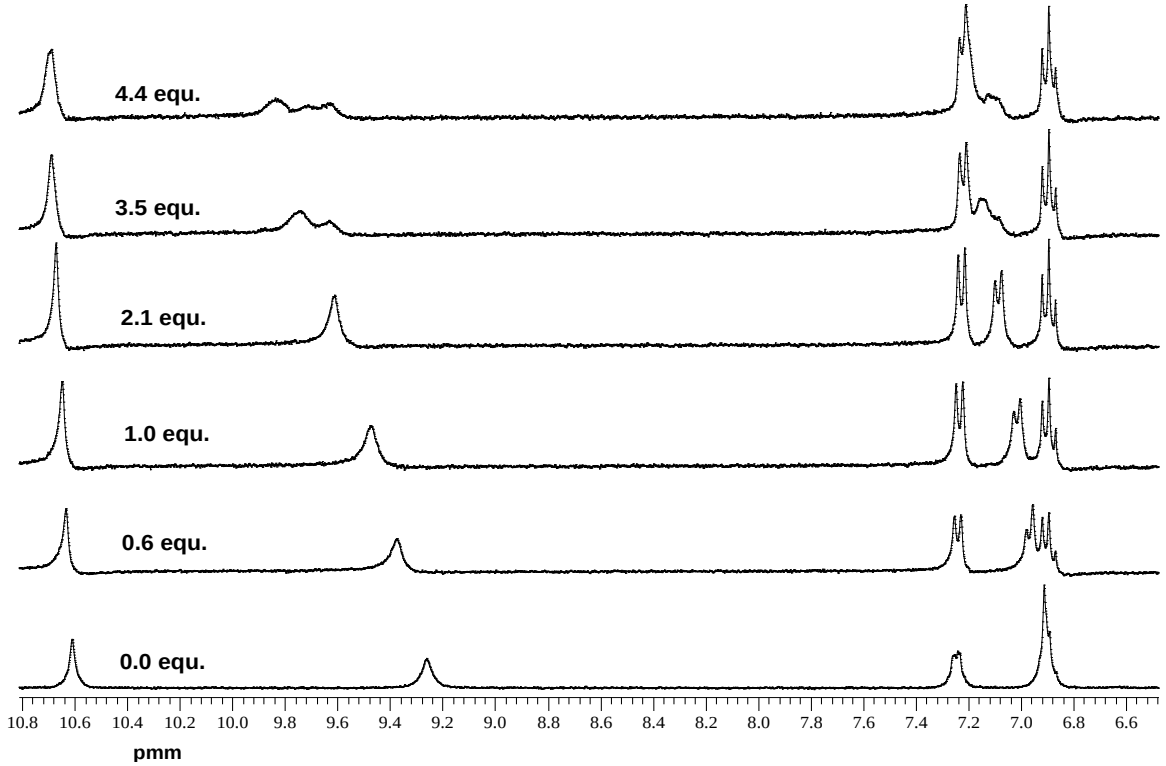

Receptor 211 *vs* TBAOAc in DMSO-d_6/H_2O 0.5% *

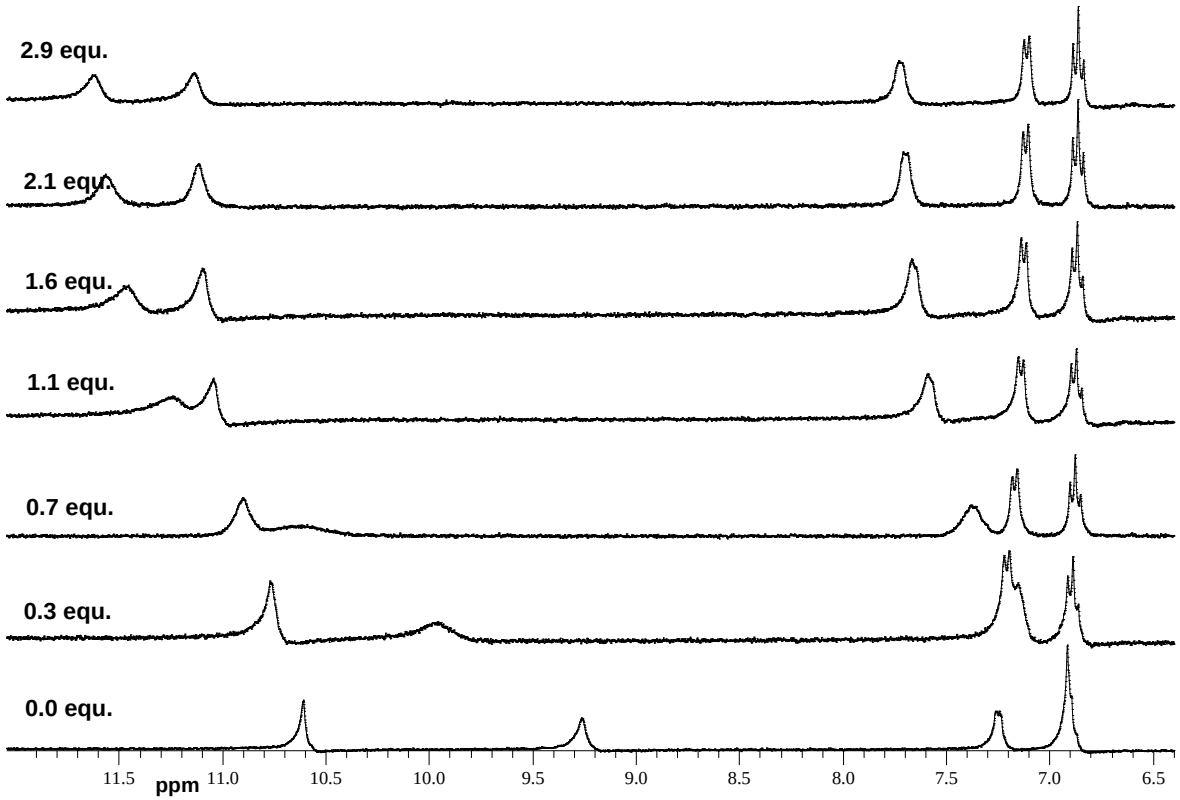

Receptor 212 *vs* TBAOAc in DMSO-d_6/H_2O 0.5% *

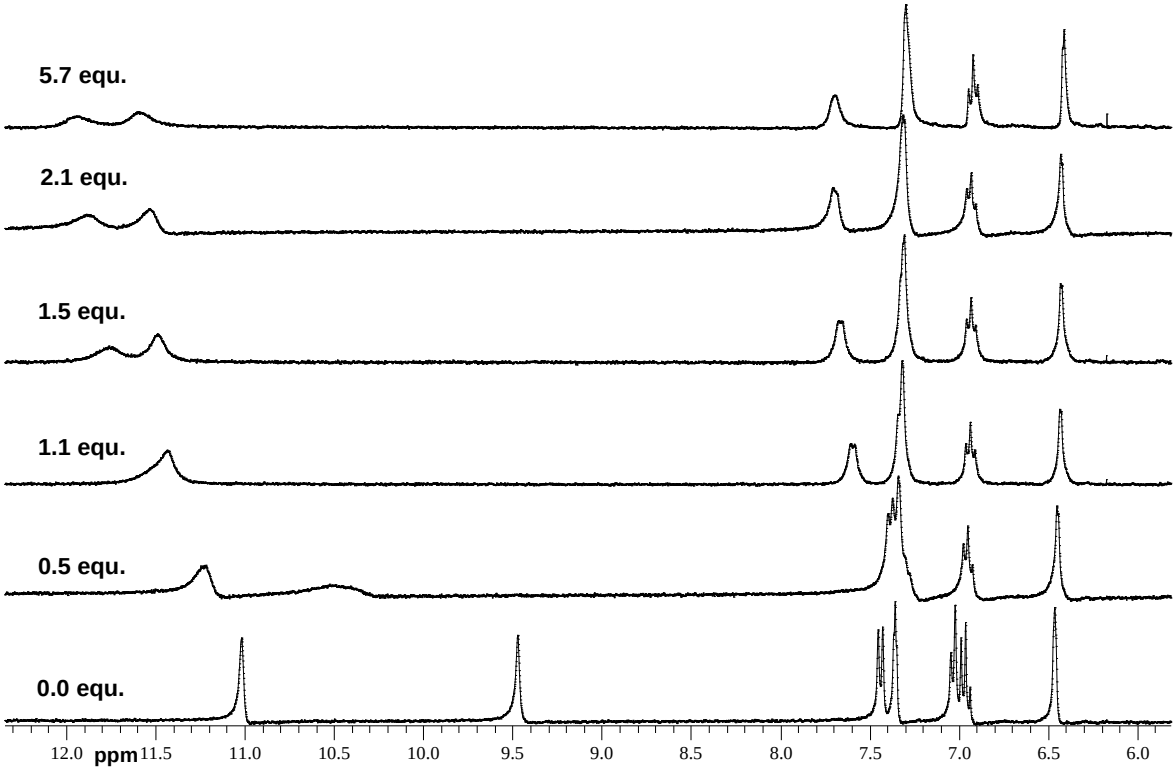

Receptor 212 *vs* TBACl in DMSO-d_6/H_2O 0.5% *

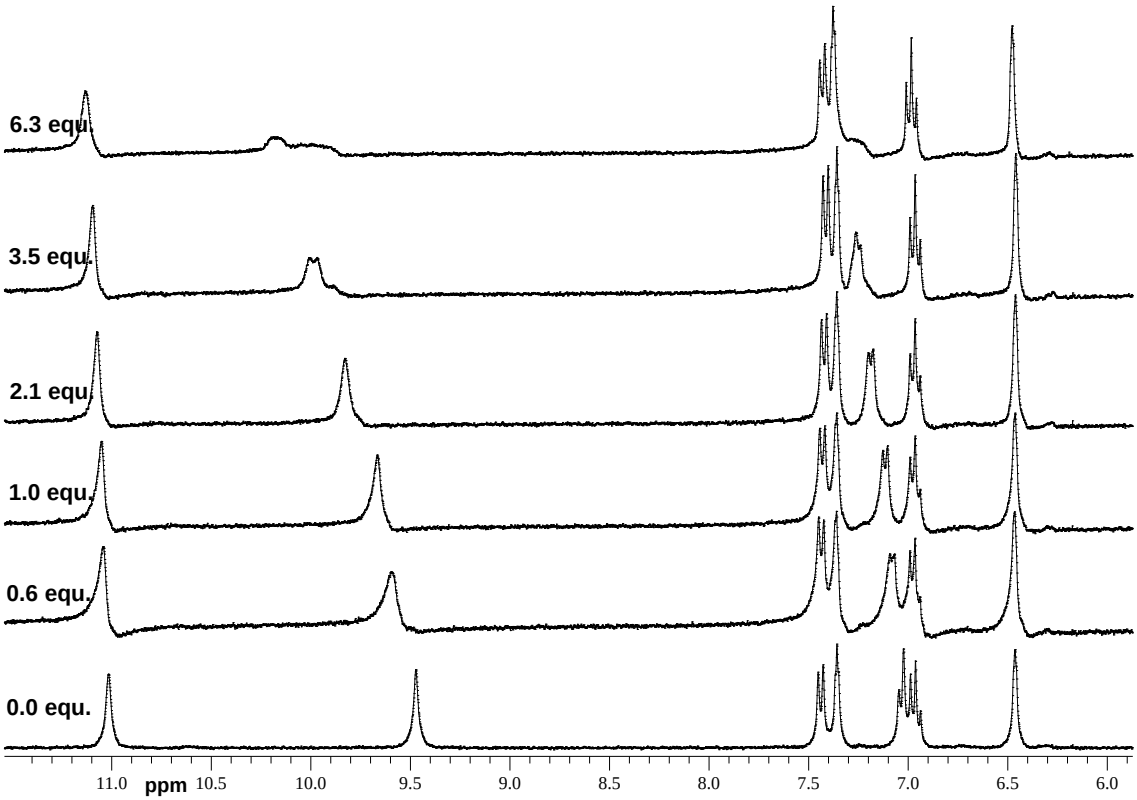

Receptor 212 *vs* TBAF in DMSO-d_6/H_2O 0.5%

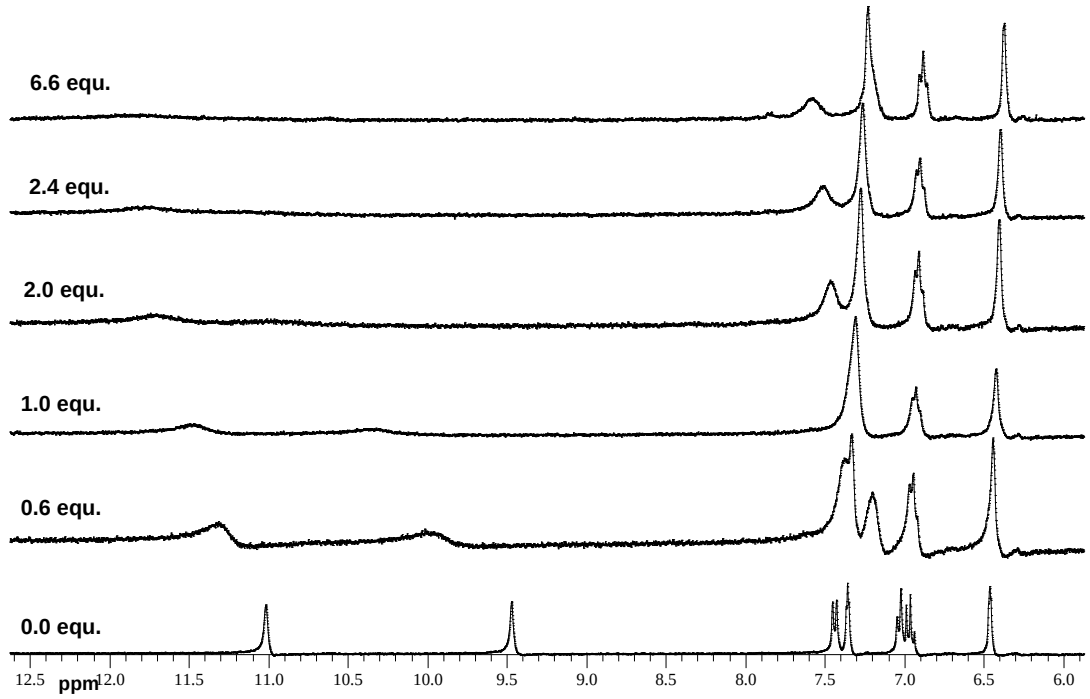

Receptor 212 *vs* TBAOBz in DMSO-d_6/H_2O 0.5% *

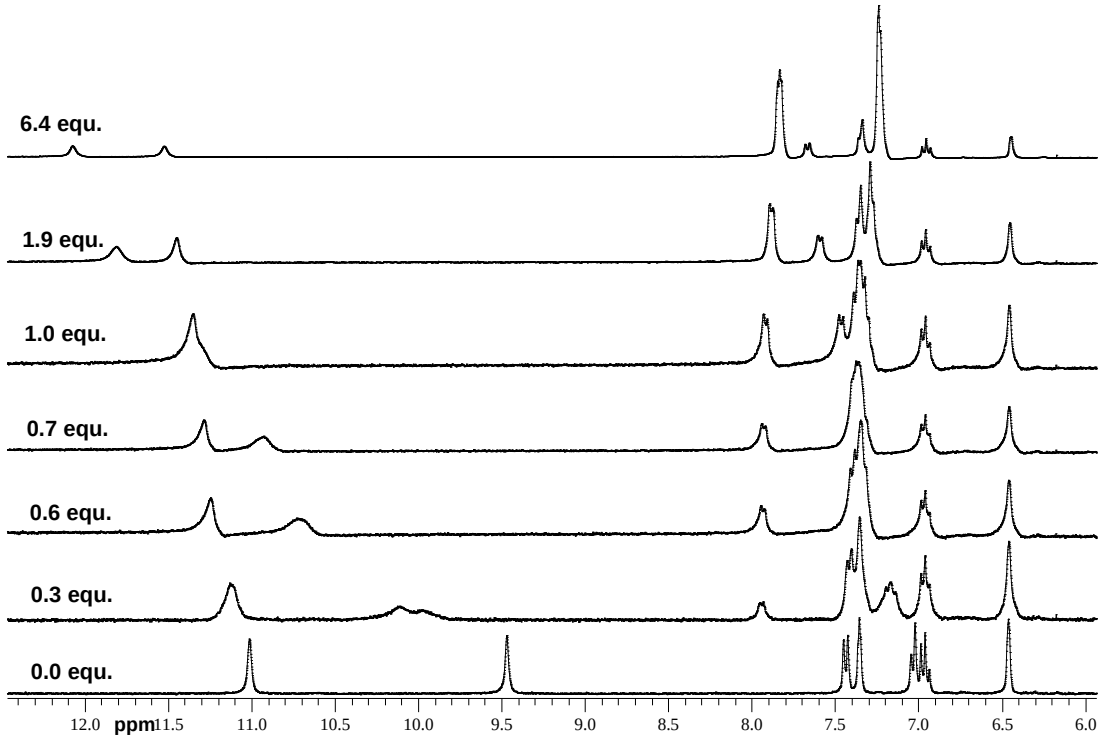

NMR Stack plots from Chapter Three

Receptor 219 *vs*. $TBAH_2PO_4$ and TBAOH in DMSO-d_6/H_2O 10%. *

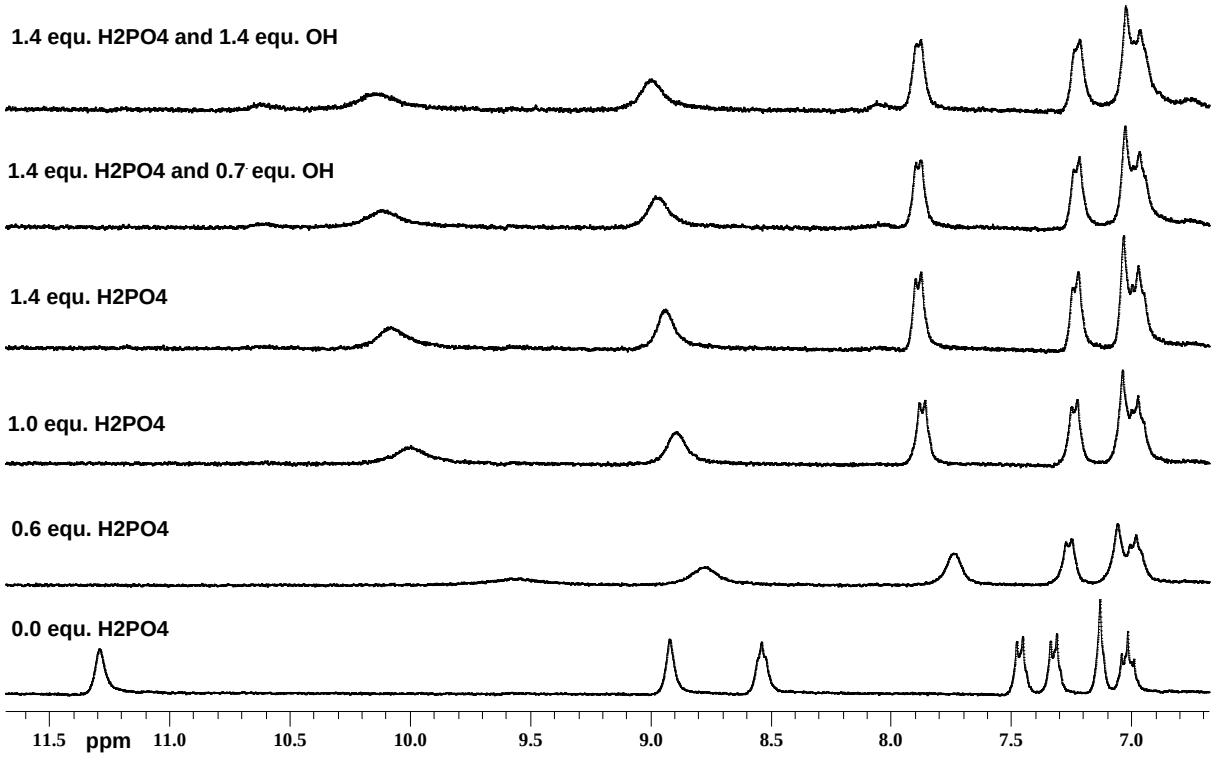

Receptor 219 *vs*. TBAOH in DMSO-d_6/H_2O 10% *

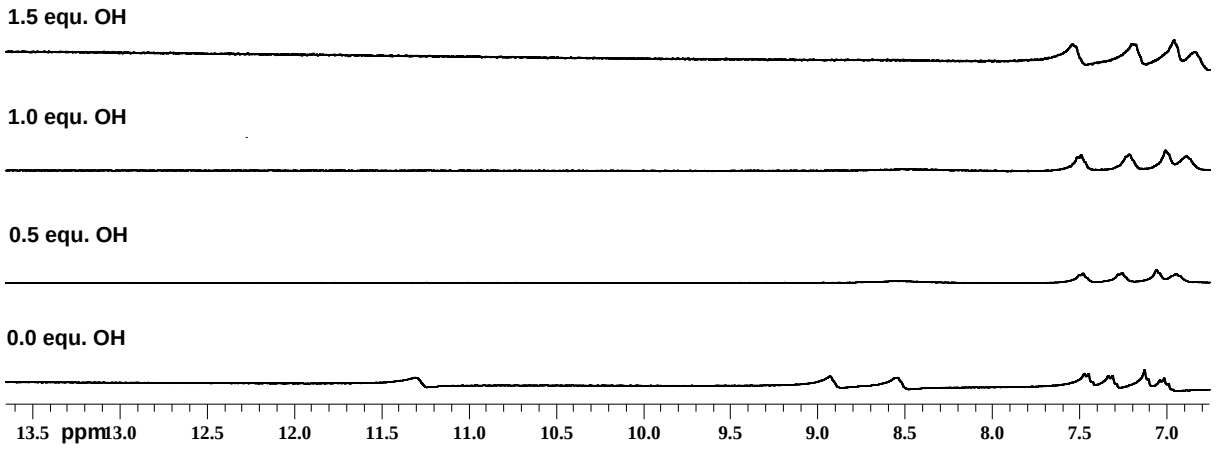

Receptor 219 with TBAOAc depicting a conformation change during the NMR titration in DMSO-d_6/H_2O 10% *

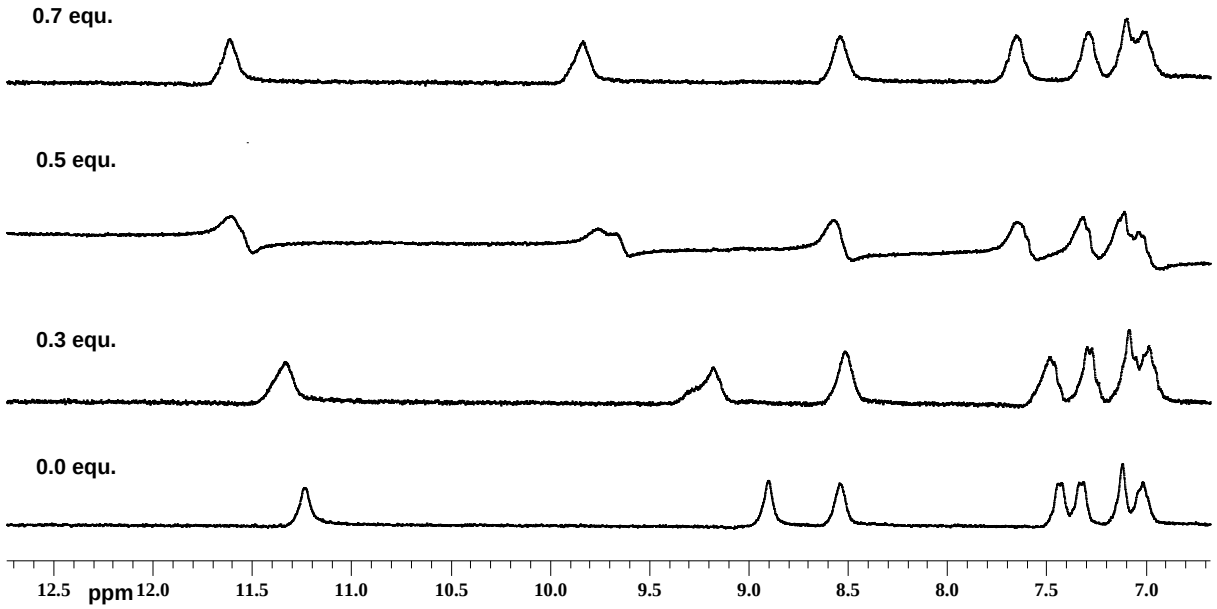

Receptor 220 *vs* $TBAH_2PO_4$ in DMSO-d_6/H_2O 0.5%

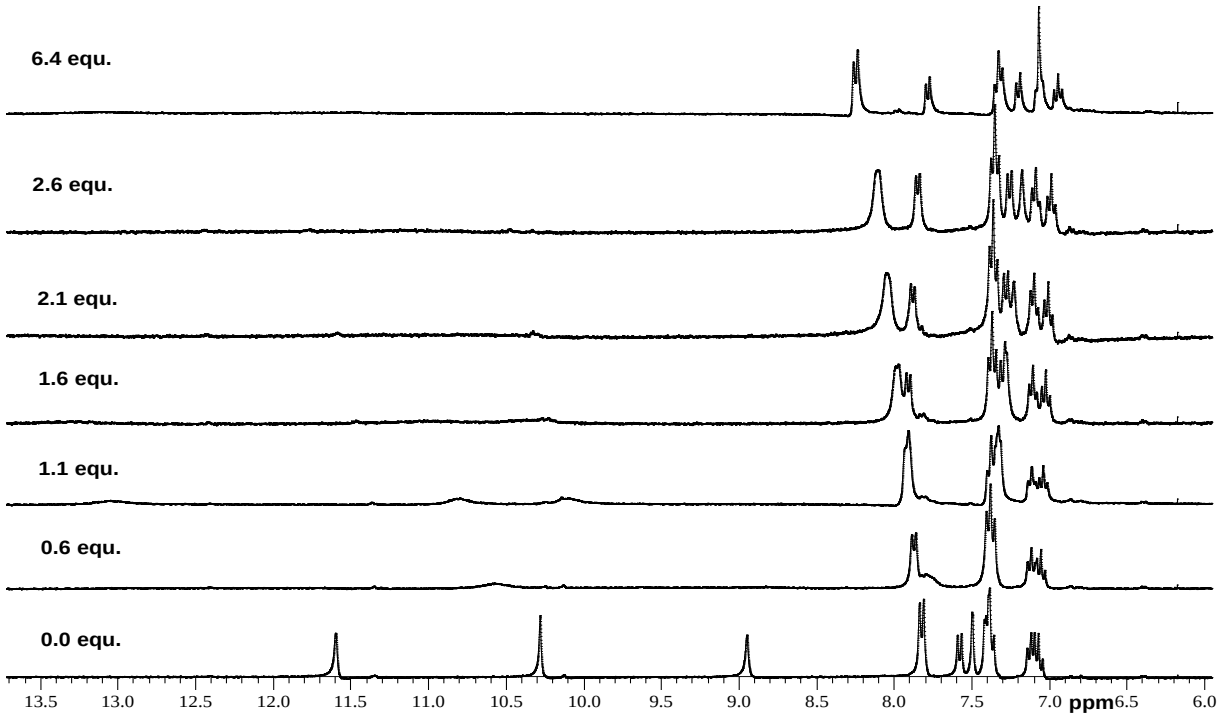

Receptor 220 *vs* TBABzO in DMSO-d_6/H_2O 0.5%

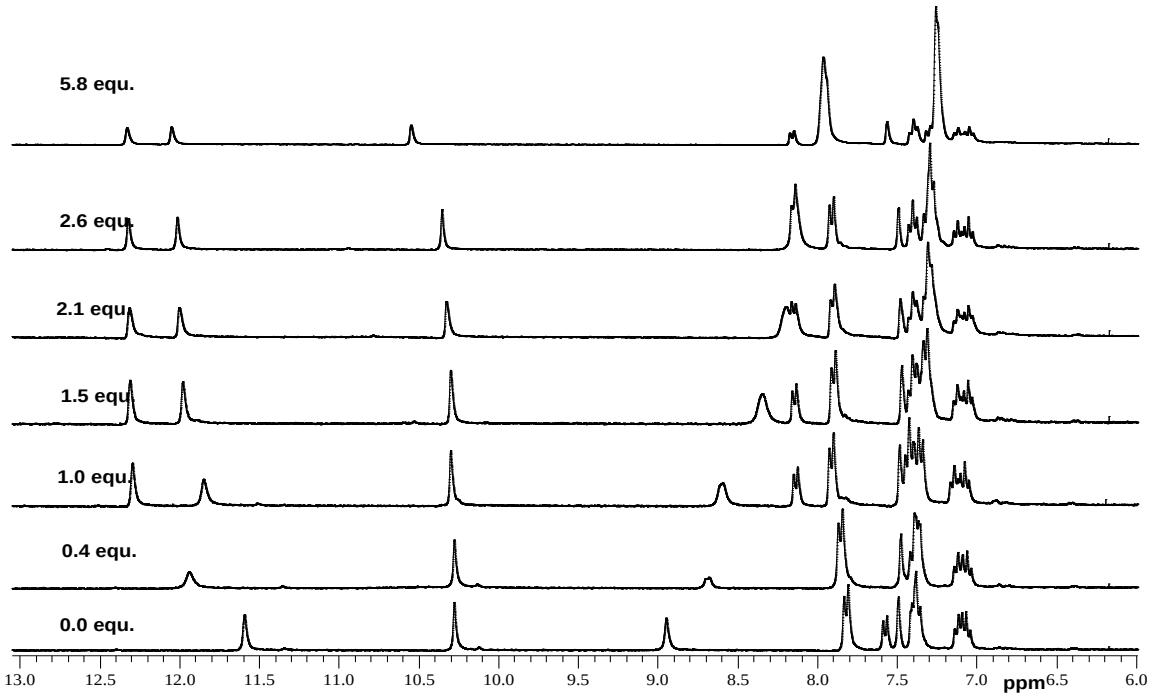

Receptor 220 vs $TBAHCO_3$ in DMSO-d6/H_2O 0.5%

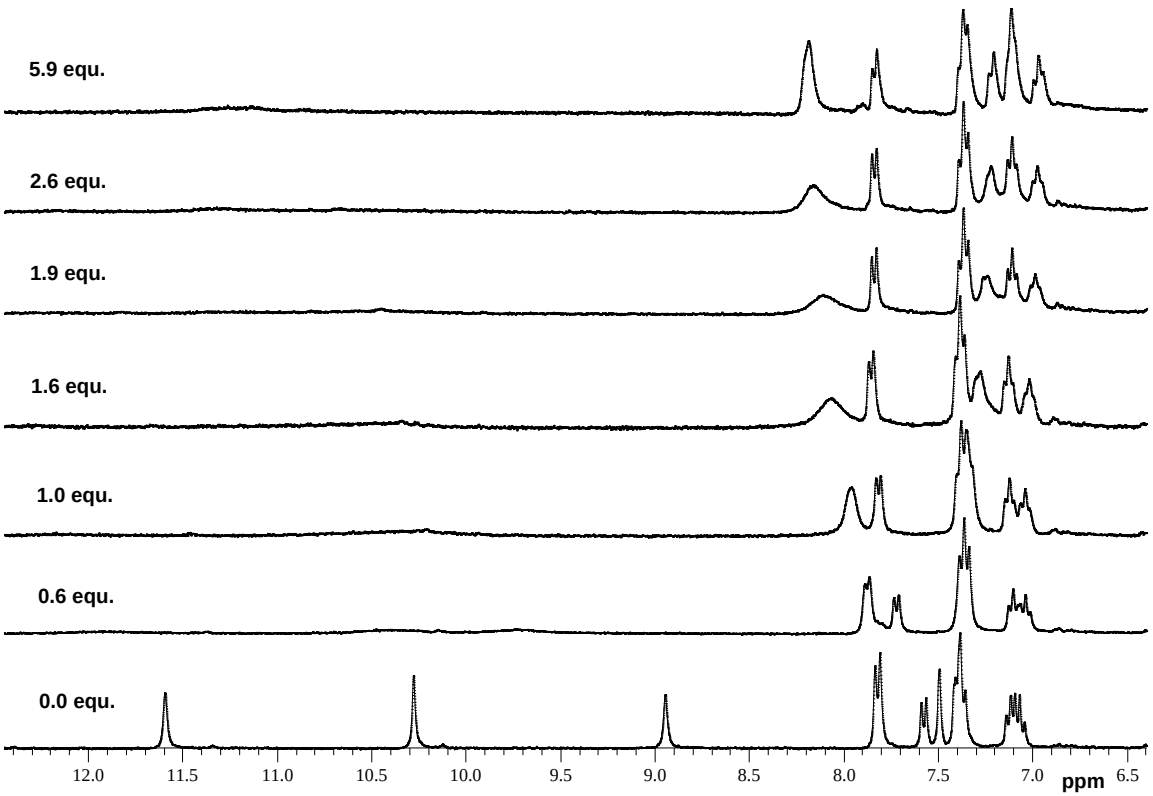

Receptor 220 *vs* TBACl in DMSO-d_6/H_2O 0.5%

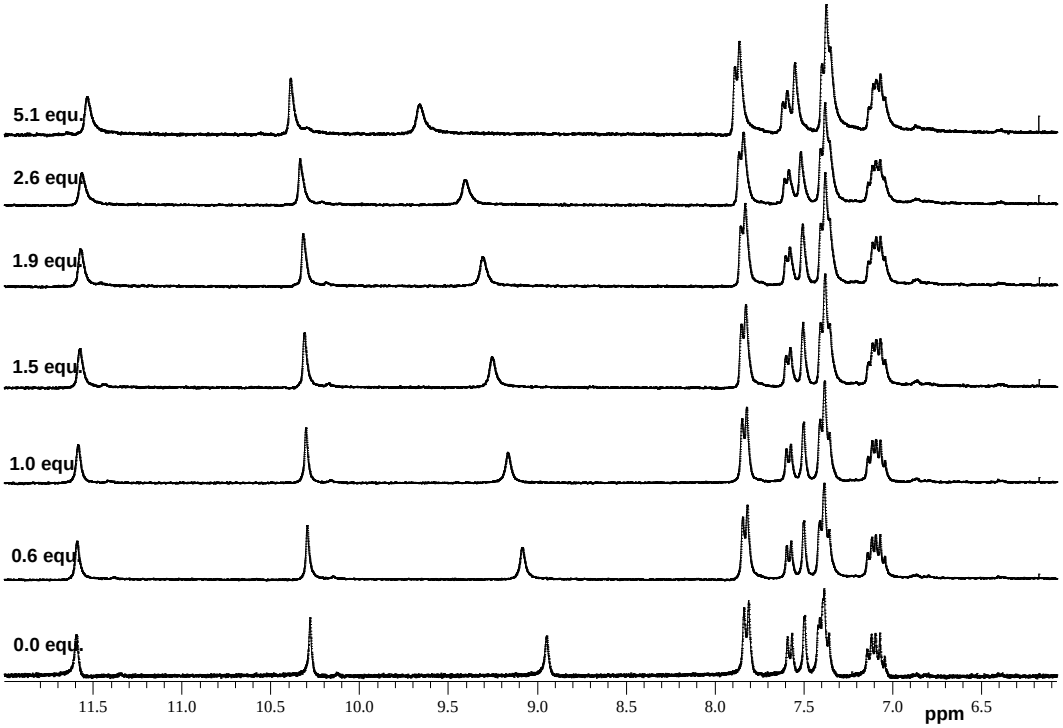

Receptor 220 *vs* TBAAcO in DMSO-d_6/H_2O 0.5%

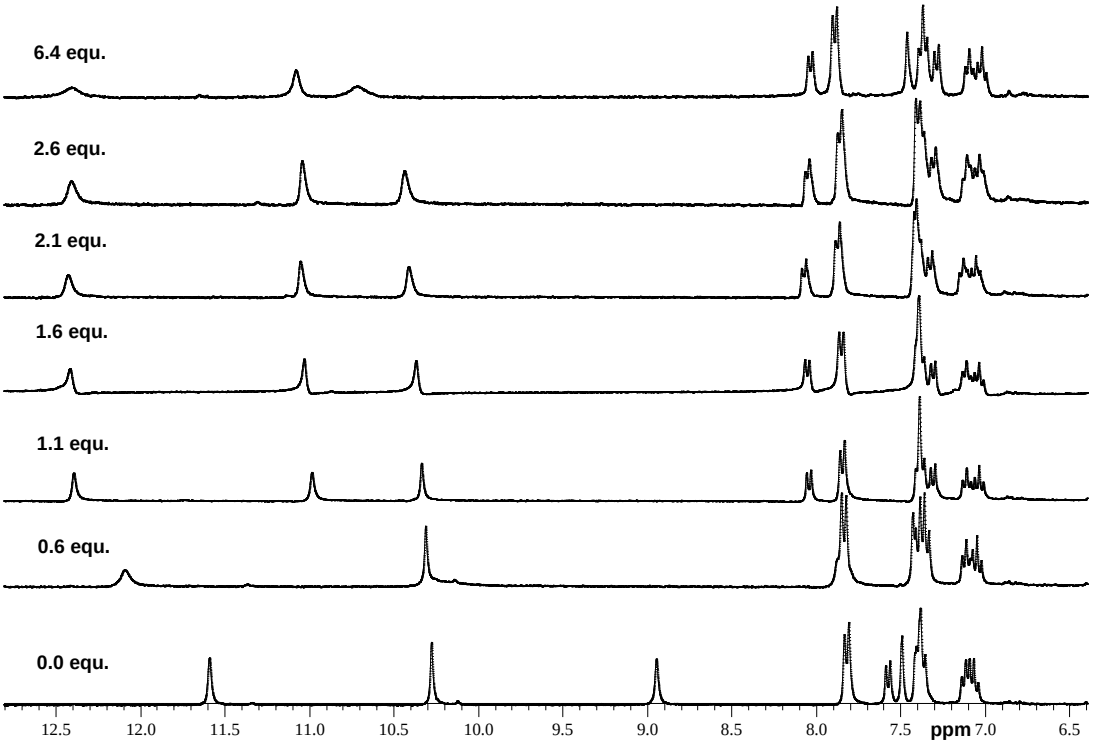

Receptor 220 *vs*. $TBAH_2PO_4$ and TBAOH in DMSO-d_6/H_2O 0.5% *

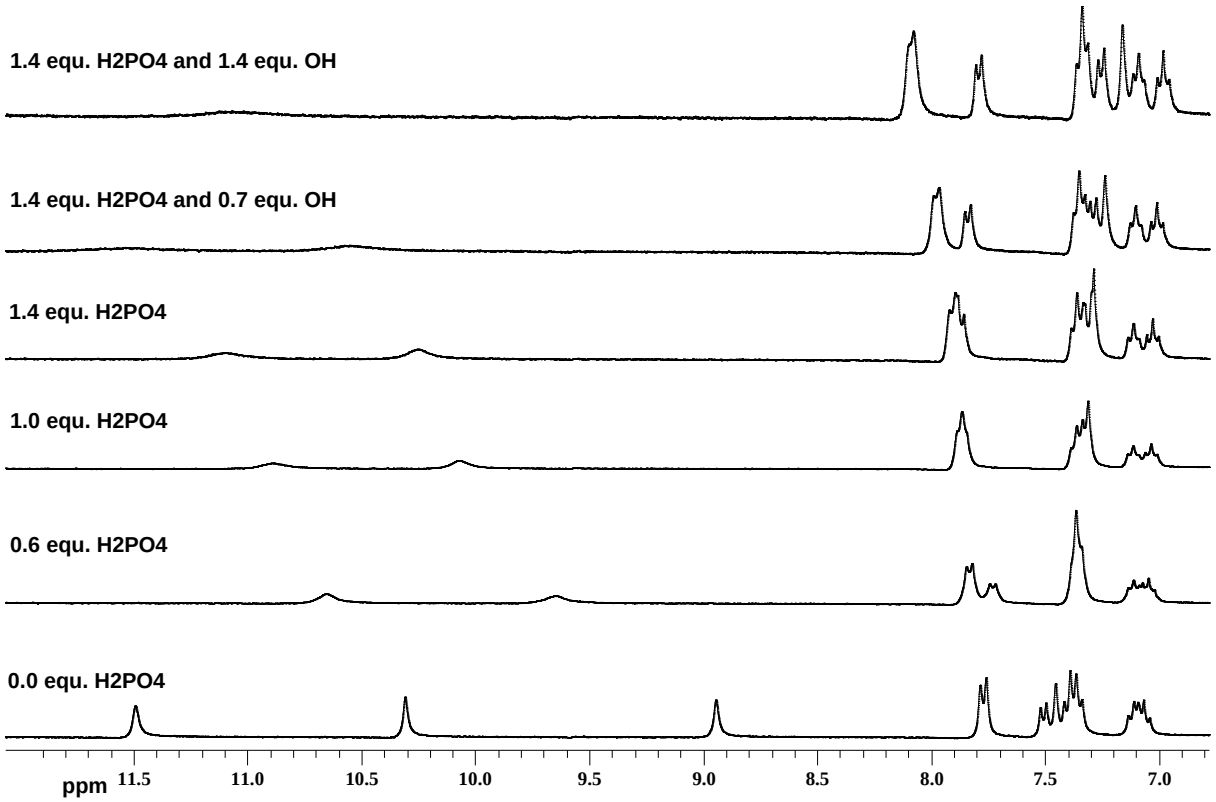

Receptor 220 *vs*. TBAOH in DMSO-d_6/H_2O 0.5% *

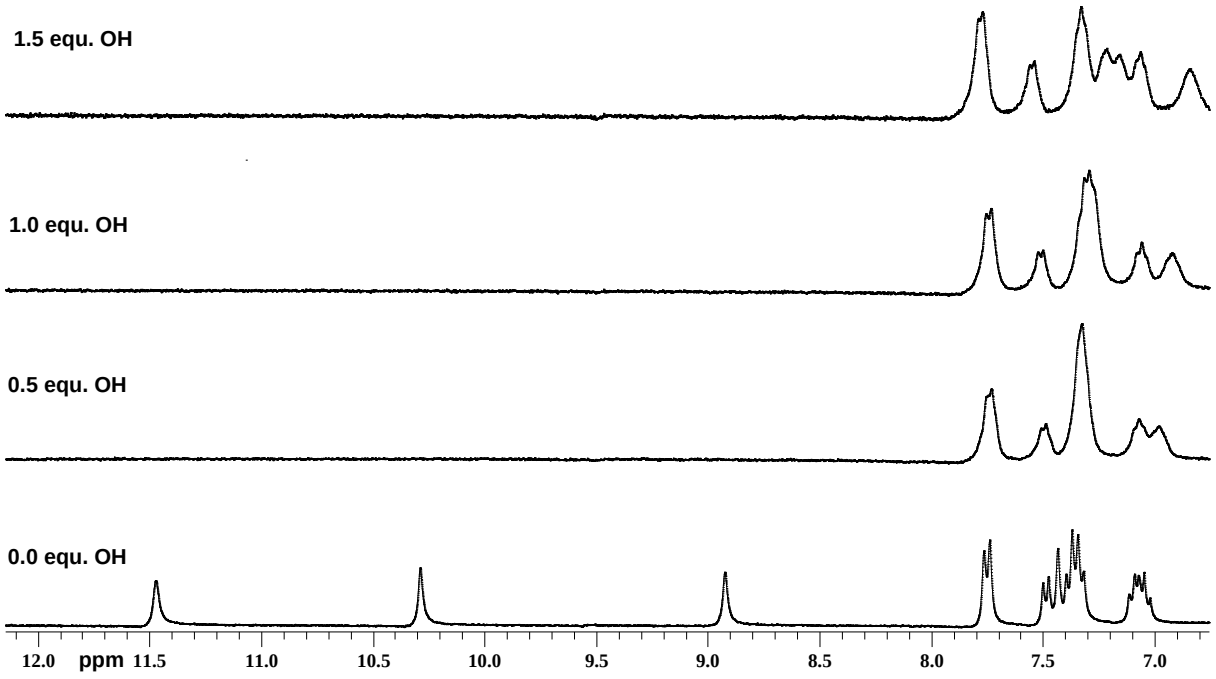

Receptor 220 *vs.* $TBAH_2PO_4$ and TBAOH in DMSO-d_6/H_2O 10% *

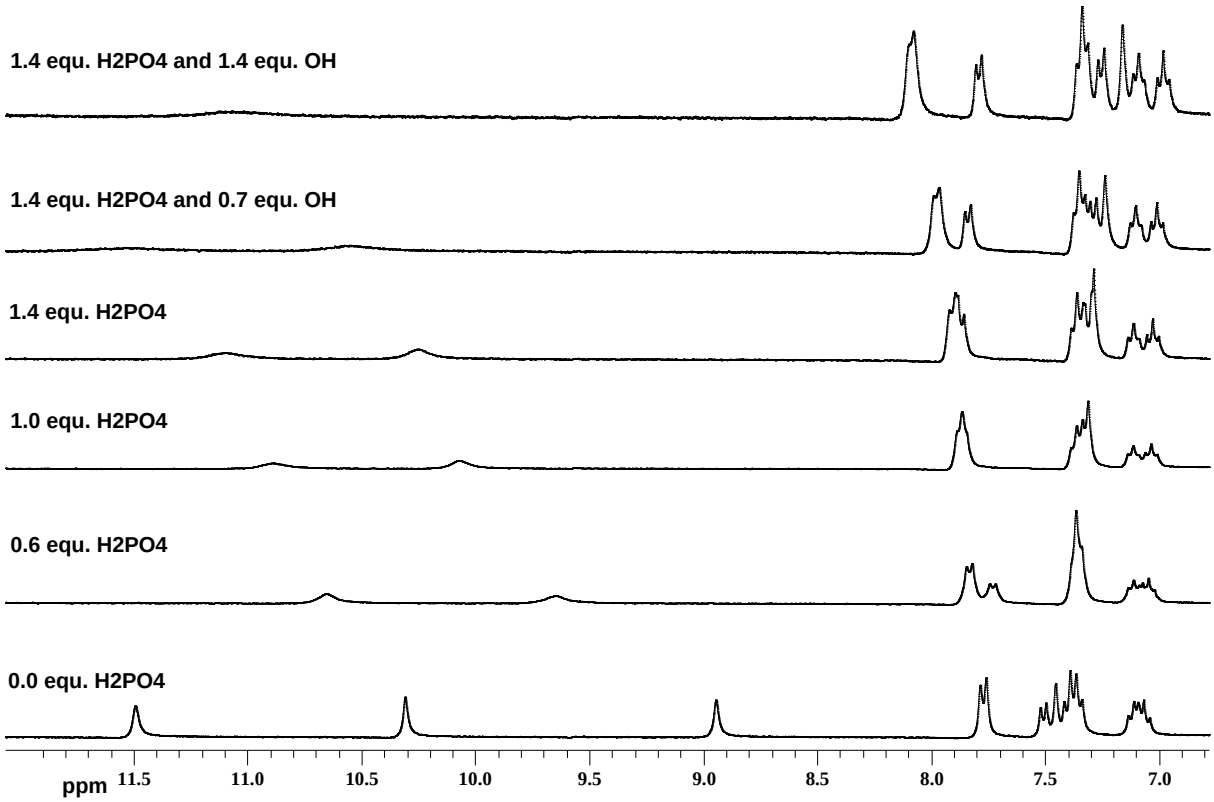

Receptor 220 *vs.* TBAOH in DMSO-d_6/H_2O 10% *

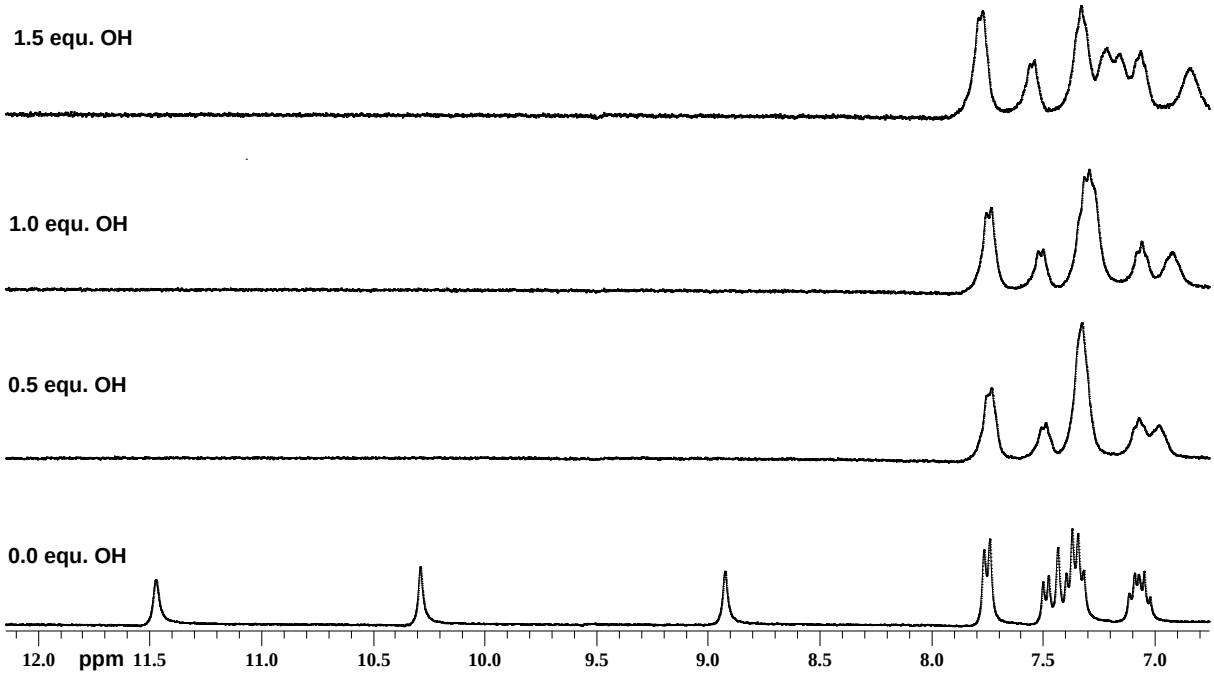

Receptor 221 *vs.* TBAOH in DMSO-d_6/H_2O 0.5% *

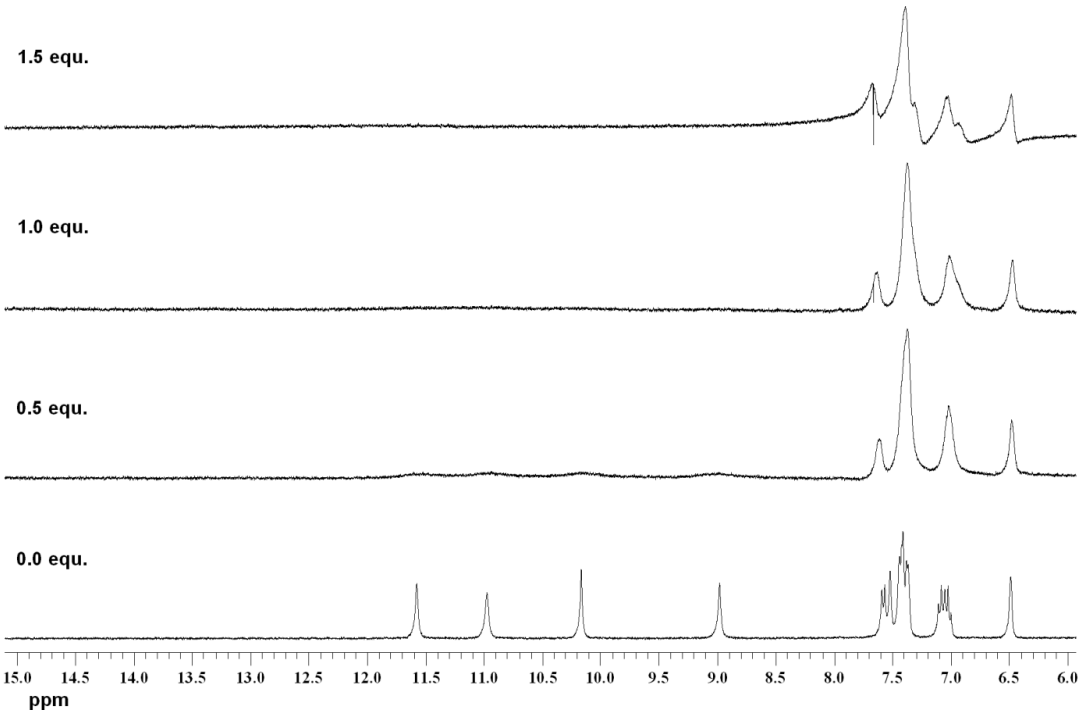

Receptor 221 *vs.* $TBAHCO_3$ and TBAOH in DMSO-d_6/H_2O 0.5% *

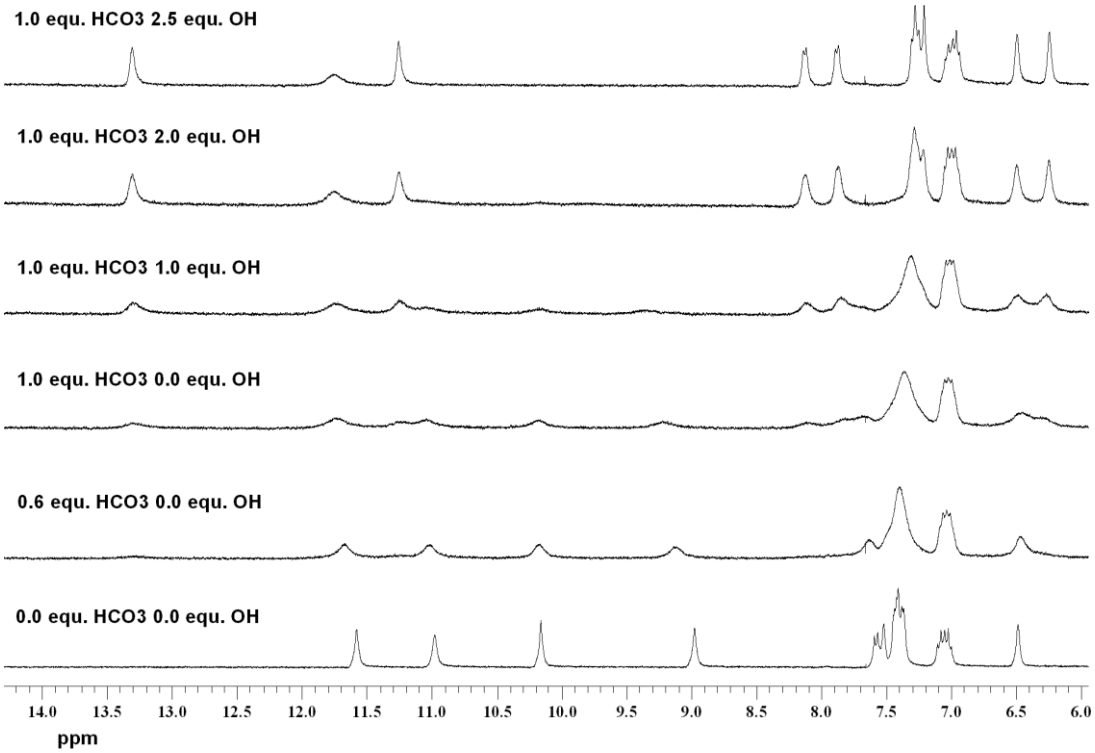

Receptor 221 *vs.* $TBAH_2PO_4$ and TBAOH in DMSO-d_6/H_2O 0.5% *

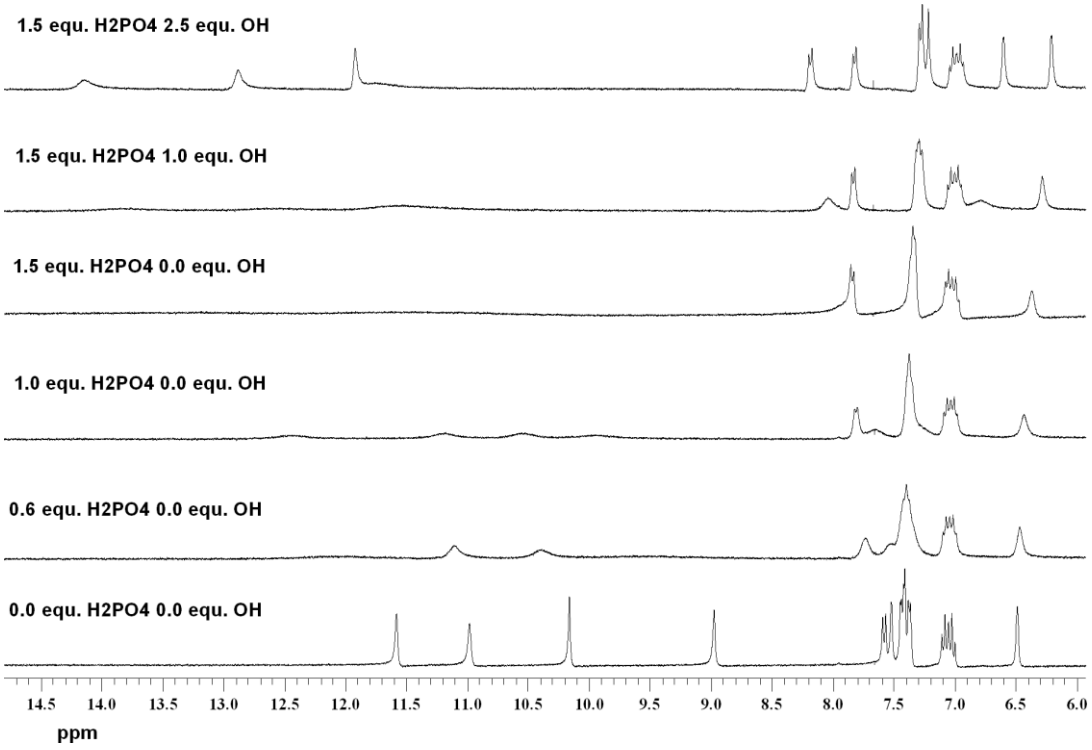

Receptor 221 *vs.* $TBAHCO_3$ in DMSO-d_6/H_2O 10% *

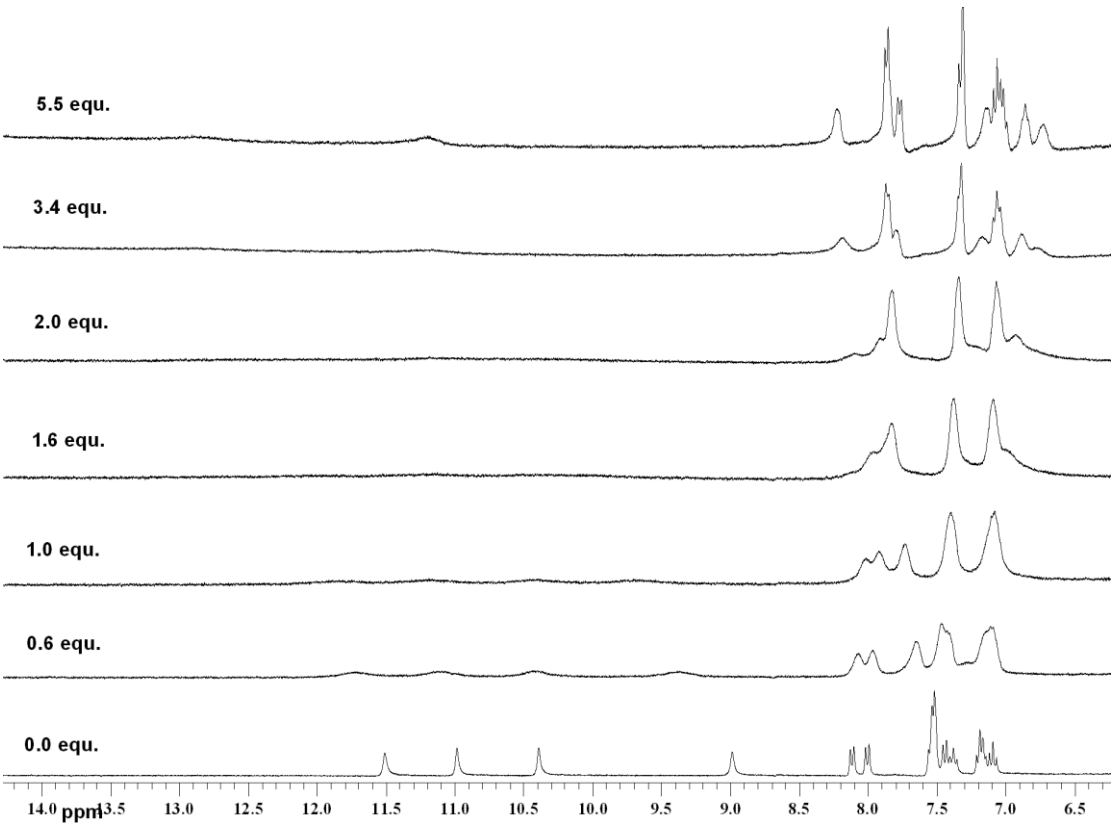

Receptor 221 *vs.* $TBAHCO_3$ and TBAOH in DMSO-d_6/H_2O 10%

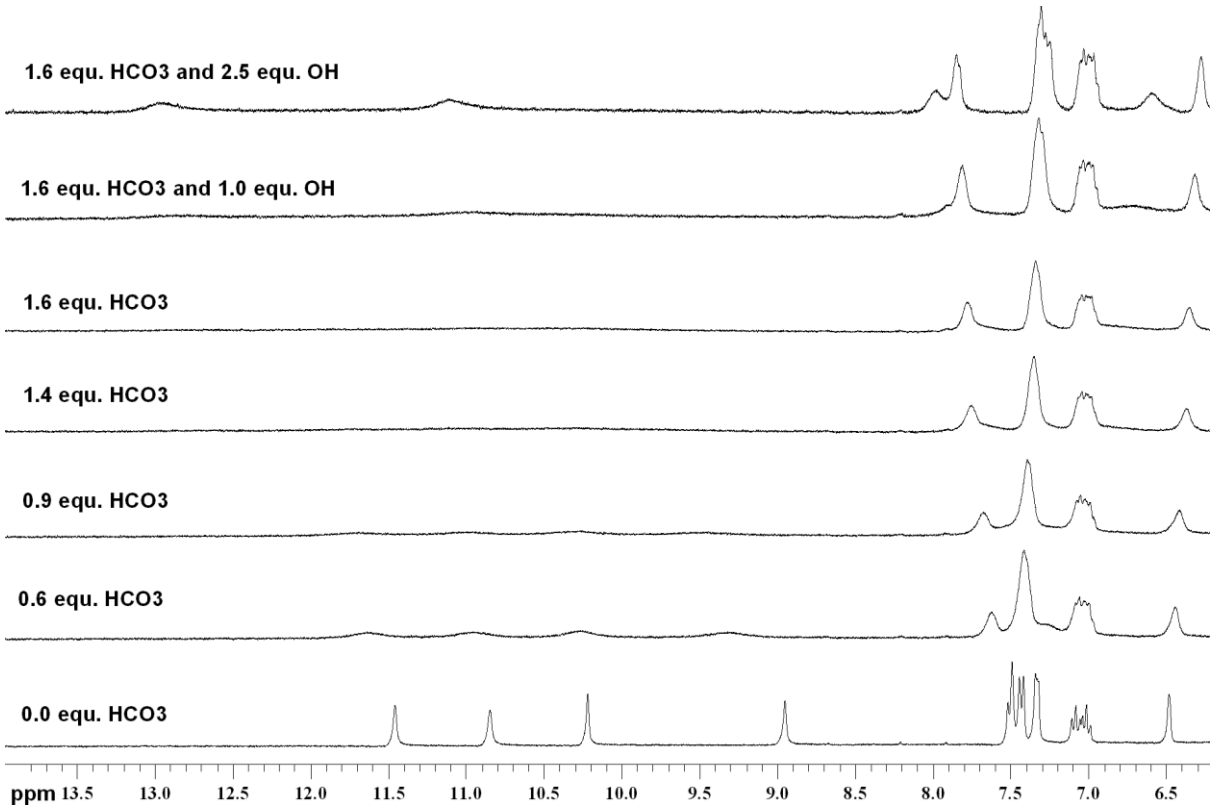

Receptor 222 *vs.* TBAOH in DMSO-d_6/H_2O 0.5% *

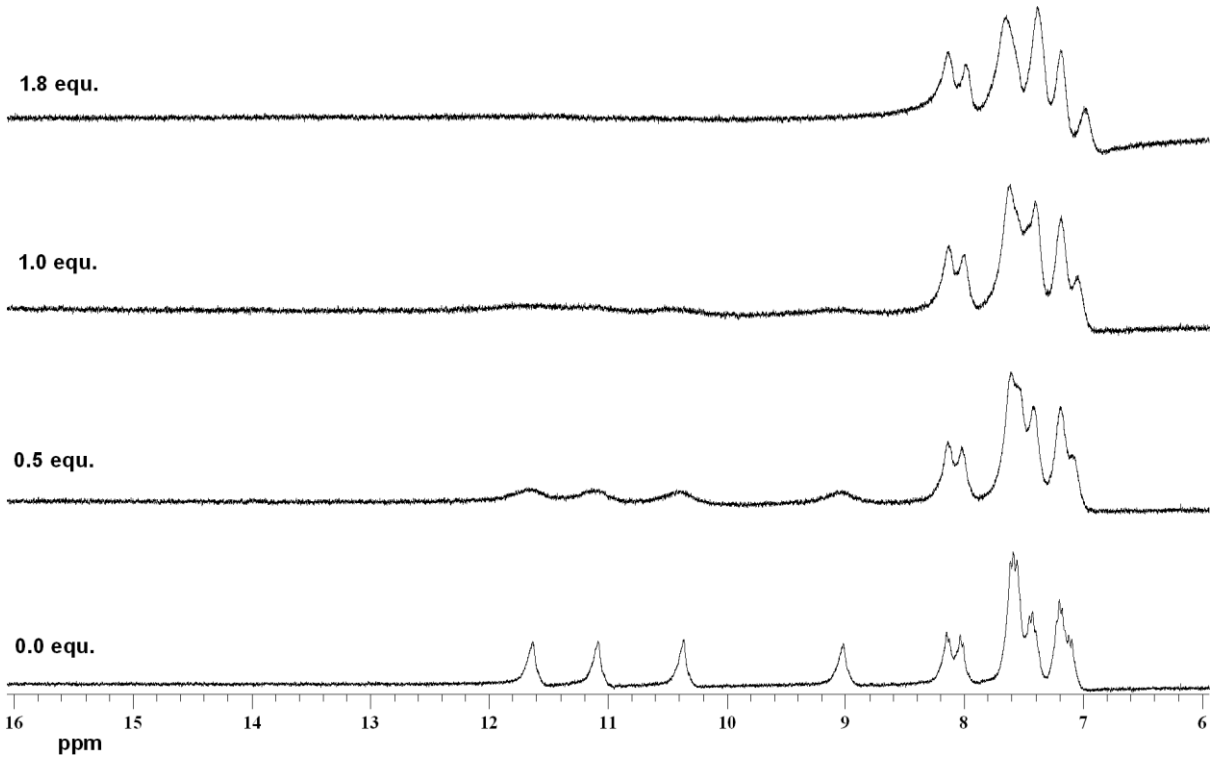

Receptor 222 *vs*. TBAHCO$_3$ in DMSO-d_6/H$_2$O 0.5% *

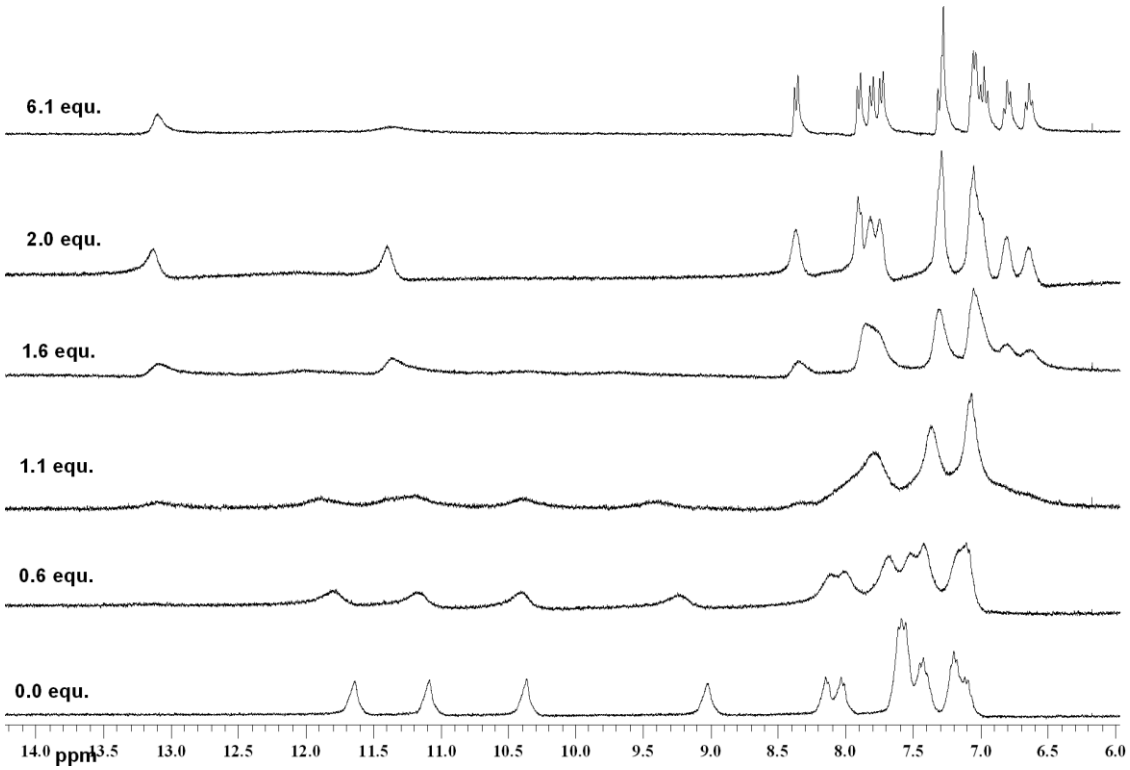

Receptor 222 *vs*. TBAHCO$_3$ and TBAOH in DMSO-d_6/H$_2$O 0.5% *

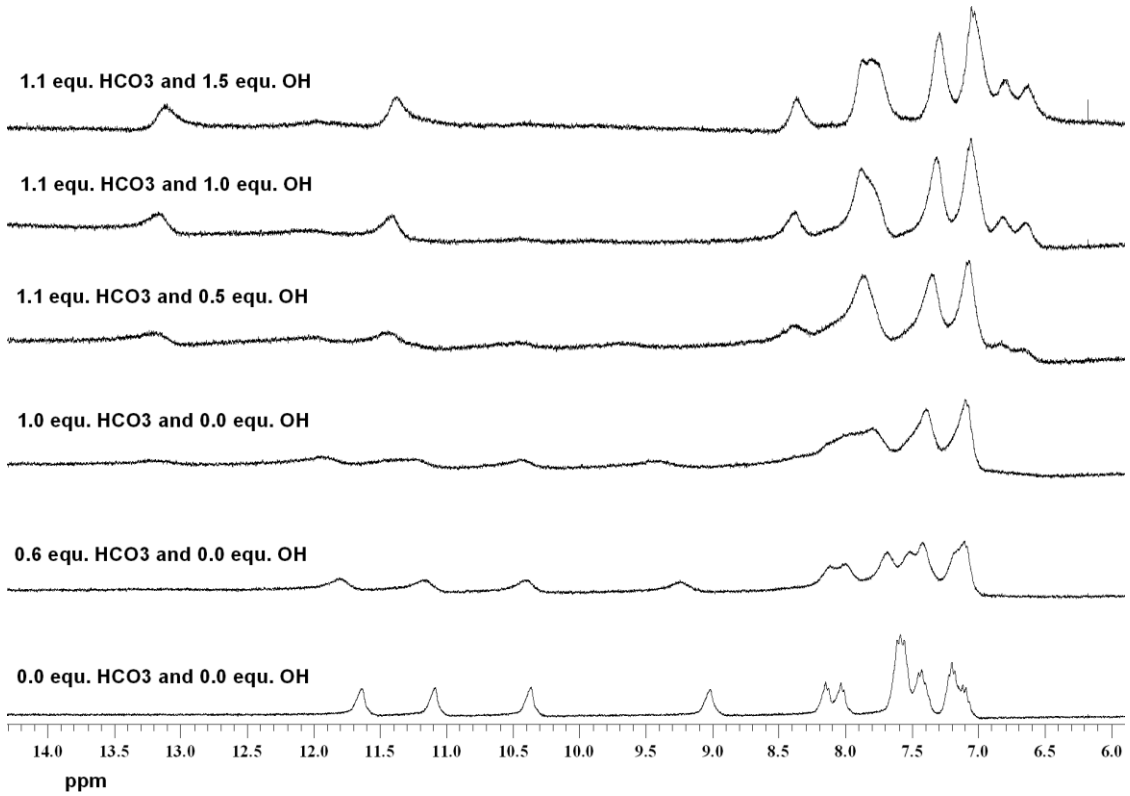

Receptor 222 *vs*. $TBAH_2PO_4$ in DMSO-d_6/H_2O 0.5% *

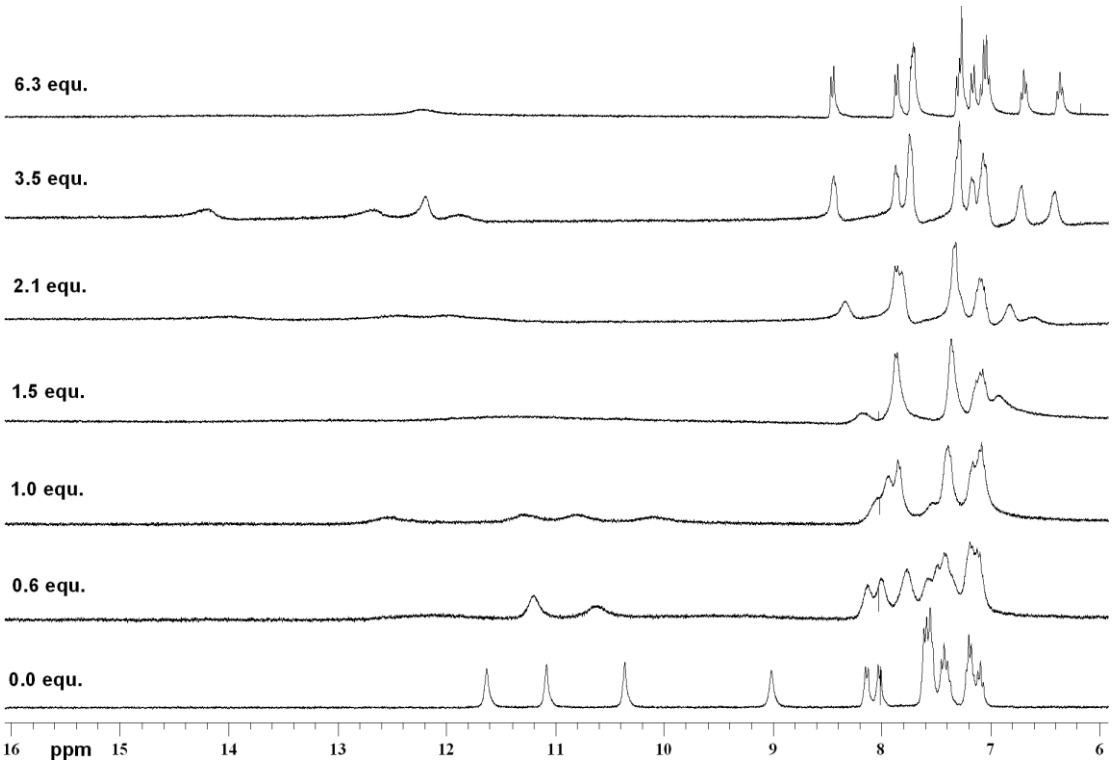

Receptor 222 *vs*. $TBAH_2PO_4$ and TBAOH in DMSO-d_6/H_2O 0.5%

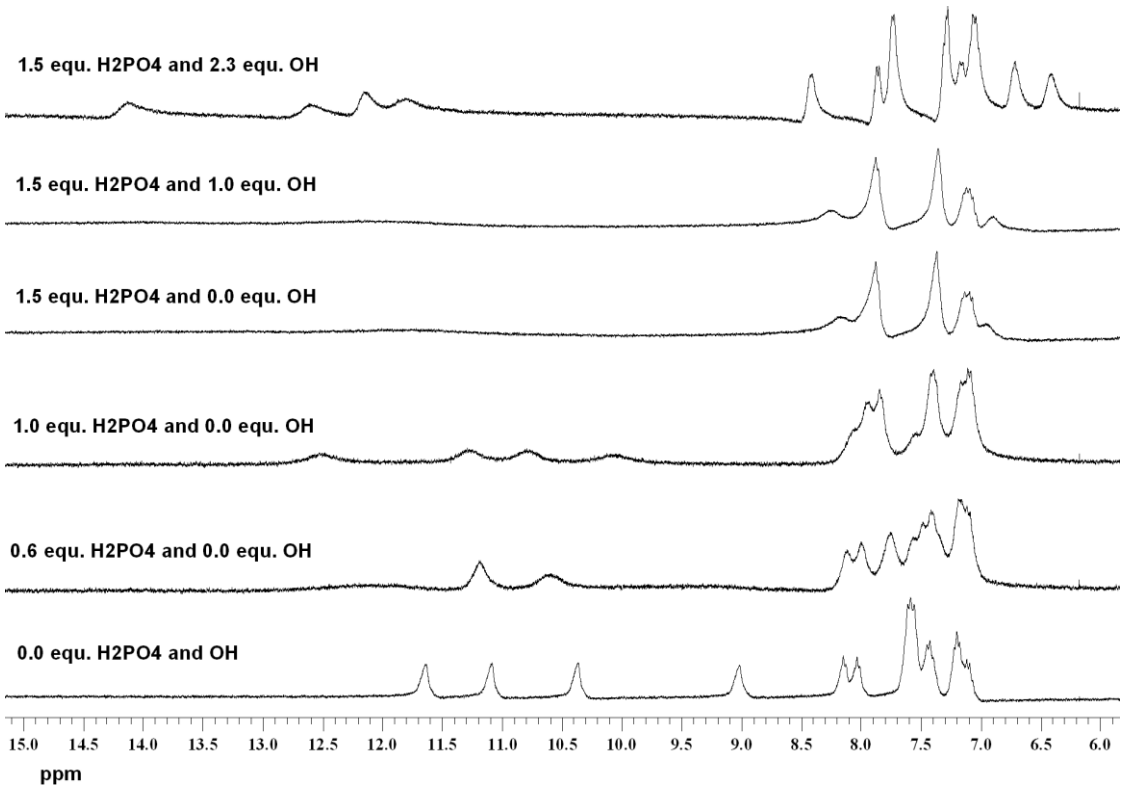

Receptor 222 *vs.* $TBAHCO_3$ in DMSO-d_6/H_2O 10% *

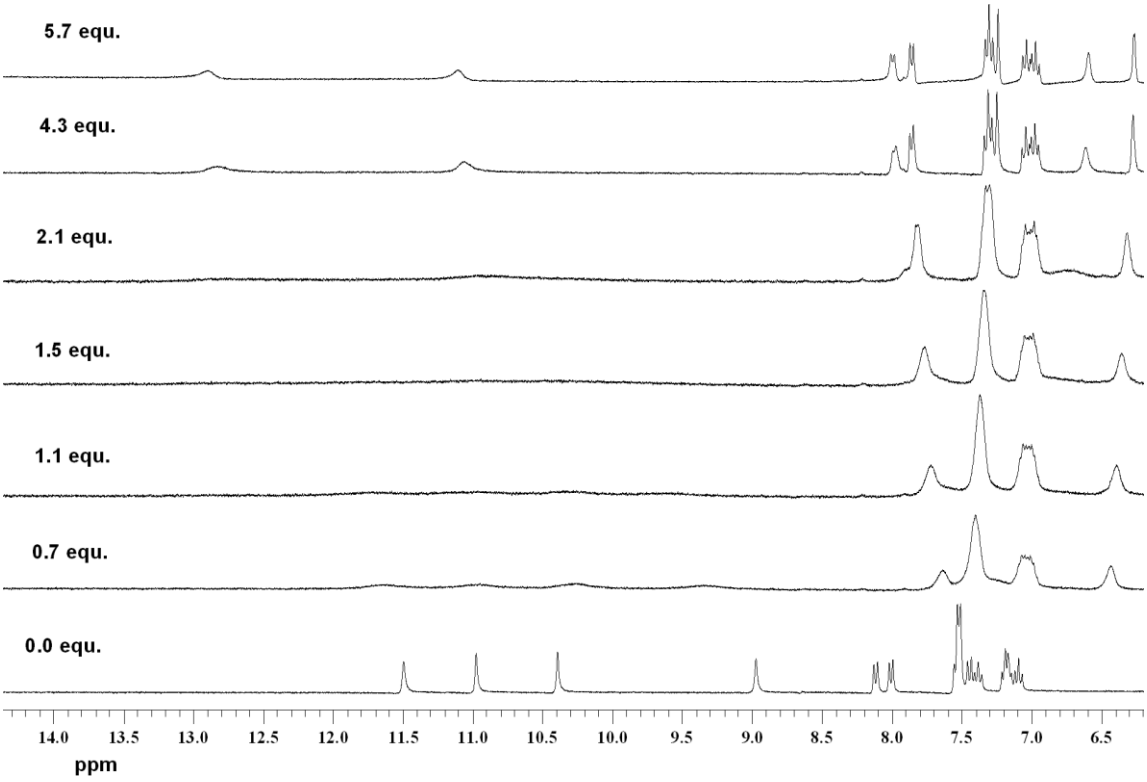

Receptor 222 *vs.* $TBAHCO_3$ and TBAOH in DMSO-d_6/H_2O 10%

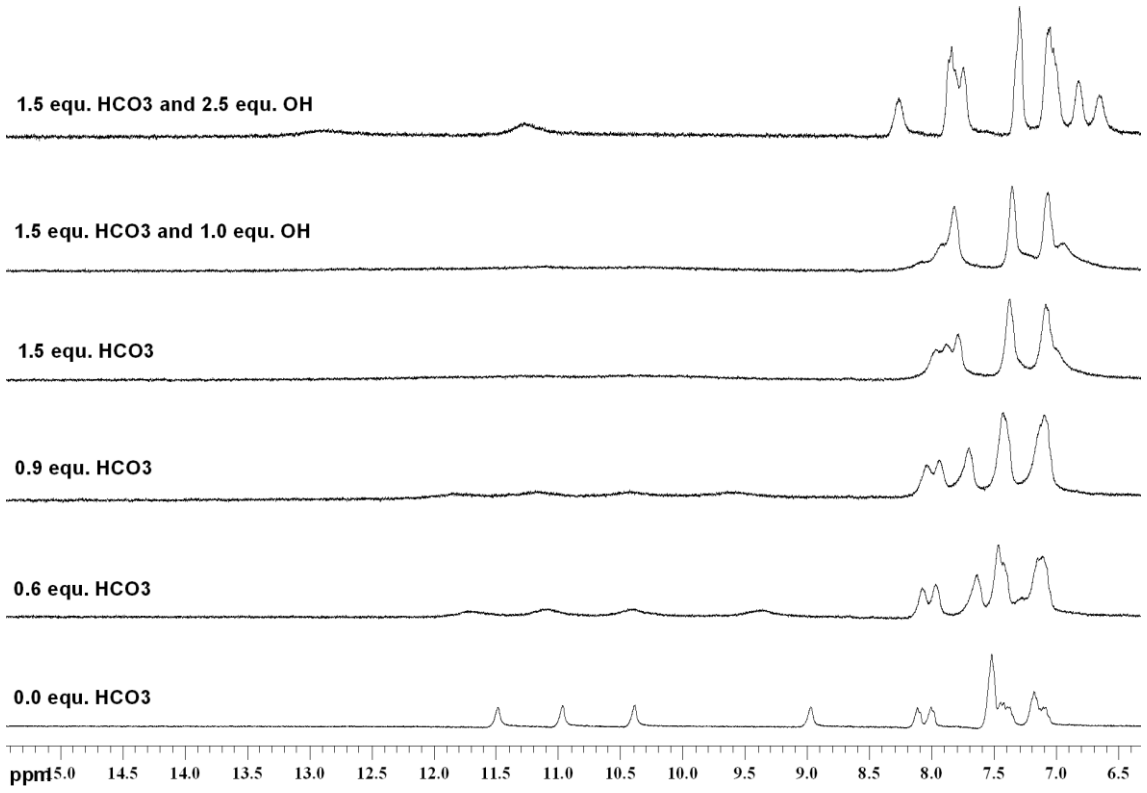

Receptor 221 (indole compound) and Receptor 222 (carbazole compound) *vs.* TBAOH in DMSO-d_6/H_2O 10%

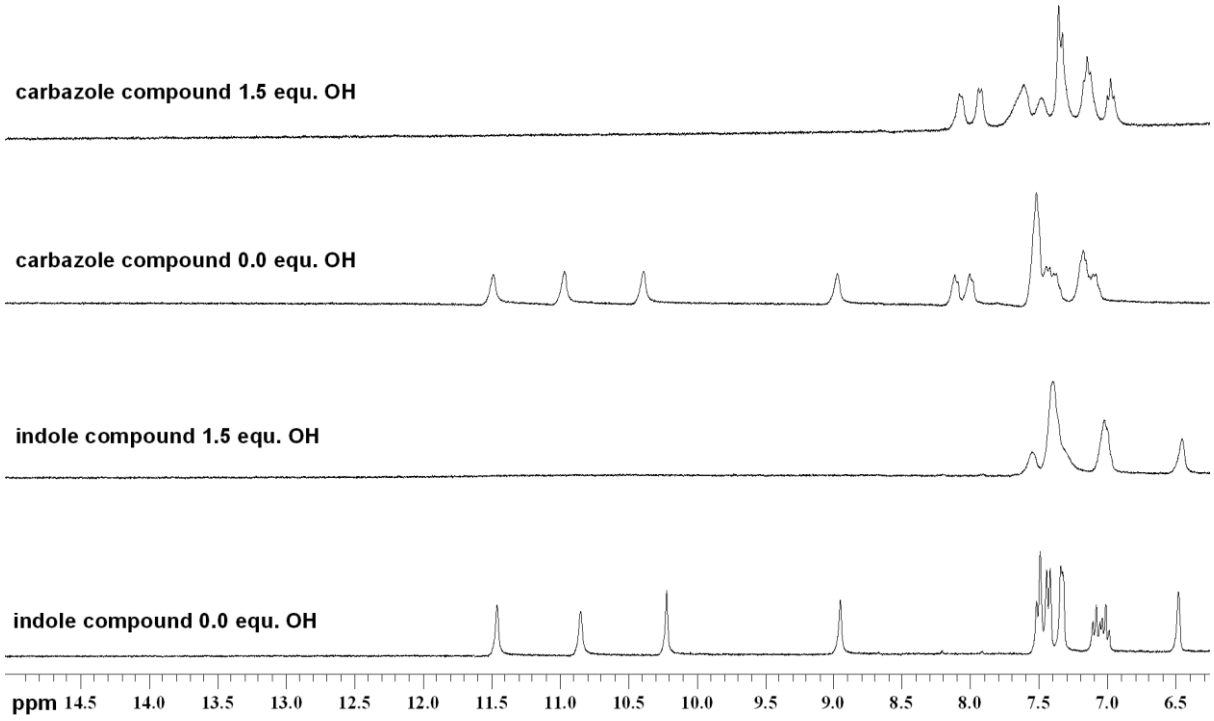

NMR Stack plots from Chapter Five

Receptor 241 *vs.* TBAF in DMSO-d_6/H_2O 0.5%

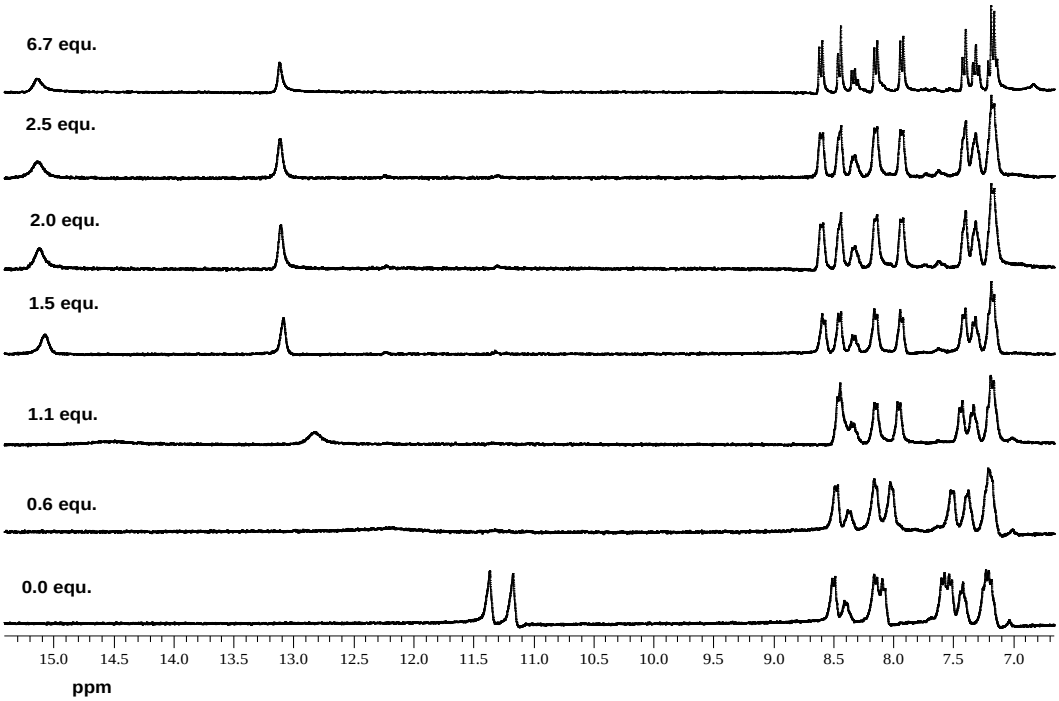

Receptor 242 *vs.* TBAF in DMSO-d_6/H_2O 0.5%

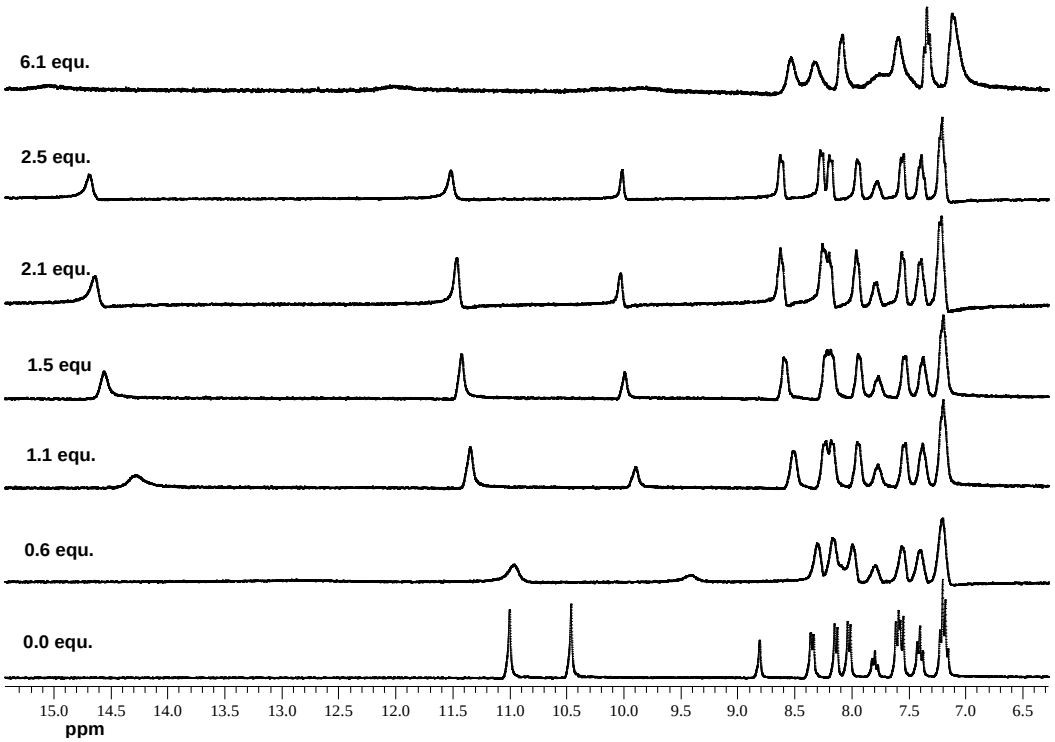

Appendix 6 – Proton NMR Titration Stack Plots

Appendix 7 – Two Dimensional NMR

NMR from Chapter Three

COSY for receptor 220 in DMSO-d_6

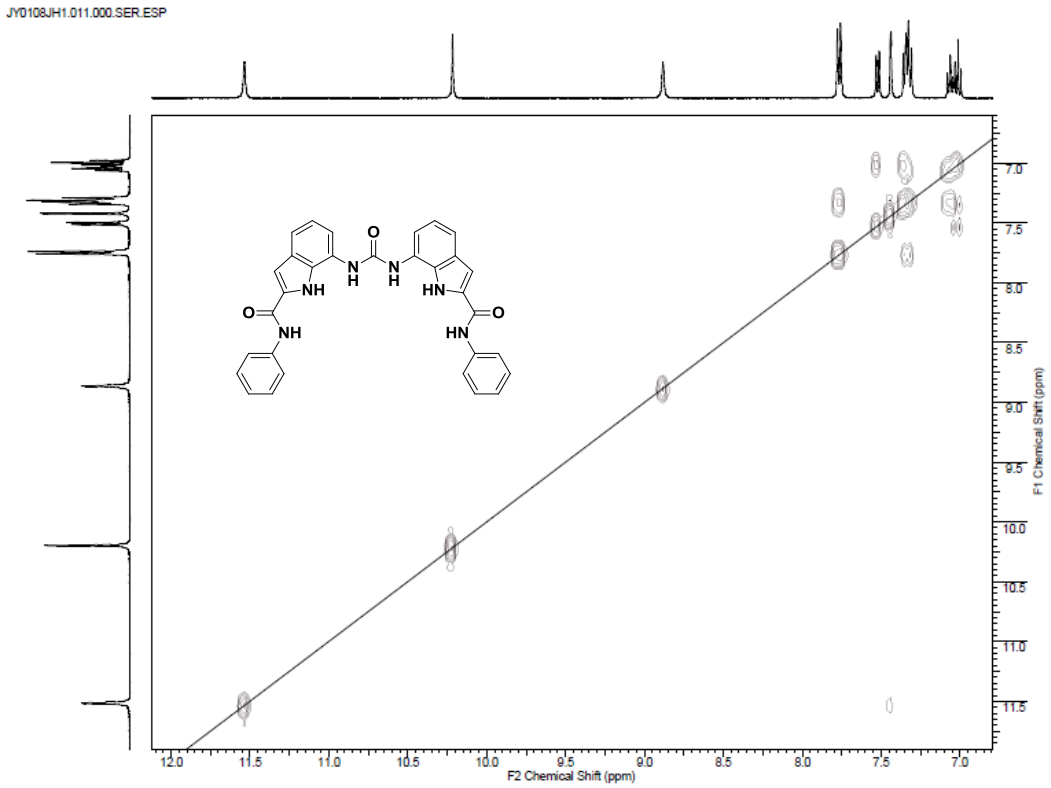

HMBC for receptor 221 in DMSO-d_6

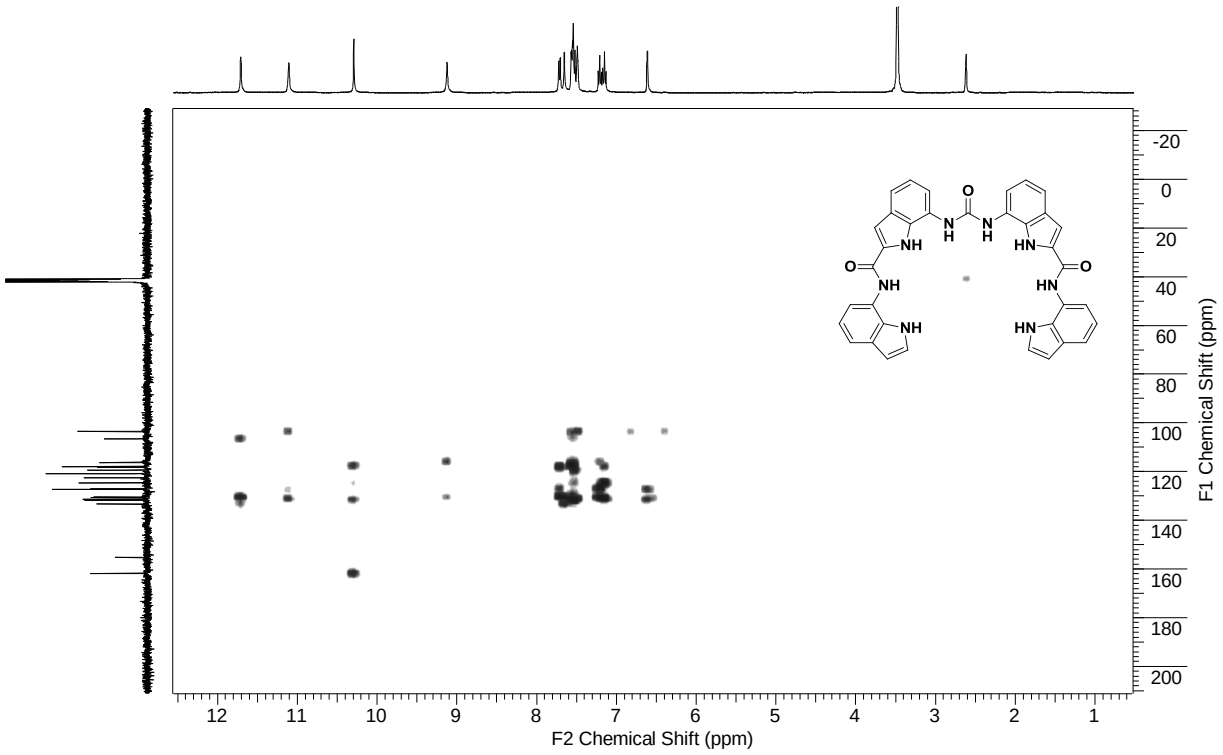

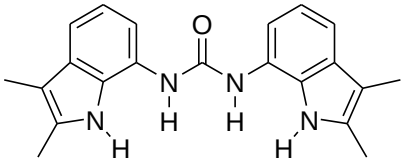

209

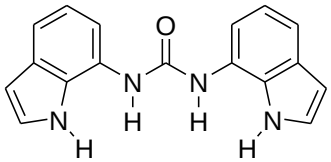

210

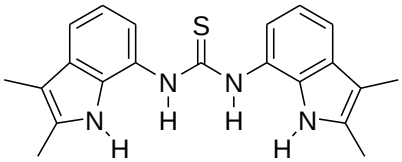

211

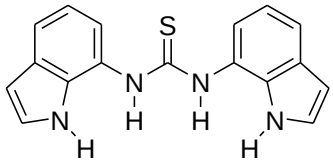

212

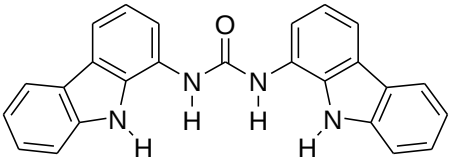

213

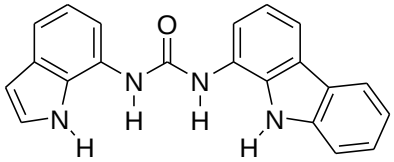

214

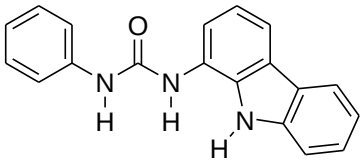

215

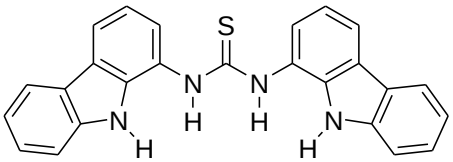

216

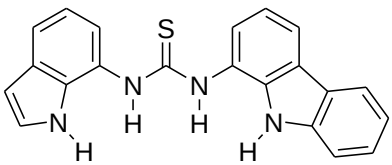

217

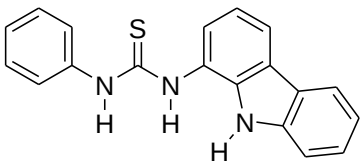

218

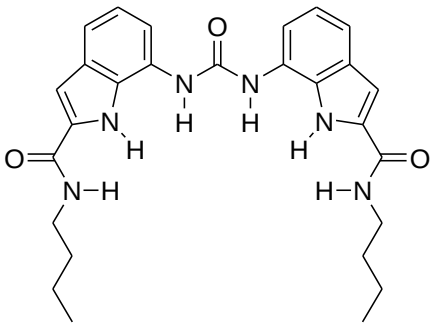

219

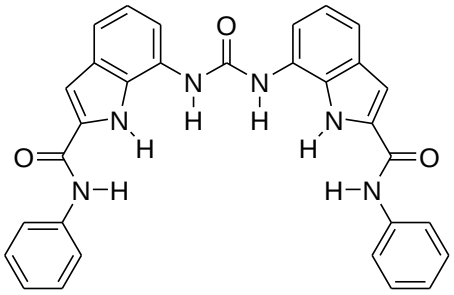

220

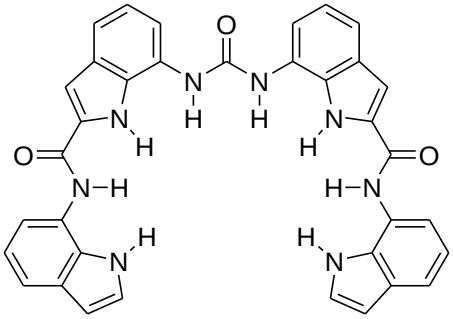

221

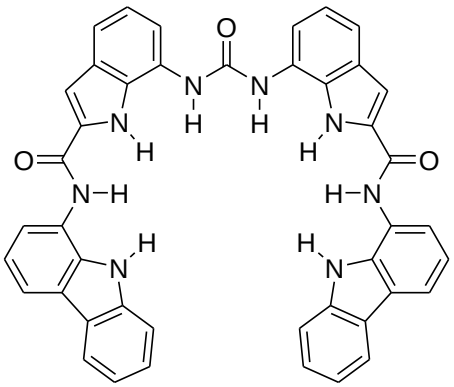

222

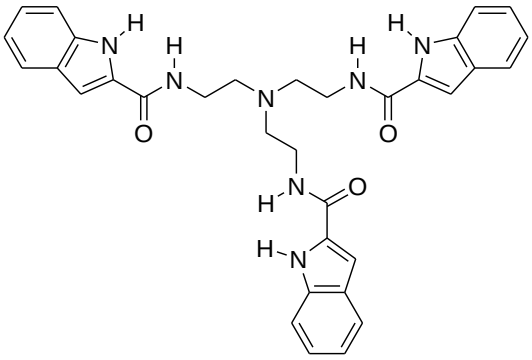

224

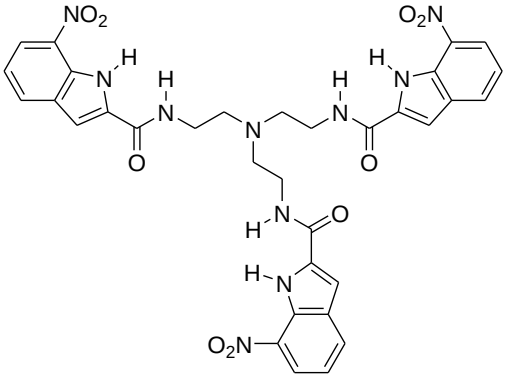

225

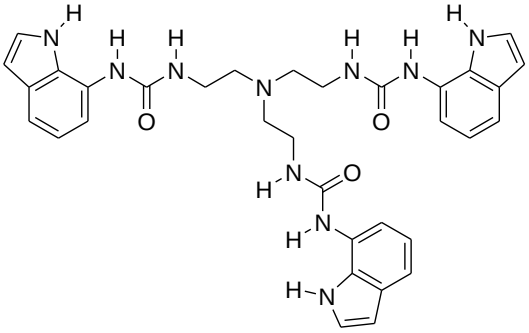

226

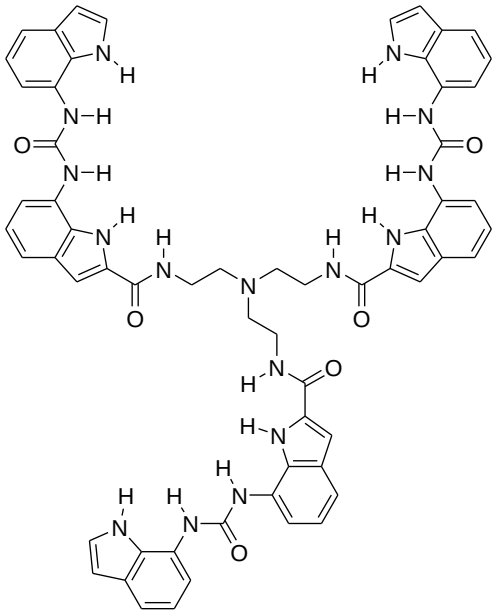

227

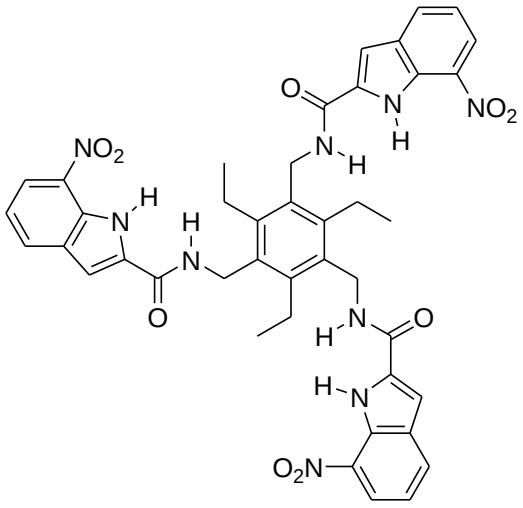

231

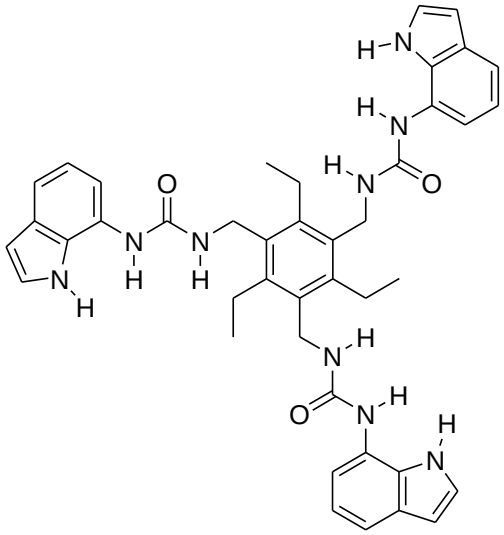

232

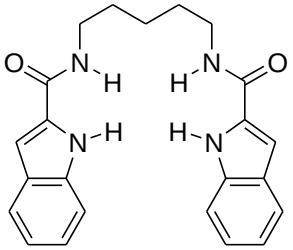

234

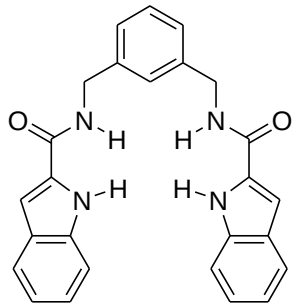

235

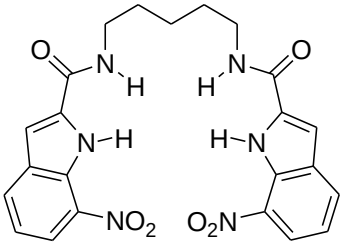

236

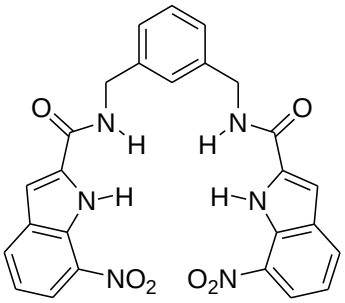

237

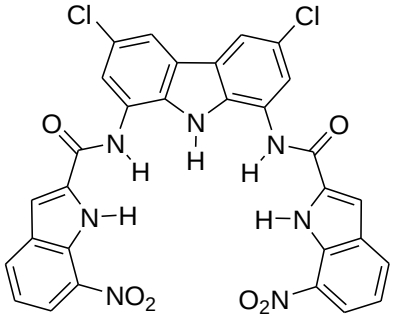

238

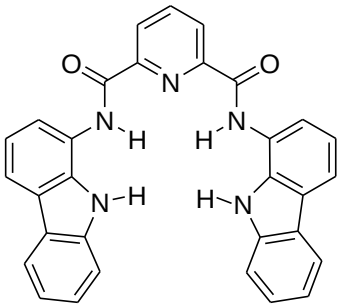

241

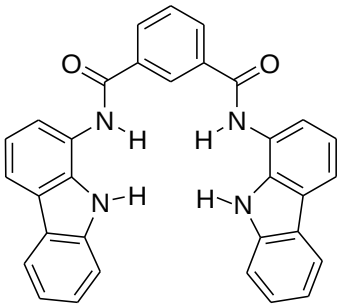

242